
Advances in

HETEROCYCLIC CHEMISTRY

VOLUME **104**

EDITORIAL ADVISORY BOARD

- A. T. Balaban, *Galveston, Texas, United States of America*
A. J. Boulton, *Norwich, United Kingdom*
D. L. Comins, *Raleigh, North Carolina, United States of America*
J. A. Joule, *Manchester, United Kingdom*
V. I. Minkin, *Rostov-on-Don, Russia*
A. Padwa, *Atlanta Georgia, United States of America*
C. A. Ramsden, *Keele, United Kingdom*
E. F. V. Scriven, *Trafalgar, Indiana, United States of America*
V. Snieckus, *Kingston, Ontario, Canada*
B. Stanovnik, *Ljubljana, Slovenia*
C. V. Stevens, *Gent, Belgium*
R. J. K. Taylor, *York, United Kingdom*
J. A. Zoltewicz, *Gainesville, Florida, United States of America*

Advances in
HETEROCYCLIC CHEMISTRY

VOLUME **104**

Editor

ALAN R. KATRITZKY, FRS

Kenan Professor of Chemistry

Department of Chemistry

University of Florida

Gainesville, Florida



Amsterdam • Boston • Heidelberg • London • New York • Oxford
Paris • San Diego • San Francisco • Singapore • Sydney • Tokyo

Academic Press is an imprint of Elsevier



Academic Press is an imprint of Elsevier
32 Jamestown Road, London, NW1 7BY, UK
Radarweg 29, PO Box 211, 1000 AE Amsterdam, The Netherlands
225 Wyman Street, Waltham, MA 02451, USA
525 B Street, Suite 1900, San Diego, CA 92101-4495, USA

First edition 2011

Copyright © 2011 Elsevier Inc. All rights reserved

No part of this publication may be reproduced, stored in a retrieval system or transmitted in any form or by any means electronic, mechanical, photocopying, recording or otherwise without the prior written permission of the publisher.

Permissions may be sought directly from Elsevier's Science & Technology Rights Department in Oxford, UK: phone (+44) (0) 1865 843830; fax (+44) (0) 1865 853333; email: permissions@elsevier.com. Alternatively you can submit your request online by visiting the Elsevier web site at <http://www.elsevier.com/locate/permissions>, and selecting *Obtaining permission to use Elsevier material*.

Notice

No responsibility is assumed by the publisher for any injury and/or damage to persons or property as a matter of products liability, negligence or otherwise, or from any use or operation of any methods, products, instructions or ideas contained in the material herein. Because of rapid advances in the medical sciences, in particular, independent verification of diagnoses and drug dosages should be made

ISBN: 978-0-12-388406-0
ISSN: 0065-2725

For information on all Academic Press publications visit our website at www.elsevierdirect.com

Printed and bound in USA
11 12 13 14 10 9 8 7 6 5 4 3 2 1

Working together to grow
libraries in developing countries

www.elsevier.com | www.bookaid.org | www.sabre.org

ELSEVIER

BOOK AID
International

Sabre Foundation

LIST OF CONTRIBUTORS

Numbers in parentheses indicate the pages on which the authors' contribution begins.

Maurizio D'Auria (127)

Dipartimento di Chimica "A. M. Tamburro", Università della Basilicata,
Via dell'Ateneo Lucano 10, 85100, Potenza, Italy

István Hermecz (1)

External Pharmaceutical Department, Technical University of Budapest,
Chinoin Ltd., 1045 Budapest, Hungary

Alexander P. Sadimenko (391)

Department of Chemistry, University of Fort Hare, Alice 5701, Republic of
South Africa

PREFACE

Volume 104 of our series comprises three chapters. In the first, Istvan Hermecz of the Technical University of Budapest, Hungary, provides an update to the chemistry of bicyclic 6–6 ring systems containing one bridge-head nitrogen and one extra heteroatom, together with their benzologs. The present update covering the literature between 2006 and 2009 and extends this subject which was previously treated in “Comprehensive Heterocyclic Chemistry,” see particularly CHEC-II, Volume 8, published in 1996, and CHEC-III published in 2008 which reviewed earlier years. These ring systems cover significant parts of the chemical space applicable to drug research, which have been intensively investigated in the past several years.

The second chapter is concerned with the photochemical and photophysical behavior of thiophene derivatives and is written by Maurizio D’Auria of the University of the Basilicata, Italy. The last readily available review of this topic is apparently the eight pages on the photochemistry of thiophene written by Lablache-Combiér, which appeared in a book on the photochemistry of heterocyclic compounds published in 1976. In recent years, photochemical and photophysical properties of thiophenes have become of great importance in a variety of technical and commercial applications; thus, the present chapter should fill an important place in the literature.

Our third contribution is by Alexander Sadimenko, of the University of Fort Hare, (Republic of South Africa) and continues the series of organometallic complexes of heterocycles. The present contribution covers a broad class of chelating ligands constituted by phosphinopyridines and related compounds. These interesting ligands possess both hard (pyridine nitrogen) and soft (phosphorus) coordination sites, which provides them with special properties in coordination chemistry.

Alan R. Katritzky
Gainesville, Florida, 2011

Recent Development in the Chemistry of Bicyclic 6–6 Systems Containing One Bridgehead Nitrogen Atom and One Extra Heteroatom and Their Benzologs: An update

István Hermecz

Contents	1. Introduction	2
	2. Pyrido[1,2- <i>b</i>][1,2]oxazines, -[1,2]thiazines, -pyridazines and Their Benzologs	5
	2.1 Structure	5
	2.2 Reactivity	6
	2.3 Synthesis	9
	2.4 Applications and important compounds	12
	3. Pyrido[1,2- <i>c</i>][1,3]oxazines, -[1,3]thiazines, -pyrimidines and Their Benzologs	12
	3.1 Structure	12
	3.2 Reactivity	15
	3.3 Synthesis	24
	3.4 Applications and important compounds	33
	4. Pyrido[2,1- <i>c</i>][1,4]oxazines, -[1,4]thiazines, pyrido[1,2- <i>a</i>] pyrazines and Their Benzologs	34
	4.1 Structure	34
	4.2 Reactivity	51

External Pharmaceutical Department, Technical University of Budapest, Chinoin Ltd., 1045 Budapest, Hungary

Advances in Heterocyclic Chemistry, Volume 104
ISSN 0065-2725, DOI 10.1016/B978-0-12-388406-0.00001-4

© 2011 Elsevier Inc.
All rights reserved

4.3 Synthesis	84
4.4 Applications and important compounds	119
List of Abbreviations	123
Acknowledgment	126

1. INTRODUCTION

This chapter covers the primary chemical literature of the title bi- and tricyclic ring systems cited in *Chemical Abstracts* Chemical Substance Indexes up to Volume 151 from Volume 144 between 2006 and 2009. Earlier literature data were systematically treated as primary subjects in *Comprehensive Heterocyclic Chemistry* series (96CHC-II(8)563, 08CHC-III(12)77).

The members of these ring systems occupy valuable parts of the chemical space for drug research, as most of their derivatives have drug-like properties and their outstanding representatives play an indispensable role in medicinal chemistry. The compounds, which were introduced into the human and veterinary therapies, are depicted in [Figure 1](#). Antofloxacin

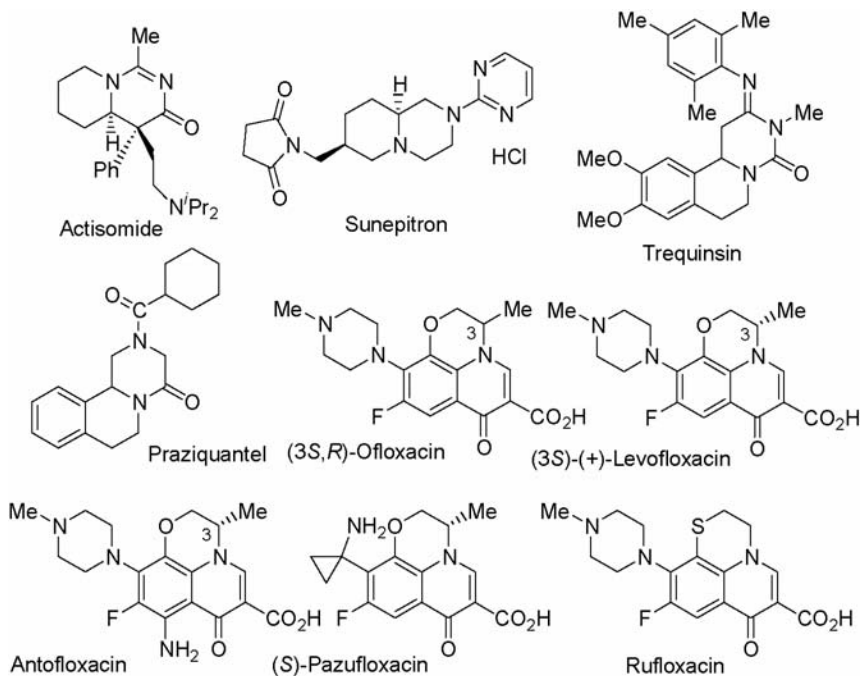


Figure 1. Outstanding representatives of ring systems that have been introduced into the human and veterinary therapy.

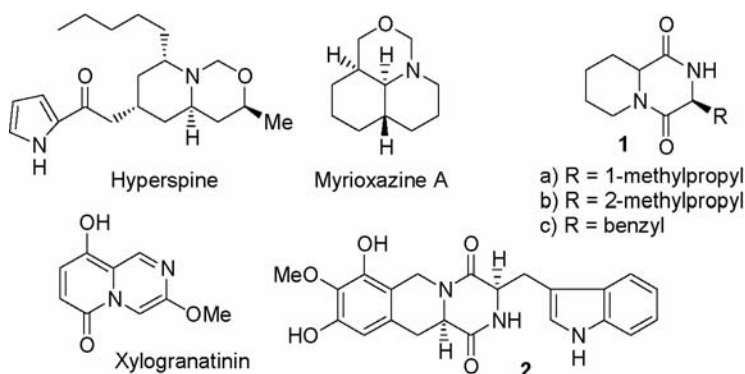


Figure 2. Representatives of the ring systems that were isolated from different natural sources.

is the newest member of this class, which has been applied to combat antibacterial infections since 2009 in China. Some prominent members were isolated from different natural sources, and their structures are shown in Figure 2.

The name of those ring systems that are treated in this chapter are indicated in *italics* in Figures 3–6. The first members of pyrido[2,1-*j*][3,1]

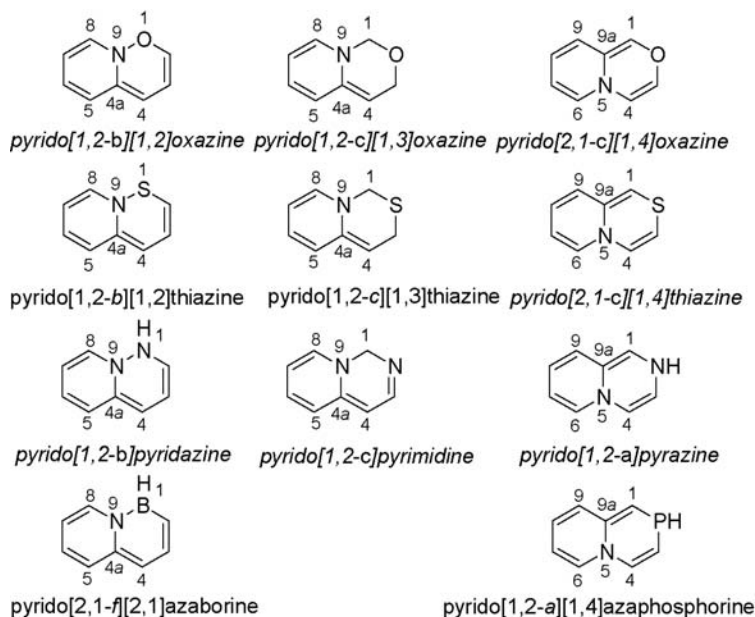


Figure 3. Overview of the known bicyclic ring systems containing one bridgehead nitrogen atom and one extra heteroatom with their numbering.

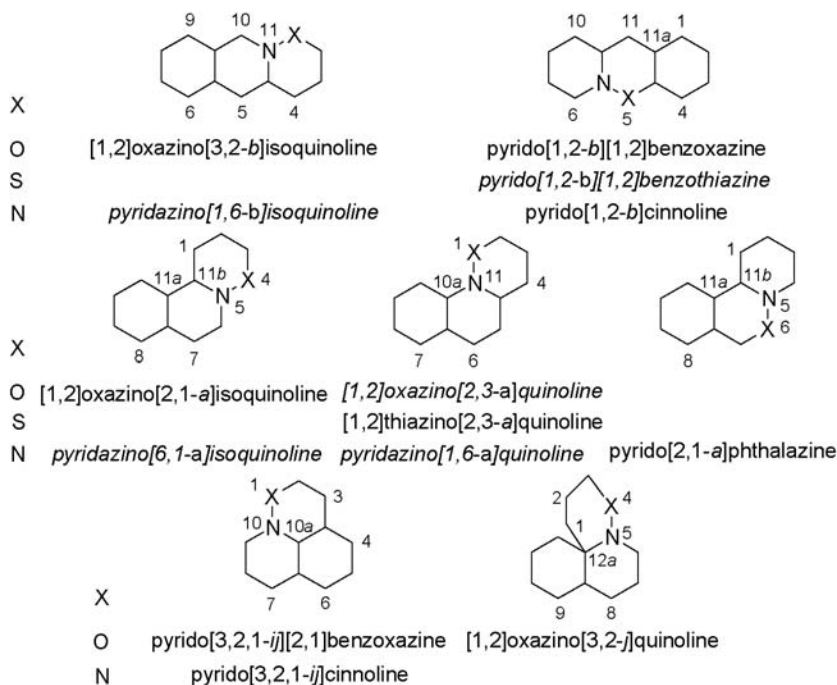


Figure 4. Overview of the known benzologs of pyrido[1,2-*b*][1,2]oxazine, -[1,2]thiazine, and -pyridazine with their numbering.

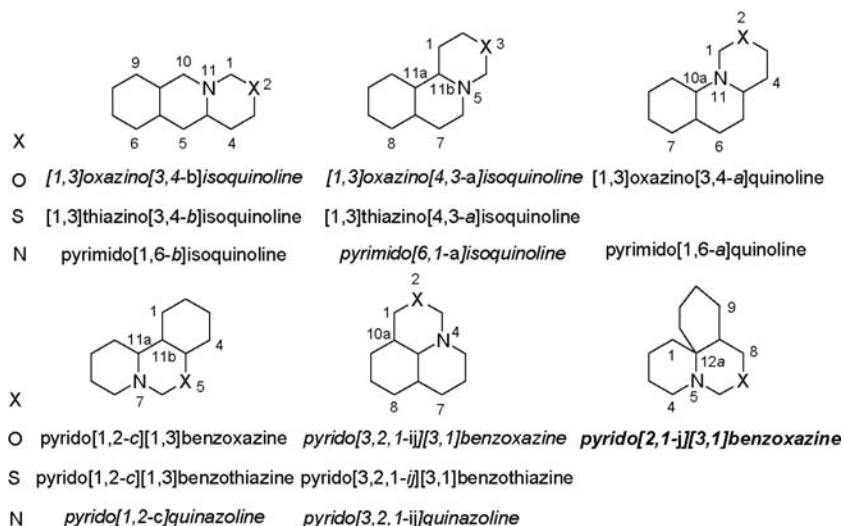


Figure 5. Overview of the known benzologs of pyrido[1,2-*c*][1,3]oxazine, -[1,3]thiazine, and -[1,2-*a*]pyrimidine with their numbering.

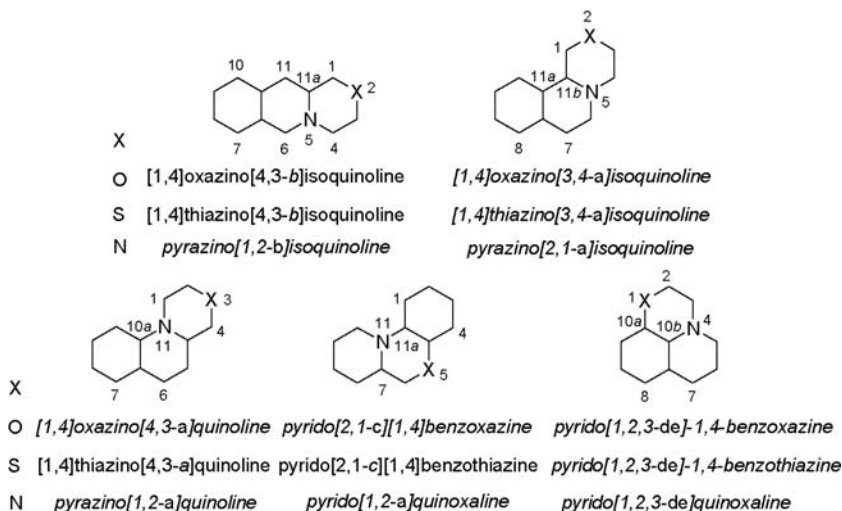


Figure 6. Overview of the known benzologs of pyrido[2,1-c][1,4]oxazine, -[1,4]thiazine, and -pyrazine with their numbering.

benzoxazine ring system were synthesized during the reviewed period, indicating in bold, as shown in Figure 5.

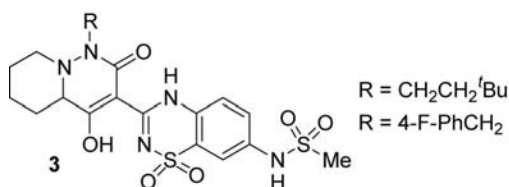
This chapter is divided into three subsections to treat separately bicycles appearing in Figure 3 with their benzo derivatives (Figures 4–6), as their basic synthesis differs from each other. Within each subsection structure, reactivity, synthesis and important compounds are discussed.

2. PYRIDO[1,2-*b*][1,2]OXAZINES, -[1,2]THIAZINES, -PYRIDAZINES AND THEIR BENZOLOGS

2.1 Structure

2.1.1 Theoretical calculations

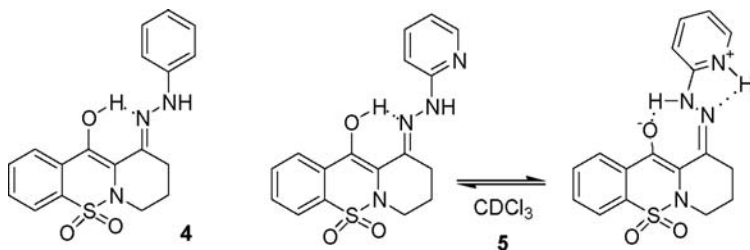
Partition coefficients of hexahydropyrido[1,2-*b*]pyridazines **3** were calculated by ACD software to be 1.49 ($R = \text{CH}_2\text{CH}_2^t\text{Bu}$) and 1.09 ($R = 4\text{-F-C}_6\text{H}_5$) (08BML5002).



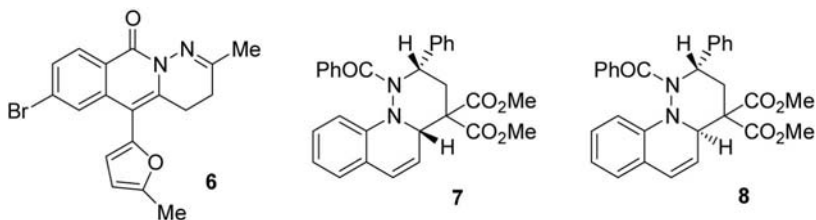
On the basis of CoMFA and CoMSIA analysis, three conformationally restricted selective D₃ ligands were successfully constructed and synthesized. One of them is *cis*-7*H*,9*aH*-7-[2-(2-benzo[*b*]thienyl)carboxylamino]ethyl]-2-(2,3-dichlorophenyl)perhydropyrido[1,2-*a*]pyrazine (06BMC5898).

2.1.2 Experimental structural methods

According to the ¹H NMR investigations hydrazone **4** exists predominantly as *E* isomer, while its pyridine analog **5** exhibits *E-Z* isomerism in CDCl₃ (08TL5711).



The structure of 3,4-dihydropyridazino[1,6-*b*]isoquinolin-10-one **6** was determined by single crystal X-ray experiment (07SL3431).

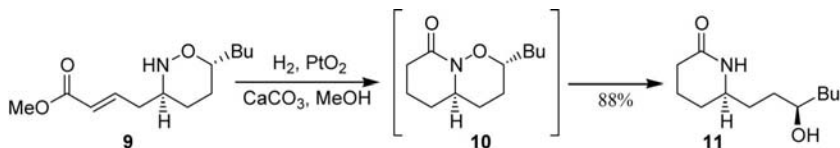


The relative configurations of diastereomers of 5*a*-H epimers **7** and **8** were established by X-ray crystallographic analysis (08OL689).

2.2 Reactivity

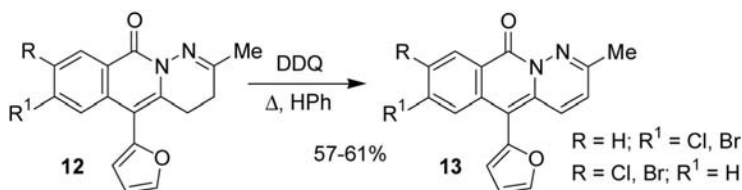
2.2.1 Ring opening

When oxazine **9** was hydrogenated over PtO₂ catalyst in the presence of CaCO₃ and the primarily formed perhydropyrido[1,2-*b*][1,2[oxazin-8-one **10** suffered an N–O cleavage to give piperidin-2-one **11** (09S655).



2.2.2 Oxidation

Oxidation of 3,4-dihydro-10*H*-pyridazino[1,6-*b*]isoquinolin-10-ones **12** with DDQ afforded the unsaturated 10*H*-derivatives **13** (07S2208).



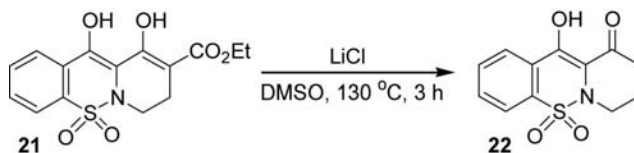
2.2.3 Hydrogenation reduction

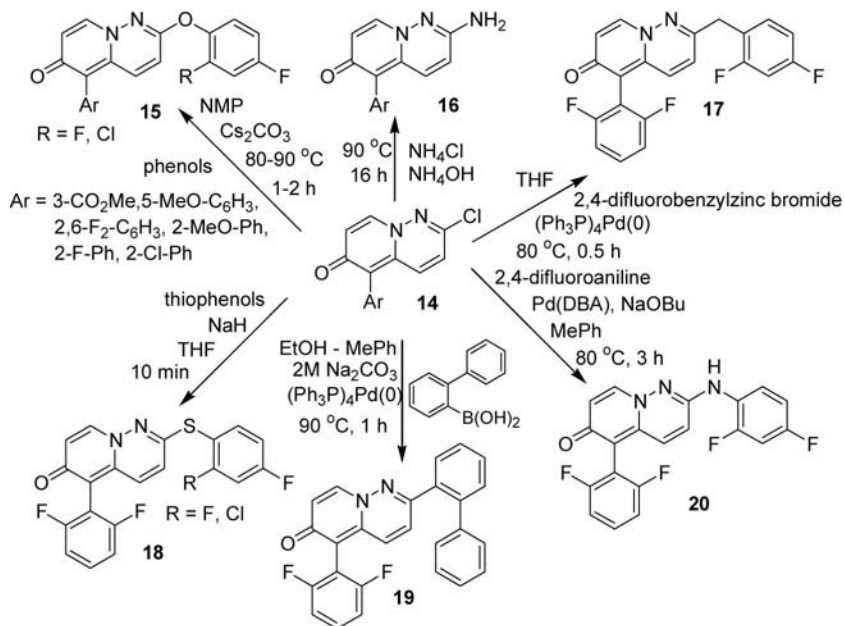
Catalytic hydrogenation of 2-(2,4-difluorophenoxy)-5-[2-vinylphenyl and 2-[(1*E*)-prop-1-enyl]phenyl]-6*H*-pyrido[1,2-*b*]pyridazin-6-ones over Pd/C in EtOAc yielded 5-(2-ethyl- and 2-propylphenyl) derivatives (07USA2007/0129372).

2.2.4 Reactivity of the ring carbon atom

Reaction of 2-chloro-6*H*-pyrido[1,2-*b*]pyridazin-6-ones **14** with phenols, thiophenols, 2,4-difluorobenzyl zinc bromide, biphen-2-ylboronic acid, 2,4-difluoroaniline, and $\text{NH}_4\text{OH}/\text{NH}_4\text{Cl}$ afforded different 2-substituted 6*H*-pyrido[1,2-*b*]pyridazin-6-ones **15–20** (Scheme 1) (07USA2007/0129372).

The treatment of pyrido[1,2-*b*][1,2]benzothiazine-2-carboxylate **21** with LiCl in DMSO at 130 °C gave decarboxylated product **22** (08TL5711).





Scheme 1

2.2.5 Reactivity of substituent attached to a ring carbon atom

Amino group of 2-amino-5-(2,4-difluorophenyl)-6H-pyrido[1,2-*b*]pyridazin-6-one was reacted with (2-fluorophenyl)isocyanate, with 2,4-difluorobenzoyl chloride to give 2-[N²-(2-fluorophenyl)ureido] and (2,4-difluorobenzoyl)amino derivatives, respectively (07USA2007/0129372).

Condensation of 10-oxopyrido[1,2-*b*][1,2]benzothiazine-5,5-dioxide **22** with arylhydrazines in boiling EtOH gave hydrazones **4** and **5** in 90–94% yield (08TL5711).

2.2.6 Reactivity of substituent present in a side chain

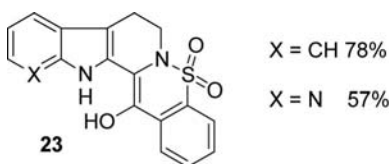
Aromatic ester group present in a side chain attached to position 5 of pyrido[1,2-*b*]pyridazine skeleton was hydrolyzed under basic conditions to the carboxyl group which was converted to the 5-methyl-1,2,4-oxadiazol-2-yl group by treatment with ClCO₂Et and NEt₃, followed by with H₂NNH₂·H₂O then with MeC(OEt)₃, and to carboxamide groups by treatment with ClCO₂Et and NEt₃, followed by with primary and secondary amines (07USA2007/0129372).

The bromo atom present in phenyl ring attached to position 5 of pyrido[1,2-*b*]pyridazine skeleton was changed for 3-fluorophenyl and

5-pyrimidyl group by treatment with respective boronic acids in the presence of $(\text{Ph}_3\text{P})_4\text{Pd}(0)$ and 2 M Na_2CO_3 in a mixture of MePh and EtOH at 90 °C for 16 h. Vinyl, (1*E*)-propen-1-yl and 2-furyl groups were introduced into phenyl group attached to position 5 of pyrido[1,2-*b*]pyridazine skeleton by the treatment of the appropriate bromo derivative with tributyl(vinyl)tin, tributyl(1-propenyl)tin, and tributyl(2-furyl)tin, respectively, in the presence of $(\text{Ph}_3\text{P})_4\text{Pd}(0)$ in MePh at 80 °C for 1 h (07USA2007/0129372).

2.2.7 Ring transformation

Heating hydrazones **4** and **5** in PPA at 180 °C for 30 min afforded pentacyclic derivatives **23** (08TL5711).

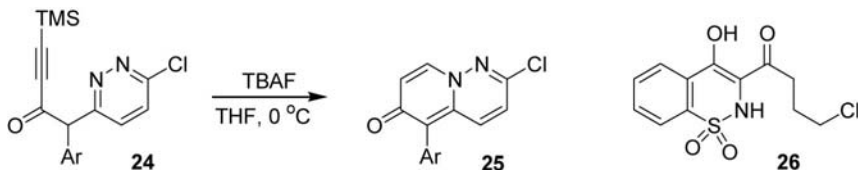


2.3 Synthesis

2.3.1 By the formation of one bond α to the bridgehead nitrogen atom [6+0(α)]

Catalytic hydrogenation of oxazine **9** over Pd/C catalyst gave pyrido[1,2-*b*][1,2]oxazin-8-one **10**, while hydrogenation over PtO_2 afforded piperidone **11** (09S655).

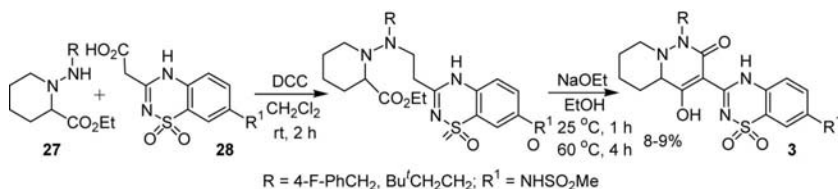
Cyclization of 1-(6-chloropyridazin-3-yl)-1-aryl-but-3-yn-2-ones **24** in the presence of TBAF gave 5-aryl-6*H*-pyrido[1,2-*b*]pyridazin-6-ones **25** (07USA2007/0129372).



The treatment of benzothiazine **26** with NaOEt in the presence of CuCO_3 in DMF at 70 °C for 5 h provided tricyclic pyrido[1,2-*b*][1,2]benzothiazine-5,5-dioxide **22** in 42% yield (08TL5711).

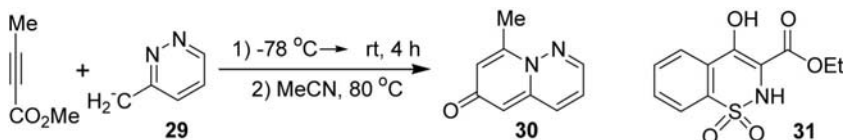
2.3.2 By the formation of one bond γ to the bridgehead nitrogen atom [6+0(γ)]

Reaction of 1-aminopiperidine-2-carboxylates **27** and (benzo[1,2,4]thiadiazin-3-yl)acetic acid **28** in the presence of DCC, followed by the treatment with NaOEt afforded pyrido[1,2-*b*]pyridazin-2-ones **3** (08BML5002, 08WOP2008/073987).



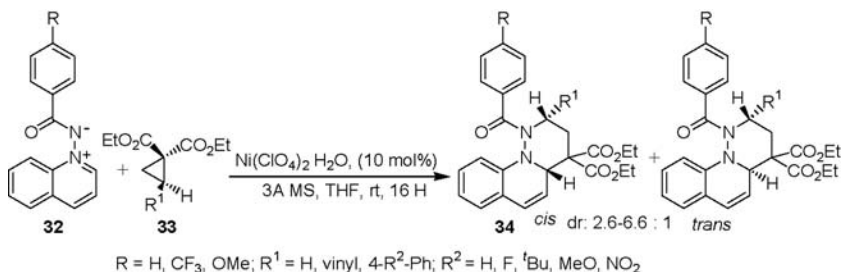
2.3.3 By the formation of two bond from [3+3] atom fragments

6-Endo-trig cyclization of anion **29**, formed from 3-methylpyridazine by LDA in THF with methyl 3-propynoate provided 6*H*-pyrido[1,2-*b*]pyridazin-6-one **30** (06TL5063).

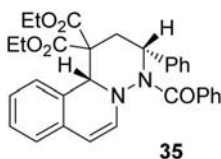


Cyclocondensation of [1,2]benzothiazine-3-ester **31** and ethyl 4-chlorobutyrate in the presence of NaOEt and CuCO_3 in a mixture of EtOH and DMF at 65 °C for 8 h gave pyrido[1,2-*b*][1,2]benzothiazine **22** in 47% yield (08TL5711).

Lewis acid $[\text{Ni}(\text{ClO}_4)_2]$ catalyzed cycloaddition of 1-iminoquinolinium ylides **32** with cyclopropanediester **33** afforded diastereoselectively *cis*-1,2,3,4-tetrahydro-4*aH*-pyridazino[1,6-*a*]quinoline-3,3-dicarboxylates **34**. Somewhat lower conversion could be achieved by the application of $\text{SC}(\text{OTf})_3$ and $\text{Mg}(\text{OCl}_4)_2$, while MgI_2 , $\text{Yb}(\text{OTf})_3$, $\text{Cu}(\text{OTf})_2$, and $\text{Cu}(\text{ClO}_4)_2$ gave little or no conversion. The presence of water had a detrimental effect on the yield. Reaction in the absence of 3 Å MS gave only 45% conversion, instead of 94% yield (**34**, $R = \text{H}$, $R^1 = \text{Ph}$) (08OL689).

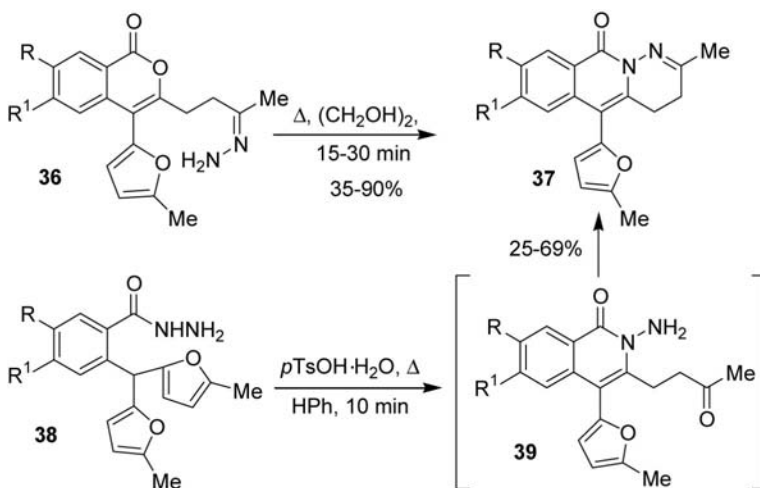


Similar reaction of *N*-benzoyl-2-iminoisoquinolinium ylide and cyclopropanediester **33** (R^1 = Ph) gave 1,2,3,4-tetrahydro-11*b*H-pyridazino[6,1-*a*]isoquinoline-1,1-dicarboxylate **35** with high diastereoselectivity [(dr) 20:1] (08OL689).



2.3.4 Ring transformation

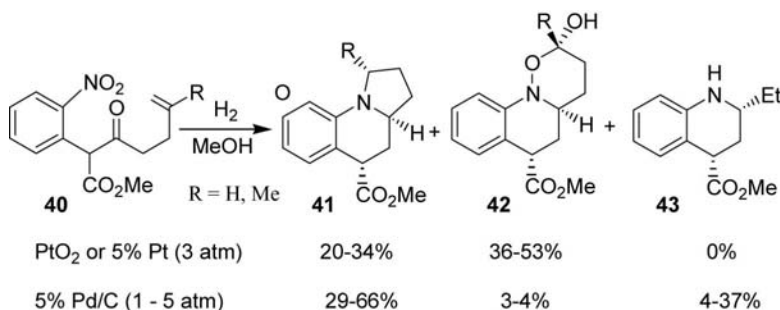
Heating hydrazones **36**, obtained from the appropriate ketones and $\text{H}_2\text{NNH}_2 \cdot \text{H}_2\text{O}$, in boiling ethylene glycol, afforded 3,4-dihydro-10*H*-pyridazino[1,6-*b*]isoquinolin-10-ones **37** (06SL3431, 07RUS2130653, 07S2208, 08JAP209609).



Recyclization of hydrazides **38** was carried out by treatment with *p*TsOH·H₂O gave 3,4-dihydro-10*H*-pyridazino[1,6-*b*]isoquinolin-10-ones **37** via tetrahydroisoquinolin-1-ones **39** (06SL3431, 07S2208).

2.3.5 Miscellaneous

Hydrogenation of 1,4-diketones **40** over PtO₂, Pt (5%) and Pd/C (5%) catalysts afforded a mixture of pyrrolo[1,2-*a*]quinoline-5-carboxylates **41**, [1,2]oxazino[2,3-*a*]quinoline-6-carboxylates **42** and quinoline-4-carboxylate **43** (06JHC1505). When palladium catalyst was applied, **41** formed only a few percent.



2.4 Applications and important compounds

Perhydropyrido[1,2-*b*][1,2]oxazine **10** was applied in the total synthesis of (–)-monomorphine I, an indolizidine alkaloid, to control the stereoselectivity (09S655).

Hexahydropyrido[1,2-*b*]pyridazin-2-ones **3** and their lower homologs exhibited HCV NS5B polymerase inhibitory activity and they may be applied in therapy to treat infections by hepatitis C virus (08BMC5002, 08WOP2008/073987). 3,4-Dihydropyridazino[1,6-*b*]isoquinolin-10-ones **37** are patented as electron-transferring agents in photoreceptors (07RUP2310653, 08JAP(K)2008/209609).

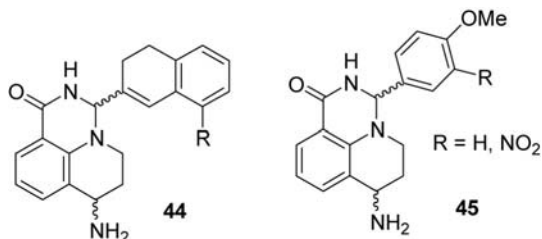
3. PYRIDO[1,2-*c*][1,3]OXAZINES, -[1,3]THIAZINES, -PYRIMIDINES AND THEIR BENZOLOGS

3.1 Structure

3.1.1 Thermodynamic aspects

Diastereomers and optical isomers of hexahydropyrido[3,2,1-*ij*]quinazoline **44** were separated by using silica gel flash column chromatography

and preparative chiral HPLC methods, respectively (07JAP(K)2007/131577):

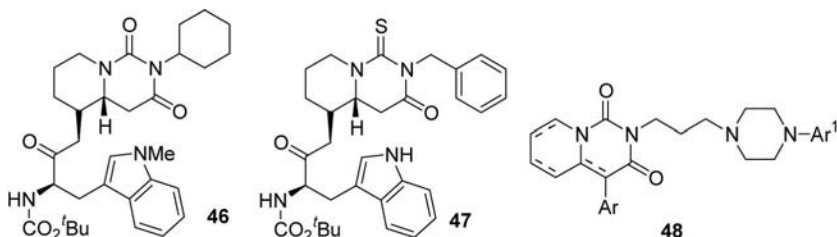


Diastereomers of nitro derivative of **45** (R = NO₂) were separated on a silica gel column chromatography, and enantiomers of *cis*-3*H*,7*H* derivative of **45** (R = H) were separated by chiral HPLC (06USA2006/0004028).

3.1.2 Theoretical calculations

Actisomide was included in a set of drugs for computational predictions of human drug clearance using different allometry methods (08MI1, 09JPS2472) and for computational predictions of volume of distribution using linear and nonlinear models (09JMC4488).

A new versatile 3D pharmacophore descriptor was developed, and perhydropyrido[1,2-*c*]pyrimidines **46** and **47** were also used to develop this method (08JCI797):



5-HT_{1a}, 5HT_{2a}, and α_1 -adrenergic receptor affinities of 4-aryl-2-{4-[4-(het)arylpiperazino]butyl}-2,3-dihydro-1*H*-, -2,3,5,6,7,8-hexahydro-1*H*- and -*trans*-4*H*,4*aH*-perhydropyrido[1,2-*c*]pyrimidine-1,3-diones **48** were analyzed by CoMFA methodology (06JGM353).

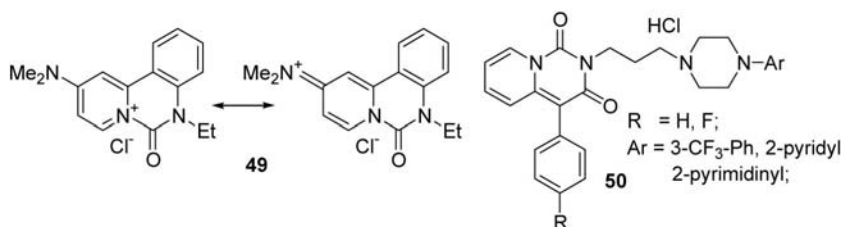
Chemical shifts of ¹³C CPMAS NMR spectra of 4-(4-fluorophenyl)-2-{4-[4-(3-trifluoromethylphenyl)piperazino]butyl}-2,3-dihydro-1*H*-pyrido [1,2-*c*]pyrimidine-1,3-dione and its hydrochloride salt were unambiguously assigned by theoretical calculations at GIAO/DFT (B3LYP/6-311 +G**) level (08JST325). Absolute energies, bond angles, and bond distances of 9,10-dimethoxy-1,6,7,11*b*-tetrahydro-2*H*,4*H*-[1,3]oxazino[4,3-*a*]

isoquinoline and its 4-oxo derivative were calculated at the B3LYP/6-31G* level (09T8021).

3.1.3 NMR spectroscopy

The temperature-dependent ^1H NMR measurements indicated that there is a substantial double character of C(10)-NMe₂ bond in **49**. The barrier to rotation is about 18.5 kcal mol⁻¹ (08T8381).

The structures of 4-aryl-2,3-dihydro-1*H*-pyrido[1,2-*c*]pyrimidine-1,3-diones hydrochlorides **50** were characterized by solid-state ^{13}C CPMAS NMR spectroscopy (08JT325).

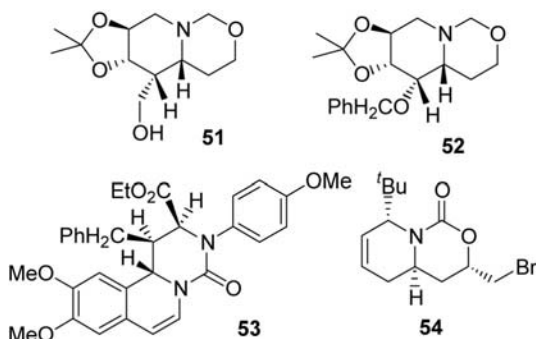


3.1.4 Mass spectrometry

6-Methyl-3,4-dihydro-1*H*,6*H*-pyrido[1,2-*c*][1,3]oxazine-1,4-dione was identified in a hemodialysate uremic sample by the LC-MS/MS technique (09RCM3194).

3.1.5 X-ray investigations

Stereostructures of perhydropyrido[1,2-*c*][1,3]oxazines **51** and **52** (06JOC8481, 06TL7923) and (+)-(3*R*,7*R*)-7-amino-3-(4-methoxyphenyl)-6,7-dihydro-3*H*,5*H*-pyrido[3,2,1-*ij*]quinazoline-1(2*H*)-one (06USA2006/0004028), the relative configuration of 1,1*b*-dihydro-2*H*,4*H*-pyrimido[6,1-*a*]isoquinolin-4-one **53** were determined by X-ray crystallographic analysis (09OL1559).



3,4,4*a*,5-tetrahydro-1*H*,8*H*-pyrido[1,2-*c*][1,3]oxazin-1-one **54** adopts an unsymmetrical half-chair conformation with deviations of the C(2), C(3), and N(1), C(4) atoms, respectively, from the main plain of the other ring atoms. The relative configurations of the asymmetric centers are (2*S**,4*R**,8*R**) (07EJO2015). Stereostructures of 7-bromo-2-bromomethyl-6-methoxy-11*b*-cyano-1,6,7,11*b*-tetrahydro-2*H*,4*H*-[1,3]oxazino[4,3-*a*]isoquinolin-1-one and its 2-methyl derivative was determined by X-ray crystal analysis (08JHC1651).

Structure of 4-(4-fluorophenyl)-2-{4-[4-(3-trifluoromethylphenyl)piperazino]butyl}-2,3-dihydro-1*H*-pyrido[1,2-*c*]pyrimidine-1,3-dione was characterized by X-ray diffraction study (08JST325). That of 6-oxopyrido[1,2-*c*]quinazolinium chloride **49** was established by X-ray single-crystal diffraction (08T8381).

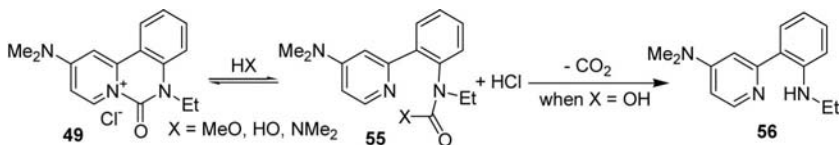
3.2 Reactivity

3.2.1 Ring opening

Ring-opened products were obtained from 3-methylene-3,4,4*a*,5-tetrahydro-1*H*,8*H*-pyrido[1,2-*c*][1,3]oxazin-1-ones (07EJC2015), different perhydropyrido[1,2-*c*][1,3]oxazines (06JOC8481, 06OBC1587, 06TL7923, 09JA11707), 4-cyano-3-phenyl-3-trifluoromethyl-2,3-dihydro-1*H*-pyrido[1,2-*c*]pyrimidin-1-one (05MI1), and 10-(*tert*-butyl)-3-methylene-3,4,4*a*,5-tetrahydro-3*H*-[1,3]oxazino[3,4-*b*]isoquinolin-1-one (07EJO2015) under either acidic or basic conditions.

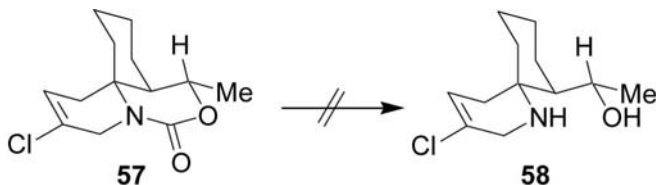
Reduction of perhydropyrido[1,2-*c*][1,3]oxazin-1-ones with Zn in AcOH yielded ring-opened products (06OBC1587).

N-(3-chloro-5-methoxycarbonylphenyl)-5-bromo-1,2,3,4-tetrahydroquinoline-8-carboxamide was obtained from 8-bromo-6,7-dihydro-1*H*,3*H*,5*H*-pyrido[3,2,1-*ij*][3,1]benzoxazine-1,3-dione with methyl 3-amino-5-chlorobenzoate in NMP at 170 °C for 16 h (07WOP2007/028789).



Pyrido[1,2-*c*]quinazolinium chloride **49** was stable when it was dissolved in MeOH, but ring opened products **55** (X = NMe₂) and **56** were obtained by treatment with HNMe₂ at room temperature in D₂O and in H₂O at 55 °C (08T8381). In MeOH the equilibrium between **49** and **55** (R = OMe) favors tricyclic form. When volatiles were removed from D₂O solution of urea **55** (X = NMe₂), it was converted back to the tricycle **49**. In H₂O

carbamic acid **55** ($X = \text{OH}$) gradually loses CO_2 to give **56** in 20% yield after 16 h.

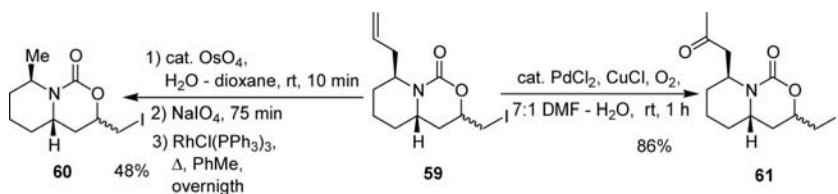


Pyrido[2,1-*j*][3,1]benzoxazin-6-one **57** could not be hydrolyzed to produce amino alcohol **58** (06TL3815).

For some more examples see Section 3.2.3.

3.2.2 Oxidation

Oxidation of 5-hydroxy-5-hydroxymethylperhydropyrido[1,2-*c*][1,3]oxazine derivative with silica supported NaIO_4 in CH_2Cl_2 at room temperature gave 8-oxo derivative (06JOC8481, 06TL7923). That of 3-azidomethyl-5,6,7-tribenzyloxy-8-hydroxymethylperhydropyrido[1,2-*c*][1,3]oxazin-1-one with 2-iodoxybenzoic acid in DMSO afforded 8-aldehyde, which was subsequently oxidized to 8-carboxyl derivative by treatment with NaClO_2 and $\text{NaPO}_4\text{H}_2 \cdot \text{H}_2\text{O}$ in MeCN with 72% yield over two steps (07CAR1813).



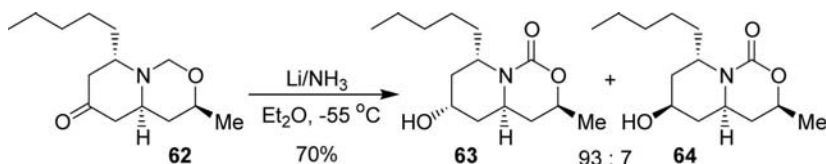
OsO_4 -mediated dihydroxylation of **59** followed by an oxidative cleavage of the formed diol with NaIO_4 gave the aldehyde, which was decarbonylated with $\text{RhCl}(\text{PPh}_3)_3$ to yield 8-methyl derivative **60** (06OBC1587). Wacker oxidation of **59** provided 8-(2-oxopropyl) derivative **61**.

For some more examples see Section 3.2.6.

3.2.3 Hydrogenation, reduction

Catalytic hydrogenation of (3*S*,4*aS*)-3-methyl-4,4*a*,7,8-tetrahydro-1*H*,3*H*-pyrido[1,2-*c*][1,3-oxazin-1-one in MeOH over Pd/C (10%) afforded perhydro derivative (09JA11707).

The treatment of a 5-oxoperhydropyrido[1,2-*c*][1,3]oxazine derivative with NaBH₄ in MeOH afforded *cis*-4*aH*,5*H*-5-hydroxy derivative (06JOC8481, 06TL7923). Reduction of (3*S*,4*aR*)-(+)-3-phenyl-4,4*a*,7,8-tetrahydro-1*H*,3*H*-pyrido[1,2-*c*][1,3]oxazin-1-one with LAH gave ring-opened 1-methyl-2-(2-phenyl-2-hydroxyethyl)-1,2,5,6-tetrahydropyridine (08S1033).



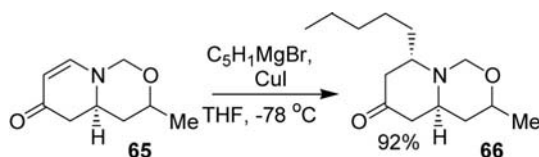
Reduction of perhydropyrido[1,2-*c*][1,3]oxazin-6-one **62** with Li and NH₃ in Et₂O gave a 93:7 diastereomeric mixture of **63** and **64** alcohols (05OL5227). Catalytic hydrogenation of 5-benzyloxy-6,7-dihydropyrido[1,2-*c*][1,3]oxazin-1-one over 10% Pd/C in EtOH for 9 h gave 5,6,7-trihydroxy derivative in 95% yield (06JOC8481). That of 3-azidomethyl-5,6,7-tribenzyloxy-8-benzyloxymethylperhydropyrido[1,2-*c*][1,3]oxazin-1-one over Pearlman's catalyst in aqueous MeOH in the presence of a few drops of AcOH for 24 h afforded 3-aminomethyl-5,6,7-trihydroxy-8-hydroxymethyl derivative in quantitative yield (07CAR1813). Similarly 3-aminomethyl-5,6,7-trihydroxy-1-oxoperhydropyrido[1,2-*c*][1,3]oxazine-8-carboxylic acid and 3-methyl-5,6,7-trihydroxy-8-hydroxymethyl-perhydropyrido[1,2-*c*][1,3]oxazin-1-one were obtained from 3-azidomethyl-5,6,7-tribenzyloxy-1-oxoperhydropyrido[1,2-*c*][1,3]oxazine-8-carboxylic acid and 3-methylene-5,6,7-tribenzyloxy-8-benzyloxymethylperhydropyrido[1,2-*c*][1,3]oxazin-1-one, respectively (07CAR1813).

7-Hydroxy- and 7-amino-3-aryl-2,3,6,7-tetrahydro-1*H*,5*H*-pyrido[3,2,1-*ij*]quinazolin-1-ones were prepared from 1,7-diones with NaBH₄ in MeOH, and by treatment with NH₄OAc in the presence of NaBH₃CN in a 1:1 mixture of CHCl₃ and MeOH at 50 °C, respectively (06USA2006/0004028). 7-Amino derivatives were also obtained from 7-hydroxyimino derivatives by catalytic hydrogenation over Pd/C catalyst in a mixture of DMF and 2.5 N HCl methanol solution at 50 °C for 12 h.

Catalytic hydrogenation of 9-(3-substituted prop-1-enyl, -2-enyl)-7-oxo-1*H*,3*H*,7*H*-pyrido[3,2,1-*ij*][3,1]benzoxazine-6-carboxylic acids (07WOP2007/054296) and 9-(3-substituted prop-1-ynyl)-7-oxo-1*H*,3*H*,7*H*-pyrido[3,2,1-*ij*][3,1]benzoxazine-6-carboxylates (06WOP2006/050940, 06WOP2006/050943, 07WOP2007/054296) over Pd/C (10%) for 5–70 h gave 9-(3-substituted propyl) derivatives.

For some more examples see Sections 3.2.6 and 3.2.7.

3.2.4 Reactivity of ring carbon atoms



Conjugate addition of dipentylcuprate, prepared from pentylmagnesium bromide and CuI , to 3,4,4a,5-tetrahydro-1H,6H-pyrido[1,2-c][1,3]oxazin-6-one **65** afforded nearly complete facial selectivity (96%) providing 8-pentylperhydropyrido[1,2-c][1,3]oxazin-6-one **66** (05OL5227).

Reaction of 4-cyano-3-trichloromethyl-1H-pyrido[1,2-c]pyrimidin-1-one with primary amines in boiling dioxane for 15 h gave 3-amino derivatives in 30–48% yields (05MI2).

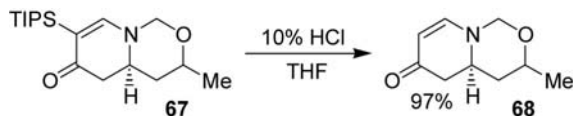
3.2.5 Reactivity of the ring nitrogen atom

The treatment of 6-chloro-4-cyclopropyl-7-fluoro-5-methoxy-1H,3H-pyrido[1,2-c]pyrimidine-1,3-dione with *O*-(2,4-dinitrophenyl)hydroxylamine in the presence of K_2CO_3 in a mixture of THF and DMF at 80°C for 2 h gave 2-amino derivative in 88% yield (09TL785).

4-Cyano-2,3-dihydro-1H-pyrido[1,2-c]pyrimidin-1- and -3-ones were *N*-alkylated with MeI in the presence of K_2CO_3 in DMF (05MI1). 4-Aryl-2,3-dihydro-1H-pyrido[1,2-c]pyrimidine-1,3-diones were *N*(2)-alkylated with 1,4-dibromobutane in the presence of K_2CO_3 in boiling acetone for 2 h in 57–95% yields (06EJM125).

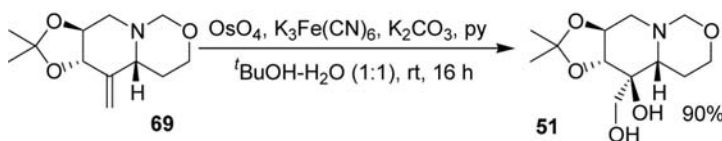
3.2.6 Reactivity of substituent attached to ring carbon atoms

Protodesilylation of 3,4,4a,5-tetrahydro-1H,6H-pyrido[1,2-c][1,3]oxazin-6-one **67** in the presence of the 10% aqueous solution of HCl gave 7-unsubstituted derivative **68** (05OL5227).

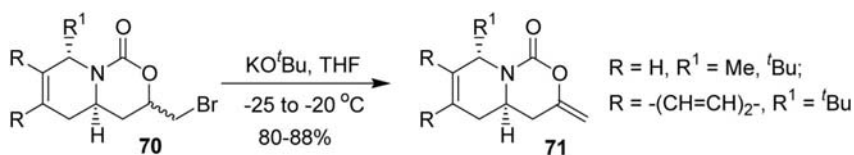


Heating 4-cyano-1-(4-methylphenyl)-1-trifluoromethyl-2,3-dihydro-1H-pyrido[1,2-c]pyrimidin-3-one in POCl_3 for 6 h provided 3-chloro-1H-pyrido[1,2-c]pyrimidine in 89% yield (05MI1).

The treatment of 5-benzyloxy-6,7-(dimethylmethylenedioxy)perhydropyrido[1,2-*c*][1,3]oxazine with 1 N HCl in MeOH at ambient temperature for 4 h gave 5-benzyloxy-6,7-dihydroxy derivative (06TL7923). Hydroxy derivatives of perhydropyrido[1,2-*c*][1,3]oxazines were *O*-benzylated with BnBr in the presence of NaH and TBAI in boiling THF (06JOC8481, 06TL7923). The 5-hydroxy group of a perhydropyrido[1,2-*c*][1,3]oxazine was *O*-mesylated with MsCl in pyridine at room temperature, and the mesyloxy group was changed for an azido group by inversion by treatment with LiN₃ in DMF at 110 °C, and hydrogenation over Pd/C in MeOH yielded an 5-amino derivative (06JOC8481). The dihydroxylation of 5-methyleneperhydropyrido[1,2-*c*][1,3]oxazine **69** using OsO₄ in the presence of K₃Fe(CN)₆ and K₂CO₃ produced 5-hydroxy-5-hydroxymethyl derivative **51** (06JOC8481, 06TL7923).



Epimeric mixture of 3-bromomethyl derivatives **70** undergoes rapid dehydrobromination with KO^{*t*}Bu to afford 3-methylene derivatives **71** (07EJO2015). The treatment of 3-iodomethyl-5,6,7-tribenzyloxy-8-benzylloxymethylperhydropyrido[1,2-*c*][1,3]oxazin-1-one with Bu₄NOH in MeCN yielded 3-methylene derivative, which was converted to 8-acetoxymethyl-3-methyl-5,6,7,8-tetrahydro-1*H*,4*aH* derivative by treatment with Ac₂O in TFA (07CAR1813).

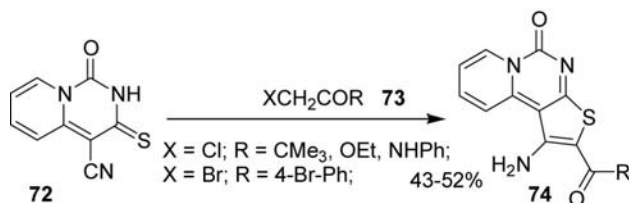


(+)-Hyperaspine, a ladybird alkaloid, was obtained in 50% yield from perhydropyrido[1,2-*c*][1,3]oxazin-6-one **62** by reduction of 6-oxo group with Li/NH₃, followed by the acylation of the hydroxyl group of a 93:7 diastereomeric mixture of **63** and **64** alcohols with pyrrole-2-carbonyl chloride in the presence of NEt₃ (05OL5227).

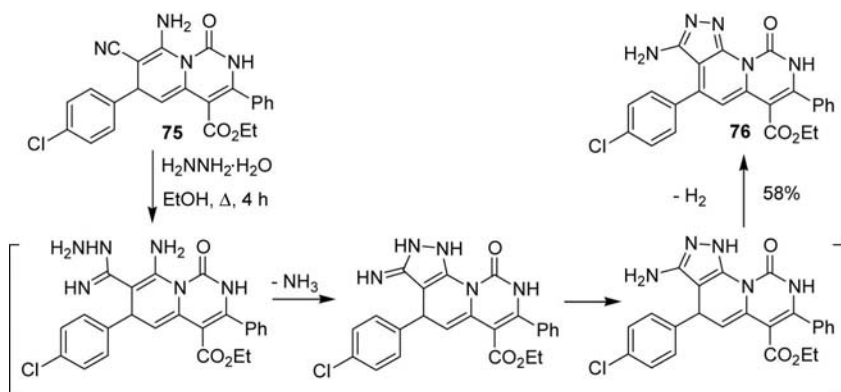
4-Amino derivatives were prepared from 4-benzamido derivatives of 4,4*a*,5,6,7,8-hexahydro-3*H*-pyrido[1,2-*c*]pyrimidin-3-ones (09S2802) and perhydropyrido[1,2-*c*]pyrimidine-1,3-diones (07SL1905) by heating in diluted H₂SO₄ solution under reflux for 45 min.

8-[(2-Hydroxyethyl)amino] derivatives were prepared from 2-(3-chlorophenyl)-8-fluoro-2,3,6,7-tetrahydro-1*H*,5*H*-pyrido[3,2-*ij*]quinazoline-1,3-dione with ethanolamine (6 equiv.) in NMP at 200 °C for 2 h under microwave irradiation. Buchwald–Hartwick reaction of 8-bromo-6,7-dihydro-1*H*,3*H*,5*H*-pyrido[3,2-*ij*]quinazoline-1,3-diones with 4-amino-1-benzylpiperidine in the presence of NaO^{*t*}Bu, Pd₂(dba)₃ and a catalytic amount of BINAP in PhMe at 80 °C for 2–16 h afforded 8-[(1-benzylpiperidin-4-yl)amino] derivatives (07WOP2007/028789).

7-Hydroxyimino-3-(4-methoxyphenyl)-2,3,6,7-tetrahydro-1*H*,5*H*-pyrido[3,2-*ij*]quinazolin-1-one was prepared from 1,7-dione with HONH₂·HCl in EtOH in the presence of pyridine at 80 °C for 3 h (06USA2006/0004028). 7-Amino-3-(4-methoxyphenyl)-2,3,6,7-tetrahydro-1*H*,5*H*-pyrido[3,2-*ij*]quinazolin-1-one was reacted with 4-dimethylaminobenzaldehyde in a mixture of CHCl₃ and MeOH containing HCl, followed by treatment with NaBH₃CN at 70 °C for 3 days to give 7-[(4-dimethylaminophenyl)methyl]amino derivative.



Reaction of 4-cyano-1-oxo-2,3-dihydro-1*H*-pyrido[1,2-*c*]pyrimidine-3-thione **72** with halogeno ketones **73** afforded tricyclic derivatives **74** (08MI2).



Reaction of 8-amino-7-cyano-2,6-dihydro-1*H*-pyrido[1,2-*c*]pyrimidin-1-one **76** and H₂NNH₂·H₂O afforded tricyclic derivative **77** (08H(75)887).

Reaction of 2-amino-6-chloro-4-cyclopropyl-7-fluoro-5-methoxy-1*H*,3*H*-pyrido[1,2-*c*]pyrimidine-1,3-dione with 3(*R*)-[(*tert*-butoxycarbonyl)amino]methylpyrrolidine in MeCN at 85 °C for 24 h gave 6-{3(*R*)-[(*tert*-butoxycarbonyl)amino]methyl-1-pyrrolidinyl} derivative in 83% yield (09TL785).

1-Aryl-4-cyano-1-trifluoromethyl-2,3-dihydro-1*H*-pyrido[1,2-*c*]pyrimidine-3-thiones were prepared from the 3-oxo derivatives by using Lawesson's reagent in boiling PhMe for 10 h in 64–67% yields. *S*-Alkylation of 1-aryl-4-cyano-1-trifluoromethyl-2,3-dihydro-1*H*-pyrido[1,2-*c*]pyrimidine-3-thiones with benzyl bromides, ethyl 2-bromoacetate, and 2-chloroacetamides in the presence of K₂CO₃ in DMF at ambient temperature gave 3-[(substituted methyl)thio]-1*H*-pyrido[1,2-*c*]pyrimidines in 51–87% yields (07MI1).

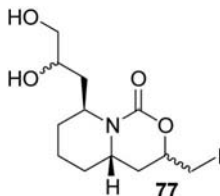
Heck couplings of 9-iodo-7-oxo-1*H*,3*H*,7*H*-pyrido[3,2,1-*ij*][3,1]benzoxazine-6-carboxylates with 3-substituted allyl derivatives in the presence of Pd(OAc)₂ and NEt₃ in boiling MeCN gave a mixture of 9-(3-substituted prop-1-enyl) and -2-enyl derivatives (07WOP2007/054296). Sonogashira couplings of 9-iodo-7-oxo-1*H*,3*H*,7*H*-pyrido[3,2,1-*ij*][3,1]benzoxazine-6-carboxylates with 3-substituted propargyl derivatives in the presence of Pd(PPh₃)₂Cl₂, CuI, and NEt₃ in a solvent (EtOH, MeCN,) at 50–100 °C, sometimes under microwave irradiation afforded 9-(3-substituted prop-1-ynyl) derivatives (06WOP2006/050940, 06WOP2006/050943, 07WOP2007/054296). Reaction of 9-iodo-3,3-dimethyl-7-oxo-1*H*,3*H*,7*H*-pyrido[3,2,1-*ij*][3,1]benzoxazine-6-carboxylate with *S*-[2-(2-*tert*-butoxycarbonylaminoethoxy)ethyl thioacetate] in the presence of CuI, K₂CO₃ and ethylene glycol in EtOH in a sealed tube at 120 °C for 1 h under microwave irradiation gave 9-[2-(2-*tert*-butoxycarbonylaminoethoxy)ethylthio] derivative (2006WOP06/050943).

Hydrolysis of alkyl 7-oxo-1*H*,3*H*,7*H*-pyrido[3,2,1-*ij*][3,1]benzoxazine-6-carboxylates under basic conditions afforded 6-carboxylic acids (06WOP2006/050940, 06WOP2006/050943, 07WOP2007/054296). An amide derivative was prepared from 9-fluoro-10-(4-methylpiperazin-1-yl)-8-methyl-1*H*,3*H*,7*H*-pyrido[3,2,1-*ij*][3,1]benzoxazine-6-carboxylic acid and an amine in the presence of DCC (07WOP2007/042504).

3.2.7 Reactivity of substituent present in a side chain

3-(4-Piperidyl)indoles were *N*-alkylated with 4-aryl-2-(4-bromobutyl)-2,3-dihydro-1*H*-pyrido[1,2-*c*]pyrimidine-1,3-diones in the presence of K₂CO₃ and a catalytic amount of KI in boiling MeCN for 4–5 h in 50–90% yields (09EJC1710). The bromo atom of 2-(4-bromobutyl)-4-aryl-2,3-dihydro-1*H*-pyrido[1,2-*c*]pyrimidine-1,3-diones was replaced by 4-(het)arylpiperazino

group by treatment with 1-(het)arylpiperazines in the presence of K_2CO_3 and KI in boiling MeCN for 10–15 h (06EJM125, 09EJM1710).



The Sharpless asymmetric dihydroxylation (AD-mix- α) of the epimeric mixture of 8-allyl-perhydropyrido[1,2-*c*][1,3-oxazin-1-one **59** in a mixture of t BuOH and H_2O at 0 °C for 17 h gave a diastomeric mixture of dihydroxy derivative **77** in 90% yield (06OBC1587).

An oxo group present in a side chain of perhydro-1*H*-pyrido[1,2-*c*][1,3-oxazin-1-one was converted into an cyclic acetal group by treatment with ethyleneglycol in the presence of p TsOH- H_2O in refluxing PhH (06OBC1587).

The iodo atom of a 3-iodomethylperhydropyrido[1,2-*c*][1,3]oxazin-1-one was changed for azido group with NaN_3 in the presence of Bu_4I in CH_2Cl_2 . The treatment of 3-azidomethyl-5,6,7-tribenzyloxy-8-benzyloxymethylperhydropyrido[1,2-*c*][1,3]oxazin-1-one with a mixture of Ac_2O and TFA at ambient temperature for 9 h gave 8-acetoxymethyl derivative, which was deacetylated to 8-hydroxymethyl derivative under Zemplén conditions by treatment with catalytic amount of Na in MeOH (07CAR1813).

Reaction of the amino group of 9-(3-aminopropyl)-3,3-dimethyl-1*H*,3*H*,7*H*-[1,3]oxazino[5,4,3-*ij*]quinoline-3-carboxylic acid and an aldehyde in MeOH in the presence of NaOAc, followed by the treatment of the formed Schiff base with $NaBH_3CN$ and AcOH gave *N*-alkylated product. This secondary amine was *N*-methylated with a mixture of 37% H_2CO aqueous solution and HCO_2H in $CHCl_3$ at 60 °C. Methanolysis of an acetoxy group, present in a side chain in the position 9 of 7-oxo-1*H*,3*H*,7*H*-pyrido[3,2,1-*ij*][3,1]benzoxazine-6-carboxylic acids, yielded hydroxy derivatives (06WOP2006/050943).

An acetoxy moiety, present in a side chain in the position 9 on 7-oxo-1*H*,3*H*,7*H*-pyrido[3,2,1-*ij*][3,1]benzoxazine skeleton, was hydrolyzed under basic condition to yield a hydroxy derivative (07WOP2007/054296). Phtalimido, and benzyloxycarbonylamino (07JP2007131577) and *tert*-butoxycarbonylamino groups (06WOP2006/050940, 06WOP2006/050943), present in a side chain on pyrido[3,2,1-*ij*][3,1]benzoxazin-7-one and pyrido[3,2,1-*ij*]quinazolin-4-one skeletons, were converted to an

amino group by treatment with $\text{H}_2\text{NNH}_2 \cdot \text{H}_2\text{O}$ in boiling EtOH for 45 min, by catalytic hydrogenation over Pd/C in MeOH, and by treatment with TFA in CH_2Cl_2 , respectively.

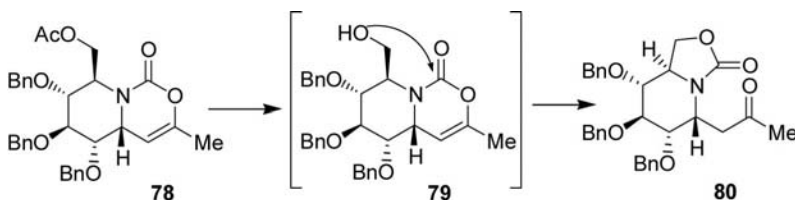
Ester and pivaloyloxy groups, present in a side chain of 1,2,3,5,6,7-hexahydropyrido[3,2,1-*ij*]quinazolin-1-ones, were hydrolyzed to carboxyl and hydroxyl groups, respectively under basic conditions (07JP2007131577).

Reaction of an amino group, present in a side chain of 7-oxo-1*H*,3*H*,7*H*-pyrido[3,2,1-*ij*][3,1]benzoxazine-6-carboxylic acids, with ethylene derivatives in the presence of a base in DMSO yielded (2-substituted ethyl)amino derivatives (06WOP2006/050940, 06WOP6006/050943).

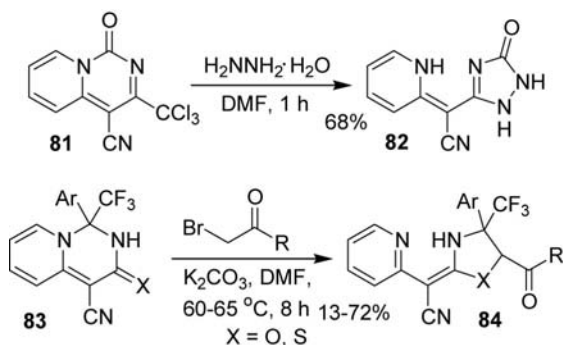
For some more examples see Section 3.2.4.

3.2.8 Ring transformation

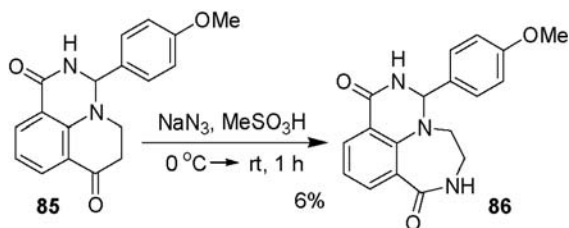
Methanolysis of 8-acetoxymethyl-5,6,7,8-tetrahydro-1*H*,4*aH*-pyrido[1,2-*a*]pyrimidin-1-one **78** under Zemplén condition in MeOH with catalytic amount of Na yielded 8-hydroxymethyl derivative **79**, which underwent ring transformation by intramolecular attack of the hydroxy group on the carbonyl group to give oxazino[3,4-*a*]pyridinone **80** in 70% yield (07CAR1813).



Ring-opening and ring-closure reaction of 1*H*-pyrido[1,2-*c*]pyrimidin-1-one **81** with $\text{H}_2\text{NNH}_2 \cdot \text{H}_2\text{O}$ afforded triazin-5-one **82** (05MI2). That of 1*H*-pyrido[1,2-*c*]pyrimidin-3-ones **83** ($\text{X} = \text{O}$) (05MI1) and 1*H*-pyrido[1,2-*c*]pyrimidin-3-thiones **83** ($\text{X} = \text{S}$) (07MI1) with bromomethyl aryl ketones gave oxazolidine and thioxazolidine derivatives **84** ($\text{X} = \text{O}$, S). Thioxazolidine derivatives **84** ($\text{X} = \text{S}$, $\text{R} = \text{OEt}$) were also obtained from ethyl 2-[(4-cyano-1-aryl-1-trifluoromethyl-1*H*-pyrido[1,2-*c*]pyrimidin-3-yl)thio]acetates in DMF at 80–90 °C for 18 h (07MI1). Heating 3-(aminocarbonylmethylthio)-4-cyano-1-(4-methylphenyl)-1-trifluoromethyl-1*H*-pyrido[1,2-*c*]pyrimidine in the presence of K_2CO_3 in DMF at 80–90 °C for 28 h gave (Z)-2-[cyano-(2-pyridyl)methylene]-1,3-tiazolidin-4-one in 67% yield (07MI1).



2,3,5,6,7,8-Hexahydro-1*H*-pyrimido[5,6,1-*jk*][1,4]benzodiazepine-1,8-one **86** was obtained when NaN_3 was gradually added to a solution of 2,3,5,6-tetrahydro-1*H*,7*H*-pyrido[3,2,1-*ij*]quinazoline-1,7-dione **85** in MeSO_3H (06USA2006/0004028).



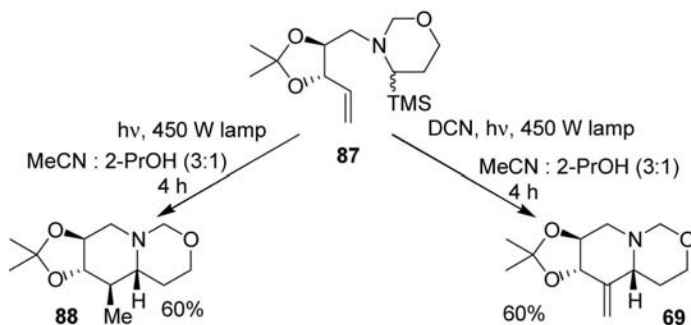
3.3 Synthesis

3.3.1 By the formation of one bond α to the bridgehead nitrogen atom [6+0(α)]

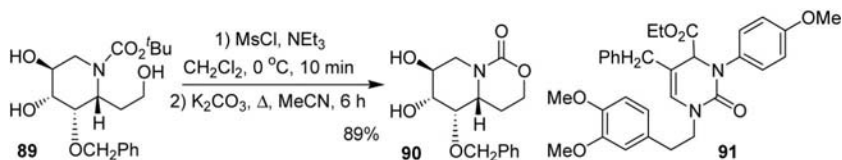
Heating 6-(4-chloro-3-hydroxybutyl)-2,4-dimethoxy-5-methylpyrimidine in MeOH saturated with gaseous NH_3 at 60°C overnight gave 7-hydroxy-3-methoxy-4-methyl-5,6,7,8-tetrahydro-1*H*-pyrido[1,2-*c*]pyrimidin-1-one in 72% yield (05MI3).

3.3.2 By the formation of one bond β to the bridgehead nitrogen atom [6+0(β)]

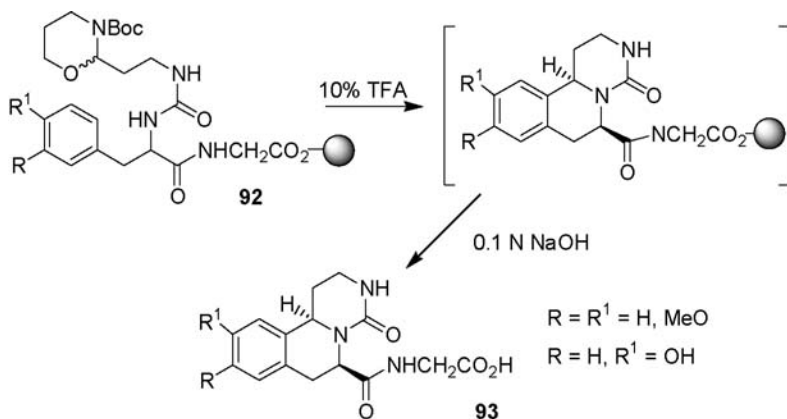
Photocyclization of the epimeric mixture of trimethylsilyloxazine **87** gave 5-methylperhydropyrido[1,2-*c*][1,3]oxazine **88** (06JOC8481, 06TL7923). If the reaction was carried out in the presence of 1,4-dicyanonaphthalene (DCN) 5-methylene derivative **69** was the product.



Perhydropyrido[1,2-*c*][1,3]oxazin-1-one **90** was obtained from 1-(*tert*-butoxycarbonyl)-2-(2-hydroxyethyl)piperidine **89** with MsCl in the presence of NEt_3 , followed by heating in boiling MeCN in the presence of K_2CO_3 (06JOC8481).



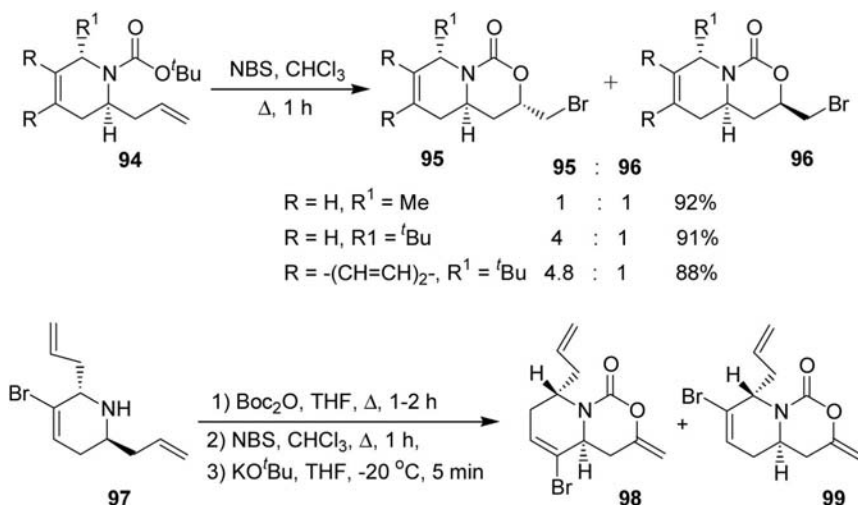
Heating a well-mixed mixture of 1-(2-hydroxyethyl)-2-ethoxycarbonyl-6,7-dimethoxy-1,2,3,4-tetrahydroisoquinoline and solid NaOMe at 130 °C for 45 min followed by extraction of the reaction mixture with EtOAc provided 9,10-dimethoxy-1,6,7,11*b*-tetrahydro-2*H*,4*H*-[1,3]oxazino[4,3-*a*]isoquinolin-4-one in 52% yield (09T8021). 1,3,4,6,7,11*b*-Hexahydro-2*H*-pyrimido[6,1-*a*]isoquinolin-4-one **53** was obtained from pyrimidinone **91** by a Pictet–Spengler reaction in CH_2Cl_2 in the action of TFA at ambient temperature (09OL1559).



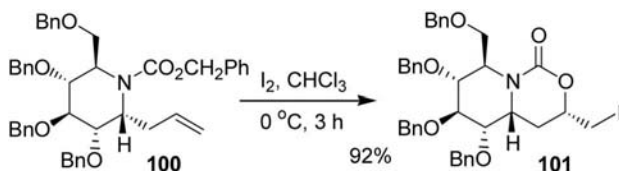
1,3,4,6,7,11*b*-Hexahydro-2*H*-pyrimido[6,1-*a*]isoquinolin-4-ones **93** were obtained, when resin bound glycine derivatives **92** were treated first with aqueous TFA, then with 0.1 N NaOH solution (06CEJ8056).

3.3.3 By the formation of one bond γ to the bridgehead nitrogen atom [6+0(γ)]

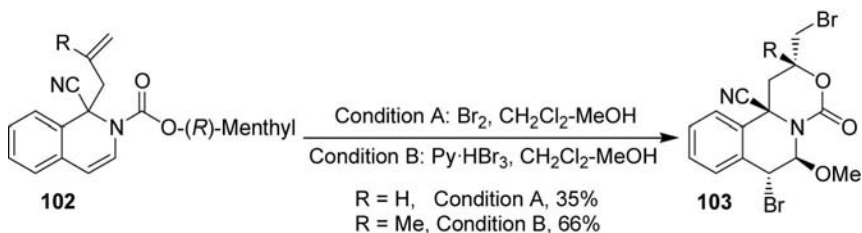
Bromocyclocarbamation reaction of 2-allyl-1-(*tert*-butoxycarbonyl)tetrahydropyridine **94** gave inseparable mixture of 3-epimers of **95** and **96**. When a bulky R^1 substituent (*t*Bu) was present in **94** a good level of diastereoselectivity was observed (07EJO2015). Reaction of 2,6-diallyl-tetrahydropyridine **97** with Boc_2O , followed by bromocyclocarbamation reaction with NBS, then the treatment of the reaction mixture with KO^tBu yielded a mixture of 5- and 7-bromo-3-methylene-tetrahydro-1*H*-pyrido[1,2-*c*][1,3]oxazin-1-ones **98** and **99**.



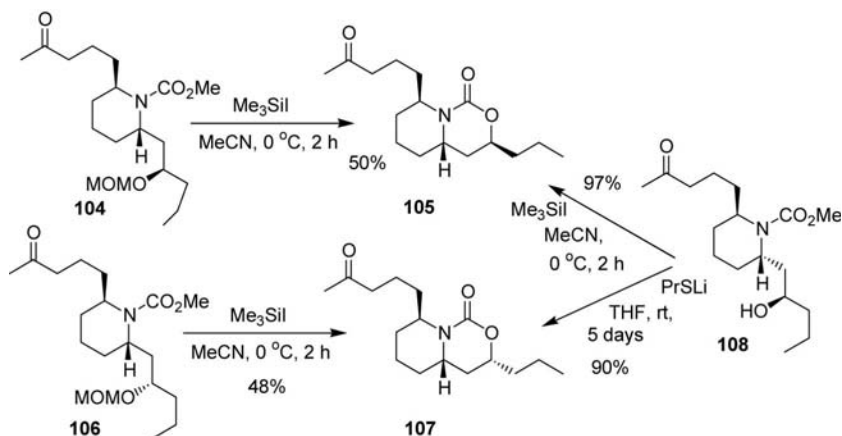
Iodocyclocarbamation reaction of *trans*-2,6-diallyl-1-(methoxycarbonyl)perhydropyridine with I_2 in CH_2Cl_2 overnight provided an 3-epimeric mixture of *trans*-4*aH*,8*H*-3-iodomethyl-8-allylperhydropyrido[1,2-*c*][1,3]oxazin-1-one in 98% yield (06OBC1587). That of 2-allyl-1-benzoyloxycarbonylpiperidine **100** gave *cis*-3*H*,4*aH*-3-iodomethylperhydropyrido[1,2-*c*][1,3]oxazin-1-one **101** (07CAR1813).



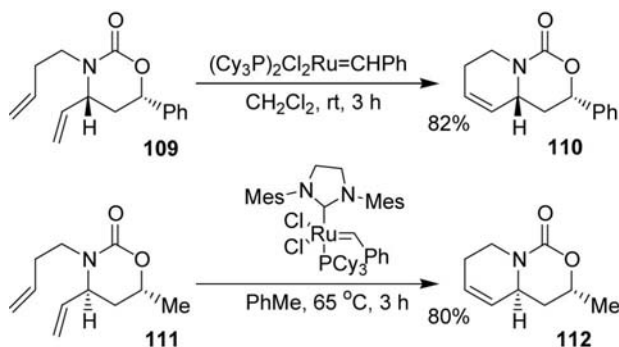
Bromocyclocarbamation reaction of 1-allyl-2-[(*R*)-menthyloxycarbonyl] derivatives of Reisert compounds **102** was accompanied by BrOMe addition to the C(3)-C(4) double bond to give 2-bromo-methyl-[1,3]oxazino[4,3-*a*]isoquinoline-4-ones **103** either under condition A with Br₂ or under condition B using pyridinium tribromides (08JHC1651).



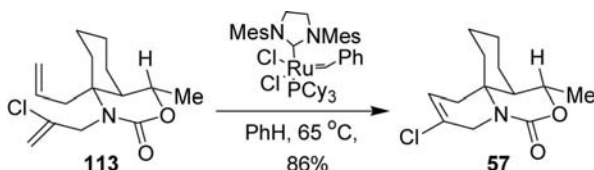
The treatment of methoxymethoxy derivatives **105** and **107** with Me₃SiI gave perhydropyrido[1,2-*c*][1,3]oxazin-1-ones **106** and **108**, respectively (06OBC1587). Better yields could be achieved when alcohol **109** was treated either with Me₃SiI or with Corey's reagent PrSLi, prepared from PrSH and BuLi.



[1,3]Oxazin-2-ones **109** and **111** underwent ring-closing methathesis on being treated with the Grubb's first-generation and second-generation catalysts to yield tetrahydro-1*H*,3*H*-pyrido[1,2-*c*][1,3]oxazin-1-ones **110** (08SI1033) and **112** (09JA11707), respectively.



The first representative **57** of pyrido[2,1-*j*]-3,1-benzoxazine ring system was synthesized by the ring-closing metathesis of perhydro-3,1-benzoxazine **113** in the presence of the second generation of Grubb's catalyst (06TL3815).

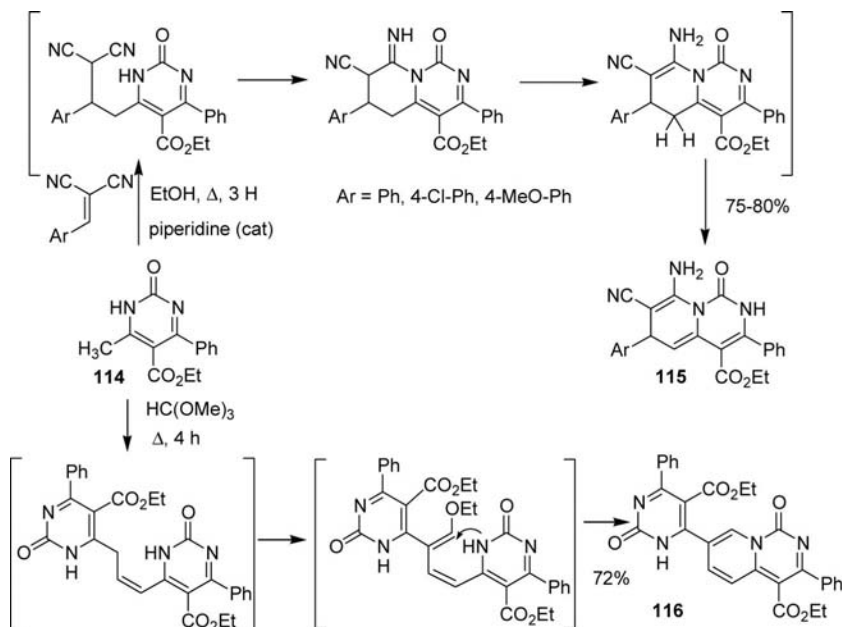


3.3.4 By the formation of two bond from [3+3] atom fragments

Cyclocondensation of 2-pyridylacetonitrile and ethoxycarbonyl isothiocyanate in MeCN gave 4-cyano-1-oxo-2,3-dihydro-1*H*-pyrido[1,2-*c*]pyrimidine-3-thione in 18% yield (08MI2). 6-Endo-trig cyclization of anion, formed from 4-methylpyrimidine by LDA in THF at -78°C , with methyl 3-propynoate provided 8-methyl-6*H*-pyrido[2,1-*c*]pyrimidin-6-one in 47% yield (06TL5063).

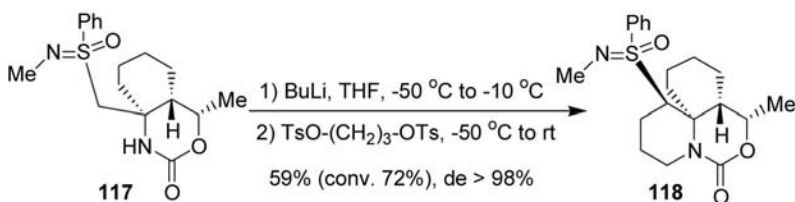
Reaction of pyrimidin-2(1*H*)-one **114** and arylmethylenemalononitrile in the presence of catalytic amount of piperidine gave 1,2-dihydro-6*H*-pyrido[1,2-*c*]pyrimidin-1-ones **115** [08H(75)887]. Heating **114** in boiling $\text{HC}(\text{OMe})_3$ yielded 1*H*-pyrido[1,2-*c*]pyrimidin-1-one **116**. The proposed reaction mechanisms are depicted in Scheme 2.

Reaction of lithium salts, formed from ethyl 4-substituted 6-methyl-2-oxo-1,2,3,4-tetrahydropyrimidine-5-carboxylates with BuLi, and 1,3-dibromopropane yielded 3-substituted 1-oxo-2,3,5,6,7,8-hexahydropyrido[1,2-*c*]pyrimidine-4-carboxylates (08T11718). Reaction of *N,C*-dianion,



Scheme 2

formed from perhydro-3,1-benzoxazine **117** with BuLi and 1,3-propanediol di-*p*-tosylate afforded 6*H*-pyrido[2,1-*j*]-3,1-benzoxacin-6-one **118** with high diastereoselectivity (07OL2155).



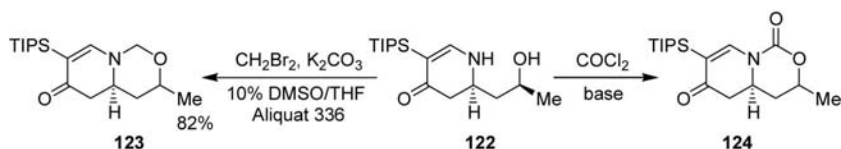
3.3.5 By the formation of two bond from [4+2] atom fragments

Reaction of 2-allylpiperidine **119** with *N,N*-di(*tert*-butoxycarbonyl)thio-urea in the presence of HgCl_2 yielded an epimeric mixtures of 3-(chloromercuriomethyl)perhydropyrido[1,2-*c*]pyrimidine **120** and 2-chloromercuriomethylperhydrofuro[3,2-*b*]pyridine **121** (07CAR1813).

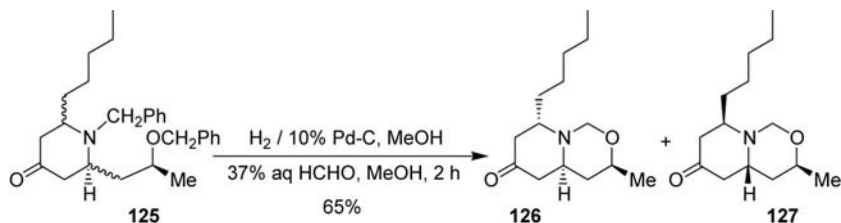


Reaction of methyl 5-fluoro-1,2,3,4-tetrahydroquinoline-8-carboxylate and (3-Cl-Ph)NCO in PhMe at 90°C for 20 h afforded 2-(3-chlorophenyl)-8-fluoro-2,3,6,7-tetrahydro-1*H*,5*H*-pyrido[3,2,1-*ij*]quinazoline-1,3-dione in 35% yield (07WOP2007/028789).

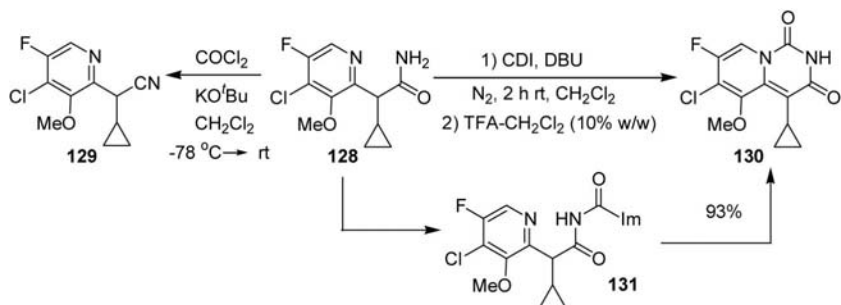
3.3.6 By the formation of two bond from [5+1] atom fragments



The treatment of tetrahydropyridin-4-one **122** with CH_2Br_2 and COCl_2 in the presence of a base afforded tetrahydro-1*H*,3*H*-pyrido[1,2-*c*][1,3]oxazin-6-one **123** and -1,6-dione **124**, respectively (05OL5227).



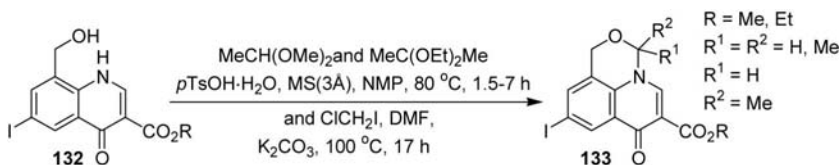
Catalytic hydrogenation of a mixture of piperidin-4-ones **125**, followed by treatment with 37% aqueous HCHO gave a 3:1 mixture of perhydropyrido[1,2-*c*][1,3]oxazin-6-ones **126** and **127** (07TL6924).



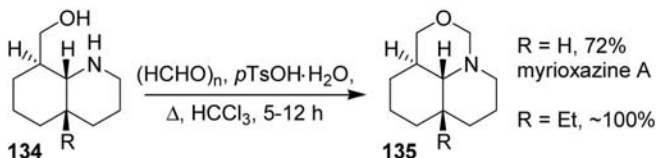
While reaction of 2-[(aminocarbonyl)cyclopropylmethyl]pyridine **128** with COCl_2 in the presence of KO^tBu led to the dehydration of the carbamoyl function of **128** to give nitrile **129**, instead of the bicyclic derivative **130**, reaction applying CDI and DBU the desired bicycle **130** formed in 20% yield, detected by HPLC (09TL785). When the cooled reaction mixture was quenched by dropwise addition of a solution of TFA in CH_2Cl_2 the isolated yield was increased up to 93%. It was suggested that acid (TFA) simply activate the carbonylimidazole (COIm) leaving group of the reaction intermediate **131**, driving cyclization. In the absence of acid, the intermediate was hydrolyzed back to the starting material **128**.

Reaction of 5-bromo-1,2,3,4-tetrahydroquinoline-8-carboxylic acid with COCl_2 in THF at room temperature for 16 h gave 8-bromo-6,7-dihydro-1*H*,3*H*,5*H*-pyrido[3,2,1-*ij*][3,1]benzoxazine-1,3-dione in 80% yield (07WOP2007/028789). 8-Bromo-2-aryl-2,3,6,7-tetrahydro-1*H*,5*H*-pyrido[3,2,1-*ij*]quinazoline-1,3-diones were also prepared in the reaction of *N*-aryl-5-bromo-1,2,3,4-tetrahydroquinoline-8-carboxamides and ClCO_2Ph in boiling 1,2-dichloroethane for 30 min.

Reaction of 8-hydroxymethyl-4-oxo-1,4-dihydroquinoline-3-carboxylates **132** with ClCH_2I , 1,1-diethoxyethane (06WOP2006/050940, 06WOP206/050943) and 2,2-dimethoxypropane (06WOP2006/050940, 06WOP206/050943, 07WOP2007/054296) yielded 7-oxo-1*H*,3*H*,7*H*-pyrido[3,2,1-*ij*][3,1]benzoxazine-6-carboxylates **133**.



The treatment of 8-hydroxymethylperhydroquinolines **134** with $(\text{HCHO})_n$ and $p\text{TsOH}\cdot\text{H}_2\text{O}$ in boiling CHCl_3 gave perhydropyrido[3,2,1-*ij*][3,1]benzoxazines **135** (09JOC2290, 09OL1515).



Reaction of 4-amino-1,2,3,4-tetrahydroquinoline-8-carboxamide and 2*H*-chromene-3-carbaldehydes in MeOH in the presence of $p\text{TsOH}\cdot\text{H}_2\text{O}$ at room temperature for 20 min then heating for 2 h afforded racemic

mixtures of *cis*-3*H*,7*H*- and *trans*-3*H*,7*H*-3-substituted 7-amino-1,2,3,5,6,7-hexahydropyrido[3,2-*ij*]quinazolin-1-ones, which were separated by flash column chromatography (07JP2007131577). Similar reactions of 4-oxo-1,2,3,4-tetrahydroquinoline-8-carboxamide and aromatic aldehydes in boiling EtOH in the presence of conc. H₂SO₄ gave 3-aryl-1,2,3,5,6,7-hexahydropyrido[3,2-*ij*]quinazolin-1,7-ones (06USA2006/0004028).

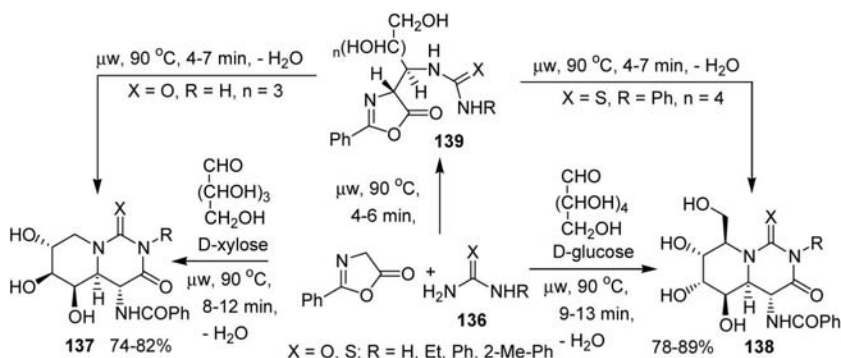
Pyrido[1,2-*c*]quinazolinium chloride **49** was obtained in 81% yield, when 2-[2-(ethylamino)phenyl]-4-dimethylaminopyridine was reacted with COCl₂ in the presence of polymer-supported diisopropylamine in CHCl₃ at ambient temperature for 0.5 h (08T8381).

Reaction of 1-(2-hydroxyethyl)-6,7-dimethoxy-1,2,3,4-tetrahydroisoquinoline with 36% H₂CO solution in MeOH at room temperature provided 9,10-dimethoxy-1,6,7,11*b*-tetrahydro-2*H*,4*H*-[1,3]oxazino[4,3-*a*]isoquinoline in 82% yield (09T8021).

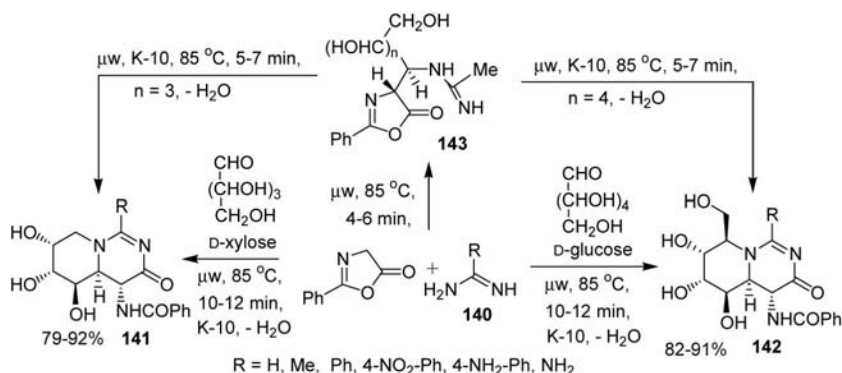
3.3.7 Ring transformation

Solvent-free three-component Biginelli reactions of 2-phenyl-1,3-oxazol-5-one, D-xylose/D-glucose and (thio)ureas **136** in the presence of Ce₂(SO₄)₃ salt (10%) under microwave irradiation produced perhydropyrido[1,2-*c*]pyrimidines **137** and **138** with 94% *trans* diastereoselectivity (Scheme 3). In the absence of Ce³⁺ salt no reaction occurred, and without microwave irradiation using conventional heating at 90 °C yields were significantly lower (39–51%) even for longer reaction times (3–5 h). If shorter reaction periods (4–7 min) was applied addition products **139** could be isolated, which then were converted to pyrido[1,2-*c*]pyrimidines **137** (X = O, R = H) and **138** (X = S, R = Ph) (07SL1905).

Similar reactions using K-10 clay and amidines **140**, instead of (thio)ureas, afforded 4,4*a*,5,6,7,8-hexahydro-3*H*-pyrido[1,2-*c*]pyrimidin-3-ones



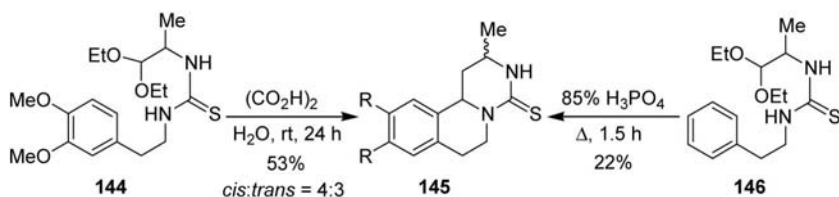
Scheme 3



Scheme 4

141 and **142** with 95% *trans* diastereoselectivity (Scheme 4). When other catalyst (CeCl₃·7H₂O, CeCl₃·7H₂O/NaI, silica gel, neutral, and acidic alumina), than K-10 clay, was applied the yield was lower. Applying shorter reaction period addition products **143** could also be isolated and then cyclized (09S2802).

Enantiomers of racemic *cis*-3*H*,7*H*- and *trans*-3*H*,7*H*-3-substituted 7-amino-1,2,3,5,6,7-hexahydropyrido[3,2,1-*ij*]quinazolin-1-ones were separated by using chiral preparative HPLC method (06USA2006/0004028, 07JP2007131577).

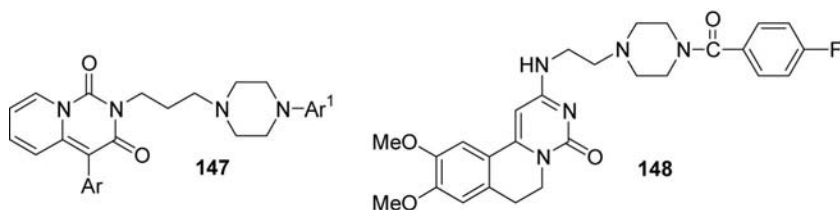


Thiourea **144** was cyclized into a 4:3 *cis*–*trans* mixture of tricyclic compound **145** (R = OMe) on the action of the saturated aqueous solution of (CO₂H)₂ at room temperature, while thiourea **146** could be cyclized only in refluxing 85% H₃PO₄ (06RJO1269).

3.4 Applications and important compounds

The affinities of 4-aryl-2-[4-[4-(het)aryl]piperazino]butyl]-2,3-dihydro-1*H*-pyrido[1,2-*c*]pyrimidine-1,3-diones **147** for 5-HT_{1A}, 5HT_{2A} and α₁-adrenergic receptors were evaluated *in vitro* (06EJM125). 4-Aryl-2-[4-[4-(1*H*-indol-3-yl)

piperidin-1-yl]butyl]-2,3-dihydro-1*H*-pyrido[1,2-*c*]pyrimidine-1,3-diones exhibit both selective 5-HT reuptake inhibitory and presynaptic 5-HT_{1a} receptor blocking activities (09EJM1710).



Trequinsin, a selective PDE3 inhibitor (07CTM221), significantly augmented glucose-dependent insulin secretion in both INS(832/13) cell and rat islets (08MI3). 9,10-Dimethoxy-2-[(2,4,6-trimethylphenyl)imino]-3-(*N*-carbamoyl-2-aminoethyl)-3,4,6,7-tetrahydro- and 9,10-dimethoxy-2-(2,6-diisopropylphenoxy)-6,7-dihydro-2*H*-pyrimido[6,1-*a*]isoquinolin-4-ones are long-acting PDE3/4 inhibitors exhibiting a broad range of broncho-protective and anti-inflammatory activities (06JEP840).

Perhydropyrido[1,2-*c*][1,3]oxazin-1-ones were applied in the total synthesis of different alkaloids [(−)-porantheridine, (−)-2-*epi*-porantheridine, (+)-*epi*-dihydropinidine, (−)-solenopsin A, precoccinelline] to control the stereochemistry (06OBC1587). Sedamine (2008S1033) and (+)-allosedridine alkaloids (09JA11707) were synthesized through pyrido[1,2-*c*][1,3]oxazin-1-one derivatives. *trans*-4*aH*,8*H*-3-methylene-8-methyl-3,4,4*a*,5-tetrahydro-1*H*,8*H*-pyrido[1,2-*c*][1,3]oxazin-1-one was used in the synthesis of the (±)-6-epipinidinone alkaloid (07EJO2015).

6,7-Dihydro-4*H*-pyrimido[6,1-*a*]isoquinolin-4-one 148 did not blocked nicotinic acid adenosine dinucleotide phosphate signaling (09NCB220).

4. PYRIDO[2,1-*c*][1,4]OXAZINES, -[1,4]THIAZINES, PYRIDO[1,2-*a*]PYRAZINES AND THEIR BENZOLOGS

4.1 Structure

4.1.1 Thermodynamic aspects

Solubility of racemic praziquantel was determined in MeOH and 2-PrOH in the temperature range between 0 °C and 40 °C. A ternary phase diagram of praziquantel enantiomers and the MeOH system was also determined (06CH259). The solubility phase and binary melting-point phase diagrams were determined. Experimental and predicted aqueous solubility of praziquantel was reported (07CPB669, 08SQE191). Dissolution of praziquantel

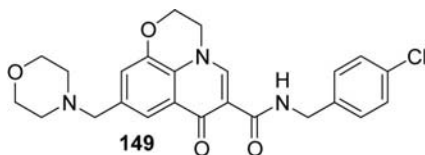
could be enhanced by melt granulation and ultrasonic spray congealing (06IJP92). Phase solubility test indicated a fivefold aqueous solubility increase of praziquantel with β -cyclodextrin (04MIP1, 06JPB1428). Thermoanalytical behavior of praziquantel-loaded PLGA nanoparticles was studied (06MI1). Taste of racemic and (*R*)-enantiomers of praziquantel was determined in humans (09PLN1). The optically active form was significantly less bitter than the racemic form. The separation of the two diastereomers of 2-(2'-phenyl-2'-methoxy-2'-trifluoromethylacetyl)-1,3,4,6,7,11*b*-hexahydro-1*H*-pyrazino[1,2-*a*]isoquinolin-4-one was performed by column chromatography (08EJO895).

Praziquantel was determined by pressurized capillary electrochromatography (CEC) using methacrylate-based monolithic columns (08ELP4463). Praziquantel was determined in formulations, processed foods, aquatics products, and biological matrixes by different HPLC methods (06BBB54, 06MI2-4, 07JPB263, 07MI2,3, 08LSJ77, 08MI4-7) and by gas chromatography (08MI6). Praziquantel and its *trans*-4'-hydroxy metabolite were simultaneously determined in plasma by HPLC-electrospray mass spectrometry (07JPB558) and by chiral LC-MS/MS [09JCH(B)3083]. The absorption of praziquantel was investigated *in vitro* in an everted rat gut sac absorption model by isocratic reversed-phase LC method (09CHR213).

Praziquantel was separated from other pharmaceutical compounds by CEC (07MI4). Enantiomers of praziquantel were separated by CEC (05ELP3921, 05ELP3930, 06ELP1050, 06MI5, 08ELP919, 08ELP3933, 08JCH(B)317) and by HPLC on different chiral stationary phases [05CHJ885, 06JCH(A)109, 06JCH(A)307, 08JCH(A)66, 08JCH(A)118, 08JCH(B)48, 08JPB882, 09JLC553]. Enantiomers of praziquantel were separated in gram quantities on microcrystalline cellulose triacetate column using MeOH as the mobile phase (09PLN1). Rapid separation of drug enantiomers, among them praziquantel, was investigated in polar organic solvent chromatography [06JCH(A)48, 06JSS1353, 08JCH(B)57].

Aqueous solubility of ofloxacin was determined in the temperature range of 293.15–323.15 K (08JCED1295, 09MI1). Intrinsic solubility of 100 drugs, among them ofloxacin and levofloxacin, was accurately measured at 25 °C and an ionic strength of 0.15 M using the CheqSol approach (08JCI1289). Water solubility of a saccharin salt of ofloxacin was determined (09JPS3788). A rapid-throughput screening assay was developed to estimate solubility parameter of the hydrochloride and citric salts of **149** (08JPS2080). Ofloxacin was also included in a set of water-insoluble drugs for the validation of pK_a determination in the MDM-H₂O mixture (MDM is a 1:1:1 mixture of MeOH, dioxane, and MeCN) by potentiometric and spectrophotometric methods (07ACA418). Protonation and fluorescence spectra of ofloxacin were studied in strong acidic solutions (09MI2). The effect of intermolecular proton transfer on the spectral properties of levofloxacin in the ground and excited electronic states was studied (08MI8).

Physicochemical properties of antibacterial agents, including 24 fluoroquinolones (levofloxacin), were analyzed (08JMC2871).



Optical activity of (*R*)-(+)-isomer of ofloxacin is $[\alpha]^{23} +76.9$ ($c = 0.385$ in 0.5 N NaOH), that of (*S*)-(–)-isomer of ofloxacin (levofloxacin) $[\alpha]^{23} -76.9$ ($c = 0.385$ in 0.5 N NaOH) (09MI3). The electrochemical behavior of ofloxacin was investigated (09RCE271). The absolute values of the triplet energies of rifloxacin, and ofloxacin were estimated by means of laser flash photolysis to be 253 kJ mol^{-1} and 262 kJ mol^{-1} , respectively [07JPC(B)7409]. Thermal stability and thermal decomposition kinetics of ofloxacin were studied by TG, DTG, and DSC (08MI9). Photoinduced degradation of ofloxacin was characterized by HPLC/high-resolution multiple-stage MS (08RCM1533).

Enantiomers of 4-aryl-6-oxo (07USA2007/0117839) and 6-aryl-4-oxo (07USA2007/0117798, 08USA2008/0207900) derivatives of (*Z*)-3-[1-[3-methoxy-4-(4-methyl-1*H*-imidazol-1-yl)phenyl]methylidene]-4-arylperhydropyrido[2,1-*c*][1,4]oxazines; furthermore, those of 2-[1-(diphenylmethyl)azetidin-3-yl]perhydropyrido[1,2-*a*]pyrazin-6-ones (07WOP2007/037743) were separated using preparative chiral HPLC methods. 9*a*-Epimers of *cis*-7*H*,9*H*-*trans*-8*H*-7,8,9-tri(pivaloyloxy)perhydropyrido[2,1-*c*][1,4]thiazin-6-ones were separated by column chromatography (06EUP1657244).

Ofloxacin was determined by different TLC methods (06MI6, 07MI5, 08ALE1909, 08MI10, 2009ACA64), by a high-performance TLC method (07MI6), and ultraperformance liquid chromatography methods [07RCM3487, 08MI11-13, 08RCM41, 09ANB1709, 09JCH(A)2529, 09JPB367, 09MI4-6], too. Levofloxacin was determined by densitometric HPTLC methods (07ASJC5647, 07MI7, 08MI14) and ultraperformance liquid chromatography (08CHR187) in tablets and biological samples. The retention of rifloxacin and ofloxacin on HPLC stationary phases supporting human serum albumin or α_1 -acid glycoprotein was investigated (07EJP211).

Different types of HPLC methods were developed for the determination of rifloxacin [05EJD249, 09JFA4535, 09JCH(A)5327, 09JFA4535, 09MI7], ofloxacin [04MI1, 05EJD249, 05JCH(A)206, 05JSS2444, 05MI4-8, 05MIP1, 06NAN16, 06ANB1228, 06JCH(A)68, 06JCH(A)83, 06JCH(A)101, 06JCH(B)1, 06JCH(B)72, 06MI3,7-12, 06ACA16, 06EST357,

06STO314, 06TAL678, 07AC9372, 07JCH(A)45, 07JCH(A)95, 07JCH(B)246, 07JSS2421, 07JSS2676, 07MI8-26, 07WRE4526, 08ACA96, 08ACA154, 08ACA230, 08ANB799, 08CHR117, 08IJE1033, 08JCH(A)66, 08JCH(A)100, 08JCH(A)162, 08JSS119, 08JSS294, 08MI7,15-32, 08MIP1, 08STO84, 09ACA68, 09ANB1685, 09ASJC3360, 09JCH(A)5949, 09JCH(A)7510, 09JCH(A)8217, 09JCH(B)961, 09JCH(B)2961, 09JFA4535, 09MI7-17, 09MIP1, 09JSS955, 09TAL1071], levofloxacin [05MI9,10 06JPB179, 06MI13-24, 07ACA147, 07BCH1045, 07CHR15, 07EJA1, 07JLC1981, 07MI26-34, 08ETC73, 08JCH(A)151, 08JCH(A)206, 08MI32-44, 09ANB927, 09JPB710, 09MI18], pazufloxacin (05EJD249, 05MI10-13, 06MI25-32, 07MI35-37, 08MI45-50), and antofloxacin (06MI33, 07MI38, 08JPP667, 08MI51) in formulation, in biological and in environmental samples.

A RP-HPLC method was developed for the separation of ofloxacin, its 3-decarboxylated, *N*-oxide, *N*-desmethyl derivatives and its 9-(4-methylpiperazino)-10-fluoro-7-oxo-2,3-dihydro-7*H*-pyrido[1,2,3-*de*][1,4]oxazine-6-carboxylic acid isomer [06JCH(A)224]. 9,10-Difluoro-7-oxo-2,3-dihydro-7*H*-pyrido[1,2,3-*de*][1,4]oxazine-6-carboxylic acid content of ofloxacin was determined by a HPLC method (05MI14). Ofloxacin, together with other drugs, was simultaneously isolated in biological samples by selective molecularly imprinted polymers combined with an HPLC method (08ACA154, 09ANB235). Stability of levofloxacin injection was investigated by UV spectrophotometry and LC-MS/MS methods (07MI34). That of pazufloxacin was studied in different infusions by UV spectrophotometry method (08MI52).

The electrochemical behavior of ofloxacin at carbon nanotubes film electrode and its voltammetric determination in biological samples were reported (07MI39, 08MI53, 08MKA227). Ofloxacin was determined by using adsorptive stripping voltammetry (08MI54) and by differential pulse stripping voltammetry (08MI55) methods in formulated products. Ofloxacin was detected in selected Northcentral and Northwestern Arkansas streams by capillary-column gas chromatography (06JEQ1078). An optical surface plasmon resonance biosensor assay was validated for the determination of ofloxacin in egg, fish, and poultry (09MI19).

Interactions of ofloxacin and levofloxacin with Al^{3+} , Fe^{3+} , and Mg^{2+} ions were investigated by capillary zone electrophoresis (07CHR489). A fluorescence enhancement phenomenon in the europium-ofloxacin-sodium dodecyl benzenesulfonate fluorescence system was observed when Gd^{3+} was added (07JFL105). A quantitative relation was found between the relative fluorescences of Zr, Mo, and V chelates of ofloxacin and the ionization of the carboxylic group and the calculated stability constants of the formed chelates (06MI34). Factors that significantly influence the stability of ofloxacin- and levofloxacin-metal (Al_3^+ , Fe_3^+ , Cu_2^+ ,

Zn^{2+} , Ca^{2+} , and Mg^{2+}) complexes were analyzed (09ACA54). Ofloxacin and levofloxacin were determined by precipitation of their Ag^+ , Cu^{2+} , and Fe^{3+} salts and the ions were analyzed in the precipitations by atomic absorption spectroscopy (07MI40).

Enantiomers of 6-(amino-1-piperidinyl)-8-fluoro-6,7-dihydro-3*H*,5*H*-pyrido[1,2,3-*de*]quinoxalin-3-one were separated by using preparative chiral HPLC method (08WOP2008/003690). Enantioseparation of ofloxacin (07JLC1497, 09MI20) and impurity determination of levofloxacin (07ACA160) were investigated by ligand exchange. Ofloxacin and its enantiomers were separated by chiral HPLC [06MI35, 07ANB2681, 08JCH(A)77, 08MI56, 09ANS931] and capillary electrophoresis [06CCL407, 06ELP872, 06JCH(A)296, 06MI36,37, 07MI41,42, 08JLC348, 08JSS177, 08MI57,58, 09MI3] on chiral stationary phases. The enantiomeric purity and quantitation of levofloxacin was determined by capillary zone electrophoresis in pharmaceutical forms (05MI15). Enantiomers of pazufloxacin were separated by capillary electrophoresis [06JCH(A)296]. Enantiomeric impurity of antofloxacin HCl was determined by means of capillary electrophoresis (07MI43) and HPLC (04MI2).

Structural requirements for drug inhibition of liver specific human organic cation transport protein 1 were analyzed. Ofloxacin was also selected for this investigation (08JMC5932). Interaction of ofloxacin-copper complex with Calf thymus DNA was studied by using voltametric method (07MKA65). Electrochemical and spectroscopic methods were applied to investigate the interaction of ofloxacin with Calf thymus DNA (09RCE271), whereas ofloxacin and DNA were investigated by using UV and synchronous fluorescence spectroscopy (09AN1840). A thermodynamic study was conducted on the interaction of (*R*)- and (*S*)-ofloxacin with DNA (09BKC1031). Interaction between pazufloxacin and calf thymus DNA was studied by fluorescence, absorption spectroscopy, and viscosity measurement [08JFL701, 08JPH(B)172]. Effect of acidity on the interaction of ofloxacin and bovine serum albumin was investigated (08MI59). Interactions between fluoroquinolones [including rufloxacin (05MI16), ofloxacin (06ANS1515, 07MI44), levofloxacin (06MI38, 06ANS1515, 07ACA101, 07MI45, 08MI60), pazufloxacin mesilate (06MI39, 07MI46, 08JLU81)], and bovine serum albumin were studied by different methods. The bindings of ofloxacin and levofloxacin to a transport protein and human serum albumin were studied under simulated physiological conditions by capillary electrophoresis-frontal analysis (08CHR969). Ofloxacin was also included in a set of drugs for investigation of the effect of electrostatic interaction and ionization on an immobilized artificial membrane retention [08JCH(A)67]. For determination of ofloxacin, an indirect competitive inhibition ELISA test was developed (07CCL1107, 07MI47). Enzyme-linked immunosorbent assay was developed for detection of ofloxacin (06JAF2822, 06MI8, 08MI61, 09JFA5971)

and levofloxacin (08MI61) in various biological matrixes. Ofloxacin (07CCL1107, 08JFA5469) was detected by an immunochromatophy strip in biological samples. Residues of ofloxacin, levofloxacin, and pazufloxacin, among other fluoroquinolones, were determined by an indirect competitive enzyme immunoassay in poultry meat (05MI17). The membrane phospholipids affinity of 10 quinolones, including rifloxacin and ofloxacin, was measured by HPLC on two different immobilized artificial membrane stationary phases (07EJP288). The interaction of pazufloxacin mesilate with catalase was studied by spectrofluorometric method (08JST96).

A microchip-atmospheric pressure thermospray ionization technique was developed to investigate ofloxacin in the presence of other compounds (09RCM3313). Ofloxacin was detected by a voltammetric method in human urine (08ELA144). The trace of ofloxacin was detected with poly (crystal violet) film modified electrodes (07MI48).

Gravimetric and spectrophotometric methods were developed for determination of ofloxacin using ammonium reineckate (05MI18). A photoinduced-fluorescence method could not apply for ofloxacin's determination (07MI49). Different spectrophotometric methods were applied for determination of ofloxacin (04MI3, 05MI19, 05EPB87, 06APP1174, 06MI40, 07ASJC5223, 07CPB1551, 07MI50,51, 08ALE837, 08MI29,62-69, 09ANS125, 09ASJC2473, 09ASJC4149, 09MI21-24), levofloxacin (05MI20,21, 06ASJC559, 06MI41-45, 07ASJC1628, 07MI28,52, 08ASJC1957, 08JKC622, 08MI40,70,71, 09ASJC528, 09MI25-27), and pazufloxacin (06MI46,47) in pharmaceuticals and different biological samples. Levofloxacin and its decarboxylated derivative were simultaneously determined by simple multivariate spectrophotometric procedure (05BPS191). Levofloxacin was determined in milk by fluorescent spectrophotometry (07MI53). Compatibility of ofloxacin with yuxingcao injection was investigated by UV spectroscopy (08MI72). Compatibility of levofloxacin with other drugs was investigated by HPLC (08MI71) and UV spectrometry (05MI22, 07MI54,55, 08MI73,74), and its dissolution by UV spectroscopy (07MI56). Charge-transfer reaction of ofloxacin with chloranilic acid (06MI48), chloranil (07MI57), bromanil [07MI58, 09SA(A)1769], and 2,3-dichloro-5,6-dicyano-1,4-benzoquinone (08JIC399) were studied by spectrophotometry. Spectrofluorometric methods were developed for the determination of levofloxacin, based on its charge-transfer reaction with chloranilic acid, 2,3-dichloro-5,6-dicyano-1,4-benzoquinone (05MI23) and bromanil (07MI58). The charge-transfer complexation of ofloxacin and levofloxacin with 2,3,5,6-tetrafluoro-*p*-benzoquinone was studied by a spectrofluorimetric method (06MI49). Ofloxacin and levofloxacin were determined by spectrofluorimetric method using 2,3,5,6-tetrachloro-*p*-benzoquinone [09SA(A)1038]. Ofloxacin was determined in pharmaceutical preparation by potentiometric and fluorometric methods (08MI735). For ofloxacin

determinations, its reaction with picric acid (05MI24,25) and sodium tetraphenylborate (05MI26,27) were investigated. A rapid identification method of ofloxacin, levofloxacin, and pazufloxacin was developed by observing color changes induced by a series of chemical reactions (06MI50).

Ofloxacin was separated by microemulsion electrokinetic chromatography [07JCH(A)333] and determined by microemulsion liquid chromatography (08MI76). Ofloxacin could be determined by microchip capillary electrophoresis with solid-state electrochemiluminescence detector (05AC7993) and capillary gas chromatography after esterification with $\text{BF}_3\text{-MeOH}$ (07MI59). Flow-injection chemiluminescence detections (06ANS1145, 07MI60, 07JFL481, 07TAL1066, 08MI77) were developed for the determination of ofloxacin in pharmaceutical preparation and biological fluids. A flow-injection chemiluminescence method was applied for the determination of ofloxacin, which could be also used for rifloxacin, but not for pazufloxacin (08LUM309). Ammonium vanadate was used for determination of ofloxacin in ophthalmic drugs (06MI51, 06OJC119). Ofloxacin residues were determined in biological samples by capillary electrophoresis [06ELP2240, 07JCH(B)145, 08JSS3740, 08JSS3765, 08MI78, 09AC3188, 09JSS118], capillary electrophoresis-conductivity measurement (08MI79), pressurized electrochromatography (05JSS2210), and micellar capillary electrophoresis (07MI61). Separation of fluoroquinolones, among them rifloxacin (05MI28) and ofloxacin (06MI52, 07ELP4101, 07ELP4180), and pazufloxacin (06MI52) were achieved by high-performance capillary electrophoresis. Ofloxacin (05MI29, 08JBS389, 08JLC2771, 09MI28) and levofloxacin (05MI29) were determined by capillary zone electrophoresis methods in formulated product and biological samples. Pazufloxacin was determined by a capillary electrophoresis method in injection and human urine (08MI80). Ofloxacin and pazufloxacin, besides other five fluoroquinolones, were separated by capillary electrophoresis (08MI79, 09TAL1667). Simultaneous separations of levofloxacin (06ACA185) and pazufloxacin (09JSS118) from other fluoroquinolones were achieved by capillary zone electrophoresis. Separation of fluoroquinolones, among them pazufloxacin was achieved by high-performance capillary electrophoresis (07ELP4101, 07MI62). Levofloxacin was determined in biological fluid by capillary electrophoresis (07JCCTAS991, 08CCL962, 08ELP3207, 09CHR1101).

Determination of ofloxacin by inductively coupled plasma mass spectroscopy was investigated (06APP80). Luminescence performance of ofloxacin was investigated (06ALE603). Stability-indicating spectrophotometric and spectrofluorimetric methods were developed for the determination of levofloxacin in pharmaceutical formulations in the presence of its decarboxylated degradate (08MI81). Levofloxacin determined in the presence of other fluoroquinolones by synchronous scanning room-temperature

phosphorimetry and Th^{4+} as the selective signal inducer [09SA(A)429]. Turbulent flow chromatography load columns were applied for on-line analysis of levofloxacin in wastewaters (09CHR239). An indirect analysis of levofloxacin was developed using flame atomic absorption spectrometry (07ATS58). A flow-injection chemiluminescence detection was developed for the determination of levofloxacin in pharmaceutical preparation and biological fluids (06ANS1145, 06MI53,54, 07TAL1066, 09SPE209). Electrochemiluminescence of Tb^{3+} -ofloxacin-sodium sulfite system was investigated in the aqueous solution [06SA(A)130]. Levofloxacin was determined by Tb^{3+} -levofloxacin complex fluorescence enhancement method (08MI82), by fluorometric methods (06MI55, 07ANS337), and by the PVC membrane ion-selective electrode (07MI63). A Eu^{3+} (06MI56) and Tb^{3+} (09MI29) sensitized fluorescent spectroscopic methods were developed for the determination of pazufloxacin mesylate. The fluorescence characteristics of levofloxacin hydrochloride were studied in micellar systems (06MI57).

Resonance Rayleigh scattering spectra of ofloxacin- and levofloxacin-Pd(II)-eosin Y systems (07MI64) and those of ofloxacin- and levofloxacin-Co(II)-Congo red (08MI83) systems were investigated. The interactions between Cu^{2+} complex of ofloxacin and levofloxacin (08MI84), furthermore levofloxacin [08SA(A)956] with erythrosine were studied by absorption, fluorescence, and resonance Rayleigh scattering spectra.

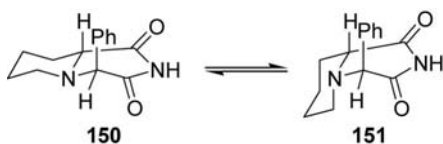
The retention behavior of levofloxacin was investigated in anionic micellar liquid chromatography (05MI30). Residual of ofloxacin in the pig viscera was determined by micellar electrokinetic chromatography (07MI65). A micellar liquid chromatography was developed for the prediction of octanol–water partition coefficients of drugs, including ofloxacin and levofloxacin, too (07MI66). Ofloxacin and levofloxacin were determined in urine by micellar liquid chromatography [09JCH(B)3975]. A micellar liquid chromatography was developed for prediction of protein–drug binding. Ofloxacin and levofloxacin were also including in the studied drugs [07JCH(A)88]. A turbulent flow chromatography coupled to LC-MS/MS was used for analysis of ofloxacin in honey (08JFA35).

A chemiluminescence method was developed for determination of pazufloxacin mesylate (08MI85). Pazufloxacin was determined in formulation using water-soluble quantum dots as fluorescent probe (08MI86). A molecularly imprinted polymer was developed, and it exhibits higher affinity and selectivity for pazufloxacin than for norfloxacin and ofloxacin (05MI31).

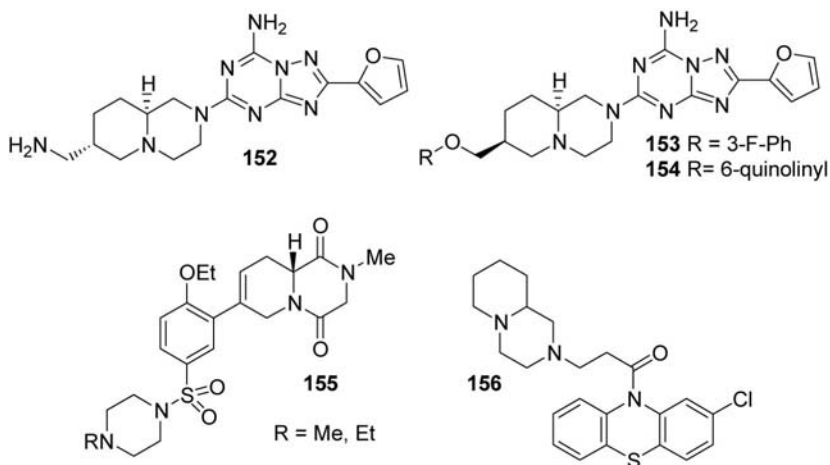
4.1.2 Theoretical calculations

There is $7.5 \text{ kcal mol}^{-1}$ free energy difference between 4,9*a*-*cis* and 4,9*a*-*trans* isomers of diethyl (4-oxoperhydropirido[2,1-*c*][1,4]oxazin-4-yl)

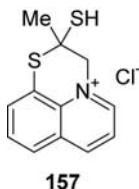
malonate by B3LYP/6-31G* calculations (09OBC655). Structures of 3-hydroxy-3-methyl-3,4-dihydro-1*H*-pyrido[2,1-*c*][1,4]oxazinium chloride (06PJC1039) and 3-hydroxy-3-phenyl-3,4-dihydro-1*H*-pyrido[2,1-*c*][1,4]oxazinium bromide (06JST36) were calculated by B3LYP/6-31G(d,p) method. Energy optimization with the AM1 semiempirical method indicated that the gas-phase conformations **150** and **151** of (4*R*,9*aR*)-4-phenyl-perhydropyrido[1,2-*a*]pyrazine-1,3-dione were essentially isoenergetic, with an energy difference of 0.1 kJ mol⁻¹ favoring the invertomer **150** (09TA1759).



2-[[2-(Methyl- and 3,4-dimethylphenyl)amino]carbonyl]perhydropyrido[1,2-*a*]pyrazines were identified by a sequential virtual screening as serotonin 2C receptor ligands, but they proved to be inactive during biochemical testing (09BMC4559). Selective A_{2A} antagonist perhydropyrido[1,2-*a*]pyrazines **152**–**154** were also used to generate a 3D pharmacophore model (07JCI613). A molecular docking study revealed that the main interaction types of **153** and **154** with A_{2A} adenosine receptors (08MI87). Computational prediction suggested that 1,2,3,4,9,9*a*-hexahydro-5*H*-pyrido[1,2-*a*]pyrazin-1,4-diones **155** exhibit larger interaction energy to PDE-5 receptors than verdenafil (08BMC7599). Compound **156** belongs to the top-ranking trypanothione reductase inhibitors identified by a ligand-based virtual screening cascade protocol (09JMC1670).



The reaction mechanism of the reaction of MeHg^+ cation with 2,3-dihydropyrido[1,2,3-*de*]-1,4-benzothiazinium chloride **157** in aqueous media was studied by a quantum chemical method (06JTC1042).



Stereostructure and electrostatic potential map of 2-(2-piperidinoethyl)-1,2,3,4,11,11a-hexahydro-6*H*-pyrazino[1,2-*b*]isoquinoline-1,4-dione was determined by *ab initio* (RHF/3-21G) and DFT [B3LYP/6-31G (d)] calculations (06T4408). 2-(3-Arylamino-3-oxopropyl)-2,3,4,6,11,11a-hexahydro-1*H*-pyrazino[1,2-*b*]isoquinolines were included in a set of compounds to carry out the 3D QSAR study (06BMC8249).

Principal component-genetic algorithm-multiparameter linear regression and principal component-genetic algorithm-artificial neural network models were applied for the prediction of melting point for 323 drug-like compounds, among them praziquantel (08BKC833). Antifungal activity of praziquantel was predicted by the support-vector machine approach (05JMT73). The molecular modeling data suggested that praziquantel/ β -cyclodextrin inclusion complexes have a 1:1 stoichiometry and isoquinoline ring moiety is embedded in the cavity of β -cyclodextrin (06JPB1428). Praziquantel was also included in a set of drugs to predict a relationship between drug absorption and melting point (09IJP24).

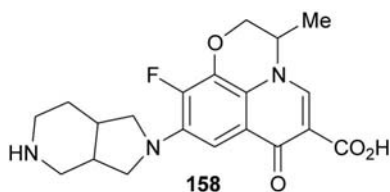
The effects of protonation states on the binding of *S*- and *R*-ofloxacin to [d(ATAGCGCTAT)]₂ oligonucleotide were investigated by molecular dynamics study (08BKC2103). The relative stability of zwitterionic and uncharged neutral forms of levofloxacin in hydrophilic and hydrophobic media was investigated using quantum mechanical calculations at the B3LYP/6-31+G level (07CPL281). The possible interaction between fenbufen and ofloxacin was investigated by quantum-chemical calculations [HF and DFT/B3LYP6-311++G(d,p)] (08STC381). Host-guest interactions between calix[4]arenes and levofloxacin were analyzed by quantum mechanical calculations at density functional and semiempirical levels (06JPO157). The interactions between levofloxacin and bovine β -lactoglobulin were investigated by computational and experimental (using ¹⁹F NMR technics) approaches (06PRO555).

Levofloxacin was included into a training set for development prediction of hERG potassium channel blockade using kNN-QSAR and local lazy regression methods (08QSR1305). QSAR models were developed to estimate the blood–brain barrier permeability of 159 compounds, including praziquantel, rifloxacin, ofloxacin, and levofloxacin (08PR1902). Praziquantel (05MI32, 07QSR653) and ofloxacin (05MI32) were included in a set of drugs to predict human intestinal absorption. Human protein binding rate, and bioavailability of different drugs, among them praziquantel, were predicted by support vector machine method combined with genetic algorithm for feature selection and conjugate gradient method for parameter optimization (08JPB677). Praziquantel and levofloxacin were also included in a set of drugs to develop QSAR models to predict human serum protein binding (06JMC7169). Praziquantel was among the 768 chemical compounds to try to develop correlation between oral bioavailability and several important molecular properties (07JCI460). Predicting Caco-2 cell permeability of 157 drugs, including praziquantel and ofloxacin, linear discriminant analysis was used to obtain quantitative models (08JPS1946).

It was suggested that the matrix of drug metabolism in the Biopharmaceutics Drug Disposition Classification System could be used to substantiate the classification of permeability by the Biopharmaceutics Classification System. Ofloxacin and levofloxacin were also included in this study (09MPH74). Blood–brain barrier permeability of rifloxacin and ofloxacin was predicted by using topological descriptors (08MI88). Experimental blood–brain partition coefficients for diverse set of 113 drug molecules, including rifloxacin, and ofloxacin, were correlated with computed structural descriptors using CODESSA-PRO and ISIDA programs to give statistically significant QSAR models (06BMC4888). Ofloxacin and levofloxacin were also included into a set of structurally diverse drugs to develop a higher correlation between logarithms of the brain/blood partition coefficients and that of the predicted *n*-octanol/alkane coefficients and that of cyclohexan/water coefficients, over the logarithms of the measure *n*-octanol/water coefficients (09CMD105). The use of classification trees for modeling and predicting the passage of drugs, including rifloxacin and ofloxacin, through the blood–brain barrier was evaluated (06JCI1410). Ofloxacin (08QSR704) and levofloxacin (08PR1902) were also including into a set of compounds for computational prediction of blood–brain partitioning of drugs. Ofloxacin was also included in a set of drugs for predicting effect of food on extent of drug absorption based on physicochemical properties (07PR1118), and to set up correlation between blood–brain penetration and human serum albumin binding (08ARK38). Levofloxacin was included into the validation set for QSAR modeling of human serum protein binding (06JMC7169).

A quantitative structure relationship study was performed to understand drug binding to human serum albumin, using an artificial neural network method and 94 drugs, including levofloxacin (07CBD19). Ofloxacin was included into a set of drug to investigate the value of a prediction method of human clearance (09MI30). Human plasma protein binding rate and oral bioavailability of ofloxacin and levofloxacin were predicted by using genetic algorithm – conjugate gradient – support vector machine method (08JPB677). Hologram QSAR models were applied for the prediction of human oral bioavailability (07BMC7738) and that of human plasma protein binding (07LDD502) of drugs. (*R*)-Ofloxacin and levofloxacin were also included into the studied drugs. Quantitative structure-pharmacokinetic/pharmacodynamic relationship techniques and chemometric methods were employed to classify fluoroquinolones (including ofloxacin, levofloxacin) with respect to their activity against *Streptococcus pneumoniae* (07PCJ82). Levofloxacin was also included in a set of drugs to study the quantitative structure–retention relationship studies with immobilized artificial membrane chromatography [07JCH(A)174]. A unified Markov model was developed to describe the biological activity of more than 70 drugs, including levofloxacin, too, from the literature tested against 96 species of bacteria (07BMC897). A quantitative structure–activity relationship models were developed for the prediction of genotoxic potential of quinolone antibacterials, including ofloxacin, levofloxacin, and pazufloxacin (07EST4806). The quantitative structure-pharmacokinetic relationship models for quinolones, including rifloxacin (07MI67), ofloxacin (07MI67), and levofloxacin (06MI58, 07MI67) were employed. Principal component analysis and hierarchical cluster analysis were employed to investigate the structure–activity relationship of 14 fluoroquinolones, including ofloxacin and levofloxacin, with the anti-*B. fragilis* activity (06MI59). Density functional theory was used to calculate molecular descriptors for 12 fluoroquinolones, including rifloxacin, ofloxacin, and levofloxacin with anti-*S. pneumoniae* activity (06MI60). The antibacterial property space of antibacterial compounds, including rifloxacin and levofloxacin, was analyzed (2008JMC2871). A quantitative retention–activity relationship model utilizing biopartitioning micellar chromatography was developed for the biological parameter estimation of drugs including rifloxacin, ofloxacin, and levofloxacin (08BCH106).

The chemical structure of levofloxacin derivatives was optimized and calculated using molecular mechanics and quantum chemical methods (05MI33). A novel approach (TOMOCOMD-CARDD) to the computer-aided “rational” drug design method indicated that compound **158** (KRQ10099) was expected to be exhibited antibacterial activity (06JMM255).



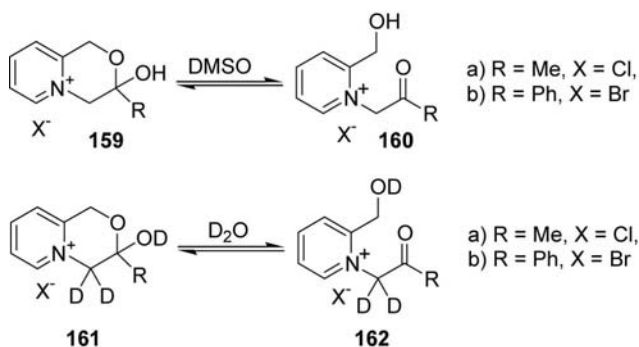
Retention indices of drug, among them levofloxacin, based on the immobilized artificial membrane chromatography were predicted using projection pursuit regression and local lazy regression (08JSS2325). The inhibiting effect and mechanism of ofloxacin on the corrosion of mild steel in $1 \text{ mol}^{-1} \text{ L HCl}$ was studied using electrochemical and quantum chemical methods at 303 K (08MI89).

4.1.3 UV spectroscopy

Ofloxacin was characterized by UV, vibrational, IR spectroscopies, ^1H -, ^{13}C -NMR spectrometry, X-ray powder diffraction pattern, single crystal X-ray diffraction, and mass spectrometry (09MI3). Levofloxacin formed a supramolecular complex with β -cyclodextrin at a molar ratio of 1:1, which was characterized by using UV, fluorescent spectra, DSC, and X-ray diffraction (07MI68).

4.1.4 IR and Raman spectroscopy

The equilibrium mixtures of 3-hydroxy-3-methyl-3,4-dihydro-1*H*-pyrido [2,1-*c*][1,4]oxazinium chloride **159a**, its 4,4-dideutero derivatives **161a** (06PJC1039) and those of 3-hydroxy-3-phenyl-3,4-dihydro-1*H*-pyrido [2,1-*c*][1,4]oxazinium bromide **159b** and **161b** (06JST36) with their ring-opened forms **160** and **162** were characterized by FTIR, ^1H , ^{13}C , and ^{15}N NMR spectra in DMSO and D_2O .

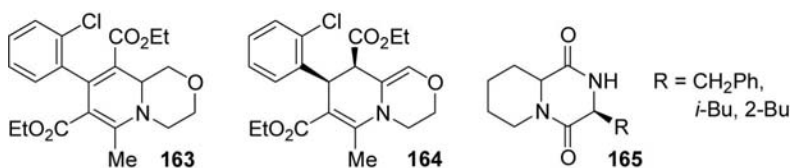


Co^{2+} and Ni^{2+} complexes of ofloxacin were prepared and they were characterized by elemental analysis, IR, electronic and fluorescence spectra, and thermal analysis (08MI90). $[\text{Cu}(\text{ofloxacin})_2 \cdot \text{H}_2\text{O}] \cdot 2\text{H}_2\text{O}$ complex was characterized by IR spectroscopy (08JCR2961). Pd complexes $[\text{PdCl}_2(\text{oxacin})]$ of ofloxacin and levofloxacin were prepared and they were characterized by IR, ^1H , and ^{13}C NMR spectroscopy (09EJM4107). The solid-state structure of $[\text{Cu}(\text{ofloxacin})_2 \cdot \text{H}_2\text{O}] \cdot 2\text{H}_2\text{O}$ complex was characterized by IR spectroscopy and single crystal X-ray diffraction analysis (09JCR1313).

IR and Raman spectra of ofloxacin and levofloxacin were measured and evaluated [06SA(A)159]. Saccharin salt of ofloxacin was prepared and characterized by FTIR, X-ray powder diffraction, thermal analysis, and ^1H and ^{13}C NMR spectroscopy in solution and in solid state (09JPS3788). Nondestructive discrimination between levofloxacin and ofloxacin containing tablets was achieved by using diffusion reflectance NIR spectroscopy (08PHA628).

4.1.5 NMR spectroscopy

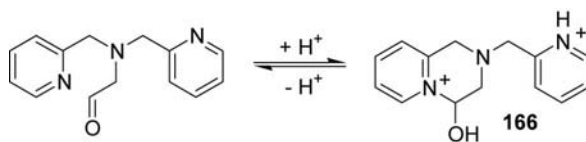
The structure of xylogranatinin (9-hydroxy-3-methoxy-6*H*-pyrido[1,2-*a*]pyrazin-6-one) was determined and characterized by ^1H and ^{13}C NMR investigations (2007CNO426, 2008CCL68). The structures of two degradation products of amlopidine, a calcium channel blocking agent, were determined by ^1H and ^{13}C NMR measurements to be 3,4-dihydro-1*H*- and 3,4,8,9-tetrahydropyrido[2,1-*c*][1,4]oxazines **163** and **164** (07MRC688).



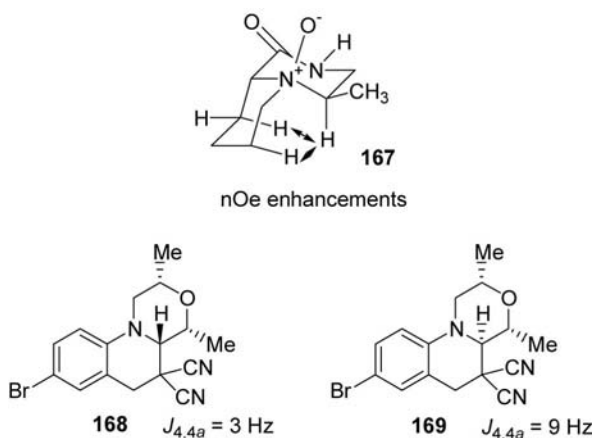
Structure of diketopiperazines **165**, isolated from the cell-free culture supernatant of the Antarctic psychrophilic bacterium *Pseudoalteromonas haloplanktis* TAC125, was characterized by ^1H and ^{13}C NMR spectroscopy (05MI34).

^1H NMR spectroscopy revealed that methyl *cis*-3*H*,9*aH*-2-acetyl- and 2-*tert*-butoxycarbonylperhydropyrido[1,2-*a*]pyrazine-3-carboxylates exist as a ca. 3.3:1 and ca. 1:1 mixtures of *cis*- and *trans*-amide rotamers, respectively, in CDCl_3 solution (08SL702).

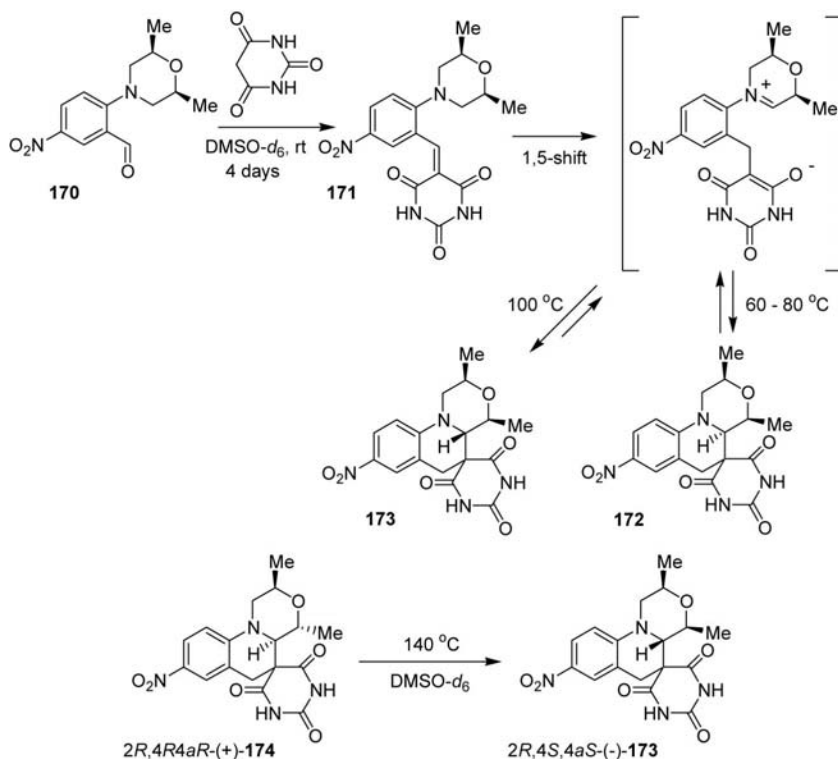
Depending upon the pH compound **166** exhibits a ring-chain tautomerism, and ring-closed form could be used as a masked aldehyde precursor (07PNA10780, 08JOC734, 08USA2008/0138292).



NMR investigations revealed, that in CDCl_3 **150** and **151** invertomers' ratio was 1:1.3, while in the more polar CD_3OD 1.5:1 (09TA1759). NOE measurement confirmed a *cis*-fused ring system of 4-methylperhydropyrindo[1,2-*a*]pyrazin-1-one *N*-oxide **167** with distorted conformation (07TL1683). Coupling constants between 4-H and 4*a*-H indicated that at 1,2,4,4*a*,5,6-hexahydro[1,4]oxazino[4,3-*a*]quinoline-5,5-dinitrile 4*a*-H **168** is in equatorial position and at its 4*a*-epimer **169** in axial position (09JA3991).

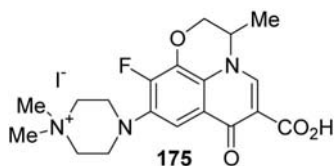


Reaction of aldehyde **170** and barbituric acid was followed by ^1H NMR spectroscopy in $\text{DMSO}-d_6$. After 4 days at room temperature condensation product **171** accumulated. Upon heating to 60 °C and then to 80 °C the signal of *cis*-2H,4H,4*a*H tricycle **172** appeared, which was isomerized into the thermodynamically more stable product **173** at 100 °C (09JA3991). Isomerization of *trans*-methyl derivative (2*R*,4*R*4*aR*)-(+)-**174** was also followed by ^1H NMR spectroscopy at 140 °C. By 22 h, the equilibrium mixture contains a cca 8:1 mixture of *cis* (2*R*,4*S*4*aS*)-(–)-**173** and *trans* isomers (2*R*,4*R*4*aR*)-(+)-**174**.



NMR ROESY experiments indicated molecular proximities (≤ 5 Å) between hydrogens 10, 11, and 12 of the aromatic ring of praziquantel and hydrogen H-3 and H-5, in the internal cavity of β -cyclodextrin (06JPB1428). Rotamers of 2-acyl-1,3,4,6,7,11*b*-hexahydro-1*H*-pyrazino [1,2-*a*]isoquinolin-4-ones were identified and analyzed by ^1H and ^{13}C NMR spectroscopy (08EJO895). Commercial praziquantel tablets were analyzed by ^1H NMR spectroscopy (07JPB263).

Fluoride in pazufloxacin mesylate samples was determined by ^{19}F NMR spectra (06MI61,62). Platina complexes of ofloxacin and levofloxacin were characterized by ^1H , ^{13}C , and ^{195}Pt NMR (09ICA2060). ^1H and ^{13}C NMR spectra of quaternary derivative **175** of ofloxacin were determined in both acidic and alkaline solutions (08MI91). Mg complexes of ofloxacin [$\text{Mg}(\text{Oflo})_2(\text{H}_2\text{O})_2 \cdot 2\text{H}_2\text{O}$] and levofloxacin [$\text{Mg}(\text{Levo})_2(\text{H}_2\text{O})_2 \cdot 2\text{H}_2\text{O}$] were characterized by ^1H and ^{13}C NMR spectra (06JIB1755).



4.1.6 Mass spectrometry

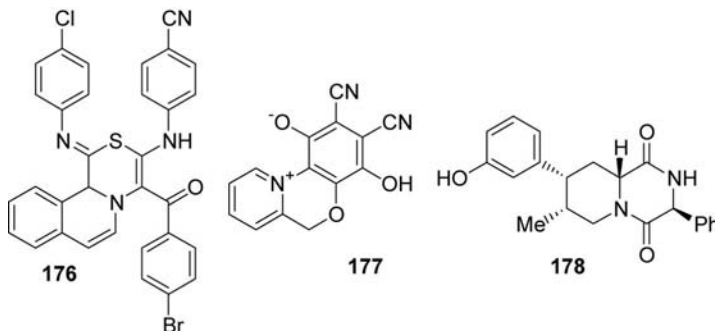
Residues of praziquantel and ofloxacin, among other animal drugs, were monitored in foods by tandem mass spectrometry (05MI35). During photostability, investigation of ofloxacin in the solid-state formation of its 10-amino and 10-dimethylamino derivatives was postulated on the basis of detailed mass spectra investigations (07PHA105). Fragmentation mechanism of ofloxacin and pazufloxacin were analyzed using electrospray ion-trap mass spectrometry (06MI63). A revised conformational code for the exhaustive analysis of conformers was proposed, which can strictly define the conformation of compounds with relatively high-symmetry substituents (e.g., levofloxacin) and is especially useful for visualizing conformational changes in ligands and protein (09JOC1231). The metabolites of antofloxacin in rat were studied by a hybrid ion-trap/time-of-flight mass spectrometer (09JPB1022).

4.1.7 X-ray investigation

The structure of a thermal degradation product **164** of amlopidine was also determined by the X-ray diffraction method (07ANS91). Solid-state structures of 3-hydroxy-3-methyl-3,4-dihydro-1*H*-pyrido[2,1-*c*][1,4]oxazinium chloride **159a** (06PJC1039), 3-hydroxy-3-phenyl-3,4-dihydro-1*H*-pyrido[2,1-*c*][1,4]oxazinium bromide **159b** (06JST36), 1-oxo-3-phenyl-1,2-dihydropyrido[1,2-*a*]pyrazin-5-ium hexafluorophosphate (06AX(E)2438), 4-hydroxy-2-(2-pyridylmethyl)-1,2,3,4-tetrahydropyrido[1,2-*a*]pyrazin-5-ylum chloride (08JOC734), methyl *cis*-3*H*,9*aH*-(3*S*,9*aR*)-2-(*tert*-butoxycarbonyl)perhydropyrido[1,2-*a*]pyrazine-3-carboxylate (08SL702), 11*b*-[1,4]thiazino[3,4-*a*]isoquinoline **176** (08S1688) racemic spiro[1,4]oxazino[4,3-*a*]quinoline **173** (09JA3991), 6,6-dimethyl-6*a*,7-dihydro-6*H*,10*H*-pyrido[2,1-*c*][1,4]benzothiazin-10-one (09S665), 2-(piperidinoethyl)-1,2,3,4,11,11*a*-hexahydro-6*H*-pyrazino[1,2-*b*]isoquinoline-1,4-dione·HCl·H₂O (06T4408), *trans*-6*H*,11*aH*-2-tosyl-6-cianomethyl-11-methylene-1,2,3,4,11,11*a*-hexahydro-6*H*-pyrazino[1,2-*b*]isoquinoline (07T6152), 6-methyl and 6-ethoxycarbonyl derivatives of *trans*-6*H*,11*aH*-2,9-dimethyl-7,8,10-trimethoxy-1,2,3,4,11,11*a*-hexahydro-6*H*-pyrazino[1,2-*b*]isoquinoline-1,4-dione (08H(76)1497), (+)-praziquantel (06CH259), zwitter ionic compound **177**

(09OL5530), (11*bR*,2'*R*)-2-(2'-phenyl-2'methoxy-2'-trifluoromethylacetyl)-1,3,4,6,7,11*b*-hexahydro-1*H*-pyrazino[1,2-*a*]isoquinolin-4-one (08EJO895), 2-aminopyrido[1,2-*a*]quinoxalinium perchlorate and its thiocyanate monohydrate (08IC9122) were determined by X-ray diffraction studies.

The absolute regio- and stereochemistry of perhydropyrido[1,2-*a*]pyrazine-1,4-dione **178** was determined by X-ray crystallography (06JMC7290).



X-Ray diffraction determination revealed that in solid state the asymmetric unit cell of (4*R*,9*aR*)-4-phenylperhydropyrido[1,2-*a*]pyrazine-1,3-dione contains two distinct invertomers **150** and **151**, and they formed a head-to-head dimer (09TA1759). The invertomer **150** adopts *trans*-chair/*sofa* conformation with a *trans*-diaxial arrangement of the N5 lone pair and the H-C9*a*. The invertomer of **151** adopts *cis*-chair/*sofa* conformation with a *cis*-axial/*equatorial* arrangement of the N5 lone pair and the H-C9*a*, with respect to the piperidine ring.

It was determined by single crystal X-ray crystallography that (–)-praziquantel enantiomer has (*R*) absolute configuration (09PLN1).

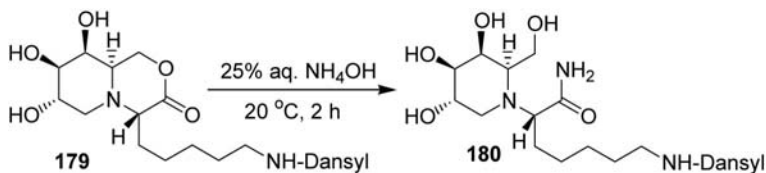
Structure of Mg complexes of ofloxacin [Mg(ofloxacin)₂(H₂O)₂·2H₂O] and levofloxacin [Mg(Levo)₂(H₂O)₂·2H₂O] were determined by X-ray crystallography (06JIB1755). [Cu(ofloxacin)₂·H₂O]·2H₂O complex was characterized by single crystal diffraction measurement (08JCR2961). {[Cu₂Br₃]_{*n*}[Cu(H-levofloxacin)₂]·2H₂O} complex was prepared and its crystal structure (orthorhombic, space group Fddd) was determined (05MI35).

For some more examples see Section 4.1.3.

4.2 Reactivity

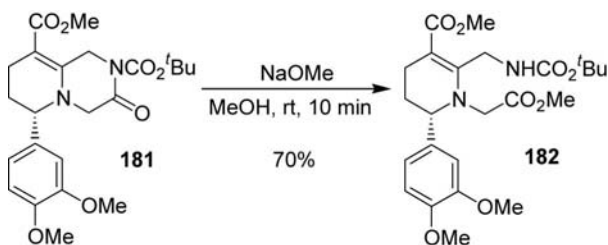
4.2.1 Ring opening

The treatment of trihydroxyperhydropyrido[2,1-*c*][1,4]oxazin-3-one **179** with 25% aqueous solution of NH₄OH provided ring opened product **180** (08BMC10216).

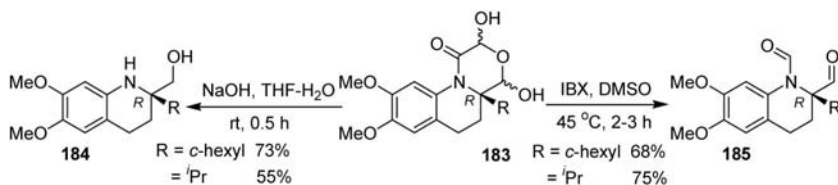


1-[1(*R*)-Phenyl-2-hydroxyethyl]-2(*S*),3(*R*)-bis(hydroxymethyl)piperidine was obtained by the reduction of methyl (4*R*,9*R*,9*Sa*)-1,6-dioxo-4-phenylperhydropyrido[2,1-*c*][1,4]oxazine-9-carboxylate with LiAlH_4 in boiling THF for 22 h (08WOP2008/076417). Catalytic hydrogenation of 3-(4-nitrophenyl)perhydropyrido[2,1-*c*][1,4]oxazin-3-ol over 20% Pd(OH)₂-on-carbon in 1 N H₂SO₄ at 20 psi for 18 h afforded 1-(4-aminophenyl)-2-[2-(hydroxymethyl)piperidin-1-yl]ethanol (08WOP2008/026046). Reduction of methyl *cis*-6*H*,9*aH*-4-phenyl-1-oxoperhydropyrido[2,1-*c*][1,4]oxazine-9-carboxylate (07LOC4) and (4*S*)-[4β*H*,7α*H*,8β*H*,9α*H*,9aβ*H*]-4-phenyl-7,8,9-tribenzyloxyperhydropyrido[2,1-*c*][1,4]oxazin-1-one (07TA1585) over Pd(OH)₂ in alcohol yielded methyl (2*S*,3*S*)-methoxycarbonylpipecolic acid and (2*S*,3*R*,4*R*,5*S*)-trihydroxypipelicolic acid, respectively.

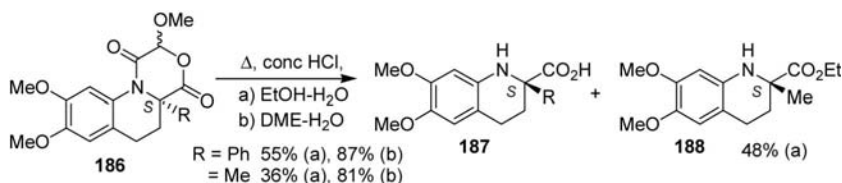
Ring opening of 3-oxo-3,4,7,8-tetrahydro-1*H*,6*H*-pyrido[2,1-*a*]pyrazine-9-carboxylate **181** occurred on the action of NaOMe to give tetrahydropyridinecarboxylate **182** (06T5697).



Tetrahydroquinoline-2-methanols **184** were obtained from the diastereomeric mixtures of cyclic hemiacetals **183** by treatment with aqueous solution of NaOH in THF (08T2321). C4*b*(*S*) epimers of **183** (R = Me, Ph) furnished the enantiomers of **184** (R = Me, Ph) in 84–90% yields. The oxidation of cyclic hemiacetals **183** with 2-iodoxybenzoic acid afforded 1-formyltetrahydroquinoline-2-aldehydes **185**. Enantiomers of **185** (R = Me, Ph, C≡CPh) were prepared similarly.



Heating 1,3,4,6,7,11*b*-hexahydro[1,4]oxazino[4,3-*a*]quinoline-1,4-diones **186** in the presence of conc. HCl in EtOH (method a) and DME (method b) at reflux yielded tetrahydroquinoline-2-carboxylic acids **187** (08T2321). Methyl derivative **187** (R = Me) was accompanied with the ethyl ester **188**, when EtOH was the solvent (method a).

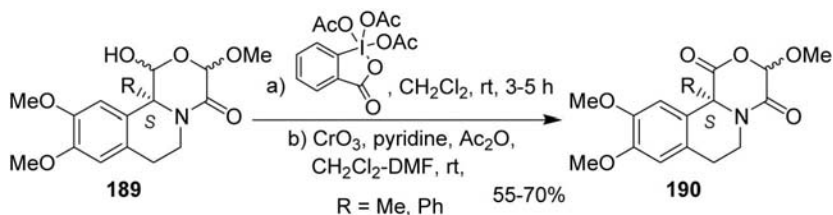


4.2.2 Oxidation, dehydrogenation

Oxidation of *trans*-4(*R*)*H*,9(*R*)*aH*-8-methylene-perhydropyrido[2,1-*c*][1,4]oxazin-1-one with OsO₄ and NaIO₄ in aqueous THF at ambient temperature provided *trans*-4(*R*)*H*,9*a*(*R*)*H*-perhydropyrido[2,1-*c*][1,4]oxazine-1,8-dione (08JOC6877).

Swern oxidation of 2-(3-cyanopyrazin-2-yl)-6-hydroxymethylperhydropyrido[1,2-*a*]pyrazine at -78 °C gave 6-aldehyde (07USA2007/037816).

Dess–Martin oxidation of 1,3,4,6,7,11*b*-hexahydro[1,4]oxazino[3,4-*a*]isoquinolin-4-ones **189** in CH₂Cl₂, or their oxidation with CrO₃ in the presence of pyridine and Ac₂O in a mixture of CH₂Cl₂ and DMF provided 1,3,4,6,7,11*b*-hexahydro[1,4]oxazino[3,4-*a*]isoquinoline-1,4-ones **190** (08T2321).



Oxidation of 3-hydroxymethyl-2,3-dihydro-5*H*-pyrido[1,2,3-*de*][1,4]benzoxazin-5-ones with *o*-iodoxybenzoic acid in DMSO and with Dess–Martin periodinate in CH₂Cl₂ afforded 3-formyl derivatives (08WOP2008/120003). Dehydrogenation of ethyl 10-[2-(*tert*-butoxycarbonyl)-1,2,3,4,6,8a-hexahydropyrrolo[1,2-*a*]pyrazin-7-yl]-9-fluoro-3(*S*)-methyl-7-oxo-2,3-dihydro-7*H*-pyrido[1,2,3-*de*][1,4]oxazine-6-carboxylates in the presence of Pd/C with air in MeOH afforded 10-[2-(*tert*-butoxycarbonyl)-1,2,3,4-tetrahydropyrrolo[1,2-*a*]pyrazin-7-yl] derivatives, which then were deprotected (09BML4933).

For some more examples see Section 4.2.6.

4.2.3 Hydrogenation, reduction

Catalytic reduction of methyl 4(*R*)-phenyl-1,6-dioxo-3,4,7,8-tetrahydro-1*H*,6*H*-pyrido[2,1-*c*][1,4]oxazine-9-carboxylate over Pd/C catalyst provided diastereoselectively *cis*-6*H*,9*H*,9*aH*-perhydro derivative in MeOH. Reduction of methyl *cis*-6*H*,9*H*,9*aH*-4-phenyl-1,6-dioxo-perhydropyrido[2,1-*c*][1,4]oxazine-9-carboxylate with two equivalents of BH₃–Me₂S in THF gave *cis*-6*H*,9*H*,9*aH*-4-phenyl-1-oxoperhydropyrido[2,1-*c*][1,4]oxazine-9-carboxylate at room temperature for 2 h, and a single isomer of *cis*-6*H*,9*H*,9*aH*-4-phenyl-1-hydroxyperhydropyrido[2,1-*c*][1,4]oxazine-9-carboxylate after 18 h reaction period, when six equivalents of BH₃–Me₂S were applied in boiling THF for 2.5 h *cis*-6*H*,9*H*,9*aH*-4-phenyl-9-(hydroxymethyl)perhydropyrido[2,1-*c*][1,4]oxazin-1-ol was the product (07LOC4).

Optically active pipelicolic acids, and their 2-substituted derivatives were prepared by the catalytic hydrogenation of the respective optically active 4-phenylperhydropyrido[2,1-*c*][1,4]oxazin-1-ones and their 9*a*-substituted derivatives over Pearlman's catalyst in good yields (05TA3858).

Atmospheric catalytic hydrogenation of 4-aryl-1,3,4,6,7,9*a*-hexahydropyrido[2,1-*c*][1,4]oxazin-6-ones (07USA2007/0117839, 08WOP2008/013213) and (4*R**,9*aS**)-6-oxo-4-(3,4,5-trifluorophenyl)-2,3,4,6,7,9*a*-hexahydro-1*H*-pyrido[1,2-*a*]pyrazine-2-carboxylate (07USA2007/0117839) over PtO₂ catalyst in MeOH gave perhydro derivatives.

Catalytic hydrogenation of the double bond and the azide group of (4*R*,9*aR*)-7-azido-9*a*-methyl-4-phenyl-3,4,9*a*-tetrahydro-1*H*,6*H*-pyrido[2,1-*c*][1,4-oxazine-1,6-dione in the presence of Boc₂O over Pd-C (10% wt) catalyst in MeOH for 18 h furnished a 9:1 mixture of (4*R*,7*S*,9*aR*)- and (4*R*,7*R*,9*aR*)-7-(*tert*-butoxycarbonylamino)perhydro derivatives in 77% yield (09JOC4429).

Reduction of perhydropyrido[2,1-*c*][1,4]oxazine-3,4-diones with *L*-selectride in THF at –30 °C to –15 °C for 3 h, followed by the treatment

with 5 N NaOH solution and 20–35% aqueous H_2O_2 afforded 3-hydroxy derivatives (07USA2007/0117798, 08USA2008/0207900).

cis-7*H*,9*H*-*trans*-8*H*,9*H*-7,8,9-Tri(pivaloyloxy)perhydropyrido[2,1-*c*][1,4]thiazine was obtained from the 6-oxo derivative by treatment with BH_3 ·THF in refluxing THF for 4 h (06EUP1657244). (6*R*,9*aS*)-2-substituted 6-arylperhydropyrido[1,2-*a*]pyrazines was prepared from the 8-oxo derivatives by reaction with *p*-toluenesulfonyl hydrazide in a mixture of MeOH and THF at room temperature for 20 h, then the formed hydrazone was treated NaBH_3CN in MeOH for 0.5 h, followed by the addition of $(\text{CF}_3\text{SO}_3)_2\text{Zn}$ and stirring at 65 °C for 5.5 h (06USA2006/0009456).

Hydrogenation of 9-benzyloxy-3,4-dihydro-1*H*,8*H*-pyrido[1,2-*a*]pyrazine-1,8-diones over Pd/C catalyst (10%) in MeOH gave 9-hydroxy derivatives (06WOP2006/066414). Transfer hydrogenation of 2-(4-nitrophenyl)perhydropyrido[1,2-*a*]pyrazine over Pd/C catalyst with H_2NNH_2 · H_2O in EtOH yielded the respective 2-(4-aminophenyl) derivative (06JMC6351).

Hydrogenolysis of 2-[1-(diphenylmethyl)azetidin-3-yl]perhydropyrido[1,2-*a*]pyrazines over Pearlman's catalyst in AcOH under hydrogen (5 bar) overnight (06WOP2006/137791) and transfer hydrogenolysis of 2-[1-(diphenylmethyl)azetidin-3-yl]perhydropyrido[1,2-*a*]pyrazin-6-ones over Pearlman's catalyst in the presence of NH_4OAc under microwave irradiation in EtOH at 120 °C for 2 min (07WOP2007/037743) yielded 2-(azetidin-3-yl) derivatives. The nitrogen atom of azetidine moiety of 2-(3-azetidiny)perhydropyrido[1,2-*a*]pyrazines (06WOP2006/137791) and their 6-oxo derivatives (07WOP037743) was reductively alkylated with aldehydes and $\text{NaB}(\text{OAc})_3\text{H}$ in the presence of DIPEA and a few drops of AcOH in CH_2Cl_2 at ambient temperature for 2–4 h.

2-Unsubstituted derivatives were obtained from 2-benzylperhydropyrido[1,2-*a*]pyrazines by transfer hydrogenation of over Pearlman's catalyst with HCO_2NH_4 (06USA2006/0009456). Catalytic hydrogenation of 2-benzyloxycarbonylbenzylperhydropyrido[1,2-*a*]pyrazine-3-carboxylate (08SL702) and 2-benzylperhydropyrido[1,2-*a*]pyrazines (06JMC7290, 07WOP2007/050802, 08WOP2008/101247, 09USP7538110) over Pd/C catalyst also provided 2-unsubstituted derivatives. That of 8-(3-benzyloxyphenyl)perhydropyrido[1,2-*a*]pyrazines (06JMC7290, 07WOP2007/050802, 09USP7538110), and *N*-(4-fluorobenzyl)-9-benzyloxy-2-(2-methoxyethyl)-1,8-dioxo-1,2-dihydro-8*H*-pyrido[1,2-*a*]pyrazine-7-carboxamide (06WOP2006/088173, 07WOP2007/049675) afforded 8-(3-hydroxyphenyl) perhydropyrido[1,2-*a*]pyrazines and 9-hydroxy-1,2,3,4-tetrahydro derivatives, respectively.

Oxo groups of perhydropyrido[1,2-*a*]pyrazine-1,4-dione were reduced to methylene groups with LAH (08WOP2008/101247). Oxo groups of perhydropyrido[1,2-*a*]pyrazine-1,4-diones and 2-acylperhydropyrido

[1,2-*a*]pyrazines were reduced with $\text{BF}_3 \cdot \text{Me}_2\text{S}$ to methylene groups (06JMC7290, 07WOP2007/050802, 09USP7538110).

Reduction of *cis*-6*H*,9*aH*-1,4-dioxoperhydropyrido[1,2-*a*]pyrazine-6-carboxylate with LAH yielded quantitatively 6-hydroxymethylperhydropyrido[1,2-*a*]pyrazine (07USA2007/037816, 07USA2007/037817).

3-Hydroxymethyl derivative was prepared from methyl 6-oxo-6,6*a*,7,8,9,10-hexahydro-5*H*-pyrido[1,2-*a*]quinoxaline-3-carboxylate by reduction with LAH (08USA2008/0161292, 09BML4050). Oxo group of 8-methoxy-3-[2-(*trans*-4-aminocyclohexyl)acetyl]-2,3,4,4*a*,5,6-hexahydro-1*H*-pyrazino[1,2-*a*]quinoline was reduced to methylene group by using LAH in boiling THF (06BML443).

Catalytic hydrogenation of 3-(2,3,4,4*a*,5,6-hexahydro-1*H*-pyrazino[1,2-*a*]quinolin-3-yl)propionitrile over Raney-Nickel in MeOH containing NH_3 gave 3-(2,3,4,4*a*,5,6-hexahydro-1*H*-pyrazino[1,2-*a*]quinolin-3-yl)propylamine in 97% yield (05WOP2005/118591).

Catalytic hydrogenation of 3-arylidene-1,2,3,4,11,11*b*-hexahydro-6*H*-pyrazino[1,2-*b*]isoquinoline-1,4-diones over 10% Pd/C gave a mixture of 3-epimeric mixture of 3-arylmethyl derivatives (09T2201). When a 6-benzyloxymethyl group was present in the starting material, 6-hydroxymethyl derivative was obtained. The 6-benzyloxymethyl group remained intact when the reduction of 3-arylidene derivative was carried out using Zn in AcOH at 125 °C, and a mixture of $\text{H}_2\text{NNH} \cdot \text{H}_2\text{O}$ and H_2O_2 in the presence of 1% aqueous CuSO_4 in EtOH at room temperature.

Catalytic hydrogenation of 6-benzyloxymethyl derivatives of 1,2,3,4,11,11*b*-hexahydro-6*H*-pyrazino[1,2-*b*]isoquinolin-4-ones in EtOH over 10% Pd/C catalyst under 3.5 atm of H_2 at 70 °C gave 6-hydroxymethyl derivatives. 6-Hydroxymethyl group was converted into esters groups with acids in the presence of 1-(3-dimethylaminopropyl)-3-ethylcarbodiimide and 4-dimethylaminopyridine in CH_2Cl_2 at room temperature (08BMC9065, 09T2201), and into a phthalimidomethyl group with phthalimide in the presence of diethyl azodicarboxylate and Ph_3P at 23 °C for 2 h (08BMC9065). The reduction of 1,2,3,4,11,11*a*-hexahydro-6*H*-pyrazino[1,2-*b*]isoquinoline-1,4-diones with $\text{LiAlH}(\text{O}^t\text{Bu})_3$ (5 equiv.) in THF at room temperature for 16 h afforded *cis*-1*H*,11*aH*-1-hydroxy-1,2,3,4,11,11*a*-hexahydro-6*H*-pyrazino[1,2-*b*]isoquinolin-4-one in excellent yields. The 2-(*iso*-propoxycarbonyl) derivatives of the latter gave 1,2,3,4,6,11,11*a*-hexahydro-1*H*-pyrazino[1,2-*b*]isoquinolin-4-ones by treatment with Et_3SiH (17 equiv.) and TFA (15.5 equiv.) in CH_2Cl_2 at -10 °C. When the reaction was performed at ambient temperature the product was accompanied by a 3,4,6,11-tetrahydro-2*H*-pyrazino[1,2-*b*]isoquinolin-4-one derivative. Due to the lability of the 2-(*tert*-butoxycarbonyl) group of a *trans*-1*H*,11*aH*-1-hydroxy-2-(*tert*-butoxycarbonyl)-2,3,4,6-hexahydro-1*H*-pyrazino[1,2-*b*]isoquinolin-4-one to TFA, this compound provided only a 3,4,6,11-tetrahydro-2*H*-pyrazino[1,2-*b*]

isoquinolin-4-one at -10°C . Reduction of a 6-(phthalimidomethyl)-2-(*iso*-propoxycarbonyl)-2,3,4,6-tetrahydro-1*H*-pyrazino[1,2-*b*]isoquinoline-1,4-dione with $\text{LiAlH}(\text{O}^t\text{Bu})_3$ (7 equiv.) in THF at room temperature afforded a 6-(1'-oxo-3'-hydroxy-1',3'-dihydro-2'-isoindolylmethyl)-1-hydroxy-2,3,4,6-tetrahydro-1*H*-pyrazino[1,2-*b*]isoquinolin-4-one as a diastereomeric mixture in excellent yield. The treatment of this mixture with Et_3SiH (50 equiv.) and TFA (50 equiv.) in CH_2Cl_2 at -30°C provided a ca. 2:1 mixture of 6-(1'-oxo-1',3'-dihydro-2'-isoindolylmethyl)-1,2,3,4-tetrahydro-6*H*-pyrazino[1,2-*b*]isoquinolin-4-one and 6-(1'-oxo-1',3'-dihydro-2'-isoindolylmethyl)-2,3,4,6,11,11*a*-hexahydro-1*H*-pyrazino[1,2-*b*]isoquinolin-4-one. The latter was also obtained by the catalytic reduction of the former over 10% Pd/C catalyst in MeOH at 70°C .

10-Amino-2-cyclohexylcarbonyl-1,3,4,6,7,11*b*-hexahydro-2*H*-pyrazino[1,2-*b*]isoquinolin-4-one was obtained in good yield from 10-nitro derivative by catalytic hydrogenation over Pd/C catalyst and reduction with $\text{SnCl}_2 \cdot 2\text{H}_2\text{O}$ (07BML4154). 1,3,4,6,7,11*b*-Hexahydro-2*H*-pyrazino[2,1-*a*]isoquinoline was obtained from 4-oxo derivative by reduction with LiAlH_4 in boiling THF in 98% yield (07WOP2007/119463).

Reduction of 8-nitro-9,10-difluoro-7-oxo-2,3-dihydro-7*H*-pyrido[1,2,3-*de*][1,4]benzoxazine-6-carboxamides with $\text{Na}_2\text{S}_2\text{O}_4$ in aqueous MeOH under reflux for 5 h gave 8-amino derivatives in 51–74% yields (09WOP2009/035634). 8-Amino derivative was obtained from (S)-8-nitro-9-fluoro-10-(1-aminocyclopropyl)-7-oxo-2,3-dihydro-7*H*-pyrido[1,2,3-*de*][1,4]benzoxazine-6-carboxylic acid by catalytic hydrogenation over Pd/C catalyst in AcOH (06MIP1).

A C=C double bond present in a side chain in position 9 on 7-oxo-2,3-dihydro-7*H*-pyrido[1,2,3-*de*][1,4]oxazine-6-carboxylic acid skeleton was catalytically reduced by H_2 over 10% Pd/C catalyst (07WOP2007/054296).

9,10-Difluoro-3(S)-methyl-7-oxo-2,3-dihydro-7*H*-pyrido[1,2,3-*de*][1,4]oxazine-6-carboxylate was obtained from 3(S)- CH_2SMe and $-\text{CH}_2\text{SCH}_2\text{Ph}$ derivatives by reductive cleavage with Raney Ni in EtOH at 30°C (04MIP2).

For some more examples see Sections 4.2.5 and 4.2.6.

4.2.4 Reactivity of ring carbon atoms

The epimerization of (4*R*,9*aR*)-4-phenylperhydropyrido[2,1-*c*][1,4]oxazin-1-one at C9*a* carbon could be achieved by treatment with $\text{KN}(\text{SiMe}_3)_2$ in THF at -78°C for 30 min to yield effectively the (4*R*,9*aS*) epimer (05TA3858). $\text{NaN}(\text{SiMe}_3)_2$ and LiN^tPr_2 proved to be less appropriate than $\text{KN}(\text{SiMe}_3)_2$, as they gave only 10% and 50% conversion, respectively. 9*a*-Substituted derivatives were obtained by alkylation of (4*R*,9*aR*)-4-phenylperhydropyrido[2,1-*c*][1,4]oxazin-1-one with alkyl iodides, allyl and benzyl bromides in THF in the presence of $\text{KN}(\text{SiMe}_3)_2$ and HMPA at -78°C for 1.5 h in 61–83% yields.

The treatment of 4-arylperhydropyrido[2,1-*c*][1,4]oxazin-6-ones (07USA2007/0117839, 08WOP2008/013213) and 6-oxo-4-(3,4,5-trifluorophenyl)perhydropyrido[1,2-*a*]pyrazine-2-carboxylate (07USA2007/0117839) with Me₃SiI and *N,N,N',N'*-tetramethylethylenediamine in CH₂Cl₂ in a N₂ atmosphere at 0 °C followed by the addition of I₂ and stirring at 0 °C for another 30 min yielded 7-iodo derivatives.

Reaction of 4-aryl-3,4,6,7,8,9-hexahydro- and -perhydropyrido[2,1-*c*][1,4]oxazin-6-ones with (Pr)₂NLi in THF at 0 °C, then with 3-methoxy-4-(4-methyl-1*H*-imidazol-1-yl)benzaldehyde afforded 7-([3-methoxy-4-(4-methyl-1*H*-imidazol-1-yl)phenyl]hydroxymethyl) derivatives, which were dehydrated by treatment first with MeSO₂Cl and NEt₃, then with a solution of NaOMe in MeOH to provide (*E*)-7-([3-methoxy-4-(4-methyl-1*H*-imidazol-1-yl)phenyl]methylene)-4-aryl-3,4,6,7,8,9-hexahydro- and -perhydropyrido[2,1-*c*][1,4]oxazin-6-ones (07USA2007/0117859).

(4*R*,9*aR*)-7-Azido-9*a*-methyl-4-phenyl-3,4,9,9*a*-tetrahydro-1*H*,6*H*-pyrido[2,1-*c*][1,4-oxazine-1,6-dione was obtained from (4*R*,9*aR*)-9*a*-methyl-4-phenyl-3,4,9,9*a*-tetrahydro derivative by addition of Br₂ in boiling CCl₄ for 2 h, then by stirring with saturated aqueous Na₂SO₃ solution at room temperature, followed by the reaction with NaN₃ in DMF at ambient temperature for 3 h and 70 °C for 4 h (09JOC4429).

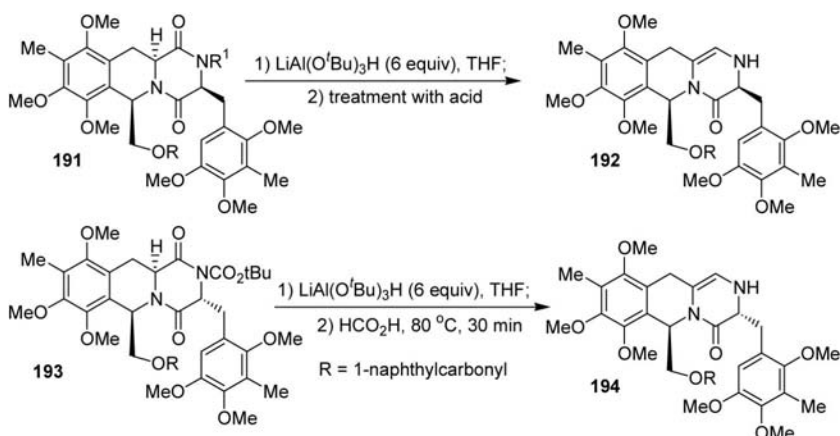
Fluorination of 9-benzyloxy-2-(4-fluorobenzyl)-6-methoxy-3,4-dihydro-1*H*,8*H*-pyrido[1,2-*a*]pyrazine-1,8-dione with Selectfluor® in the presence of Ce₂CO₃ in MeCN at ambient temperature for 6 h provided 7-fluoro derivative. Reaction of 6-bromo-3,4-dihydro-1*H*,8*H*-pyrido[1,2-*a*]pyrazine-1,8-diones with phenol cyclohexyl-, and cyclopropylmethanols in the presence of Ce₂CO₃ in DMF in a sealed tube at 25–60 °C for 12–24 h afforded 6-phenoxy, 6-cyclohexyl-, and 6-cyclopropylmethoxy derivatives, respectively (06WOP2006/066414).

Upon stirring of 1,2,4,4*a*,5,6-hexahydro[1,4]oxazino[4,3-*a*]quinoline-5,5-dinitrile **168** in 4 N HCl/dioxane for 1 h epimerization occurred in position C4*a* to provide the thermodynamic product **169** (09JA3991).

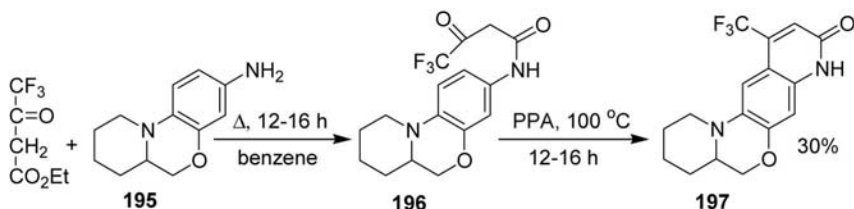
Epimerization of a *trans*-6*H*,11*aH*-1,2,3,4,11,11*a*-6*H*-hexahydropyrazino[1,2-*b*]isoquinoline-1,4-dione occurred at position 11*a* by heating in the presence of DMAP (2 equiv.) in CH₂Cl₂ at 70 °C to yield a 1:1 mixture of the *trans*- and the *cis*-6*H*,11*aH* derivatives (08BMC9065).

Reaction of 2-acyl-1,2,3,4,11,11*a*-6*H*-hexahydropyrazino[1,2-*b*]isoquinoline-1,4-diones with aromatic aldehydes in the presence of KO^{*t*}Bu in CH₂Cl₂ afforded 2-unsubstituted-3-arylidene derivatives (09T2201). From a similar reaction of *cis*-6*H*,11*aH*-6-benzyloxymethyl-9-methyl-7,8,10-trimethoxy-2-pivaloyl-1,2,3,4,11,11*a*-6*H*-hexahydropyrazino[1,2-*b*]isoquinoline-1,4-dione and 3-methyl-2,4,5-benzaldehyde 2-unsubstituted-3-(3-methyl-2,4,5-trimethoxyphenyl)methylene and 2-pivaloyl-3,3-dihydroxy derivatives were isolated in 20% and 39% yields, respectively.

The treatment of 1,2,3,4,11,11a-hexahydro-6*H*-pyrazino[1,2-*b*]isoquinoline-1,4-dione **191** ($R = \text{cinnamoyl}$, $R^1 = \text{CO}_2^i\text{Pr}$) with $\text{LiAl}(\text{O}^t\text{Bu})_3\text{H}$ (6 equiv.), and followed by treatment of the reaction mixture with HCO_2H at 80°C , and then with $\text{TFA}/\text{H}_2\text{SO}_4$ gave 1,2,3,4-tetrahydro-6*H*-pyrazino[1,2-*b*]isoquinoline-1,4-dione **192** ($R = \text{H}$) in 62% yield (09T2201). Compound **192** ($R = \text{H}$) was also obtained in 82% yield from **191** ($R = \text{CO}_2^t\text{Bu}$, $R^1 = \text{CO}^t\text{Bu}$) when after the reduction the reaction mixture was treated with boiling TFA . When TFA was applied as acid at room temperature in the case of **191** ($R = 1\text{-naphthylcarbonyl}$, $R^1 = \text{CO}_2^t\text{Bu}$), **192** ($R = 1\text{-naphthylcarbonyl}$) was obtained in 70%. The treatment of the reaction mixture of **193**, after reduction, with HCO_2H at 80°C afforded a mixture, which contains 22% of **194**.

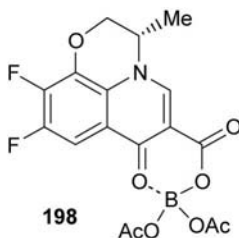


Nitration of praziquantel with a mixture of $\text{HNO}_3/\text{H}_2\text{SO}_4$ provided 10-nitro derivative in 39% yield (07BML4154).



Tetracyclic compound **197** was obtained when 4,4,4-trifluoroacetate and 3-amino-6,6a,7,8,9,10-hexahydropyrido[2,1-*c*][1,4]benzoxazine **195** was heated in benzene, then the condensation product **196** was cyclized by heating in PPA (07JMC2486).

Nitration of 9,10-difluoro-7-oxo-2,3-dihydro-7*H*-pyrido[1,2,3-*de*][1,4]benzoxazine-6-carboxylic acids (09WOP2009/035634) and ethyl ester (07WOP2007/106537) with solid KNO₃ in conc. H₂SO₄, furthermore that of (S)-9-fluoro-10-(1-aminocyclopropyl)-7-oxo-2,3-dihydro-7*H*-pyrido[1,2,3-*de*][1,4]benzoxazine-6-carboxylic acid with a mixture of HNO₃/H₂SO₄ (06MIP1) afforded 8-nitro derivatives.



Reaction of diacetatoboron chelate **198** with cyclic amines (09USA2009/0156577), 2-aminomethylaziridine (06CCCL1431), followed by hydrolysis provided 10-substituted 3(*S*)-methyl-9-fluoro-7-oxo-2,3-dihydro-7*H*-pyrido[1,2,3-*de*][1,4]oxazine-6-carboxylic acids.

The 10-fluoro atom of 9,10-difluoro-7-oxo-2,3-dihydro-7*H*-pyrido[1,2,3-*de*][1,4]oxazine-6-carboxylic acids and an amide derivative was replaced by secondary amines [03MIP1, 05MIP2-4, 05WOP2005/123746, 06WOP2006/030452, 06WOP2006/048889, 07MIP1, 07WOP2007/003308, 07WOP2007/141900, 08MI92, 08MIP2, 08WOP2008/143343, 09JAP(K)2009/198177, 09MIP2-4, 09USA2009/0156577, 09WOP2009/064836]. Similar reactions were carried out with 9,10-difluoro-2,2-dimethyl- and -3,3-dimethyl-6-carboxylic acid derivative and cyclic amines in DMSO at 70–100 °C in the presence of a base (05MIP2). That of 9,10-difluoro-3(*S*)-methyl-7-oxo-2,3-dihydro-7*H*-pyrido[1,2,3-*de*][1,4]oxazine-6-carboxylic acid-difluoroborane complex with cyclic amines [06WOP2006/123792, 07WOP2007/141900, 08WOP2008/082009, 2008WOP2008/122384, 09JAP(K)2009/198177, 09USA2009/0029980] gave 10-substituted carboxylic acid derivatives. That of bis(acetate-*O*)[(3*S*)-9,10-difluoro-3-methyl- and -3-fluoromethyl-7-oxo-2,3-dihydro-7*H*-pyrido[1,2,3-*de*][1,4]oxazine-6-carboxylato-*O*⁶,*O*⁷]borons were reacted with cyclic amines in the presence of Et₃N in MeCN at 30–60 °C for 1–6 h (08JMC3238, 09EJM4063, 09MIP5). The 10-fluoro atom of 9,10-difluoro-3-methyl-7-oxo-2,3-dihydro-7*H*-pyrido[1,2,3-*de*][1,4]benzoxazine-6-carboxylic acid was reacted with *p*-methoxybenzylamine in pyridine at 110 °C for 48 h to give 10-[(*p*-methoxyphenyl)methyl]amino derivative (08EJM2453). That of 8-amino-9,10-difluoro-6-cyano-, and -6-(1*H*-tetrazol-5-yl)-2,3-dihydro-7*H*-pyrido[1,2,3-*de*][1,4]benzoxazine-7-ones were reacted with 3-substituted propylamines in DMSO

at 120 °C for 1–3 h to give 10-(3-substituted propylamino) derivative in 15–37% yield (09WOP2009/035634).

Levofloxacin was obtained in 92% when 9,10-difluoro-3(*S*)-methyl-7-oxo-2,3-dihydro-7*H*-pyrido[1,2,3-*de*][1,4]benzoxazine-6-carboxylic acid was reacted with 4-methylpiperazine dihydrochloride in the presence of Et₃N and BF₃·THF complex in MeCN at room temperature (08WOP2008/126384).

It is interesting while the reaction of enantiomers of 8,9,10-trifluoro-3-phenyl-7-oxo-2,3-dihydro-7*H*-pyrido[1,2,3-*de*][1,4]oxazine-6-carboxylate with *N*-2-pyridyl-1,2-ethylenediamine in DMSO in the presence of Et₃N at 100 °C afforded 10-substituted derivatives, that of 8,9,10-trifluoro-3(*S*)-benzyl-7-oxo-2,3-dihydro-7*H*-pyrido[1,2,3-*de*][1,4]oxazine-6-carboxylate with benzylamine in boiling MePh in the presence of Et₃N afforded 8-substituted derivative (07WOP2007/106537). The 10-substituted derivative was also obtained in the reaction of 3-fluoromethyl-9,10-difluoro-8-amino-7-oxo-2,3-dihydro-7*H*-pyrido[1,2,3-*de*][1,4]oxazine-6-carboxylic acid and *N*-2-pyridyl-1,2-ethylenediamine in DMSO in the presence of Et₃N at 120 °C. Reaction of 4-methoxybenzylamine with the enantiomers of 10-[2-(2-pyridylamino)ethylamino]-8,9-difluoro-3-benzyl-7-oxo-2,3-dihydro-7*H*-pyrido[1,2,3-*de*][1,4]oxazine-6-carboxylic acid in DMSO at 150 °C gave 8-(4-methoxybenzylamino) derivatives.

Reaction of ethyl 9,10-difluoro-7-oxo-2,3-dihydro-7*H*-pyrido[1,2,3-*de*][1,4]oxazine-6-carboxylates with MeNO₂ in DMSO in the presence of NaH afforded 10-nitromethyl derivatives (07BMC7274). Pazufloxacin intermediate, 10-cyanomethyl-9-fluoro-3(*S*)-methyl-7-oxo-2,3-dihydro-7*H*-pyrido[1,2,3-*de*][1,4]oxazine-6-carboxylic acid was prepared from 9,10-difluoro ethyl ester by reacting with ethyl cyanoacetate in the presence of 20–60% NaOH solution and PEG-200 as phase transfer catalyst below 0 °C, then by treatment with 6–18% H₂SO₄ at 60 °C for 6 h in 94% yield (06MIP2), and in the presence of NaH in DMF between 0 °C and 50 °C, then by treatment with HCl and *p*TSA in dioxane at reflux for 24 h in 85% yield (05MI36, 07MI69).

Reaction of 9-fluoro-7-oxo-2,3-dihydro-7*H*-pyrido[1,2,3-*de*][1,4]oxazine-6-carboxylate and *tert*-butyl (2-mercaptoethyl)carbamate in DMSO at 100 °C for 5 h gave 9-[2-(*tert*-butoxycarbonylamino)ethylthio] derivative (06WOP2006/050943). The iodo atom of 9-iodo-7-oxo-2,3-dihydro-7*H*-pyrido[1,2,3-*de*][1,4]oxazine-6-carboxylic acids was coupled with 4'-*O*-(2-allyloxyethyl)azithromycin in MeCONMe₂ in the presence of Bu₃N and *trans*-di- μ -acetato-bis[2-(di-*o*-tolylphosphino)benzyl]dipalladium(II) and di(*tert*-butyl)-4-methylphenol at 110–115 °C for 15–17 h to give a mixture of 9-(3-substituted prop-1- and -2-enyl) derivatives (07WOP2007/054296). 10-methoxy and 10-cyano-3-hydroxymethyl-2,3-dihydro-5*H*-pyrido[1,2,3-*de*][1,4]benzoxazin-5-ones were obtained from 10-bromo derivative by reaction with NaOMe in the presence of Cu(I)I at 140 °C in DMF,

and with Cu(I)CN at 180 °C in NMP, respectively (08WOP2008/120003). Palladium-mediated coupling of ethyl 9-fluoro-10-[(trifluoromethylsulfonyl)oxy-3(*S*)-methyl-7-oxo-2,3-dihydro-7*H*-pyrido[1,2,3-*de*][1,4]oxazine-6-carboxylate with 1,2,3,4,6,8*a*-hexahydropyrrolo[1,2-*a*]pyrazin-7-yl boronic esters in the presence of CsF and Pd(PPh₃)₄ afforded 10-(1,2,3,4,6,8*a*-hexahydropyrrolo[1,2-*a*]pyrazin-7-yl) derivatives (09BML4933).

Reaction of 8-fluoro-5*H*-pyrido[1,2,3-*de*][1,4]benzoxazine-3,7(2*H*,6*H*)-dione and triphenyl(methoxymethyl)phosphonium chloride in the presence of KO^{*t*}-Bu gave 7-[(methyloxy)methylidene]-3-oxo derivative, which was reacted with Me₃SiCl in the presence of NaI in MeCN at ambient temperature for 18 h to yield 7-carbaldehyde derivative (08WOP2008/116815).

4.2.5 Reactivity of the ring nitrogen atom

The treatment of 2-*tert*-butoxycarbonylperhydropyrido[1,2-*a*]pyrazines with an acid (4 N HCl solution, TFA) gave 2-unsubstituted derivatives (05USA2005/0282811, 07USA2007/037817, 08SL702). 2-Unsubstituted *cis*- and *trans*-4*H*,9*aH*-4-(3,4,5-trifluorophenyl)-7-{1-[3-methoxy-4-(4-methyl-1*H*-imidazol-1-yl)phenyl]-(*E*)-methylene}perhydropyrido[1,2-*a*]pyrazin-6-ones were obtained from the 2-methoxycarbonyl derivatives by treatment with Me₃SiI in boiling CH₂Cl₂ for 3 h (07USA2007/0117839).

Reactions of perhydropyrido[1,2-*a*]pyrazine with aldehydes in the presence of NaB(OAc)₃H and NaBH₃CN in AcOH (05USA2005/0282811) and in acidified EtOH (07USA2007/0117839) afforded 2-substituted derivatives. 2-(1-Diphenylmethylazetididin-3-yl) derivative was obtained in the reaction of perhydropyrido[1,2-*a*]pyrazine and diphenylmethyl-3-azetididin-3-one in the presence of (polystyrylmethyl) trimethylammonium cyanoborohydride in MeOH containing 10% AcOH at 120 °C for 5 min under microwave irradiation (06WOP2006/137791).

2-Unsubstituted perhydropyrido[1,2-*a*]pyrazin-6-ones were reacted with MeSO₂Cl and Me₂NCOCl in CH₂Cl₂ to give 2-methanesulfonyl and dimethylaminocarbonyl derivatives, respectively (07USA2007/0117839). Reaction of Na salt of perhydropyrido[1,2-*a*]pyrazine with ClCO₂CH₂Ph in THF gave 2-benzyloxycarbonyl derivative (08WOP2008/101247). Methyl perhydropyrido[1,2-*a*]pyrazine-3-carboxylate was reacted with ClCO₂CH₂Ph in the presence of Et₃N in CH₂Cl₂ at room temperature, and with L-2-(^{*t*}BuCONH)EtCO₂H in the presence of ClCO₂Et and *N*-methylmorpholine in THF at -20 °C to yield 2-substituted derivatives (08SL702). 2-*tert*-Butoxycarbonyl derivatives of 3,4,7,8-tetrahydro-1*H*,6*H*-pyrido[2,1-*a*]pyrazine-9-carboxylate **181** (06T5697) and perhydropyrido[2,1-*a*]pyrazine-3-carboxylate (08SL702) were prepared from the 2-unsubstituted derivatives by treatment with (Boc)₂O. Racemic and optically

active *cis*-6*H*,9*aH*-6-(4-methoxy-2,3-dimethylphenyl)perhydropyrido[1,2-*a*]pyrazines were *N*(2)-acylated with 6-trifluoromethylnicotinic acid in the presence of benzotriazol-1-yloxy-tris(dimethylamino)phosphonium hexafluorophosphate and 5% Et₃N in DMA at ambient temperature and with 6-trifluoromethylnicotinic acid chloride in the presence of NEt₃ and DMAP in CH₂Cl₂ at room temperature, respectively (06USA2006/0009456).

N(2)-(Het)arylation of perhydropyrido[1,2-*a*]pyrazine was carried out with methyl 2-chloropyrimidine-5-carboxylate in the presence of ^tPr₂NEt at ambient temperature, with 5-chloropyrazine-2-carboxamide derivatives in DMSO at 100 °C, with methyl 4-iodobenzoate in the presence of Ce₂CO₃, Cu(I)I and acetylcyclohexanone in DMF at 90 °C (08WOP2008/075068), with 6-bromo-1-(triisopropylsilyl)-1*H*-indole in the presence of ^tBuONa, ^tBu₃P, and Pd(OAc)₂ in xylene at 110 °C (08WOP2008/101247), and with 2,4,6-trichloro-5-fluoropyrimidine in DMSO in the presence of ^tPr₂NEt at room temperature (09WOP2009/061879). 2-(Het)arylperhydropyrido[1,2-*a*]pyrazines were obtained from perhydropyrido[1,2-*a*]pyrazine with 1-chloro-4-nitrobenzene (06JMC6351), a *N*-substituted 6-chloronicotinamide (07BML5300), 2,4-dibenzyl-6,8-dichloro-3-oxo-3,4-dihydro-2*H*-benzo(*e*)-2,4-thiadiazine 1,1-dioxide (07WOP2007/108569), 4-trifluoromethylsulfonyloxy-2-morpholino-7-benzyl-5,6,7,8-tetrahydropyrido[3,4-*b*]pyrimidine (07CHE640), 7-chlorofuro[2,3-*c*]pyridine, 7-chlorothieno[2,3-*c*]pyridine 1-chloro-7-methoxyisoquinoline, (09CPB34), and 2-chloro-6-methoxybenzothiazole (07WOP2007/110364). 7-Hydroxymethylperhydropyrido[1,2-*a*]pyrazine was *N*(2)-arylated by 1-bromo-2,3-dichlorobenzene in the presence of Pd₂(dba)₃, BINAP, and NaO^tBu in toluene at 80 °C (06BMC5898).

The *N*(2)-atom of perhydropyrido[1,2-*a*]pyrazine-1,4-ones was alkylated, arylated, acylated, and sulfonylated by reacting with aldehydes under reductive amination condition using NaCNBH₃, resin-supported cyano borohydride, and BH₃·pyridine as reducing agent, by coupling with potassium phenyltrifluoroborate in the presence of Cu(OAc)₂ and Et₃N, furthermore by reacting with acyl chlorides and sulfonyl chlorides, respectively (06JMC7290, 07WOP2007/050802, 09USP7538110). Reaction with PhNCO, BrCH₂CO₂^tBu, and CH₂=CHCO₂^tBu gave 2-(phenylamino)carbonyl (06JMC7290), 2-(*tert*-butoxycarbonyl)methyl, and 2-[2-(*tert*-butoxycarbonyl)ethyl] (07WOP2007/050802, 09USP7538110) derivatives, respectively.

N(2)-acylation of perhydropyrido[1,2-*a*]pyrazines with carboxylic acid was achieved in the presence of HATU and Hünig's base in CH₂Cl₂ (08BML215), with 2-(trifluoromethyl)pyrimidine-5-carbonyl chloride (08WOP2008/0977483) and with Ac₂O (08SL702). Reaction of perhydropyrido[1,2-*a*]pyrazin-6-one and 2-FPhSO₂Cl in the presence of Et₃N in a mixture of CH₂Cl₂ and MeCN provided 2-substituted derivative (09EUP2098526, 09WOP2009/103176). Reaction of *cis*-6*H*,9*aH*-6-hydroxymethylperhydropyrido[1,2-*a*]pyrazine with (Boc)₂O in CH₂Cl₂ at 0 °C

for 1 h, and 3-chloropyrazine-2-carbonitrile in the presence of Et_3N in THF at 35 °C overnight furnished 2-*tert*-butoxycarbonyl (07USA2007/037817) and 2-(3-cyano-2-pyrazinyl) derivatives, (07USA2007/037816), respectively.

A 8-(3-benzyloxyphenyl)perhydropyrido[1,2-*a*]pyrazine was prepared from a 8-(3-hydroxyphenyl)perhydropyrido[1,2-*a*]pyrazine by protecting the *N*(2)-atom first by reacting with di-*tert*-butyl dicarbonate, followed by *O*-alkylation with PhCH_2Br , and the removal of the *N*-protecting group by heating in the presence of 2 N solution of HCl in Et_2O in MeOH at room temperature for 18 h (06JMC7290).

N(3)-acylation of 8-methoxy-2,3,4,4*a*,5,6-hexahydro-1*H*-pyrazino[1,2-*a*]quinoline with *trans*-(4-*tert*-butoxycarbonylaminocyclohexyl)acetic acid in the presence of 1-(3-dimethylaminopropyl)-3-ethylcarbodiimide hydrochloride, 1-hydroxybenzotriazole hydrate and Hünig's base in CH_2Cl_2 at room temperature was carried out (06BML443). 10-Methoxy-2,3,4,4*a*,5,6-hexahydro-1*H*-pyrazino[1,2-*a*]quinoline was *N*(3)-alkylated with 4-(phthalimido)butyl bromide in the presence of K_2CO_3 and KI in refluxing MeCN overnight (07MIP2). Reaction of acrylonitrile with 2,3,4,4*a*,5,6-hexahydro-1*H*-pyrazino[1,2-*a*]quinoline in MeOH afforded 3-(2,3,4,4*a*,5,6-hexahydro-1*H*-pyrazino[1,2-*a*]quinolin-3-yl)propionitrile in 78% yield (05WOP2005/118591). Acylation of 1,3,4,6,7,11*b*-hexahydro-2*H*-pyrazino[2,1-*a*]isoquinolin-4-one with cyclohexanecarbonyl chloride in the presence of K_2CO_3 in afforded praziquantel (05MIP5, 09WOP2009/115333). 1,3,4,6,7,11*b*-hexahydro-2*H*-pyrazino[2,1-*a*]isoquinoline was *N*(2)-arylated with 2-chloro-3-methyl-6-(4-pyridyl)-3*H*-pyrimidin-4-one in the presence of Et_3N in DMF at room temperature overnight in 95% yield (07WOP2007/119463).

Reaction of 7,10-dimethoxy-3-[(2,4-dimethoxyphenyl)methyl]-6-methyl-1,2,3,4,11,11*a*-hexahydro-6*H*-pyrazino[1,2-*b*]isoquinoline-1,4-dione with $\text{ClCO}_2\text{CH}_2\text{Ph}$ in the presence of NaH in THF at 0 °C gave 2-benzyloxycarbonyl derivative in 93% yield (07T8781). 2-(*iso*-Propoxycarbonyl), 2-(*tert*-butoxycarbonyl), 2-methyl derivatives were prepared from 2-unsubstituted 1,2,3,4,11,11*b*-hexahydro-6*H*-pyrazino[1,2-*b*]isoquinoline-4-ones by the treatment with $^\text{i}\text{PrO}_2\text{CCl}$ in the presence of Et_3N and 4-dimethylaminopyridine in CH_2Cl_2 at room temperature, with Boc_2O in the presence of catalytic amount of 4-dimethylaminopyridine in MeCN at ambient temperature (08BMC9065, 09T2201), and with a mixture of H_2CO and HCO_2H at 70–100 °C for 1 h, respectively (08BMC9065). When a 6-hydroxymethyl side chain was present in the case of *N*(2)-methylation the hydroxyl group was partly formylated by HCO_2H . 2-Unsubstituted were obtained by deprotection of 2-(2-propoxycarbonyl), 2-(*tert*-butoxycarbonyl), and 2-acetyl derivatives by the treatment with TFA.

Reductive *N*(2)-cycloalkylation of 1,3,4,6,7,11*b*-hexahydro-2*H*-pyrazino[1,2-*a*]isoquinolin-4-one with 4-spiro derivatives of cyclohexanone in

dichloroethane in the presence of $\text{NaB}(\text{OAc})_3\text{H}$ at room temperature afforded mixtures of diastereomeric racemates in 47–70% yields (08EJO895). Acidic hydrolysis of 2-(2'-phenyl-2'-methoxy-2'-trifluoromethylacetyl)-1,3,4,5,6,11*b*-hexahydro-1*H*-pyrazino[1,2-*b*]isoquinolin-4-one in H_3PO_4 at 100 °C for 3.5 days afforded optically active 2-unsubstituted tricycle. Racemate and optically active enantiomers of 1,3,4,5,6,11*b*-hexahydro-2*H*-pyrazino[1,2-*b*]isoquinolin-4-one were *N*(2)-acylated with MeCO_2H at room temperature in CHCl_3 for 8 h and with different carboxylic acids in the presence of benzotriazol-1-yloxy-tripyrrolidinophosphonium hexafluorophosphate and *N*-methylmorpholine in DMF and DMSO at room temperature for 7–8.5 h. According to this protocol racemic 1,3,4,5,6,11*b*-hexahydro-2*H*-pyrazino[1,2-*b*]isoquinolin-4-one was *N*(2)-acylated with Mosher's acid [(*R*)- α -methoxy- α -(trifluoromethyl)phenylacetic acid], and the diastereomeric mixture of 2-acyl derivative was separated on a silica column with Et_2O as eluent. 1,3,4,5,6,11*b*-Hexahydro-2*H*-pyrazino[1,2-*b*]isoquinolin-4-one was reacted in position 2 with (1*S*,2*R*,5*S*)-menthyl (5*R*)-*p*-toluenesulfinate and (–)-menthyl chloroformate.

4.2.6 Reactivity of substituent attached to the ring carbon atom

Epimerization of *trans*-4(*R*),9*a*(*R*)-4-phenyl-8-benzyloxymethyl-3,4,9,9*a*-tetrahydro-1*H*,6*H*-pyrido[2,1-*c*][1,4]oxazin-1-one to *cis*-4(*R*),9*a*(*S*)-*H* derivative in 30% yield was achieved by treatment with KHMDS in THF at –78 °C, followed by the addition of HMPA and AcOH at same temperature and after 15 min stirring the reaction mixture was quenched with the saturated NH_4Cl solution (08JOC6877). A solution of *cis*-4(*R*),9*a*(*S*)- and *trans*-4(*R*),9*a*(*R*)-4-phenyl-8-benzyloxymethyl-3,4,9,9*a*-tetrahydro-1*H*,6*H*-pyrido[2,1-*c*][1,4]oxazin-1-ones in DMF containing HCO_2H and NEt_3 was added to a solution of allyl palladium chloride dimer and 2-di-*tert*-butylphosphino-2'-methylbiphenyl in DMF at 10 °C for 6 h and room temperature for 16 h under nitrogen afforded *cis*-4(*R*),9*a*(*S*)- and *trans*-4*H*,9*aH*-(4*R*,9*aR*)-4-methyleneperhydropyrido[2,1-*c*][1,4]oxazin-1-one, respectively.

Reaction of 4-aryl-7-iodoperhydropyrido[2,1-*c*][1,4]oxazin-6-ones (07USA2007/0117839, 08WOP2008/013213) and 7-iodo-6-oxo-4-(3,4,5-trifluorophenyl)perhydropyrido[2,1-*a*]pyrazine-2-carboxylate (07USA2007/0117839) with $\text{P}(\text{OEt})_3$ at 120 °C for 2 h afforded 7-phosphonic acid diethyl esters. 3-Hydroxy-6-arylperhydropyrido[2,1-*c*][1,4]oxazin-4-ones first were reacted with triphenylphosphonium bromide in refluxing MeCN, then with 3-methoxy-4-(4-methyl-1*H*-imidazol-1-yl)benzaldehyde at ambient temperature in the presence of NEt_3 to provide (*Z*)-3-{1-[3-methoxy-4-(4-methyl-1*H*-imidazol-1-yl)phenyl]methylidene} derivatives (07USA2007/0117798, 08USA2008/0207900).

7-[1-[3-Methoxy-4-(4-methyl-1*H*-imidazol-1-yl)phenyl]-(*E*)-methylidene] derivatives of 4-arylperhydropyrido[2,1-*c*][1,4]oxazin-6-ones (07USA2007/0117839, 08WOP2008/013213) and 6-oxo-4-(3,4,5-trifluorophenyl)perhydropyrido[1,2-*a*]pyrazine-2-carboxylate (07USA2007/0117839) were prepared from the respective 7-phosphonic acid diethyl esters by treatment with LiOH·H₂O and 3-methoxy-4-(4-methyl-1*H*-imidazol-1-yl)benzaldehyde in a mixture of THF and EtOH at ambient temperature. 7-[1-[3-Methoxy-4-(4-methyl-1*H*-imidazol-1-yl)phenyl]-(*E*)-methylidene]-4-phenylperhydropyrido[2,1-*c*][1,4]oxazin-6-one was also obtained by the treatment of 7-[1-[3-methoxy-4-(4-methyl-1*H*-imidazol-1-yl)phenyl]-1-hydroxymethyl] derivative with MeSO₃Cl and NEt₃ in CH₂Cl₂ at room temperature for 45 min, then with NaOMe in MeOH for 30 min (07USA2007/0117839). 7-[1-[3-Methoxy-4-(4-methyl-1*H*-imidazol-1-yl)phenyl]-1-hydroxymethyl] derivative was prepared from the 7-unsubstituted perhydro derivative with LDA in THF at 0 °C for 30 min, followed by the addition of 3-methoxy-4-(4-methyl-1*H*-imidazol-1-yl)benzaldehyde and stirring at 0 °C for 35 min.

1-Methoxy derivative was obtained from 1-hydroxy-4-(3,4,5-trifluorophenyl)perhydropyrido[2,1-*c*][1,4]oxazin-6-one by reacting with CH(OMe)₃ in the presence of (+)-10-camphosulfonic acid at ambient temperature. Reaction of 1-methoxy-4-(3,4,5-trifluorophenyl)perhydropyrido[2,1-*c*][1,4]oxazin-6-one with Et₃SiH in TFA at 70 °C for 15.5 h provided a mixture of *cis*- and *trans*-4*H*,9*aH*-4-(3,4,5-trifluorophenyl)perhydropyrido[2,1-*c*][1,4]oxazin-6-ones. The treatment of 1-hydroxy-4-(4-fluorophenyl)perhydropyrido[2,1-*c*][1,4]oxazin-6-one with Et₃SiH and CF₃SO₃SiMe₃ in CH₂Cl₂ at room temperature for 1.5 h, then at 60 °C for 2 h gave a mixture of *trans*-4*H*,9*aH*-4-(4-fluorophenyl)perhydropyrido[2,1-*c*][1,4]oxazin-6-one and 4-(4-fluorophenyl)-3,4,6,7,8,9-hexahydropyrido[2,1-*c*][1,4]oxazin-6-one (07USA2007/0117839).

The treatment of *cis*-7*H*,9*H*-*trans*-8*H*,9*H*-7,8,9-tri(pivaloyloxy)perhydropyrido[2,1-*c*][1,4]thiazine with NaOMe in MeOH at room temperature for 8 h gave 7,8,9-trihydroxy derivative (06EUP1657244). Heating 9-methoxy-2-(4-fluorophenyl)-3,4-dihydro-1*H*,8*H*-pyrido[1,2-*a*]pyrazine-1,8-diones in the HBr-AcOH solution (38%) at 100 °C overnight afforded 9-hydroxy derivatives (06WOP2006/066414).

Reaction of *cis*-6*H*,9*aH*-2-(*tert*-butoxycarbonyl)perhydropyrido[1,2-*a*]pyrazine-6-aldehyde with ylide, formed from (3-chlorobenzyl)(triphenyl)phosphonium bromide with BuLi, furnished 6-[(*E*)-2-(3-chlorophenyl)vinyl] derivative (07USA2007/037817). The treatment of *cis*-6*H*,9*aH*-2-(3-cyanopyrazin-2-yl)perhydropyrido[1,2-*a*]pyrazine-6-aldehyde with dimethyl (1-diazo-2-oxopropyl)phosphonate in the presence of K₂CO₃ in MeOH at ambient temperature for 1 h provided 6-ethynyl derivative (07USA2007/037816), which was reacted with 3-iodobenzonitrile in the presence of PdCl₂(PPh₄)₂, CuI, and Et₃N in THF under microwave

irradiation at 90 °C for 6 min to give 6-[(3-cyanophenyl)ethynyl] derivative in 73% yield (07USA2007/037817). Reaction of 6-formyl-2-(3-cyano-2-pyrazinyl)perhydropyrido[1,2-*a*]pyrazine with $\text{NH}_2\text{OH}\cdot\text{HCl}$ in the presence of NaOAc in EtOH at room temperature for 3 h gave 6-[(*E*)-(hydroxyimino)methyl] derivative, which was chlorinated with NCS to *N*-hydroxy-6-carboximidoyl chloride in DMF containing 2 *N* etheral solution of HCl at 60 °C for 40 min (07USA2007/037816). This *N*-hydroxy-6-carboximidoyl chloride derivative was reacted with 3-ethynylbenzonitrile in the presence of Et_3N at room temperature overnight to furnished 6-[5-(3-cyanophenyl)-3-isoxazoly] derivative in 5% yield. Reaction of 6-formyl-2-(3-cyanopyrazin-2-yl)perhydropyrido[1,2-*a*]pyrazine with Li salt of 1-chloro-3-ethynylbenzene gave 6-[3-(3-chlorophenyl)-1-hydroxy-2-propynyl] derivative. Its Swern oxidation provided the appropriate ketone, which was reacted with $\text{NH}_2\text{OH}\cdot\text{HCl}$ and Na_2CO_3 to yield 6-[5-(3-chlorophenyl)-3-isoxazoly]-2-(3-cyanopyrazin-2-yl)perhydropyrido[1,2-*a*]pyrazine. Reaction of 6-ethynyl-2-(3-cyano-2-pyrazinyl)perhydropyrido[1,2-*a*]pyrazine with 3-iodobenzonitrile, NaN_3 , $\text{CuSO}_4\cdot 7\text{H}_2\text{O}$, *L*-proline, *Na* ascorbate, Na_2CO_3 in the presence of H_2O in DMSO at 68 °C overnight, with *N*-hydroxy-2-pyridinecarboximidoyl chloride, and with 3-chloro-*N*-hydroxybenzenecarboximidoyl chloride in CH_2Cl_2 in the presence of Et_3N at room temperature overnight provided 6-[5-(3-cyanophenyl)-1,2,3-triazol-4-yl], 6-[5-(2-pyridyl)-3-isoxazoly] and 6-[5-(3-chlorophenyl)-3-isoxazoly] derivatives, respectively.

9-Hydroxy derivatives were obtained from a 9-benzyloxy-1,8-dioxo-1,2-dihydro-8*H*-pyrido[1,2-*a*]pyrazine-7-carboxamide and a 9-methoxy-1,2-dihydro-8*H*-pyrido[1,2-*a*]pyrazine-7-carboxamide by stirring in TFA at room temperature for 1.5 h and by heating in pyridinium hydrochloride at 180 °C for 5 min (06WOP2006/088173, 07WOP2007/049675). The treatment of a 4-hydroxy-1,2,3,4-tetrahydro-8*H*-pyrido[1,2-*a*]pyrazine-1,8-dione with methyl *N*-(triethylammoniumsulfonyl)carbamate in MeCN at 70 °C, and that of a 3-hydroxy-1,2,3,4-tetrahydro-8*H*-pyrido[1,2-*a*]pyrazine-1,8-dione with MeSO_2Cl in the presence of Et_3N in THF at room temperature gave 1,2-dihydro-8*H*-pyrido[1,2-*a*]pyrazine-1,8-dione derivatives.

Hydrolysis of methyl perhydropyrido[1,2-*a*]pyrazine-3-carboxylates with LiOH in aqueous MeOH gave 3-carboxylic acids, which were converted into amides by treatment amines in the presence of EDC , HOBt , and Hünig's base (08SL702).

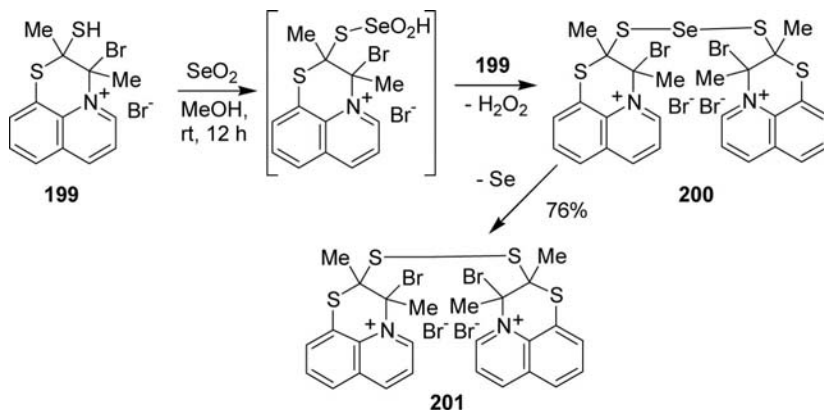
Reaction of ethyl 9,10-difluoro-7-oxo-2,3-dihydro-7*H*-pyrido[1,2,3-*de*]-1,4-benzothiazine-6-carboxylate with 1-methylpiperazine in the presence of K_2CO_3 in DMF at 80 °C for 4.5 h gave 10-(4-methylpiperazino)-5-carboxylate in 88% yield (08MI93). Acidic hydrolysis of this ester in aqueous AcOH containing HCl at 90 °C for 3 h afforded rifloxacin· HCl in 91% yield.

The bromo atom of (S)-8-bromo-9-fluoro-10-(1-aminocyclopropyl)-7-oxo-2,3-dihydro-7H-pyrido[1,2,3-de][1,4]benzoxazine-6-carboxylic acid was changed for amino groups by primary and secondary aliphatic amines and cyclopropylamine (06MIP1).

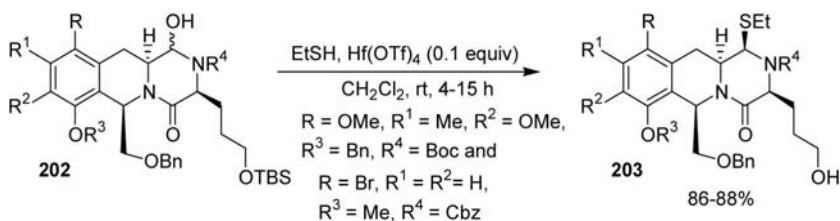
Enantioselective hydrolysis of ofloxacin's alkyl and 4-nitrophenyl esters was investigated by using *Yarrowia lipolytica* CL180 esterase (07AMB820, 07MIP3). 7-Oxo-2,3-dihydro-7H-pyrido[1,2,3-de][1,4]oxazine-6-carboxylic acids were prepared from their ethyl ester by acidic (05MIP2, 05MIP4, 05WOP2009/123746, 06SL963, 06WOP2006/048889, 07BML7274, 07WOP2007/106537, 08MI92, 09MIP2) and basic hydrolysis (07WOP2007/054296, 07WOP2007/106537, 09BML4933).

Levofloxacin hemihydrate was prepared by the hydrolysis of its ethyl ester in aqueous EtOH in the presence of NaOH (06WOP2006/070275) and crystallization of anhydrous levofloxacin from EtOH and acetone containing 2 v/v% of water [06JAP(K)2006/273718].

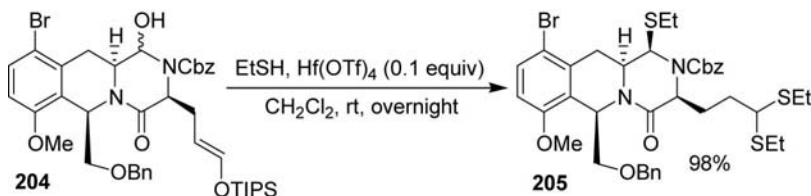
Dithioselenide **200** was formed in the reaction of **199** and SeO₂, which was stable only at 20 °C, and it was converted into disulfide **201** during work-up (06CHC1478).



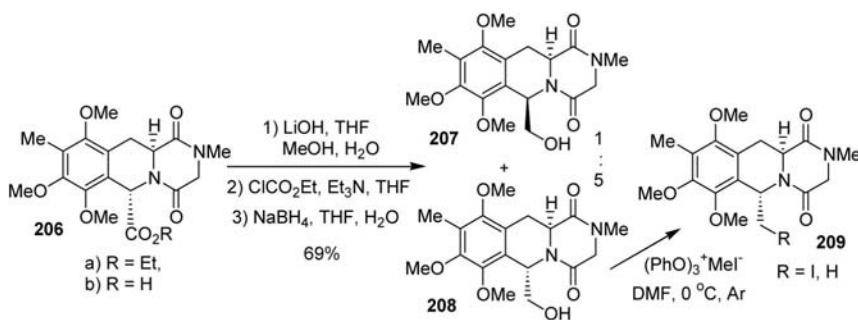
Phenolic hydroxyl groups were liberated from *tert*-butyldimethylsilyloxy groups present in position 7 and a side-chain phenyl group of 1,2,3,4,11,11a-hexahydro-6H-pyrazino[1,2-*b*]isoquinolin-4-one on the action of Bu₄NF in THF at 0 °C for 1 h (09T5709).



The treatment of an epimeric mixture of 1-hydroxy-1,2,3,4,11,11a-hexahydro-6*H*-pyrazino[1,2-*b*]isoquinolin-4-ones **202** with EtSH in the presence of $\text{Hf}(\text{OTf})_4$ gave 1-ethylthio derivatives **203** with concurrent removal of *O*-TBS group as a single isomer (08JA7148, 09JOC2046). Similar reaction of 1-hydroxy-1,2,3,4,11,11a-hexahydro-6*H*-pyrazino[1,2-*b*]isoquinolin-4-one **204** afforded 1-ethylthio derivative **205** (08JA7148).



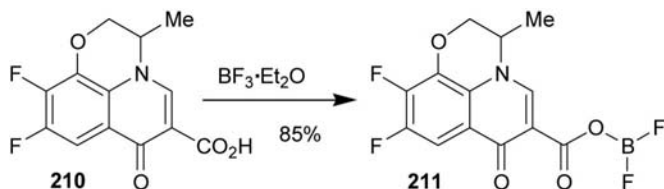
The amino group of 10-amino-2-cyclohexylcarbonyl-1,3,4,6,7,11*b*-hexahydro-2*H*-pyrazino[1,2-*b*]isoquinolin-4-one was acylated with AcCl in pyridine and rhodamine (07BML4154).



When ester **206** ($\text{R} = \text{Et}$) was hydrolyzed with 10% aqueous NaOH in EtOH gave 1:1 mixture of diastereomeric 6-acids **206** ($\text{R} = \text{H}$) in 65% yield [08H(75)1497]. Alternatively, hydrolysis with LiOH afforded a mixture of acid **206** ($\text{R} = \text{H}$). The major isomer was treated with ClCO_2Et to give a mixed anhydride, which was reduced with NaBH_4 to furnish 1:5 mixture alcohols **207** and **208**. The alcohol **208** was transformed into 6-iodomethyl derivative **209** ($\text{R} = \text{I}$) by treatment with $(\text{PhO})_3\text{P}^+\text{MeI}^-$ in 87% yield, which was catalytically hydrogenated over Pd/C catalyst in the presence of NaOAc in MeOH to yield 6-methyl derivative **209** ($\text{R} = \text{H}$) quantitatively.

9,10-Difluoro-3(*S*)-methyl-2,3-dihydro-7*H*-pyrido[1,2,3-*de*][1,4]benzoxazin-7-one was obtained in 28% yield by decarboxylation of levofloxacin using PPA (06MI64). Carboxy group of ofloxacin was reacted with silicagel functionalized with 3-chloropropyltrimethoxysilane (08MI94).

The carboxy group of levofloxacin was converted into 6-(2-benzothiazolyl) group with 2-aminophenol in PPA at 170–250 °C for 4 h in 51% yield (09JMC5649).



Reaction of 7-oxo-2,3-dihydro-7H-pyrido[1,2,3-*de*][1,4]benzoxazine-6-carboxylic acid **210** (07WOP2007/090579) and its (*S*) enantiomer (07WOP2007/141900, 09JAP(K)2009/198177, 09USA2009/0029980, 09USA2009/0156577) with $F_3B \cdot O_2Et$ gave mixed anhydride **211** and its (*S*) enantiomer. That of ethyl ester of (*S*) enantiomer of **210** (08JMC3238, 09MIP5), and its 3-fluoromethyl derivative (08JMC3238) with $B(OH)_3$ and $ZnCl_2$ in Ac_2O at 60 °C for 2 h gave **198** and its 3-fluoromethyl derivative in 88% and 83% yields, respectively.

Acid chlorides formed from ofloxacin and levofloxacin with $SOCl_2$ were reacted with 3'-azido-3'-deoxythymidine to give ester derivatives (09NNN89). Levofloxacin, through its acid chloride, was esterified with glycolic acid, and then the product was conjugated to L-Asp hexapeptide (08PR92). Levofloxacin was esterified with glycolic acid, which was conjugated to L-Asp hexapeptide. This conjugate selectively distributed to bone, reaching concentration up to 100-fold those of nonconjugated fluor-quinolones (08PR2881).

Reaction of coumarinoyl hydrazides **213** and 3-methyl-2,3-dihydro-7-oxo-7H-pyrido[1,2,3-*de*][1,4]benzoxazine-5-carboxylic chlorides **212** in the presence of H_2NSO_3H in DMF at 125 °C for 4–5 h, or under microwave irradiation for 4–5 min afforded 2,5-diaryl-1,3,4-oxadiazines **214** in excellent yields (09JHC289).



6-Carboxamides were prepared when suspensions of 8-nitro-9,10-difluoro-7-oxo-2,3-dihydro-7H-pyrido[1,2,3-*de*][1,4]benzoxazine-6-carboxylic acids were heated in boiling $SOCl_2$ for 2–3 h until clear solutions

were obtained. Upon completion of the reactions, SOCl_2 was removed under vacuo, the remaining solids were dissolved in dioxane, and the solutions were treated with conc. NH_4OH under cooling. The treatment of 8-amino-9,10-difluoro-7-oxo-2,3-dihydro-7H-pyrido[1,2,3-de][1,4]benzoxazine-6-carboxamides with POCl_3 in CH_2Cl_2 in the presence of Et_3N at 0°C for 5 h provided 6-carbonitriles (09WOP2009/035634). 8-Amino-6-cyano-9,10-difluoro-3(S)-methyl-2,3-dihydro-7H-pyrido[1,2,3-de][1,4]benzoxazin-7-one was reacted with NaN_3 in the presence of ZnCl_2 in a 1:1 mixture of H_2O and $i\text{PrOH}$ at 110°C for 18 h to provide 6-(1H-tetrazol-5-yl) derivative.

The oxidation of 9-fluoro-10-nitromethyl-7-oxo-2,3-dihydro-7H-pyrido[1,2,3-de][1,4]oxazine-6-carboxylates with KMnO_4 in the presence of NaB_4O_7 and KOH in aqueous MeOH at -5°C gave 10-formyl derivatives (07BMC7274). 10-Formyl derivatives were reacted with primary amines in boiling EtOH , then the formed Schiff bases were reduced with NaCNBH_3 to yield 10-(substituted amino)methyl derivatives. Reduction of 10-formyl derivatives with NaBH_4 in MeOH provided 10-hydroxymethyl derivatives, which were converted into 10-bromomethyl derivatives by treatment with PBr_3 in CH_2Cl_2 , and finally the 10-bromomethyl derivatives were reacted with amines in the presence of K_2CO_3 to give 10-aminomethyl derivatives.

The treatment of 3-(2-tetrahydropyranyloxymethyl)-9,10-difluoro-7-oxo-2,3-dihydro-7H-pyrido[1,2,3-de][1,4]benzoxazine-6-carboxylate with $p\text{TsOH}\cdot\text{H}_2\text{O}$ gave 3-hydroxymethyl derivative in 92% yield (06WOP2006/009143, 08JMC3238). The 3-hydroxymethyl derivative was converted to 3-fluoromethyl compound by treatment with DAST in boiling THF for 0.5 h in 65% yield (08JMC3238).

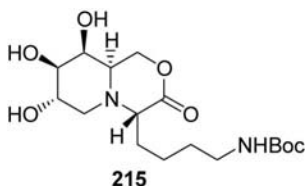
5-Oxo-2,3-dihydro-5H-pyrido[1,2,3-de][1,4]benzoxazine-3-carbaldehydes were reacted with *tert*-butyl piperidin-4-ylcarbamate, then the reaction mixture was treated with sodium triacetoxyborohydride to give 3-[4-(*tert*-butoxycarbonylamino)piperidin-1-yl)methyl derivatives (08WOP2008/120003). 8-Fluoro-3-oxo-2,3,6,7-tetrahydro-5H-pyrido[1,2,3-de][1,4]benzoxazin-7-carbaldehyde was similarly reacted with cyclic amines, then with (polystyrylmethyl)trimethylammonium cyanoborohydride in acidified MeOH (08WOP2008/116815).

4.2.7 Reactivity of substituent present in a side chain

The amino group of 3-(4-aminophenyl)perhydropyrido[2,1-c][1,4]oxazine was sulfonylated with 4- $i\text{PrPhSO}_2\text{Cl}$ in the presence of $i\text{Pr}_2\text{NEt}$ in MeCN at room temperature (08WOP2008/026046).

Reaction of 4-phenyl-9-hydroxymethylperhydropyrido[2,1-c][1,4]oxazin-1-ol and TBDMSCl in the presence of imidazole in CH_2Cl_2 at room temperature for 24 h gave 9-(*tert*-butyl,dimethylsilyloxy)methyl derivative (2007LOC4).

4-Methyl-1*H*-imidazol-1-yl group, present in a side chain of perhydropyrido[2,1-*c*][1,4]oxazin-6-one skeleton was quaternized by reacting with chloromethyl di-*tert*-butyl phosphate in the presence of NaI and Hünig's base in DME at 80 °C for 2 h, followed by treatment TFA in CHCl₃ to give methylphosphonic acid derivative (08WOP2008/013213).



A side-chain NH-Boc group of perhydropyrido[2,1-*c*][1,4]oxazin-3-one **215** was changed for a NH-dansyl group by treatment first in a 30:1 mixture of MeOH and AcCl at room temperature for 20 h, then the residue of the evaporated reaction mixture was dissolved in DMF and was reacted with dansyl chloride in the presence of NEt₃ at room temperature for 4 h (08BMC10216).

Trans-7*H*,9*aH*-2-*tert*-butoxycarbonyl-7-hydroxymethylperhydropyrido[1,2-*a*]pyrazine was *O*-alkylated with 1-(3-chloropropyl)piperidine in the presence of NaO^{*t*}Bu in THF at 50 °C for 45 min (05USA2005/0282811).

6-(4-Hydroxy-2,3-dimethylphenyl)perhydropyrido[1,2-*a*]pyrazines were prepared from 6-(4-methoxy- and 4-allyloxy-2,3-dimethylphenyl)perhydropyrido[1,2-*a*]pyrazines by the treatment ethereal solution of HCl in CH₂Cl₂ for 10 min, then with BBr₃ at –70 °C for 20 min and the reaction mixtures were allowed to warm at room temperature for 18 h, and by treatment with morpholine and (PPh₃)₄Pd in CH₂Cl₂ at ambient temperature for 1 h, respectively (06USA2006/0009456). The phenolic 4-hydroxyl group was *O*-alkylated with 2-bromoethyl methyl ether, (2-bromoethoxy)-*tert*-butyldimethylsilane, (*S*)- and (*R*)-2-(*tert*-butyl-dimethylsilyloxy)propyl *p*-toluenesulfonates, chloroacetone, 3-chloropropyl iodide, 1,4-dibromobutane, and *N*-(3-bromopropyl)phthalimide. From a side-chain TBDMSO-group hydroxyl group was liberated by the treatment with Bu₄NF. Reaction of a side-chain oxo group with NH₂OH·HCl in the presence of NaOAc gave oxime derivative. A side-chain chloro atom was replaced by the morpholino group, and a side-chain bromo atom by a dimethylamino group. The treatment of a side-chain phthalimido group with N₂H₄·H₂O provided an amino group, which was *N*-acylated with MeCOCl.

The hydroxy group of 7-hydroxymethyl-2-(2,3-dichlorophenyl)perhydropyrido[1,2-*a*]pyrazine was mesylated, which was reacted with Bu₄NCN to give 7-cyanomethyl derivative (06BMC5898). Its reduction

with LiAlH_4 furnished 7-aminoethyl derivative, and the amino group was acylated with benzo[b]thiophene-2-carboxylic acid in the presence of TBTU.

The hydroxy group of a 8-(3-hydroxyphenyl)perhydropyrido[1,2-*a*]pyrazine was reacted with $\text{PhN}(\text{SO}_2\text{CF}_3)_2$ in the presence of Et_3N in CH_2Cl_2 , and the 8-(3-trifluoromethylsulfonyloxyphenyl) derivative was treated with HCO_2H in the presence of Et_3N , PPh_3 , and $\text{Pd}(\text{OAc})_2$ in DMF, furthermore with CO in the presence of Et_3N , dppf, MeOH, and $\text{Pd}(\text{OAc})_2$ in DMSO to give 8-phenyl and 8-(3-methoxycarbonylphenyl) derivatives, respectively (06JMC7290, 07WOP2007/050802, 09USP7538110). The ester group was hydrolyzed, and then the carboxyl group was converted to carboxamide group by treatment with NH_4Cl , TBTU, and Et_3N , in DMF. 2-(Carboxymethyl and 2-carboxyethyl)perhydropyrido[1,2-*a*]pyrazines were obtained from their *tert*-butyl esters by treatment with the 1 N solution of HCl in Et_2O in dioxane at room temperature for 2 days.

The amino group of 2-(4-aminophenyl)perhydropyrido[1,2-*a*]pyrazine was arylated with 4-chloro-2,3-dimethylquinoline (06JMC6351).

A side-chain carboxylate group of perhydropyrido[1,2-*a*]pyrazines was reacted with pyrazole-3-amines in the presence of Me_3Al in MePh to give the corresponding amides (08WOP2008/075068).

2-(1*H*-Indol-6-yl)perhydropyrido[1,2-*a*]pyrazine was obtained from 2-(1-triisopropyl)-1*H*-indol-6-yl) derivative by treatment with KF in MeOH at room temperature for 4 h in 60% yield (08WOP2008/101247).

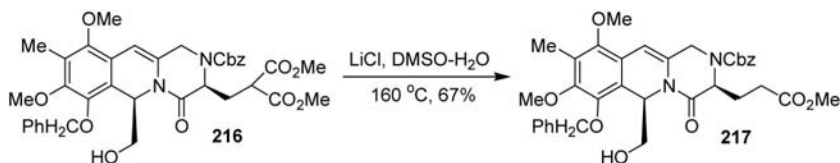
3-Aminomethyl derivatives were obtained from 3-hydroxymethyl-6,6*a*,7,8,9,10-hexahydro-5*H*-pyrido[1,2-*a*]quinoxalin-6-one with secondary amines under standard Mitsunobu conditions using PPh_3 and di-*tert*-butyl azodicarboxylate in THF (08USA2008/0161292, 09BML4050). 3-Pyrrolidin-1-ylmethyl derivative was also prepared with pyrrolidine from 3-methanesulfonyloxymethyl derivative, obtained in the reaction of 3-hydroxymethyl derivative and MeSO_2Cl (08USA2008/0161292). Conversion of the alcohol to the amines via bromide was unsuccessfully due to the instability of the bromide (09BML4050).

A side-chain amino group in a 2,3,4,4*a*,5,6-hexahydro-1*H*-pyrazino[1,2-*a*]quinoline skeleton was liberated from *tert*-butoxycarbonylamino group by the treatment with 4 N HCl in dioxane at ambient temperature for 4 h, and was acylated with aromatic carboxylic acids in the presence of 1-(3-dimethylaminopropyl)-3-ethylcarbodiimide hydrochloride, 1-hydroxybenzotriazole hydrate, and Hünig's base at room temperature in CH_2Cl_2 (06BML443). The amino group was liberated from phthalimido group of 3-[4-(phthalimido)butyl]-10-methoxy-2,3,4,4*a*,5,6-hexahydro-1*H*-pyrazino[1,2-*a*]quinoline by treatment with $\text{H}_2\text{NNH}_2 \cdot \text{H}_2\text{O}$ in boiling EtOH, and then amino group was acylated with different acyl chloride (07MIP2). Reaction of 3-(2,3,4,4*a*,5,6-hexahydro-1*H*-pyrazino[1,2-*a*]quinolin-3-yl)propylamine

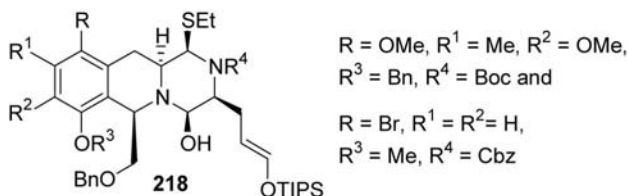
with *cis*-1,2,3,6-tetrahydrophthalimide in boiling MePh provided 2-[3-(2,3,4,4a,5,6-hexahydro-1*H*-pyrazino[1,2-*a*]quinolin-3-yl)propyl]-3a,4,7,7a-tetrahydroisindole-1,3-dione (05WOP2005/118591).

The treatment of a *tert*-butoxycarbonylamino group present in a side chain of 6,7-dihydro-3*H*,5*H*-pyrido[1,2,3-*de*]quinoxalin-3-one with 4 N HCl in a dioxane liberated amino group, which was reductively alkylated using heteroaromatic aldehydes followed by the treatment of the formed Schiff bases with NaB(OAc)₃H (08WOP2008/003690).

Hydrolysis of methyl 9-chloro-2,3-dione-2,3,6,7-tetrahydro-1*H*,5*H*-pyrido[1,2,3-*de*]quinoxalin-5-ylacetate gave acetic acid derivative, which was converted into an acetamide derivative by using ^tBuCOCl in the presence of Et₃N in CH₂Cl₂, followed by the treatment with an aniline derivative (06CTM733). A ^tBuO₂CNHCH₂ group, present in a side chain of 2,3,6,7-tetrahydro-1*H*,5*H*-pyrido[1,2,3-*de*]quinoxaline-2,3-dione skeleton, was treated with MeCO₂H containing 6 N HCl to yield a H₂NCH₂ derivative.



Krapcho decarbomethoxylation of diester **216** provided monoester **217** (06SL1691). Chemoselective Swern oxidation of 3-(3-hydroxypropyl)-1,2,3,4,11,11*a*-hexahydro-6*H*-pyrazino[1,2-*b*]isoquinolin-4-ones **203** followed by silyl enol ether formation with TIPSOTf and Et₃N in Et₂O for 12 h at room temperature gave compounds **218** as a single isomer in excellent yields (08JA7148, 09JOC2046).



N-Desmethyl-levofloxacin was *N*-alkylated with 3-bromo-2,5-dihydro-4*H*-1-benzopyran-4-one oxime (09AP405) and a mesylate (06MI65).

Alkylation of the *N*(4)-atom of 10-piperazino group of *N*-desmethyl-levofloxacin was carried out with phenacyl halogenides, phenacyl halogenides oxime, and their *O*-benzyl derivatives in DMF in the presence of NaHCO_3 at room temperature yielded antibacterial compounds, somewhat less active than levofloxacin (07EJM985). *N*-Desmethyl-levofloxacin was *N*-arylated with 2-chloro-5-(nitroaryl)-1,3,4-thiadiazoles in boiling EtOH in the presence of NaHCO_3 (06AP621). The piperazino group, in the presence, in position, 10 of 7-oxo-2,3-dihydro-7*H*-pyrido[1,2,3-*de*][1,4]benzoxazine skeleton, was *N*-alkylated with 2-(substituted phenyl)ethyl mesylates (07MIP4), 10-[2-(4-Substituted phenyl)ethyl]- (07MIP5) and -(1-oxoethyl)piperazinyl derivatives (07MIP6) were prepared from 10-(piperazin-1-yl)-9-fluoro-7-oxo-2,3-dihydro-7*H*-pyrido[1,2,3-*de*][1,4]oxazine-6-carboxylic acids by *N*(4)-alkylation and acylation, respectively. *N*-Desmethyl ofloxacin was reacted with aroyl chlorides and substituted benzenesulfonyl chlorides in the presence of K_2CO_3 and KI in DMF at 80 °C (09JCTAS374). Resin-bound oligonucleotides were *N*-acylated with levofloxacin in the presence of HATU, HOAt, and Hünig's base in DMF, then *N*-acylated oligonucleotides were cleaved from resin (07JCO306).

Nitration of 6-(benzothiazol-2-yl)-10-(4-methylpiperazin-1-yl)-9-fluoro-3(*S*)-methyl-2,3-dihydro-7*H*-pyrido[1,2,3-*de*][1,4]benzoxazin-7-one with conc. HNO_3 in conc. H_2SO_4 gave 6-(6-nitrobenzothiazol-2-yl) derivative (09JMC5649).

Heating ofloxacin in CH_2Cl_2 at reflux for 72 h led to the formation of 4-chloromethyl-4-methylpiperazinium chloride derivative, which was characterized by ^1H -NMR spectroscopy (08ASJC5573). Reaction of MeI with ofloxacin gave quaternary salt **175** (08MI91).

A side-chain *tert*-butoxycarbonylamino group present on a 7-oxo-2,3-dihydro-7*H*-pyrido[1,2,3-*de*][1,4]oxazine skeleton was hydrolyzed into an amino group by treatment with an HCl solution (06WOP2006/050943, 06WOP2006/123792, 08WOP2008/082009). The amino group present in side chain attached to 2,3-dihydro-5*H*-pyrido[1,2,3-*de*][1,4]benzoxazin-5-ones (08WOP2008/120003, 08WOP2008/128953) and in a 7-side-chain of 2,3,6,7-tetrahydro-5*H*-pyrido[1,2,3-*de*][1,4]benzoxazin-3-ones (08WOP2008/116815) was liberated from NHCO_2^tBu and $\text{NHCO}_2\text{CH}_2\text{Ph}$ groups by acidic hydrolysis (08WOP2008/116815, 08WOP2008/128953) and catalytic hydrogenation over 10% Pd/C catalyst (08WOP2008/116815, 08WOP2008/128953), respectively. The amino group present in a 10-side-chain of a 2,3-dihydro-7-oxo-5*H*-pyrido[1,2,3-*de*][1,4]benzoxazine-6-carboxylic acid was liberated from an acetamido group by the treatment with an NaOH solution (05MIP2) and an 1,3-dioxo-1,3-dihydroisoindol-2-yl group by treatment with 10% aqueous HCl (09USA2009/0156577). Amino groups were reacted with

2,3-dihydro[1,4]dioxino[2,3-*c*]pyridine-7-carboxaldehyde (08WOP2008/116815, 08WOP2008/120003, 08WOP2008/128953), with 3-oxo-3,4-dihydro-2*H*-pyrido[3,2-*b*][1,4]oxazine-6-carboxaldehyde, with 3-oxo-3,4-dihydro-2*H*-pyrido[3,2-*b*][1,4]thiazine-6-carboxaldehyde (08WOP2008/116815), and the formed Sciff bases were reduced with sodium triacetoxymethylborohydride in CH_2Cl_2 and with (polystyrylmethyl)trimethylammonium cyanoborohydride in acidified MeOH. 2(*E*)-3-[3(*R*)-({4-[(2,3-Dihydro[1,4]dioxino[2,3-*c*]pyridin-7-ylmethyl)amino]-1-piperidinyl)methyl}-10-fluoro-5-oxo-2,3-dihydro-5*H*-pyrido[1,2,3-*de*][1,4]benzoxazin-8-yl)-2-propenoic acid was obtained from the ethyl ester by alkali hydrolysis (08WOP2008/128953). A side-chain amino group, present in the position 10 of 7-oxo-2,3-dihydro-7*H*-pyrido[1,2,3-*de*][1,4]benzoxazine-6-carboxylic acid, was liberated from a phthalimido moiety by treatment with H_2NNH_2 in boiling MeOH (09USA2009/0029980). Treatment of 9-fluoro-10-[(*p*-methoxyphenyl)methyl]amino-7-oxo-3-methyl-2,3-dihydro-7*H*-pyrido[1,2,3-*de*][1,4]oxazine-6-carboxylic acid with 30% solution of TFA in CH_2Cl_2 at room temperature for 5 h afforded 10-amino derivative, which was then *N*-alkylated with {4-[(phenylaminocarbonyl)amino]phenyl)methyl chloride in the presence of NaHCO_3 in HMPA at 130 °C for 24 h in 90% yield (08EJM2453). Reaction of an amino group, present in a side chain of a 7-oxo-2,3-dihydro-7*H*-pyrido[1,2,3-*de*][1,4]benzoxazine-6-carboxylic acid with an ethylene derivative in the presence of NEt_3 in DMSO at 80 °C for 16 h yielded (2-substituted ethyl)amino derivative (06WOP2006/050943).

The hydroxy group of 3(*R*)-hydroxymethyl-2,3-dihydro-5*H*-pyrido[1,2,3-*de*][1,4]benzoxazin-5-ones was sulfonylated with MeSO_2Cl in the presence of Et_3N in CH_2Cl_2 then the mesyloxy group was substituted with cyclic amines in MeCN at 60–70 °C in the presence of a base (pyridine, K_2CO_3) (08WOP2008/128953). Reaction of 2-(mesyloxymethyl)-2,3-dihydro-5*H*-pyrido[1,2,3-*de*][1,4]benzoxazin-5-ones with NaN_3 in DMF at 70 °C for 20 h yielded 3-azidomethyl derivatives. The azido group was treated with PPh_3 and H_2O in THF at 60 °C for 2 h to give 3-aminomethyl derivatives, which were alkylated with 6-(5(*S*)-iodomethyl-2-oxo-oxazolidin-3-yl)-4*H*-benzo[1,4]thiazin-3-one in DMSO in the presence of Hünig's base at 70 °C (09WOP2009/104147).

9-Fluoro-10-(piperazin-1-yl)-7-oxo-2,3-dihydro-7*H*-pyrido[1,2,3-*de*][1,4]benzoxazine-6-carboxylic acids and esters were reacted with NaNO_2 in aqueous AcOH at room temperature for 4.5 h to give 10-(4-nitrosopiperazin-1-yl) derivatives, which were reduced with activated Zn to yield 10-(4-aminopiperazin-1-yl) derivatives (09WOP2009/064836).

Phase transfer alkylation of cyanomethyl group of 10-cyanomethyl-9-fluoro-3(*S*)-methyl-7-oxo-2,3-dihydro-7*H*-pyrido[1,2,3-*de*][1,4]oxazine-6-carboxylic acid with 1,2-dibromoethane in the presence of $(\text{PhCH}_2)\text{Et}_3\text{NBr}$

and NaOH provided 10-(1-cyanocycloprop-1-yl) derivative in 90% yield. The cyano group was hydrolyzed under acidic condition to a carboxamide (04MI4, 05MI36, 07MI69), and its Hofmann rearrangement using NaOCl in an aqueous NaOH solution gave pazufloxacin in 76% yield (04MI4, 05MI36, 07MI69,70).

Reaction of potassium 9-fluoro-3-methyl-10-(4-methylpiperazin-1-yl)-2,3-dihydro-7H-pyrido[1,2,3-de][1,4]benzoxazine-6-carboxylate with 2-[3-(2,4-dichlorophenoxy)propyl]-3-[(2-chloroacetyl)amino]quinoxalin-4(3H)-one gave ester derivative of 2,3-dihydro-7H-pyrido[1,2,3-de][1,4]benzoxazine-6-carboxylic acid. 3-Amino-2-(aryloxymethyl)quinoxalin-4(3H)-ones were *N*-acylated with 9-fluoro-3-methyl-10-(4-methylpiperazin-1-yl)-2,3-dihydro-7H-pyrido[1,2,3-de][1,4]benzoxazine-6-carboxylic acid chloride in the presence of K_2CO_3 in boiling benzene for 6 h (07MI71).

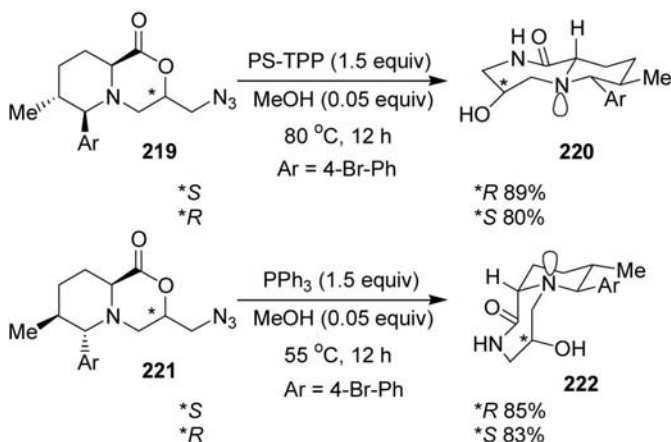
8-Amino-7-oxo-2,3-dihydro-7H-pyrido[1,2,3-de][1,4]oxazine-6-carboxylic acids were obtained from 8-(4-methoxyphenyl)amino derivatives by treatment with TFA at room temperature in CH_2Cl_2 , and 8-amino-3-esters from 8-benzylamino- and 8-nitro-3-ester derivatives by catalytic hydrogenation over Pd/C catalyst in acidified EtOH and DMF in 60% and 87% yields, respectively (07WOP2007/106537). The nitro group of 8-nitro-9,10-difluoro-3(S)-methyl-7-oxo-2,3-dihydro-7H-pyrido[1,2,3-de][1,4]oxazine-6-carboxylic amide was reduced with $Na_2S_2O_4$ in a suspension in boiling aqueous EtOH for 5–8 h.

6-Carboxamides were prepared when suspensions of 8-nitro-9,10-difluoro-7-oxo-2,3-dihydro-7H-pyrido[1,2,3-de][1,4]benzoxazine-6-carboxylic acids were heated in boiling $SOCl_2$ for 2–3 h until clear solutions were obtained. Upon completion of the reactions, $SOCl_2$ was removed under vacuo, and the remaining solids were dissolved in dioxane, and the solutions were treated with conc. NH_4OH under cooling. The treatment of 8-amino-9,10-difluoro-7-oxo-2,3-dihydro-7H-pyrido[1,2,3-de][1,4]benzoxazine-6-carboxamides with $POCl_3$ in CH_2Cl_2 in the presence of Et_3N at 0 °C for 5 h provided 6-carbonitriles (09WOP2009/035634).

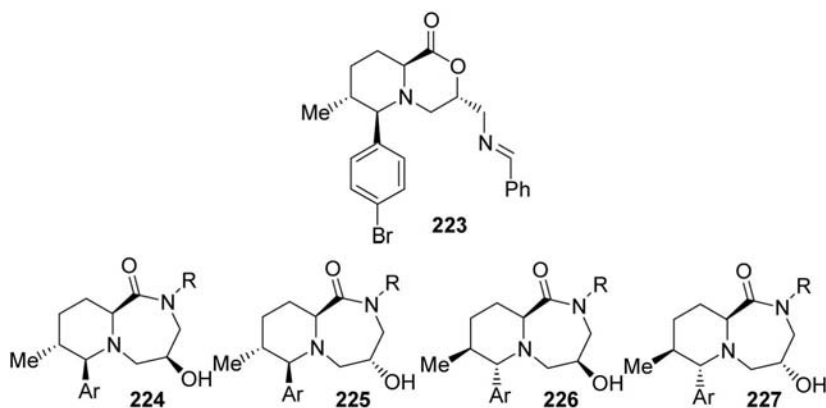
For some more examples see Section 4.3.5.

4.2.8 Rearrangement, ring transformation

The treatment of 6(S)-(iodomethyl)-4(R)-phenyl-1(R)-(trifluoromethyl)-3,4,7,8-tetrahydro-1H,6H-pyrido[2,1-c][1,4]oxazin-1-ol with NaH and I_2 under microwave irradiation in $CHCl_3$ gave 6(S)-(iodomethyl)-4(R)-phenyl-9a-(trifluoromethyl)-9-iodoperhydropyrido[2,1-c][1,4]oxazin-1-one in 90% yield (08OL605).

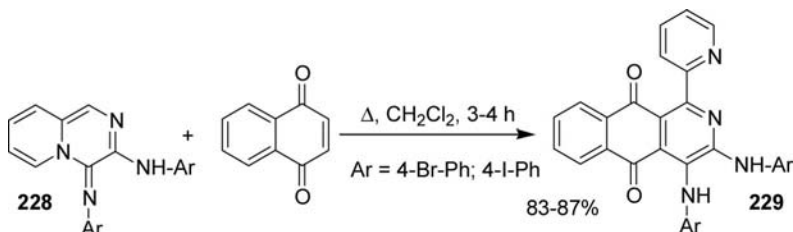


The treatment of *cis*-6*H*,9*aH*-3-azidoperhydropyrido[2,1-*c*][1,4]oxazin-1-ones **219** with polystyryl triphenylphosphine (PS-TPP) in a sealed tube gave ring expansion products **220** (07OL1529). At temperature exceeding 60 °C, *trans*-6*H*,9*aH*-3-azidoperhydropyrido[2,1-*c*][1,4]oxazin-1-ones **221** epimerized at C9*a* to yield enantiomers of **220**. Below this temperature with Ph₃P (instead of PS-TPP) complete conversion of **221** occurred to pyridodiazepinones **222** without epimerization. When **219** and **221** were reacted first with aromatic aldehydes in the presence of Ph₃P in a sealed tube at 55 °C for 20 h, the isolated crude imine derivatives were formed, for example, **223**, were treated with NaBH₄ or NaBH₃CN in MeOH or THF at 10 °C for 12 h to provided *N*-substituted pyridodiazepinones **224**–**227** in 50–98% yields.

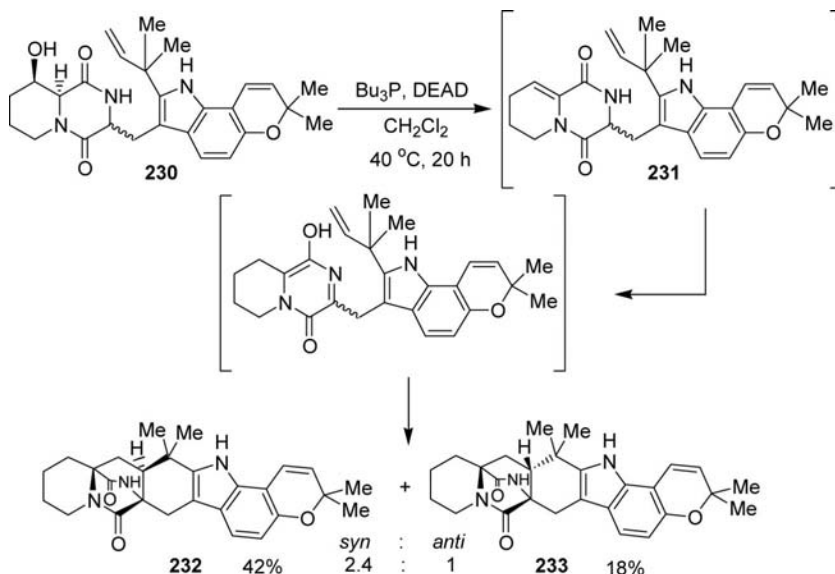


R = PhCH₂, 3-NO₂-PhCH₂, 4-Cl-PhCH₂, cyclohexylCH₂; Ar = 4-Br-Ph, 3-Br-Ph.

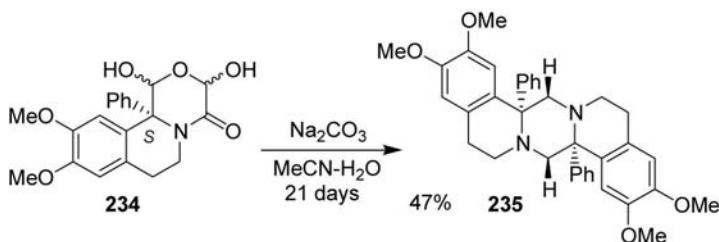
Reaction of 3-arylmino-4-arylimino-4*H*-pyrido[1,2-*a*]pyrazines **228** and 1,4-naphthoquinone gave tricyclic derivatives **229** [05ZN(B)771].



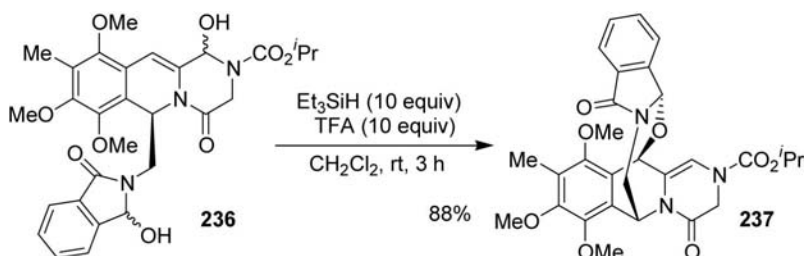
The Mitsunobu reaction of perhydropyrido[1,2-*a*]pyrazine-1,4-dione **230** at ambient temperature gave dehydrated product **231** in 15% yield. When the reaction was carried out with excess PBU_3 and diethyl azodicarboxylate at 40 °C the incipient **231** spontaneously underwent enolization and tautomerization, [4+2] aza-Diels–Alder reaction to provide a 2.4:1 mixture of diastereomers **232** and **233** (07T6124). No reaction occurred when isolated **231** was treated under similar conditions.



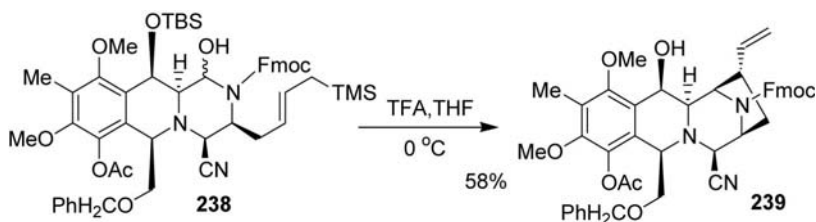
In the presence of Na_2CO_3 in aqueous MeCN a very slow hydrolysis of the diastereomeric mixtures of cyclic hemiacetal **234** proceeded to give pentacyclic derivative **235** (08T2321).



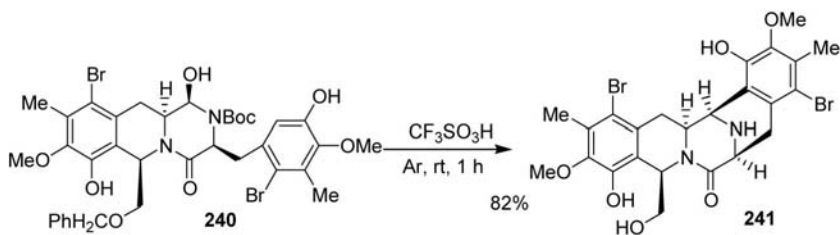
The treatment of a diastereomeric mixture of 1-hydroxy-1,2,3,4-tetrahydro-6*H*-pyrazino[1,2-*b*]isoquinolin-4-one **236** with Et_3SiH and TFA gave pentacyclic derivative **237** (08BMC9065).



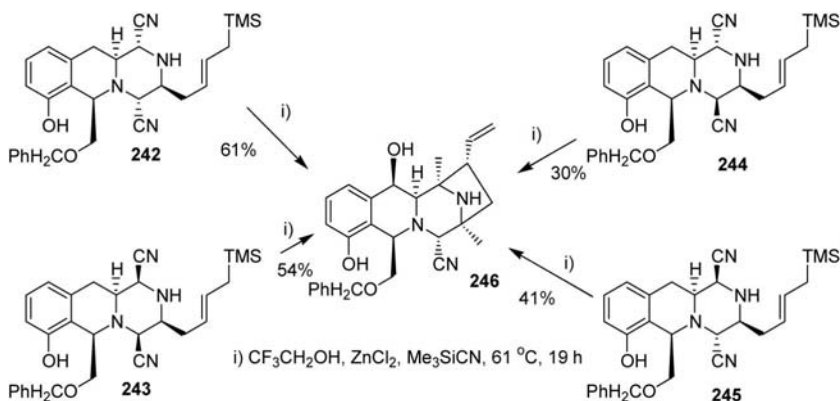
The treatment of tricycle **238** with TFA in THF triggered a cascade reaction, which led to the formation of tetracycle **239**, an intermediate of (–)-lemonomycin alkaloid (08SL2443).



Intramolecular Pictet–Spengler reaction of hemiacetal **240** on the action of $\text{CF}_3\text{SO}_3\text{H}$ provided the pentacyclic compound **241** (09T5709). Cyclization did not occur when HCO_2H , AcOH , MeSO_3H , or $\text{BF}_3\cdot\text{OEt}_2$ was applied.



Cyclization of diastereomers **242–245** into the tetracyclic product **246** occurred in $\text{CF}_3\text{CH}_2\text{OH}$ in the presence of ZnCl_2 and Me_3SiCN at 61°C for 19 h at different rates and with different efficiencies (05JA16796).

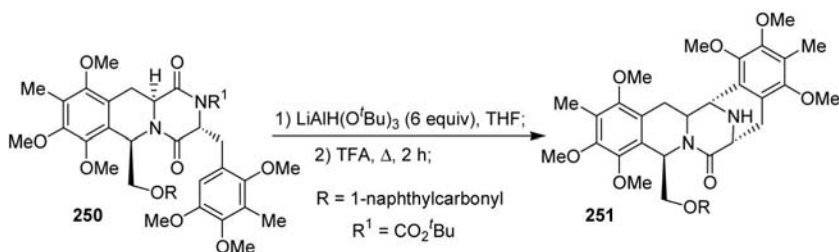


Reduction of tetrahydro-1*H*-pyrazino[1,2-*b*]isoquinolin-4-one **217** with $\text{LiAlH}_4(\text{OEt})$ in Et_2O at 0°C gave tetracyclic compound **247** in 44% yield (06SL1691). The intramolecular Mannich reaction of 1-ethylthio derivatives **218** in the presence of AgBF_4 in THF for 6–8 h at ambient temperature afforded tetracyclic aldehydes **248** in good yield (08JA7148, 09JOC2046).



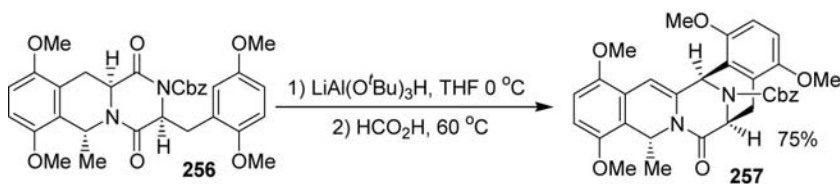
When 1-hydroxy-1,2,3,4,11,11a-hexahydro-6*H*-pyrazino[1,2-*b*]isoquinolin-4-one **202** ($R = \text{Br}$, $R^1 = R^2 = \text{H}$, $R^3 = \text{Me}$, $R^4 = \text{Cbz}$) was treated with PhSH , instead of EtSH as a nucleophile, tetracyclic compound **249** was formed under the same conditions (08JA7148).

Reduction of 1,2,3,4,11,11a-hexahydro-6*H*-pyrazino[1,2-*b*]isoquinoline-1,4-dione **250** ($R = \text{cinnamoyl}$, $R^1 = \text{CO}_2^t\text{Bu}$) with $\text{LiAlH}(\text{O}^t\text{Bu})_3$ (6 equiv.), and followed by treatment of the reaction mixture with boiling TFA gave a mixture of tricyclic **250** ($R = \text{cinnamoyl}$, $R^1 = \text{H}$) and pentacyclic compounds **251** (09T2201).



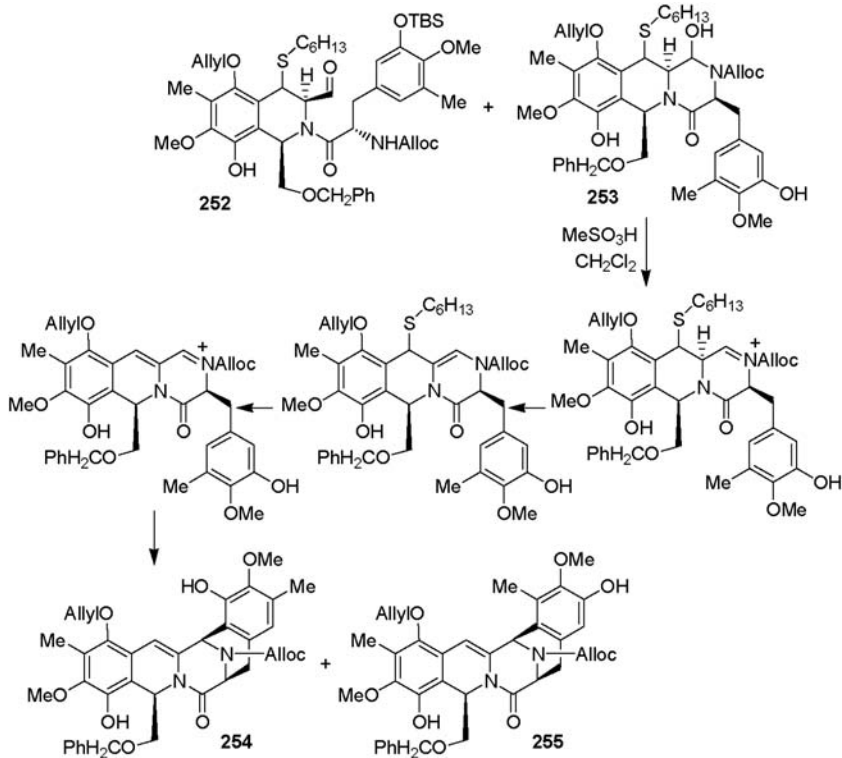
The treatment of a mixture of tetrahydroisoquinoline-3-aldehyde **252** and tricyclic pyrazino[1,2-*b*]isoquinolin-4-one **253** with MeSO_3H lead to an efficient domino process with the formation of a mixture of pentacyclic compounds **254** and **255** (Scheme 5) (07AGE3962).

Selective reduction of 1-oxo group of compound **256** with $\text{LiAl}(\text{O}^t\text{Bu})_3\text{H}$, followed by heating in HCO_2H gave pentacyclic compound **257** (07T8781).



4.2.9 Miscellaneous

Enantiomers of 4-(4-fluorophenyl)-7(*E*)-{[3-methoxy-4-(4-methyl-1*H*-imidazol-1-yl)phenyl]methylene}-3,4,6,7,8,9-hexahydro-, and *cis*- and *trans*-4*H*,9*aH*-4-aryl-7(*E*)-{[3-methoxy-4-(4-methyl-1*H*-imidazol-1-yl)phenyl]methylene}perhydropyrido[2,1-*c*][1,4]oxazin-6-ones, furthermore ethyl *cis*- and *trans*-4*H*,9*aH*-6-oxo-4-(3,4,5-trifluorophenyl)-7(*E*)-{[3-methoxy-4-(4-methyl-1*H*-imidazol-1-yl)phenyl]methylene}perhydropyrido[1,2-*a*]



Scheme 5

pyrazine-2-carboxylates were separated by means of chiral HPLC (07USA2007/0117839).

Rufloxacin phototoxicity on yeast was evaluated by measuring DNA fragmentation using single-cell gel electrophoresis assay (07PPS181). DNA-photosensitization by rufloxacin and ofloxacin was investigated (06PAC2277). Process control was important for the crystallization of rufloxacin aspartate to improve crystal quality (06MI66).

Biotransformation of praziquantel was investigated by using human cytochrome P450 3A4 isoenzyme (06MI67).

Resolution of racemic 1,3,4,6,7,11*b*-hexahydro-2*H*-pyrazino[1,2-*a*]isoquinolin-4-one into enantiomers was unsuccessful either through the crystallization of diastereomeric chiral salts prepared from enantiopure acids in different solvent mixtures, or with kinetic resolution by an enzymatic acylation using different enzymes (08EJO895).

Hydrates of levofloxacin hydrochloride were prepared from levofloxacin in the presence or absence of antisolvent (09MIP6). Levofloxacin

aspartate was prepared from levofloxacin and aspartic acid (06MIP3). Pazufloxacin mesylate was prepared from pazufloxacin and MeSO_3H in acetone (09MIP7).

UV light-induced photodegradation of liposome-encapsulated ofloxacin was investigated [08JPH(A)268]. Photostability of ofloxacin was investigated besides other drugs [09JPH(B)57]. Degradation of ofloxacin in wastewater was investigated by microwave irradiations (04CTA35) and its photocatalytic one by using polycrystalline TiO_2 and a nanofiltration membrane reactor (06CTO205). Decomposition characteristics of levofloxacin by ozonation were investigated (07MI72).

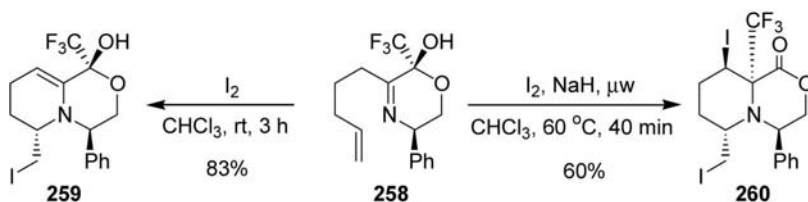
Metal complexes (Ag^+ , V^{3+}) of ofloxacin were synthesized and characterized (07JIC1205). Platina complexes with general formula $[\text{PtCl}_2\text{L}]$ (09ICA2060), and copper(II) complexes with $[\text{CuL}(\text{phen})\text{H}_2\text{O}]\text{NO}_3 \cdot 2\text{H}_2\text{O}$ (pen = 1,10-phenanthridine) (08ZNK766) were formed from ofloxacin and levofloxacin (L). $[\text{Cu}(\text{ofloxacin})_2 \cdot \text{H}_2\text{O}] \cdot 2\text{H}_2\text{O}$ (08JCR2961) and $[\text{Zn}(\text{ofloxacin})_2 \cdot \text{H}_2\text{O}] \cdot 2\text{H}_2\text{O}$ (09JCR1313) complexes were formed in the hydrothermal reaction.

4.3 Synthesis

4.3.1 By the formation of one bond α to the bridgehead nitrogen atom [6+0(α)]

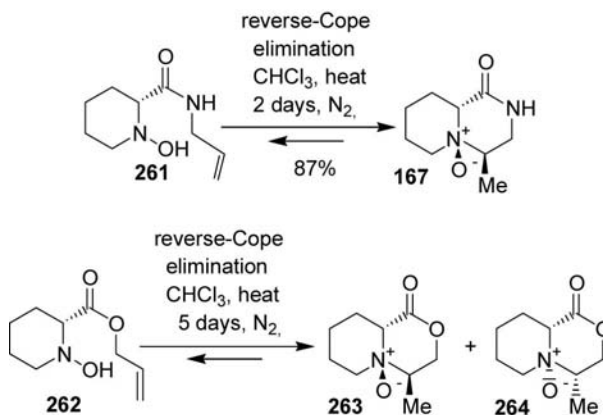
Optically active 4-phenylperhydropyrido[2,1-c][1,4]oxazin-1-ones were prepared by the cyclization of 3-(4-iodobutyl)-5-phenylmorpholin-2-ones on the action of Hünig's base in refluxing CH_2Cl_2 for 6 h (05TA3858).

Iodoamination of 1,4-oxazine **258** with I_2 afforded 3,4,7,8-tetrahydro-1*H*,6*H*-pyrido[2,1-c][1,4]oxazin-1-ol **259**, as a single isomer. In the presence of NaH under microwave irradiation, a rearrangement product **260** was obtained (08OL605).



cis-4(*R*),9*a*(*S*)-4-(3,4,5-Trifluoromethylphenyl)perhydropyrido[2,1-c][1,4]oxazin-6-one and its enantiomer were obtained by intramolecular condensation of 4-[(3*S*,5*R*)-5-(3,4,5-trifluorophenyl)morpholin-3-yl]butanoic acid and its enantiomer (09WOP2009/081959).

Perhydropyrido[1,2-*a*]pyrazin-1-one *N*-oxide **167** was formed from 1-hydroxypipercolic acid amide **261** by reverse Cope elimination by heating in CHCl_3 . Similar reaction of 1-hydroxypipercolinate **262** resulted an 1:5:30 equilibrium mixture of **262**, **263**, and **264** (07TL1683).

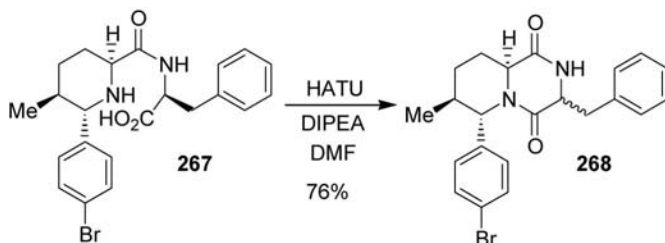


(6*R*,9*aS*)-Perhydropyrido[1,2-*a*]pyrazin-8-ones **266** were obtained by heating 2(*S*)-(4-aryl-2-oxo-3-buten-1-yl)piperazines **265** in MeOH in the presence of 2 M AcONH_4 (06USA2006/0009456). Catalytic hydrogenation of 2-[4-(4-methoxy-2,3-dimethylphenyl)-4-oxo-butyl]pyrazine over 5% PtO_2 catalyst in MeOH containing AcOH provided *cis*-6*H*,9*aH*-6-(4-methoxy-2,3-dimethylphenyl)perhydropyrido[1,2-*a*]pyrazine.

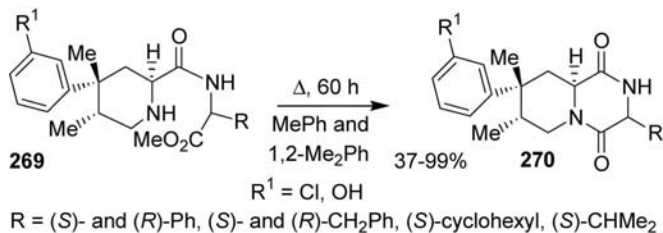


The treatment of *N*-(2-hydroxyethyl),*N*-(4-fluorophenyl)-4-benzyloxy-3-methoxypyridine-2-carboxamides with a mixture of polystyryldiphenylphosphine, imidazole, and I_2 in CH_2Cl_2 at ambient temperature overnight yielded 9-methoxy-2-(4-fluorophenyl)-3,4-dihydro-1*H*,8*H*-pyrido[1,2-*a*]pyrazine-1,8-diones (06WOP2006/066414). When *N*-(2-hydroxyethyl),*N*-(4-fluorophenyl)-4-benzyloxy-3-methoxy-6-bromopyridine-2-carboxamides was heated in HBr-AcOH solution (38%) at 100 °C for overnight 6-bromo-9-hydroxy-2-(4-fluorophenyl)-3,4-dihydro-1*H*,8*H*-pyrido[1,2-*a*]pyrazine-1,8-diones were the products.

Cyclization of pipecolic acid amide **267** on the action of HATU and Hünig's base afforded a 1:1 diastereomeric mixture of perhydropyrido[1,2-*a*]pyrazine-1,4-dione **268** (06JOC8934).



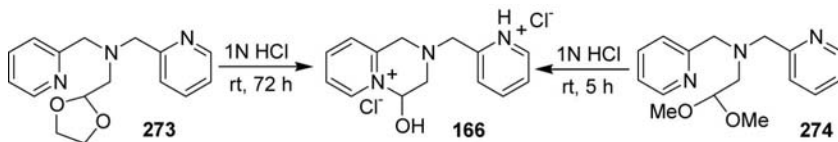
Heating picolinic acid amides **269** in boiling toluene and *o*-xylene for 60 h provided perhydropyrido[1,2-*a*]pyrazine-1,4-dione **270** (06JMC7290, 07WOP050802, 09USP7538110). 3-Unsubstituted derivative **270** ($R = H$, $R^1 = OH$) was obtained from 1-(*tert*-butoxycarbonyl) derivative of **269** ($R = H$, $R^1 = OSiMe_2^tBu$) by treatment first with the 4 N solution of HCl in dioxane in refluxing MeOH for 2 h, then for 60 h in the presence of Et_3N in quantitative yield (07WOP2007/050802).



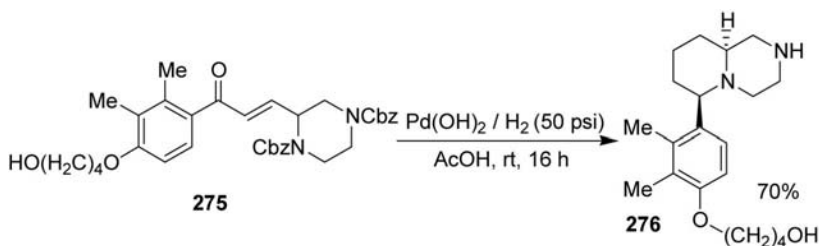
Heating 1,4-dihydropyridine-2-carboxamide **271** in dioxane containing 2 N HCl solution at 70 °C for 0.5 h gave 4-hydroxy-1,2,3,4-tetrahydro-8H-pyrido[1,2-*a*]pyrazine-1,8-dione **272** (06WOP2006/088173, 07WOP2007/049675).



On the action of 1 N aqueous HCl solution both **273** and **274** provided bicyclic salt **166** (08JOC734, 08USA2008/0138292).

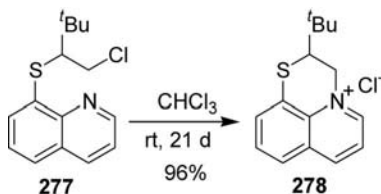


Catalytic hydrogenation of piperidine **275** over Pearlman's catalyst in AcOH afforded perhydropyrido[1,2-*a*]pyrazine **276** (08WOP2008/097483).

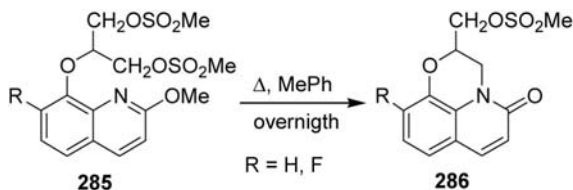


Catalytic hydrogenation of ethyl 4-pyrazin-2-yl-butylate over Pd/C catalyst in EtOH at 50 psi for 20 h afforded perhydropyrido[1,2-*a*]pyrazine-6-one in 57% yield (09EUP2098526, 09WOP2009/103176).

Cyclization of quinoline **277** in CHCl₃ at room temperature for 21 days afforded tricyclic salt **278** (05CHE771). When **277** was kept in MeNO₂ in the presence of LiClO₄ cyclization occurred within 1 day to give perchlorate salt in 92% yield.

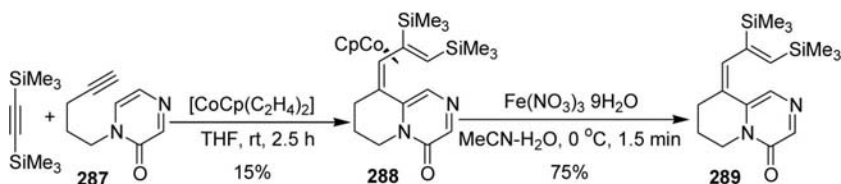


A mixture of oxolan-2-one **280** and 2,3-dihydropyrido[1,2,3-*de*]-1,4-benzothiazinium betaine **281** was obtained when a solution of disulfide **279** and CH₂=CH(CH₂)₂CO₂H was electrolyzed in the presence of Bu₄NBr in CH₂Cl₂ [05H(65)2861].



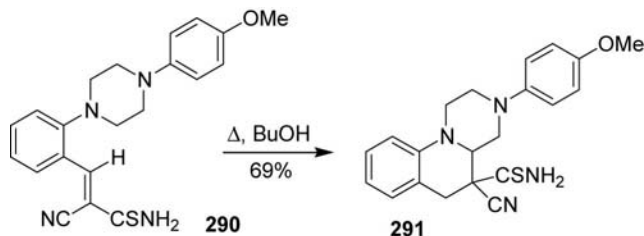
4.3.2 By the formation of one bond β to the bridgehead nitrogen atom [6+0(β)]

Cobalt-mediated C-H activation of pyrazone **287** with bis(trimethylsilyl) acetylene in the presence of cyclopentadienylcobaltbis(ethene) [CpCo (C₂H₄)₂] afforded pyrido[1,2-*a*]pyrazin-4-one complex **288**, and its decomplexation with Fe³⁺ furnished 6,7,8,9-tetrahydro-4*H*-pyrido[1,2-*a*]pyrazin-4-one **289** (07CEJ7443).

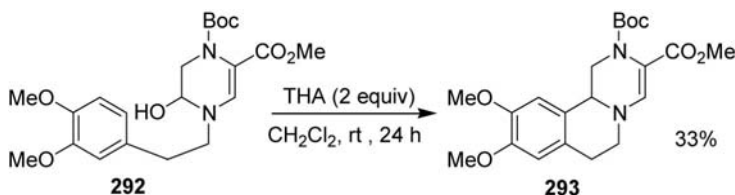


Stirring the solution of dimethyl 2-(2-morpholinobenzylidene)malonate in MeCN in the presence of Gd(OTf)₃ (5 mol%) at 40 °C for 12 h provided dimethyl 1,2,4,4*a*,5,6-hexahydro-[1,4]oxazino[4,3-*a*]quinoline-5,5-dicarboxylate in 78% yield (09OL129).

Cyclization of thioamide **290** in boiling BuOH occurred stereospecifically to give a single diastereomer of hexahydro-1*H*-pyrazino[1,2-*a*]quinoline **291** in 95–98% yield (08CHE759). Similarly, amide analog of **290** could not be cyclized.



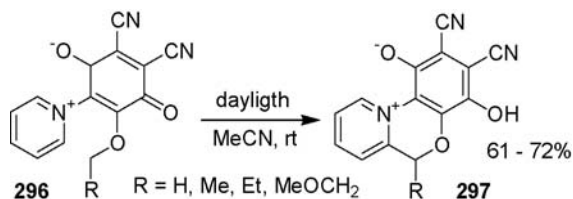
Intramolecular cyclization of hemiacetal **292** in CH₂Cl₂ in the presence of 2 equiv. of TFA provided 1,6,7,11*b*-tetrahydro-2*H*-pyrazino[1,2-*b*]isoquinoline-3-carboxylate **293** (09TL3679).



Heating a diastereomeric mixture of pyrazine-2,5-dione **294** in TFA gave a mixture of pyrazino[1,2-*b*]isoquinoline-1,4-dione **206a**, spiro derivative **295** and the starting material **294** [08H(761497)]. Cyclization of **294** in boiling CH_2Cl_2 in the presence of $\text{BF}_3 \cdot \text{OEt}_2$ (1.5 equiv.) for 22 h, and boiling $\text{ClCH}_2\text{CH}_2\text{Cl}$ in the presence of *p*TsOH (1.2 equiv.) for 36 h afforded **206a** in 64% and 93% yield, respectively. Compound **206a** was also prepared in 93% yield from 1-methyl-3-[(2,4,5-trimethoxy-3-methylphenyl)methyl]perhydropyrazine-2,5-dione by treatment with Me_3SiCl in the presence of Et_3N in $\text{ClCH}_2\text{CH}_2\text{Cl}$ at room temperature for 2 h, followed by the addition of $(\text{EtO})_2\text{CCO}_2\text{Et}$ than that of TMSOTf and the reaction mixture was stirred at ambient temperature for 16 h, and at 100 °C for 4 h.

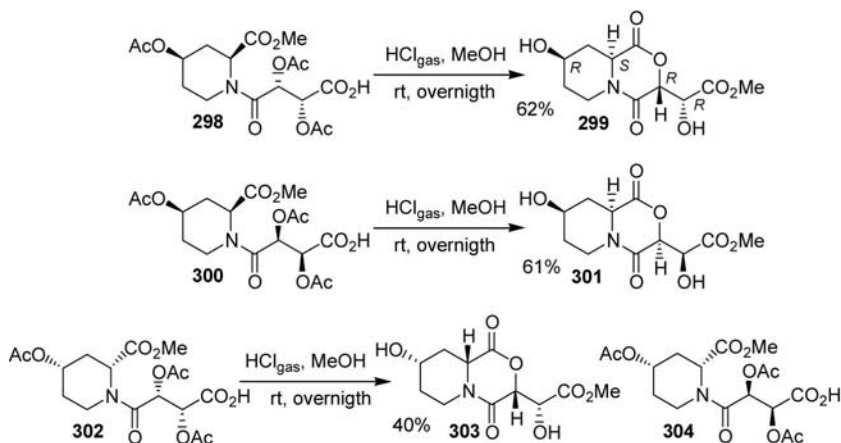


A photoinduced intramolecular dehydrogenative-coupling reaction of stable semiquinone radicals **296** yielded 6H-pyrido[2,1-*c*][1,4]benzoxazinium inner salts **297** (09OL5530).



4.3.3 By the formation of one bond γ to the bridgehead nitrogen atom [6+0(γ)]

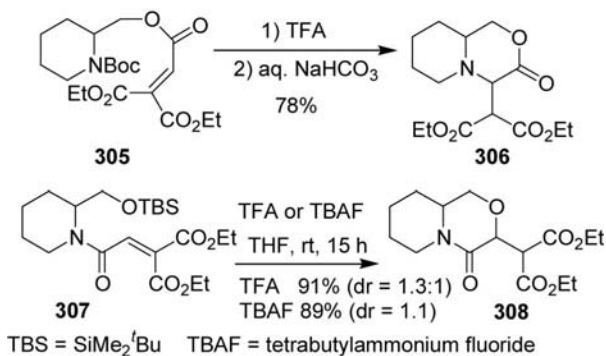
Boiling 1-(4-aminophenyl)-2-[2-(hydroxymethyl)piperidin-1-yl]ethanol in 48% aqueous HBr for 3.5 h yielded 3-(4-aminophenyl)perhydropyrido[2,1-*c*][1,4]oxazine (08WOP2008/026046).



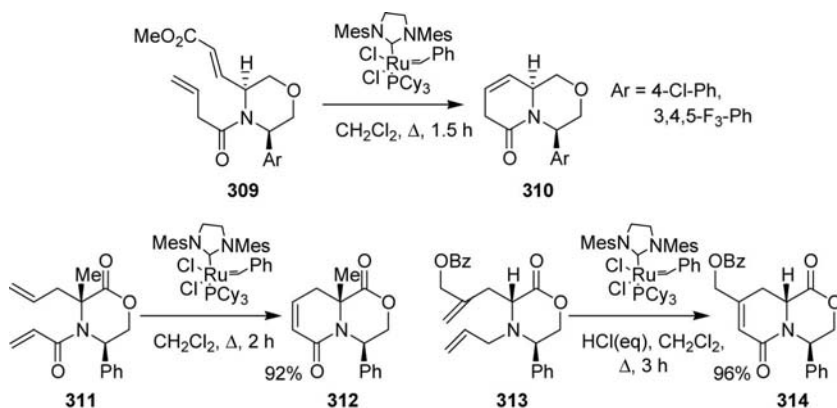
Perhydropyrido[2,1-*c*][1,4]oxazine-1,4-diones **299**, **301**, and **303** were obtained from piperidine derivatives **298**, **300**, and **302** stirring in MeOH saturated with HCl gas overnight, but stereoisomer **304** gave only tarry material (07EJO3028).

While the treatment of 3,4,5-tribenzyloxy-1-(2'-hydroxy-1'(*R*)-phenylethyl)-[1' α ,2 β ,3 α ,4 β ,5 α]piperidine-2-carbonitrile provided (4*S*)-[4 β ,7 α ,8 β ,9 α ,9 α]-4-phenyl-7,8,9-tribenzyloxyperhydropyrido[2,1-*c*][1,4]oxazin-1-one in 60% yield on the action of TiCl_4 in the presence of K_2CO_3 in acetone at -20°C , then stirring the solution at 40°C for 1 day, isomeric 3,4,5-tribenzyloxy-1-(2'-hydroxy-1'(*R*)-phenylethyl)-(1-[1' α ,2 β ,3 α ,4 β ,5 β]piperidine-2-carbonitrile did not yield the appropriate pyrido[2,1-*c*][1,4]oxazin-1-one bicyclic product (07TA1585).

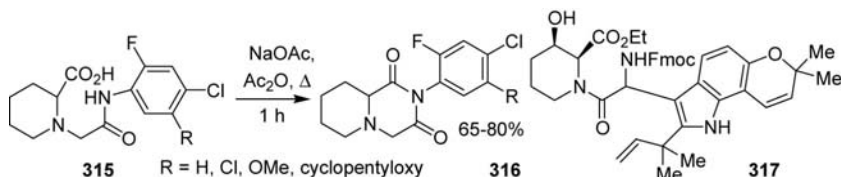
Deprotection of the *N*-Boc group of piperidine **305** by TFA to afford a TFA salt, followed by basic aqueous workup with aqueous NaHCO_3 solution gave a single racemate of perhydropyrido[2,1-*c*][1,4]oxazin-3-one **306**, while that of the *O*-TBS protected piperidine **307** by TFA or TBAF yielded diastereomeric mixtures of **308** (09OBC655).



Ring-closing metathesis of [1,4]oxazines **309**, [1,4]oxazin-2-ones **311** and **313** in the presence of Grubbs second-generation catalyst provided hexahydropyrido[2,1-*c*][1,4]oxazin-6-ones **310** (07USA2007/0117839, 08WOP2008/013213), (4*R*,9*aR*)-hexahydropyrido[2,1-*c*][1,4]oxazine-1,6-dione **312** (09JOC4429), and hexahydropyrido[2,1-*c*][1,4]oxazin-1-one **314** (08JOC6877), respectively. Methyl (4*R**,9*aS**)-6-oxo-4-(3,4,5-trifluorophenyl)-1,2,3,4,6,7-hexahydropyrido[1,2-*a*]pyrazine-2-carboxylate was similarly prepared from methyl 4-(3-butenoyl)-3-(2-ethoxycarbonylvinyl)-5-(3,4,5-trifluorophenyl)piperazine-1-carboxylate (07USA2007/0117839).



Heating pipecolic acids **315** in refluxing Ac₂O in the presence of catalytic amount of NaOAc for 1 h afforded perhydropyrido[1,2-*a*]pyrazine-1,3-diones **316** (05MOL119). The treatment of piperidine **317** with morpholine in THF at ambient temperature for 2 h afforded diketopiperazine **230** as an inseparable mixture of diastereomers (07T6124).

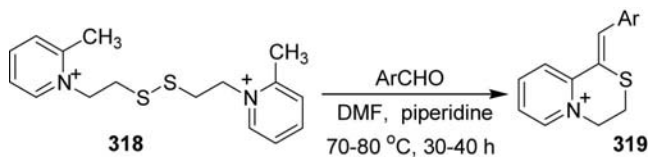


For the treatment of 1-(2-hydroxy-1-phenylethyl)-2-hydroxymethyl-6-piperidone with *p*TsCl and NEt₃ in CH₂Cl₂ at ambient temperature overnight, the reaction mixture was added dropwise to a solution of KO^{*t*}Bu in

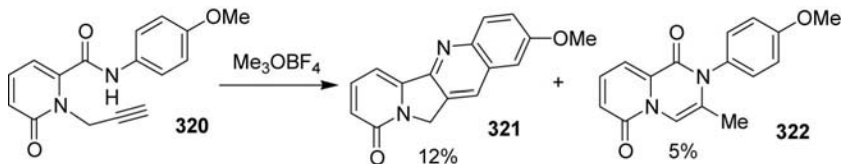
THF at room temperature for 220 min to give 4-phenylperhydropyrido[2,1-*c*][1,4]oxazin-6-one (07USA2007/0117839). Reduction of ethyl 1-[1-aryl-2-hydroxyethyl]-6-oxopiperidine-2-carboxylates with NaBH_4 in MeOH at 0 °C for 80–100-min-yielded 1-hydroxy-4-arylperhydropyrido[2,1-*c*][1,4]oxazin-6-ones.

For ozonolysis of ethyl [*cis*-2*H*,6*H*-2-(4-fluorophenyl)-6-vinylpiperidin-1-yl]oxoacetate in MeOH at -78 °C for 20 min, the treatment of the reaction mixture with NaBH_4 at the same temperature for 0.5 h afforded *cis*-6*H*,9*aH*-3-hydroxy-6-(4-fluorophenyl)perhydropyrido[2,1-*c*][1,4]oxazin-4-one (07USA2007/0117798).

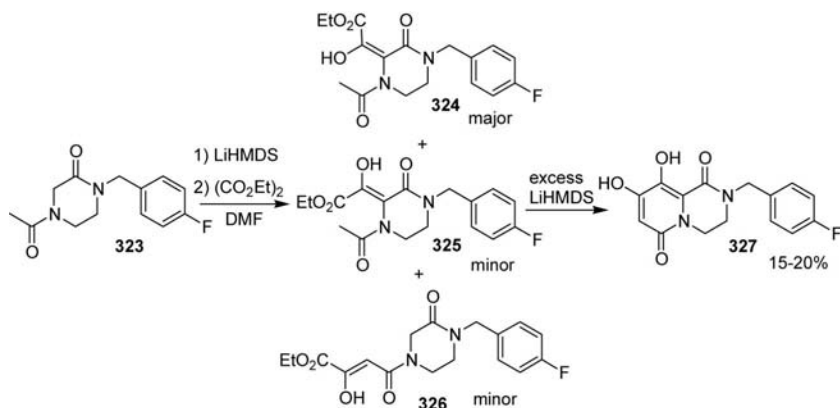
Reactions of bispyridinium salts **318** with benzaldehydes in the presence of a catalytic amount of piperidine in DMF at 70–80 °C for 30–40 h yielded 1-arylmethylene-3,4-dihydro-1*H*-pyrido[2,1-*c*][1,4]thiazinium salts **319** (06WOP2006/136617, 07WOP2007/003506, 07WOP2007/039527).



The treatment of 1-propargyl-6-oxo-1,6-dihydropyridine-2-carboxamide **320** with Me_3OBF_4 gave a mixture of tetracyclic **321** and 1*H*,6*H*-pyrido[1,2-*a*]pyrazine-1,6-dione **322** in low yields (07OL2003).



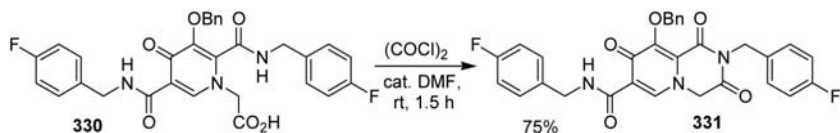
The treatment of 4-acetylpiperazinone **323** with LiHMDS, followed by addition of $(\text{CO}_2\text{Et})_2$ gave three condensation products **324–326**. Upon addition of excess LiHMDS 8,9-dihydroxy-3,4-dihydro-1*H*,6*H*-pyrido[1,2-*a*]pyrazine-1,6-dione **327** was obtained in low yield (07BML5595). The major isomer **324** could be isomerized into **325** on the action of TFA in aqueous MeCN, which readily cyclized to pyrido[1,2-*a*]pyrazine-1,6-dione **327**. ^{14}C -labeled **327** was also prepared using ^{14}C -labeled diethyl oxalate.



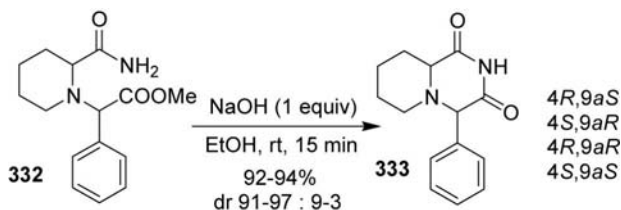
Heating piperidine **328** in DMF in the presence of Cs_2CO_3 at 62°C provided 4-oxoperhydropyrido[1,2-*a*]pyrazine-1-carboxylate **329** (07T8017).



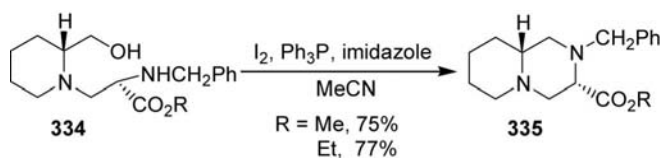
The treatment of 1-(carboxylmethyl)-4-oxo-1,4-dihydropyridine-2-carboxamide **330** with $(\text{COCl})_2$ in the presence of catalytic amount of DMF at room temperature for 1.5 h afforded 1,3,8-trioxo-1,2,3,4-tetrahydro-8*H*-pyrido[1,2-*a*]pyrazine-7-carboxamide **331** (06WOP2006/000824).



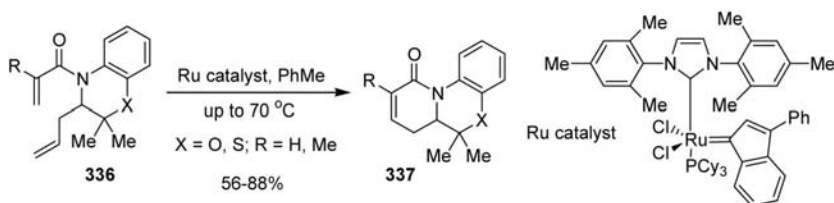
Cyclization of the optically active enantiomers of methyl α -(2-carbamoylpiperidinyl)- α -phenylacetate **332** with 1.0 equiv. of NaOH in EtOH provided almost pure optically active 1-phenylperhydropyrido[1,2-*a*]pyrazine-2,4-diones **333** (09TA1759).



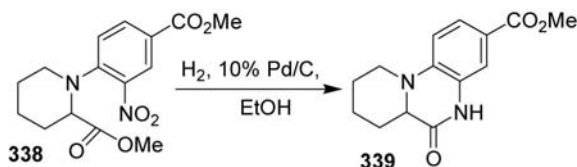
Cyclization of alcohols **334** under Mitsunobu condition was very sluggish, but it happened easily when alcohol was treated with Ph_3P , imidazole and I_2 to give perhydropyrido[1,2-*a*]pyrazine-3-carboxylates **335** (08SL702). C3 Epimer of **335** was prepared similarly.



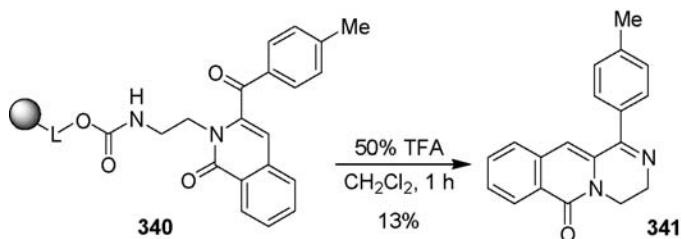
Ring-closing metathesis of α -allyl acrylamides **336** using a Ru catalyst provided triyclic derivatives **337** (09S665).



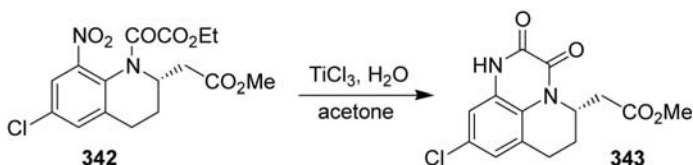
Catalytic hydrogenation of 1-arylpipicolinate **338** over 10% Pd/C catalyst yielded 6-oxo-6,6*a*,7,8,9,10-hexahydro-5*H*-pyrido[1,2-*a*]quinoxaline-3-carboxylate **339** (08USA2008/0161292, 09BML4050).



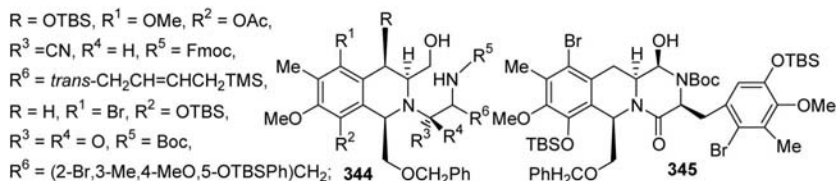
3,4-Dihydro-5*H*-pyrazino[1,2-*b*]isoquinolin-5-one **341** was obtained by cleavage of 2-[(4-methylbenzoyl)-1-oxo-1,2-dihydroisoquinolin-2-yl]ethylamino moiety from resin **340** with 50% TFA (09JCO851).



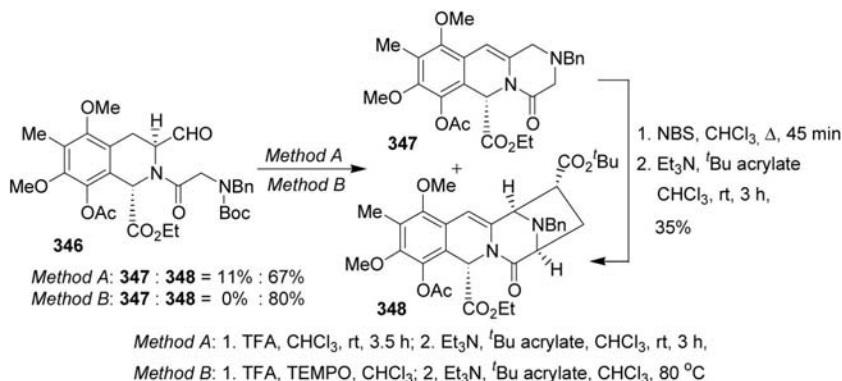
Reduction of 8-nitro-1,2,3,4-tetrahydroquinoline **342** with aqueous $TiCl_3$ in acetone gave 2,3,6,7-tetrahydro-1*H*,5*H*-pyrido[1,2-*de*]quinoxaline-2,3-dione **343** after a spontaneous cyclization (06CTM733).



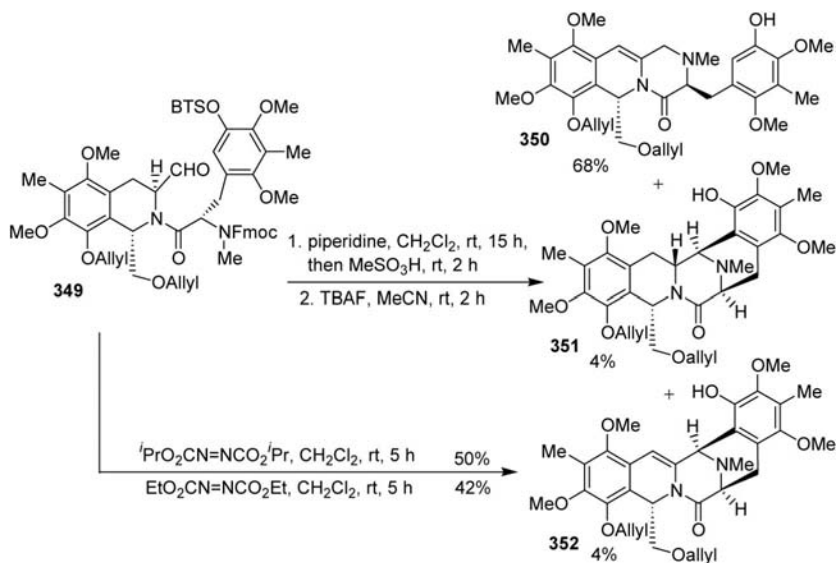
Dess–Martin oxidation of tetrahydroisoquinoline-3-methanols **344** in CH_2Cl_2 at room temperature resulted the formation of aldehydes, which immediately cyclized into hexahydro-1*H*-pyrazino[1,2-*b*]isoquinolines **238** and **345** (08SL2443, 09T5709).



Aldehyde **346** gave a mixture of tricyclic **347** and tetracyclic derivatives **348** on the action of TFA followed by treatment with Et_3N and tBu acrylate [07H(72)385]. When the oxidation of tricycle **347** was promoted by adding TEMPO the unsaturated cycloadduct **348** was the only product. Tricycles **347** could be transformed into tetracycle **348** by treating with NBS followed by treatment with Et_3N and tBu acrylate in 35% yield.

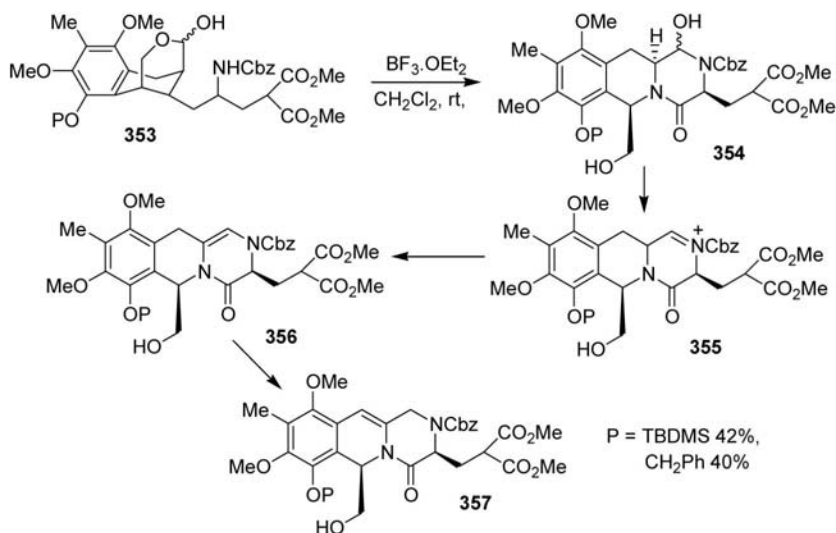


When aldehyde **349** was treated with piperidine, with MeSO_3H , and finally with $^t\text{Bu}_4\text{NF}$ 2,3,4,6-tetrahydro-1*H*-pyrazino[1,2-*b*]isoquinolin-4-one **350** was obtained in 68% yield, which was accompanied by a small amount of tetracyclic derivatives **351** and **352**. Tetracyclic compound **352** could be obtained from aldehyde **349** in higher yield by treatment with alkyl azodicarboxylate [07H(72)385].

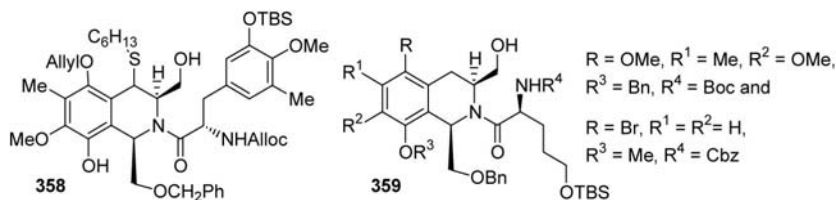


The treatment of lactols **353** with $\text{BF}_3 \cdot \text{OEt}_2$ provided 2,3,4,6-tetrahydro-1*H*-pyrazino[1,2-*b*]isoquinolin-4-ones **357**, through the formation of

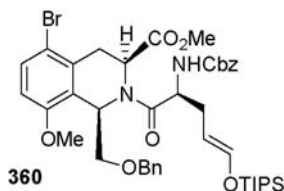
epimeric mixture of 1-hydroxymethyl derivatives **354** followed by dehydration under Lewis acidic conditions, and then iminium-enamine tautomerization (**355** \rightarrow **356**) and finally isomerization to **357** (06SL1691). Applying other promoters [$\text{TiCl}_4 \cdot \text{Et}_3\text{N}$, $\text{TiCl}_4 \cdot \text{pyridine}$, TiCl_4 , SnCl_4 , AlCl_3 , $\text{Yb}(\text{OTf})_3$, TFA, $\text{CF}_3\text{SO}_3\text{H}$] usually led to the degradation of the starting material **353**.



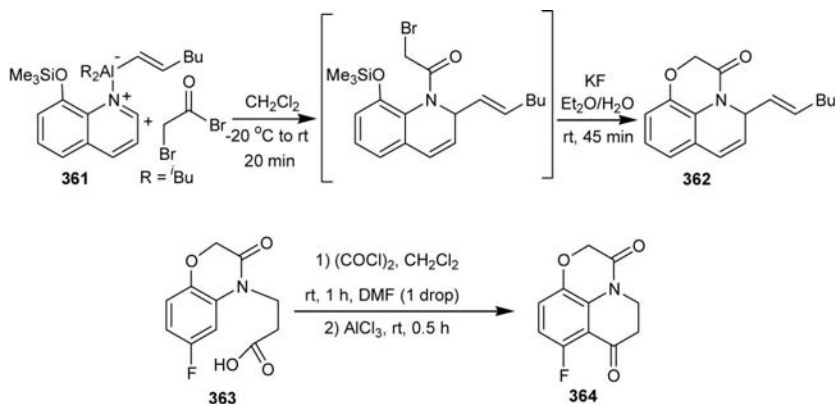
Swern oxidation of 3-hydroxymethyltetrahydroisoquinoline **358**, followed by the treatment of the reaction mixture with Bu_4NF gave a mixture of 3-phenyltetrahydroisoquinoline **252** and 2,3,4,6,11,11a-hexahydro-1*H*-pyrazino[1,2-*b*]isoquinolin-4-one **253** (07AGE3962). That of 3-hydroxymethyltetrahydroisoquinolines **359** afforded a 3:2 mixture of epimeric mixture of 1-hydroxy derivatives **202** in excellent yields (08JA7148, 09JOC2046).



1-Hydroxy-1,2,3,4,11,11a-hexahydro-6*H*-pyrazino[1,2-*b*]isoquinolin-4-one **204** was obtained in 83% overall yield, when tetrahydroisoquinoline-3-carboxylate **360** was reduced with LiBH_4 in a mixture of MeOH and Et_2O at room temperature for 4 h, followed by Swern oxidation (08JA7148).

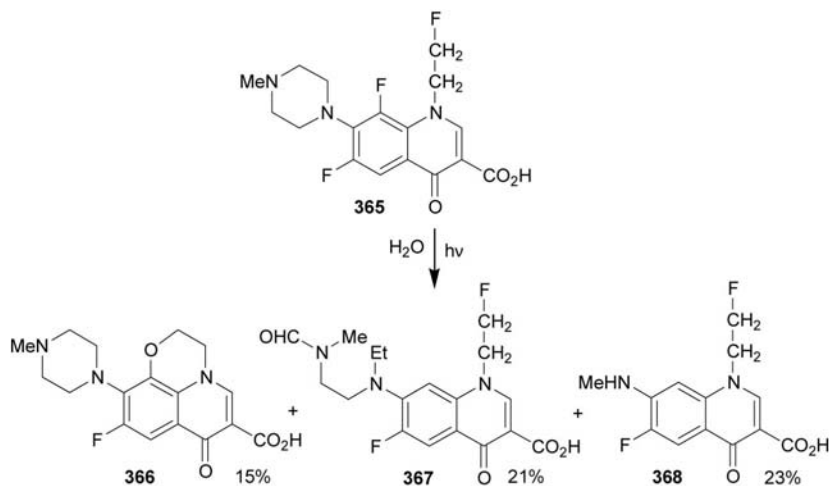


5(*E*)-(Hex-1-enyl)-2,3-dihydro-5*H*-pyrido[1,2,3-*de*][1,4]oxazine-3-one **362** was obtained in the reaction of BrCH_2COBr and quinoline **361**, prepared from 8-trimethylsilyloxyquinoline with di-*i*-butyl hex-1-enylaluminum (08T197).

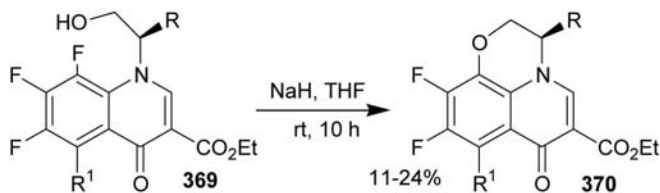


The treatment of propionic acid **363** with $(\text{COCl})_2$ than with AlCl_3 at room temperature afforded 5*H*-pyrido[1,2,3-*de*][1,4]benzoxazine-3,7 (2*H*,6*H*)-dione **364** (08WOP2008/116815).

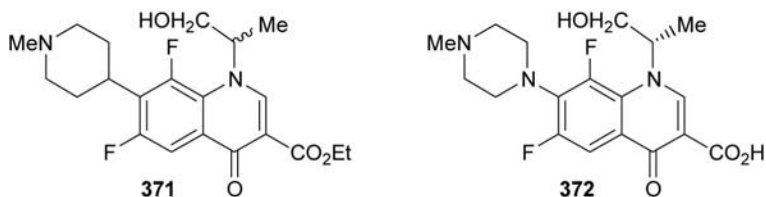
Flash photolysis of fleroxacin **365** in water gave a mixture of 7-oxo-2,3-dihydro-7*H*-pyrido[1,2,3-*de*][1,4]oxazine-6-carboxylic acid **366** and 4-oxo-1,4-dihydroquinolone-3-carboxylic acids **367** and **368** (09OL1875).



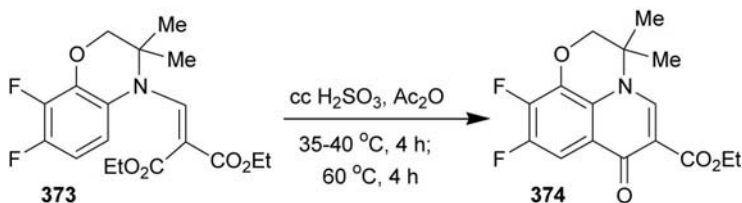
Cyclization of quinolone **369** ($R = Ph$, $R^1 = F$) in the presence of NaH (60% in oil) afforded 8,9,10-difluoro-7-oxo-2,3-dihydro-7H-pyrido[1,2,3-*de*][1,4]oxazine-6-carboxylate **370** ($R = Ph$, $R^1 = F$) (07WOP2007/106537). Similarly enantiomers of **369** ($R = CH_2SMe$, CH_2SCH_2Ph , $R^1 = H$) were cyclized by stirring in CH_2Cl_2 in the presence of NaOH and $PhCH_2NEt_3Cl$ at 30 °C to give enantiomers of **370** ($R = CH_2SMe$, CH_2SCH_2Ph , $R^1 = H$) (04MIP2).



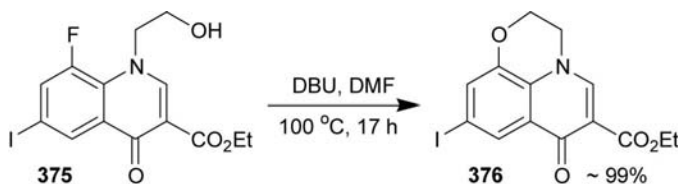
Ethyl esters of ofloxacin and levofloxacin were obtained by the cyclization of racemic and optically active forms of quinolinone **371**, respectively (05WOP2005/123746). Heating quinoline-3-carboxylic acid **372** and its ethyl ester in boiling 96% EtOH in the presence of KOH afforded levofloxacin in 76–78% yield (08EUP1939206).



Cyclization of aminomethylenemalonate **373** and its 2,2-dimethyl analog in a mixture of cc H_2SO_4 and Ac_2O afforded 7-oxo-2,3-dihydro-7*H*-pyrido[1,2,3-*de*][1,4]benzoxazine-6-carboxylate **374** and its 2,2-dimethyl analog (05MIP2).

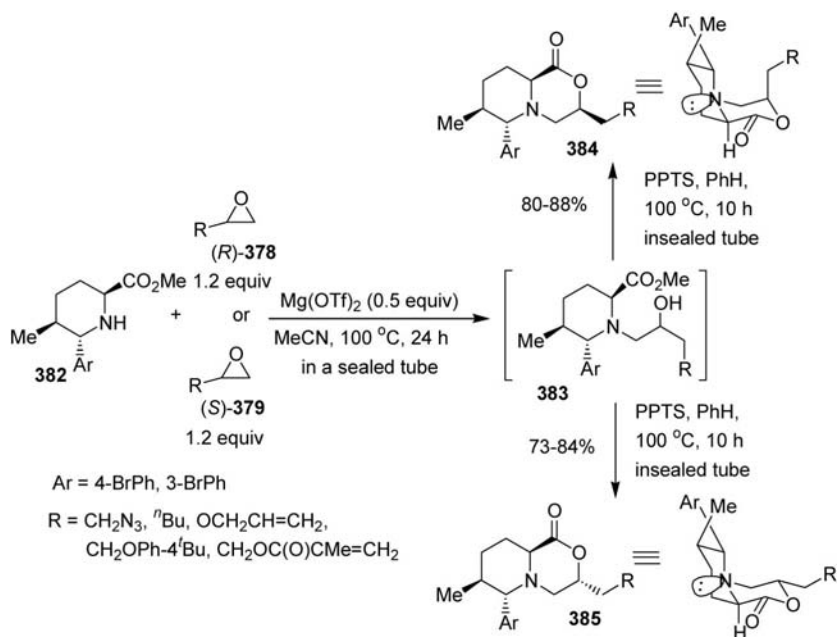
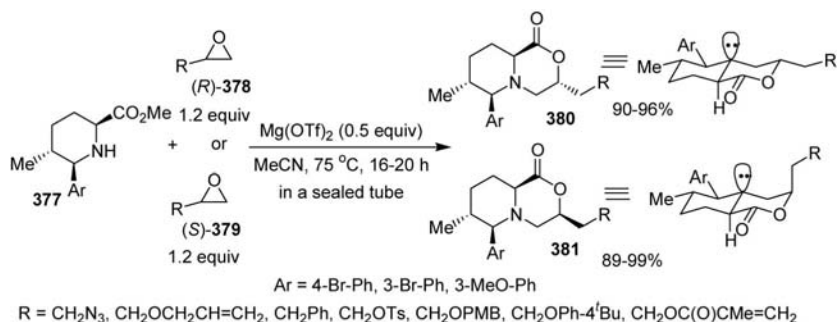


The treatment of 1-(2-hydroxyethyl)-8-fluoro-4-oxo-1,4-dihydroquinoline-3-carboxylate **375** with DBU provided 9-iodo-7-oxo-2,3-dihydro-7*H*-pyrido[1,2,3-*de*][1,4]benzoxazine-6-carboxylate **376** (07WOP2007/054296).



4.3.4 By the formation of two bond from [3+3] atom fragments

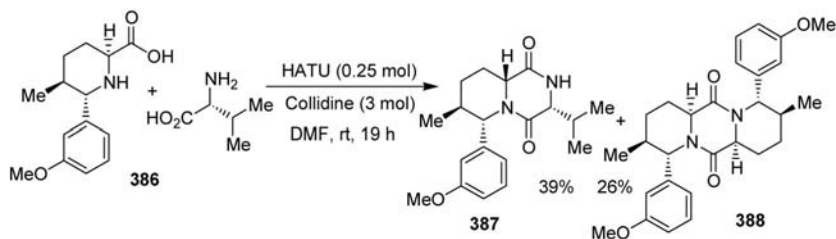
Cyclocondensation of *cis*-2*H*,6*H*-pipercolates **377** with optically active oxiranes **378** and **379** in the presence of $\text{Mg}(\text{OTf})_2$ in MeCN at 75 °C in a sealed tube yielded perhydropyrido[2,1-*c*][1,4]oxazin-1-ones **380** and **381**, respectively (07OL1529). The reactions of *trans*-2*H*,6*H*-pipercolates **382** with optically active **378** and **379** required higher reaction temperature and longer reaction period to give **384** and **385**. In the case of **382** (Ar = 4-Br-Ph) and **378** (R = CH_2N_3) besides 40% of **384** (Ar = 4-Br-Ph, R = CH_2N_3) 50% of **383** (Ar = 4-Br-Ph, R = CH_2N_3) was obtained. Compound **383** (Ar = 4-Br-Ph, R = CH_2N_3) could be cyclized on the action of pyridinium *p*-toluenesulfonate in a sealed tube at 50 °C. The lower reactivity observed in the conversion of **383** (Ar = 4-Br-Ph, R = CH_2N_3) to **384** (Ar = 4-Br-Ph, R = CH_2N_3) may be a result of destabilizing 1,3-diaxial interaction during the formation of the tetrahedral intermediate leading to **384** (Ar = 4-Br-Ph, R = CH_2N_3).



6-Endo-trig cyclization of anion, formed from 2-methylpyrazine by LDA in THF at -78°C , with methyl 3-propynoate provided 6-methyl-8*H*-pyrido[1,2-*b*]pyridazin-8-one in 52% yield (06TL5063).

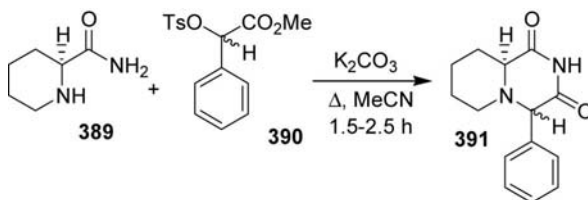
Reaction of 2-hydroxymethylpyridine with ClCH_2COMe (06PJC1039) and BrCH_2COPh (06JST36) in acetone at 40°C for 2–3 weeks afforded **159a** and **159b** in 62% and 67% yields, respectively.

Cyclocondensation of pipecolic acid **386** and isoleucine gave a mixture of bi- and tricyclic heterocycles **387** and **388** (06JOC8934).

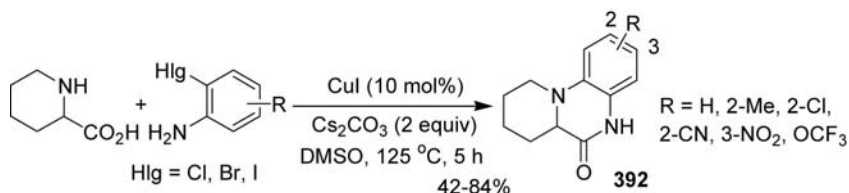


Heating 2-cyanopyridine and 2-bromoacetophenone at 90 °C for 2 h, and then the treatment of the aqueous solution of the reaction mixture with KPF₆ gave 1-oxo-3-phenyl-1,2-dihydropyrido[1,2-*a*]pyrazin-5-ium hexafluorophosphate [06AX(E)2438].

Cyclocondensation of optically active (*S*)-pipecolinamide **389** and enantiomers of methyl 2-(4-methylphenylsulfonyloxy)phenylacetates **390** in the presence of an excess of K₂CO₃ in MeCN led to 67–81:33–19 mixture of (4*R*,9*aS*)- and (4*S*,9*aS*)-4-phenylperhydropyrido[1,2-*a*]pyrazine-1,3-diones **391**, regardless of whether (*S*)-**390**, (*R*)-**390**, or *rac*-**390** was used as starting material (09TA1759).



Copper-catalyzed coupling reaction of 2-bromoanilines and pipecolinic acid provided 6,6*a*,7,8,9,10-hexahydro-5*H*-pyrido[1,2-*a*]quinoxalin-6-ones **392** (09BML4119). Using [Pd(η^3 -C₃H₅)Cl₂]₂ with (2-biphenyl)di-*tert*-butylphosphine catalyst system and Cu(I)Br gave lower yields.



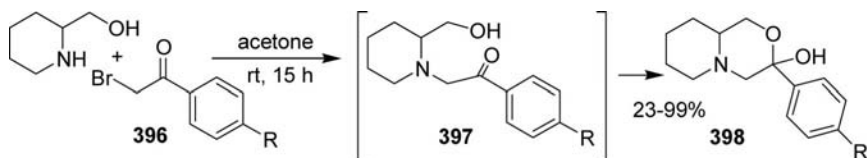
Cyclocondensation of 2-methoxy-8-quinolinols **393** with (*S*)-glycidyl nosylate **394** in the presence of NaH gave 3(*R*)-hydroxymethyl-2,3-dihydro-5*H*-pyrido[1,2,3-*de*][1,4]benzoxazin-5-ones **395** (08WOP2008/128953).

That of 7-bromo- and 7-fluoro-8-hydroxyquinolin-2(1*H*)-ones with epichlorohydrin in the presence of catalytic amount of piperidine in DMF at 85 °C gave 10-substituted 3-hydroxymethyl-2,3-dihydro-5*H*-pyrido[1,2,3-*de*][1,4]benzoxazin-5-ones (08WOP2008/120003).

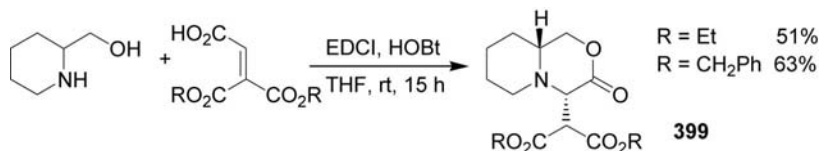


4.3.5 By the formation of two bond from [4+2] atom fragments

A spontaneous cyclization of 1-(2-aryl-2-oxoethyl)-2-piperidinemethanol **397**, prepared from 2-piperidinemethanol and bromomethyl aryl ketones **396**, yielded 3-aryl-3-hydroxyperhydropyrido[2,1-*c*][1,4]oxazines **398** (08JMC5861, 08WOP2008/026046).



Oxalyl chloride was added dropwise into a CHCl_3 solution of the diastereomer mixture of (*S*)-1-[(2*R*,6*S*)- and (*R*)-1-[(2*R*,6*S*)-6-(3,4,5-trifluorophenyl)piperidine-2-yl]ethanols in the presence of pyridine at 0 °C to give a diastereomeric mixture of (1*R*,6*S*,9*aR*)- and (1*SR*,6*S*,9*aR*)-1-methyl-6-(3,4,5-trifluorophenyl)perhydropyrido[2,1-*c*][1,4]oxazine-3,4-diones (08USA2008/0207900). Reaction of $(\text{CO}_2\text{Et})_2$ with 2-piperidinemethanols at 120 °C for 1 h gave perhydropyrido[2,1-*c*][1,4]oxazine-3,4-diones (07USA2007/0117798).



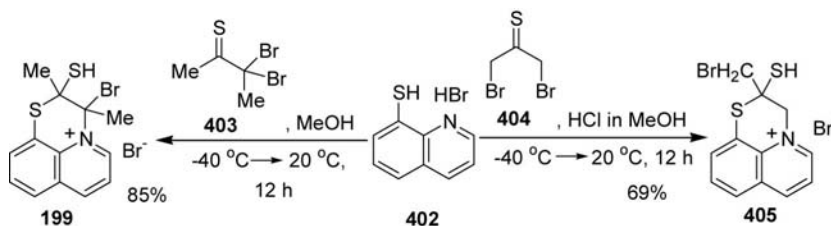
Cyclocondensation of hydroxycarbonylmethylenemalonates and 2-piperidinemethanol in the presence of EDCI and HOBT gave *cis*-4*H*,9*aH*-perhydropyrido[2,1-*c*][1,4]oxazin-3-ones **399** (09OBC655).

Cyclocondensation of 2-aminomethylpyridine with oxalyl acid bis(4-bromophenylimidoyl) chloride yielded 3-(4-bromophenylamino)-4-(4-bromophenylimino)-4*H*-pyrido[1,2-*a*]pyrazine [05ZN(B)771].

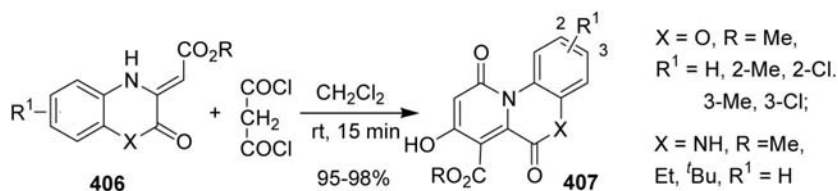
Reaction of 8-quinolinesulfonyl chloride and ethylene derivatives **400** in the presence of LiClO₄ afforded 2,3-dihydropyrido[1,2,3-*de*]-1,4-benzothiazinium perchlorates **401** (09MC49).



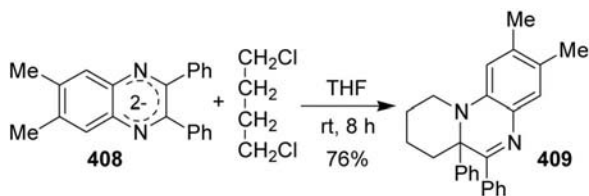
Reactions of 8-mercaptoquinolinium bromide **402** with dibromothiones **403** and **404** provided 1,2-dihydropyrido[1,2,3-*de*]-1,4-benzothiazinium bromides **199** and **405**, respectively (06CHC1478). Bromide anion of **405** was changed for ClO₄[−] anion in MeOH with NaClO₄.



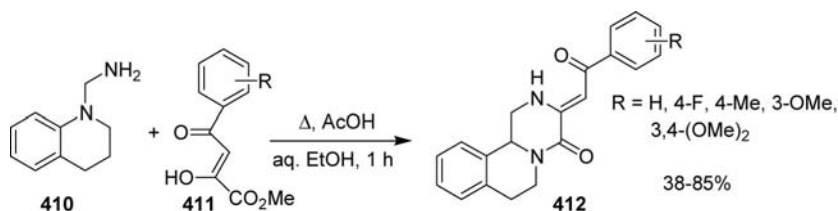
Cyclocondensation of acetates **406** and CH₂(COCl)₂ at room temperature provided tricyclic derivatives **407** (09SL1921).



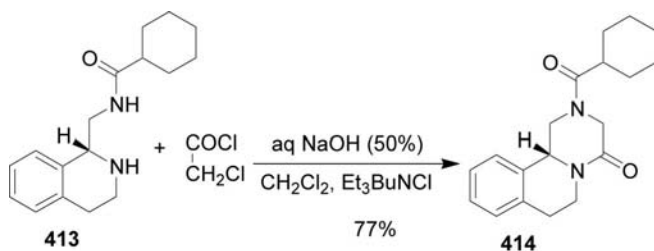
That of 1,4-dichlorobutane and quinoxaline sodium salt **408**, prepared from quinoxaline with metal Na in THF, provided 7,8,9,10-tetrahydro-6*aH*-pyrido[1,2-*a*]quinoxaline **409** (08M669).



Cyclocondensation of 1-aminomethyl-1,2,3,4-tetrahydroquinoline **410** and 3-aryl-2-hydroxyacrylates **411** in boiling aqueous EtOH in the presence of AcOH afforded 3-arylmethylene-1,3,4,6,7,11*b*-hexahydro-2*H*-pyrazino[2,1-*a*]isoquinolin-4-ones **412** (05CHC1041).



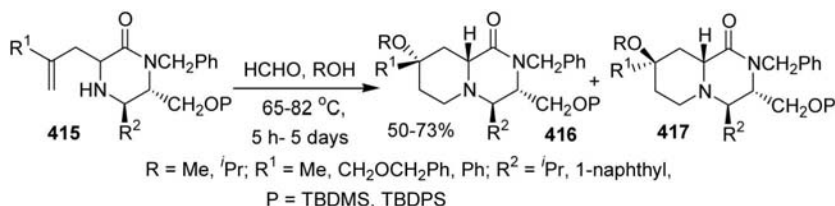
(1*R*)-(–)-Praziquantel **414** was prepared in the reaction of 1,2,3,4-tetrahydroisoquinoline **413** and ClCH_2COCl under phase transfer conditions (06TA1415). Praziquantel was obtained in 85% yield in the reaction of racemic **413** and ClCH_2COCl in the presence of K_2CO_3 in AcOEt at 80 °C for 4 h (09MIP8).



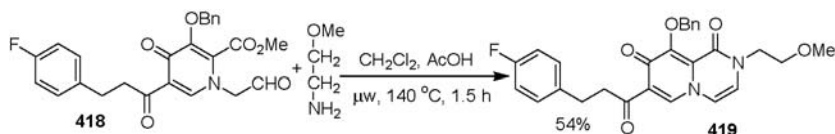
4.3.6 By the formation of two bond from [5+1] atom fragments

2-Benzylperhydropyrido[1,2-*a*]pyrazine-1,4-dione was obtained in the reaction of methyl 1-(2-chloroacetyl)piperidine-2-carboxylate and benzylamine in the presence of Et_3N in CH_2Cl_2 at ambient temperature for 48 h in 75% yield (08WOP101247).

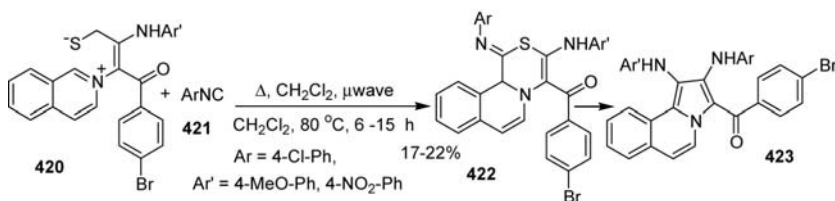
Pictet–Spengler–Grieco cyclization of 3-allylpiperazin-2-ones **415** with H_2CO and alcohols afforded usually highly diastereoselectively perhydro-pyrido[1,2-*a*]pyrazin-1-ones **416**. When starting **415** contained a bulky R^1 ($\text{CH}_2\text{OCH}_2\text{Ph}$) or R^2 (1-naphthyl) groups, diastereomeric mixtures of **416** and **417** were obtained (08T11580). The alkene-iminium cyclization did not proceed in the absence of a nucleophilic alcohol as solvent (THF-PhCH₂OH) or less reactive aldehyde (PhCHO) were employed.



Reaction of 1-(2-oxoethyl)-4-oxo-1,4-dihydropyridine-2-carboxylate **418** and 2-methoxyethylamine in the presence of AcOH at 140°C for 0.5 h under microwave irradiation provided 1,2-dihydro-8*H*-pyrido[1,2-*a*]pyrazine-1,8-dione **419** (06WOP2006/088173, 07WOP2007/049675).

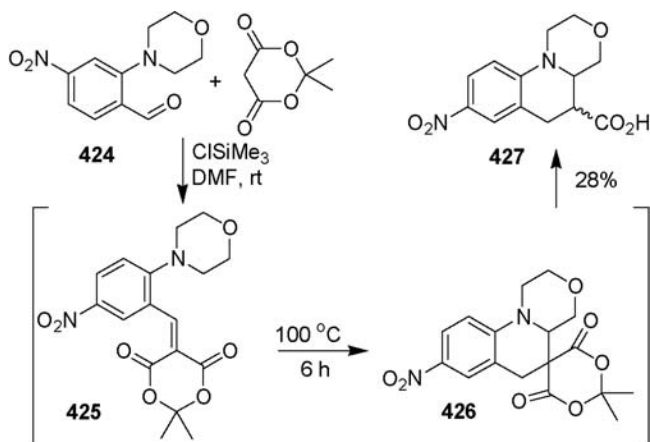


Heating isoquinolinium zwitterions **420** and isocyanides **421** in CH_2Cl_2 under microwave irradiation afforded [1,4]thiazino[3,4-*a*]isoquinoline-1-imines **422** in low yields (08S1688). Reactions, either at higher temperature or for longer reaction time, led to the formation of pyrrolo[2,1-*a*]isoquinolines **423** through **422**.

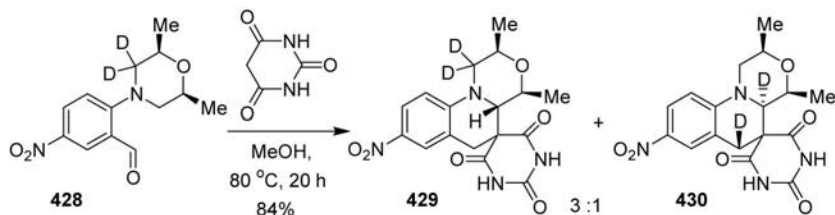


For the reaction of aldehyde **424** and Meldrum's acid in DMF with dropwise addition of TMSCl at room temperature, the closed reaction

vessel was heated on a water bath for 6 h to give a 84:16 diastereomeric mixture of hexahydro[1,4]oxazino[4,3-*a*]quinoline-5-carboxylic acid **427** (08SC3032). Better yield (62%) could be achieved when the reaction mixture was heated at 60 °C for 12 h to form the condensation product **425** followed by cyclization, then the formed **426** was hydrolyzed and decarboxylated by heating at 100 °C for 6 h to afford tricycle **427**. Spiro compound **426** could also be isolated.

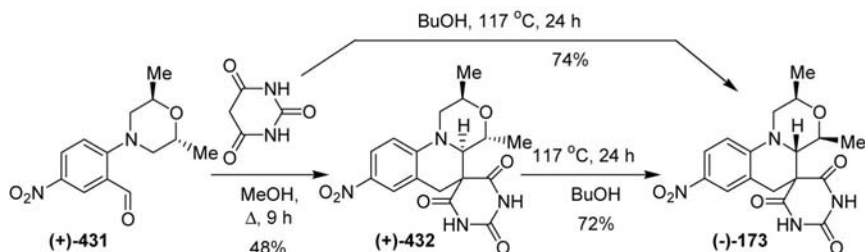


For the cyclocondensation of 5-bromo-2-(*cis*-2,6-dimethylmorpholin-4-yl)benzaldehyde with malononitrile in DMSO at 23 °C for 1 h, at 130 °C for 20 h furnished 1,2,4,4*a*,5,6-hexahydro[1,4]oxazino[4,3-*a*]quinoline-5,5-dinitrile **168** in 54% yield (09JA3991). Similar cyclocondensation of dideuterated **428** provided a 3:1 mixture of spiro derivatives **429** and **430**, which were separated by using preparative HPLC.

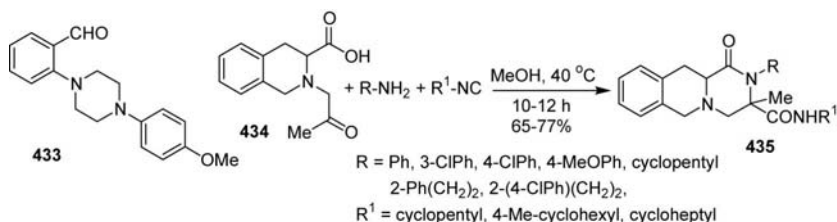


Reaction of *trans*-methyl **431** and barbituric acid in boiling MeOH provided **432**, which contained cca 10% of *cis*-methyl derivative, estimated by ¹H NMR. Optically active (+)-**431** gave optically active (+)-**432**, which could be isomerized into optically active (–)-**173**. One-pot reaction of

(+)-**431** with barbituric acid in boiling BuOH yielded directly optically active (–)-**173** in 74% yield (09JA3991).

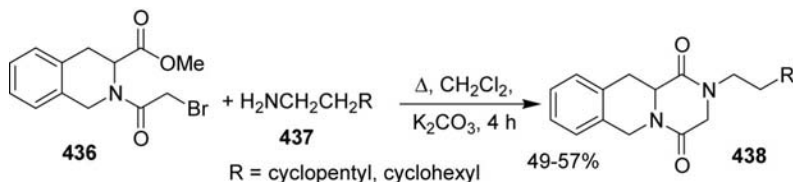


The Knoevenagel condensation of aldehyde **433** with cyanothioacetamide followed by cyclization in boiling BuOH yielded hexahydro-1*H*-pyrazino[1,2-*a*]quinoline **291** (08CHE759). Cyanoacetamide gave only condensation product under similar conditions.



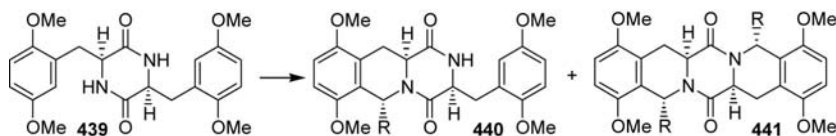
Reaction of tetrahydroisoquinoline-3-carboxylic acid **434** with primary amines and isonitriles provided 1,2,3,4,11,11*a*-hexahydro-6*H*-pyrazino[1,2-*b*]isoquinolin-1-ones **435** (06HEC107).

Cyclocondensation of (*S*)-2-(2-bromoacetyl)tetrahydroisoquinoline-3-carboxylate **436** with amines **437** gave (*S*)-1,2,3,4,11,11*a*-hexahydro-6*H*-pyrazino[1,2-*b*]isoquinoline-1,4-diones **438** (06T4408).

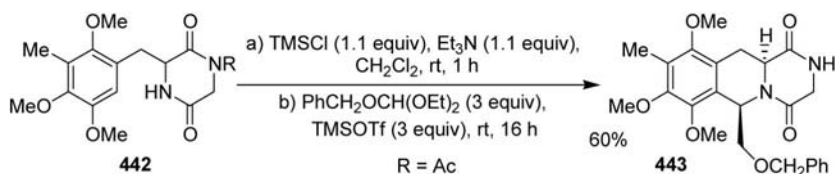


Stereoselective Pictet–Spengler cyclization of piperazine-1,4-dione **439** with MeCHO and EtCHO on the action of a 1–3:5 mixture of CF_3CO_2H and

AcOH at 70–80 °C for 4–16 h was investigated (07T8781). Usually, a mixture of tricyclic **440** and pentacyclic **441** compounds were obtained.

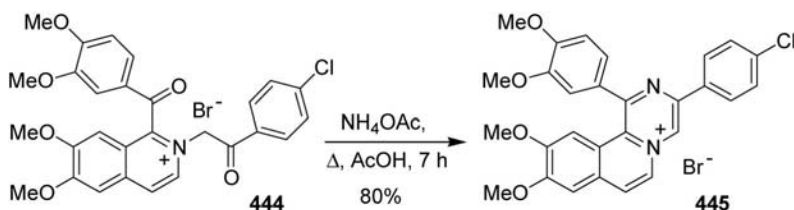


1,2,3,4,11,11a-hexahydro-6*H*-pyrazino[1,2-*b*]isoquinoline-1,4-dione **443** was prepared in a one-pot procedure from perhydropyrazine-2,5-dione **442** (R = Ac) through *in situ* activation of the C(4)-lactam of **442** to a *O*-trimethylsilyl-lactim with TMSCl followed by the treatment with PhCH₂OCH₂CH(OEt)₂ in the presence of TMSOTf (08BMC9065).



Reaction of the methyl derivative of **442** (R = Me) with (H₂CO)_x and MeCHO (both 10 equiv.) in a 1:4 mixture of AcOH and TFA under reflux for 1–6 h provided 2,9-dimethyl-7,8,10-trimethoxy-2,3,4,6,11,11a-hexahydro-1*H*-pyrazino[1,2-*b*]isoquinoline-1,4-dione and its *trans*-6*H*,11a*H*-6-methyl derivative in 85% and 54% yields, respectively [08H(76)1497]. Similar reaction with OHCCO₂Et gave only a few percent (6–8%) of 6*H*,11a*H*-6-ethoxycarbonyl derivative, even for a much longer reaction time, 120 h.

The treatment of quaternary salt **444** with excess NH₄OAc in boiling AcOH gave pyrazino[2,1-*b*]isoquinolinium salt **445** (06RJO776).



For some more examples see Section 4.3.2.

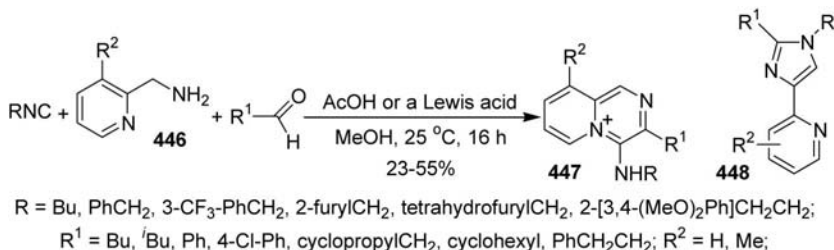
4.3.7 By the formation of three bond from [3+2+1] atom fragments

For reaction of dimethyl *cis*-2*H*,6*H*-piperidine-2,6-dicarboxylate, BrCH_2COCl in the presence of Na_2CO_3 at 0°C , then the treatment of the reaction mixture with the aqueous conc. NH_4OH solution afforded methyl *cis*-6*H*,9*aH*-1,4-dioxoperhydropyrido[1,2-*a*]pyrazine-6-carboxylate in 83% yield (07USA2007/037816, 07USA2007/037817).

In a multicomponent reaction 1,11*b*-dihydro-[1,4]thiazino[3,4-*a*]isoquinoline-1-imine **176** was obtained in 32% yield, when 2-[2-(4-bromophenyl)-2-oxoethyl]isoquinolinium bromide was reacted with 4-CNPhSCN in the presence of diethylaminomethyl polystyrene in CH_2Cl_2 overnight at room temperature, then 4-ClPhNC was added into the reaction mixture, which was heated under microwave irradiation at 90°C for 6 h (08S1688).

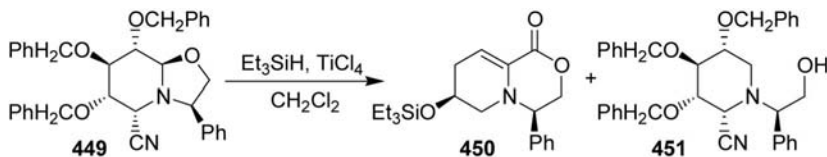
4.3.8 By the formation of three bond from [4+1+1] atom fragments

A three-component one-pot condensation of 2-aminomethylpyridines **446**, aldehydes, and isocyanides afforded 3-substituted 4-aminopyrido[1,2-*a*]pyrazinium salts **447** (05OL2517) and not 4-(2-pyridyl)imidazols **448**, as was stated earlier (05OL39).

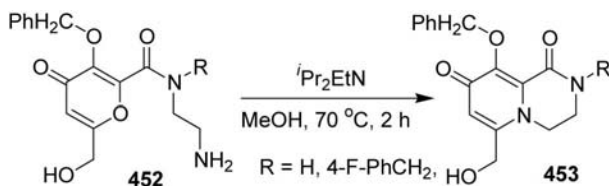


4.3.9 Ring transformation

The treatment of oxazolo[3,2-*a*]pyridine **449** with Et_3SiH in the presence of TiCl_4 afforded two different products depending on the reaction temperature (07TA1585). At 0°C 1,3,4,6,7,8-hexahydropyrido[2,1-*c*][1,4]oxazin-1-one **450** was the product in 35% yield, while below -40°C piperidine derivative **451** was obtained.



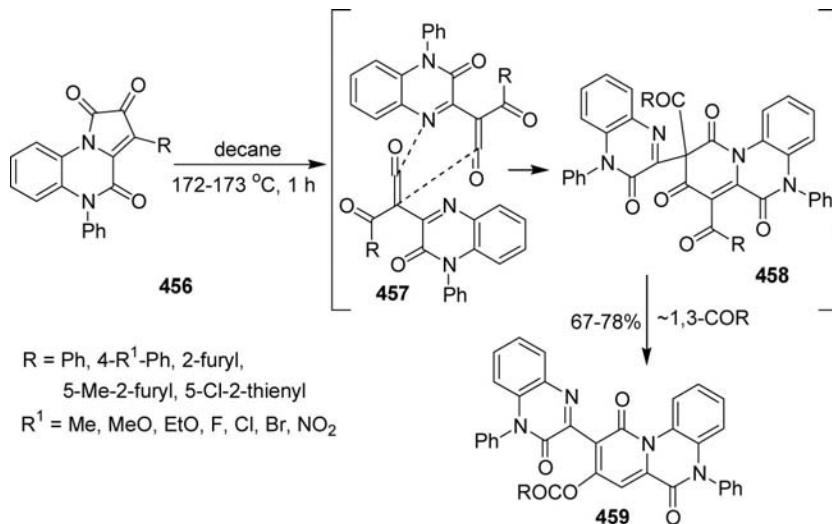
Heating 4*H*-pyran-2-carboxamides **452** in MeOH in the presence of Hünig's base at 70 °C provided 3,4-dihydro1*H*,8*H*-pyrido[1,2-*a*]pyrazine-1,8-diones **453** (06WOP2006/066414).



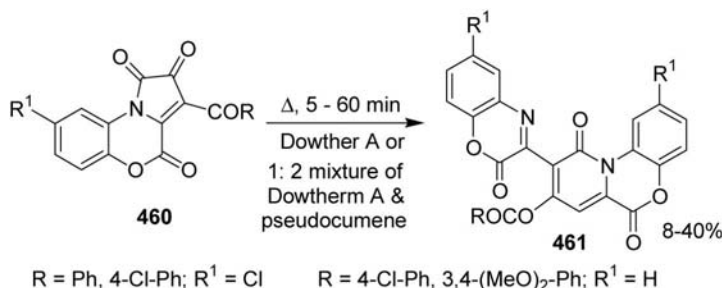
Oxidation of dihydroxy-pyrroloisoquinolines **454** with NaIO₄ in aqueous MeCN provided cyclic hemiacetals **455** (R¹ = H) (08T2321). When the oxidation was carried out in aqueous MeOH methoxy derivatives of **455** (R¹ = Me) were obtained. 10*b*-(*R*) epimers of **454** yielded similarly 11*b*-(*R*) epimers of **455** (R = *c*-hexyl, ^{*i*}Pr; R¹ = H, Me).



Heating tetrahydropyrrolo[1,2-*a*]quinoxaline-1,2,4-trione **456** in decane at 172–173 °C provided 5,6-dihydro-10*H*-pyrido[1,2-*a*]quinoxaline-6,10-dione **459** via the [4+2] cycloaddition of primarily formed ketene **457** followed by the 1,3-migration of the COR group of **458** (05RJO1081).

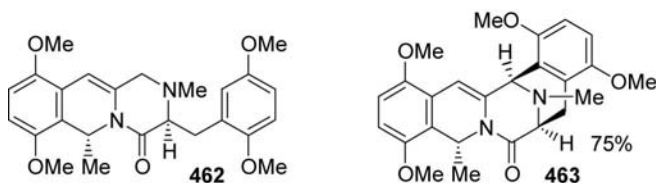


In a similar reaction of tricycles **460** afforded 6*H*,10*H*-pyrido[2,1-*c*][1,4]benzoxazine-6,10-diones **461** (05RJ01222).



Tetracyclic compound **249** was converted to 1-ethylthio-1,2,3,4,11,11*a*-hexahydro-6*H*-pyrazino[1,2-*b*]isoquinolin-4-one **203** ($\text{R} = \text{Br}$, $\text{R}^1 = \text{R}^2 = \text{H}$, $\text{R}^3 = \text{Me}$, $\text{R}^4 = \text{Cbz}$) by treatment with EtSH in the presence of $\text{Hf}(\text{OTf})_4$ in CH_2Cl_2 at ambient temperature for 15 h in 88% yield (08JA7148).

Hydrogenation of pentacyclic compound **257** over Pd/C catalyst in MeOH, followed by an *in situ* *N*-methylation with H_2CO afforded a 1:4 mixture of *N*-methyl derivatives of tricyclic **462** and pentacyclic **463** ring systems (07T8781).

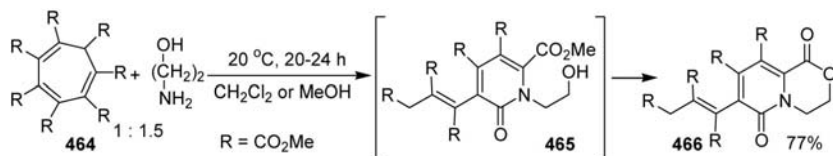


For some more examples see Section 4.3.7.

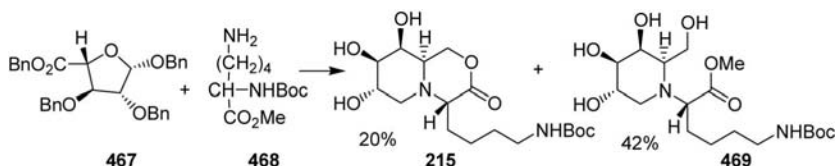
4.3.10 Miscellaneous

The asymmetric Rh-catalyzed [2+2+2] cycloaddition of 4-methoxyphenylacetylene and 3-(2-isocyanatoethoxy)prop-1-ene in the presence of $[\text{Rh}(\text{C}_2\text{H}_4)_2\text{Cl}]_2$ (5 mol%) and (3*aR*,8*aR*)-*N,N*,2,2-tetramethyl-4,4,8,8-tetraphenyltetrahydro[1,3]dioxolo[4,5-*e*][1,3,2]dioxaphosphepin-6-amine ligand (10 mol %) in refluxing PhMe for 16 h leads to the formation of 6-(4-methoxyphenyl)-1,3,4,8,9,9*a*-hexahydropyrido[2,1-*c*][1,4]oxazin-8-one in 41% yield with 96% enantioselectivity (09JA15717).

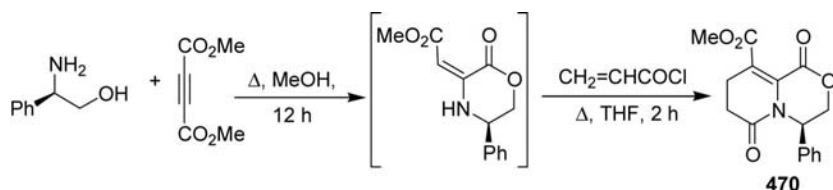
Reaction of 2-aminoethanol with cycloheptatriene-1,2,3,4,5,6,7-heptacarboxylate **464** afforded 3,4-dihydro-1*H*,6*H*-pyrido[2,1-*c*][1,4]oxazine-1,6-dione **466** via 2(1*H*)-pyridone **465** (09TL5605).



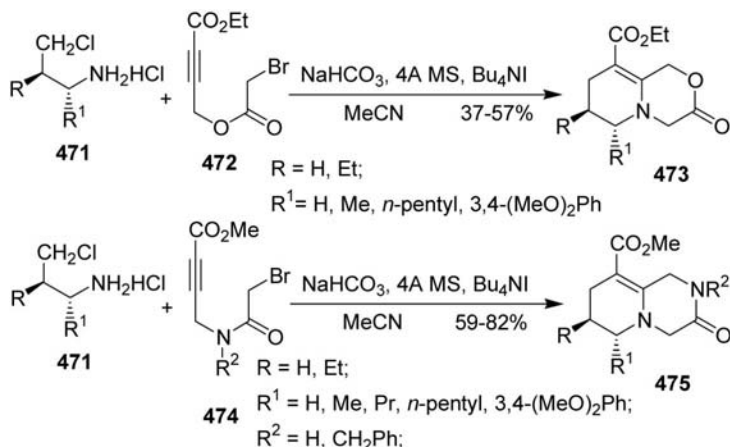
Catalytic reduction of compound **467** over Pd(OH)₂/C catalyst in MeOH for 1 h, then reaction with L-lysine derivative **468** for 24 h gave an inseparable mixture of perhydropyrido[2,1-*c*][1,4]oxazin-3-one **215** and piperidine **469** (08BMC10216).



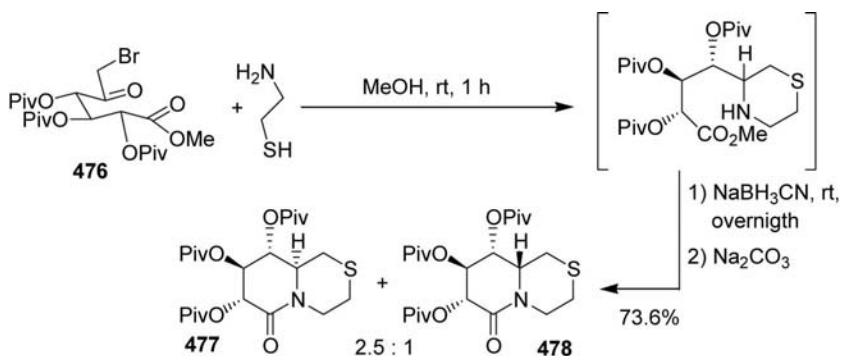
Reaction of (*R*)-phenylglycinol with dimethyl acetylenedicarboxylate in boiling MeOH 12 h, followed by the treatment of the reaction mixture with acryloyl chloride yielded 1,6-dioxo-3,4,7,8-tetrahydro-1*H*,6*H*-pyrido[2,1-*c*][1,4]oxazine-carboxylate **470** (07LOC4).



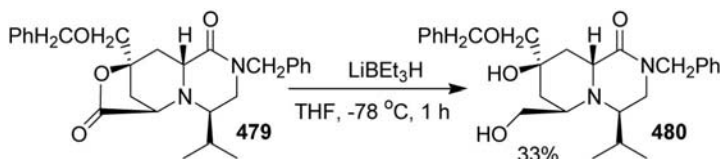
Reactions of γ -chloropropylamines HCl **471** and acetylene compound **472** in MeCN in the presence of a base, 4 Å MS and Bu₄NI afforded 3-oxo-3,4,7,8-tetrahydro-1*H*,6*H*-pyrido[2,1-*c*][1,4]oxazine-9-carboxylates **473** (06T5697). Similar reactions of acetylene derivatives **474** provided 3-oxo-3,4,7,8-tetrahydro-1*H*,6*H*-pyrido[2,1-*a*]pyrazine-9-carboxylates **475**.



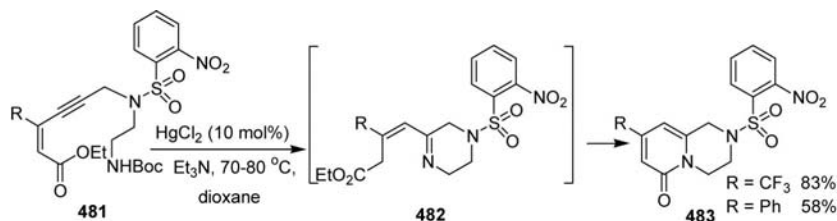
A solution of 2-aminoethanethiol and compound **476** in MeOH was stirred at ambient temperature for 1 h, followed by addition of NaBH₃CN and stirring was continued overnight, and then Na₂CO₃ was added to the reaction mixture to provide a 2.5:1 diastereomeric mixture of perhydro-pyrido[2,1-*c*][1,4]thiazin-6-ones **477** and **478** (06EUP1657244).



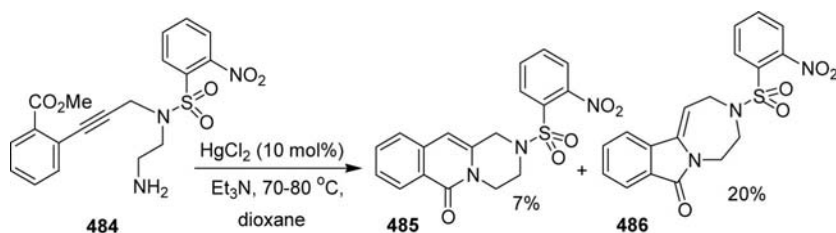
The chemoselective reduction of lactone **479** with LiEt₃H provided diol **480** with recovered starting material **479** (08T11580).



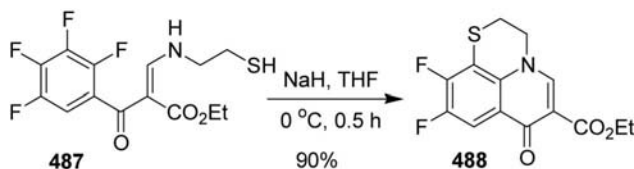
9-Hydroxy-1-methyl-1,2,3,4-tetrahydro-8*H*-pyrido[1,2-*a*]pyrazin-8-one was determined in zymolite of pork by the solid-state phase micro-extraction and gas chromatography-mass spectrometry (05MI37).



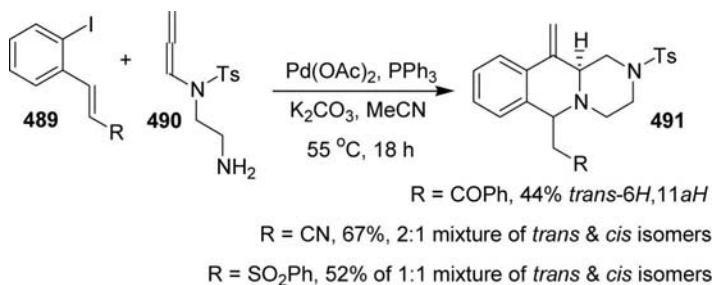
Intramolecular cascade cyclization of compounds **481** in the presence of catalytic amount of HgCl_2 gave 1,2,3,4-tetrahydro-6*H*-pyrido[1,2-*a*]pyrazin-6-ones **483** (09TL4050). NMR investigations indicated that the reaction goes through intermediate **482**, which then cyclized to **483**. In the absence of catalyst, the cyclization was found to be sluggish. When instead of (2- NO_2 -Ph) SO_2 derivative *N*-benzyloxycarbonyl derivative was used, no cyclized product was obtained. Similar reaction of compound **484** provided a mixture of tricyclic compounds **485** and **486**.



The treatment of compound **487** with NaH provided 7-oxo-2,3-dihydro-7*H*-pyrido[1,2,3-*de*]-1,4-benzothiazine-6-carboxylate **488** (08MI93).



Palladium-catalyzed two component cascade cyclization of 1-iodovinylbenzenes **489** and sulfonamide **490** gave 6-substituted 2-tosyl-11-methylene-2,3,4,6,11,11*a*-hexahydro-1*H*-pyrazino[1,2-*b*]isoquinolines **491** (07T6152).

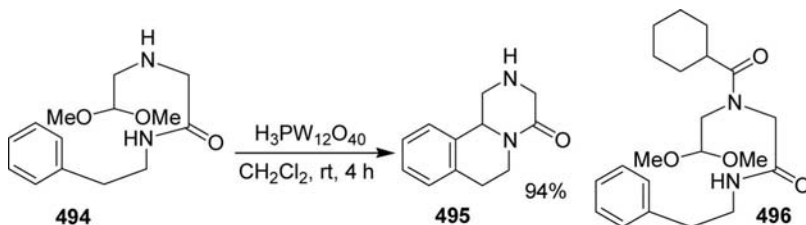


Cleavage of bis-amide **492** from polyethylene glycol grafted polystyrene resin with 20% MeSO_3H afforded 2-acyl-1,3,4,6,7,11*b*-hexahydro-2*H*-pyrazino[2,1-*a*]isoquinolin-4-ones **493** (06TL1287).

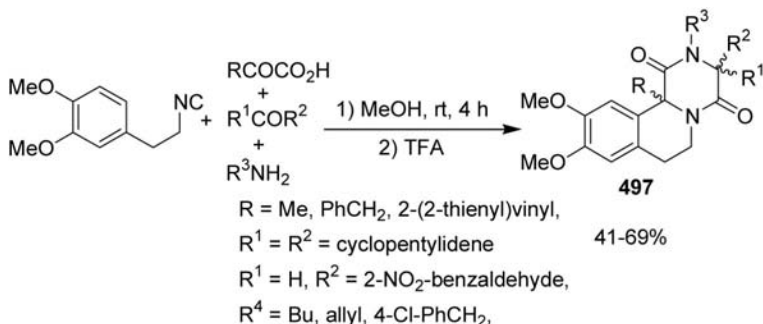
New diketopiperazine alkaloid **2** was isolated from the algicolous aspergillus flavus strain (08PHA323).



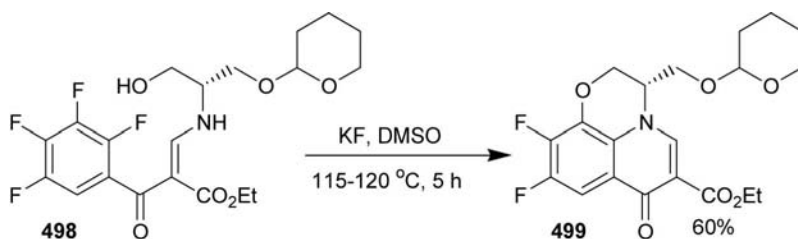
The treatment of acetal **494** with phosphotungstic acid ($\text{H}_3\text{PW}_{12}\text{O}_{40}$) in CH_2Cl_2 at room temperature for 4 h provided 1,3,4,6,7,11*b*-hexahydro-2*H*-pyrazino[2,1-*a*]isoquinolin-4-one **495** (05MIP5). Cyclization of hydrochloride salt of **494** was also carried out in H_2SO_4 at ambient temperature for 3.5 h in 75–98% yield (07WOP2007/119463, 08EJO895, 09MIP9). The treatment of compound **494** with 3 equiv. of MeSO_3H in CH_2Cl_2 in the presence of MgSO_4 at 80°C for 5 h gave compound **495** in 68% yield (09WOP2009/115333). Praziquantel was similarly prepared in 69% yield by cyclization of compound **496** in CH_2Cl_2 in the presence of MeSO_3H (09GEP102008015250, 09WOP2009/115333).



The diastereomeric mixture of 1,3,4,6,7,11*b*-hexahydro-2*H*-pyrazino [1,2-*b*]isoquinoline-1,4-diones **497** was prepared in four-component Ugi/Pictet–Spengler two-step procedure when aldehydes/ketones, α -ketoacids, 2-(3,4-dimethoxyphenyl)ethyl isocyanide and primary amines were stirred in MeOH, and then the evaporated reaction mixture in TFA (07SL500).

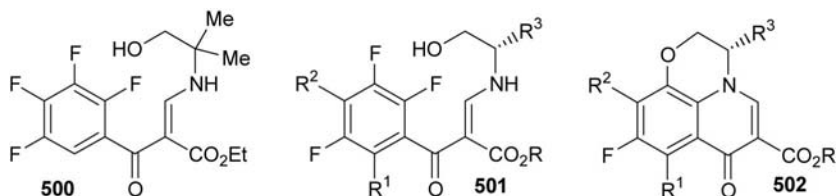


Heating enamine **498** in DMSO in the presence of KF at 115–120 °C afforded 7-oxo-2,3-dihydro-7*H*-pyrido[1,2,3-*de*][1,4]benzoxazine-6-carboxylate **499** (06WOP2006/009143, 08JMC3238).



For double cyclization of enamine **500** in DMSO in the presence of K_2CO_3 at 70 °C for 4 h, at 120 °C for 2 h yielded 7-oxo-2,3-dihydro-7*H*-pyrido[1,2,3-*de*][1,4]benzoxazine-6-carboxylate **374** in 75% yield (05MIP2). When enamine **500** was treated with crushed pellets of KOH under ice-cooling for 1.5 h, 10% aqueous KOH was added and the reaction mixture was heated at 85 °C for another 2 h the appropriate 9,10-difluoro-3,3-dimethyl-7-oxo-2,3-dihydro-7*H*-pyrido[1,2,3-*de*][1,4]benzoxazine-6-carboxylic acid was obtained in 83% yield (09WOP2009/035634). 7-Oxo-2,3-dihydro-7*H*-pyrido[1,2,3-*de*][1,4]benzoxazine-6-carboxylate **502** ($\text{R} = \text{Et}$, $\text{R}^1 = \text{H}$, $\text{R}^2 = \text{F}$, $\text{R}^3 = \text{Me}$) and its racemic form was obtained similarly from

501 ($R = \text{Et}$, $R^1 = \text{H}$, $R^2 = \text{F}$, $R^3 = \text{Me}$) (05MIP4, 06WOP2006/048889, 07MIP7, 08MI92, 08MIP3, 09MIP2) and its racemic form (05MIP4, 09MIP2), respectively. By heating compound **501** ($R = \text{Et}$, $R^1 = \text{Me}$, $R^2 = \text{F}$, $R^3 = \text{H}$) in MeCN at 65 °C in the presence of K_2CO_3 for 16 h, mixed the reaction mixture with 10% aqueous solution of KOH and stirring at 90 °C gave carboxylic acid **502** ($R = \text{H}$, $R^1 = \text{Me}$, $R^2 = \text{F}$, $R^3 = \text{H}$) in 80% yield [07JAP(K)2007/210914]. Methyl ester of racemic derivative of **501** ($R = R^3 = \text{Me}$, $R^1 = \text{H}$, $R^2 = \text{F}$) was cyclized by treatment with NaH in refluxing dioxane for 4 h to afford methyl ester of racemic **502** ($R = R^3 = \text{Me}$, $R^1 = \text{H}$, $R^2 = \text{F}$) in 76% yield (06SL963). Heating enamine **501** ($R = \text{Et}$, $R^1 = R^2 = R^3 = \text{H}$) in DMF in the presence of DBU at 70 °C for 2 days provided **502** ($R = \text{Et}$, $R^1 = R^2 = R^3 = \text{H}$) in 87% yield (06WOP2006/050943). For the treatment of the phenyl derivative of compound **501** ($R = \text{Et}$, $R^1 = R^2 = \text{F}$, $R^3 = \text{Ph}$) in THF with NaH (60% inoil) at 0 °C for 0.5 h, 1 h at room temperature, and finally at reflux temperature afforded 3(*S*)-phenyl derivative **502** ($R = \text{Et}$, $R^1 = R^2 = \text{F}$, $R^3 = \text{Ph}$) in 24% yield (07WOP2007/106537). 3(*S*)-benzyl derivative **502** ($R = \text{Et}$, $R^1 = \text{F}$, $R^3 = \text{CH}_2\text{Ph}$) was obtained in 26% yield by the cyclization of enamine **501** ($R = \text{Et}$, $R^1 = R^2 = \text{F}$, $R^3 = \text{CH}_2\text{Ph}$) in the presence of NaH in DMSO at 90 °C.



Enantiomers of 3-[(4-aminopiperidin-1-yl)methyl]-5-oxo-2,3-dihydro-5*H*-pyrido[1,2,3-*de*][1,4]benzoxazine-10-carbonitril and 10-methoxy-3-((4-[(3-oxo-3,4-dihydro-2*H*-pyrido[3,2-*b*][1,4]oxazin-6-yl)methylamino]piperid-1-yl)methyl)-2,3-dihydro-5*H*-pyrido[1,2,3-*de*][1,4]benzoxazin-5-one were separated by chiral HPLC (08WOP2008/120003).

4.4 Applications and important compounds

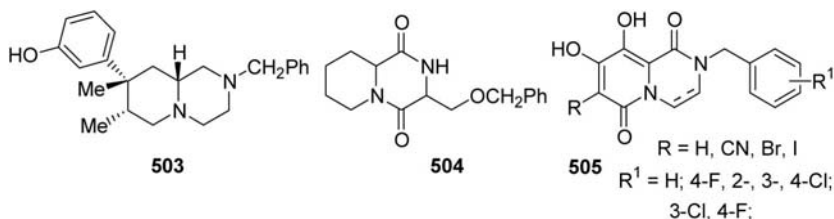
Optically active pipercolic acids were synthesized via perhydropyrido[1,2-*a*]pyrazin-1-ones to control their stereochemistry (05TA3858, 07LOC4, 07TA1585, 08JOC6877).

Three diketopiperazines **165** were isolated from the cell-free culture supernatant of the Antarctic psychrophilic bacterium *P. haloplanktis* TAC125 (05MI34). Xylogranatinin (9-hydroxy-3-methoxy-6*H*-pyrido[1,2-*a*]pyrazin-6-dione) was isolated from the fruit of a Chinese mangrove

Xylocarpus granatum (07NPO426) and from *Solanum cathayanum*, a folk medicine of Hubei Provance (China) (08CCCL68).

1,2,3,4,11,11a-Hexahydro-6*H*-pyrazino[1,2-*b*]isoquinolines are advanced intermediates in the total synthesis of different alkaloids [(–)-lemonomycin (2006SL1691, 2008SL2443), (–)-quinocarcin (05JA16796), (–)-cribrostatin 4 (renieramycin H) (07AGE3962), (–)-renieramycin G (09T5709), (–)-quino-carcin (08JA7148)] and asymmetric synthesis of lemonomycinone amide (09JOC2046).

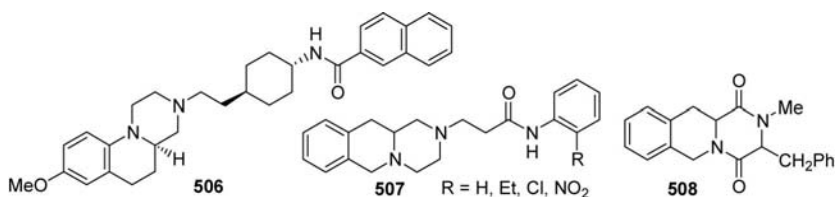
2-(4-Chloro-5-cyclopentyloxy-2-fluorophenyl)perhydropyrido[1,2-*a*]pyrazine-1,4-dione exhibited significant herbicidal activity (05MOL1119). 4-[4-(Perhydropyrido[1,2-*a*]pyrazin-2-yl)phenylamino]-2,3-dimethylquinoline had a good antagonist potency against the α_{2c} -adrenoceptor with excellent subtype selectivity over α_{2A} - and α_{2B} -adrenoceptors (06JMC6351). 2-[3-[4-(*o*-*N*-Propylaminocarbonylphenyl)piperazin-1-yl]propyl]perhydropyrido[1,2-*a*]pyrazine-1,4-dione was found to be inactive on 5-HT₁ serotonin receptor in a virtual screening-like experiment (06JMC205). Perhydropyrido[1,2-*a*]pyrazine **503** exhibited high affinity toward the μ -opoid receptor ($K_i = 0.47$ nM), potent *in vitro* antagonistic activity ($IC_{50} = 1.8$ nM) and improved binding selectivity profile μ/κ and μ/δ to compare to its perhydroquinolizine analog (06JMC7290). Perhydropyrido[1,2-*a*]pyrazine-1,4-dione **504** preferentially interacts with the S100B region of S100 proteins, over the S100A13 region (07CHM1648).



Pyrido[1,2-*a*]pyrazine-1,6-diones **505** exhibit potent HIV-1 integrase inhibition (07BML5595). In a quantitative structure–affinity relationship of 5-HT_{1A} ligands the contribution of 1,4-dioxoperhydropyrido[1,2-*a*]pyrazin-2-yl fragment to affinity 5-HT_{1A} receptors was also estimated (08SQE213). Sunepitron anxiolytic drug was also including into the studied compounds during the assessment of three human *in vitro* systems (pooled human liver microsomes, liver S-9 fraction, and hepatocytes) in the generation of major human excretory and circulating metabolites (09CRT357).

(2*R*,4*S*,4*aS*)-Enantiomer of spiro[1,4]oxazino[4,3-*a*]quinoline **173** is a promising member of a novel class of antibacterial agents with novel mechanism of action (09JA3991).

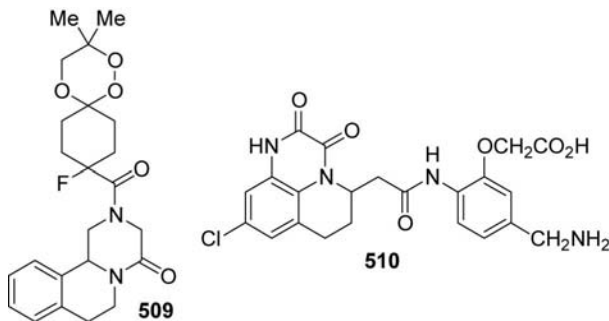
In vitro antitrypanosomal activity of 3-nitro-6,6*a*,7,8,9,10-hexahydro-5*H*-pyrido[1,2-*a*]quinoxalin-6-one was in agreement with the theoretical prediction (06BML1898). 2-Substituted derivatives of 6,6*a*,7,8,9,10-hexahydro-5*H*-pyrido[1,2-*a*]quinoxalin-6-ones **392** exhibited promising cytotoxic activities toward HaLaS3 cell lines (09BML4119). 2,3,4,4*a*,5,6-Hexahydro-2,3,4,4*a*,5,6-hexahydro-1*H*-pyrazino[1,2-*a*]quinoline **506** (08JMC5905) and its derivatives, containing bicyclic heterocyclic-carbonyl moieties, instead of 2-naphthylcarbonyl group (06BML443), are potent and selective D3 ligand.



1,2,3,4,11,11*a*-Hexahydro-6*H*-pyrazino[1,2-*b*]isoquinolines **507** exhibit potent antihistaminic H_1 activity (06BMC8249). 1,2,3,4,11,11*a*-Hexahydro-6*H*-pyrazino[1,2-*b*]isoquinoline-1,4-dione **508** was included into a set of compounds to study the transport across the blood-brain barrier (07JA11802). The *in vitro* antitumor potential of 1,2,3,4-tetrahydro-6*H*-, 1,2,3,4,11,11*a*-hexahydro-6*H*-pyrazino[1,2-*b*]isoquinolin-4-ones and 1-hydroxy-1,2,3,4,11,11*a*-hexahydro-6*H*-pyrazino[1,2-*b*]isoquinolin-4-ones was explored in three cancer lines (08BMC9065). *In vitro* cytotoxicity of 3-(2,4-dimethoxyphenyl)methylene and 3-(2,4-dimethoxyphenyl)methyl derivatives of *cis*-6*H*,11*aH*-6-methyl-7,10-dimethoxy-1,2,3,4,11,11*a*-hexahydro-6*H*-pyrazino[1,2-*b*]isoquinoline-1,4-dione and *cis*-6*H*,11*aH*-2-acetyl-6-phenyl-7,10-dimethoxy-2,3,4,6-tetrahydro-1*H*-pyrazino[1,2-*b*]isoquinoline-1,4-dione was investigated (07BMC112).

Praziquantel has been used for the treatment of schistosomiasis and other trematode-inflicted diseases since the 1970s, as an orally active drug (06MI68). It was suggested to use the active component of racemic praziquantel, the (*R*)-enantiomer, in schistosomiasis treatment, which is significantly less bitter (09PLN1). The oral bioavailability of praziquantel was enhanced by incorporation into solid lipid nanoparticles (09PHA86). Praziquantel is capable of inhibiting P-glycoprotein-mediated efflux in Caco-2 cells (06EJP70). The 1,2,4-trioxane pharmacophore unit of antimalarial artemisinin and pyrazinoisoquinolinone moiety of praziquantel

were unified within single molecules, for example, **509**, and the activities of new molecules were evaluated in mice infected with *Schistosoma mansoni* (08EJO895).



Alkaloid **2** was isolated from the *Aspergillus flavus* strain, collected in Putian, Pinghai, China, and its weak cytotoxic activity was reported against HL-60 cell line (08PHA323). 3,4,11,11a-Tetrahydro-1H,6H-[1,4-oxazino[4,3-b]isoquinoline was patented as selective cytochrome P450 2A13 isoenzyme inhibitor (09USA2009/0137592, 09WOP2009/070579). 2,3,6,7-Tetrahydro-1H,5H-pyrido[1,2,3-de]quinoxaline-2,3-dione **510** exhibited NMDA receptor antagonist activity, and has shown efficacy in several animal stroke models using intravenous infusion protocols (06CTM733).

Antofloxacin, a new member of fluoroquinolonone antibacterial agent was introduced into the human therapy in 2009 in China. Fluoroquinolones, for example, ofloxacin were proved to be effective ligands in the Heck reaction (08MI95). Reaction between butyl acrylate and 4-bromobenzonitril afforded butyl *trans*-4-cyanocinnamate in the presence of 0.1 mol% of Pd(OAc)₂, 0.2 mol% of ofloxacin, and K₂CO₃ in DMA in 91% yield. A composition was developed, containing ofloxacin, for the stabilization of ceruloplasmin (04MIP3). Ofloxacin was found to be a good internal standard for the determination of ciprofloxacin by matrix-assisted laser desorption/ionization mass spectrometry (06RCM1517). Ofloxacin selective electrode was prepared and used in pharmaceutical analysis (08MI96). The trace of Zn²⁺ and Pb²⁺ could be extracted from biological and natural water with ofloxacin-modified-silica gel (08IJE857). Levofloxacin (06MI69) and ofloxacin (07AC8242) imprinted polymers were prepared and used for selective adsorption of levofloxacin and ofloxacin, respectively.

CoMSIA	comparative molecular similarity indices analysis
CPMAS	cross polarization magic angle spinning
d	day
DAST	(diethylamin)sulfur trifluoride
DBU	1,8-diazabicyclo[5.4.0]undec-7-ene
DCC	<i>N,N'</i> -dicyclohexylcarbodiimide
DCN	1,4-dicyanonaphthalene
DDQ	2,3-dichloro-5,6-dicyano- <i>p</i> -benzoquinone
DEAD	diethyl azodicarboxylate
DFT	density functional theory
DIPEA	<i>N,N</i> -diisopropylethylamine
DMAP	4-(dimethylamino)pyridine
DME	1,2-dimethoxyethane
DMF	<i>N,N</i> -dimethylformamide
DMSO	dimethyl sulfoxide
DNA	deoxyribonucleic acid
DSC	differential scanning calorimeter
DTG	differential thermogravimetry
EDC	1-[3-(dimethylamino)propyl]-3-ethylcarbodiimide
EDCI	1-[3-(dimethylamino)propyl]-3-ethylcarbodiimide hydrochloride
Et	ethyl
EtOAc	ethyl acetate
FTIR	Fourier transformed infrared
GIAO/DFT	gauge including atomic orbitals/density function theory
h	hour
HATU	<i>O</i> -(7-azabenzotriazol-1-yl)- <i>N,N,N',N'</i> -tetramethyluronium hexafluorophosphate
HCV NS5B	hepatitis C virus NS5B
HOAt	1-hydroxy-7-azabenzotriazole
HOBt	1-hydroxybenzotriazole
HPh	benzene
HPLC	high-pressure thin-layer chromatography
HPTLC	high-pressure liquid chromatography
ⁱ Pr	isopropyl
IR	infrared
ISIDA	<i>in silico</i> design and data analysis
LAH	lithium aluminum hydride
LC	liquid chromatography
LiHMDS	lithium bis(trimethylsilyl)amide

LDA	lithium diisopropylamide
MDM	1:1:1 mixture of methanol, dioxane, and acetonitrile
Me	methyl
MeCN	acetonitrile
MePh	toluene
MS	molecular sieve
Ms	methanesulfonyl
NBS	<i>N</i> -bromosuccinimide
NCS	<i>N</i> -chlorosuccinimide
NMDA	<i>N</i> -methyl-D-aspartastate
NMR	nuclear magnetic resonance
O-TBS	<i>tert</i> -butyldimethylsilyloxy
Pd(DBA)	tris(dibenzylideneacetone)dipalladium(0)
PDE	phosphodiesterase
Ph	phenyl
PLGA	poly-(lactic-coglycolic acid)
PPA	polyphosphoric acid
Pr	propyl
PS-TPP	polystyryl triphenylphosphine
<i>p</i> TsOH	<i>p</i> -toluenesulfonic acidl
PVC	polyvinylchloride
Py	pyridine
QSAR	quantitative structure–activity relationship
ROESY	rotating frame overhause effect spectroscopy
RP-HPLC	reversed-phase high-pressure thin-layer chromatography
rt	room temperature
TBAF	tetrabutylammonium fluoride trihydrate
TBAI	tetrabutylammonium iodide
TBDMSCl	<i>tert</i> -butyl(chloro)dimethylsilane
TBDMSO	<i>tert</i> -butyl(chloro)dimethylsilyloxy
TBTU	<i>O</i> -(benzotriazol-1-yl)- <i>N,N,N'</i> -tetramethyluronium tetrafluoroborate
^t Bu	<i>tert</i> -butyl
TEMPO	2,2,6,tetramethyl-1-piperidinyloxyI
TFA	trifluoroacetic acid
TG	termogravimetry
THF	tetrahydrofuran
TLC	thin layer chromatography
TMSCl	trimethylsilyl chloride
TOMOCOMD-CARDD	topological molecular computer design-computer aided “rational” drug design

UV

ultraviolet

 μ w

microwave

 μ wave

microwave

ACKNOWLEDGMENT

The author gratefully acknowledges the support through ProProgressio fellowship.

CHAPTER 2

Photochemical and Photophysical Behavior of Thiophene

Maurizio D'Auria

Contents		
	1. Introduction	128
	2. Photophysical properties of thiophene derivatives	128
	2.1 Thienyl derivatives and oligomers	128
	2.2 Condensed thienyl derivatives	150
	2.3 Photophysical properties in organized media	160
	3. Photochemical and photobiochemical properties of naturally occurring thiophenes and related structures	162
	4. Photochemical isomerization	165
	5. Norrish-type I reaction	171
	6. Dimerization	171
	7. Cycloaddition reactions	171
	8. Photochemical reactivity of halogeno-substituted derivatives	179
	8.1 Photochemical coupling of halogeno-substituted derivatives with thiophene	179
	8.2 Photochemical arylation	180
	9. Styrene-like cyclization	196
	10. Photochromism	206
	11. Photolysis of azido derivatives	229
	12. Photopolymerization	230
	13. Optically active thiophene materials	232
	13.1 Oligothiophenes	233
	13.2 Polythiophenes	285
	14. Photooxidation	339
	15. Photochemical cyclization	342

Dipartimento di Chimica "A. M. Tamburro", Università della Basilicata, Via dell'Ateneo Lucano 10, 85100 Potenza, Italy

Advances in Heterocyclic Chemistry, Volume 104
ISSN 0065-2725, DOI 10.1016/B978-0-12-388406-0-00002-6

© 2011 Elsevier Inc.
All rights reserved

16. Photochemistry of thiophene s-oxide and sulphone	343
17. Dihydrothiophenes	350
18. Photochemistry of inorganic complexes	353
References	357

1. INTRODUCTION

The photochemistry of heterocyclic compounds was the object of a book published in 1976 and edited by Buchardt (76MI1). Here, the photochemistry of thiophene covers eight pages written by Lablache-Combier (76MI123). Some reviews have appeared since on the photochemical behavior of pyrrole and furan derivatives (89G419; 96H(43)1305; 96H(43)1529) but apparently none on thiophene photochemistry.

2. PHOTOPHYSICAL PROPERTIES OF THIOPHENE DERIVATIVES

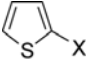
2.1 Thienyl derivatives and oligomers

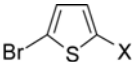
UV properties of some thienyl derivatives appear in Table 1 (59G540) along with some 3-substituted derivatives (58SA350). UV and IR spectra of 2,2'-bithienyl derivatives appear in Table 2 (67T4419; 91JCP(95)4783). Optical spectra of oligothiophene derivatives (n T) with $n = 2-11$ have been studied in solution (93SM(60)23; 94JCP(101)1787; 95JPC16991; 95PAC9; 96JPC18683), in thin films (93JCP(97)7427; 94JCP(101)1787; 98CP(227)33), and in crystals (96CPL(260)125). Spectra of n T in the gas phase have been reported for 1T and 2T (94JCP(98)3031). The absorption and emission spectra show systematic red shifts with increasing size of oligothiophenes (95JPC16991; 96JPC18683; 97SM(87)127). The singlet state energy was found at 29,940 cm^{-1} for 2T to 20,198 cm^{-1} for 7T, while the triplet state energy was found at 18,003 cm^{-1} for 2T and at 12,923 cm^{-1} for 7T (99JCP(111)5427).

Fluorescence-excitation, hole-burning, and dispersed-fluorescence spectra of 2,2'-bithiophene in a supersonic jet were measured (94JPC12893).

In order to obtain information on the torsional potential in the S_0 state, dispersed-fluorescence spectra were measured with the excitation of the origin bands of the main and second component, respectively. The UV spectra of some naturally occurring thienyl, bithienyl, and terthienyl derivatives appear in Table 3 (82PP(35)615). Their spectra were related to their

Table 1. UV spectra of some thienyl derivatives

	λ_{max} (Å)	Log ϵ	λ_{max} (Å)	Log ϵ
X = COOH	2460	3.93	2640	3.76
X = COOCH ₃	2480	3.97	2680	3.86
X = COOC ₂ H ₅	2490	3.95	2690	3.89
X = CONH ₂	2480	3.78	2720	3.87
X = COCH ₃	2600	3.89	2820	3.84
X = CHO	2600	4.02	2850	3.85
X = CH=CH-COOH	2720	4.29	2970	4.27
X = CH=CH-COOCH ₃	2780	3.98	3110	4.26
X = CH=CH-COOC ₂ H ₅	2790	3.98	3110	4.26
X = CH=CH-COCH ₃	2760	3.84	3215	4.29

	λ_{max} (Å)	Log ϵ	λ_{max} (Å)	Log ϵ
X = H	2370	3.96		
X = COOH	2570	3.94	2690	4.00
X = COOCH ₃	2590	3.93	2790	4.09
X = COOC ₂ H ₅	2590	3.95	2785	4.11
X = CONH ₂	2260	3.54	2760	4.06
X = COCH ₃	2680	3.92	2930	4.09
X = CHO	2670	3.91	2955	4.07
X = CH=CH-COOH	2435	3.79	3080	4.30
X = CH=CH-COOCH ₃	2660	3.67	3195	4.36
X = CH=CH-COOC ₂ H ₅	2640	3.68	3190	4.32
X = CH=CH-COCH ₃	2220	3.65	3300	4.26
	2720	3.54		

biological activity, showing that the compounds at the entries 1 and 2 were the most efficient, 3 and 4 intermediate, while 5 and 6 exerted low activity. Other tested dithienylethenes had no effect on enzymic activities (see below) (82PP(35)615). For terthienyl, an absorption maximum was reported at $28,350\text{ cm}^{-1}$ at 298 K; the fluorescence was observed at $23,600\text{ cm}^{-1}$ (99JPC(A)795).

α,ω -Dicyanoterthiophene showed absorption at 325 nm (02MI699).

The UV/Vis and fluorescence spectra of other thienyl derivatives are reported in Figure 1 (85PP(41)1; 89JCP(90)3506; 88H(27)1731; 90G793). 2,5-Bis(2-tellurienyl)thiophene showed absorptions at 406, 391, 328, and 244 nm, while 2,5-bis(2-thienyl)tellurophene has absorptions at 406, 388, 265, and 250 nm (00H(52)159).

The compound with four thienyl rings (4T) showed an absorption at 390.6 nm, 5T at 412.0 nm, and 6T at 429.2 nm (88JCP(89)5535; 99JPC(A)3864). UV/Vis spectra of 4T and 5T films under polarized light are known

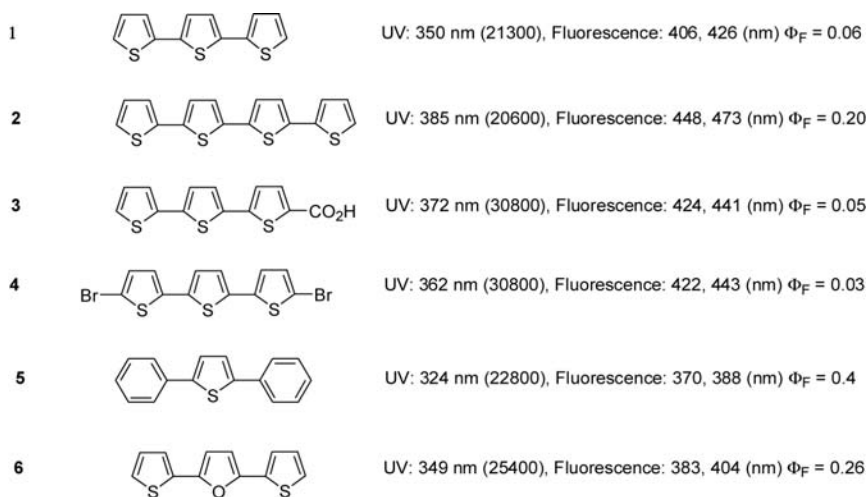
Table 2. UV spectra of some bithienyl derivatives

Compound	UV		Electron transfer band, mμ (ε)
	$\eta-\sigma^*$, mμ (ε)	$\pi-\pi^*$, mμ (ε)	
2,2'-bithienyl	206 (4200)	246 (6400)	301 (12,800)
2,2'-5,2''-Terthienyl	210 (12,420)	252 (9220)	350 (22,650)
5-Formyl-2,2'-bithienyl	207 (7960)	244 (7240)	350.5 (22,400)
5-Acetyl-2,2'-bithienyl	207 (9730)	245 (8710)	348 (21,900)
5-Dichloromethyl-2,2'-bithienyl	210 (10,100)	248.5 (8150)	342 (20,560)
5-Methoxycarbonyl-2,2'-bithienyl	206 (8720)	257 (5610)	332 (19,700)
5-(But-3-en-1-ynyl)-2,2'-bithienyl	210 (12,645)	249 (8820)	341 (22,930)
<i>Trans</i> -5-(4-hydroxybut-1-enyl)-2,2'-bithienyl	210 (9860)	245 (8630)	339-341 (20,300)
<i>Cis</i> -5-(4-hydroxybut-1-enyl)-2,2'-bithienyl	207 (12,700)	243 (9330)	333-337 (20,900)
5-(4-Hydroxybut-1-ynyl)-2,2'-bithienyl	207 (8270)	242 (6580)	328 (22,060)
5-(4-Chloro-3-hydroxy-but-1-ynyl)-2,2'-bithienyl	214 (9540)	245 (9120)	334 (22,280)
5,5'-Diformyl-2,2'-bithienyl	207 (11,100)	260 (6310)	331 (25,120)
5,5'-Diacetyl-2,2'-bithienyl	208 (12,800)	260 (7410)	336 (25,570)
5-Chloro-2,2'-bithienyl	207 (7210)	247 (5880)	358 (24,000)
5-Bromo-2,2'-bithienyl	209 (5590)	249 (5400)	357 (29,500)
5-Iodo-2,2'-bithienyl	210 (6570)	248 (5640)	311 (13,800)
5-Methyl-2,2'-bithienyl	210 (5570)	245 (5820)	311 (13,660)
5,5'-Dichloro-2,2'-bithienyl	206 (5060)	250 (6300)	314 (15,700)
5,5'-Dibromo-2,2'-bithienyl	208 (6320)	255 (6910)	308 (13,230)
5,5'-Diiodo-2,2'-bithienyl	209 (9650)	246 (6740)	318 (16,500)
5-Iodo-5'-methyl-2,2'-bithienyl	204 (9370)	239.5 (6770)	318 (15,210)
5-Chloro-5'-methoxycarbonyl-2,2'-bithienyl	207 (11,780)	245 (7774)	324 (19,880)
5-Bromo-5'-methoxycarbonyl-2,2'-bithienyl	210 (8490)	245 (5950)	320 (17,070)
5-Iodo-5'-methoxycarbonyl-2,2'-bithienyl	210 (10,380)	251 (6750)	339 (18,820)
5-Formyl-5'-iodo-2,2'-bithienyl	210 (11,950)	258 (11,222)	339 (22,230)
5-(But-3-en-1-ynyl)-5'-methyl-2,2'-bithienyl	207 (14,710)	252 (9210)	344 (23,090)
5-(But-3-en-1-ynyl)-5'-methoxycarbonyl-2,2'-bithienyl	207 (15,600)	263 (9010)	350 (27,300)
5-(But-3-en-1-ynyl)-5'-hydroxymethyl-2,2'-bithienyl	207 (12,100)	252 (5220)	358 (23,730)
5-Acetoxymethyl-5'-(but-3-en-1-ynyl)-2,2'-bithienyl	208 (16,700)	252 (9700)	348 (24,400)
			348 (28,200)

Table 3. Absorption maxima and molecular extinctions of some naturally occurring and synthetic thiophenes

Entry	Compound	λ_{max} (nm)	ϵ
1	2,2'-5,2''-terthienyl	350	24,000
2	5-methyl-2,2'-dithienyl	307	13,500
3	5-phenyl-2,2'-dithienyl	337	26,000
4	5,5'-dichloro-2,2'-dithienyl	327	11,560
5	<i>trans</i> -1-(2-thienyl)-2-(5-chloro-2-thienyl)-ethene	347	31,600
6	<i>trans</i> -1,2-di(5-chloro-2-thienyl)-ethene	352	33,100
7	<i>trans</i> -1,2-di(2-thienyl)-ethene	337	28,000
8	<i>trans</i> -1-(2-thienyl)-2-(5-methyl-2-thienyl)-ethene	343	30,600
9	<i>trans</i> -1-(2-thienyl)-2-/3-methyl-2-thienyl)-ethene	342	22,590
10	<i>trans</i> -1-(2-thienyl)-2-(3-thienyl)-ethene	317	26,670

(97AM389) along with UV/Vis spectra from 3T to 11T (91SM(41–43)473). 2,5''-dinitroterthiophene derivatives showed an absorption maximum at 444 nm (03JA2524). The fluorescence quantum yield for 2T is 0.01, for 3T 0.06, for 4T 0.18, for 5T 0.32, and for 6T 0.40 (96SM(76)249). The emission of 5T is at 20,540 cm^{-1} (02SM(127)221). Both the fluorescence quantum yield and fluorescence lifetime increase with increasing oligomer size (93SM(60)23; 95JPC16991; 96JPC18683) from about 0.014 and 51 ps for 2T up to 0.34 and 1018 ps for 6T (93SM(60)23; 95JPC16991; 96JPC18683). The low fluorescence quantum yield is caused by effective intersystem crossing (ISC) connected with a high triplet quantum yield (99% for 2T, 95–93% for 3T

**Figure 1.** Photophysical properties of some terthienyl derivatives.

and 80–70% for 4T (96JPC18683), depending on the solvent). The population of triplets detected in nanosecond flash experiments, in which transient spectra were also measured, were identified as triplet–triplet absorption (TTA) (90PP(52)655).

Laser excitation at 355 nm of deoxygenated 3T (terthienyl) in dichloromethane (absorption maximum at 354 nm) immediately generates a transient with an absorption maximum at 470 nm (94JPC228). This transient corresponds to the triplet state $^3T^*$ with a lifetime longer than 50 μ s.

Similar results have been obtained with 4T (quaterthiophene) in dichloromethane (absorption maximum at 390 nm). The observed transient spectrum appears structured with two maxima at 560 nm and 610 nm. The lifetime of the corresponding triplet $^3T^*$ is on the order of 35 μ s. The excitation of 6T in dichloromethane (absorption maximum at 432 nm) leads to a transient triplet with an absorption maximum at 680 nm and a lifetime of about 24 μ s.

The lifetime and the quantum yield of fluorescence for these three compounds in dichloromethane are 0.135 ns and 0.055, respectively, for 3T, 0.24 ns and 0.16 for 4T, and 1.1 ns and 0.32 for 6T (sexithiophene) (93JPC513). The energy level of the first excited singlet state is 3.12, 2.82, and 2.52 eV, respectively, for 3T, 4T, and 6T.

The molecules have relatively high singlet-to-singlet molar extinction coefficients and high-to-moderate fluorescence quantum yields in all solvents. This demonstrates the π – π^* character of the lowest excited singlet state (85PP(41)1). Upon excitation with 353 nm laser flashes, N_2 -saturated solutions gave rise to intense transient absorption bands. The transient decay rate was strongly increased by the presence of oxygen, suggesting that an excited triplet state had been formed. The bimolecular rate constant (k_c) for this quenching follows a Stern–Volmer law showing that the quenching seems to be mostly physical since it does not give rise to new transient absorption bands.

The excitation profile for two-color 1+1 photoionization of 2,2'-bithiophene seeded in a supersonic helium expansion showed that its two-photon photoionization is significantly enhanced by resonance with the S_1 state, but the observed dynamics clearly show that the dominant channels for photoionization involve long-lived triplet state into which S_1 decays (94JPC4990). To fit the observed temporal profiles, sequential decay of S_1 through two triplet states must be invoked.

The kinetic analysis establishes that the decay rate for the final triplet state is $1.79 (\mu s)^{-1}$ (lifetime = 550 ns) and that both triplet states contribute to the photoionization.

The $(1)^1Bu$ state is the lowest excited singlet state in all α -oligothiophenes from 2T to an including 7T (96JPC18683) while the $(2)^1A_g$ is 6570 cm^{-1} above the lowest state (92JCP(96)2492; 93SM(60)23). The photo-physical properties of these thiophene oligomers are collected in Table 4.

Table 4. Photophysical and Φ_{Δ} data for α -oligothiophenes in benzene (96JPC18683)^a

Compound	Φ_F	τ_F (ns)	k_F^0	k_{NR}	Φ_T	Φ_{Δ}	k_{IC}	k_{ISC}	τ_T (μ s)
2T	0.026	0.046	0.55	21	0.99	0.96	0.11	22	104
3T	0.07	0.16	0.44	5.8	0.95	0.81	0.03	5.9	88
4T	0.18	0.44	0.41	1.9	0.73	0.72	0.20	1.7	38
5T	0.34	0.82	0.41	0.81	0.59	0.56	0.098	0.72	24
6T	0.44	0.97	0.45	0.58		~ 0.36			≥ 17
7T	0.36	0.82	0.43	0.79	≤ 0.6		0.049	0.73	21

^a ks are 10^9 s^{-1}

Table 4 presents comprehensive photophysical data of 2T–7T (di-*n*-butyl), including singlet oxygen quantum yields (ϕ_{Δ}) in benzene. Considering the absorption and emission spectra, there is a relatively small effect of solvent on these maxima. In the fluorescence excitation spectra, there is a considerable red shift, $\sim 1600 \text{ cm}^{-1}$, in the maxima with an excellent linear correlation between $1/n$ and the maximum of the first transition, as well as the 0–0 energy particularly for 4T–7T.

These data plus photophysical results indicate that 2T, and even 3T, are not yet legitimate representatives of a polythiophene and that such a representation seemingly begins with 4T. However, additional consideration of all the photophysical data indicates that the first true representative of a polythiophene is 5T.

Of notable importance, there is almost no red shift ($100\text{--}200 \text{ cm}^{-1}$) in the fluorescence maxima between room temperature and 77 K and no phosphorescence in three different laboratories for $n = 2$ or $n = 3$ at 77 K in various glasses. No phosphorescence was observed for dodecyl-substituted 6T, 7T, and longer ones (94JCP(101)1787). Very interestingly, a weak phosphorescence of thiophene with a maximum at $\sim 430 \text{ nm}$ and a 0–0 band near 362 nm ($27,600 \text{ cm}^{-1}$) was observed.

Considering TTA data, there is a shift of the absorption maximum to progressively longer wavelengths as the number or rings increase.

The ϕ_F and ϕ_T values are remarkably solvent independent, but ϕ_F clearly increases and ϕ_T clearly decreases as the number of rings increase and both become essentially constant from 5T to 7T. The τ_F values are also quite solvent independent, but clearly, the τ_F increases as the number of rings increase, becoming essentially constant from 5T to 7T.

The k_{NR} values show a clear decreasing trend with increasing number of rings, but apparently, k_{NR} attains a nearly constant value from 5T to 7T. Clearly, k_{ISC} decreases with increasing number of rings, reaching a constant value from 5T to 7T.

The $^3\pi \rightarrow \pi^*$ transition in thiophene was found at 3.7 and 4.6 eV (76CPL (41)535). Triplet yields for 3T of 0.2 (85PP(41)1), ≥ 0.9 (90PP(52)655), and

0.95 (93JPP(A)(70)59) exist. Based on all available data, a ϕ_T for 3T of 0.2 cannot be correct. For 4T, a value of 0.2 (85PP(41)1) exists for ϕ_T while values of 0.63–0.73 were found (96JPC18683). On the basis of ϕ_T data and ϕ_Δ for 4T (0.69) (95JF165), ~ 0.2 for ϕ_T of 4T was not correct.

Triplet state lifetimes are shown in Table 4. For 3T, a value of 30 μs in methanol at zero laser dose and concentration has been given (86PP(44)441). Nonetheless, this is much shorter than values ranging from ~ 62 (acetonitrile) to 108 μs (dioxane) (96JPC18683). For 3T and 4T, others (85PP(41)1) reported a value of 57 (3T) and 45 μs (4T) in ethanol while other found values of 91 (3T) and 43 μs (4T) in the same solvent (96JPC18683). The lifetime of 5T in dioxane under nitrogen has been given [95JF165] to be 7.7 μs (0.24 μs in air) (96JPC18683).

Calculations showed that the *trans* conformer of 2T, albeit twisted around the inter-ring bond, is lower in energy (68AX(B)(24)467; 74JA1305; 76CPL(38)489; 93SM(59)259). Some data propose that for 2T in the ground state, both *cis* and *trans* conformers coexist in an 2T-seeded free-jet expansion and that the inter-ring twisting is about the same in both conformers (94JPC3631). The ΔH between *cis* and *trans* was given to be $1.16 \pm 0.13 \text{ kcal mol}^{-1}$ ($406 \pm 46 \text{ cm}^{-1}$) with the *trans* conformer being the more stable. On the other hand, different but parallel supersonic jet experiments (94JPC12893) involving 2T and using the same emission techniques, plus hole burning, point to the existence of a torsionally twisted equivalent pair (a double minimum) around the *trans* conformer in the ground state in place of identifying the coexistence of *cis* and *trans* conformers as done earlier (94JPC3631). In the first excited state by contrast, 2T was found to be *trans* and planar with a deep, steep single minimum torsional potential well around the equilibrium structure. For 3T, higher level calculations (*ab initio*) predict the *tt* conformer as the more stable as does the MM2 approach and with a fairly comparable ΔH . The ΔH between *tt* and *cc* in general seems to be in the $2.0 \text{ kcal mol}^{-1}$ range (± 0.4) for *ab initio* methods. For 4T and 5T, all methods predict the all-*t* conformer as the most stable.

X-ray data of terthiophene (3T) (89SM(30)381) give a clear indication that the *tt* is the more stable: this is the conformer in the crystal with inter-ring angles of about 6° – 9° . Also, a dibutyl-substituted terthiophene has a *tt* configuration (93JA12158) with a higher angle of inter-ring twist than for 3T itself. However, the barrier to rotation was given to be $19.7 \text{ kcal mol}^{-1}$ in the ground state and $4.2 \text{ kcal mol}^{-1}$ in the lowest excited singlet state using ^1H NMR. A reinvestigation (93JA12158) of the same molecule at higher resolution suggested a ground state barrier of 0.5 – 1 kcal mol^{-1} with the excited state barrier similar to that reported earlier. In the case of 5T essentially all the calculation methods give near planar geometry for all-*cis* conformers. Some X-ray data on 4T and 6T (93SM(57)4714) give evidence for an all-*trans*, nearly planar (0 – 10° twist) geometry. There is no reason to believe 5T should be different. For 5T, all the methods of

geometry optimization show that all-*trans* conformer spectral data are very much closer to experimental results than the all-*cis* (96JPC18683).

For 2T, two-photon spectroscopy (92JCP(96)165) has located the ^1Ag above the ^1Bu . Theoretically, it has been predicted (93JCP(98)8819) that the ^1Ag state would be below the ^1Bu state for 2T–4T with crossing between 4T and 5T. Other calculations (94JCP(100)2571) for 1T–4T predicted that the ^1Ag state (0 level) would be below the ^1Bu state (0 level). They believed the ^1Ag state observed was the (3) ^1Ag state. On thiophene, the (2) $^1\text{A}_1$ state was below the $^1\text{B}_2$ (93CPL(211)125). Other calculations (95CP(201)309) used CNDO/S both with single and single plus double CI to calculate transition energies and state orders. Good results compared with experimental results were obtained with single CI but not with single plus double CI. From experimental data, the k_F^0 values in benzene show that the k_F^0 is remarkable constant (96JPC18683). The k_F^0 values for all the α -oligothiophenes in all the solvents only vary from $(0.28\text{--}0.45) \times 10^9 \text{ s}^{-1}$, most values being in a narrower range still. These correspond to τ_F^0 values of 2.3–3.5 ns, which is clearly typical of emission lifetimes from allowed π, π^* states. All these considerations provide experimental evidence that the lowest excited state for 2T–7T is of allowed character and is (1) ^1Bu and not (2) ^1Ag (96JPC18683).

Relative to the question of whether the (1) ^1Bu and (2) ^1Ag state cross and, if so, when, the authors believed crossing might occur between $n = 9$ and $n = 11$ (96JPC18683).

They noted the very significant red shift ($\sim 1600 \text{ cm}^{-1}$) of the absorption maxima of 2T–7T upon going from 298 to 77 K (96JPC18683). All the absorption results were interpreted to mean that for 2T the ground state becomes more planar, as it is for all $n\text{T}$ s, and a greater population of a more singular conformer exists for 2T compared to other $n\text{T}$ s at low temperature. One source of support regards the spectroscopic studied of bithiophene (2T) is a supersonic jet (94JPC12893) where there is a clear indication that in S_1 the 2T is *trans* planar with a single minimum and that a deep, steep potential well exists.

The dependence of ϕ_F on temperature showed that ϕ_F for 2T and 3T clearly increase from 298 to 77 K by 2.9-fold and 2-fold, respectively (96JPC18683). However, there is essentially no change in ϕ_F for the other $n\text{T}$ s (4T–7T). Others (93JPP(A)(70)59) also found a very similar change for 3T and, furthermore, by assuming that the only temperature-dependent process was nonradiative, calculated an activation energy of $\sim 1.2 \text{ kcal mol}^{-1}$. The effect of temperature on ϕ_T of 3T showed little or no change over the range 290–140 K (96JPC18683). Others (93JPP(A)(70)59) believed that the activation energy was for $S_1 \rightarrow T_n$ and that about 55% of the ϕ_T arose from this path.

Significant inter-ring bond torsional (twisting) coupling to the ground state could occur, resulting in a large radiationless rate constant for $T_1 \rightarrow S_0$

with a quenching of phosphorescence emission. Recall that the lifetime of the triplet state undergoes a substantial decrease from 2T to 7T in all solvents by five to tenfold. If the lifetimes are considered to be essentially the radiationless lifetimes, then the radiationless ISC $T_1 \rightarrow S_0$ would strongly dominate and phosphorescence would be "absent." Some two-photon photoionization experiments (94JPC4990) assign the final state as a triplet state. τ_T was 100–146 μ s (solvent dependent) at room temperature in a fluid solution (96JPC18683). The τ_T given for the triplet state of 2T in the supersonic jet experiment was 550 ns (94JPC4990). This triplet lifetime seems to be extraordinarily short for a molecule in a nearly isolated condition presumably without external intermolecular interaction and where, although it is not strictly possible to define the temperature, a temperature in the order of 10 K seems reasonable.

These considerations make very doubtful the assignment of the T_1 triplet state (of 2T) as the state to be associated with the 550 ns lifetime.

Transient absorption study by using femtosecond apparatus appeared (93CPL(211)135) showing that, for all the studied oligomers, a transient absorption band with a lifetime < 1 ps was observed in the spectral region 450–750 nm. Because both absorption and fluorescence decay have the same time behavior in the pico second time region, it was assumed that they come from a common state, the excited singlet state (96JPC18683).

In Table 4, it can be seen that the ϕ_Δ decreases with an increase in the number of rings. Note that for 3T, the efficiency of triplet energy transfer to produce 1O_2 , $\Delta = \phi_\Delta / \phi_T$, is 0.85 while for 2T, 4T, and 5T it is near 1. These results clearly indicate that energy transfer is highly efficient from many oligothiophenes to ground state oxygen. Although the authors are not totally confident about the ϕ_Δ for 7T (or ϕ_T), it appears to be in 0.2–0.3 range, giving a S_Δ that is relatively low (~ 0.5). This may be because of the presence of two *n*-butyl groups preventing efficient encounter transfer and the fact that the triplet is expected to be quite low for 7T (9–12,000 cm^{-1}). The situation for 6T is unclear, although based on ϕ_T data in two solvents for 5T and one for 7T, it seems that ϕ_T for 6T should be in 0.5 area. There are several literature values for ϕ_Δ of 3T: 0.15 (85PP(41)1), ~ 0.8 (95PAC9; 95JF165), 0.73 (90PP(52)655), and 0.6 or 0.86 depending on the technique used (94JPP(A)(83)1) compared with values of 0.81 in benzene and 0.74 in acetonitrile (94JPC18683). The 0.15 value is very probably incorrect (85PP(41)1).

The ϕ_Δ values of other *n*Ts have been given to be ~ 0.7 for 4T, ~ 0.5 for 5T, and ~ 0.36 for 6T (95JF165). Elsewhere, a value of 0.24 has been determined for 4T (85PP(41)1). The ϕ_Δ values of some substituted bithiophenes (acetylenic, olefinic) are known (88G633) and these all seem to be quite low, ~ 0.05 , compared to what we obtain for bithiophene itself, ~ 0.97 .

The primary processes, which take place directly after light absorption, proceed on the picosecond time scale as seen from both time-resolved

fluorescence and pump-probe measurements (93SM(60)23; 94JPC228; 95JPC16991).

The time-resolved spectra of the oligothiophenes (92CPL(192)566; 95JPC16991) were found to consist of excited state absorption (ESA) from the S_1 state to a higher singlet state and of the TTA spectra, which were identical with the TTA spectra observed previously (90PP(52)655; 93JPP(A)(70)59; 94JPC228). The temporal development of the TTA spectra of oligothiophenes was detected by picosecond time-resolved studies (95JPC16991).

The depletion of the state S_1 is mainly due to ISC followed by occupation of the lowest triplet state.

Because of its long lifetime, the triplet state T_1 is able to store energy, which may be essentially for the mechanism of photoconductivity or other photochemical processes, which proceed on a microsecond time scale.

Although the triplet spectra and the ISC quantum yield of oligothiophenes are well characterized, the location of the lowest triplet state T_1 could not be determined in solution and in isolated molecules so far because of a lack of phosphorescence (95PAC9; 96JPC18683). Attempts have also been made to detect an S_0 - T_1 transition by absorption measurements in highly concentrated solutions, but these attempts were not very successful. The only S_0 - T_1 spectrum that has been reported was measured for 3T (90PP(52)655).

The energy of the triplet states of α -oligothiophenes with $n = 1$ -4 monomer units was determined (99PCCP1707).

The results of detailed picosecond time-resolved spectroscopic studies on a series of oligothiophenes with $n = 2$ -6 repeat units was reported (92SM(48)167; 92SM(52)213; 93SM(55-57)4740; 95JPC16991).

The fast rising transient absorption bands which appeared at all thiophene oligomers nT could be identified by their kinetics as transitions from S_1 to higher singlet states.

Whereas the thiophene monomer absorbs at about 250 nm, the oligomer bands are located at longer wavelengths and shift bathochrom with increasing repeat units per molecule due to the lengthening of the conjugated system. The structureless absorption bands exhibit increasing absorption coefficients ϵ with increasing oligomer size. The fluorescence bands also shift bathochrom with size, but they are well structured with a very similar band shape for all nT . The influence of solvents on both absorption and fluorescence spectra is insignificant.

At all studied nT ($n = 3$ -6), the first spectra which arise during absorption of the exciting pulse (FWHM 25 ps) are the induced fluorescence F and the absorption A_1 . With a long delay, the second transient spectrum A_2 appears in the spectral region between F and A_1 . Both these decays of each member of the nT series are identically. The comparison of both fluorescence and absorption decay times demonstrates that the A_1 band of each nT stems from the corresponding fluorescence state S_1 .

The bands A_2 arise during the decay of the corresponding A_1 bands, and then they remain constant in shape and value during observation time of 2 ns. These long-living transients could be identified as triplet absorption bands from the corresponding lowest triplet state T_1 of nT by comparison with the literature. From studies of triplet and fluorescence quantum yield of nT , it can be concluded that nonradiative decay processes are dominated by ISC.

Time-resolved pump-probe experiments, low-temperature phosphorescence spectroscopy of high sensitivity and photodetachment photoelectron spectroscopy (PD-PES) were used. Spectra ΔA of dodecylquaterthiophene showed that immediately after excitation the S_1 - S_0 fluorescence band appears as negative ΔA values and, on the long wavelength side, part of the excited state absorption can be seen. At the spectral region where fluorescence is situated, the TTA emerges. After S_1 depletion, the pure TTA spectrum is detected. The smaller nT shows a similar spectral behavior (95JPC16991). TTA is a transition from the lowest triplet state T_1 to a higher state with an energy difference of about 2 eV.

The measurements of the luminescence of 2T and 3T were performed in dilute ethanolic solutions at 77 K. The fluorescence quantum yields were roughly estimated to be 0.07 (2T) and 0.11 (3T) from the relationship of the fluorescence intensities of dilute solutions at 77 K and room temperature. These results agree with the reported data (96JPC18683). The attempts to measure the phosphorescence were successful for 2T. A weak emission at 600 nm was found. The decay time was determined to be (800 ± 200) μ s. The attempt to measure the phosphorescence of 3T under the same experimental conditions failed.

A very interesting fact is the observation of the second triplet state T_2 near the corresponding S_1 states of 3T and 4T via photodetachment photoelectron spectroscopy (PD-PES). The triplet energies obtained by PD-PES were 2.28 eV for 2T, 1.92 eV for 3T, and 1.76 eV for 4T. The S_1 levels obtained from PD-PES were 3.88 eV for 2T, 3.05 for 3T, and 2.69 eV for 4T. T_2 states determined for the first time by PD-PES were 3.4 eV for 3T and 3.13 eV for 4T.

The results of a picoseconds spectroscopic study of nT are summarized in Table 5 (97JPC107).

Both transient bands, A_1 and A_2 , shift with increasing n to longer wavelengths. The increase of the fluorescence lifetime with n is mainly caused by decreasing triplet formation. Open questions were how fast the occupation of the lowest excited singlet state takes place and whether there are processes to observe during this procedure.

The optical density difference $\Delta D(\lambda, t)$ during and after excitation with 350 fs pulses at 308 nm with subpicosecond delay step was measured. The measurements were performed on nT in solution. For 2T, the maximum of

Table 5. Photophysical properties of oligothiophenes

Compound	UV λ_{max} (nm)	Emission λ_{max} , nm	A_1 λ_{max} , nm	A_2 λ_{max} (nm)	τ (ps)
2T	306		495		51 ± 5
3T	355	408	600	460	135 ± 13
4T	392	450	710	560, 595	531 ± 53
5T	414	483	845	630	880 ± 88
6T	435	507	905		
6T1	426	509	900	680	1018 ± 102

A_1 is located at $\lambda = 495$ nm. The decay of A_1 was found to be single exponential with a decay time of 51 ps. A similar decay time was found for the fluorescence of 2T. A_1 was assigned to absorption from the relaxed S_1 state to a higher electronic state.

For 3T, a broad A_1 band was observed that becomes spectrally narrower within the first picosecond. The maximum of A_1 lies at $\lambda = 600$ nm. Additionally, small positive values of ΔD at very small delay times, indicating a further transient absorption A_0 , were found. The transient behavior of 4T showed that the maximum of A_1 was found at about $\lambda = 770$ nm. It was found that the whole absorption band A_1 decays simultaneously and single exponentially with $\tau = 530$ ps. Positive ΔD values due to an absorption A_0 seem to appear weak at zero decay.

For 5T A_0 decays within about 500 fs, whereas A_1 increases to a terminal value within about 2 ps. The induced fluorescence appears delayed because of the superposition by A_0 . The whole absorption A_1 was found to decay single exponentially with a decay time of about $\tau = 900$ ps.

The results for 6T1 (dodecylsexithiophene) after one-photon excitation are very similar to that of 5T. At first, the transient absorption A_0 was observed. The maximum of the excited-state absorption A_1 was found by picosecond spectroscopy at 900 nm with a decay time $\tau = 1100$ ps. With excitation by two photons ($\lambda_{\text{exc}} = 616$ nm, 80 fs), a broad A_0 band appears first followed by the A_1 and fluorescence bands. A_0 is seen for about 500 fs; later, the fluorescence predominates.

Stimulated fluorescence appears with a delay of about 500 fs relative to the A_1 absorption, although both absorption and fluorescence stem from the same state, proved by decay measurements with picosecond time-resolved spectroscopy. This delayed appearance of stimulated fluorescence is caused by a quickly increasing and short-lived absorption A_0 located in nearly the same spectral range as the fluorescence. The authors assumed that the “instant” absorption A_0 is caused by a state located slightly below the level reached by excitation with 4 eV. This state 2,

occupied by relaxation of the excited state 3, decays down to the known electronic state 1 from which the fluorescence and the ($S_n \leftarrow S_1$)-absorption start.

In the case of 5T and 6T, the excited states with B symmetry near 4 eV can be occupied by allowed one-photon excitation from the A ground state. For 3T and 4T, states of A symmetry lie next to the excited state. They need vibronic coupling to be excited. The initially occurring absorption A_0 is assumed to start from one of the higher electronic states near 4 eV. Relaxation processes from these states may be responsible for the decay of A_0 during the first picosecond and for the delayed increase of stimulated fluorescence of 3T–6T.

A femtosecond-spectroscopic investigation of 3T in solution using wavelengths in the range of the absorption band in the near-UV for excitation and probing has been described (98CPL(292)607). After a few hundred picoseconds, the optical density difference $\Delta D(t)$ reaches a value that remains constant up to the longest delay times of 1.2 ns. The fast time constant τ_1 remains constant within the precision of the measurement and amounts to ≈ 2 ps, the slower one τ_2 decreases with shorter excitation wavelengths, that is, higher energies. At 400 nm, a time constant τ_2 of (126 ± 4) ps was observed, whereas at shorter wavelengths τ_2 is significantly smaller. The decay curves consist of two exponential functions with time constants τ_1 of ≈ 2 ps and τ_2 varying from ≈ 50 to 130 ps.

Another process which has to be considered is the conformation change from the nonrelaxed nonplanar to the planar excited state, which could be connected with a fast increase of absorption. The most important radiationless decay process in oligothiophenes is ISC. Therefore, a fast channel of ISC was suggested, which is effective before the lowest vibronic state of S_1 is occupied. The fast decay of the $\Delta D(t)$ kinetics is caused by an effective formation of triplets.

The excitation with an ultrashort laser pulse populates an electronic state with extremely strong spin–orbit coupling character. If there are triplet levels isoenergetic to S_1 state, an effective ISC would be expected. Therefore, it can be assumed that the ISC is strongly enhanced by coupling between suitable vibrational modes of the singlet and triplet manifold. The fast decay component is mainly caused by an effective ISC mediated by vibrations of the primary excited state and those of the triplet manifold. The successive energy relaxation processes within the triplet ladder are assumed to proceed via vibrational states only, because electronic triplet states near by the S_1 state could not be detected. A fast process of triplet formation in addition to that associated with the known S_1 depopulation characterized by τ_2 was found. The fast ISC process observed is the key to understanding the high triplet quantum yields in thiophene oligomers and polymers.

High-resolution energy-loss spectroscopy (HREELS) spectra of the oligothiophenes 4T through 8T have been reported (94JCP(101)6344; 95JST(348)405).

In typical UV/Vis absorption spectra of thick films, three principal regions of absorption A, C, and E can be distinguished. Absorption band A consists of a high energetic main part forming a broad continuum with the maximum at A_{\max} , which shifts to shorter wavelengths with decreasing film thickness, and a low energetic edge revealing a structure (A_0 , A_1 , A_2 ,...) with spacings of $\approx 1750 \text{ cm}^{-1}$ and of $\approx 1500 \text{ cm}^{-1}$, independent of chain length. The position of the absorption A can be directly related to the S_1 -transition of single molecules dissolved in a polyethylene matrix. The A_0 -peaks of the thick film spectra are red shifted by 1100 cm^{-1} versus the S_1 -transition of the dissolved molecule, while the maximum A_{\max} is blue shifted versus the S_1 -transition of a few thousands of wavenumbers. The second absorption band C can be located only in 6T–8T films, in solution also in 5T.

The optical constants of vapor-deposited films of quinquethiophene (T5) are presented and compared to those of suspensions of colloidal T5 nanoparticles, which serve as model systems for the films [99MI395]. In nanoparticles, the maximum value of the absorption constant in the direction of the optical axis is $k_z = 1.8$. It is reached at $\nu \approx 26,000 \text{ cm}^{-1}$ and is due to the HOMO–LUMO- $(S_{1,1*})$ -transition. The maximum of the absorption constant for the directions perpendicular to the optical axis, $k_x, y = 0.3$, is found at $\nu = 28,500 \text{ cm}^{-1}$, and is probably due to the $S_{1,2*}$ transition.

In film, the absorption maximum at $\nu = 29,500 \text{ cm}^{-1}$, which is blue shifted by $\Delta\nu \approx 5500 \text{ cm}^{-1}$ against the absorption maximum in solution.

Optical spectra with narrow and well-resolved lines can be accomplished when the films are prepared on microscopically clean a structurally defined surfaces (98CP(227)33). 6T film was deposited on a glass substrate at room temperature. Obviously, all peaks are rather broad (about 500 cm^{-1}) which is the main reason why other vibrational modes are not resolved. The vibrational energies are $1430 \pm 30 \text{ cm}^{-1}$ and $1570 \pm 50 \text{ cm}^{-1}$ in emission and absorption, respectively. The mode at 1430 cm^{-1} stems from a ring-breathing mode of the thiophene ring and is systematically found with strong intensity in photoluminescence spectra of isolated and condensed oligothiophenes. The mode at 1570 cm^{-1} is also typical for oligothiophene films and is close to the C=C stretching mode observed for isolated 4T. The highest energy line in emission is found to be about 1645 cm^{-1} below the lowest energy line in absorption (A_0), and is thus strongly red shifted with respect to A_0 . The most likely explanation for this is that a small concentration of structural defects is contained in the film or that very small regions with a different crystal structure (minority phase) are present. These can both act as highly

effective radiative traps in which the exciton energy is significantly lowered due to a modified local packing of the molecules.

The second interesting observation is the appearance of small additional peaks, which are systematically shifted with respect to the dominant photoluminescence lines by 545 cm^{-1} to higher energies. With respect to the lowest energy line in absorption (A_0), this component is also significantly red shifted by 1100 cm^{-1} . The intensity of these peaks increases systematically for smaller film thicknesses.

These traps close to the substrate are related to structural defects, which are generated when the 6T crystallites nucleate on the glass surface.

If the films are prepared on HOPG (highly oriented pyrolytic graphite), the photoluminescence and the absorption spectra both show much narrower peaks. Additional fine structure is thus resolved. This is consistent with the fact that a higher structural order with respect to the film on glass is indeed obtained, leading to a smaller inhomogeneous line broadening.

The lowest energy line belonging to the absorption spectrum of the 6T majority phase is a very weak shoulder at $18,350\text{ cm}^{-1}$. The line a_0 of the dominant trap ($17,325\text{ cm}^{-1}$) is found very close to the position of the above-mentioned small peak at $17,450\text{ cm}^{-1}$ in the absorption spectrum. The important finding is that additional lines (which were not observed on glass) are found at $18,340\text{ cm}^{-1}$ ($0-0$); $17,645\text{ cm}^{-1}$ (v_3); $16,885\text{ cm}^{-1}$ (v_4 , intense); and $15,400\text{ cm}^{-1}$ ($2v_4$). The very small Stokes shift of $<10\text{ cm}^{-1}$ points again to the high structural order in this phase.

At least three different photoluminescence components or species are observed for 6T films on HOPG ($0-0$, b_0 , a_0) with origins at $18,340\text{ cm}^{-1}$; $17,870\text{ cm}^{-1}$; and $17,325\text{ cm}^{-1}$. The two lower energy components are due to rather deep traps, which are very likely related to structural modifications, since their intensity varies for different preparation conditions.

It is likely that oligothiophenes, as many other organic materials, exhibit an intrinsic tendency to form several polymorphic phases, such that small grains of structural minority phases can be easily formed. The respective vibronic energies can be obtained which are in very close agreement ($\Delta E \leq 15\text{ cm}^{-1}$) to those reported for matrix isolated 4T. This result clearly indicates that the observed luminescence come from undistorted 4T molecules.

Contrary to 6T, no indications for an additional luminescence from deep traps are found in the 4T spectra. The reason for this difference between 4T and 6T may be that in the case of 4T one type of structure is energetically more strongly favored than in the case of 6T, possibly due to the reduced molecular size of 4T. In agreement with the above finding, the $0-0$ transition of 4T in photoluminescence ($21,025\text{ cm}^{-1}$) is observed to be in resonance with the lowest line observed in absorption ($21,035\text{ cm}^{-1}$). Since the lines have a considerable overlap, the Stokes shift is below 10 cm^{-1} .

The influence of the crystal lattice on the optical spectra comes into play for the molecules considered here at two points. First, due to the polarization of the local environment the transition energy is shifted with respect to the transition energy, which is observed for the isolated molecules (solvent shift). In the case of 4T, the shift has a size of $(1158 \pm 20) \text{ cm}^{-1}$.

All spectra exhibit a well-resolved fine structure, which broadens at about 1200 cm^{-1} wavenumbers above the onset of absorption. The important point is that a consistent interpretation of the spectra is only possible, if the excited electronic levels of 4T and 6T are split into two components, and the higher energy component (0–0) is the origin of the progressions in the absorption spectra. The lower energy components of the transitions are observed as additional weak lines for 4T and 6T about 150 cm^{-1} below the 0–0 lines.

Solid-state photoluminescence of quaterthiophene was found at 2.43, 2.24, and 2.07 eV (05TSF(474)230).

Fluorescence excitation and fluorescence spectra of bithiophene seeded into a supersonic helium expansion show complete vibronic resolution (94JPC3631). Bithiophene is expected to exist in two isomeric forms. Vibrationally resolved optical spectra of 4.2 K solutions of terthiophene in *n*-decane and bithiophene in *n*-hexane were reported. The electronic spectra of *s-cis* and *s-trans* bithiophene were studied. The S_1 origin excitation energies of bithiophene ($31,203 \text{ cm}^{-1}$ for *cis* and $31,111 \text{ cm}^{-1}$ for *trans*, corresponding to absorption wavelengths of 3214 and 3205 Å, respectively) are significantly lower than that of the thiophene ($41,680 \text{ cm}^{-1}$, corresponding to absorption wavelength 2399 Å) indicating the kind of strong interaction that is only expected if the two rings interact significantly.

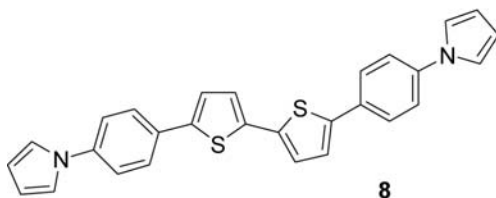
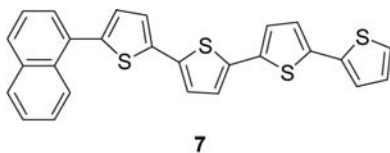
The radical ions of oligothiophenes chemical and electrical generated and also light-induced were investigated in the past few years in order to contribute to the understanding of electrical conductivity of oligo- and polythiophenes. Radical ions of oligothiophene exhibit well-defined absorption bands in the visible and near infrared spectrum; their spectral position remains unchanged by the preparation.

In order to understand the rotational freedom intrinsic to the oligomer so that we may ultimately know the limits to ordering attainable in the synthesis of poly(3',4'-dibutyl-2,2':5',2''-terthiophene) poly(DBTT), the rotational isomerization in the first excited singlet state using fluorescence lifetime measurements has been performed (93JA12158). The S_0 barrier to rotation for DBTT is $19.7 \text{ kcal mol}^{-1}$, and its S_1 barrier to rotation is $4.2 \text{ kcal mol}^{-1}$, showing that the first excited singlet-state barrier to rotation is significantly smaller than the ground-state barrier. The fluorescence lifetime of the oligomer depends linearly on the solvent viscosity.

With time-resolved fluorescence investigations on *n*T the fluorescence quantum yields ϕ_F and the fluorescence lifetime τ_S for the complete series

2T–6T have been determined (95CP(201)309). A computational work in this field appeared (02JCC(23)824). Two photon absorption in thiophene and bithiophene induces triplet formation with a phosphorescence decay within about 20 ps (99SM(101)624).

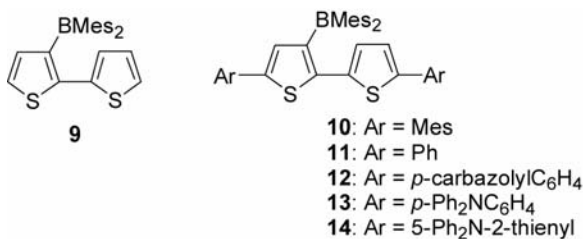
A femtosecond time-resolved study on dodecyl-sexithiophene appeared (94CPL(228)651). A transient absorption forms immediately after excitation and remains stable between 400 fs and 15 ps. Induced fluorescence raised about 400 fs after excitation and increases further up to 15 ps.



Two-substituted naphthalene thienyl oligomers have been characterized for their photophysical properties (09PCCP8706). The compound **7** showed absorption at 405 nm and an emission at 475 and 502 nm. The fluorescence quantum yield was 0.27 and τ_F 0.56 ns. The quantum yield for the internal conversion was 0.05, while the triplet quantum yield resulted to be 0.68.

Phenyl pyrrol-substituted bithiophene **8** showed absorption bands at 308 and 395 nm (08MI122).

While π systems bearing boryl groups generally have strong fluorescence in solution, the introduction of bulky dimesitylboryl groups at the side positions of the electron-donating π framework is, particularly, effective for obtaining fluorescence quantum yields close to unity, even in the solid state (07AGE4273). This property is attributable to two factors: first, the steric bulk of the boryl groups prevents intermolecular interaction. Second, a large Stokes shift resulting from the intramolecular charge-transfer (CT) transition from the electron-donating π system to the electron-accepting boron moiety diminishes the self-quenching in the condensed phase. 3-Boryl-2,2'-bithiophene-based π -conjugated materials **9–14** as a new highly emissive system were described.



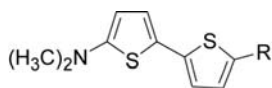
The parent compound **9** showed an intense sky-blue fluorescence with a maximum wavelength of 477 nm (Φ_F 0.66) in THF. To demonstrate its uniqueness, it was compared to its regioisomer 5-dimesitylboryl-2,2'-bithiophene.

The longest wavelength absorption maximum of both compounds are comparable (around 370 nm) in the UV/Vis spectra, although the molar extinction coefficient of **9** is much smaller ($\log \epsilon = 3.65$) than that of the regioisomer ($\log \epsilon = 4.51$). In contrast to this similarity in the absorption spectra, significant differences are observed in the fluorescence properties. First, the wavelength of the emission maximum (λ_{em}) of **9** is more than 40 nm longer than that of the regioisomer. The Stokes shift of **9** exceeds 100 nm (5990 cm^{-1}), whereas that of the regioisomer is only 56 nm (3500 cm^{-1}). Second, the lifetime of the singlet excited state (τ_s) of **9** (12 ns) is much longer than that of the regioisomer (1.7 ns). It is also worth noting that the fluorescence spectra of **9** show only a subtle solvent effect ($\lambda_{em} = 457$ (cyclohexane), 477 (THF), 478 nm (MeOH)), which is indicative of a less-polarized excited state produced by the intramolecular charge-transfer transition, unlike ordinary donor-acceptor-type π -electron system.

The extension of the π conjugation with mesityl (**10**) or phenyl (**11**) groups shifts the emission maximum to 510 nm (green) and 543 nm (greenish yellow), respectively. The introduction of electron-donating carbazolyl (**12**) or diphenylamino (**13**) groups to the terminal phenyl rings causes further red shifts to 557 nm (yellow) and 600 nm (reddish orange). Moreover, the introduction of an electron-donating 5-(diphenylamino)-2-thienyl group further shifts the emission wavelength. Thus, **14** has a deep-red emission at 660 nm with a Stokes shift of 195 nm in THF.

The 3-borylbithiophene derivatives **9–14** show intense fluorescence not only in solution, but also in the solid state. The decrease in the Φ_F value of the spin-coated film relative to that of the THF solution is within 20% for **9** and **10–12** and about 33% and 21% even for the orange-emissive **13** and red-emissive **14**, respectively. No significant difference in the fluorescence spectra of the THF solution and the spin-coated film, in terms of both the emission maximum (FWHM), is observed for all the compounds.

The presence of both donor and acceptor substituents on bithiophene, such as in **15–17**, induces a large shift (95JOC2082).



15: R = CN: λ_{max} 398 nm

16: R = CH=C(CN)₂: λ_{max} 529 nm

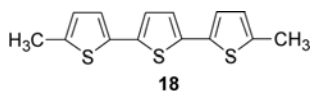
17: R = SO₂CH₃: λ_{max} 389 nm

In a study on substituted terthiophenes, if methoxy substitution induces a bathochromic shift of the absorption and emission bands, it has little or no effect on fluorescence quantum yields and lifetimes of the excited states (93JPC513). The bathochromic shifts induced by the end disubstitution by bromine atoms can be rationalized as previously described for the methoxy groups and thus this substituent effect is only limited at the five first terms of the oligothiophene series.

Only the nitro-substituted oligothiophenes display large bathochromic shifts, large Stokes shifts, high fluorescent quantum yields, and long lifetimes for excited states. As for the other substituents, the trend is mostly noticeable for the short oligomers like terthiophenes and seems to disappear for sexithiophenes. As can be inferred from their solvatochromic effect, an intramolecular charge transfer takes place in the excited states of these molecules.

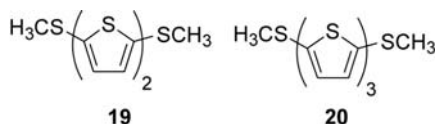
Radical cations of conjugated thiophene oligomers, nT^+ , can be obtained from the photogenerated triplet $^3nT^*$ by electron transfer to an electron acceptor present in the solution, as already described by Scaiano for 3T (89JPP(B)(3)411; 90JA2694). Using tetracyanoethylene (TCNE) as electron acceptor, an electron transfer occurs from $^3T^*$, generating $3T^+$ with a rate constant for electron transfer of $2.3 \times 10^{10} \text{ M}^{-1} \text{ s}^{-1}$. The radical cation $3T^+$ has been characterized by its absorption spectrum, which has an absorption maximum at 550 nm (2.25 eV) in acetonitrile. The absorption spectrum of the radical cation $3T^+$ has a second absorption band located at 850 nm (1.46 eV). These two absorption bands decay following the same second-order kinetics pathway, which corresponds to the back electron transfer from TCNE^{-1} to $3T^+$. The radical cation $3T^+$ is not formed through the triplet state $^3T^*$ but directly from the excited singlet state. $3T^+$ leads directly to a dimer $6T$ by homocoupling and, by further oxidation, to the radical cation $6T^+$.

The cation radicals of terthiophene **18** reversibly dimerize even at low concentration (92JA2728). As a consequence, π -dimers and π -stacks deserve attention as entities responsible for the properties of oxidized polythiophene and other conducting polymers.



During oxidation, the band at 360 nm due to the reactant disappeared and three new bands grew in at longer wavelengths. Several experimental observations indicated that the new absorbance at 572 nm was due to one species (assigned as monomeric cation radical), while the bands at 466 and 708 nm were due to a second species (assigned as a cation radical dimer). Diamagnetic π -dimers can be an alternative to diamagnetic bipolarons as an explanation for the small ESR signal from highly oxidized polythiophenes.

The UV/Vis spectroelectrochemical oxidation of **18** at 21°C shows that as neutral **18** is oxidized in the thin-layer cell, the initial band at 360 nm gives way to four new bands at longer wavelengths (92CM1106). Several experimental observations indicated that the absorbances at 572 nm and >800 nm (beyond the spectrometer range) are due to one species (assigned as the monomeric cation radical, $\mathbf{18}^+$), while the bands at 466 and 708 nm are due to a second species (assigned to cation radical dimer $(\mathbf{18}^+)_2$).



For **19**, the initial absorbance at 356 nm diminishes while new bands grow in at 461, 570, 688, and >800 nm. By using **20**, a set of high-temperature peaks at 665 and 1100 nm was assigned to $\mathbf{20}^+$, and a set of low-temperature peaks at 524, 838, and 1094 nm were assigned to $(\mathbf{20}^+)_2$.

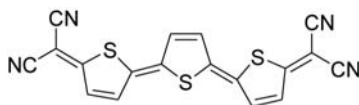
Ng et al. have found that conducting regioregular poly[1,4-bis(3-alkyl-2-thienyl)phenylenes] were strongly fluorescent with a maximum fluorescence yield of 26% and presented a bandgap energy of 2.5 eV (98SM(92)33). The same authors have shown that the fluorescence quantum efficiency of alternating block copolymers, incorporating 3-alkyl-substituted thiophene and aniline repeat units, decreased from about 16% to 5% upon increasing pendant alkyl chain length from methyl to dodecyl, which may be explained by the concomitant decrease of the number of monomeric repeating units (98SM(94)185). Sato et al. have observed the dual photoluminescence of electrosynthesized polybithiophene and polyterthiophene thin films, with emission lifetimes in a few tens and few hundreds of picosecond suggesting the existence of at least two distinct excitons in the films, in agreement with the observation of both amorphous and microcrystalline regions (98SM(95)107).

Also, the optical and photophysical characteristics of poly(3-methoxythiophene) (PMOT) films, electrochemically prepared in an aqueous anionic micellar medium and mainly constituted of hexamers, were investigated (00POLLDG4047; 00SA1391; 02JCP(116)10503). Important solvent

effects on the absorption and fluorescence spectra, and fluorescence quantum yields of PMOT, were determined, leading to quantitative solvatochromic correlations. As a result, the PMOT dipole moment was found to be significantly higher in the first excited singlet state than in the ground state, while the specific solute-solvent interactions included the contribution of notable solvent hydrogen-bond abilities (00POLLDG4047). Strong red shifts of the PMOT absorption and fluorescence emission bands relative to unsubstituted sexithiophene and 3-methoxythiophene suggested a marked electronic delocalization resulting from the methoxy group electrodonating mesomer effect and an extended conjugation in the hexamer singlet excited state (00SA1391). In addition, a significant fluorescence quenching of PMOT takes place in the presence of various quenchers; modified Stern-Volmer relationships were obtained with large bimolecular rate constants (2.7×10^9 – 6.1×10^{11} L mol⁻¹ s⁻¹), which indicates electronic energy migration throughout the PMOT hexamer repeat units. In the case of electrosynthesized composite PMOT-bithiophene (BT) oligomers, electronic absorption and fluorescence spectra properties were found to depend on the bithiophene initial concentration used during electrosynthesis and on the film composition and oligomer chain length; biexponential fluorescence decays were observed (00JF107).

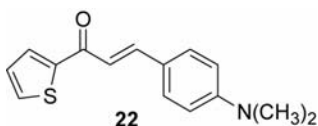
α -Oligothiophenes are able to form self-organized films if the molecules are carefully deposited from the vapor phase on planar metallic or dielectric substrates and if the chain length n exceeds three thienylene rings (96TSF (284/85)267). On metals and graphite, the molecules can be arranged in the monolayer region with their conjugated ring skeleton parallel to the substrate surface. On dipolar substrates such as fused silica, oxidized silicon, or alumina, the molecules can be arranged perpendicular to the surface. The main absorption band was HOMO-LUMO $S_{1,1^*}$ long-axis polarized. Then, the authors observed a HOMO-LUMO+1 $S_{1,2^*}$ short-axis polarized band and a HOMO-1-LUMO+1 $S_{2,2^*}$ long-axis polarized band.

Oligomers with 11 thiophene units showed an absorption maximum at 462 nm (91JA5887). The terthiophene derivative **21** and some other oligothiophene derivatives were studied because the coexistence of an electron-rich moiety (the terthiophene spine) and electron-deficient moiety (the dicyanomethylene groups on either side of the molecule) is expected to cause intramolecular charge-transfer (89BCJ1539; 95BCJ2363; 98BCJ2229; 98JCP(109)2543): the compound showed an absorption maximum at 1.92 eV.

**21**

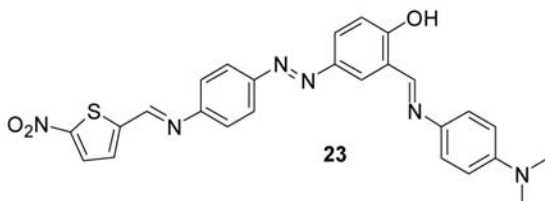
Quinodimethane derivatives of terthiophene and other oligomers showed an absorption maximum at 583–688 nm (02JOC6015; 03OL1535). Bis(dicyanoethylene) oligothiophene derivatives have been characterized and the compound with four thienyl rings showed an absorption band at 790 nm (02JA12380). This type of compounds was used in thin film transistors (see below) (02JA4184).

The thienyl chalcone **22** is an example of a compound with a significant solvatochromic properties (08MI528). It showed absorption at 390 nm in heptane and at 430 nm in DMSO. A crystalline solid gave an excimer-like emission at 570 nm. A dye solution in chloroform gave a good laser emission in the range 480–560 nm with an emission maximum at 530 nm upon pumping by nitrogen laser.



Thienyl-substituted benzoxazoles have been studied for their potential application for fluorescent sensors of metals. They showed absorption bands near 315 nm and emission at 393–394 nm ($\Phi_F = 0.66$ –0.80) (07MI2096). Thienyl-substituted imidazopyridines show absorption bands in the range 309–340 nm and emit in the range 474–533 nm (09T5062). Bithienyl-imidazo-anthraquinone derivatives were studied showing an absorption band at 444 nm (07OL3201).

Thienyl imines have been characterized for their absorption properties and both fluorescence and phosphorescence spectra (09JPC(C)19677). New dyes containing nitrothienyl ring have been described, able to coordinate Cu^{2+} (97DP(33)319; 07DP(75)11). The compound **23** has an absorption maximum at 487 nm and emissions at 537 and 577 nm. Some other azo dyes showed absorptions in the range 581–671 nm (99JCS(P1)3691).



Some others azo dyes containing aminothiophenes with absorptions in the range 485–538 nm were reported (99DP(42)249; 00JCS(P1)4316). Methoxythienyl derivatives showed absorptions over 381–418 nm (08DP

(78)89). A thienyl azo dye with an electron donor (amino group) and an electron withdrawing group (dicyanoethylene) has absorption at 646 nm (08MI973).

2.2 Condensed thienyl derivatives

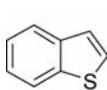
Some benzo[*b*]thiophene derivatives have been studied (99MI259; 05JPP(A)(170)181). Benzo[*b*]thiophene showed absorption bands at 228, 258, 281, 289, 291, and 297.5 nm (56JA549). Its fluorescence properties were measured in ethanol at 77 K, showing 0–0 emission band at 304 nm and emission quantum yields between 0.035 and 0.02 (85ZN497; 89ZN205). Some azo dyes containing benzothiophene ring showed absorption bands in the range 419.2–546.8 nm (97DP(35)219).

Dibenzothiophene emission maxima were found at 427, 450, and 482 nm (73JPC1478; 00TAL807). The singlet excitation energy of dibenzothiophene oxide is 85 kcal mol⁻¹, while the triplet energy of dibenzothiophene is 70 kcal mol⁻¹; the oxide showed a triplet energy of 61 kcal mol⁻¹ and the sulfone a triplet energy of 64 kcal mol⁻¹ (94JPC2282). Triplet states act as channels to decrease the efficiency of a LED device. The introduction of emissive triplets in polymers or copolymers through coupling of known emissive fragments is consequently a valid strategy to improve the emissive response of an organic light-emitting device.

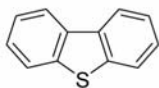
For the molecules **24–26**, the absorption band progressively move to longer wavelength (red shift) with the number of benzene rings, that is, with the “size” of the molecule (08JPP(A)(194)67). In the fluorescence spectra, a red shift of the emission bands is observed with the progressive addition of benzene rings, with **26** presenting the longest wavelength maxima. The values for ϕ_{Δ} (singlet oxygen quantum yields) and ϕ_T are similar for **27–29** indicating that they sensitize singlet oxygen formation with near unit efficiency. However, for **24–26**, and with the exception of **26**, this efficiency is decreased to $\approx 50\%$.

With **26** the $S_1 \rightarrow S_0$, internal conversion deactivation channel becomes operative (inoperative with **25**) which leads to high ϕ_{IC} for **26**. This increase in ϕ_{IC} (from **25** to **26**) is made at the expenses of a decrease of the triplet yield from 0.97 in **26** to 0.66 in **25** and also by a decrease in the phosphorescence quantum yield, ϕ_{Ph} .

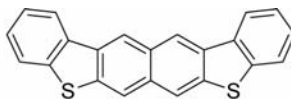
In the case of **27–29**, with the exception of the borderline **28**, the radiative rate constant is one order of magnitude lower than the value found for **24–26**. This observation, together with the longer values obtained for the natural radiative lifetime (see $\tau_F^0 = \tau_F/\phi_F$), is clearly compatible with the forbidden nature of the lowest lying transition/state. The nature of this transition seems to be a π, π^* symmetry forbidden transition/state.

**24**

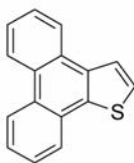
λ_{max} 228 nm
 $\lambda_{\text{F max}}$ 309 nm
 $\lambda_{\text{Ph max}}$ 453 nm

**25**

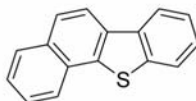
λ_{max} 236 nm
 $\lambda_{\text{F max}}$ 328 nm
 $\lambda_{\text{Ph max}}$ 424 nm

**26**

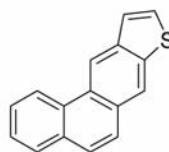
λ_{max} 300 nm
 $\lambda_{\text{F max}}$ 379 nm
 $\lambda_{\text{Ph max}}$ 559, 606 nm

**27**

λ_{max} 262 nm
 $\lambda_{\text{F max}}$ 370 nm
 $\lambda_{\text{Ph max}}$ 495 nm

**28**

λ_{max} 252 nm
 $\lambda_{\text{F max}}$ 347 nm
 $\lambda_{\text{Ph max}}$ 514 nm

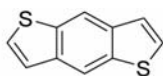
**29**

λ_{max} 279 nm
 $\lambda_{\text{F max}}$ 382 nm
 $\lambda_{\text{Ph max}}$ 499 nm

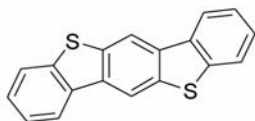
The fluorescence lifetime increases in the order **24**, **25** (\approx **26**), **28**, **29**, **227**. In all cases, the fluorescence decays are single exponentials, indicating that no additional species or quenching (besides internal conversion and ISC) deactivation channels exist during the decay.

Compounds **27–29** display nearly identical phosphorescence spectra (in shape and maxima) and are particularly valid for **29** and **27** where the 0–0 band and wavelength maxima are identical, with the exception of **27** that displays more resolved spectra than **29**. The transient triplet–triplet spectra for **27–29** are different in maxima although similar in shape. This shows that the thiophene unit, when found in a terminal position of the phenanthrene ring, shifts the longer wavelength $T_1 \rightarrow T_n$ transition and yet the relative position of the thiophene ring does not seem to affect the energy of the 0–0 for T_1 . The above data seem to establish that the gradual increase in the π -electron path by adding additional benzene rings does not change the nature of the state order and the relative positions of the S_1 , S_2 , and T_1 states. In **27–29**, the phenanthrene ring seems to determine the relative position of the lowest lying states as well as of the nature of the S_1 state (of forbidden nature).

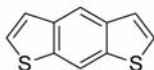
Spectral data for **30** and **31** were also reported (07OL4499).



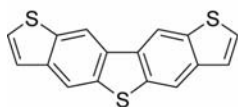
30 λ_{max} 335 nm, E_g 3.6 eV



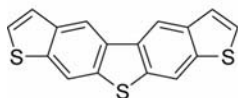
31 λ_{max} 369 nm, E_g 3.3 eV



32 λ_{max} 248 nm; λ_{max}^F 328, 336, 344 nm; Φ_F 0.009
 $\lambda_{\text{max}}^{\text{Ph}}$ 484, 498, 512, 522 nm; Φ_{Ph} 0.1



33 λ_{max} 261 nm; λ_{max}^F 381, 401 nm; Φ_F 0.14
 $\lambda_{\text{max}}^{\text{Ph}}$ 509, 523, 542, 556, 569 nm; Φ_{Ph} 0.04



34 λ_{max} 263 nm; λ_{max}^F 365, 386 nm; Φ_F 0.012
 $\lambda_{\text{max}}^{\text{Ph}}$ 471, 487, 497, 510 nm; Φ_{Ph} 0.56

The fusion of one thiophene ring onto the *f*-bond of benzothiophene results in a 38 (30) nm bathochromic shift of the longest wavelength absorption band of **30** (**31**) (06JPC(A)13754). Two thiophene rings fused on the terminal bonds of dibenzothiophene (**25**) affect a 52 (37) nm bathochromic shift for **33** (**34**). A molecule in the *anti*-orientation shows a greater bathochromic shift, indicating a more effective conjugation in the *antigeometry* compared to the *syn* isomer. A bathochromic shift of emission of 38 nm for *anti*-**30** and 30 nm for *syn*-**32** is observed upon extending the ring system by one thiophene ring.

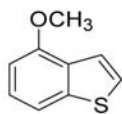
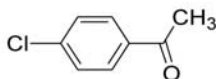
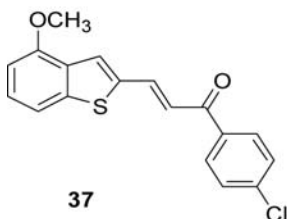
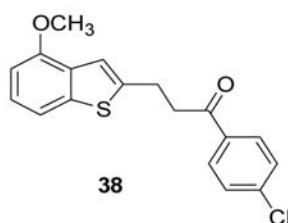
Two thiophene rings result in a shift in the fluorescence of 54 and 38 nm, respectively, for *anti* and *syn* **33** and **34**.

Marginal fluorescence quantum yields (1%) are generally observed though **25** and **33** fluorescence with 8% and 14% yields, respectively. Such low quantum yields are indicative of the effective competition of radiationless processes such as the $S_1 \rightarrow T_1$ ISC and fast internal conversion ($S_1 \rightarrow S_0$). The rate constants for radiative decay of S_1 (k_F) range from 8×10^6 to $1.3 \times 10^8 \text{ s}^{-1}$, and the nonradiative decay rate constants (k_{NR}) range from 1.9×10^8 to $3.5 \times 10^9 \text{ s}^{-1}$. The nonradiative deactivation pathway is thus six times faster than the radiative one for **33** (*anti*) and about 110 times faster for **32** (*syn*).

The phosphorescence emission of **30** is red shifted by 82 nm compared to the emission of **24**, but the emission is only 60 nm red shifted for **32**, while **30** and **33** resulted in a 100 nm bathochromic shift. The phosphorescence lifetimes were about twofold longer in the *syn* isomers compared to the *anti*-isomers. Only a negligible phosphorescence quantum yield of below 5% was observed for *anti*-**30** and *anti*-**33** in a glass matrix at 77 K. Higher phosphorescence quantum yields are observed only for the *syn* (**32** = 0.10, **34** = 0.57). For **24**, **25**, and **34** >40% of the excited molecules decay via phosphorescence.

Femtosecond laser excitation of benzothiophene (**24**) resulted in one broad absorption band with $\lambda_{\text{max}} = 550$ nm. With time, this band decreased, while a new band grew in at 430 nm. The signals are connected by two clear isosbestic points at 400 and 450 nm. The absorption signal at 550 nm was fitted to a lifetime of about 0.35 ns, a value close to the reported fluorescence lifetime of 0.28 ns and was therefore assigned to the decay of $S_1 \rightarrow S_n$ absorption of **24**. The absorption at 430 nm was assigned to the triplet state. Dibenzothiophene (**25**) showed immediately after excitation a strong absorption band at 630 nm, which decayed with a lifetime of 0.9 ns. The signal was connected to the rising signal at 390 nm, with an isosbestic point at $\lambda = 435$ nm and assigned to the triplet state of **25**. Compound **30** exhibited several absorption bands. The decay signal of the negative transient absorption at 350 nm and the decay at 400 nm each had a time constant of 260 ps. Transient absorptions for **25** were detected at 460 and >690 nm. The decaying trace at 755 nm was composed of two components 26 and about 1020 ps. The longer component was assigned to the decay of the singlet excited state. For **33**, the slow rise and decay profiles as observed at 513 and 780 nm could not be fitted due to the long-time constants expected from the long fluorescence lifetime. For **34**, the decay of the singlet state and the rise of the triplet state populations were observed with time constants of 0.57 ns.

An investigation with the electron donor 4-methoxybenzo[*b*]thiophene (**35**) and electron acceptor *p*-chloroacetophenone (**36**) and with the bichromophores **37** and **38**, where the above donor and acceptor moieties are connected by an olefinic (unsaturated as well as saturated) spacer, was performed (02JPP(A)(152)41). The absorption spectra of the donor **35** in the presence of the electron acceptor **36** were measured in *n*-heptane and highly polar acetonitrile solutions. In both nonpolar and highly polar media, it was found that the spectra of the mixture of **35** and **36** are just the superposition of the absorption bands of the individual components. This observation excludes the possibility of formation of any ground state charge transfer (CT) complex.

**35****36****37****38**

However, the absorption spectra of the bichromophore **37** do not show the spectra of components but instead an overlapping of the two new long wavelength bands of broad nature spanning between 330 and 420 nm in both polar and nonpolar solutions. These bands seem to be due to the two CT bands: one resides at 351 nm and the other at 380 nm. In the case of bichromophore **38**, however, both the absorption spectra of the donor and the acceptor part are apparent but additionally a long wavelength (low energy) tail extending down to 410 nm was observed. This tail seems to originate from the ground-state CT interaction between **35**, the donor, and **36**, the acceptor.

When the donor part of bichromophore **37** using the excitation wavelength 307 nm was excited, it was surprisingly observed that the fluorescence band of **35**, spanning between 320 and 350 nm, was completely quenched but a long wavelength band of large intensity peaking at about 518 nm, in cases of both **37** and **38**, appeared. Moreover on direct excitation of the CT absorption band of bichromophore **37** situated at 351 nm and **38** at 400 nm region, a fluorescence band of considerable intensity at the same energy position 518 nm was found. The 518 nm band should be the CT emission band whose formation is largely facilitated in the intramolecular system comprising the donor and the acceptor moieties. Thus, it is inferred that both in the ground and excited singlet (S_1) states, a particular conformation through mutual orientation of the donor and acceptor sites is responsible for the formation of a CT complex.

The biexponential nature of the fluorescence emission of this bichromophore was clearly observed from the decay analysis. There

should be two different species involved in fluorescence emission of the bichromophore **37**. In high probability, these two species should be due to the presence of two geometrical isomers, *cis*- and *trans*-forms, of **37**. Thus, the excited CT band is composed mainly of two overlapping emission spectra: one due to *cis* (folded) and the other to *trans*-type (extended) geometry of **37**. On irradiation of this *trans*-isomer and excited species would be produced, which is usually lower in energy than that of the corresponding *cis*-isomer. The parameters associated with fluorescence lifetimes demonstrates that 2.6 ns species dominates at longer wavelength region and should correspond to the *trans*-isomer and 1 ns should be responsible due to the presence of the *cis*-form of **37**.

In the case of bichromophore **38**, measurements of CT fluorescence lifetimes demonstrate the formation of the two different species having 1.7 and 3.5 ns. The two different species are the two different conformations of the bichromophore, viz. “gauche” and “staggered.”

Upon 355 nm laser pulse excitation of the mixture of **35** and **36** in acetonitrile, transient species at around 370, 440, and 480 nm are observed. The band near 480 nm corresponds to the band of dissociated anions (36^-) or the anions of the solvent separated species. The bands at 370 and 440 nm are due to the cation of benzothiophene. The decays of the bichromophores show unimolecular first-order decays. This indicates that the 480 nm band observed with **37** and **38** should be assigned to a mixture of contact ion-pair (CIP) of the acceptor anion.

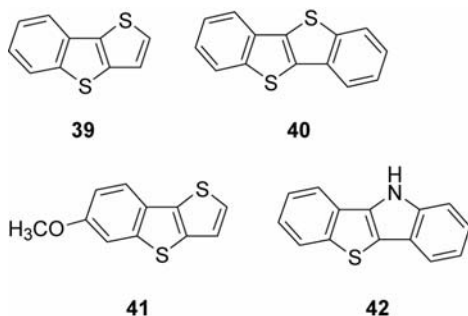
All the above parameters were also measured from the cationic decay (using 440 nm wavelength of the transient absorption spectra). As the contribution of k_{CST} is very small relative to k_{CR} , the observed τ_{ip} show approximately the charge recombination within the ion-pair complex.

In bichromophoric systems, k_{CR} values computed from the cationic decays are found to be similar to those obtained from the analysis on the decay of the anionic species.

Main absorption bands in the region 240–270 and 290–330 nm for **40**, 245–275 and 290–315 nm for **39**, 230–270 and 310–355 nm for **42**, and 250–280 and 290–320 nm for **41** were observed (02JF231; 03JOC9813). The shortest-wavelength bands can be attributed to $\pi \rightarrow \pi^*$ ^1B transitions, whereas the long-wavelength bands, with weaker, but still quite high, molar absorption coefficients belong to the $\pi \rightarrow \pi^*$ ^1La and ^1Lb transitions. The presence of weaker shoulders at long wavelength can be ascribed to the overlapping of n, π^* bands due to the thiophene ring by π, π^* bands.

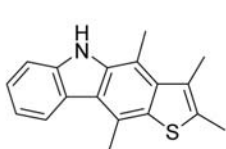
The excitation spectra contain bands generally located at wavelength values closed to those of the absorption spectra where **40** and **39** exhibited two emission bands situated in the 320–360 nm region for most solvents,

whereas **42** and **43** presented generally only one wide emission band in the 340–375 nm region. Important red shifts of the emission bands ($\Delta\lambda_{\text{em}} = 34\text{--}43$ nm, according to the solvent) were observed when changing from **39** to **42**.

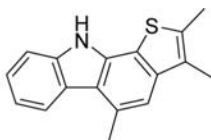


Except for water, weak blue shifts of the emission bands ($\Delta\lambda_{\text{em}} = 3\text{--}9$ nm, according to the compound) were noted upon increasing the solvent polarity, which confirms the existence of a small negative solvatochromism. The fluorescence quantum yields (ϕ_F) varied strongly from 0.0002–0.56. An important increase of ϕ_F occurred upon increasing the solvent polarity. Solvatochromic plots indicate the existence of a weak negative solvatochromism. Therefore, the excited singlet-state dipole moment (μ_e) of the fused benzothiophene derivatives under study should be slightly smaller than their ground-state counterparts (μ_g). It allows us to predict that these fused benzothiophenes are less polar in the excited singlet state than in the ground state.

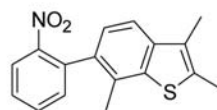
The fluorescence excitation and emission spectra of the electrogenerated fused benzothiophene oligomers [poly(**39**) and poly(**41**)] show the existence of dramatic red shifts of the fluorescence maxima and important increases of the fluorescence intensity relative to the parent monomers. These results suggest the existence of extended electronic conjugation in the oligomer chains. Poly(**39**) and poly(**41**) showed a well-structured excitation band with maxima at about 335 nm and 395 nm, respectively. These excitation maxima are strongly red shifted by about 50 and 108 nm, respectively, against the **39** and **41** excitation spectra. The emission spectra are characterized by a relatively wide, poorly structured band, centered at 410 nm and 445 nm, respectively. These emission maxima also present dramatic red shifts relative to the emission spectra of the parent monomers.



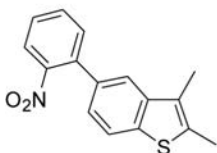
43



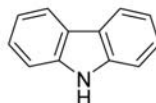
44



45



46



47

With **44** and **43**, three major bands are observed in the UV spectra, corresponding to the $S_0 \rightarrow S_1$, $S_0 \rightarrow S_2$, and $S_0 \rightarrow S_3$ transitions (03PP(77)121). In the thienocarbazoles, there is a clear red shift of the longer-wavelength-absorbing band of **43** relative to **44**. Similarities are observed between these and the UV spectra of the nitro precursors, except that with **45** an additional band occurs in the 280–320 nm region. With **46** this band is not observed, but the lower wavelength band at 260 nm is red shifted relative to **45**.

As observed in the case of the absorption spectra, the maximum fluorescence of **43** also is red shifted, now by ~ 30 nm relative to **44**. The phosphorescence spectra of **43** are red shifted relative to **44**. With the precursors, the less methylated compound **46** shows a blueshift relative to the more methylated **45**.

The low values obtained for Φ_F and Φ_{Ph} values of the precursors **46** and **45** are consistent with the nonradiative decay processes being the preferred deactivation channels in these compounds. This is also reflected in the comparison of their radiation-less (k_{NR}) and radiative rate constants. The less methylated **46** have fluorescence lifetime value of about 16 times larger than that of **45**. The lowest lying singlet excited state for these two compounds is of n, π^* origin. Assignment of triplet-state configurations is based on (1) the relative large gap, ΔE_{ST} , between the lowest singlet and emitting triplet when T_1 is π, π^* and (2) the characteristic phosphorescence lifetimes ($\tau_{Ph} < 0.01$ s for n, π^* states and of seconds for π, π^* states). The long phosphorescence lifetimes observed for the compounds (0.35 and 0.45 s) indicate that emission is from a triplet π, π^* state. This is supported by the relatively large S_1-T_1 energy gap observed (~ 6000 cm^{-1}), which again is characteristic of a $^3(\pi, \pi^*)$ state. Smaller ΔE_{ST} values are normally observed with $^3(n, \pi^*)$

states. This suggests that an additional triplet of n,π^* origin exists between S_1 and T_1 and could be responsible for the low triplet yield value. This, together with the very-efficient radiation-less deactivation pathway between T_1 and S_0 , explains the low phosphorescence yield of these compounds.

The ring closure of the nitro-precursors to thienocarbazoles leads, first, to a strong red shift of the longer wavelength-absorbing bands. These redshifts of **43** and **44** relative to their precursors also are observed in fluorescence and phosphorescence and are a direct consequence of the increase in the π -electron path, with subsequent decrease in the energetic difference between the HOMO and the LUMO. Comparison between the thienocarbazoles and their nitro-precursors also shows that the radiative parameters (Φ_F , τ_F , Φ_{Ph}) are all greater than the former, and the radiative rate constants now display typical values for allowed π,π^* transitions. There is no change in the Φ_F value from RT to LT, indicating that no structural change is expected to occur.

Although the two compounds show similar photophysical behavior, the same is not true for their spectroscopic characteristics such as absorption, fluorescence, and phosphorescence maxima, where the bands in **43** are all red shifted relative to **44**, suggesting less conjugation in the angular **44**. In the case of **44**, there is strong evidence for TTA in the singlet region.

An interesting observation from the photophysics of these compounds is the differences obtained in their ISC yields. It can be seen that the linear compound has a Φ_T value lower (0.84) than that obtained for the angular compound (0.94). The explanation for this difference can be found when their **47** and benzothiophene counterparts are compared, where benzothiophene has a Φ_T value of 0.98, whereas for **47** this value is 0.36. Comparison between these suggests that in the case of the angular compound, a disconnection between the two **47** and benzothiophene ring systems is induced, with the latter unit having a higher Φ_T value that dominates ISC in **44**, whereas in the case of the **43** there is only a partial decoupling.

With the phosphorescence spectra, similarities are observed between **44** and the nitro-precursor **45**. In fact, their phosphorescence maxima are practically identical, and the shapes of their bands are fairly similar, which again supports the idea that there is a partial decoupling between the benzothiophene ring system and the carbazole unit in the angular compound, with the π -electron path responsible for the phosphorescence being essentially located in the benzothiophene ring.

The photophysical properties of bithienyl derivatives **48**–**50** have been reported (98JCS(F)3331; 03JOC2921; 05T11055).

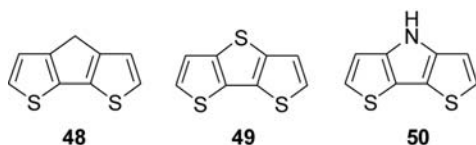


Table 6. Photophysical properties of bithienyl derivatives

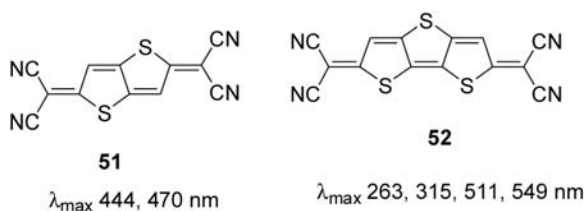
Compound	Fluorescence λ_{\max} (nm)	Φ_F	Phosphorescence λ_{\max} (nm)
2T	362	1.3×10^{-12}	374
48	365	3.7×10^{-13}	375
49	333	1.0×10^{-13}	384
50	337	7.7×10^{-15}	400

Compound **50** showed a maximum absorption peak at 300 nm. After irradiation at 300 nm, they showed the fluorescence emissions reported in Table 6. In the presence of benzophenone, the authors observed also the phosphorescence spectra and the observed emissions are collected in Table 6.

The electron transfer process in the presence of dinitrobenzene derivatives was also studied. In the presence of *p*-dinitrobenzene in acetonitrile, the following results were observed (Table 7).

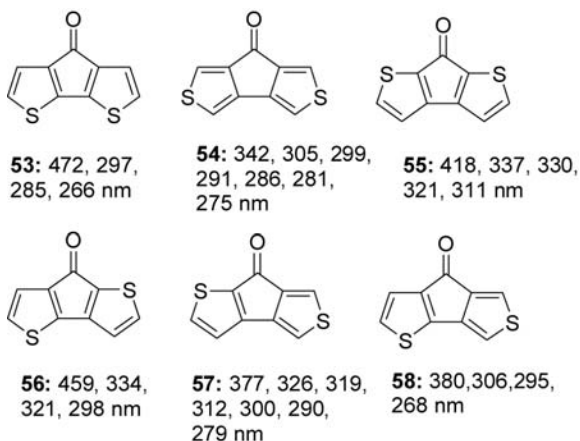
Compound **49** absorbs in a crystal at 30,650; 31,120; 31,590; 32,060; 33,400; 34,630; 35,860; 38,880; 40,120; and 42,460 cm^{-1} (83JPC2317).

The compounds **51** and **52**, analogs of the corresponding oligothiophene derivatives (see below), have been studied for their conductivity properties (89BCJ1547).

**Table 7.** Electron transfer process in bithienyl derivatives

Compound	λ_{\max} (nm)	K	ΔG (kJ mol $^{-1}$)
2T	417, 600	1.5×10^{10}	−39.7
48	395, 560	2.0×10^{10}	−59.8
49	406, 586	2.4×10^{10}	−83.9
50	Reacts	—	−115.8

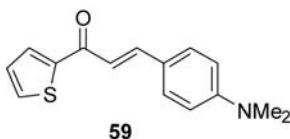
Cyclopentadithiophenone derivatives **53–58** have been characterized (79JCS(P2)393).



2.3 Photophysical properties in organized media

Organized media including micellar solutions and cyclodextrins (CDs) have been the subject of continuous interest. These media are able to solubilize hydrophobic compounds in water and modify significantly their physicochemical properties.

Quinque thiophene gave an inclusion complex in perhydrotriphenylene with emission at 2.52 and 2.37 eV (97CPL(278)146). The absorption and emission characteristics of a hetero-chalcone derivative, 3-(4'-dimethylaminophenyl)-1-(2-thienyl)prop-2-en-1-one (**59**), in aqueous micellar solutions of sodium dodecyl sulfate (SDS), cetyltrimethylammonium bromide (CTAB), and Triton X-100 (TX-100) as well as in β -CD solutions were reported (08PPS257).



This is to understand how **59** molecules which exhibit an ICT fluorescence translate their association with these substrates fluorometrically. Due to high sensitivity of the fluorescence characteristics of **59** to solvent polarity, its spectral properties have been studied in SDS, CTAB, and TX-100 micelles to characterize the properties of these micelles by calculating

the dielectric constant (ϵ), micropolarity at the $E_T(30)$ scale and determining the critical micelle concentration (CMC).

As the water content increases from 5% to 90%, the absorption maximum is red shifted (about 31 nm) relative to that in dioxane, due to increasing the polarity of the medium. Similarly, the fluorescence maximum is shifted to the red upon increasing the water contents in dioxane but with a larger magnitude. The 485 nm emission of **59** in dioxane is shifted to 559 nm in water.

The spectral properties of **59** have been investigated in different concentrations of SDS, CTAB, and TX-100 as examples of anionic, cationic, and neutral micelles, respectively.

The data indicate that the absorption band of **59** in water is blue shifted by about 9 and 14 nm in CTAB and TX-100, respectively. In fact, the addition of SDS has no effect on the absorption maximum of **59**. The spectral shift and enhancement of the fluorescence intensity can be rationalized in terms of binding of this hydrophobic probe to less polar sites in micelles (most probably the micellar core). It has been shown that **59** posses a fluorescent ICT excited state, therefore, lowering the polarity of the medium destabilizes this state more than the ground state. As a consequence, the energy gap between the emitting and the ground state increases; thus, the emission maximum is blue shifted. The UV/Vis absorption spectra of **59** were recorded in aqueous solutions having different β -CD concentrations. The long wavelength absorption band, with a maximum at 446 nm, suffers almost no shift with a pronounced gradual increase in the molar absorption coefficient on adding β -CD. This can be attributed to the enhanced solubilization of **59** molecules through the detergent action of β -CD and indicates the formation of the **59**: β -CD inclusion complex.

In contrast, the fluorescence emission spectrum of **59** is highly sensitive to changing the concentration of β -CD. The emission spectrum, which exhibits a broad structureless band located at 559 nm in water, is shifted to 543 nm on adding β -CD with a great enhancement in the emission intensity. Quantitatively, the fluorescence quantum yield shows 21-folds increase on going from water to 6.4×10^{-3} M β -CD solution ($\phi = 0.005$ to 0.109, respectively). These observations confirm the formation of an inclusion complex between **59** and β -CD, which increases the energy of the first excited singlet state of **59** and decreases the rates of radiationless deactivation processes. The blue shift in the emission maximum of **59** on adding β -CD suggests that the NMe_2 group of the chalcone molecule is buried in the hydrophobic cavity of β -CD; thus, the bulk water molecules are not available to solvate it, while the hydrophilic carbonyl group resides at the hydrophilic gate and/or in the water bulk.

A study on Langmuir–Blodgett films obtained from 4-[5-(dicyanomethanido)thien-2-yl]-*N*-(*n*-hexadecyl)pyridinium and 1-[*N*-(*n*-

hexadecyl-4-pyridinio)]-2-[5-(dicyanomethanido)thien-2-yl]ethene was reported (99TSF(340)218). Two relatively sharp peaks were present in the UV/Vis spectra at 420 and 467 nm. These peaks were significantly blue shifted with respect to the monomers absorptions: for instance, the CT bands of the compounds occurred at about 550 and 635 nm in ethanol solution. The presence of the 420 and 467 nm peaks and their sharpness represented clear evidence of the H-type aggregation arrangement, respectively, in the mixed LB.

The LB film was submitted to irradiation at 467 nm for 30 h. After irradiation the 467 nm peak was fully bleached but no effect was observed on the 420 nm peak.

The latter was bleached after a subsequent independent irradiation at 420 nm for 30 h. The same selective photobleaching could be obtained by irradiating the same kind of mixed LB film at 420 nm for 30 h: the 420 nm peak was bleached but no significant effect could be observed on the 476 nm peak; the latter was bleached by irradiating the film at 467 nm for 30 h. The observed bleaching phenomenon was probably caused by the disruption of the H-type molecular aggregates followed by the photochemical degradation of the monomers.

3. PHOTOCHEMICAL AND PHOTOBIOCHEMICAL PROPERTIES OF NATURALLY OCCURRING THIOPHENES AND RELATED STRUCTURES

Bithiophenes and terthiophenes were isolated in several members of the *Compositae*. α -Terthiophene was found in *Tagetes minuta* (47JA270; 47JA273). After this first identification, several different compounds were found in all the family of the *Compositae* (58ACSA765; 58ACSA771; 62CB2934; 65CB155; 65JCS7109; 66TL4227; 70CB834; 76P1309; 78P2097; 80P2760; 81P743; 81P825; 82P1795; 85P615). From a biogenetic point of view, there derived from the fat acids metabolism, such as polyacetylenes (65CB876; 66CB984). These compounds, and in particular α -terthienyl, have been extensively studied for their biological properties.

The first study on the biological activity of polythiophene derivatives has been published in 1958: Uhlenbroek e Bijloo found an interesting nematocidal activity (58MI1005). The authors found that LD₅₀ on *Heterodera rostochiensis* was <12.5 ppm. They were able to correlate the biological activity of the compound to the presence of bithienyl moiety in the structure (60MI1181). However, direct use on the field did not show nematocidal activity (63MI357).

Several years later Gommers found that in the presence of light (sun light or UV-A), the nematocidal activity of α -terthienyl increased (LD₁₀₀

1 ppm) (72MI458; 79JBC(254)1841; 80MI369). On the basis of this result, during few years several examples of biological activity in the presence of light appeared. Thus, photomediated antibiotic activity on *Candida albicans*, *Candida utilis*, and *Escherichia coli* was reported (75P2295; 75PP(14)2295; 80PP(31)465; 81PP(33)821; 96MI374). Furthermore, ovicidal activity on *Drosophila melanogaster* with LD₅₀ 0.5 ppm was reported (83E402). The presence of UV irradiation was needed also to show algicidal and antifungal activity (81MI54; 94MI377).

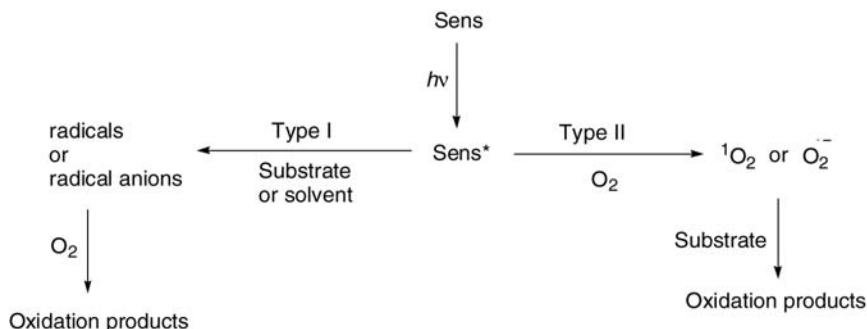
This way, phototoxic activity on insect larvae at the first development stages was observed. A 100% mortality was observed in the presence of 0.5 ppm of polythiophenes (81MI59; 82MI2565; 83MI377; 84BBA(802)442). On larvae of flies (*Aedes aegypti*), a concentration of 0.019 ppm of the polythiophene was sufficient to kill 50% of flies, while DDT gave a value of 0.070 ppm (81MI59; 81MI63; 92MI261; 94MI745). In the presence of UV irradiation, both inhibition of germination and growth in 5 cm plants of dicotyledonous (*Asclepias siriaca*) and herbicidal activity were observed (82MI961). Antifeedant activity against larvae of *Euxoa messoria* was observed: larvae, after a diet containing 100 ppm of a polythiophene derivative in the presence of light decreased the growth rate until death within four weeks (84E577; 84MI104). Polythiophene showed also antiviral and anti-HIV activity (81MI67; 89MI1329; 92PP(56)479; 93MI33; 93PP(58)246; 93MI447; 94MI329; 94PP(60)591). Unfortunately, some phototoxic activity has been found in fishes and some other superior animals (84MI1115; 86MI49; 86MI781; 87MI176).

Polythiophene derivatives can represent a risk also for the men. They can induce phototoxic dermatitis (77MI215; 79MI140), and, in the presence of light, lysis of erythrocytes through a damage to the cellular membrane (79MI134; 80PP(32)167; 80MI309; 84MI124; 85BBA(821)488). These compounds are not able to induce chromosome modifications (80E1096). Polythiophenes can interact with supercoiled c-DNA (91PP(53)463; 93PP(58)49).

Photodynamic activity is usually divided into two processes named *Type I* and *Type II* (91PP(54)659). In *Type I* reaction, triplet sensitizer reacts with oxygen to give, *via* energy transfer, singlet oxygen or, *via* electron transfer, superoxide ion (Scheme 1). Polythiophenes are usually singlet oxygen sensitizers; however, the presence of some other reactive species of oxygen has been postulated in some reactions (84MI25; 84PP(39)177; 93JPP(A)(70)59).

Time-resolved phosphorescence detection (TRPD) was employed to check the yields obtained with the 1,3-diphenylisobenzofuran (DPBF) bleaching procedure for some oligothiophene (94JPP(A)(83)1).

α -Terthienyl showed a τ_T value of 180 ns, $\Phi_T = 0.95$, and $\Phi_\Delta = 0.86$. An extensive study on bithienyl and terthienyl derivatives appeared (96JPP(A)(93)39). The results are summarized in Table 8.



Scheme 1

Table 8. Photosensitizing properties of oligothiophenes

Compound	Φ_{Δ}
5'-iodo- α -terthienyl	0.26
5'-formyl- α -terthienyl	0.60
5'-(3-hydroxy-1-butyryl)- α -terthienyl	0.77
5'-(3-methyl-2-buten-1-yl)- α -terthienyl	0.76
5'- <i>t</i> -butyl-5''-trimethylsilyl- α -terthienyl	0.57
Ethyl 3-(5'- α -terthienyl)-2-amino-propionate	0.58
5'- α -terthienyl- <i>N</i> -benzyl-sulfonamide	0.76
5'- α -terthienyl- <i>N,N</i> -diethyl-sulfonamide	0.77
5'- α -terthienyl- <i>N</i> -allyl-sulfonamide	0.68
5'- α -terthienyl- <i>N</i> -butyl-sulfonamide	0.65
5'- α -terthienyl-benzyl-sulfide	0.44
5'- α -terthienyl-benzyl-sulfoxide	0.30
5'- α -terthienyl-benzyl-sulfone	0.60
5-phenyl-bithienyl	0.80
5-propynyl-bithienyl	0.62
5-(1-hexynyl)-bithienyl	0.52
5-(1-octynyl)-bithienyl	0.70
5-(4-hydroxy-1-butyryl)-bithienyl	0.51
5-(5-hydroxy-1-pentyryl)-bithienyl	0.73
5-(3,4-dihydroxy-1-butyryl)-bithienyl	0.63
5-(4-ethoxy-1-butyryl)-bithienyl	0.72

The presence of UV-A to have biological activity can be explained considering that this type of compounds are photosensitizers of singlet oxygen and that singlet oxygen quenchers inhibit the enzymatic inactivation by α -terthienyl (79JBC(254)1841; 80MI369; 84MI177; 91MI87; 91PP(53) 181; 94TL3151). An electron transfer mechanism and formation of

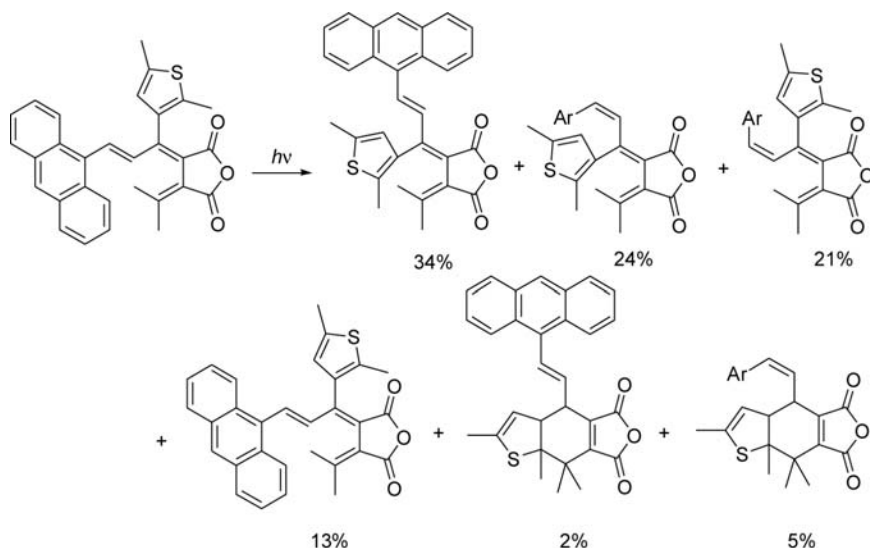
superoxide anion has been invoked in aqueous medium (89JPP(B)(3)165); however, other experiments did not confirm this finding (85PP(41)1): the efficiency of the electron transfer was found $<1\%$ (89JPP(B)(3)411).

Because of their biological properties, these compounds are potentially useful against infesting insects (87MI1). Furthermore, it is known that several plants containing thiophenes are used in the traditional medicine of China, India, Pakistan, Guyana, and Malaysia against conjunctivitis, mumps, sore eyes, and in the treatment of skin infections (88MI139).

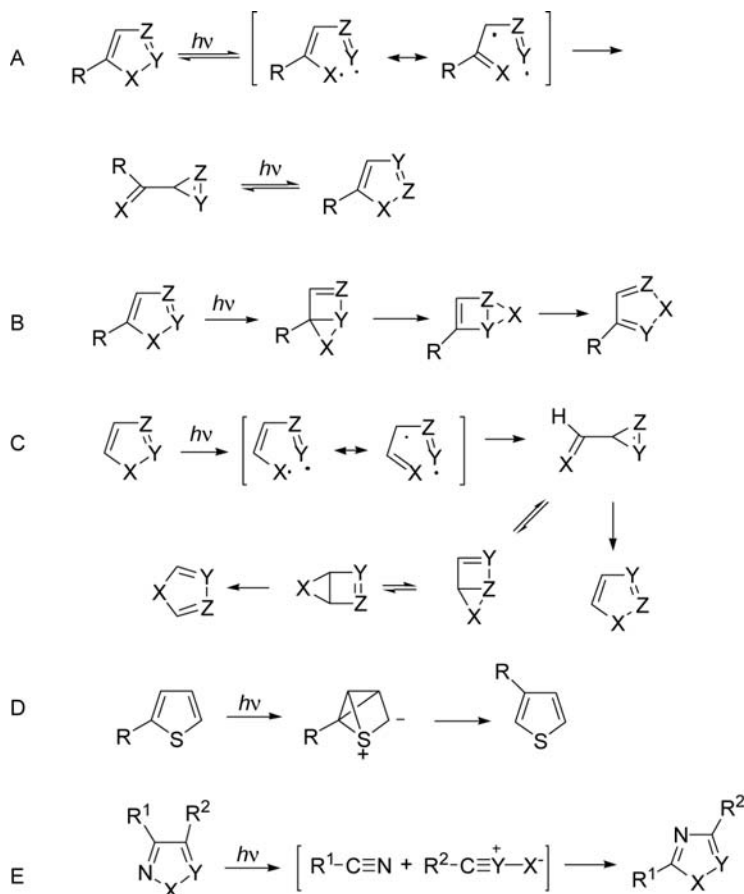
4. PHOTOCHEMICAL ISOMERIZATION

A photochemical isomerization of thienyl alkenes has been described (Scheme 2) (92CB2583). In this case, the cyclization reaction plays only a marginal role.

The photochemical isomerization of pentaatomic heterocyclic compounds has been the object of several reviews, starting with that of Lablache-Combier in 1971 (71BSF679). After this work, reviews of the whole field (76MI123; 77CRV473; 80MI501) or part of it (85MI745; 95MI803; 95MI1063) appeared. In spite of the amount of work done in this field, the description of the photochemical behavior of pentaatomic heterocyclic compounds is confused. Five mechanisms can be invoked to justify the observed behaviors: (1) the ring contraction–ring expansion



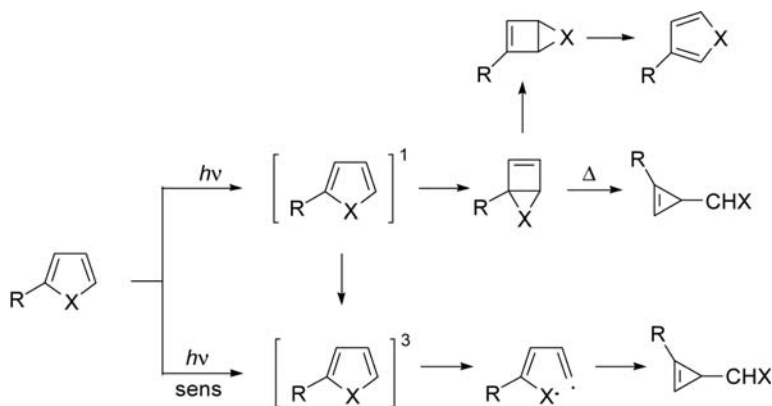
Scheme 2



Scheme 3

route (RCRE) (Scheme 3A); (2) the internal cyclization–isomerization route (ICI) (Scheme 3B); (3) the van Tamelen–Whitesides general mechanism (VTW) (Scheme 3C); (4) the zwitterion–tricyclic route (ZT) (Scheme 3D); (5) the fragmentation–readdition route (FR) (Scheme 3E).

Recently, it was reported some attempts to reach a unified description of the photochemical isomerization of pentaatomic heterocyclic compounds (99H(50)1115; 99MI233; 01AHC41). If the first excited state of a molecule is populated, this molecule can convert into the corresponding triplet state or into the corresponding Dewar isomer. The efficiency of these processes will depend on energetic factors. If the Dewar isomer is formed, an isomeric product is obtained. If the triplet state is formed, cleavage of the $X-C_\alpha$ bond can occur to give ring-opening products,

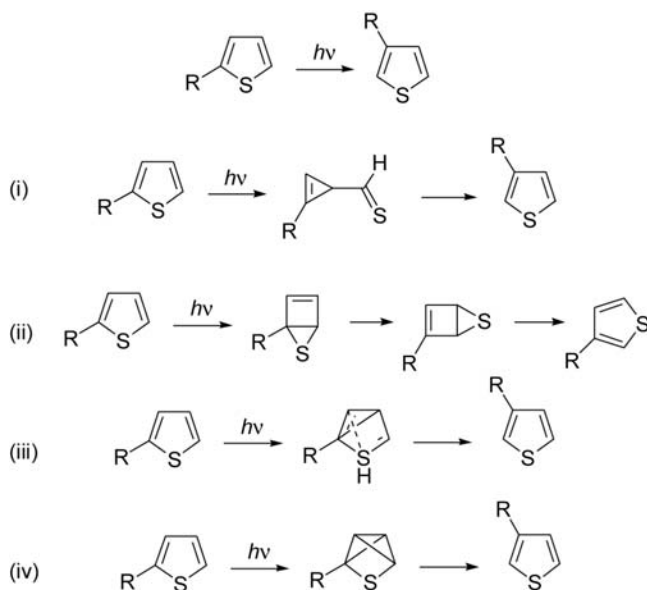


Scheme 4

decomposition products, or ring-contraction products. However, if the radical formed after the $X-C_\alpha$ cleavage shows a higher energy than the triplet state, the triplet state will not be able to give the biradical with high efficiency, and then it will be quenched in radiative and nonradiative processes. In this case, the Dewar isomer could be responsible for the isomerization reaction, but the isomerized product will probably be produced in very low quantum yields (Scheme 4).

Exposure to light of thiophene, 2-methylthiophene, 3-methylthiophene, and benzothiophene induces decomposition of the starting material (56JA5213). The irradiation of thiophene in gas-phase yields ethylene, allene, methylacetylene, carbon disulfide, and vinylacetylene. No Dewar thiophene or cyclopropene derivatives were isolated (69CJC2965). The irradiation in liquid phase gave the Dewar thiophene which can be trapped as a Diels–Alder adduct with furan (85JA723). The Dewar thiophene and cyclopropene-3-thiocarbaldehyde can be obtained by irradiation in argon matrices at 10 K (86JA1691).

Wynberg has discovered the most interesting reaction in the photochemical reactivity of thienyl derivatives. The irradiation of 2-substituted thiophenes gave the corresponding 3-substituted derivatives (Scheme 5). Several studies have been performed on the mechanism of this photoisomerization showing that the reaction takes place from the singlet excited state of the molecule (68TL5895), that the interchange between C_2 and C_3 occurs without the concomitant interchange between C_4 and C_5 , and that the bonds between ring carbons and the substituents are not broken (67JA3501). Four mechanisms have been proposed (Scheme 5). Wynberg preferred (iii) (71ACR65; 72TL1429). More recently, however, several studies showed that mechanism (ii) is the most probable (83TCA(63)55; 91JOC129).



Scheme 5

Calculation results on a possible unified approach fit the experimental data (Figure 2) (99H(50)1115). *Ab initio* calculations showed a different level in the Dewar thiophene (02JPP(A)(149)31). More recently, the possible presence of a cage thiophene structure into the photoisomerization has been studied in order to explain some results that cannot be rationalized by using the above-described approach (09H(78)737).

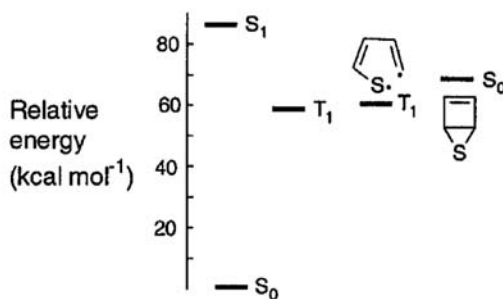


Figure 2. Relative energy of the excited states of thiophene and of some reactive intermediates.

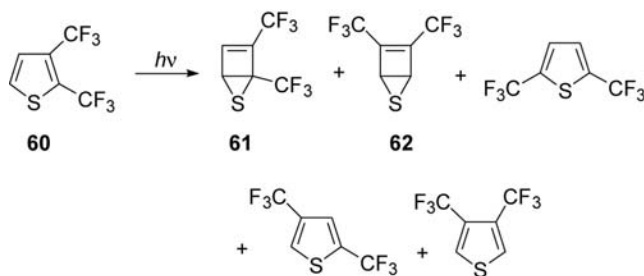
In fact, the singlet excited state can evolve giving the Dewar thiophene (and then isomeric thiophenes) or the corresponding excited triplet state. This triplet state cannot be converted into the biradical intermediate because this intermediate shows a higher energy than the triplet state, thus preventing the formation of the cyclopropenyl derivatives.

Alkylthiophenes reacted to give the corresponding transposition products, but they showed low reactivity (70JOC2737). Better results were obtained using perfluoroalkyl derivatives. The tetrakis(trifluoromethyl) Dewar thiophene, isolated in 1970 by vapor-phase irradiation of the thiophene (70MI1), was the first Dewar isomer isolated in this series. The presence of trifluoromethyl groups induces fast formation and slow decomposition of strained systems. The slow decomposition may be partly due to the “siphoning” of vibrational energy into perfluoroalkyl groups (80T1161). The Dewar structure was accepted with some equivocations (71JA3432) until confirmed by a ^{19}F NMR study (72JC2821) and an X-ray structure of the tetramethylfuran adduct (74TL2941; 75CPB2772; 75TL1639).

The irradiation of 2,3-di(trifluoromethyl)thiophene (**60**) gave a mixture of products where the authors found both isomeric thiophenes and an 8:2 mixture of Dewar isomers **61** and **62** (Scheme 6) (83H(20)174; 84TL1917).

The irradiation of the 2,5-di(trifluoromethyl)thiophene gave the corresponding 2,4 isomer, while 3,4-di(trifluoromethyl)thiophene gave the 2,4 isomer only in traces. 2,3,4-Tri(trifluoromethyl)thiophene gave the 2,3,5 isomer and a mixture of the corresponding Dewar isomers (83H(20)174).

As reported for the furan derivatives, thiophenes, when irradiated in the presence of an amine, gave the corresponding pyrroles (69JCS(CC)524; 71JCS(CC)891; 71T1059; 75T785). The authors proposed the formation of a cyclopropenyl intermediate. Subsequently, however, a Dewar thiophene derivative, treated with aniline, gave the corresponding pyrrole, showing that it is probably the true intermediate in this reaction (80JOC2968).

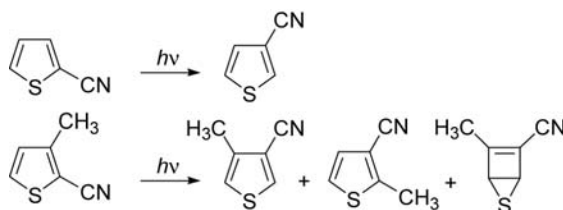


Scheme 6

Arylthiophenes were used as substrates in the photoisomerization described in Scheme 5 (65JA3998; 66JA5047; 66JCS(CC)203; 67JA3487; 67JA3495; 67JA3498). The dithienyls gave this reaction efficiently, while 2-(2-pyridyl)thiophene and 2-(2-furyl)thiophene did not give this reaction in a reasonable yield (69JOC3175; 71JOC1011). Carbonyl and olefinic substituents inhibit the rearrangement (71ACR65; 74CJC1681; 75CJC1; 86G747; 86JCS(P1)1755; 87JCS(P1)1777; 87JOC5243; 89G381; 89JPP(A)(47) 191; 94G195; 94JCS(P1)1245).

The results of theoretical calculations on 2-phenylthiophene fit the experimental results (99H(50)1115; 00JOC2494). In fact, in this case, the formation of the triplet state of 2-phenylthiophene cannot allow the formation of the biradical intermediate allowing the formation of the Dewar thiophene.

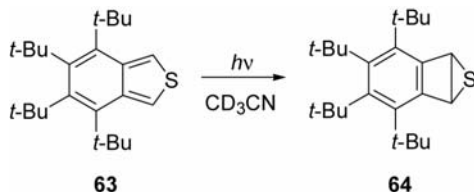
The irradiation of 2- and 3-cyanothiophene gave interesting results in agreement with the scheme described above (Scheme 7). The photoisomerization reaction involved only the π, π^* excited singlet state and Dewar thiophene were isolated when the reactions were carried out at -68°C and shown to be intermediates in the isomerization reaction (79JCS(CC)881; 79JCS(CC)966).



Scheme 7

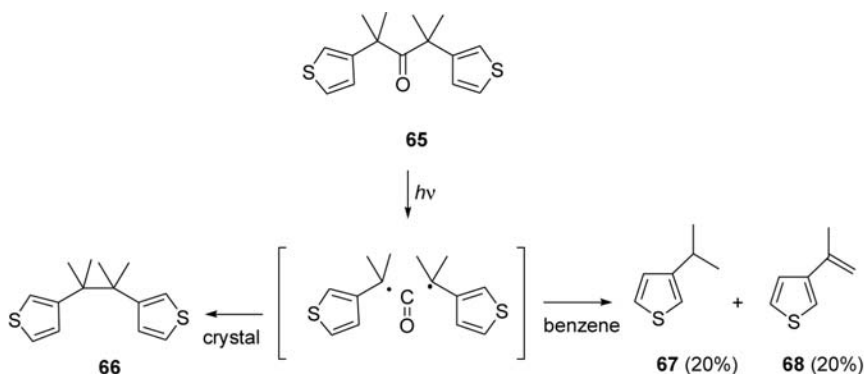
When 2-cyanothiophene is used in calculations, the results fit the experimental results. In fact, the formation of the triplet state of 2-cyanothiophene cannot allow the formation of the biradical intermediate allowing the formation of the Dewar thiophene (99H(50)1115).

Irradiation of a benzothiophene derivative **63** gave the corresponding Dewar isomer **64** (95TL3177).



5. NORRISH-TYPE I REACTION

UV irradiation of **65** in benzene (about 4 mM) with a medium-pressure Hg Hanovia lamp using Pyrex glassware as a filter ($\lambda > 290$ nm) revealed products that are consistent with the expected α -cleavage and decarbonylation followed by radical–radical reactions (07OL4351). 2,3-Dithiophenylbutane **66** is obtained by a radical–radical combination reaction, while 3-isopropylthiophene **67** and 3-(propen-2-yl)thiophene **68** form by a radical–radical disproportionation process. The solid-state reaction was shown to be highly temperature dependent. While irradiation of powdered samples at 20°C led to no observable product after 2 days, samples exposed to the same UV source for 24 h at ca. 45°C gave **66** as the only product in ca. 5–10% yield. Photochemical reactions were carried out with nanocrystalline suspensions of **65** in a Pyrex tube acting both as a container and a light filter ($\lambda > 290$ nm).

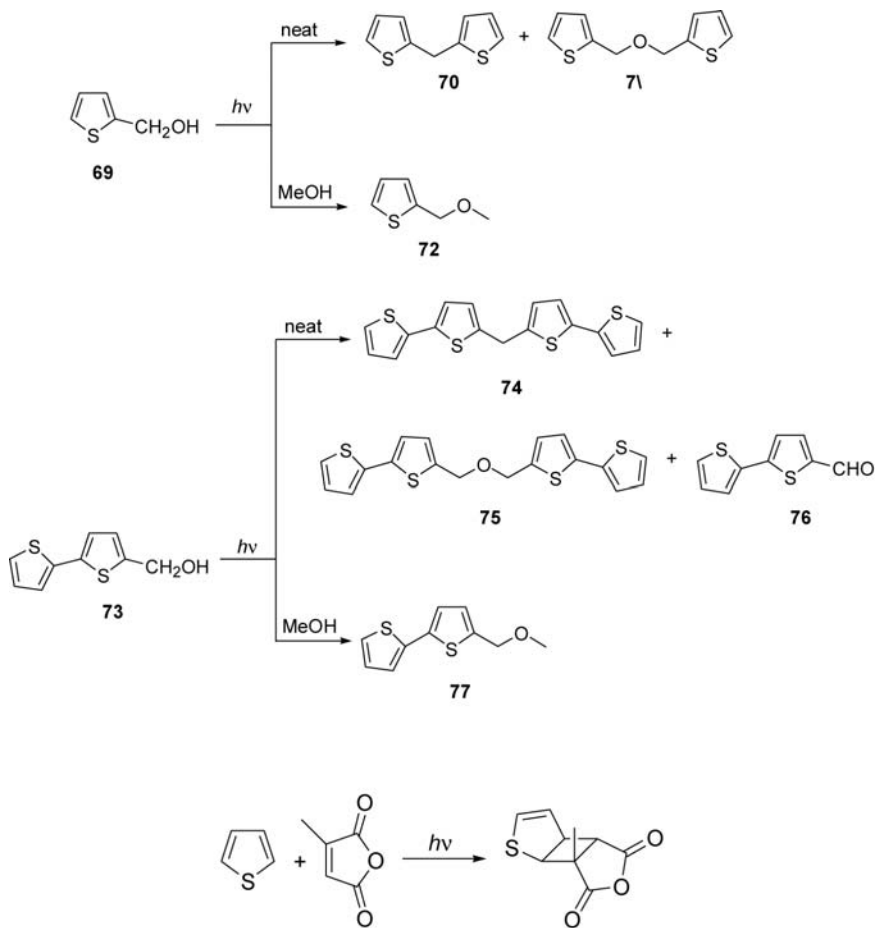


6. DIMERIZATION

The irradiation of 2-thiophenemethanol (**69**) gave dimeric products **70** and **71** (91JCR(S)166). The same behavior was observed when a bithienyl derivative **73** was used as substrate. A photosubstitution reaction to give **77** was observed in methanol.

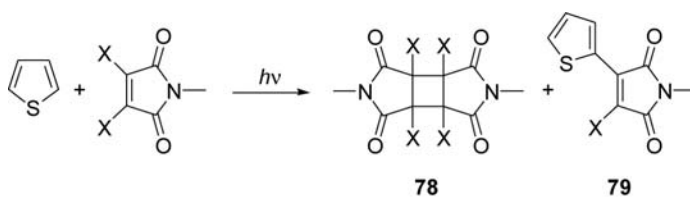
7. CYCLOADDITION REACTIONS

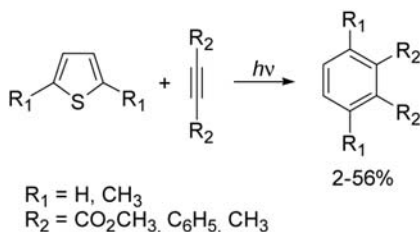
Thiophene gave a 2+2 cycloaddition reaction when irradiated in the presence of maleic anhydride (Scheme 8) (63CB498; 70 JCS(CC)1474; 70MI28; 71MI9; 73JCS(P1)2322; 86JP(32)363). But performed in the presence of benzophenone as triplet sensitizer, the main product was the Paternò-Büchi adduct.



Scheme 8

Thiophene reacts with phthalimide (78TL125). With halogenated phthalimide, the main reaction is the formation of the dimer **78** of the starting material, while a substitution product **79** was obtained in very low yields (5.8% when $X = \text{Cl}$, 4.5% when $X = \text{Br}$, 15% when $X = \text{I}$).



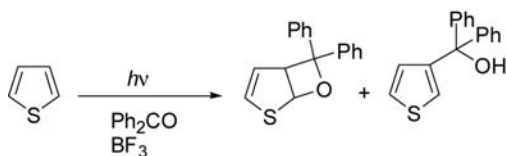


Scheme 9

Thiophene reacts with alkynes to give the corresponding benzene through a photochemical Diels–Alder reaction followed by extrusion of a sulfur atom (Scheme 9) (72TL1909; 73CB674). Thienyl derivatives with electron withdrawing substituents allow adducts isolation (78CJC1970).

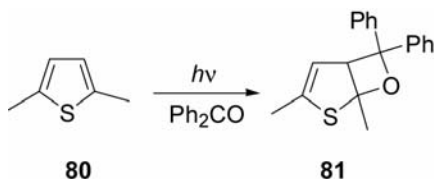
The reactivity of pentaatomic aromatic heterocycles other than furan toward carbonyl compounds to give oxetanes has been reviewed (95MI536). They show lower reactivity than furan. The reason is not clear, but could be related to their different aromaticity, or, as reported below, to the quenching properties of the heterocycles.

Thiophene does not react with benzophenone alone (81JP(17)91; 82JP(19)95; 83JP(22)91) but reacts when irradiated in the presence of BF_3 (Scheme 10) (96JPP(A)(93)169) where BF_3 is able to catalyze the ring opening of the oxetane. The initial step of Lewis acid catalysis appears to be the complexation of the organic compound with the Lewis acid. In the case of ketones and aldehydes, bonding takes place through one of the lone pairs of the carbonyl oxygen atom. Subsequently, the base which has been activated by complexation and further by light in the case of photoreactions undergoes attack by another reactant which could be an olefin or a conjugated system such as that present in a heterocyclic ring. The benzophenone– BF_3 complex is capable of reacting with thiophene to yield an unstable oxetane that opens to an alcohol. The benzophenone– BF_3 complex excited by light leads to an exciplex whose excitation energy is lower than the lowest triplet energy of thiophene which under the circumstances cannot act as a quencher and then, presumably, the electron-rich heterocycle interacts with the electron-deficient donor base complexed to BF_3 . In the benzophenone– BF_3 complex, the $n \rightarrow \pi^*$ band of the ketone is shifted from 250 to 280 nm; this may provide a spectroscopic support.



Scheme 10

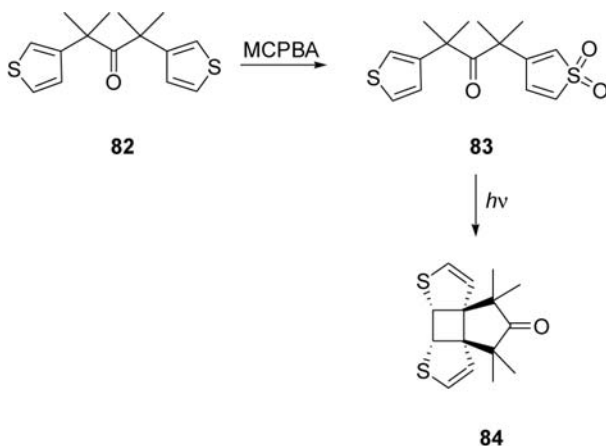
On the contrary, 2,5-dimethylthiophene (**80**) reacts with benzophenone at -10° to give the corresponding cycloadduct **81** with high regioselectivity in 62% yield (70JCS(CC)1474; 82JHC529).



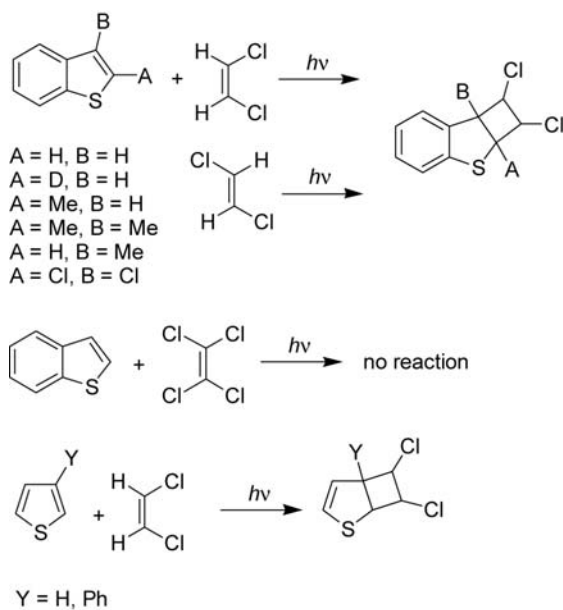
The product can also be obtained by using 1-naphthaldehyde (50%), 2-, 3-, and 4-benzoylpyridine (62, 58, and 60%, respectively), and 2-benzoylthiophene (50%), while 2-naphthaldehyde, benzaldehyde, and acetophenone do not react (73JHC967). 2,3-Dimethylthiophene also gave the corresponding oxetane when irradiated in the presence of benzophenone (60%) (81JHC1065). 2,3-Dimethyl- and 2,3,5-trimethylthiophene do not react.

2-Thienylthioamide reacts with alkenes giving the corresponding cycloadducts that, then, give the products. Here, the thiophene ring does not participate (93CPB1299; 98CPB1522).

Photolysis on crystals of **82** reacted smoothly to give a single product in 100% conversion in a very clean solid-to-solid reaction. The product was the 2+2 adduct **84** (08JOC638).



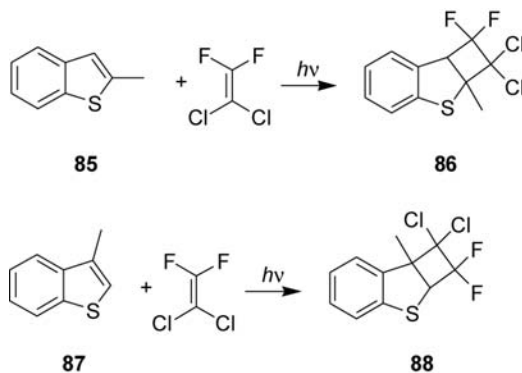
Vinylthiophene reacts with singlet oxygen giving the corresponding [4+2] adduct (75TL4471). 1:1 Adducts were obtained from the photosensitized (benzophenone and acetophenone) addition of *cis* or *trans*-1,2-dichloroethylene to benzo[*b*]thiophene (Scheme 11) (70JOC1582).



Scheme 11

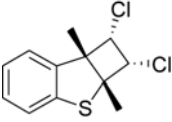
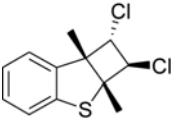
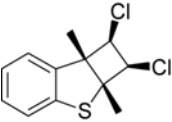
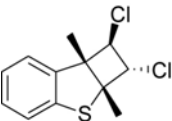
The distribution of products from the addition of *cis*- or *trans*-1,2-dichloroethylene to 2,3-dimethylbenzo[*b*]thiophene is shown in Table 9.

These additions suggest that product control depends, at least in part, on the stability of the intermediate biradical. Thus, 2-methylbenzo[*b*]thiophene (**85**) gives adduct **86** exclusively, while 3-methylbenzo[*b*]thiophene (**87**) gives adduct **88** in major proportions.

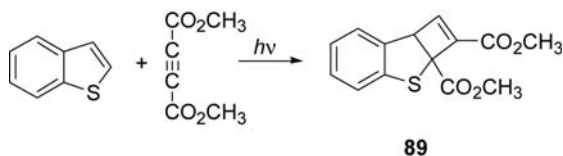


The reaction of 2,3-dichlorobenzo[*b*]thiophene with bromoethene has been described and a mixture of isomeric adducts was obtained

Table 9. Reaction of benzothiophene with 1,2-dichloroethene

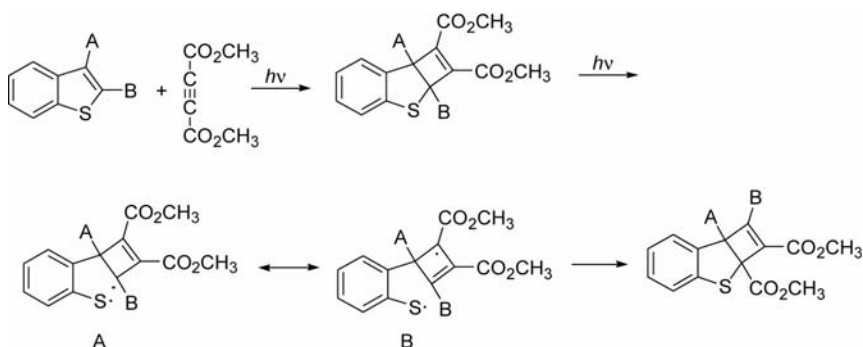
Isomer	% <i>cis</i>	% <i>trans</i>
 <i>cis, endo</i>	1	1
 <i>trans</i>	40	60
 <i>cis, exo</i>	47	27
 <i>trans</i>	11	12

(81JOC3939). Benzo[*b*]thiophene reacts with acetylenes to give coupling products **89** (69TL2913).

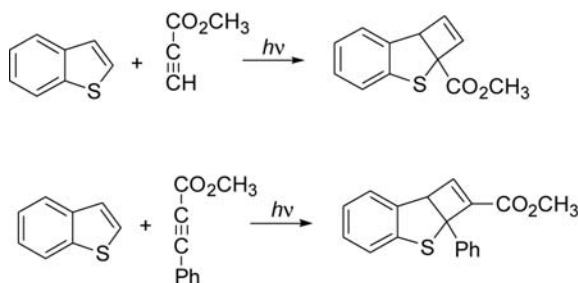


The formation of **89** was explained assuming the formation of the usual 2+2 cycloadduct followed by photochemical isomerization (Scheme 12).

After these results, the same authors found that asymmetric acetylenes gave this type of reaction with very high regioselectivity (Scheme 13) (71JOC3755). Two other possible mechanisms were proposed.



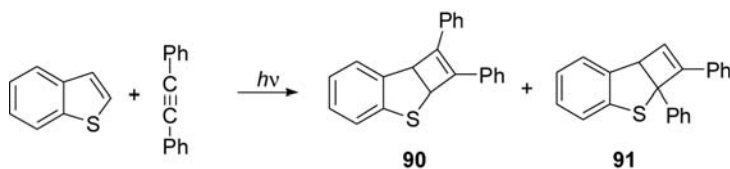
Scheme 12



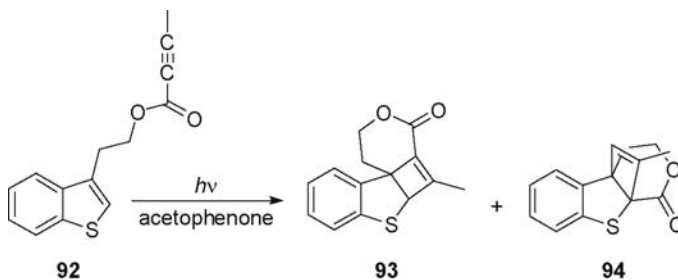
Scheme 13

The C_{α} -S cleavage in thiophene is a well-known reaction. In this case, the rearrangement is governed by the different weights of the resonance structure A and B in Scheme 12. Since the contribution of the resonance structure B when the substituent is phenyl is greater than that of A, the theory supports the experimental result.

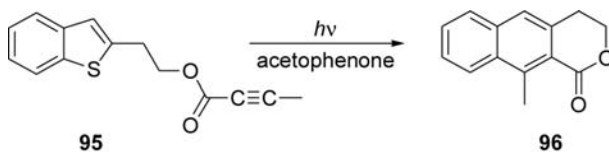
The reaction of diphenylacetylene with benzothiophene allowed the isolation of low quantity of the first cycloadduct **90**, but this reaction occurs with a mechanism different from that of propiolate considering that the excited states of diphenylacetylene is probably involved (69TL4791; 71JOC3755).



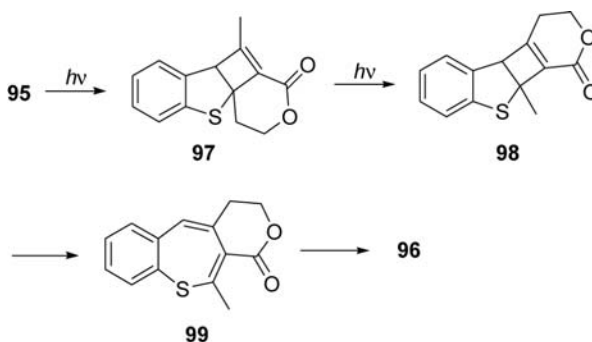
Intramolecular reactions were performed. Sensitized irradiation (acetophenone) of **92** gave **93** in 2% yield while the main product was the isomer **94** (42%) (78JOC2493). Irradiation at 300 nm of **93** gave **94**.



Sensitized irradiation of **95** gave **96** in 18% yield (78JOC2493).



The formation of **96** can be explained considering the formation of cycloadduct **97** and the following rearrangement to **98**. Then, **98** undergoes ring opening to the benzo[*b*]thiepine **99**.

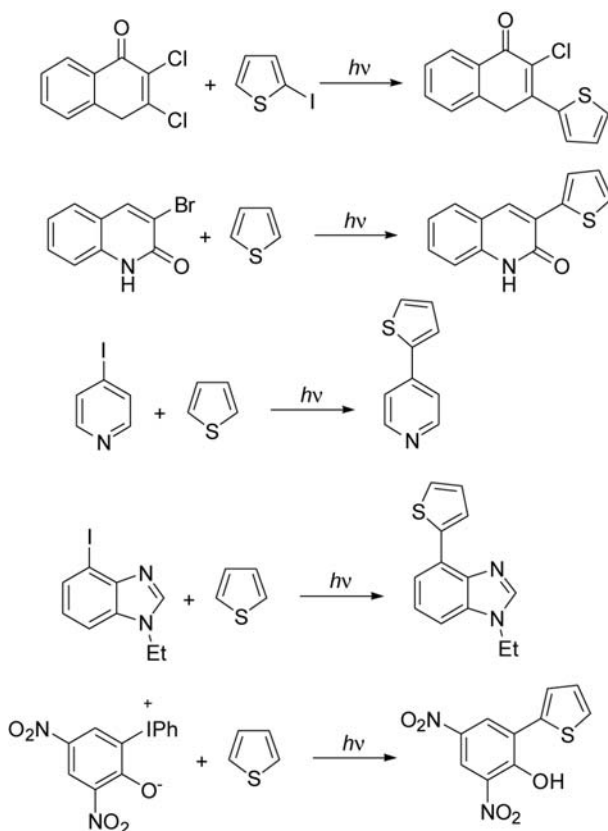


It is not surprising that **99** could not be detected since it is known that benzo[*b*]thiepine easily lose sulfur and convert into the corresponding naphthalenes, such as **96**.

8. PHOTOCHEMICAL REACTIVITY OF HALOGENO-SUBSTITUTED DERIVATIVES

8.1 Photochemical coupling of halogeno-substituted derivatives with thiophene

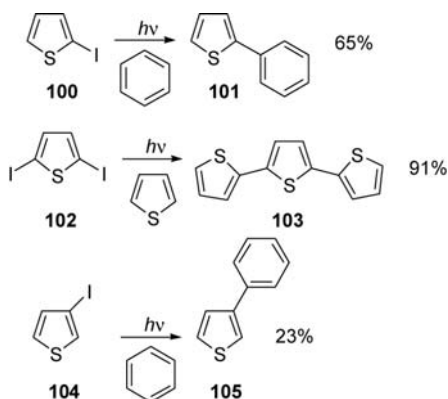
Allyl iodide reacts with thiophene giving a mixture of 2-allylthiophene (63.8%) and 3-allylthiophene (36.2%) (77JOC1570). Some other halogeno-substituted derivatives react with thiophene giving the corresponding thienyl derivatives (Scheme 14) (82JOC4520; 86H(24)799; 86JOC3453; 87BCJ1847; 91JHC1481).



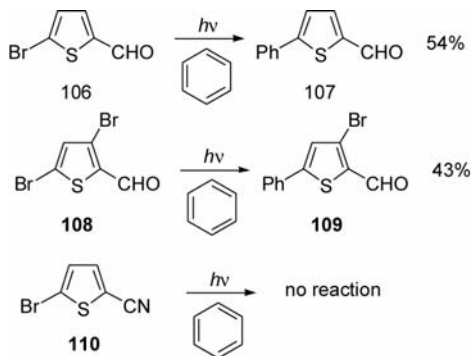
Scheme 14

8.2 Photochemical arylation

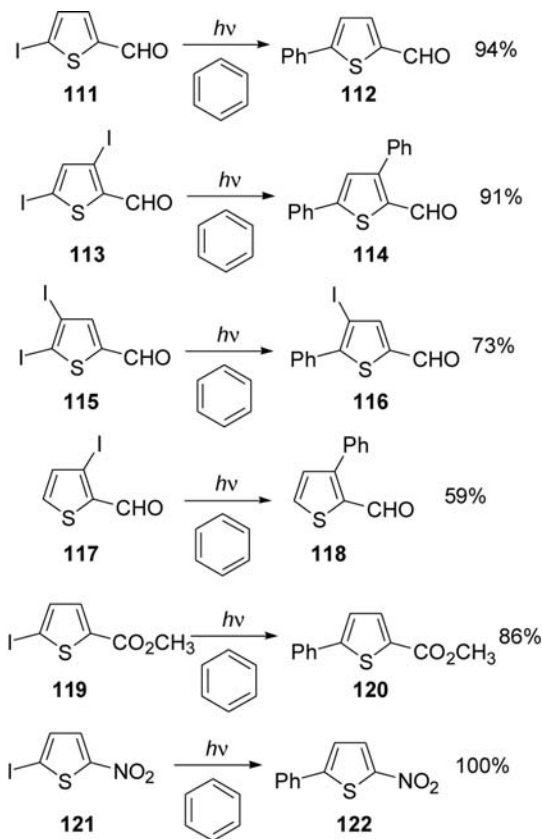
2-Iodothiophene reacts with PhS^- to give the coupling product through an $\text{S}_{\text{RN}}1$ reaction (87JOC5382). 2-Iodothiophene (**100**) can be arylated in good yields when irradiated in aromatic solvents (65JOC2493; 66MI45). Also, 2,5-diiodothiophene (**102**) gave the corresponding arylation product when irradiated in the presence of thiophene (90MI479799). However, 3-iodothiophene (**104**) gave the arylation product only in low yields (68JCS (B)901). This conversion probably occurs through the formation of the thienyl radical by the homolytic cleavage of the carbon iodine bond. The subsequent reaction with the solvent gives the product.



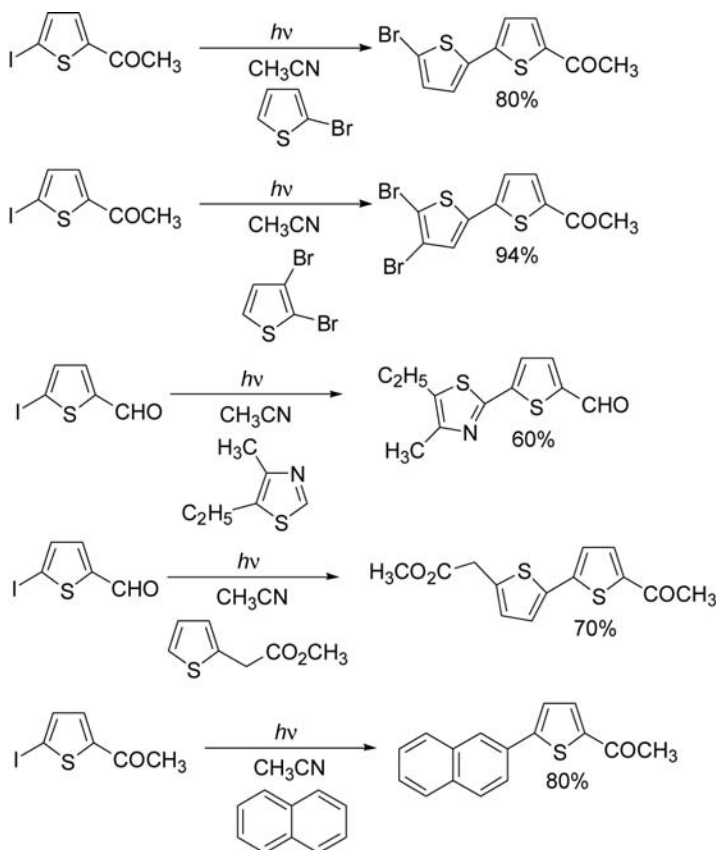
The presence of electron withdrawing substituents on the ring does not alter the reactivity of the halogenated substrates. 5-Bromothiophene-2-carbaldehyde (**106**) gave the phenyl derivative **107** in 54% yield. 3,5-Dibromothiophene-2-carbaldehyde (**108**) gave 5-phenyl-3-bromothiophene-2-carbaldehyde (**109**) in 43% yield, but 5-bromothiophene-2-carbonitrile (**110**) gave no reaction (89JPP(A)(47)191).



Better results can be obtained by using iodine-substituted heterocycles. 5-Iodothiophene-2-carbaldehyde (**111**) (86JCS(P1)1755), 3,5-diiodothiophene-2-carbaldehyde (**113**) (86JCS(P1)1755), 4,5-diiodo-2-acetylthiophene (**114**) (86JCS(P1)1755), 3-iodothiophene-2-carbaldehyde (**117**) (86JCS(P1)1755), methyl 5-iodothiophene-2-carboxylate (**119**) (89JPP(A)(47)191), and 5-iodo-2-nitrothiophene (**121**) (94G195; 95JPP(A)(91)187; 95MI542) gave the phenyl derivatives in very good yields. 5-Iodothiophene-2-carbonitrile gave only the dehalogenation product (86JCS(P1)1755).



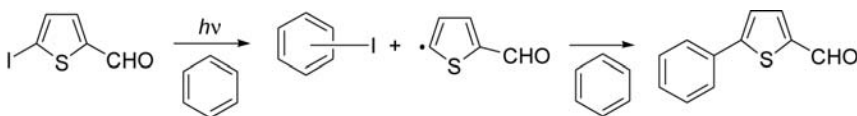
All these reactions show a limitation of this methodology: the need for an aromatic compound as solvent limits the choice of substrates to liquid, low-boiling materials. Acetonitrile was found to be the best solvent. This way, 5-iodo-2-acetylthiophene or 5-iodothiophene-2-carbaldehyde reacted with halogenothiophenes (87JCS(P1)1777), 2-thienylacetic acid derivatives (94JCS(P1)1245), and substituted thiazoles (89G381) (Scheme 15); similar results were obtained irradiating methyl 5-iodothiophene-2-carboxylate and 5-iodo-2-nitrothiophene in the presence of naphthalene or thiophene (Scheme 15) (86H(24)1575; 89JPP(A)(47)191; 95PP(60)542).



Scheme 15

This type of reaction failed on irradiating 5-iodothiophene-2-carbaldehyde with 2-thienylmethanol or 2-thienylacetonitrile (94JCS(P1)1245).

The mechanism of this reaction shows that excitation of the substrate gave an n,π^* triplet state, but this excited state was unable to dissociate the carbon-iodine bond. This was demonstrated by showing that the n,π^* triplet state, when sensitized by chrysene, did not produce coupling products. Probably, the reaction occurred in an excited σ,σ^* triplet state mainly localized on the carbon-iodine bond, and the interaction between this triplet state and aromatic compounds led to homolytic cleavage of the C-I bond with the formation of both a 5-thienyl radical and a complex between the aromatic compound and the halogen atom. The formation of this complex was demonstrated by the presence of a short-lived transient with $\lambda_{\text{max}} = 510 \text{ nm}$, showing a second-order decay kinetics and a half-life of ca. $0.4 \mu\text{s}$ in laser flash photolysis. The thienyl radical thus formed



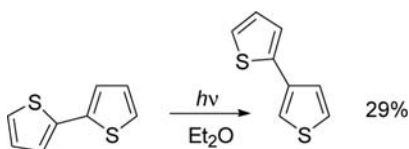
Scheme 16

reacted rapidly with the aromatic compound to form the corresponding arylation product (Scheme 16) (95JPC5365; 01PCCP2765). These data seem not to be in agreement with a previously reported hypothesis. The kinetic data appeared to fit the hypothesis that the reaction occurs through a single electron transfer process from the aromatic compound (the donor) to the heteroaromatic derivative (the acceptor) (85G595).

The reaction kinetics in four solvents (benzene, chlorobenzene, toluene, and anisole) showed an increasing order of reactivity: benzene < anisole < chlorobenzene < toluene. Hence, the aromatic substrates are involved in the key photochemical step, an electron transfer process. With the exception of the anisole, all the kinetic data fit the equation $\left(\frac{1}{\phi} - 1\right) = \beta \times IP$ where IP is the ionization potential of the donor and can be explained considering that the reaction occurs only when a complex between an iodine atom and aromatic compounds is formed. The ability of the aromatic compounds to give these complexes can be estimated on the basis of their ionization potentials (or electrochemical properties).

Furthermore, it is noteworthy that in all these experiments no isomerization products were recovered in appreciable yields. The photochemical isomerization of the thienyl derivatives is a well-known reaction (Scheme 17) (71ACR65).

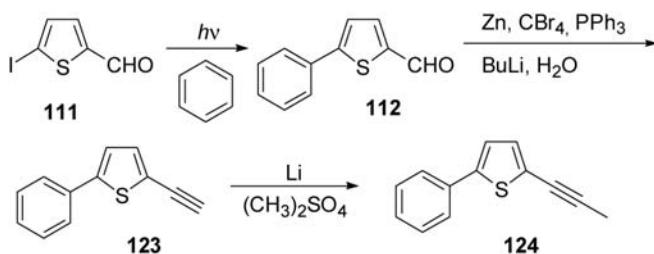
However, these results can be understood considering that (a) the above-described isomerization was obtained after 6 h irradiation while the above-described reactions used shorter irradiation time, (b) in ether, Kellogg et al. reported $\phi = 0.07$ but also observed that in ethanol ϕ was ≤ 0.01 and that in benzene isomerization did not work (70JOC2737). Furthermore, thiophenes-bearing electron-withdrawing substituents, such as NO_2 , CHO, and COMe, did not rearrange photochemically (71ACR65).



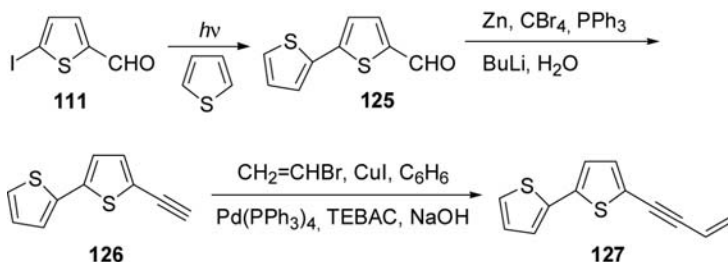
Scheme 17

The most important synthetic applications of the above-described reactions were the synthesis of several naturally occurring bithienyl compounds.

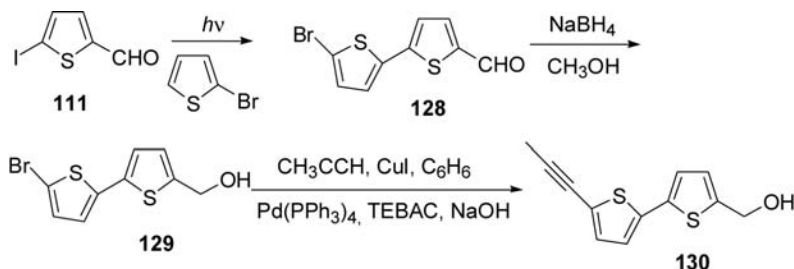
The irradiation of 5-iodothiophene-2-carbaldehyde (**111**) in the presence of benzene gave the corresponding phenyl derivative **112** as described before, and this compound can be converted into the corresponding acetylene **123** by Corey's procedure (72TL3769). The corresponding acetylide can be methylated with dimethylsulfate to give a natural thiophene **124** isolated from *Coreopsis grandiflora* (87JCS(P1)1777).



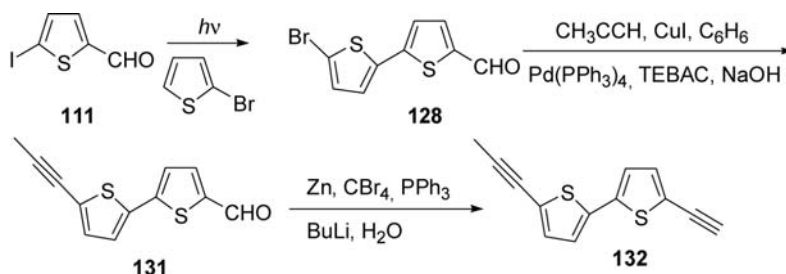
When the irradiation was carried out in the presence of thiophene, the corresponding bithienylcarbaldehyde **125** was obtained. The aldehydic function can be converted into the acetylene **126** and the product was treated with vinyl bromide, copper iodide, and tetrakis(triphenylphosphine) palladium (0) under phase-transfer conditions to give a natural bithiophene **127** isolated from *Tagetes minuta* (87JCS(P1)1777).



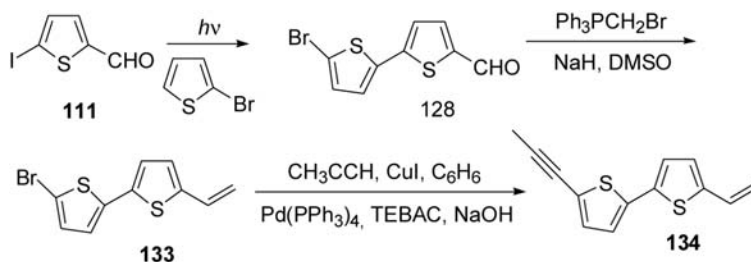
5-Bromo-2-thienyl-thiophene-2-carbaldehyde (**128**), obtained from the photochemical coupling of 5-iodothiophene-2-carbaldehyde and 2-bromothiophene, can be reduced with NaBH₄; **129** was treated with propyne, copper iodide, and Pd(PPh₃)₄ under phase-transfer conditions to give a natural bithiophene **130** isolated from *Arctium lappa* (87JOC5243).



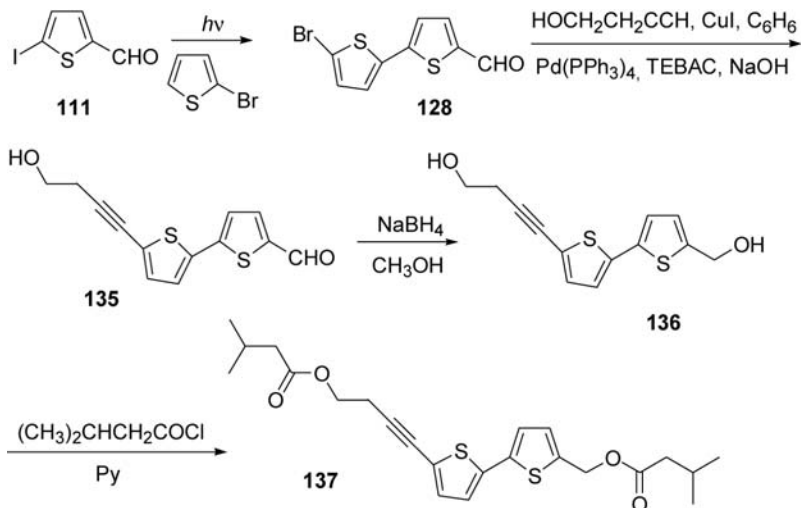
When **128** was treated with propyne, it gave a natural bithiophene **131** also isolated from *Arctium lappa* (87JOC5243); **131** could also be treated according to Corey's procedure to give the corresponding acetylene **132**, a natural bithiophene isolated from *Tagetes erecta* (87SC491).



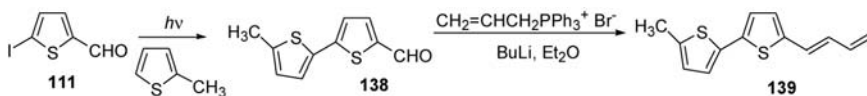
The use of methyltriphenylphosphonium bromide and MeSOCH_2^- on 5-bromo-2-thienylthiophene-2-carbaldehyde (**128**) furnished the corresponding olefin **133**. The reaction with propyne in this case furnished a natural bithiophene **134** isolated from *Tagetes minuta* (86G747).



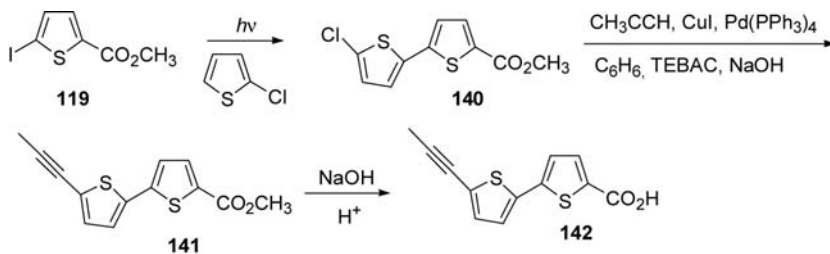
Furthermore, the treatment of the same bithienyl synthon with 2-butyn-1-ol, copper iodide and $\text{Pd(PPh}_3)_4$ gave the corresponding bithiophene **135**. The reduction with NaBH_4 and the treatment of the resulting diol **136** with isovaleryl chloride gave a natural bithiophene **137** isolated from *Eclipta erecta* (87JOC5243).



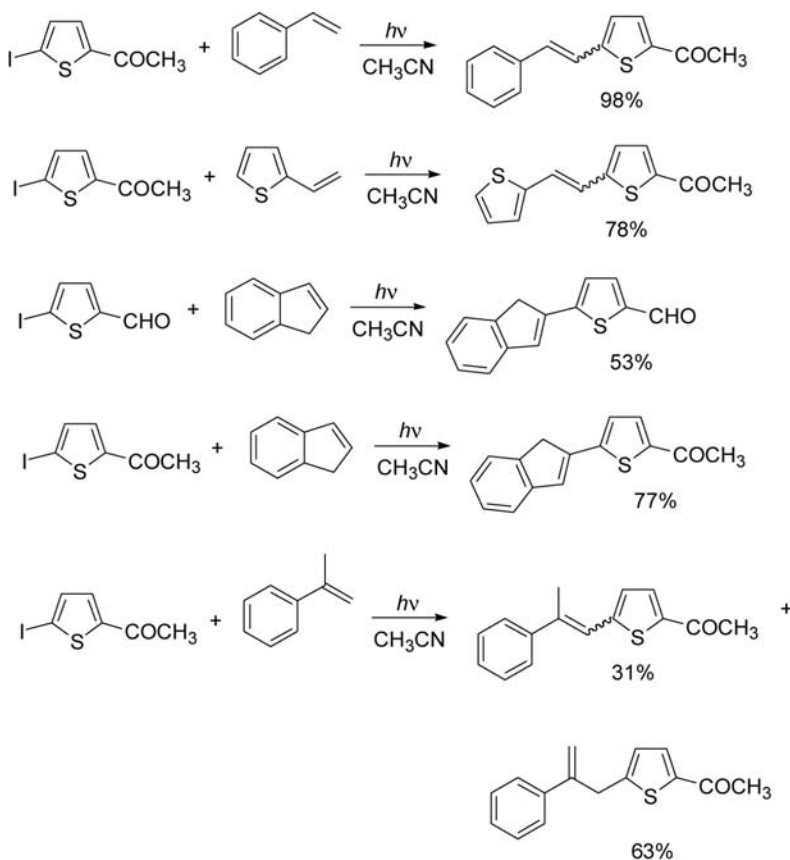
5-Iodothiophene-2-carbaldehyde can react with 2-methylthiophene. The corresponding bithiophene **138** reacted with allyltriphenylphosphonium bromide and BuLi to give a natural bithiophene **139** isolated from *Bidens radiata* (87JOC5243).



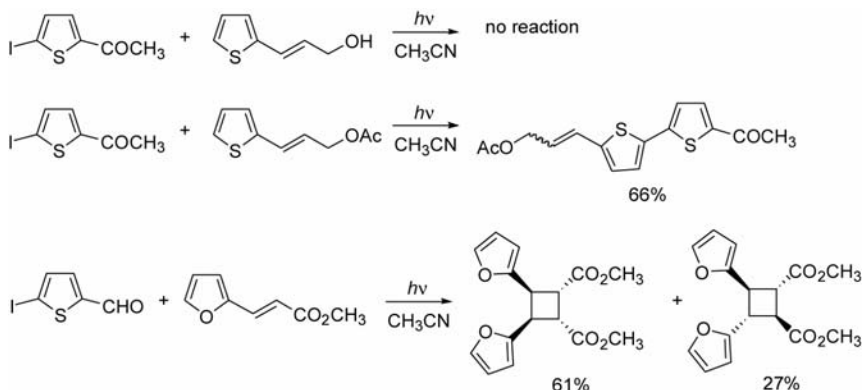
The photochemical coupling between methyl 5-iodothiophene-2-carboxylate (**119**) and 2-chlorothiophene gave the corresponding bithiophene **140**. Also, in this case the reaction with propyne gave a naturally occurring bithiophene **142** isolated from *Arctium lappa* (89JPP(A)(47)191).



One of the problems connected with this type of research was: How do halogenoheterocyclic compounds react when they are in the presence of a substrate containing functionalities able to react with them? To answer this question, the reactivity of halogenoheterocyclic derivatives with arylalkenes was tested. In fact, it is well known that these compounds could give photoaddition reactions on the carbonyl group. The irradiation of halothiényl derivatives in the presence of arylalkenes gave good yields of a *cis-trans* mixture of the corresponding photosubstitution products on the alkenes (Scheme 18) (90JOC4019). When the reaction was carried out on β -alkyl substituted compounds, the same behavior was observed (Scheme 18) (89H(29)1331). However, when an α -alkyl substituent is present, a mixture of two products was obtained (Scheme 18) (93G129).



Scheme 18



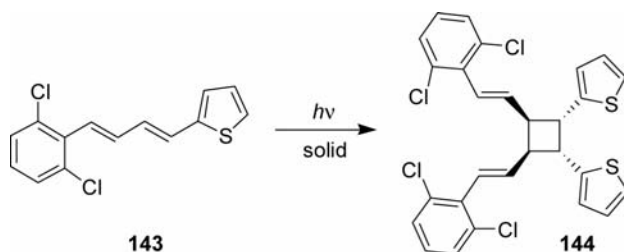
Scheme 19

The irradiation of thienyl derivatives in the presence of arylalkenes-bearing functional groups induced different behaviors. In the presence of an allylic alcohol no reaction occurred, while, in the presence of the corresponding acetate the coupling reaction occurred on the aromatic ring (Scheme 19) (94JCS(P1)1245).

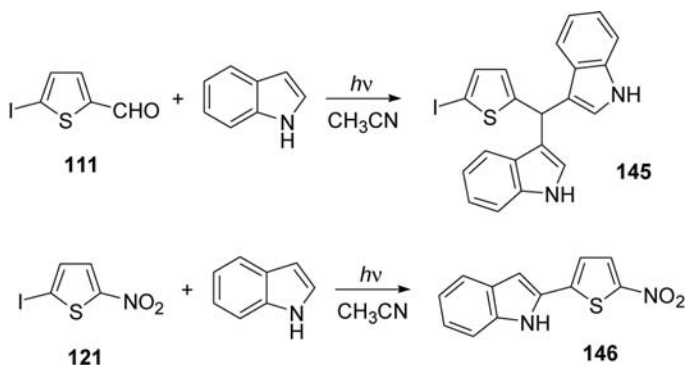
These bithienyls can be used in the synthesis of polyhydroxylated bithienyl compounds, as pointed out in a research devoted to synthesize polar compounds able to interact with DNA (95JPP(A)(91)187). When 5-iodothiophene-2-carbaldehyde was irradiated in the presence of methyl 2-furylacrylate only dimers of this compound were obtained (Scheme 19) (90JCS(P1)2999; 92T9323; 96H(43)959; 02MI65).

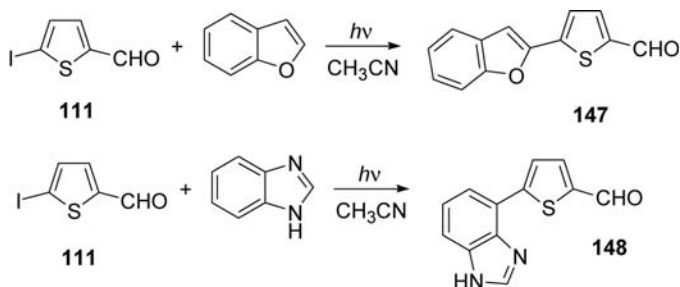
In the above-described reactivity, the reasons of different behaviors between the alcohol and the corresponding acetate are not clear. However, it seems that the presence of an electron-withdrawing substituent on the alkene lowers the reactivity of both the double bond and all the molecules. The dimerization reaction occurred also with 2-furylacrolein or with the corresponding methyl ketone. Instead of 5-iodothiophene-2-carbaldehyde, benzophenone can be used as sensitizer. This reaction did not work with methyl cinnamate, but, if methoxy-substituted cinnamic derivatives were used as starting material, the dimerization reaction occurred in good yields (92T2523). When furylidenetetralones were used as substrates, a transposition reaction occurred (90T7831). The mechanism of the photochemical dimerization of methyl 2-furyl-acrylate was carefully studied. Laser flash photolysis experiments showed that this reaction occurred *via* an energy transfer process from the sensitizer (92T9323). The regiochemistry of this reaction can be justified on the basis of the interaction between LSOMO of the triplet state and the HOMO of the other molecule. The stereochemistry can be explained considering that the obtained

compounds were the most stable ones (96H(43)959; 02MI65). Irradiation of the yellow needles (in the solid phase) of **1433** gave the topochemically expected dimer **144** (73JA2058).

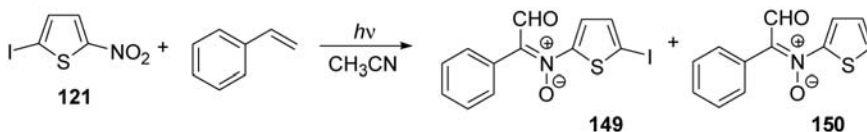


Different behaviors were also observed when the double bond is a part of a heterocyclic ring. The reaction of 5-iodothiophene-2-carbaldehyde with indole gave a completely different product **145** (91T9225). This behavior was in agreement with the previously reported reactivity of the indole with the carbonyl group (90T2367). In this case, a cycloaddition between the double bond C2-C3 of the indole and the carbonyl group was proposed. While this hypothesis was in agreement with the evidence that, when 5-iodo-2-nitrothiophene was used as substrate, the coupling product **146** was obtained, the reactivity of aromatic and heteroaromatic aldehydes with pyrrole to give the same type of product is not in agreement with a cycloaddition reaction (97T1157). In this case, then, an electron transfer mechanism was proposed to account for the observed reactivity. On the contrary, benzofuran gave the expected photosubstitution product **147** (90JOC4019). When benzimidazole was used as substrate the photosubstitution occurred but on the benzenic ring of the molecule giving **148** (91H(32)1059). It is difficult to explain this different behavior. Probably, in the case of benzofuran and benzimidazole, the side of attack could be determined by the different reactivity of the rings within the molecules.

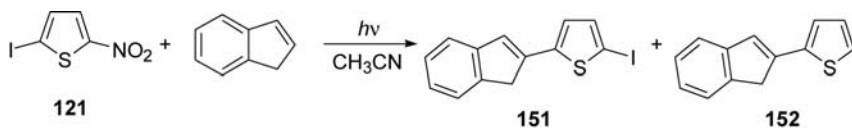




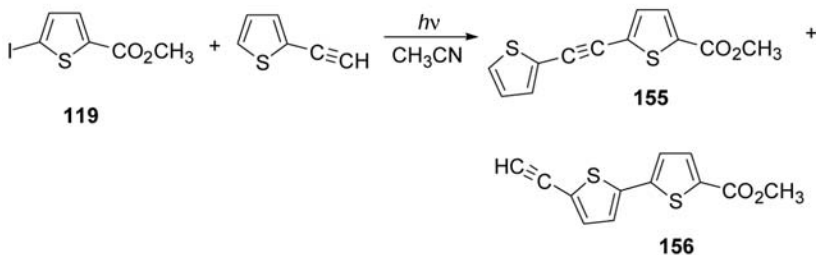
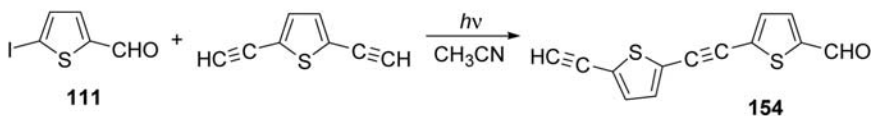
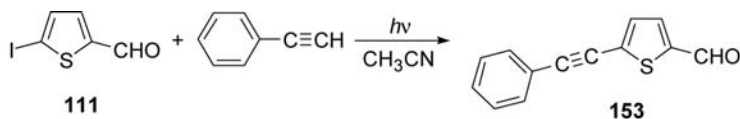
A completely different behavior was reported for the photochemical interaction between halogenonitrothiophenes and arylalkenes. When 5-iodo-2-nitrothiophene (**121**) was irradiated in the presence of styrene, the formation of a mixture of nitrones **149** and **150** was observed. The same behavior was observed by using nitroarenes, such as nitrothiophene or nitrobenzene (94JPP(A)(79)67). The reaction can be explained on the basis of a work published in 1955 where an electron transfer mechanism was proposed. The radical thus formed can give the product of addition of the nitro group to the double bond that, then, can be converted into the product (55JOC1086).



A similar behavior was observed when the same substrates reacted with 1,1-diphenylethylene. In this case, benzophenone was obtained as the main product, together with the formation of nitrones or products deriving from an unusual substitution of the nitro group (96T14253). *Trans*-stylylene showed a low reactivity and the main product was benzaldehyde (96T14253). Indene showed a very complex behavior. When it reacts with 5-iodo-2-nitrothiophene (**121**), the main product was the unusual product **151** deriving from the substitution of the nitro group (94TL633). However, in the presence of nitrobenzene, the main product is due to an oxidative fission of the double bond of indene (96T14253). These different behaviors can be explained considering that nitrobenzene and nitrothiophene show different triplet states (n,π^* and π,π^* , respectively) and the interaction between the LSOMO of the triplet state of the nitroarene with the HOMO of indene can be different. A further factor that affects the reactivity of the substrates is that styrene does not show a dipole moment while indene shows a dipole moment that selects the way of the approaching of the nitro derivatives (96T14253).



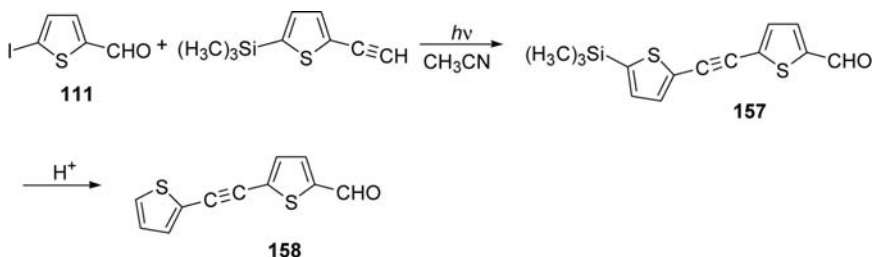
Finally, when 2-nitrothiophene reacts with β -methoxystyrene, a mixture of two products was obtained. The first was an oxidized dimer of the starting material while the second was an amide (95CL109). The irradiation of halogenothiényl derivatives with phenylacetylene gave the corresponding coupling product **153** on the alkyne in 52–54% yields (90JOC4019). The product thus obtained was a naturally occurring thiophene isolated in several *Bidens* plants and in *Coreopsis grandiflora*.



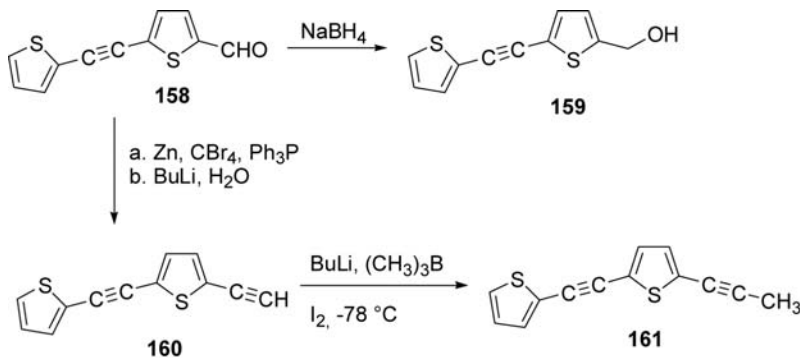
The same behavior was observed using 2,5-diethynylthiophene as substrate to obtain **154**. Unfortunately, the extension of this reaction to other arylalkynes such as 2-thienylacetylene or 2-furylacetylene gave a mixture of two products **155** and **156** (90JOC4019). By using usual reaction conditions, **155** was obtained in 22% yield, while **156** was obtained in 72% yield. Interestingly, using more diluted reaction conditions, **155** (a naturally occurring thiophene isolated in *Berkheya* species) was obtained in 68% yield in the presence of 20% of the other product (89G201).

In order to avoid tedious separation of the isomers and to increase the scale of the reaction, protected alkynes were used. 2-Ethynyl-5-trimethylsilylthiophene was used. The irradiation of 5-iodothiophene-2-carbaldehyde in the presence of this compound gave only the expected substitution

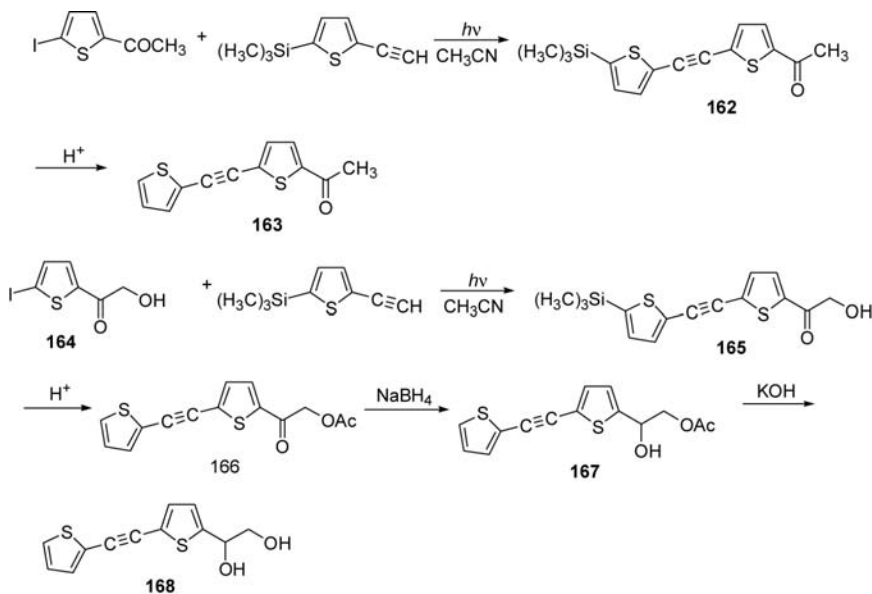
product **157** in 65% yield. The coupling product can be converted into the naturally occurring thiophene **158** in acidic medium in 85% yield (92T9315).



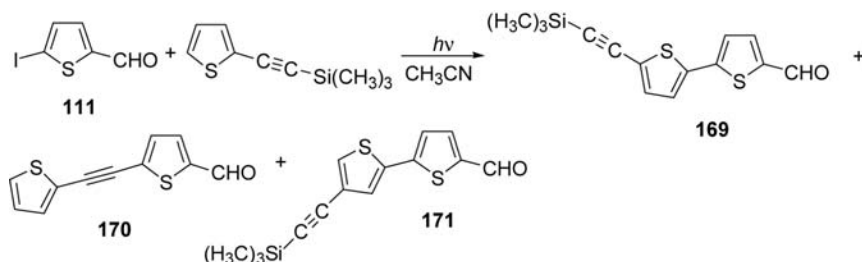
The naturally occurring thienylacetylene **158** can be converted into other naturally occurring thienylacetylenes. The aldehydic group can be reduced to the alcohol **159** or converted into the corresponding acetylene **160**. The acetylide can react with trimethylborane and iodine to give the methylated compound **161** (89G201). All these compounds are naturally occurring thiophenes isolated in *Berkheya* species.



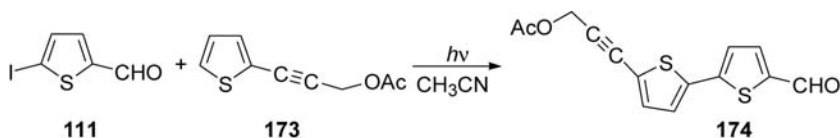
The above-described synthetic sequence using trimethylsilyl derivatives can be used in the synthesis of other naturally occurring thienylacetylenes. In fact, the irradiation of 2-acetyl-5-iodothiophene in the presence of 2-ethynyl-5-trimethylsilylthiophene gave the coupling product **162** in 81% yield (the deprotection reaction gave a naturally occurring thienylacetylene **163** in 91% yield). Furthermore, the irradiation of 2-hydroxyacetyl-5-iodothiophene **164** in the presence of 2-ethynyl-5-trimethylsilylthiophene gave the coupling product **165**. The subsequent deprotection reaction and reduction gave the corresponding diol **168** (92T9315). This is a naturally occurring thiophene isolated in *Centaurea sphaerocephala*.



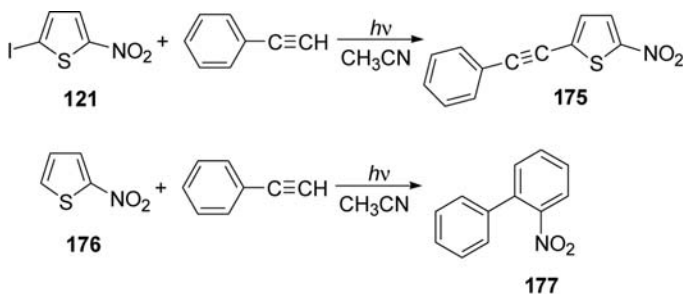
The reaction of 5-iodothiophene-2-carbaldehyde with 2-propynylthiophene gave a mixture of products (94JCS(P1)1245). Also, the reaction of 2-thienyl-trimethylsilylacetylene with 5-iodothiophene-2-carbaldehyde did not give any interesting result. In fact, with the expected coupling product **169**, the authors obtained a product deriving from the desilylation reaction **170** and from the isomerization of the acetylene **171**. In fact, the irradiation of 2-thienyl-trimethylsilylacetylene gave 3-thienyl-trimethylsilylacetylene.



The presence of electron withdrawing substituents on the triple bond decreased the reactivity of the molecule. Using 2-thienyl-1-propyn-3-ol acetate (**173**) as substrate, a photochemical reaction occurred, giving the product of photoarylation **174** (94JCS(P1)1245).

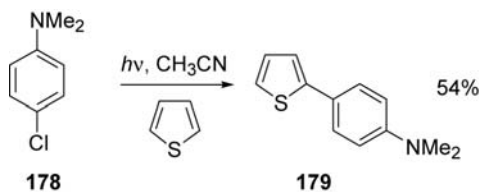


The above-reported data show that the regiochemical behavior of the photochemical coupling is a real question. In the presence of an alkene, the reaction occurs on the alkene, usually. However, if a CH_2OAc group is present, the reaction occurs on the aromatic ring. In the presence of an alkyne, the reaction gives a mixture of products. Only when a CH_2OAc group is present, the arylation occurs selectively. The regiochemical behavior of these reactions can be understood on the basis of the dipoles of the reagents. The assumptions that a reagent approaches the other on parallel planes and that the prevalent interaction is between the SOMO of the thienyl radical and the LUMO of the other reagent have been accepted. This way, the interaction between these two orbitals oriented by the dipoles of the molecules explained the regiochemical behavior of the reaction (95JOC8360). Furthermore, we have to note a different behavior when phenylacetylene is used as substrate. The reaction of 2-iodo-5-nitrothiophene (121) with phenylacetylene gave the corresponding substitution product 175 (94G195).

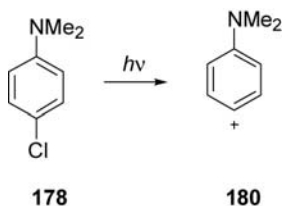


However, 2-nitrothiophene (176), but also 2-acetylthiophene and thiophene-2-carbaldehyde, irradiated in the presence of phenylacetylene, gave the corresponding diphenyl derivative *ortho* substituted 177. The reaction is probably a photo Diels–Alder reaction with extrusion of sulfur from the adduct to give the observed product (95TL6567).

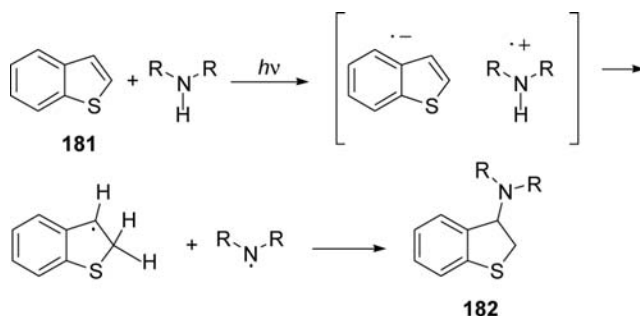
Thiophene reacts with aryl chloride derivatives 178 giving the corresponding arylation product 179 (00T9383).



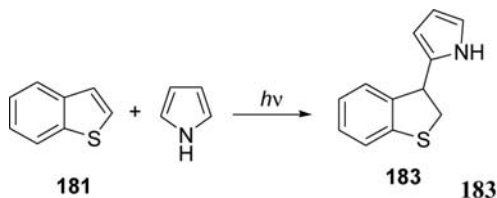
ISC is deemed to be very efficient in aniline and even more with chloro-substituted compounds (Φ_{ISC} ca. 0.9, $k_{\text{ISC}} > 1 \times 10^9 \text{ s}^{-1}$). Thus, photodecomposition of **178** is expected to occur in the triplet manifold and to give cation **180** in the triplet state.



Benzothiophene **181** reacted with a secondary amine to give an electron transfer reaction (71JCS(CC)892; 73T651). The coupling of the radical gave the corresponding addition product **182**.



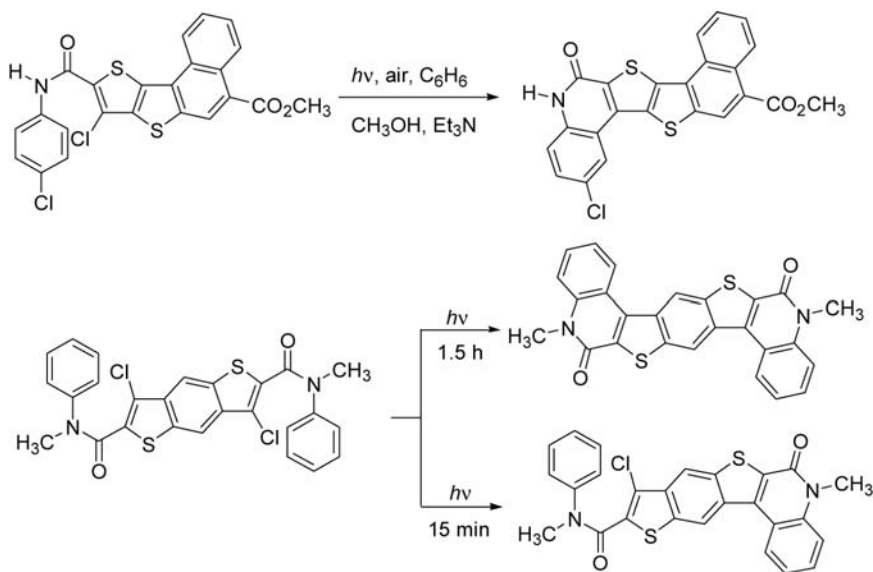
The reaction can also be used with pyrrole. In this case, the reaction occurs on the carbon atom of the pyrrole giving **183**.



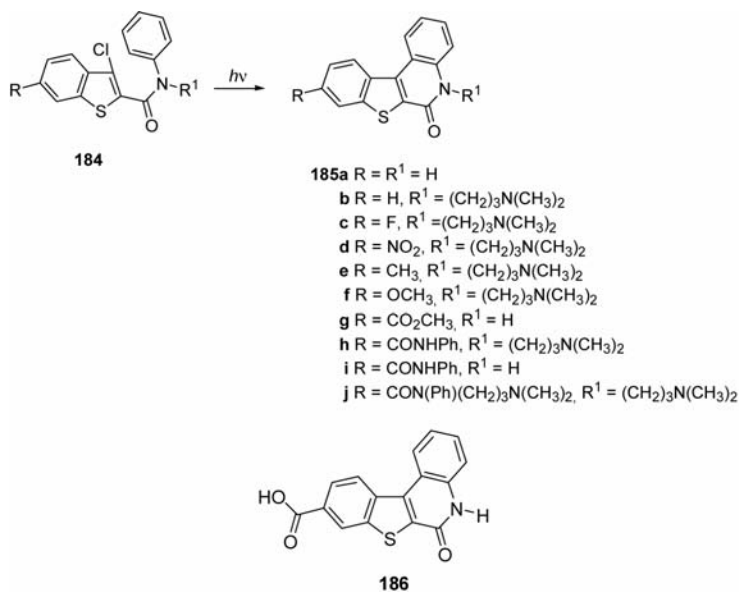
9. STYLBENE-LIKE CYCLIZATION

In an approach intermediate between photochemical arylation and stylobene cyclization, the reaction of chlorothiénylanilides has been described (Scheme 20) (75JOC3001; 89SC1325; 91H(32)2323; 91JHC1997; 95H(41)1659; 95H(41)2691). It is noteworthy that this reaction can be selectively performed.

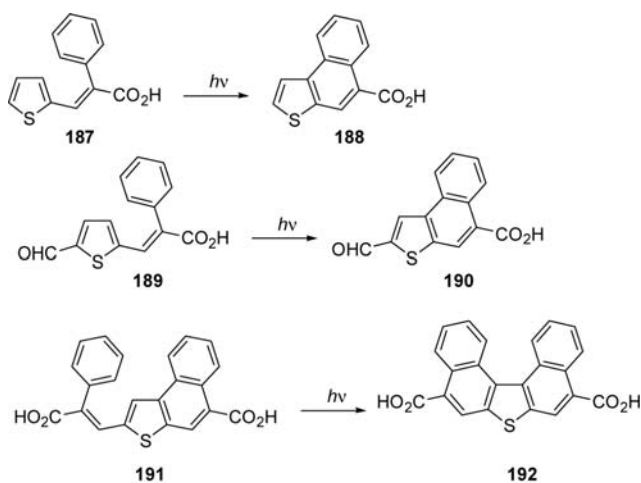
This type of reaction has been used in the synthesis of biological active compounds (03JMC4516). Compounds **185f**, **185h**, and **186** had the strongest inhibition, considering the antitumor activity. Compound **185h** also mostly inhibited HBL cells ($IC_{50} = 0.79 \mu M$), as well as MCF-7, CaCo-2, and Hep-2 cell lines ($IC_{50} = 0.47\text{--}0.65 \mu M$). Compound **185f** was not as toxic for HBL cells ($IC_{50} = 1.58 \mu M$) as for CaCo-2 ($IC_{50} = 0.47 \mu M$) and MIA PaCa-2 cells ($IC_{50} = 0.51 \mu M$).



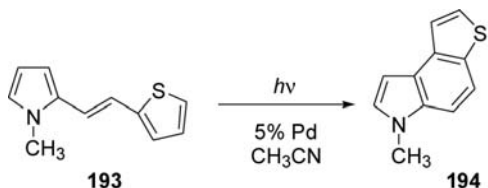
Scheme 20



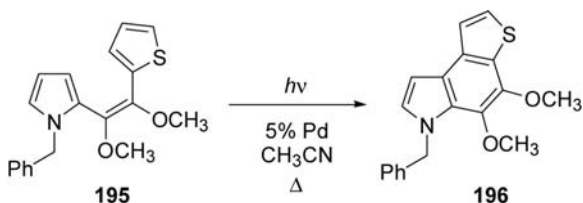
The photocyclization of 1,2-diarylethylenes is a well-known reaction and several reviews appeared in this field (83MI185; 84OR1; 89MI163). The photochemical reactivity of styrylthiophene derivatives bearing electron withdrawing groups has been investigated (92CCA835). The irradiation of **187** gave the coupling product **188** in 47% yield (Scheme 79). When an aldehydic group is present on the thiophene (**189**), the observed yield increased (60%). The double anellation reaction gave low yields of the corresponding coupling product **192** (92CCA835; 96CCA261).



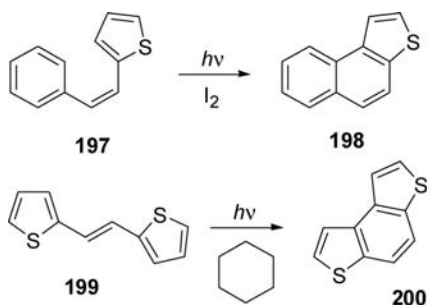
1-(2-Thienyl)-2-(2-pyrrolyl)ethylene derivatives such as **193** react in the presence of 5% Pd/C and with a nitrocompound to avoid the reduction of the carbon–carbon double bond. The reaction seems to be a very useful and general synthetic procedure to obtain **194** (85TL2423).

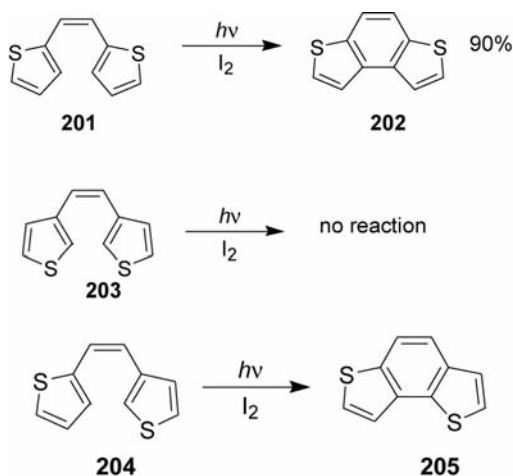


This synthetic procedure was used to synthesize thiophene analogs of PDE-I and PDE-II such as **196**, compounds able to inhibit cyclic adenosine-3',5'-monophosphate phosphodiesterase (86JCS(CC)826). In this case, the photochemical reaction by using Pd on carbon methodology gave the product in 64% yield.

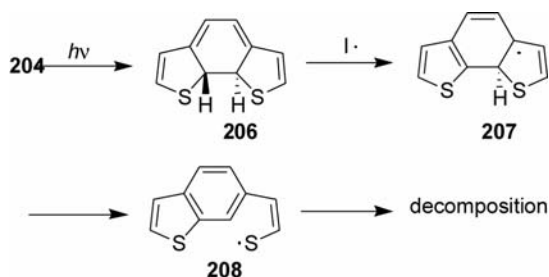


Thienyl-styrene **197** gave the corresponding arylation product **198** in quantitative yields (65TL301; 65JCS6221). The irradiation of the dithienyl derivative **199** gave the coupling product **200** in 30% yield (67JCS(C)6221). Better results can be obtained in the presence of iodine (67JOC3093). The oxidative photocyclization of di-2-thienylethylene **201** proceeds in excellent yield, whereas that of di-3-thienylethylene **203** fails (67JOC3093; 69ZN(B)12).



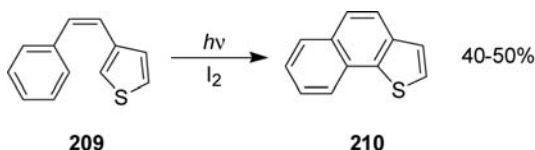


The problem with the latter photocyclization lies in the oxidative trapping of the dihydro intermediate **206**. Abstraction of an allylic hydrogen atom from **206** gives radical **207**, a species that readily suffers carbon-sulfur bond cleavage because of the large driving force associated with the formation of a benzene ring; the resulting thiyl radical **208** gives intractable products.

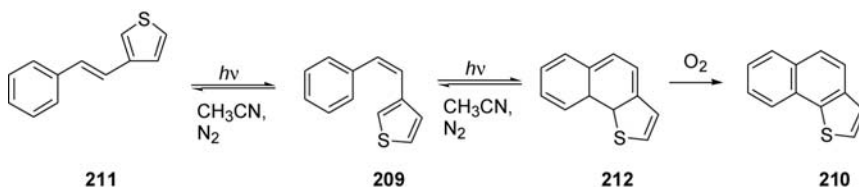


The partial success in the oxidative photocyclization of the mixed dithienylethylene **204–205** can be rationalized by assuming that the two different allylic hydrogen atoms in the dihydro intermediate are abstracted with about equal probability, leading to comparable amounts of **205** and intractable material.

The modest yield in the oxidative photocyclization of 3-styrylthiophene **209** can be accounted for by a similar assumption (70JCS(C)2504).

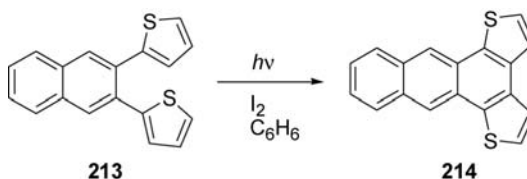


3-Styrylthiophene exists as two isomers: *trans*-3-styrylthiophene (**211**) and *cis*-3-styrylthiophene (**209**). While **211** undergoes only *trans*–*cis* isomerization, **209** may undergo a photochemical ring closure reaction to form dihydronaphtho-[1,2-*b*]thiophene (**212**) in addition to the *cis*–*trans* isomerization. It was found that **212** was oxidized to naphtho-[1,2-*b*]thiophene (**210**) by air during the isolation. The yield of this product was 100% based on the consumption of the starting material **211** and **209** (00TL1951).

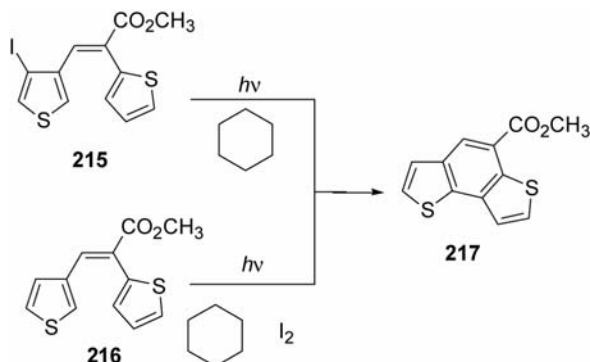


Photoirradiation of oxygen-saturated solutions of the mixture of **211** and **209** in acetonitrile containing 9,10-dicyanoanthracene (DCA) gave 3-thiophenecarboxyaldehyde and benzaldehyde.

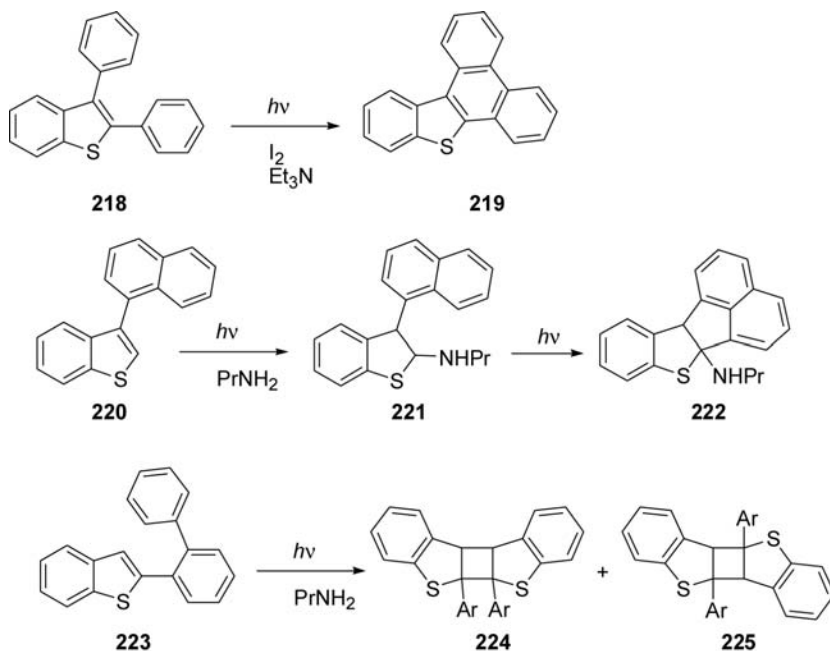
The cyclization has also been described with naphthalene derivatives such as **213**. In this case, the aromatization product **214** was obtained in 54% yield (98S1303).



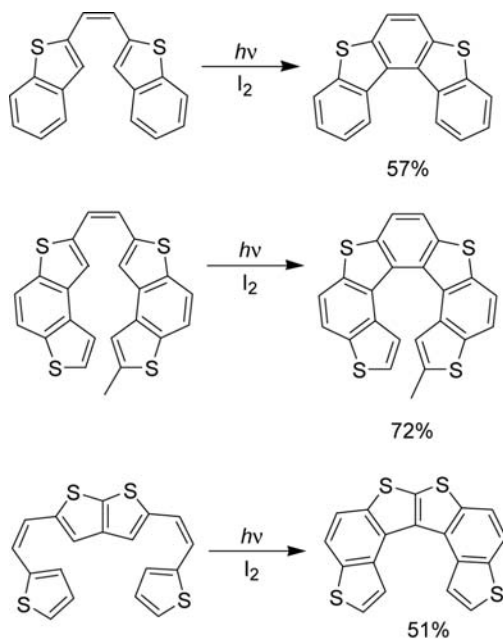
The same reaction can be performed with 3-substituted substrates. In this case, the reaction has been carried out on **216** in cyclohexane in the presence of iodine, or on iodine-substituted derivatives **215** (70JCS(C)2504; 75JCS(CC)106).



The irradiation of the benzothiophene **218** in the presence of a tertiary amine gave the cyclization product **219** (81T75). In the presence of a primary amine, the benzothiophene **220** gave an addition product **221** followed by cyclization to give **222**. The benzothiophene **223** gave only the dimers **224** and **225**.



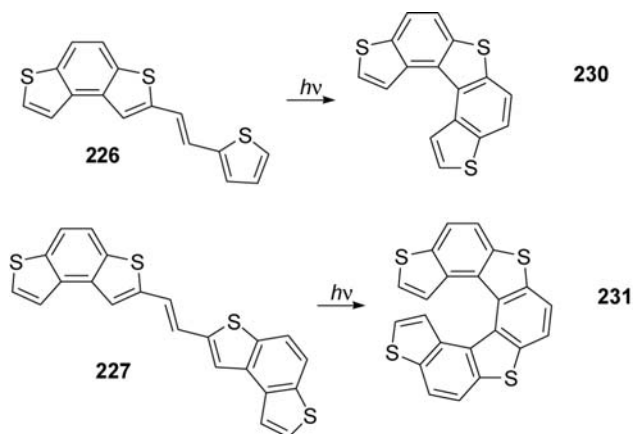
Thiophene analogs of higher polynuclear aromatic systems are readily available by oxidative photocyclization, as illustrated by the conversion of the following olefins to heterohelicenes (Scheme 21) (68JA5339; 70JA6664;

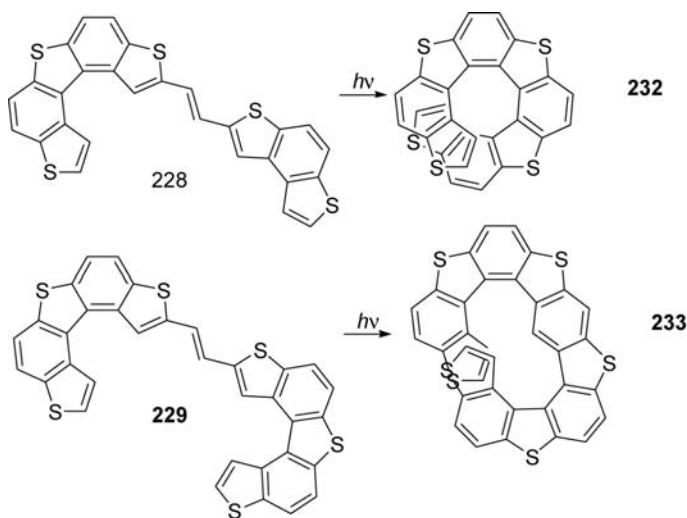


Scheme 21

71ACR65; 71JOC2797; 73JA3692; 74AJC315; 75JCS(CC)106; 83JHC1453; 84JHC185).

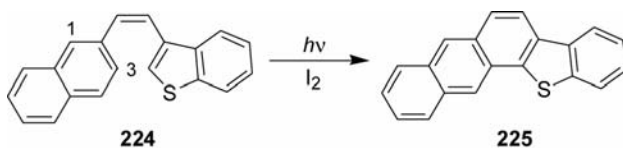
Thiohelicenes **230–233** are stable materials which can be synthesized in good yields via photochemical irradiation (96ACSA71; 96ACSA77; 96ACSA83; 00JCS(CC)1139; 01CM3906; 01SM(119)79).



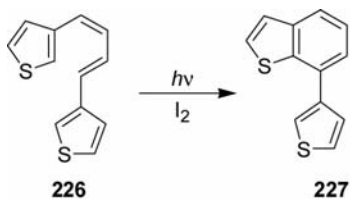


Compound **232** showed the following absorption band at λ_{\max} 293 (12,375), 315 (10,250), 328 (9750), 348 (9500), 401 (9375), and 423 (10,500), while **233** gave absorptions at λ_{\max} 305 (8500), 355 (6000), 345 (6625), 363 (6750), 380 (9375), 425 (3875), and 445 (2500). The emission quantum yields are, respectively, 1.64×10^{-12} (**230**), 4.53×10^{-12} (**231**), 4.42×10^{-12} (**232**), and 1.2×10^{-12} (**233**).

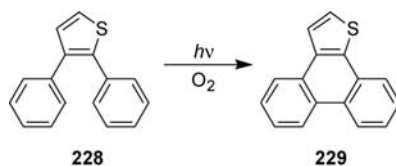
2-Styrylnaphthalene analog **224** photocyclizes at C-3 rather than C-1 (75JCS(CC)106).



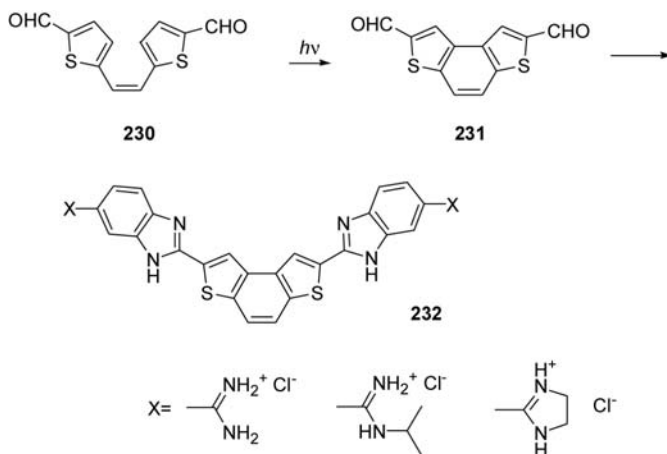
The conversion of the diene **226** to the benzothiophene **227** is an example of a vinyl cyclization involving a thiophene ring (74CJC132).



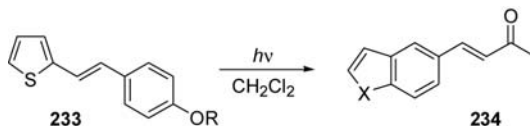
Oxygen is sufficiently reactive to trap the dihydro intermediate generated by photocyclization of 2,3-diphenylthiophene (**228**) (67JA3487).



Tetraphenylthiophene fails to undergo oxidative photocyclization (67JA3487), perhaps because its phenyl groups at C-3 and C-4 are nearly orthogonal to the rest of the π system and hence not involved in the photoexcitation. Alternatively, this failure may be attributed to low reactivity as judged by free-valence indices. Dialdehyde **230** was photochemically dehydrocyclized into **231** by the reaction of photochemical dehydrogenation described earlier (03HAC218). The obtained compound can be decorated to give bis-benzimidazole derivatives **232** with potent fungicidal activity.

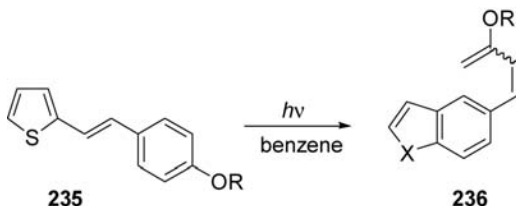


Styrylthiophene derivatives **233** can also be transformed photochemically in dichloromethane solution into the corresponding heterocycles **234** through oxidative cyclization (99OL1039).



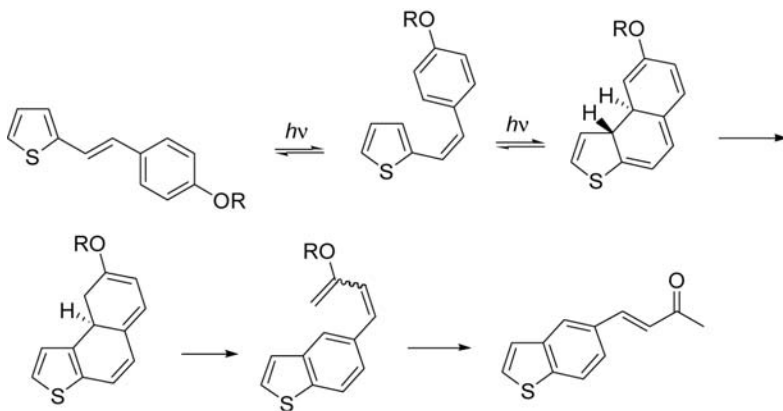
R = Me Yield 88% E/Z ratio 93/7
 R = Et Yield 90% E/Z ratio 88/12
 R = *n*-Bu Yield 93% E/Z ratio 94/6
 R = Ph Yield 98% E/Z ratio 97/3
 R = PhMe Yield 90% E/Z ratio 87/13
 R = 1-naphthyl Yield 96% E/Z ratio 96/4

In dehydrated benzene, upon irradiation of a 1×10^{-12} M *p*-ethoxystyrylthiophene (**235**), the isolate product **236** is considered to be 5-(3-ethoxy-1,3-butadieny)benzo[*b*]thiophene.



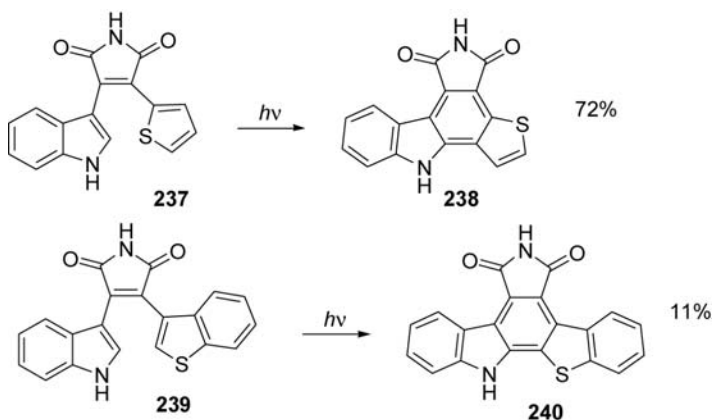
R = Me Yield 72% E/Z ratio 68/32
 R = Et Yield 77% E/Z ratio 92/8
 R = PhMe Yield 64% E/Z ratio 61/39

The mechanism of this novel photochemical rearrangement involves a photochemical conrotatory cyclization, a novel 1,9-hydrogen shift, lateral ring opening, and finally photochemical conversion of the dienol ether to the conjugated ketone (Scheme 22).



Scheme 22

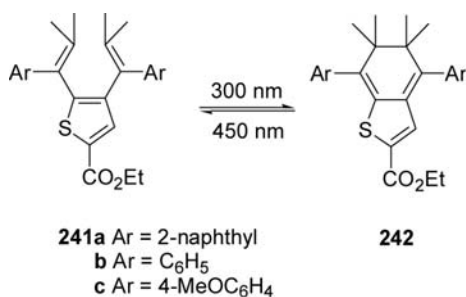
The indolo[2,3-*a*]pyrrolo[3,4-*c*]carbazolo alkaloids (such as **238** and **240**) represent an interesting class of compounds that exhibit diverse biological activities and can be obtained through the following procedure (03JOC8008).



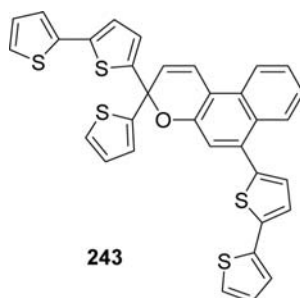
10. PHOTOCHROMISM

Several reviews consider the photochromic properties of thiophene derivatives (98BCJ985; 02MI167; 04CSR85; 04JPP(C)(5)169; 05JPC(A)7343; 06CL1204; 07JCS(CC)781; 08MI1617).

A photochromic system between the colorless trienes **241a–c** and their corresponding closed-ring species **242** of yellow color was devised (02JOC5208; 02OL1099).



The various photochromic parameters which were taken into account in the case of **243** were absorption wavelengths of the closed and open forms, rate constants of thermal bleaching (k_A) and coloration ability or “colorability” (measured as the absorbance A_0 immediately after the irradiation flash) (00JPO523).

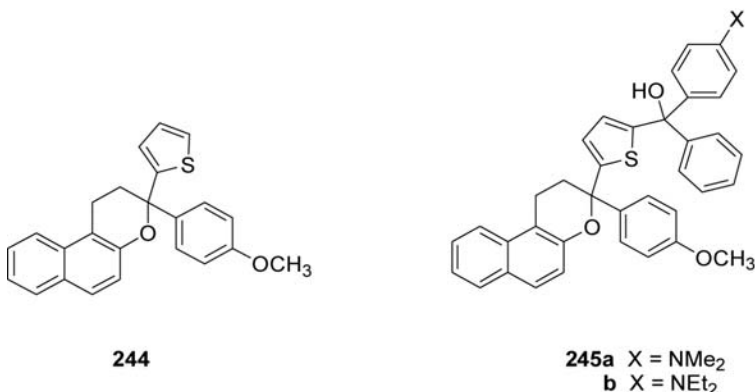


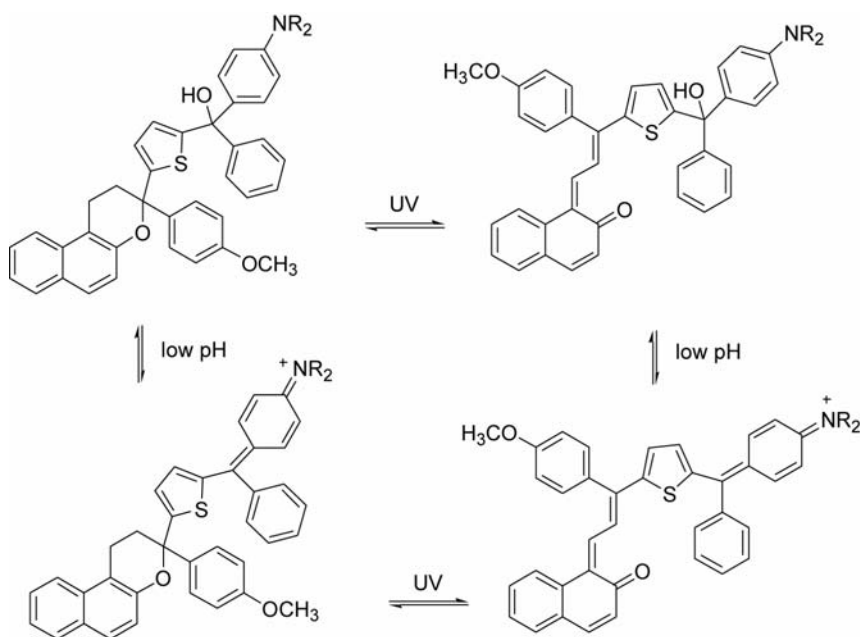
A_0 is expressed by $A_0 = \epsilon_{\text{OF}}\Phi_{\text{col}}k[\text{CF}]_0$ (at low concentration), where k depends on the experimental conditions, ϵ_{OF} is the molar absorptivity of the open form at λ_{max} , Φ_{col} is the photocoloration quantum yield, and $[\text{CF}]_0$ is the initial concentration of the closed form. All the photochromic parameters are very sensitive to the substitution on the naphthopyran ring. There is an important bathochromic shift of the absorption wavelength of the open forms (up to 88 nm) when a bithienyl entity is fixed at position 3. Moreover, the closed-form absorption spectra show minor but significant variations with a maximum shift of 20 nm.

On the other hand, a considerable increase in the coloration ability, A_0 , is observed for the product **243**, which bears five thiophene rings. Amplitude ratios between rapid ($k_{\Delta 1}$) and slow ($k_{\Delta 2}$) kinetics range from 98:2 for **243** to 25:75 for other compounds.

Irradiation with UV light (365 nm, 8 W) to a steady state affected the ring opening of the original colorless naphthopyran unit in each case to generate the orange-red colored species which upon cessation of irradiation readily reverted to their original colorless state (08EJO2031).

It is evident that the incorporation of the diarylmethanol unit induces an ~ 12 nm bathochromic shift in λ_{max} of these compounds with **245** adsorbing at ca. 486 nm and **244** at 474 nm.





Scheme 23

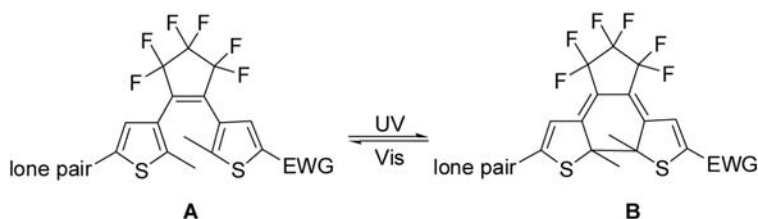
Acetone solution of **245b** was irradiated which resulted in the reversible development of an orange solution. Once the orange color had faded, two drops of MeSO₃H were added to the solution and the gradual development of a violet color was noted. This solution was then irradiated and the reversible evolution of dull purple-brown shade was noted. Once this shade had faded, the acidic solution was neutralized with aq. NaOH solution which resulted in the immediate formation of a virtually colorless solution (Scheme 23).

Photochromic compounds are classified into two types: P-type (thermally stable of the photogenerated isomer) and T-type (thermally unstable of the photogenerated isomer). Among various photochromic compounds, diarylethenes with heterocyclic aryl rings have been developed as a P-type photochromic compound because of some excellent characteristics such as thermal stability of both isomers and fatigue-resistant property (88JOC803; 00CR1685; 04BCJ195). Such materials can be potentially used for application to optical memory media, switching devices, display materials, and photo-mechanical actuators (92NAT(355)624; 99AM910; 01SCI(291)1769; 07NAT(446)778).

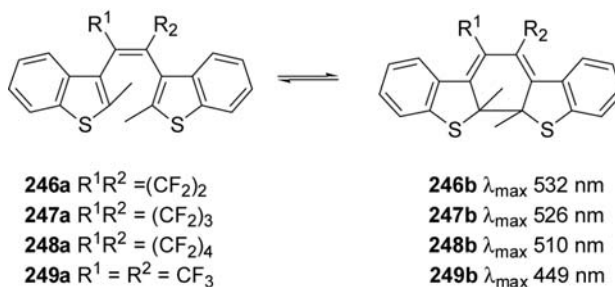
Diarylethenes with thiophene or benzothiophene moieties exhibit excellent thermal stability and outstanding fatigue resistance (88JOC803;

90BCJ1311). Different authors (04JCS(CC)72; 05TL5409) reported the triangular terthiophene derivatives that showed reversible photochromic reactions with high cyclization quantum yields. Yamaguchi et al. (04JCS(CC)1010) developed a new type of 6π -conjugated photochromic system with a bis(2,3'-benzothiényl) unit showing efficient photochromism and thermal stability for the colored isomers.

Photoresponsive compounds containing the dithienylcyclopentene (DTCP) backbone are particularly well studied to modulate chemical reactivity because they undergo rapid and reversible cyclization reactions, when exposed to UV and visible light, between two isomers (**A** and **B**) that have distinct geometric and electronic properties. Another appealing property of this photoresponsive architecture is the fact that the ring-open (**A**) and ring-closed (**B**) isomers tend to exhibit excellent thermal stability across a wide range of temperatures providing potential candidates for use as the “on” and “off” functions to start and stop chemical reactions using light. The two thiophenes in the ring-open isomer **A** are electronically insulated from each other such that any nucleophilic lone-pair electrons located on the one side of the molecular backbone will not sense the electronic effects of an electron-withdrawing group located on the other side. Photocyclization of **A** to the ring-closed isomer (**B**) creates a linearly conjugated π -electron pathway connecting the two groups, allowing the lone-pair electrons to be subjected to the electronic “pull” of the electron-withdrawing group, thus lowering their nucleophilic strength. Consequently, the ring-open isomer **A** is expected to react faster with an electrophile than its ring-closed counterpart **B**. The effect of electronic perturbation on the efficiency of the process has been studied (05CEJ6414).



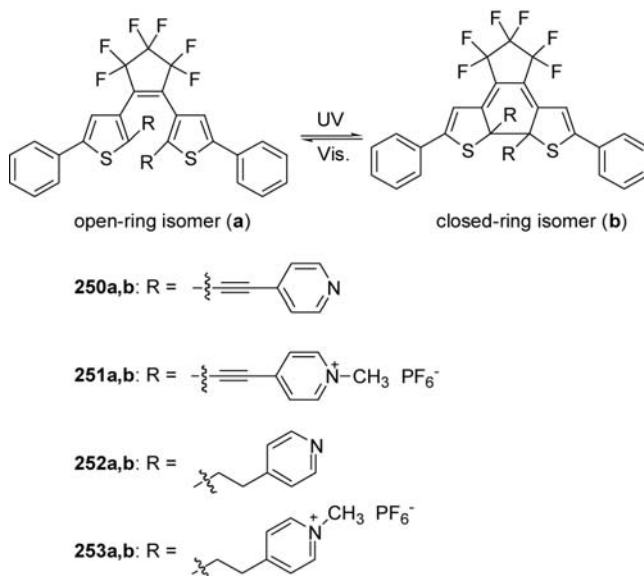
Irie developed some interesting results performed on single crystals of dithienylethene derivatives, showing change in the color and in shape of the crystals (04MI23). To prohibit *cis-trans* isomerization completely and so gain access to fatigue-resistant photochromic compounds, 1,2-diaryl-perfluorocycloalkenes **246–249**-containing heterocyclic rings have been synthesized (92JCS(CC)206; 95CL69; 02MI271).



When a hexane solution of **247a** (λ_{max} 258 nm, ϵ 1.4×10^4 dm³ mol⁻¹ cm⁻¹), upon irradiation with light at 313 nm, a new band appeared at 517 nm (ϵ 9.1×10^3 dm³ mol⁻¹ cm⁻¹) ascribable to the closed-ring form. Under photostationary conditions, the ratio of the closed- to the open-ring form was 45:55. This new band disappeared upon irradiation with light of wavelength ≥ 500 nm.

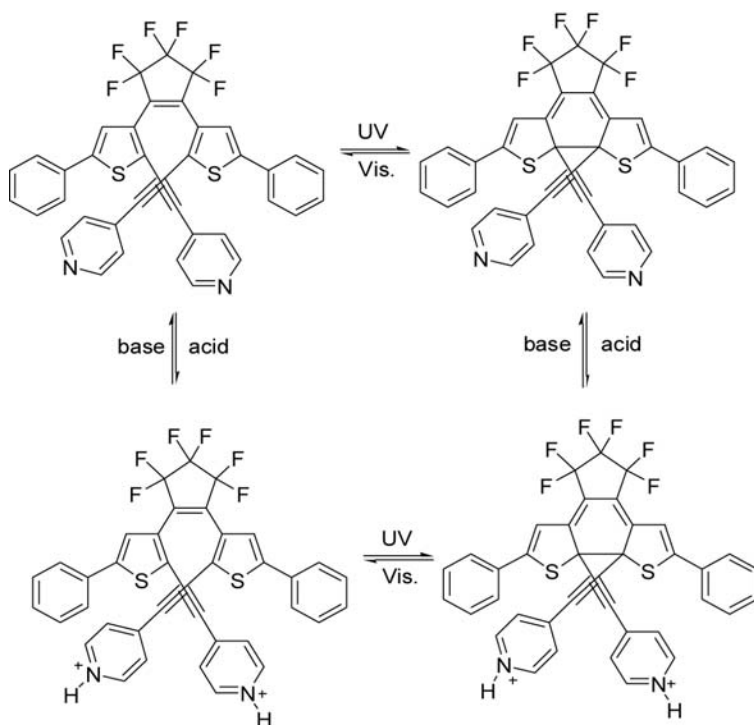
Donor-acceptor substituents on the dibenzothienylethene structure induced an increased reactivity (06T6814).

Substituents on the reactive position greatly influence the photoreactivity. 2-Thienyl derivatives have been reported to work very well (03JA3404). The control of the photoreactivity by external stimuli such as pH or electric potential is important for the practical application of diarylethenes, because a controlled photoreactivity, namely a gated reactivity, can provide a non-destructive readout capability. Pyridyl group is one of the external stimuli-responsive substituents that are quaternized by alkylating reagent or protic acid. Dithienylethene derivatives **250–253** have been reported.



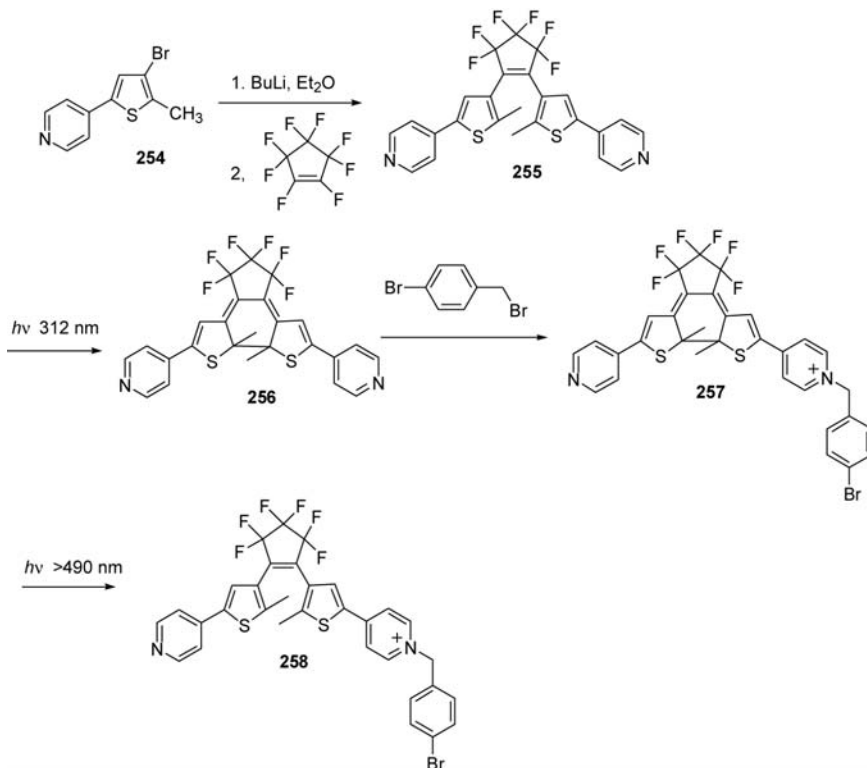
Upon irradiation of **250a** with 313 nm light, a new band appeared in the visible region (08OL2051). The solution turned blue, which suggests the formation of the closed-ring isomer **250b**. The absorption maximum of **250b** was observed at 581 nm. The cycloreversion of **250b** back to the opening isomer occurred by irradiation with visible light ($\lambda > 480$ nm). However, cationic species **251a** did not show any spectral change upon irradiation in any solvent. Both **252** and **253** showed reversible photochromism by irradiation with UV and visible light.

The cyclization quantum yields of diarylethenes **252** and **253**, which have single-bond linker, are more than three times larger than that of diarylethene **250**, which has triple-bond linker. The cycloreversion quantum yields of **252** and **253** are much smaller than that of **250**. After the addition of TFA, the absorption edge of diarylethene **250a** showed a bathochromic shift, which is also observed for **251**. After the addition of an excess amount of TFA, a new band did not appear in the visible region upon 313 nm light irradiation. The generated quaternary cation species **250aH₂²⁺** did not undergo the cyclization reaction (Scheme 24).



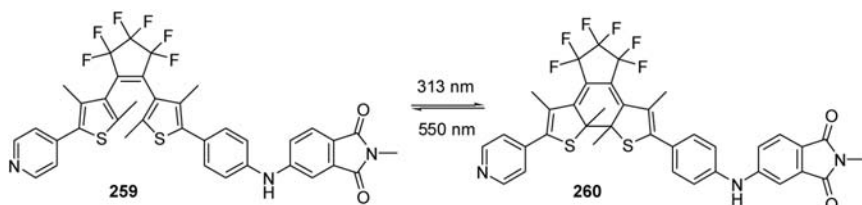
Scheme 24

The monobenzilated DTCP **258** is prepared in four steps via the ring-closed isomer of the bis(pyridine) **255** by lithiating the known pyridylthiophene **254** followed by quenching with octafluorocyclopentene (95CEJ275; 03CL1178; 08T8292).

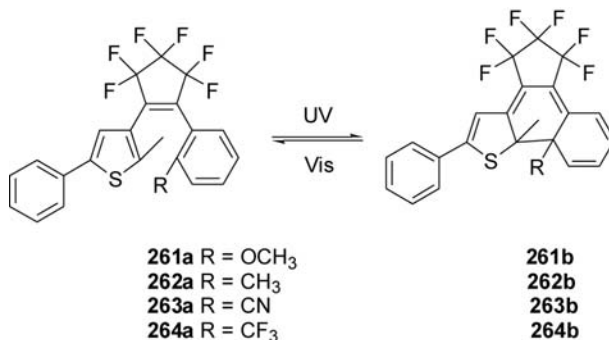


Irradiating a CH₃CN solution of compound **258** with 365 nm light triggers the photocyclization reaction and generated a solution of the ring-closed isomer **257**. The visual demonstration of this photoreaction is the change in the color of the solution from colorless to greenish-blue due to the formation of the extended π -conjugated backbone in the ring-closed isomer. The high-energy bands (356 nm) in the spectra become less intense as a broad band centered at 649 nm appears. Irradiating the colored solution with light of wavelengths >490 nm results in the complete regeneration of the ring-open isomer **258**. The use of dithienothiophene spacers between dithienylethene and pyridinium rings has been reported (95AGE1119). Dithienylethene derivatives bearing imino nitroxide and nitronyl nitroxide moieties have been prepared (05OL3777).

Dithienylethene derivatives bearing a phthalimido group **259** have been studied (08EJO2531). The open form absorbs at 370 nm and irradiation at 313 nm resulted in a rapid appearance of the characteristic absorption band of the closed form **260** at 573 nm.



Compound **261a** exhibited a sharp absorption peak at 275 nm in hexane, which was arisen from $\pi \rightarrow \pi^*$ transition (08T9464). Upon irradiation with 297 nm light, a new visible absorption band centered at 581 nm emerged, while the original peak at 275 nm decreased, indicating the formation of the closed-ring isomer **261b**.

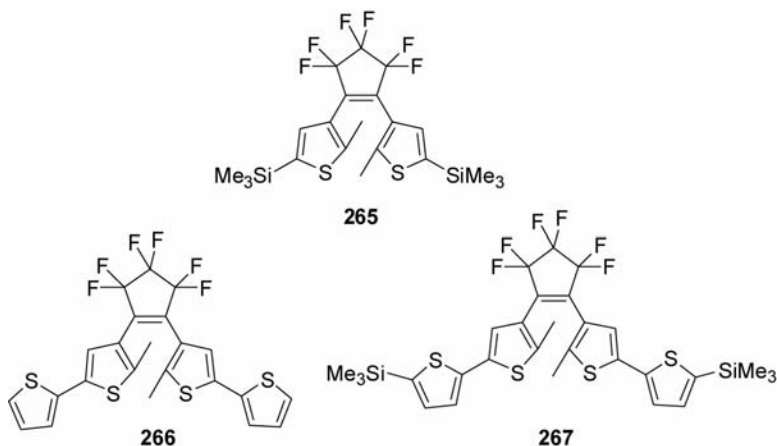


The blue-colored solution turned colorless by irradiation with visible light ($\lambda > 500$ nm), indicating that **261b** returned to the initial state **261a** and a clear isosbestic point was observed at 309 nm. Compounds **262b**, **263b**, and **264b** showed absorptions at 554, 545, and 544 nm, respectively. All the solutions of **262b**, **263b**, and **264b** can be decolorized upon irradiation with visible light ($\lambda > 450$ nm) attributable to reproduce the open-ring isomers. In the photostationary state, the isosbestic points for diarylethenes **262**, **263**, and **264** were observed at 300, 301, and 297 nm, respectively.

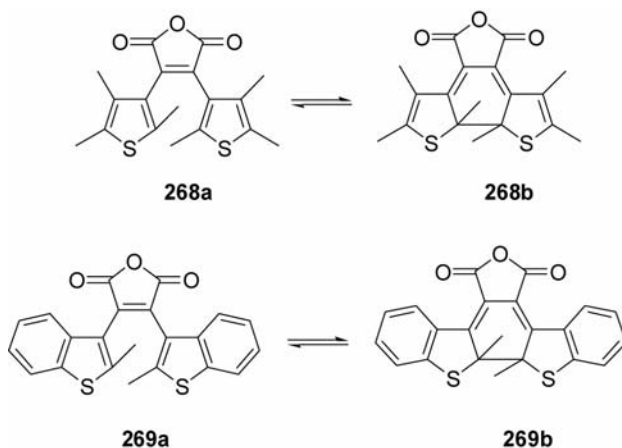
The results indicated that the cycloreversion quantum yields enhanced significantly when the electron-donating groups were substituted at 2-position of the benzene ring of these diarylethenes, while the cyclization quantum yields improved remarkably when the electron-withdrawing groups were substituted at the same position.

In PMMA (polymethylmethacrylate) amorphous film, diarylethenes also showed good photochromism. At 80°C, the blue color of **261b** disappeared completely after 3 min. In general, dithienylethene derivatives bearing electron-donating substituents show good thermal stability, but those with strong electron-withdrawing substituents, such as dicyanovinyl group, show thermal instability. The fatigue-resistant characteristics of **261** and **262** in solution indicated that ~70% of each **261b** and **262b** was destroyed after 10 repeat cycles, but only 27% of **263b** and 12% of **264b** were destroyed after 11 repeat cycles at the same conditions. The fatigue resistances of diarylethenes **261–264** in the solid state (PMMA amorphous film) are much stronger than those in solution. After 200 repeat cycles, these compounds still showed good photochromism with only ~37% degradation of **261b**, 22% of **262b**, 9% of **263b**, and 7% of **264b**, respectively. Compounds **261a**, **262a**, and **264a** showed no photochromism in the crystalline phase. Fluorescent emissions of **261a**, **262a**, **263a**, and **264a** were at 353, 409, 475, and 436 nm, respectively, when excited at 285 nm; while those of them were observed at 435, 417, 471, and 445 nm when excited at 295 nm in PMMA film. The fluorescence quantum yields of **261a**, **262a**, **263a**, and **264a** were 0.047, 0.021, 0.010, and 0.041, respectively. The introduction of methoxy group at 2-position of benzene ring in diarylethene system can significantly enhance the fluorescence quantum yield.

Triphenyl imidazol-substituted derivatives have also been described (01JOC5419). *n*-Hexane solutions showed photochromism owing to photocyclizations from the open-ring forms **265–267** to closed-ring forms by irradiation with 350 nm light for several minutes (94JCS(CC)2123). The absorption maxima of the closed-ring forms appeared in the Vis region. The closed-forms were fairly stable at room temperature and were converted back to open-ring forms by irradiation with Vis light. Dithienylethylene derivatives bearing oligothiophenes in position five of the thienyl rings have been reported. In this case, the photochromism has also been studied on poly(methylmethacrylate) film showing the same behavior observed in solution. Passing from the open form to the closed one, the fluorescence was quenched (06MI3685). Oligothiophenes linked in position 5 on the thienyl ring have also been reported (96CEJ1399). The same behavior was shown by organoboron derivatives (06OL3911).



Dithienylethene derivatives can also be linked to a fluorescent bis(phenylethynyl)-anthracene residue, showing that the irradiation at 313 nm, able to give the closed form of the photochromic device, the fluorescence of the anthracene moiety at 530 nm is efficiently quenched ($\Phi_F < 0.001$) (01JCS(CC)711).



The alkene moiety in this type of compounds can also be another heterocyclic ring, such as thiophene or thiazole (07EJO3212). On exposure to 405-nm light **268a** changed to **26b8**, and a new peak appeared at 564 nm (the yellow solution of **268a** turned to red). **268b** returned to **268a** upon irradiation with 546-nm light, and the peak at 564 nm disappeared (92JPC7671; 94CPL(230)249).

The conversion from **268a** to **268b** in the photostationary state under irradiation with 405-nm light decreased with the increasing solvent polarity. The conversion of 73% in hexane decreased to 39% in THF. The ring-closure quantum yield of 0.12 in hexane decreased to 0.03 in acetonitrile, while the ring-opening quantum yield remained almost constant even the solvent was changed from benzene to acetonitrile.

Absorption maxima of the open-ring form in benzene, THF, and acetonitrile were observed in the wavelengths ranging from 335 to 340 nm. Although the maximum showed a small hypsochromic shift in hexane, the solvent shift in the absorption spectrum was rather small. On the other hand, the fluorescence spectra showed remarkable Stokes shifts depending on the solvent polarity. The maximum at 488 nm in hexane shifted to 560 nm in THF. At the same time, the intensity decreased. The fluorescence intensity in acetonitrile was <1% of the intensity in hexane. The results indicate that the excited state of the open-ring form has a polar structure with a large dipole moment.

Compounds **268a** and **269a** showed large Stokes shifts in polar solvents. Such large Stokes shifts have been observed in many TICT (twisted intramolecular charge transfer) molecules. Fluorescence decay time measurement indicated that there were two kinds of excited states, fast and slower decaying components, and the latter was the emission from the more polar state.

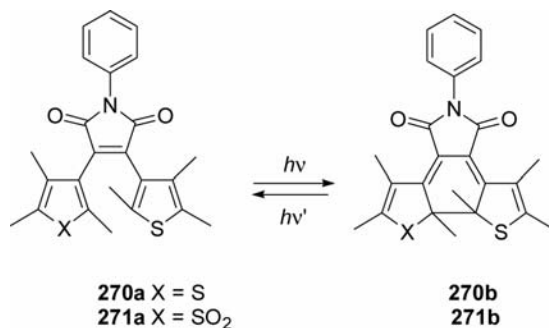
Compound **268a** consists of two thiophene rings and a maleic anhydride moiety: the former is a donor and the latter an acceptor. Compound **269a** has two benzothiophene rings as the electron donating group. Compound **268a** is considered to change its conformation by the rotation of the single bond between the thiophene ring and the maleic anhydride in the excited state, depending on the solvent polarity. In less polar solvents, a planar less polar conformation is energetically more stable than twisted polar one. In polar solvents, the twisted charge transfer state becomes more stable than the planar state. Decrease of the ring-closure quantum yields in polar solvents implies that the TICT state is not responsible for the photochromic reaction, and the interconversion between the TICT state and the planar geometry state is not possible. In less polar solvents, the excited state stabilizes to a planar conformation with a low dipole moment and undergoes a concerted ring-closure reaction in the conrotatory mode. The planar geometry is closed to the structure of the closed-ring form. In polar solvents, on the other hand, the Franck–Condon state converts to the energetically more stable charge-separated state. This state with a large dipole moment undergoes a twist which forces the plane of the thiophene ring to become perpendicular to that of the maleic anhydride moiety. The perpendicular geometry is disadvantageous to the ring-closure reaction and deactivates to the ground state without any reaction. In this geometry, the two moieties are orbitally decoupled, and the radiative transition from

the excited state to the ground state is overlap forbidden. The low fluorescence yields and longer decay time in polar solvent are thus expected.

A picosecond laser flash photolysis study appeared on **268a–b** (94CPL (230)249). After excitation at 355 nm of **268a**, the absorption maximum at ca. 560 nm is ascribed to the closed form and the depletion below 450 nm is due to the bleaching of the open-form, respectively.

First, a broad absorption spectrum whose intensity increases toward the blue region with a maximum at ca. 450 nm appears within the time resolution of the apparatus, followed by the growth of a shoulder around 540–570 nm in a several tens of picoseconds time region. Second, the absorbance around 450 nm gradually decreases in a several hundreds of picoseconds region, together with the appearance of the two absorption peaks at 470 and 565 nm as well as the broad spectrum in the wavelength region longer than 650 nm. Third, almost no evolution of the spectra was observed on and after ca 1 ns from the excitation. The absorption maximum at 565 nm observed in the time region longer than 1 ns can be safely assigned to that of the closed-form of **268a**. The time profile at 450 nm shows a time constant of 360 ps. The maximum at 450 nm may be attributed to the S_1 state of the open-form.

The increase of the absorbance at 675 nm is ascribed to the formation of other species such as the triplet state. Some conformational rearrangement seems to be responsible for the relaxation process in the S_1 potential surface to produce the fluorescent state, which has a large dipole moment. During this relaxation process in the S_1 state, some of the **268a** may undergo the cyclization reaction and others relax to the fluorescent state. Closed-form of **268a** in benzene solution was excited with a picoseconds 532 nm laser pulse. The depletion around 560 nm and positive absorption around 600–750 and 400–500 nm are observed. The former negative absorption can be safely assigned to the bleaching of the closed form. The ring-opening reaction took place with the time constant of <2–3 ps.



Upon irradiation of **270a** with 405 nm light, the yellow color solution turned to red-purple, and new absorption bands appeared at 526 and

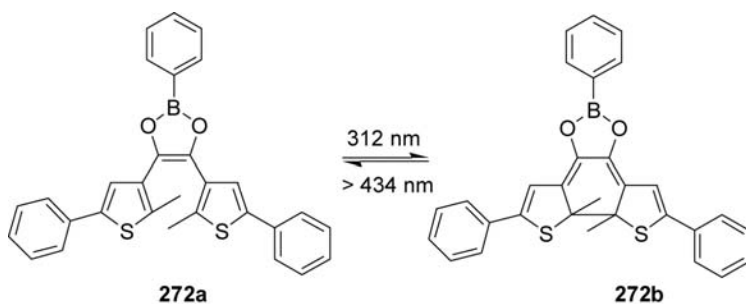
377 nm (07T9482; 08JCS(CC)3281). The color change is attributed to the photocyclization reaction from the open-ring isomer (**270a**) to closed-ring isomer (**270b**). Upon irradiation with visible light ($\lambda > 500$ nm), the peaks at 536 and 377 nm gradually decreased and finally disappeared.

The conversion from the open- to the closed-ring isomer in the photo-stationary state under irradiation with 405 nm light decreased with increasing solvent polarity. The cyclization quantum yield decreased to 0.097 in THF, 0.029 in ethanol and 0.013 in acetonitrile, respectively.

Upon irradiation of **271a** in cyclohexane solution with 405 nm light, the yellow color solution turned to red, and new absorption bands appeared at 498 and 331 nm. Upon irradiation with visible light ($\lambda > 500$ nm), the peaks at 498 and 331 nm gradually decreased and finally disappeared.

The conversion from **271a** to **271b** in cyclohexane was 80%, which is much higher than that of **270a** in the same solvent. **271a** was efficiently converted to **271b** even in polar solvents such as ethanol and acetonitrile. The weak solvent dependence observed in **271a** can be attributed to the weak electron donating ability of the *S,S*-dioxide thiophene ring.

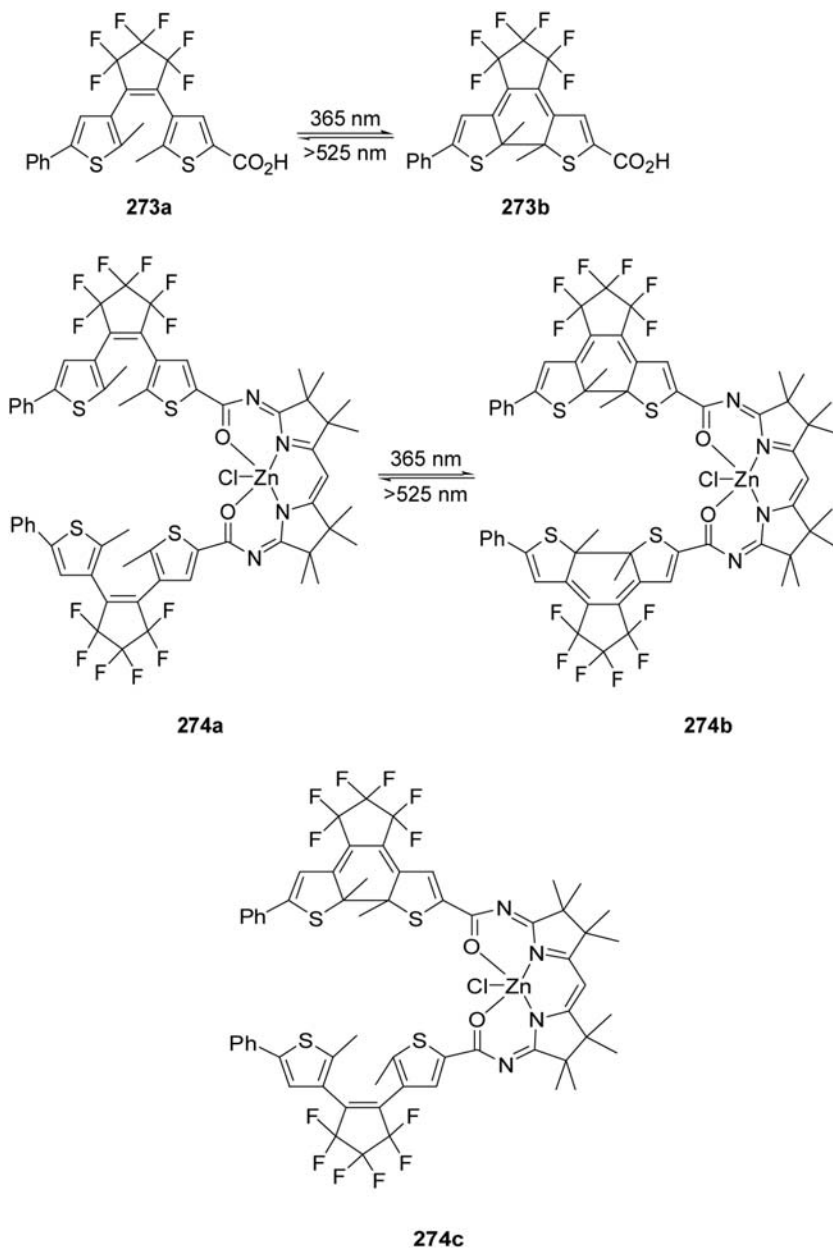
Irradiating a benzene solution (anhydrous and degassed) of compound **272a** with 312 nm light triggers the photocyclization reaction and generates the ring-closed isomer **272b** (08AGE5034). The visual demonstration of this photoreaction is the change in color of the solution from colorless to purple due to the formation of the extended π -conjugated backbone created in the ring-closed isomer.



The synthesis of a fluorescent photochromic system **274a** with a high fluorescence contrast ratio by covalently joining a highly fluorescent zinc bis(acylamidine) allowing effective energy transfer from the excited state of the dye to the photochromic component has been reported (08JPP(A) (200)74).

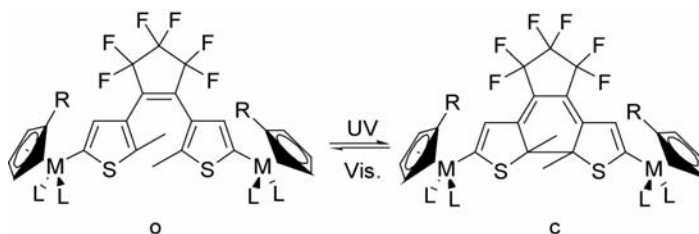
Irradiating a solution of the complex with UV light (365 nm) results in a decrease in the high-energy absorption bands corresponding to the ring-open isomer and an accompanying appearance of a broad absorption band

in the visible spectral region that corresponds to ring-closed isomer ($\lambda_{\text{max}} = 665 \text{ nm}$).



These spectral changes are responsible for the change in color of the solution from yellow to blue-green as the photostationary state is reached. Irradiation of the colored solution containing the ring-closed isomer (**274c**) with visible light at wavelength of 525 nm and greater regenerates the original spectrum corresponding to the ring-open isomer and the color of the solution changes back to yellow.

A CH_2Cl_2 solution of the ring-open isomer of the hybrid compound (**274a**) displays intense fluorescence at 502 nm when excited at 470 nm. Converting isomer **274a** into its ring-closed counterpart by irradiating a solution of it with 365 nm light results in a decrease in the fluorescence intensity at 502 nm to one that is at lower limits of the fluorescence detector showing the effective photoregulation of fluorescence by the photochromic component. The fluorescence quantum yield of **274a** in CH_2Cl_2 is 0.12 ± 0.02 . Fluorescence lifetimes are 1.40 ± 0.05 ns as measured for two different solutions using time-resolved techniques. The fluorescence decay is mono-exponential and the same lifetime is measured, which implies the presence of only one fluorescent species.



275: L = CO M = Fe R = H

276: L = CO M = Ru R = H

277: L = CO L = PPh₃ M = Fe

278: L = CO L = PPh₃ M = Ru R = H

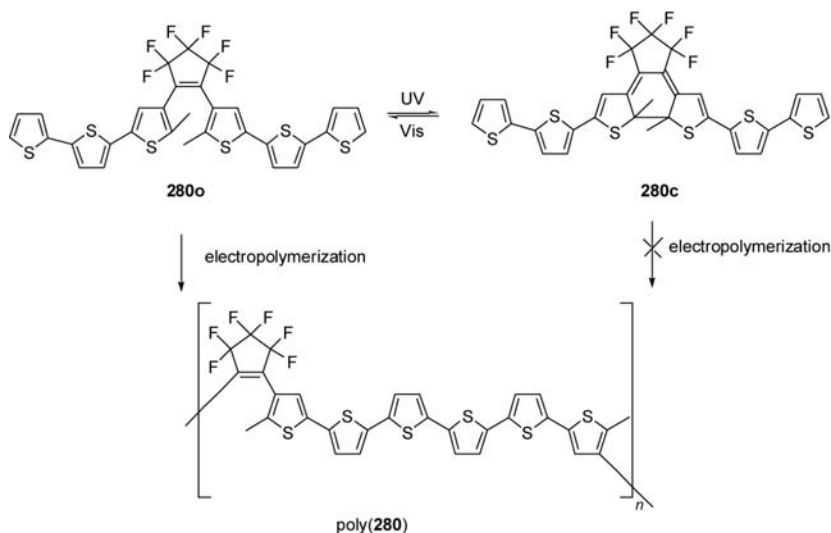
279: L = dppe M = Fe R = Me

The hybrid Zn bis(acylamide) **274a** can be immobilized in thin films of PMMA (Poly(methyl methacrylate)) by spin-casting CHCl_3 solutions of it onto quartz substrates. All films of **274a**-PMMA can be irradiated with 365 nm light to trigger the ring-closing reactions and generate colored films containing the ring-closed isomer (**274c**). Photobleaching is accomplished by using light with wavelengths longer than 525 nm, which as it does for the solutions, regenerates the ring-open isomer. When excited at 470 nm, the films emit light at 499 nm when the hybrid is in its ring-open form.

UV irradiation of the dithienylethene complexes **275–279** caused ring closure to form the purple- or deep-blue-colored closed isomer showing

the absorption maxima in the visible region (550–600 nm) (08JCS(CC) 5812). The ruthenium complexes cyclized more efficiently than the iron derivatives, and introduction of the phosphine ligands retarded the cyclization. The Fe-dppe derivative **279** did not undergo the photochemical cyclization at all. Dithienylethene derivatives with Fe(η^5 -C₅Me₅(dppe) termini have been described (07JCS(CC)1169).

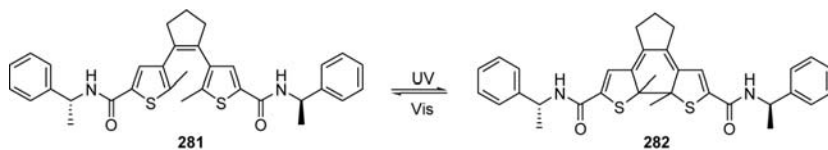
The ability to switch off and on the electropolymerizability of the monomer **280** with UV and visible light was reported (08JA12850).



The bithiophene-substituted photochromic dithienyl perfluorocyclopentene (**280**) can be switched reversibly by UV and visible light between a colorless open state (**280o**) and a colored closed state (**280c**), respectively. In the open state (**280o**), electropolymerization yields alkene bridged sexithiophene polymers (poly(**280**)) through oxidative α,α -terthiophene coupling, while in the closed state electropolymerization does not occur.

The absence of color change with irradiation with UV light confirms that ring closing does not occur in the redox polymer film.

A diarylethene switch (**281**–**282**) that combines excellent photochromic properties with the ability to undergo self-assembly has been reported (05AGE2373).



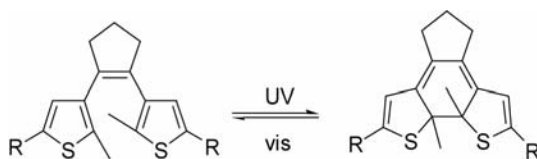
Pronounced self-assembly of **281** and **282** in nonpolar solvents (e.g., aliphatic and aromatic hydrocarbons) takes place as a result of hydrogen bonding between amide groups to result in the formation of gels above a critical gelation concentration.

Irradiation ($\lambda = 313$ nm) of a solution of **281** (1.5 mM) in toluene at room temperature results in a transition to a gel of **282** (red colored), whereas subsequent irradiation of this gel with visible light ($\lambda > 420$ nm) causes it to dissolve to give a solution of **281**.

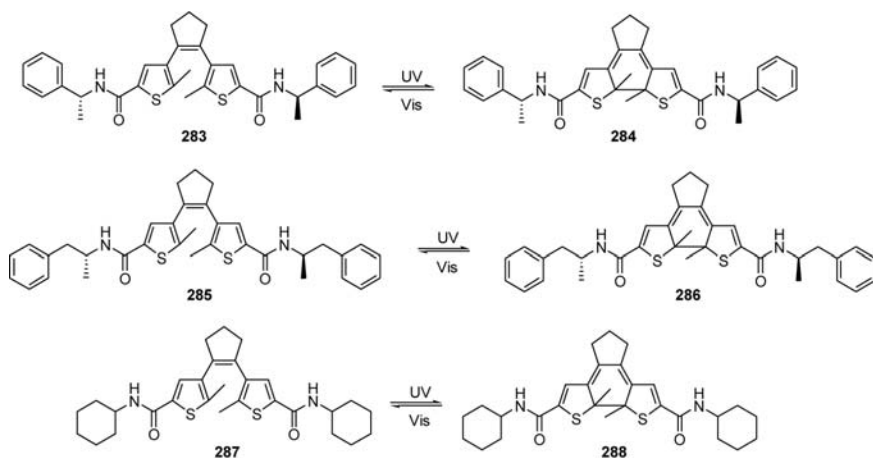
The supramolecular chirality of the gel governed the dynamic molecular chirality through the hydrogen bonding networks formed and upon photochemical ring closure of the dithienylethene, which allows for locking of the molecular chirality of the gel molecules stereoselectively. Furthermore, it was shown that switching between gels of different aggregate (fiber) stability could be achieved with the gel-to-liquid transition being achieved by photochemical ring opening of gelator molecules (Scheme 25) (08OBC1544). Indeed, photochemical control of supramolecular aggregation was used to achieve dynamic holographic pattern formation.

The coassembly of achiral (soldier) with chiral (sergeant) diarylethene photochromic switches (**283–284**, **285–286**, **287–288**), accompanied by a dynamic selection and amplification in a supramolecular system was reported (05JA13804). The highly specific self-assembly features of low-molecular-weight gelators (LMWG) bearing multiple hydrogen bonding groups, which can be addressed and controlled by incorporation of a diarylethene photoresponsive unit, were described.

Diarylethene switches are present in two, rapidly exchanging conformations (*P* and *M* helicity), which upon photochemical ring-closure lead to the *RR* or *SS* enantiomers in equal amounts. The authors showed that aggregation of a chiral diarylethene switch in the open form **283** leads to selection of only one of the helical forms of **283** in the gel state. Subsequent photochemical ring-closure of **283** to **284** in the gel state proceeds with 96% diastereoisomeric excess and a photostationary state (PSS) of 40%, whereas in solution, no stereoselection is observed.



Scheme 25

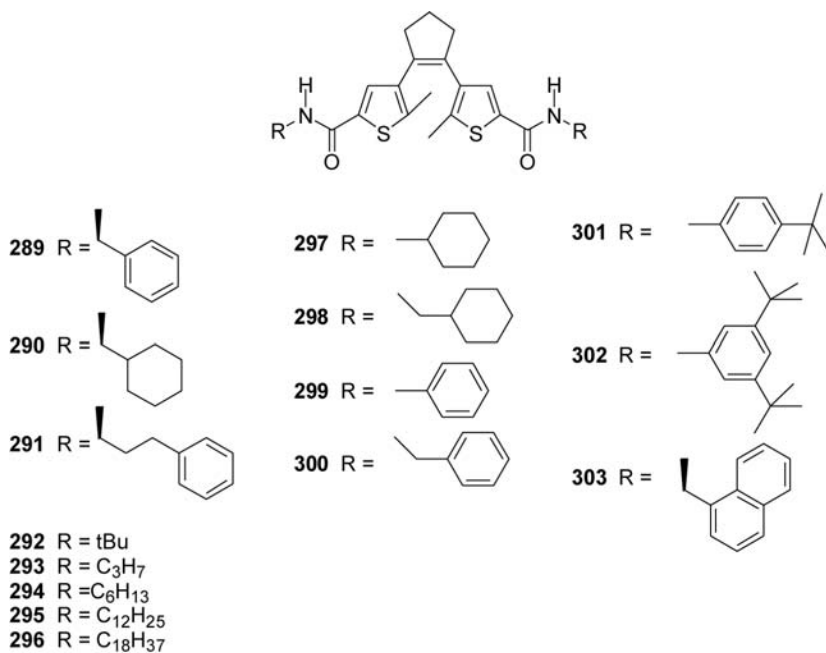


287 must be capable to coassembly with both 283 and 285. Neither 283, 285, nor 287 (0.6 mM in toluene) on their own form gels at 0°C. However, for a sample containing 0.6 mM of 287 and 0.6 mM of either 283 or 285, a gel is obtained, indicating that in the mixed system at 0.6 mM cooperative assembly occurs. Indeed, the circular dichroism (CD) spectra reveal a dramatic increase of the helicity for mixtures of 287 with 283 or 285 at low concentration (0.3 mM) at which 283–287 alone do not gelate.

An innovative system based on regulation of the intramolecular interactions, with which the on/off photoactivity of photochromism can be achieved was reported (08OL3639).

Construction and destruction of the specific hydrogen bonding interaction in the photochromic molecules is one of the best ways of fastening and unfastening the rotating thiophene rings of the photochromic unit. The “lock” process could be realized by fabricating specific intramolecular hydrogen bonding interactions in the photochromic molecules and the photoactivity was lost, in which the photoswitchable unit was fastened in a photoinactive conformation. Reversely, the “key” process can be achieved by destroying the corresponding hydrogen bonding interaction and the photoactivity would be reactivated.

Low-molecular-weight organic gelators (LMWGs), containing responsive perhydrodithienylcyclopentene photochromic switches (289–303), offer the possibility to control the self-assembly of individual molecules into supramolecular structures (01JCS(CC)759; 04SCI(304)278; 08T8324).



In methanol solution at λ_{exc} 312 nm, the photostationary (PSS) reached is >95% in favor of the closed state with the exception of **289** (77%) and **294** (87%).

It is apparent that the amide functionalized dithienylethene switches in the open state capable of gelating both apolar and aprotic solvents with gelation occurring spontaneously upon cooling. The driving force for gelation is expected to be primarily due to the hydrogen bonding interactions between the amide functional group.

The transfer of chirality of the amide component to the photochromic components of achiral LMWGS co-assembled within the same gel fibers, the effect of solvent on the transfer, and the interaction between chiral and achiral molecular units of the gel fibers are examined.

LMWGs (chiral) **289o–291o** were co-assembled with achiral LMWGS **293o–300o**. The chirality is expected to be controlled by the chiral “sergeant” molecule, which guide the assembly of the achiral “soldier” molecules. It appears that after co-gelation of **289o** with the series of achiral gelators, **293o–295o** and **297o–300o**, in toluene, the CD signal observed indicates that the helicity of the gel fibers is the same as observed for gels of **289o** alone. This indicates that **289o** is directing the chirality of the aggregates by chiral induction during co-aggregation occurring in the same manner in each case.

For **290o**, a different situation is observed. Gel formation with **290o** shows positive helicity; however, the sign of the CD signal of the co-

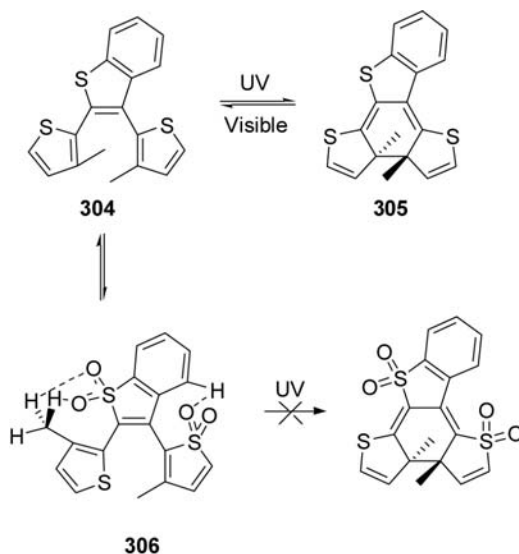
assemblies varies considerably with **293o**, **294o**, **298o**, and **300o** showing negative helicity and **295o** and **297o** positive helicity.

Assembly of **289o** into the gel state in cyclohexane is stereoselective, leading to CD absorptions with a negative exciton coupling. Upon irradiation with UV light ($\lambda = 312$ nm), the supramolecular chirality inverts to a meta-stable state, and heating and subsequent cooling to release and reform the **289c** aggregates results in an inversion of helicity.

Upon irradiation ($\lambda = 312$ nm) of the gel of **290o**, an absorption appears at longer wavelength, and after heating and subsequent cooling to release and reform the gel fibers the CD absorption changes but does not invert. Subsequent irradiation with visible light ($\lambda > 420$ nm) leads to a gel containing **290o**; however, no inversion of chirality is observed.

Usually, the thienyl ring is linked to the alkene in position 3. Derivatives with a thienyl ring linked in position 3 and another thienyl ring linked to the alkene in position 2 of the thienyl ring have been prepared, as well as derivatives with both the thienyl rings linked at the alkene in position 2 of the thienyl ring (04JA15382; 05OL3315). Irradiation with 254 nm light of the colorless THF solution of **304** brought about an immediate increase of the intensity of the absorption bands in the visible region centered at 465 nm due to the formation of the ring-closed form **305**. A well-defined isosbestic point appeared at 292 nm.

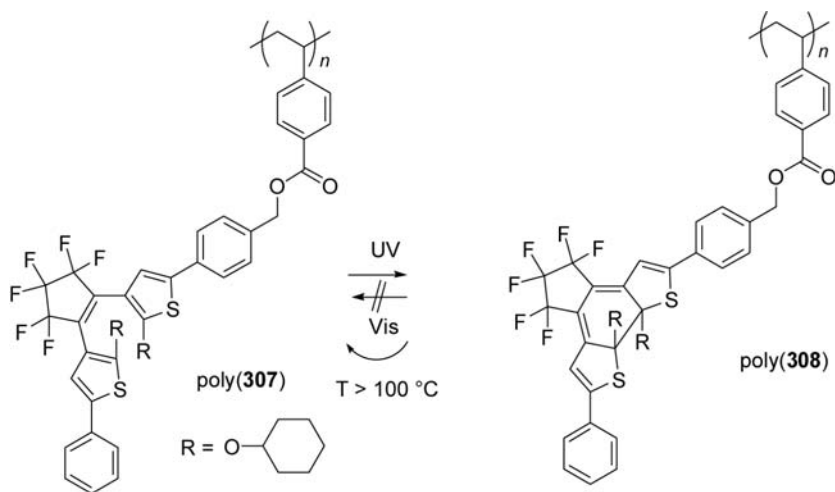
The yellowish solution can be easily bleached upon irradiation with visible light ($\lambda \geq 405$ nm), producing an absorption spectrum identical with that of the initial solution of **304**.



Compound **306** did not exhibit photochromic behavior like **304** in THF solution when irradiated with 254 nm light, which suggested no

photocyclization occurred. The sulfone moieties provide the probability for the formation of intramolecular hydrogen bonds between *S,S*-dioxide moieties and corresponding hydrogen atoms, which fastened the two pensile thiophene rings in the photoinactive conformation.

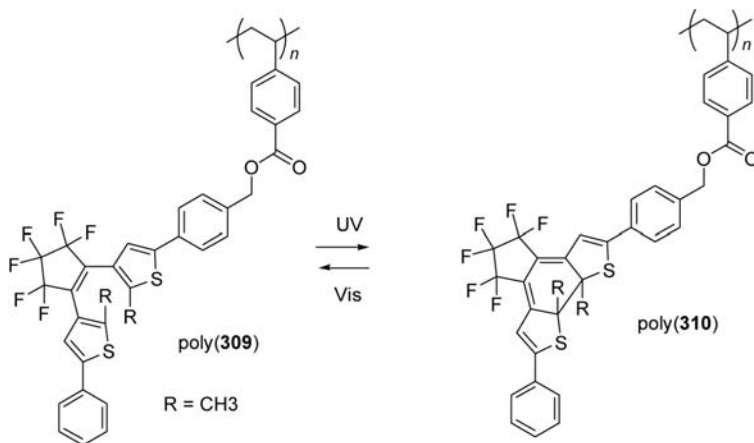
The photogenerated colored isomer of a typical diarylethene derivative, 1,2-bis(2-methyl-5-phenyl-3-thienyl)perfluorocyclopentene, is stable for >1900 years at 30°C in the dark (99JCS(CC)747; 00JA4871). However, the colored isomer returns to the initial colorless isomer under room light even at room temperature. For the recording application, diarylethene molecules having very low photodecoloration quantum yields and thermal stability at room temperature have been developed (01CL618; 02JOC4574). The photodecoloration quantum yield is strongly suppressed by the introduction of methoxy groups at the reactive 2- and 2'-positions of the thiophene rings (01CL618). Furthermore, for the reusability of the materials, the colored isomers can return to the colorless isomers thermally at high temperature above 100°C by the introduction of the cyclohexyloxy groups at 2- and 2'-positions (02JOC4574). Upon irradiation with ultraviolet (UV) light, the toluene solution of poly(**307**) turned blue and the colored state was thermally and photochemically stable (08T7611).



Upon irradiation with UV light, the new absorption band of the closed-ring appeared at 650 nm. The conversion to the closed-ring form was determined to be 92%. The photochromism in the film on a quartz glass reached to 60% conversion at a photostationary state. The quantum yield in toluene was determined to be 0.40. The quantum yield of the polymer in the film was determined to be 0.26.

In the case of the solid-state film, the decrease in the population of the photoactive conformations of diarylethene moieties may result in the

smaller photocyclization quantum yields. Poly(**308**) was thermally stable at room temperature and also stable under visible light. A diarylethene polymer (poly(**309**)) having the methyl groups instead of the cyclohexyloxy has photoreversibility between open- and closed-ring form (06CL628).

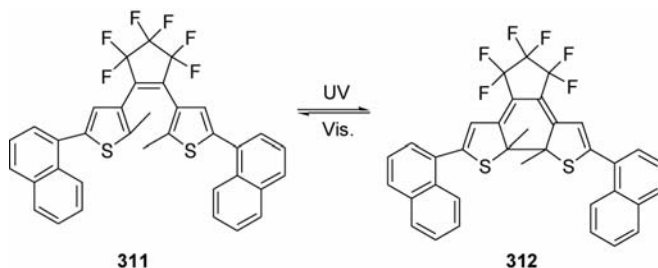


When the colored state of poly(**308**) is heated at high temperature above 100°C, it is expected to return to the colorless state to give poly(**307**). The color disappeared completely within 10 min at 150°C to reproduce poly(**307**).

Polymer showing photochromic properties was also obtained using oligomers with a diarylethene moiety obtained starting from a benzothiophene unit, and *p*-phenylenevinylene (02MM8684).

Compound **311** underwent a thermally irreversible photochromic reaction in solution (08JCS(CC)335). Upon alternate irradiation with UV and visible light, a hexane solution of **311** reversibly changed its color from colorless to bluish purple due to the isomerization between the open- and closed-ring isomers, **311** and **312**.

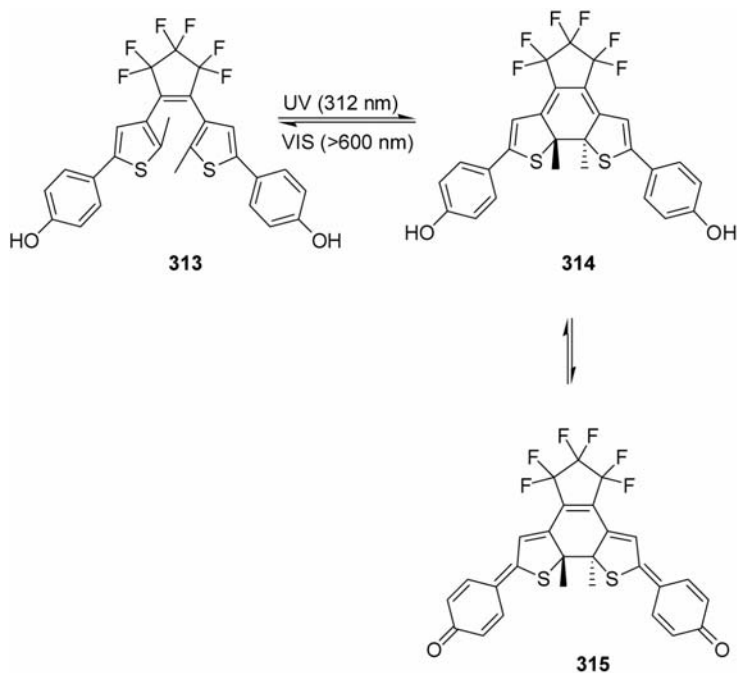
Compound **311** formed stoichiometric co-crystals with perfluorinated aromatic molecules, hexafluorobenzene (**Bz**^F) and octafluoronaphthalene (**Np**^F), by intermolecular Ar–Ar^F interactions, and **311** showed photochromic reactivity in the co-crystals as well as in the one-component crystal of **311**.



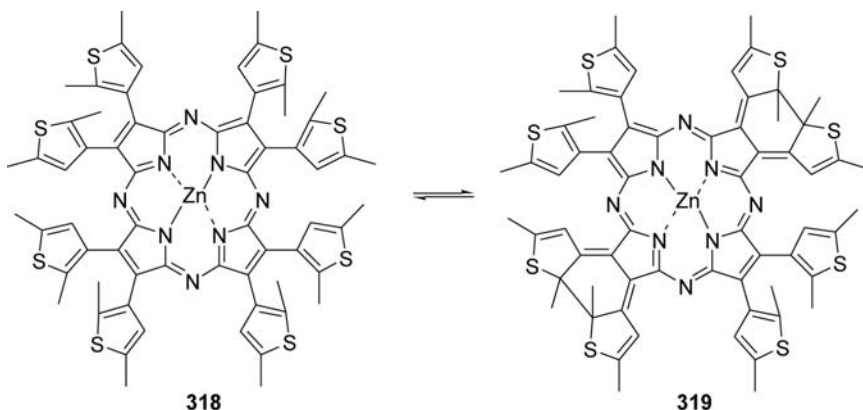
All the **311** molecules adopt a *P*-helical conformation in the central hexatriene part (this crystal is named (*P*)-**311**·Np^F). Single crystals with the opposite chirality, (*M*)-**311**·Np^F, in which **311** is in an *M*-helical conformation, were also obtained from the same sample batch. The chiral co-crystals underwent photochromism. Upon irradiation with 365 nm light, the colorless crystal turned blue.

The absorption spectrum at 0° has a maximum at 600 nm. Upon rotation of the direction of the incident polarized light by as much as 90°, the absorption intensity decreases. The anisotropy of the absorption spectra reflects the regular orientation of the photogenerated closed-ring isomers and indicates that the photochromic reaction occurred in the single-crystalline phase. The blue color disappeared by irradiation with visible light ($\lambda > 480$ nm). Anthracene-substituted derivatives also showed photochromic properties (01JPC(A)1741).

The quinoid compound **315** was synthesized by photochemically converting **313** to its deep-blue closed form **314** in acetonitrile, followed by the addition of excess potassium ferricyanide and aqueous potassium hydroxide. Irradiation of a solution of **313** resulted in the appearance of a deep-blue color and absorption bands at 590 and 340 nm due to the generation of the closed isomer **314** (94JCS(CC)1011; 95CEJ285).



The conversion at the photostationary state was determined to be >98%. Once cyclized, the solutions were cleanly decolorized by exposure to visible light of >60 nm. While photochemical closure of **315** could also be carried out at 254 nm, it was found that an additional process ensued resulting in the appearance of bands at 534 and 386 nm, corresponding to the formation of the quinoid form **317**, which does not open by irradiation with visible light.

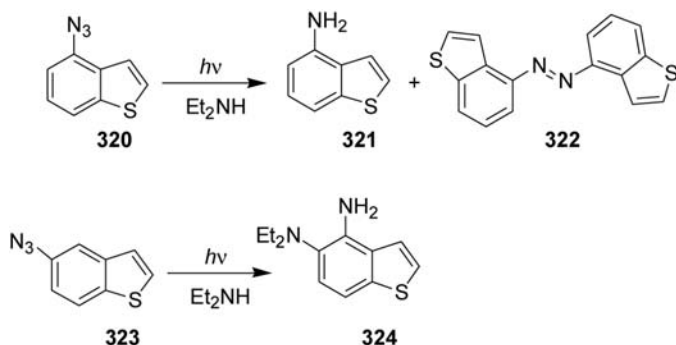


Photochromism has also been observed when two porphyrinic groups are linked to a dithienylethene scaffold. The closed form showed an absorption band at 560 nm (01JA1784). The same behavior was observed in the system **318–319** (02AM918). Dithienylethene photochromic systems have also been described to be linked to single-walled nanotubes (07JA12590).

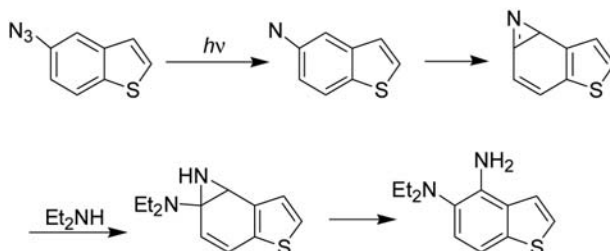
Dimers and trimers of dithienylethene derivatives were irradiated showing a complex behavior allowing us to obtain black, blue, red, and yellow colors (02JPP(A)(152)141; 03AGE3537; 05JA8922). Dibenzothienylethene sulfone derivatives have been described to have photochromic properties (05JCS(CC)2503; 06T5855).

11. PHOTOLYSIS OF AZIDO DERIVATIVES

Photolysis of 4-azidobenzo[*b*]thiophene (**320**) in diethylamine gave 4-aminobenzo[*b*]thiophene (**321**) (35%) and 4-(4-benzo[*b*]thienyl)azobenzo[*b*]thiophene (**322**) (20%) (72JCS(CC)879). However, photolysis of 5-azidobenzo[*b*]thiophene (**323**) gave **324** (24%) (72JCS(CC)879).



The proposed mechanism involved the ring opening reaction of an azirine (Scheme 26).



Scheme 26

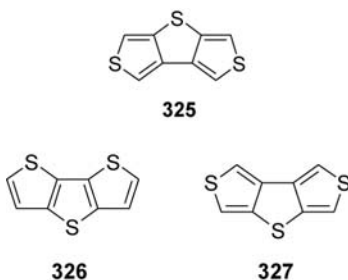
12. PHOTOPOLYMERIZATION

2-iodothiophene has been mixed with an aqueous solution of hydriodic acid, HI, by a ratio of 1:1. The entire mixture has been spin-coated on a silicon substrate, after all the fluid solution has been irradiated by UV-laser light with a wavelength of 248 nm (02MI34).

After irradiation, a silver-colored thin polymer layer totally covers the liquid phase. During the irradiation process, the color of the liquid phase has changed from yellow to a deep red one. The red color is due to a charge transfer complex between iodine and the thiophene ring dissolved in the liquid. The polymerization process takes place only at the surface of the irradiated sample. However, it was observed that when the UV-irradiation by excimer laser is over, the polymerization process continues, but only at the surface of the irradiated sample; a postpolymerization without incident UV-photons takes place. It was also observed that the presence of oxygen during

the UV-irradiation strongly inhibits the formation of the thin polymeric layer. Together with the thiophene ring, the iodine molecules form a charge transfer complex, a strong UV-absorber. The polymerization mechanism of iodinated thiophene is explained by a photochemical polymerization of cationic radicals. A photochemical procedure can be used in the photopolymerization of benzo[*c*]thiophene in carbon tetrachloride in the presence of TBABr (91JCS(CC)1618). Bithiophene and terthiophene gave the corresponding polymer if irradiated in carbon tetrachloride in the presence of *p*-dinitrobenzene (95CL99).

Photochemical polymerization of dithiophene **325** in acetonitrile in the presence of CCl_4 and TBABr leads to a thin film with electrochromic properties in the visible region (94JCS(CC)1911; 95SM(69)309). Laser flash photolysis in the presence of CCl_4 showed absorption at 417 nm due to the radical cation.



Irradiation at 500 nm of the monomers **326** and **327** in acetonitrile in the presence of dinitrobenzene (electron acceptor) showed the formation of polymeric materials (GPC) (96CL285).

In laser flash photolysis, the absorption band at 384 nm appeared in the irradiation of **326**. This transient absorption is assigned to that of triplet excited state. In the absence of the electron acceptor, its decay lifetime was estimated to be 6.2 μs . In the presence of DNB, the absorption band at 384 nm decayed within a few hundred ns, and new bands appeared at 406 and 586 nm. They were assigned to the radical cation of **326**. The initial stage of the photochemical polymerization is the generation of the radical cation. The corresponding polymers seem to be generated by the polymerization mechanism involving successive coupling and deprotonation reaction of the radical cation.

The photopolymerization of thienyl derivatives in the presence of phenyliodonium hexafluorophosphate in dichloromethane has been reported (09JCS(CC)6300). The reaction probably occurs through the formation of thienyl derivative radical cation via an electron transfer process, and subsequent coupling of two radical cations.

13. OPTICALLY ACTIVE THIOPHENE MATERIALS

Organic thin-film transistors have received intense interest in recent years for their potential as a low-cost alternative to amorphous hydrogenated silicon thin-film transistors for various electronic applications. OTFT-based array/circuits are particularly suited for large-area devices where high transistor density and switching speeds are not essential; they may also be attractive for applications in low-end microelectronics where the high cost of packaging silicon circuits becomes a prohibitive factor to ubiquitous usage (08CEJ4766).

An OTFT comprises three electrodes (source, drain, and gate), a gate dielectric layer, and an organic or polymer semiconductor layer. In operation, an electric field is applied across the source–drain electrodes, and the transistor is turned on when a voltage (V_G) is applied to the gate electrode, which induces a current flow (I_D) from the source electrode to drain electrode. When $V_G = 0$, the transistor is turned off, I_D should in theory be 0, that is, no current is flowing.

The transistor performance is generally characterized by field-effect transistor (FET) mobility (μ), current on/off ratio (I_{on}/I_{off}), and threshold voltage (V_T).

For many useful applications, μ is required to be $\geq 0.1 \text{ cm}^2 \text{ V}^{-1} \text{ s}^{-1}$ while $I_{on}/I_{off} \geq 10^4$. Ideally, desirable TFTs will have a V_T close to zero.

Applications for organic semiconductors include organic thin film transistors (OTFTs), light-emitting diodes (OLEDs), photovoltaic cells (PVC), sensors, and radio frequency identification (RF-ID) tags, for integration into low-cost, large-area electronics. The main advantages of using organic materials lie in cost and processability. Organic materials that are suitably modified are compatible with solution-processing techniques, thereby eliminating the need for expensive lithography and vacuum deposition steps necessary for silicon-based materials.

The main logic units in these circuits are field-effects transistors (FETs), comprising a gate electrode, a gate dielectric, a semiconductor, and a source/drain electrodes [01ACR359]. The device is generally in an insulating state until a gate voltage is applied (relative to the source), which establishes a “channel” of charge at the semiconductor–dielectric interface, turns the device on, and allows conductivity between the source and the drain.

FETs can be viewed partly as capacitors, with the gate and semiconductor functioning as parallel-plate electrodes. As long as the semiconductor has accessible orbitals for the injection of charge and is sufficiently continuous, the gate–source voltage charges the capacitor.

The layer of charge on the semiconductor side provides carriers for the current flowing between the source and the drain, provided that the

semiconductor forms a continuous film with intermolecular π -overlap in a direction parallel to the intended current flow.

If the doping level is too high, the device does not display its intended switching function, but rather acts as a poorly modulated resistor.

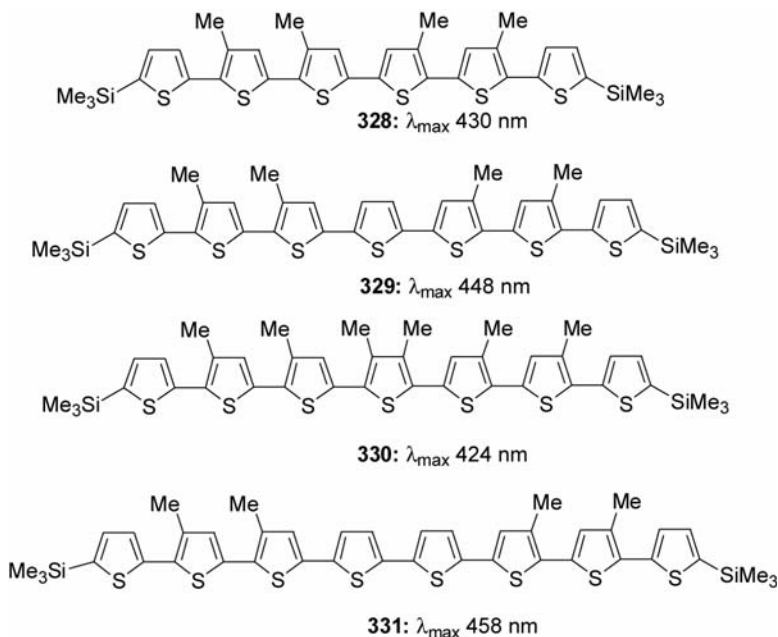
There are three basic types of semiconductor materials depending on their ability to conduct hole (p-type), electrons (n-type), or both (ambipolar) under different gate bias conditions. In semiconductor materials, reduction of the bandgap (E_g) will enhance the thermal population of the conduction band and thus increase the number of intrinsic charge carriers. The decrease of E_g can lead to true organic metals showing intrinsic electrical conductivity.

There are several reviews on this field (86CJC76; 88CRV183; 97CRV173; 98AGE402; 98AM93; 98AM365; 99ACR209; 99MI1875; 00AM227; 00AM481; 01AM1201; 01BCJ1789; 01MI1; 02MI2565; 04CM4413; 04CM4436; 04CM4824; 04MI1077; 05AM1581; 05AM1705; 05AM2281; 05MI53; 06CRV5028; 07AM2045; 07CRV1066; 07MI954; 08CEJ4766; 10CR3).

13.1 Oligothiophenes

α -Sexithiophene has been used for organic semiconductor device fabrication, and other unsubstituted oligomers have been studied for their electronic properties while encapsulated in zeolites (91JA600). Hence, the oligomers exhibit many of the desirable electronic characteristics that have been evident in the polymers, and soluble oligomers should find electronic applications where effective dissolution of the material is required. The photoinduced absorption spectra of sexithiophene are strikingly similar to that of $6T^+$. The spectra consist of two strong bands, peaked at 0.80 eV and at 1.54 eV, respectively (94AM64; 95SM(69)401). Stable radical cation of 6T was obtained in the presence of Keggin-type heteropolyanions (93AM646). Film of 6T showed a photochemical generation of polarons (95SM(69)401). A theoretical work on the electronic excitations and nonlinear optical properties of the oligomers of thiophene has appeared (93JCP(98)8819).

Poly(3-alkyl- α -thiophene) systems show significant third-order nonlinear susceptibilities ($\chi^{(3)}$). Though, oligothiophenes have been studied for their third-order susceptibilities, accurate third-order optical nonlinearity data obtained by degenerate four-wave mixing or electric-field-induced second harmonic generation (EFISH) are difficult to attain reliably on samples with poor solubility characteristics (92MM1901).

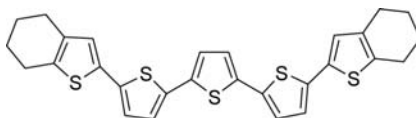


The UV-visible data for some oligo(α -thiophene)s (**328–331**) are summarized. The values for absorption maxima (λ_{max}) increase throughout the series, and although smaller consecutive increases in λ_{max} are noticed for each additional thiophene unit, no apparent saturation was reached. First, the alkyl groups can induce an hypsochromic shift when steric interactions are severe enough to cause further distortions of the conjugated system from planarity. This is most pronounced in systems when one of the thiophene units possesses dimethyl substituents. This same lowering in λ_{max} has been observed in poly(3,4-dialkylthiophene)s. Conversely, when steric interactions are not particularly severe, methyl groups can induce a bathochromic shift which has been explained by inductive and hyperconjugative effects. Moreover, the $d\pi-\pi$ -conjugative interaction between the terminal silicon atoms and the conjugated system must also be considered. The silicon group induces a bathochromic shift while the effects of the alkyl groups are less well defined.

While the octamer **331** has $\lambda_{\text{max}} = 458$ nm, electrochemically generated poly(3-alkyl- α -thiophene)s have a noticeable smaller λ_{max} value of 430–440 nm in solution. These data support the notion that the effective conjugation length in conjugated thiophene polymers may only be 6–7 monomer units long.

α,ω -Dialkylsexithiophene showed an absorption maximum at 364 nm, while the isolated molecule showed an absorption maximum at 444 nm (94CM1809; 95JPC9155). Other thiophene-phenylene oligomers have been used in the preparation of field effect transistors (03JA9414). Cyano

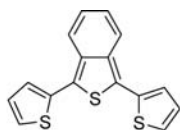
substituted terthiophene derivatives have been described: 2-cyanoterthiophene showed an absorption maximum at 377 nm and an emission band at 459 nm ($\Phi_F = 0.115$) (97CM981; 97JPC(B)4553). 2,3-Substituted thiophene derivatives have been studied showing interesting absorption properties in their UV spectra and emissions in the range 442–602 nm; these compounds also showed electroluminescence properties (02CM1884). Film of 4T showed an absorption at $20,985\text{ cm}^{-1}$ (96SM(83)227). End-capped oligothiophenes, such as **332**, have been proposed as models for polythiophene derivatives (92AM102; 93SM(61)143).



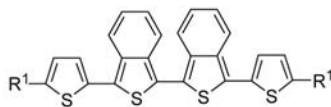
332 λ_{\max} 431 nm
 λ_{\max}^F 528.8 nm
 Φ_F 0.25

The enhanced photoluminescence behavior of 1,3-dithienylbenzo[*c*]thiophene derivatives **333–338** during photobleaching has also been observed (98JOC3105; 07TL779; 09T822).

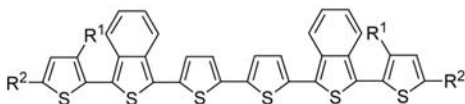
Monomeric benzo[*c*]thiophene analogs exhibited a highly intense absorption band around 400 nm due to $\pi-\pi^*$ electron transfer of the entire conjugated backbone (05TL4225; 08EJO3798). As expected, benzannulation of the quaterthienyl system (**338h**) caused a red shift of the λ_{\max} value of 75–90 nm. The introduction of α -alkyl substituents (*n*-hexyl, 2-ethylhexyl, and *n*-butyl) into **333** increased the longer wavelength absorption from 412 to 440 nm.



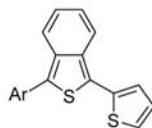
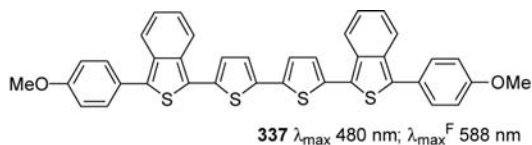
333 λ_{\max} 433 nm
 λ_{\max}^F 532 nm



334a $R^1 = \text{H}$; λ_{\max} 520 nm; λ_{\max}^F 661 nm
334b $R^1 = n\text{-C}_6\text{H}_{13}$; λ_{\max} 468 nm; λ_{\max}^F 531 nm
334c $R^1 = n\text{-C}_4\text{H}_9$; λ_{\max} 494 nm; λ_{\max}^F 602 nm



335 $R^1 = \text{C}_6\text{H}_{13}$, $R^2 = \text{H}$; λ_{\max} 484 nm; λ_{\max}^F 582 nm
336a $R^1 = \text{H}$, $R^2 = n\text{-C}_4\text{H}_9$; λ_{\max} 504 nm; λ_{\max}^F 600 nm
336b $R^1 = \text{H}$, $R^2 = 2\text{-ethylhexyl}$; λ_{\max} 510 nm; λ_{\max}^F 587 nm
336c $R^1 = \text{H}$, $R^2 = \text{C}_6\text{H}_{13}$; λ_{\max} 520 nm; λ_{\max}^F 630 nm



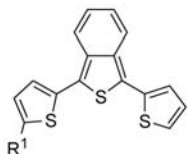
338a Ar = p-Me₂NC₆H₄; λ_{\max} 416 nm; λ_{\max}^F 566 nm

338b Ar = p-MeSC₆H₄; λ_{\max} 476 nm; λ_{\max}^F 518 nm

338c Ar = 3,4-(MeO)₂C₆H₃; λ_{\max} 445 nm; λ_{\max}^F 526 nm

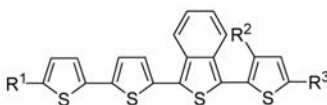
338d Ar = p-O₂NC₆H₄; λ_{\max} 470 nm; λ_{\max}^F 611 nm

338e Ar = p-MeOC₆H₄; λ_{\max} 412 nm; λ_{\max}^F 525 nm



338f R¹ = n-C₆H₁₃; λ_{\max} 440 nm; λ_{\max}^F 561 nm

338g R¹ = 2-ethylhexyl; λ_{\max} 442 nm; λ_{\max}^F 600 nm



338h R¹ = H, R² = H, R³ = n-C₆H₁₃; λ_{\max} 468 nm; λ_{\max}^F 592 nm

The introduction of an electron-releasing group such as NMe₂, OMe, or Me at one end of the benzo[*c*]thiophene caused a red shift of the absorption maxima of 10–25 nm. However, with the electron-releasing SMe group, the λ_{\max} value was shifted to a maximum extent (ca. 50 nm). The presence of electron-withdrawing groups at one end of the benzo[*c*]thiophenes (**338d**) resulted in a red shift of the λ_{\max} value, which confirms the enhancement of π -electron delocalization. Increasing of benzannelations significantly enhanced the λ_{\max} value (ca. 25 nm).

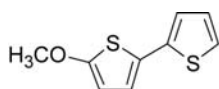
Dimerization of one-end-blocked benzo[*c*]thiophene (**334a–c**) caused a red shift of the absorption maxima of ca. 70 nm. Compared to the parent α,α' -dihexylsexithiophene (ca. 444 nm), the benzannelated sexithienyl system **336c** exhibited a λ_{\max} value at a higher wavelength (520 nm) which confirms the enhancement of conjugation through anellation.

The photoluminescence spectra of the benzo[*c*]thiophene analogs exhibited emission in the orange region, which was gradually red shifted with increasing conjugation. Between the benzo[*c*]thiophene analogues **338a–e**, only **338b** emitted light in the relatively high-energy region of 510–518 nm. As in the case of the absorption spectra, the luminescence of the benzo[*c*]thiophenes was also red shifted with increasing π -conjugation.

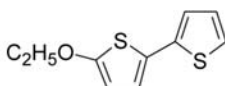
For the practical application of second-order NLO materials, not only a high hyperpolarizability but also good thermal stability is required. Heteroaryl diazo chromophores could also act as organic second-order nonlinear optical materials suitable for applications such as second

harmonic generation (00SM(115)213; 01MI445; 05T8249; 06TL3711; 08DP(77)657; 08T5878). As an efficient segment of π -electron conjugation bridge, diazo ($N=N$) bond is widely used in the design of NLO-chromophores.

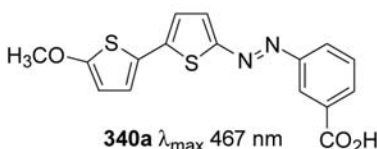
In agreement with other solvatochromic studies for heteroaryl-azo dyes, the increase of the electron-withdrawing strength of the substituent of the diazo component and/or the increase of the electron-donating strength of the coupling moiety was found to cause pronounced bathochromism as shown in 339–342. In general, red shifts in absorption were accompanied by positive solvatochromic shifts. Especially noteworthy is the extremely large positive solvatochromism exhibited by 5-acceptor-substituted 2-amino- or 2-alkoxy-(oligo)thiophenes. This red shift suggests an increase of molecular hyperpolarizability, according to theoretical and experimental NLO studies.



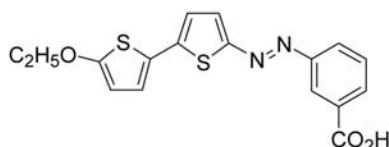
339a λ_{\max} 319 nm



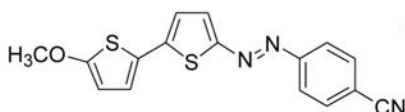
339b λ_{\max} 319.5 nm



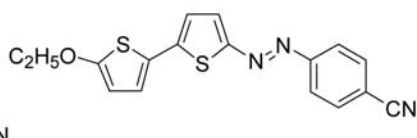
340a λ_{\max} 467 nm



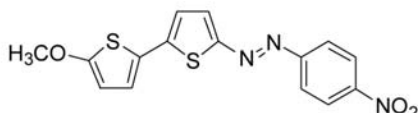
340b λ_{\max} 371.5 nm



341a λ_{\max} 496 nm



341b λ_{\max} 499 nm



342 λ_{\max} 509 nm

Table 10. Spectroscopic properties of selected compounds

Compound	λ_{abs} (nm) (log ϵ)	λ_{F} (nm)	Φ_{F}
343	370, 280 (4.66,4.41)	445, 457	0.44
344	321, 280 (4.65,4.64)	441, 384	0.42
345	403, 280 (4.61,4.63)	500, 472	0.20
346	410, 305 (4.69, 4.67)	505, 474	0.31

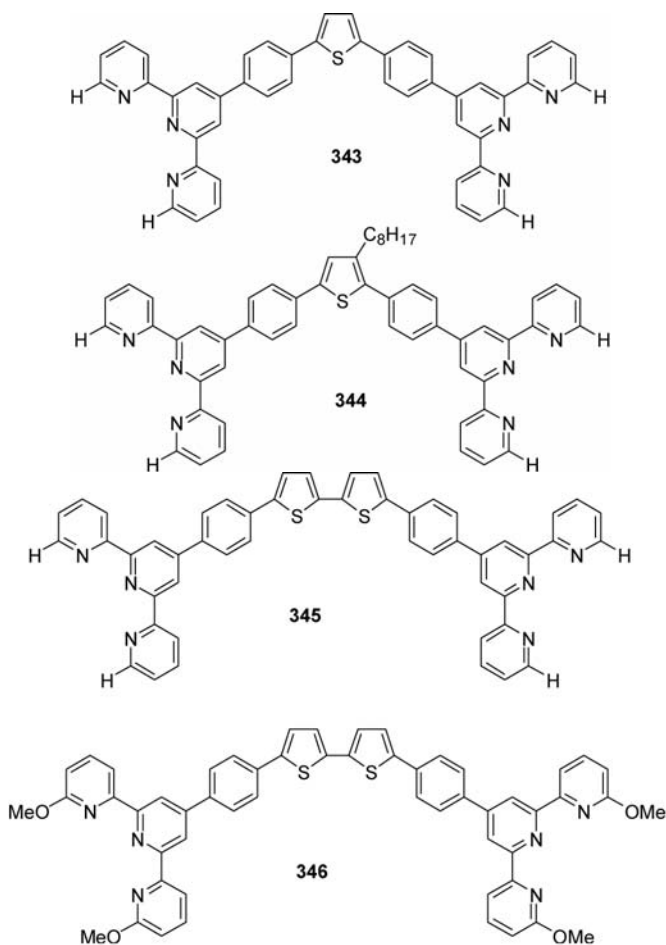
The hyper-Rayleigh scattering (HRS) method to measure the first hyperpolarizability β of 5'-alkoxy-2,2'-bithiophene azo dyes **340–342** using the 1064 nm fundamental wavelength of a laser beam was used. The experimental results obtained for the nonlinearities β of chromophores **341a** and **342** show that compound having strong acceptor groups at the *para* position of the aryl ring, CN and NO₂, exhibits the highest β values. Compounds **340a** and **341a** having the acceptor carboxylic group at the *meta* position of the aryl ring exhibit the lowest β and β_0 values.

All the chromophores are thermally stable with decomposition temperatures varying from 230 to 263°C. Thienyl azodyes linked to a polyester matrix were obtained for optical storage material, where the *trans-cis* photoisomerization was used at this purpose (07MI4477).

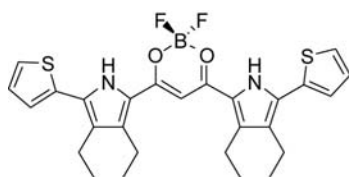
The λ_{abs} red shifts significantly to ca. 370 nm by introducing a thiophene group in the spacer region (**343**) (Table 10), and moves further to >400 nm when a bithiophene group (**345** and **346**) is incorporated (08T9108). It should be noted that, while interposing a thiophene ring without substituent at 3- or 4-position in the spacer region leads to a large red shift of λ_{max} , attaching an octyl alkyl chain at the 3-position of thiophene unit moves the absorption maximum from 370 to 321 nm as a comparison of **343** and **344** shows, indicating that substitution at 3- or 4-position of thiophene ring affects markedly on the absorption behavior of bis-terpyridine derivatives.

This observation is attributed to the introduction of a long alkyl chain, which causes a twist between the thiophene and phenylene rings, and ultimately, resulting in a decreased π -conjugation between the aromatic rings.

Compounds **343** and **344**, which contain one thiophene ring in the spacer region, exhibit bright blue emission color with λ_{F} at ca. 450 nm for **343**. More excitingly, by further increasing the number of thiophene from one to two units, the emitting wavelength of **345** and **346** is red shifted to >500 nm paired with a shoulder at ca. 470 nm, showing that a large Stoke's shift occurred (> 90 nm). Consequently, the emission colors of **345** and **346** are bright green.



Bithiophene was inserted into a polypeptide scaffold. The nanostructured compound showed absorption at 320 nm and an emission at 380 nm (08JA13840).



347 λ_{\max} 527 nm; λ_{\max}^F 570; Φ_F 0.5

Compound **347** showed interesting properties (08OL3179). Thienylpyrrolylbenzothiazole derivatives showed nonlinear optical properties (07T4258).

Radical cations and dications of oligothiophenes have been investigated by many research groups to understand the nature of polarons and bipolarons in polythiophenes which are responsible for the electrical and optical properties of these π -conjugated polymers.

Dithieno[3,2-*b*:2',3'-*d*]thiophene has been investigated as a monomer for a conducting polymer or a donor for a conducting charge-transfer complex. Furthermore, dithieno[3,4-*b*:3',4'-*d*]thiophene has been known as a monomer for a small bandgap polymer. The absorption spectra of the radical cations of dithienothiophenes (DTTs) can be generated by γ irradiation in frozen (77 K) freon solutions (97JPC(A)1056). Mobile holes on the molecules, which were generated by γ irradiation, react with DTT and then generate the radical cation of DTT. In the case of **326**, characteristic and intense absorption bands appeared in the visible region at 595, 411, and 351 nm. For **327**, absorption bands appear both in the near-IR and visible regions at 918, 880, and 410 nm.

In the laser flash photolysis of deaerated acetonitrile solutions containing 200 μ M **326**, a transient absorption band appeared at 384 nm immediately after laser pulse excitation. In the case of **327**, an absorption band appeared at 422 nm accompanied by a weak broad band at 470–570 nm. Since the absorption bands were readily quenched by oxygen, these absorptions could be assigned to the triplet excited states of **326** and **327** ($^T(326)^*$ and $^T(326)^*$), respectively. Absorption-time profiles of the absorption bands showed second-order decay indicating triplet–triplet annihilation when the concentration of DDT was higher than 200 μ M. At low concentrations, first-order decays were observed and their triplet lifetimes were estimated to be 45 and 30 μ s for **326** and **327**, respectively. These lifetimes are longer than the reported value for 2,2'-bithiophene. The transient absorption bands assigned to triplet excited states were readily quenched in the presence of the electron acceptor DBN (*p*-dinitrobenzene). In the laser flash photolysis of solutions containing **326** and DNB, the absorption band of $^T(326)^*$ (384 nm) disappeared within few hundred nanoseconds, and new absorption bands appeared at 586, 406, and <350 nm. These new absorption bands are attributed to $(326)^+$; their peak positions correspond well to those of $(326)^+$ generated by γ irradiation. The observed time profile at 410 nm was resolved with curves of $8.9 \times 10^6 \text{ s}^{-1}$ of the decay rate constant and $9.1 \times 10^6 \text{ s}^{-1}$ of the rate constant for $(326)^+$ growth.

In a solution containing **327** and DNB, new absorption bands appeared at 910, 880, 820, 780, and 396 nm, after the decay of $^T(327)^*$ (422 nm). The absorption bands at 880, 820, and 396 nm can be attributed to $(327)^+$ and the 910, 820, and 780 nm bands to $\text{DNB}^{\cdot-}$. The rate constant for the growth

of $(327)^{\cdot+}$ and $\text{DNB}^{\cdot-1}$ was estimated to be $1.4 \times 10^7 \text{ s}^{-1}$. The fluorescence lifetime of **327** was estimated to be $6.5 \times 10^2 \text{ ps}$ when the solution contained 5 mM of **327**. In the presence of DNB, fluorescence lifetime became shorter; when the solution contained 5 mM **327** and 9 mM DNB, the fluorescence lifetime was estimated to be $5.1 \times 10^2 \text{ ps}$. From the Stern–Volmer equation, a rate constant for quenching of fluorescence of **327** was estimated to be $4.4 \times 10^{10} \text{ M}^{-1} \text{ s}^{-1}$.

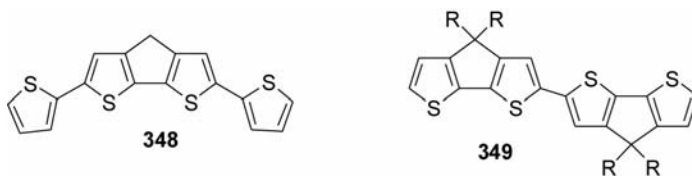
The absorption ascribable to the radical ions decays after reaching a maximum. The decay of absorption can be attributed to the back-electron-transfer reaction and radical coupling of $\text{DTT}^{\cdot+}$ yielding dimers. The back-electron-transfer rate (k_{bet}) was estimated to be $1.1 \times 10^{10} \text{ M}^{-1} \text{ s}^{-1}$ using an evaluated ϵ for $\text{DNB}^{\cdot+}$ at 910 nm ($5.9 \times 10^3 \text{ M}^{-1} \text{ cm}^{-1}$).

When laser flash photolysis was carried out in acetonitrile solution containing DTT and CCl_4 , absorption bands ascribable to $\text{DTT}^{\cdot+}$ were observed immediately after laser excitation.

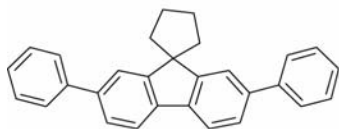
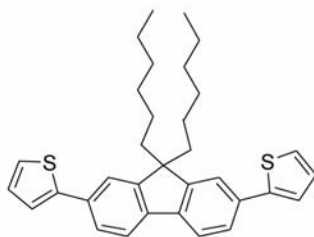
Fast generation of the radical ions can be attributed to electron-transfer reaction from the singlet excited state and slow radical generation to that from triplet excited state. Fluorescence of both **326** and **327** was quenched in the presence of CCl_4 according to the Stern–Volmer equation. The Stern–Volmer constants were estimated to be 1.55 and 17.7 M^{-1} for **326** and **327**, respectively, and quenching rate constants were estimated to be $\sim 10^{10}$ and $2.7 \times 10^{10} \text{ M}^{-1} \text{ s}^{-1}$.

Upon laser flash photolysis of a cyclohexane solution containing DTT and DNB, no transient absorption band ascribable to the products of electron-transfer reactions was observed. The transient absorption due to $^T(326)^*$ disappeared within 500 ns after laser excitation, and a new absorption band appeared at wavelengths $< 350 \text{ nm}$. The new band can be attributed to the triplet excited state of DNB. The result indicates that $^T(326)^*$ is quenched by energy transfer to DNB. The decay rate constant of $^T(326)^*$ for the energy transfer was estimated to be $8.8 \times 10^9 \text{ M}^{-1} \text{ s}^{-1}$. As for cyclohexane solution of **327** and DNB, quenching of $^T(327)^*$ by energy transfer was also observed and the rate constant was $1.1 \times 10^{10} \text{ M}^{-1} \text{ s}^{-1}$.

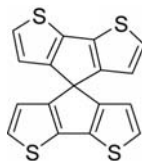
Cyclopentabithiophene derivatives were described (99T14985; 00SM (113)129; 04SM(146)251). The absorption energy ($\lambda_{\text{max}} = 407 \text{ nm}$) and profile of **348** are almost identical to those of the DTP oligomer (see below) (05OL5253). Its reported fluorescence is slightly lower in energy ($\lambda = 457$) but was measured in more polar THF solvent.



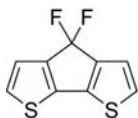
In the case of **350–352**, both absorption and emission spectra of thin films or powders are quite similar (01SM(121)1647; 02MI37).z

**350****351****352**

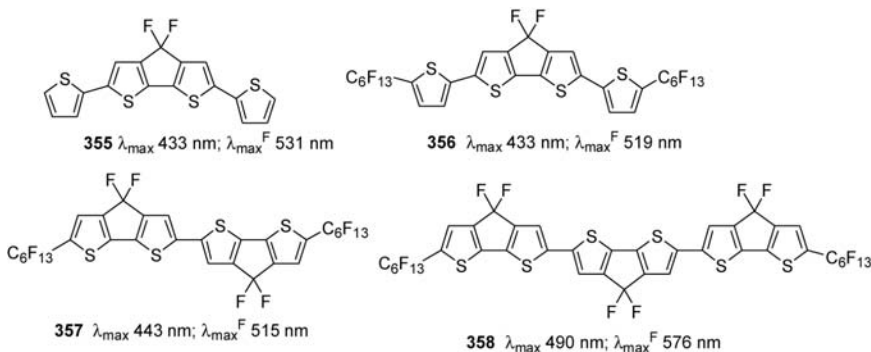
A theoretical work on the photophysical properties of **353** appeared (06CPL(429)180). **353** can be a promising OLED material in view of its luminous efficiency and transfer rate. Substituted analogs of **353** have been reported showing an absorption band at 431 nm and an emission at 486 and 516 nm (Φ_F 0.27) (01JCS(P1)740).

**353**

It has been systematically unveiled that the π -conjugated systems incorporated with electron-withdrawing groups, especially perfluoroalkyl groups, dramatically increase n-type character. In addition, the synthesis of the hexafluorocyclopenta[*c*]thiophene unit **354** and its oligomers has been reported (07OL2115).

**354** λ_{\max} 348 nm

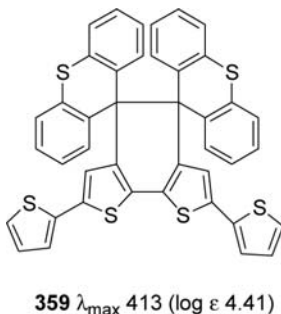
The substitution of fluorine atoms for the hydrogens at the bridging position results in a bathochromic shift of the absorption maximum by 38 nm and shifts to more positive potentials for both the oxidation and reduction processes. Some oligomers (**355–358**) have been investigated.



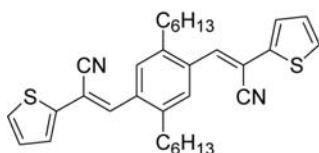
The absorption maxima are red shifted with an increase in the number of $2T_f$ units as seen for **356** and **357**, indicating effective conjugation between the $2T_f$ units. Although the electronic spectra of **358** were successfully measured, its low solubility precluded the investigation of electrochemical properties.

These compounds showed n-type FET behavior with field-effect mobility of $1.8 \times 10^{-12} \text{ cm}^2 \text{ V}^{-1} \text{ s}^{-1}$ ($I_{\text{on}}/I_{\text{off}}$: 1.3×10^3) for **356** and $1.4 \times 10^{-13} \text{ cm}^2 \text{ V}^{-1} \text{ s}^{-1}$ ($I_{\text{on}}/I_{\text{off}}$: 5.4×10^2) for **357**.

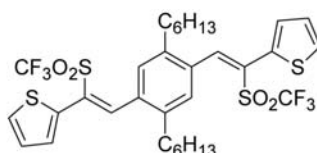
Thienyl derivatives hexarylethane unit **359** has been prepared for molecular wires applications (04OL2523).



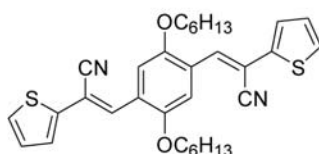
The photoluminescence emission maxima (measurements in dichloromethane) for styryl derivatives **360–363** are given (97AM233).



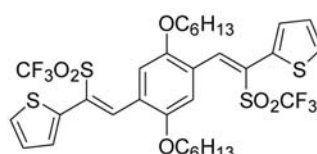
360 $\lambda_{\text{max}}^{\text{F}}$ 476, 498 nm
 Φ_{F} 0.013



361



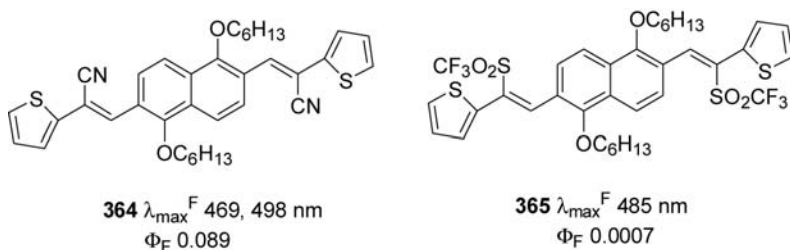
362 $\lambda_{\text{max}}^{\text{F}}$ 526 nm
 Φ_{F} 0.25



363 $\lambda_{\text{max}}^{\text{F}}$ 550 nm
 Φ_{F} 0.0027

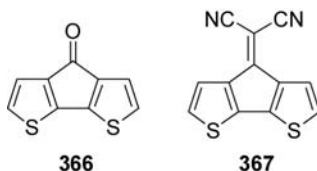
The stronger inductive effect of alkoxy groups in **362** compared to the alkyl groups in **360** can explain why the alkoxy-substituted model compounds **362–363** show emission maxima at longer wavelengths than the parent alkylsubstituted model compounds **360–361**. On the other hand, substitution with acceptor groups in vinylene moiety of arylenevinylenes should lead to an overall stabilization of the HOMO and LUMO levels. The LUMO level is thereby more affected upon substitution with acceptor groups. The asymmetry of stabilization again causes a decrease in the HOMO–LUMO gap and consequently a shift to longer wavelengths of the emission maxima. Thus, a strong bathochromic shift is observed when comparing the emission maxima of the cyano-substituted derivative **362** with the corresponding unsubstituted analogs. Introduction of the stronger triflyl acceptor leads to an even larger shift to longer wavelengths in the emission maxima as observed for the triflyl substituted **363** compared with the cyano-substituted analog **362**. Practically no emission is observed in the triflyl-substituted compound **361**.

Heteroaromatic naphthalene derivatives generally have a lower HOMO–LUMO gap than the analogous phenylene-based compounds, leading to a bathochromic shift of the PL emission maxima. By superimposing the PL spectra of **364** ($\lambda = 469$ nm/498 nm) and the corresponding triflylone **365** ($\lambda = 485$ nm), it can be shown that replacement of cyano by triflyl does not shift the spectral position of the nathylenevinylenes.



The UV/Vis spectrum of **367** displays a 100 nm (0.48 eV) red shift of the long wavelength absorption band compared to **366** ($\lambda_{\max} = 472$ nm, $\epsilon = 1250$) (91JCS(CC)1268). This band was assigned as a $\pi-\pi^*$ absorption for **366**. The analogous absorption in **367** was assigned to a $\pi-\pi^*$ transition based in the presence of structure in this band, its 20 nm red shift from hexane to methanol, and by analogy with **367**. Upon polymerization, this band shifts to 950 nm in neutral poly**367**, a red shift of ≈ 0.9 eV compared to the monomer and similar in magnitude and direction to that observed upon polymerization of **366**.

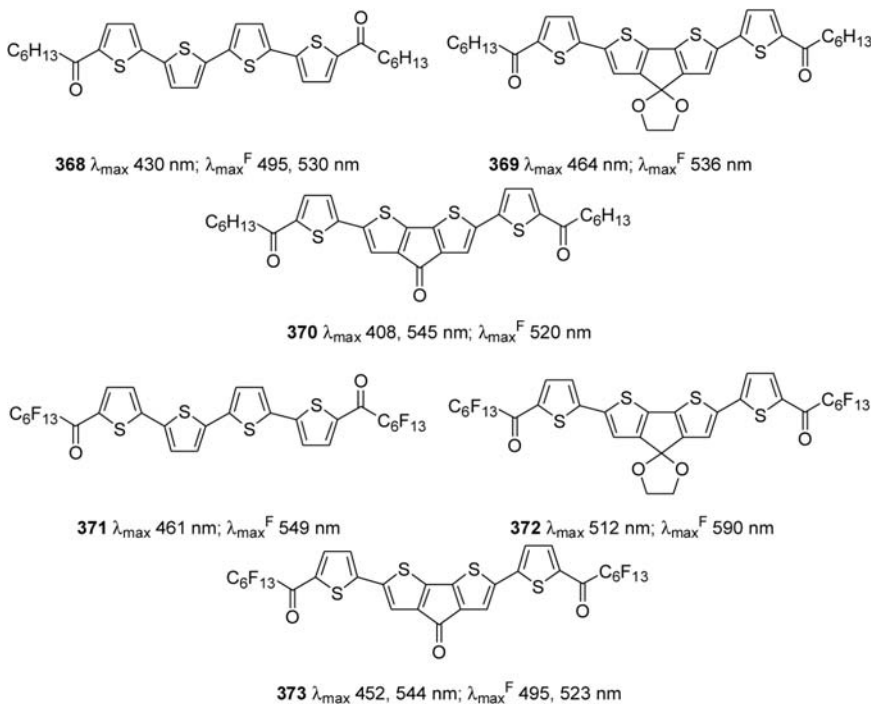
The UV/Vis/near IR spectrum of neutral poly**367** shows the long wavelength band edge (E_{gap}) at ≈ 0.8 eV, making it one of the lowest bandgap polymers reported to date. Furthermore, poly**367** appears stable to both p- and n-doping.



UV/Vis absorption and photoluminescence spectra of semiconductors **368–373** were measured in solution to assess the effect of carbonyl functionalization on the optical absorption/emission spectra and resultant optical HOMO–LUMO energy gaps (E_{gap}) (07CM4864).

The general trend in the adsorption maxima is a red shift of the $\pi-\pi^*$ transition band with chemical modification of the quaterthiophene core, in the λ_{\max} ordering: 430 (**368**) < 464 (**369**) < 545 nm (**370**) in the acyl family, and 461 (**371**) < 512 (**372**) < 544 nm (**373**) in the perfluoroacyl family. Carbonyl group incorporation at peripheral locations in conjunction with hexyl and perfluorohexyl substituents induces a significant λ_{\max} red shift ($\Delta\lambda_{\max} = +28$ (**368**) and $+63$ nm (**371**)) and reduction in E_{gap} ($\Delta E_{\text{gap}} = -0.23$ (**368**) and -0.45 eV (**371**)) compared to α,ω -di-*n*-hexylquaterthiophene, and α,ω -diperfluorohexylquaterthiophene. Such large changes in optical properties are directly attributed to the effective conjugation of the peripheral

carbonyl groups with the oligothiophene core π system. Furthermore, the addition C=O group in **370** and **373** cores further enhances the red shifts in the absorption maxima by extending the conjugation, thereby significantly compressing the optical band gap compared to **368** ($\Delta E_{\text{gap}} = -0.43$ eV) and **370** ($\Delta E_{\text{gap}} = -0.35$ eV), respectively. E_{gap} reduction by carbonyl group introduction is significantly more pronounced in the perfluoroacyl series than in the acyl series, implying that extending the core conjugation is more effective from the combination of perfluoroalkyl and carbonyl substituents than for the combination of alkyl and carbonyl substituents.

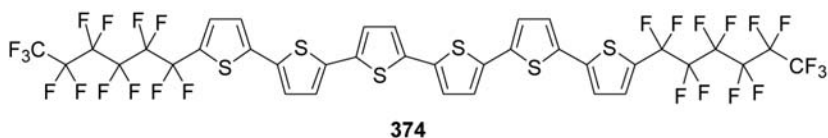


It was found that **368** exhibits ambipolar activity with appreciable electron ($0.12 \text{ cm}^2 \text{ V}^{-1} \text{ s}^{-1}$) and hole ($0.008 \text{ cm}^2 \text{ V}^{-1} \text{ s}^{-1}$) mobilities at the substrate growth temperature of 70°C , and **371** shows monopolar n-type activity with a high mobility of $0.32 \text{ cm}^2 \text{ V}^{-1} \text{ s}^{-1}$ for semiconducting films deposited at a substrate temperature of 25°C . **373** exhibits stable n-type activity even in the air although the observed electron mobility in the air ($0.01 \text{ cm}^2 \text{ V}^{-1} \text{ s}^{-1}$) is somewhat lower than that under vacuum ($0.08 \text{ cm}^2 \text{ V}^{-1} \text{ s}^{-1}$). In the case of **368** films grown at 70°C , both n- and p-type mobilities as well as current on-off ratios are enhanced by orders of magnitude compared to films grown at 25°C . **369** exhibits only p-type activity, with no detectable n-type behavior. Hole mobility extracted from the transfer plot is $5 \times 10^{-14} \text{ cm}^2 \text{ V}^{-1} \text{ s}^{-1}$ with

a current $I_{\text{on}}/I_{\text{off}} \sim 10^4$. **370** exhibits ambipolar activity with electron and hole mobilities of 0.002 and $2 \times 10^{-14} \text{ cm}^2 \text{ V}^{-1} \text{ s}^{-1}$, respectively.

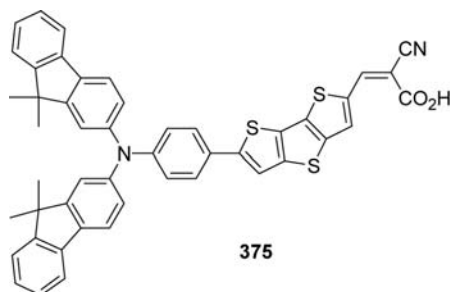
Depending on the chemical modification of the conjugated core, either n- or p-type behavior is observed, while the fluorine-free acyl analogs behave as either ambipolar or p-type semiconductor. Insertion of the dioxolane group into the thiophene core inverts the majority charge carrier type from electrons (**371**) to holes (**372**) in a very similar fashion to **369**. The **373** data reveal that n-type activity is recovered with mobility and on-off ratio $0.07 \text{ cm}^2 \text{ V}^{-1} \text{ s}^{-1}$ and 10^6 .

The synthesis of the first n-type sexithiophene conductor, α,ω -diperfluorohexylsexithiophene (**374**) has been described (00AGE4547); the synthesis of other oligomers of the same shape has been reported (04CM4715).



The solution spectrum are nearly superimposable with that of 6T, which suggests that the energy differences between the ground and excited states of the 6T core are only marginally sensitive to α,ω -substitution. The spectra of the films exhibit both differences and similarities. While **374** exhibits strong green fluorescence ($\lambda_{\text{max}} \approx 588 \text{ nm}$), the emission intensity of non-fluorinated compound is several orders of magnitude weaker and red shifted by about 30 nm. Transistor action is observed only for positive gate voltages ($V_g > 0$), which indicates that a layer of mobile electrons accumulates at the interface between **374** and SiO_2 .

A sensitizer is of paramount importance to photovoltaic performance. The sensitizer is attached to the surface of a mesoporous wide band-gap semiconductor serving as electron transporter. While the trivial ultraviolet absorption for **375** with a molar extinction coefficient (ϵ) of $50.0 \times 10^3 \text{ M}^{-1} \text{ cm}^{-1}$ peaks at 372 nm, the ϵ value of its low-energy band at 525 nm (mainly stemming from the intramolecular charge transfer transition) is $44.8 \times 10^3 \text{ M}^{-1} \text{ cm}^{-1}$ (08JA9202).

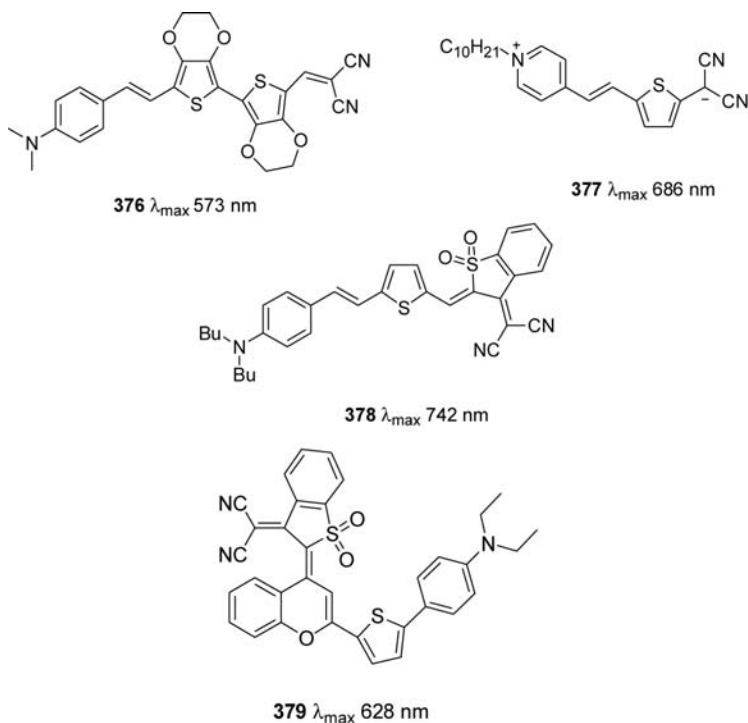


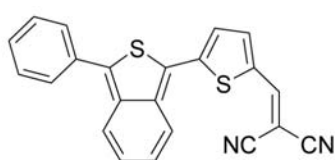
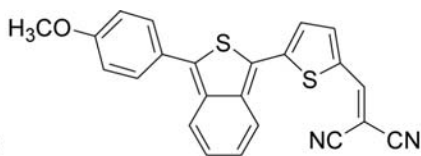
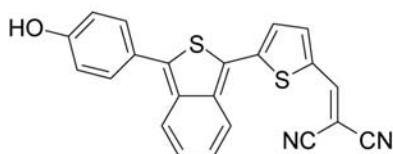
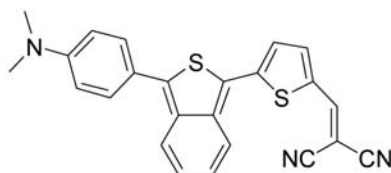
Two devices are prepared. In the case of the device A, the incident photon-to-collected electron conversion efficiency (IPCE) exceeds 80% from 410 to 590 nm, reaching the maximum of 93% at 530 nm. The short-circuit photocurrent density (J_{sc}), open-circuit photovoltage (V_{oc}), and fill factor (FF) of device A with an acetonitrile-based electrolyte under an irradiance of AM 1.5 G full sunlight are 14.33 mA cm^{-2} , 734 mV, and 0.76, respectively, yielding an overall conversion efficiency (η) of 8.0%. The photovoltaic parameters of device B with a solvent-free ionic liquid electrolyte are 14.06 mA cm^{-2} , 676 mV, 0.74, and 7.0%, respectively.

Some other NLO chromophores (**376–378**) with the same type of structure have been reported (95JOC2082; 97L3434; 97L4182; 99OL1847; 03CEJ1991; 03CEJ3670; 04JPC(B)8626; 04T4071; 07JOC8332). These types of compounds were also inserted in a polyamine scaffold (09MI1533). Thienyl-tiazolyl derivatives were described with absorption peaks in the range 418–718 nm (00EJO1327). Thienyl-pyrrole derivatives showed absorption band in the range 408–519 nm (05T11991).

Nonlinear optical properties were also found in thienyl derivatives bearing a chromone moiety in the structure such as **379** (99AM452; 02CL984).

Some isothiaphthene derivatives (such as **380–383**) have been described (08OL2991).

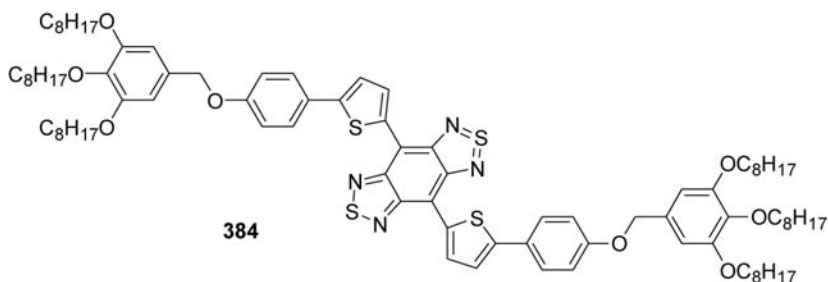


**380** λ_{\max} 525 nm; λ_{\max}^F 637 nm**381** λ_{\max} 537 nm; λ_{\max}^F 672 nm**382** λ_{\max} 545 nm; λ_{\max}^F 684 nm**383** λ_{\max} 579 nm; λ_{\max}^F 785 nm

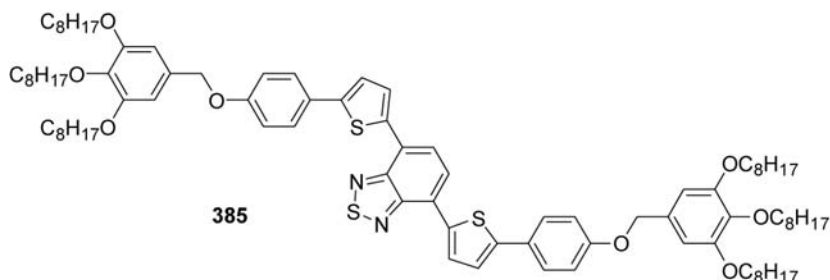
Columnar mesophase liquid crystals (LC) have attracted considerable academic and commercial interests because of their unique structures and properties in organic semiconductors. The planar uniaxial alignment with edge-on orientation of the molecules and columns parallel to the substrate is needed for FETs to ensure the charge migration between the source and the drain, while the homeotropic alignment with a face-on orientation of the discs and the columnar axes perpendicular to the substrate is expected to be beneficial for the performance in PVC and LEDs. Generally, columnar mesophases are generated from discotic LC molecules.

To capture the infrared energy, low band gap or NIR-absorbing organic columnar mesophase LC semiconductors are urgently needed for PVCs. NIR materials have potential applications for telecommunications, thermal imaging, and biological imaging.

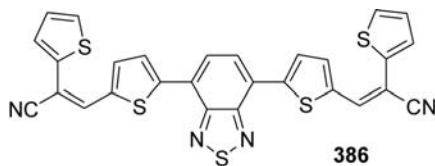
Compound **384** is strongly NIR-absorbing with peaks at 836 nm in solution (chloroform) and at 890 nm in film (08OL3785).



Emission of **384** is in the NIR region as well, as is evident from the emission peaks at 1060 nm in solution and 1160 nm in film. A film of **385** has a maximum absorption at 533 nm and emits a deep red color at 665 nm.



The compound **386** showed absorptions at 304, 399, and 478 nm and an emission at 578 nm (09SM(159)1471).



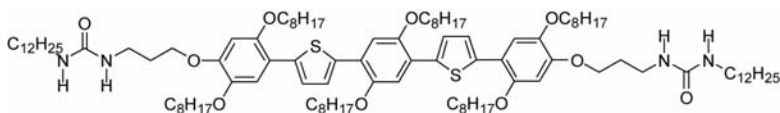
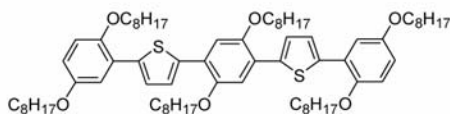
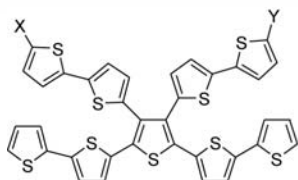
One of the most promising “bottom-up” approaches in nanoelectronics is to assemble π -conjugated molecules to build nano-sized electronic and opto-electronic devices in the 5–100 nm length scale. This field of research, called “supramolecular electronics,” bridges the gap between molecular electronics and bulk “plastic” electronics. In this contest, the design and preparation of nanowires are of considerable interest for the development of nano-electronic devices such as nanosized transistors, sensors, logic gates, LEDs, and photovoltaic devices.

Numerous nanostructures such as nanorods, nanotubes, or nanorings have been obtained by this approach. In particular, the use of organogelators as directors to control the morphologies of the aggregates has been explored recently. Cholesterol- and phospholipid-thethered *trans*-stylobenes are able to gelate different organic solvents in which the steroid and the lipid units serve as templates to form one-dimensional stacks.

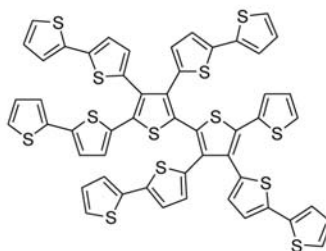
The thiophene moieties formed closely packed arrays enforced by the urea hydrogen-bonding units, thereby creating an efficient pathway for charge transport. The synthesis of **387**, a sequence of five 1,4-dialkoxypheylene and thiophene units functionalized with two urea moieties, was reported (08CEJ4201). This oligo(phenylenethienylene) derivative was found to be capable of forming one-dimensional supramolecular assemblies, leading to gelation of several solvents. To confirm the influence of the urea moieties on the supramolecular organization of **387** in the solid state, the otherwise identical unsubstituted conjugated segment **388** was

prepared, and the structural and optical properties of the two compounds were established and compared.

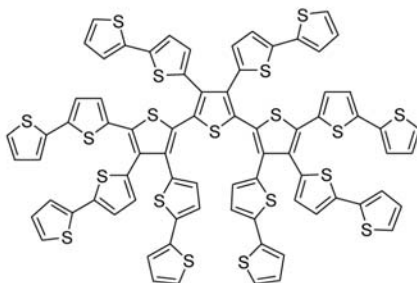
The UV/Vis absorbance of **387** was blue-shifted from 413 nm in solution to 406 nm in the solid state, accompanied by a broadening and decrease in intensity of the $\pi-\pi^*$ absorption bands. These spectral changes can be attributed to a strong exciton coupling between the phenylenethienylene moieties.

**387****388**

389: X = Y = H
 λ_{max} 345, 419 nm



390 λ_{max} 341, 420 nm



391 λ_{max} 338, 421 nm

Apparently, the phenylenethienylene chromophores of **387** are present in the solid state as π -stacked *H*-aggregates. On the other hand, the red

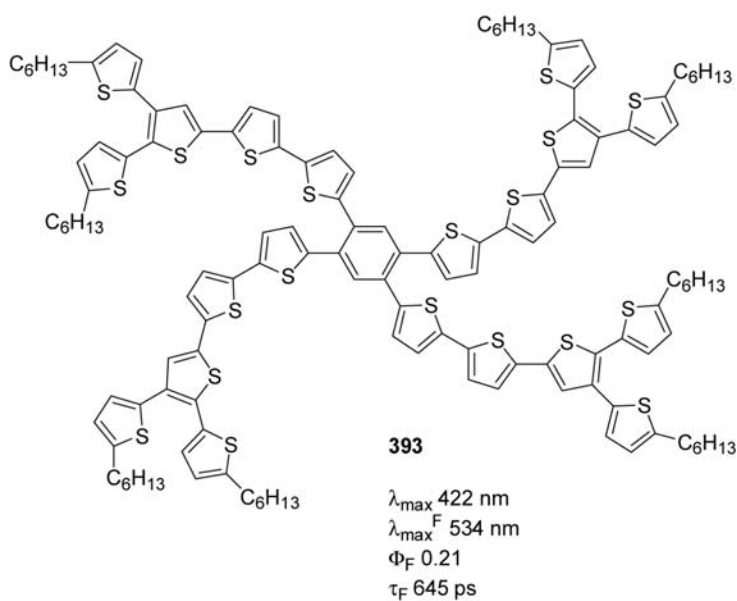
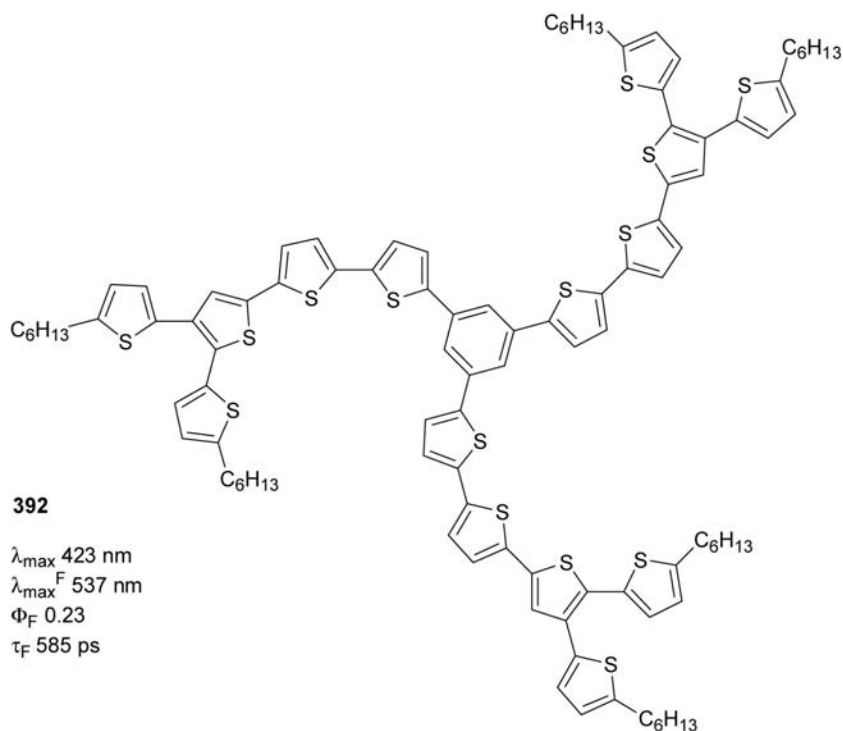
shift from 405 to 434 nm observed for **388** suggests a different supramolecular organization with the formation of *J*-aggregates.

Some dendrimers (**389–391**) have been reported. The thiophene-containing dendrimers are promising materials, due to the unique properties of oligothiophenes and their derivatives, such as high charge carrier mobility, efficient fluorescence, excellent stability in ambient conditions (even at elevated temperatures), and easy functionalization.

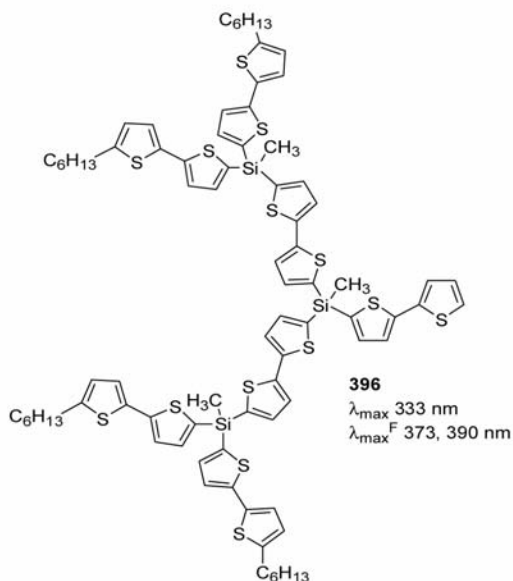
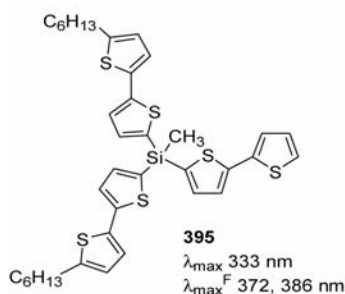
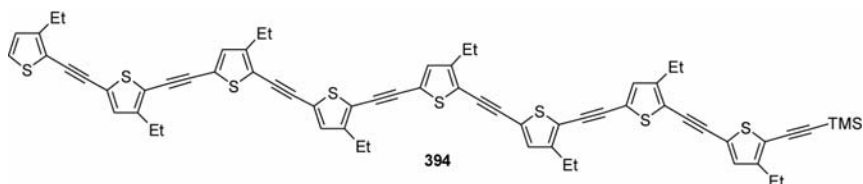
The first absorption peaks are in agreement with the observations on which the structural design of spider-like oligothiophene was based: (a) **389**, **390**, and **391** show a π -conjugation efficiency equivalent to or even slightly higher than linear oligothiophenes having the same number of α -linked thiophene units; (b) the energy gap values progressively decrease as *n* increases up to the critical value of 8–9, and then the trend flattens for higher *n* values; (c) the energy gap values flatten when five α -conjugated thiophene units are present, independently of the whole number of thiophene units constituting the molecule (06MI3177; 07MI1163; 08CEJ459). Indeed, the three compounds display nearly identical $E_g(\lambda)$ and very similar $E_g^*(\lambda)$ values, independently of the length of the main α -conjugated sequence (*n* = 5, 6, 7) and of the overall number of thiophene units constituting the molecule (*n* = 9, 14, 19), which is more than doubled on passing from **389** to **391**.

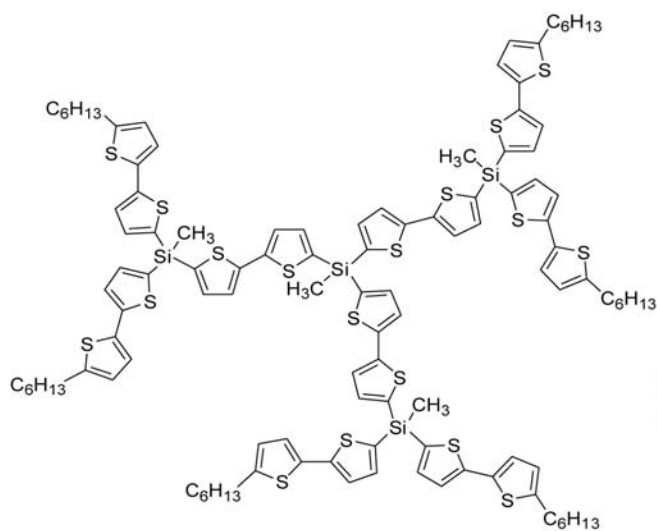
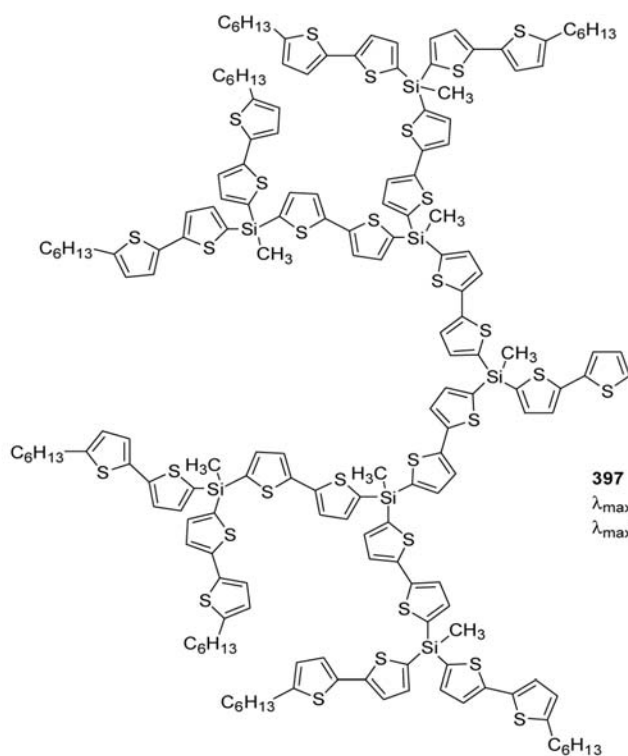
The band occurring at about 345 nm could be assigned to absorptions involving the spider legs, as suggested by the extinction coefficient values ϵ which are linearly dependent on the number of bithienyl pendants present in the molecule (2, 4, and 6). The extinction coefficient is known to be dependent upon the number of the thiophene units also in linear α -oligothiophenes.

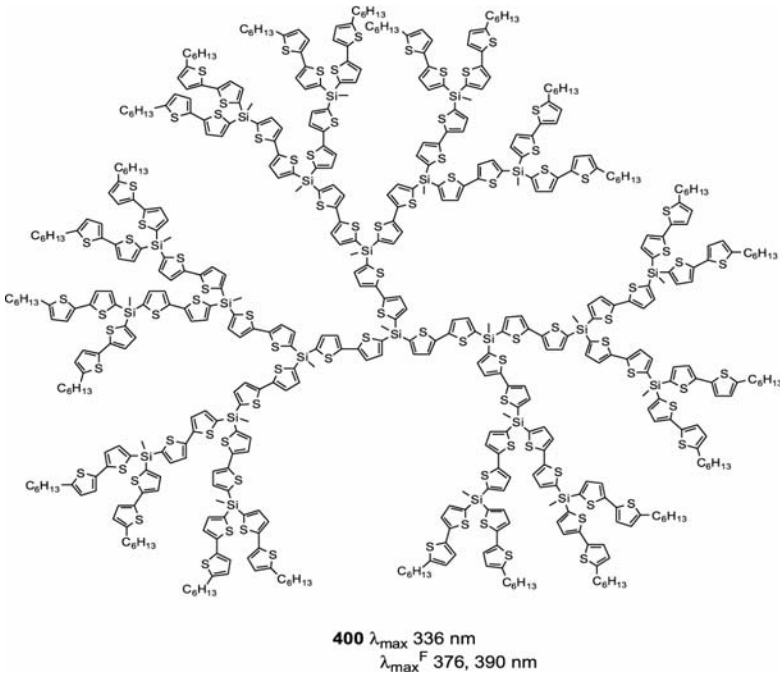
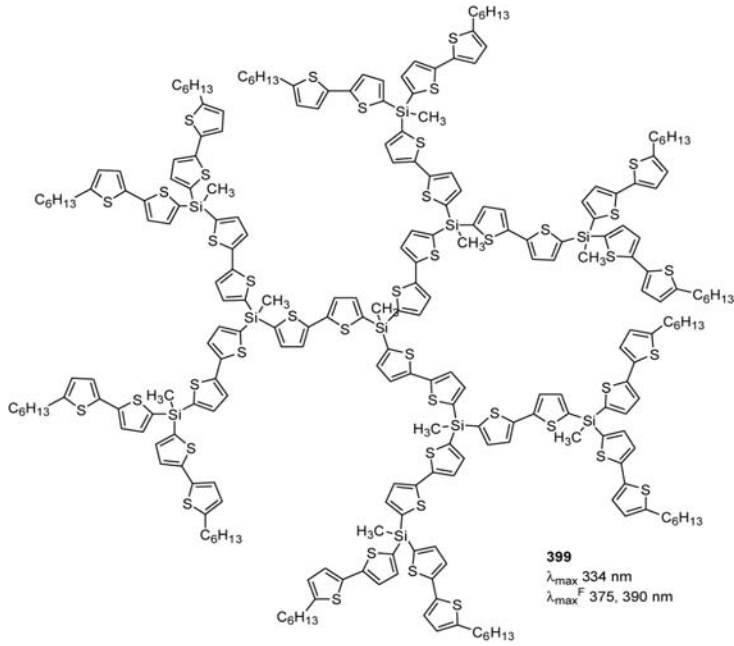
The emission of **390** is red shifted with respect to that of **389** (emission maximum at about 569 and 524 nm, respectively). This behavior can be explained if we assume that the lowest excited state geometry corresponds to a planarized structure. The UV/Vis absorption spectra of [**389**]_m and [**390**]_m films shift to significantly longer wavelengths with respect to the corresponding monomers, thus confirming that coupling has indeed occurred resulting in a more extended π -conjugated system. This conjugation improvement is significantly higher than the expected one considering oligomers in solution. Consistently with absorption, the photoluminescence spectra of [**389**]_m and [**390**]_m are at lower energy with respect to the ones of the corresponding monomers, confirming the longer effective π conjugation in the films. The maximum emission wavelengths of [**389**]_m and [**390**]_m are located at about 630 and 610 nm, respectively, again suggesting a more extended conjugation in [**389**]_m with respect to [**390**]_m. Some other dendrimers of thiophene have been reported (07AGE1679). Some phenyl-cored dendrimers (**392**, **393**) have been prepared and their photophysical properties collected (09CM287).



Oligothiényleneethynylenes have been prepared: the compound **394** has an absorption band at 426 nm and showed nonlinear optical properties (96CM819). Derivatives with terminal thioester moiety have also been synthesized (97JOC1376).







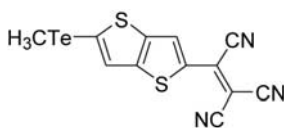
A number of dendrimers (**395–400**) of the first generation containing bithiophene or terthiophene units linked directly to silicon atoms have been reported (06MI3040; 07OM5165; 08OL2735).

The absorption spectra of the monodendrons and dendrimers of all three generations are quite similar: all of them are slightly broadened and red shifted with respect to the model 5-hexyl-2,2'-bithiophene due to the influence of the silicon atom to a π system of the bithiophenes. It is noteworthy that attachment of the methylsilyl group to 5-hexyl-2,2'-bithiophene leads to an increase of the molar extinction coefficient (ϵ) from 13,000 to 19,000 $\text{M}^{-1} \text{cm}^{-1}$.

All of the monodendrons **395–397** and dendrimers **398–400** exhibit apparently identical violet-blue light emission with two maxima at 373 and 390 nm. Triarylamine dendrimers with terminal 2,5-diarylthiophene moiety have been synthesized (03JA8104).

As a model approach toward electronic property modulation, chromophore sequences are arranged in such a way that electron-donor (D) and/or acceptor (A) units are linked through conjugation to the electron relay (π -center) at the ends. Electronic properties obtained from such molecules provide valuable information for understanding of relay role and also for developing functional tuning and enhancing the efficiency of electronic/photonic materials. The eligibility of oligothiophenes (π -center) for potential property modulator is associated with the role of sulfur d orbital that mix well with aromatic π -orbitals, such that electron transfer (or transport) across the relay to the terminal unit is facilitated, thereby anticipating a pronounced alteration in electronic/photonic properties. This is noticeable when the terminal groups are redox-active moieties, particularly involving metal complexes or D/A pair components as in nonlinear optical (NLO) chromophores.

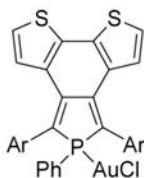
Some thienothiophene derivatives, such as **401**, showed nonlinear optical properties (96JCS(P2)1377).



401 λ_{max} 538 nm

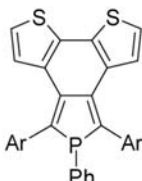
The ring-annulated polycyclic π -conjugated systems such as dibenzo[*b,d*]phospholes and dithieno[*b,d*]phospholes have attracted growing interest, as they possess rigid and elongated π networks that are beneficial for designing efficient light-emitting and electron-conducting materials. The UV/Vis absorption spectra of **403a** and **405a** display broad absorption bands attributable to the $\pi-\pi^*$ transition in the visible region (08EJO255;

08CEJ8102). In the fluorescence spectra, **403a** and **405a** show single emission bands in the orange region with relatively high quantum yields (**403a**, $\Phi_F = 17.6\%$; **405a**, $\Phi_F = 9.7\%$). The absorption and fluorescence maxima of **403a** (462 nm; 600 nm) and **405a** (472 nm; 609 nm) are remarkably red shifted relative to those of **408** (354 nm; 466 nm), exhibiting the effective π -extension in the present fused π systems. In marked contrast, **407a** exhibits a weak absorption peak (sh) at 395 nm and is far less emissive ($\Phi_F = 0.64\%$).



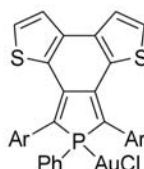
402a = Ph; λ_{\max} 502 nm
 λ_{\max}^F 661 nm

402b = 2-thienyl; λ_{\max} 535 nm
 λ_{\max}^F 710 nm



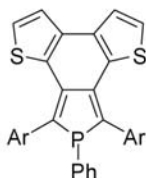
403a λ_{\max} 462 nm
 λ_{\max}^F 600 nm

403b λ_{\max} 483 nm
 λ_{\max}^F 646 nm



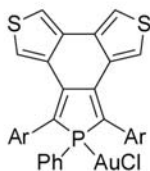
404a λ_{\max} 503 nm
 λ_{\max}^F 675 nm

404b λ_{\max} 539 nm
 λ_{\max}^F 720 nm



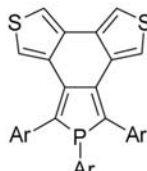
405a λ_{\max} 472 nm
 λ_{\max}^F 609 nm

405b λ_{\max} 491 nm
 λ_{\max}^F 656 nm



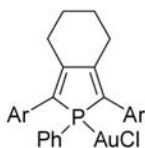
406a λ_{\max} 420 nm
 λ_{\max}^F 596 nm

406b λ_{\max} 435 nm
 λ_{\max}^F 606 nm



407a λ_{\max} 395 nm
 λ_{\max}^F 548 nm

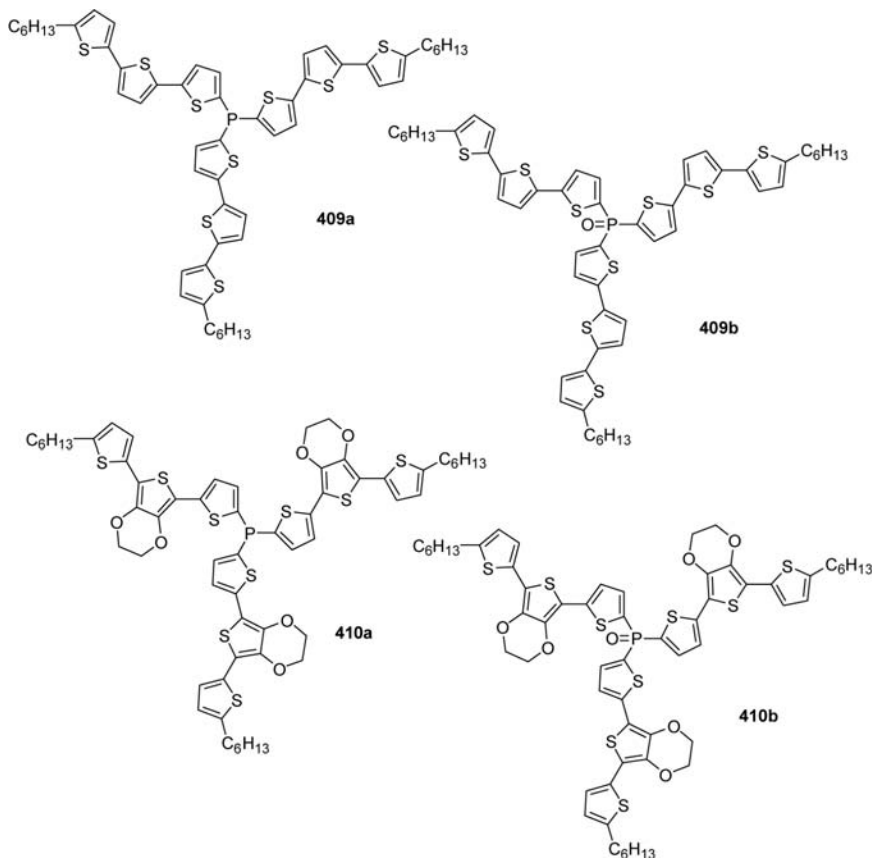
407b λ_{\max} 409 nm
 λ_{\max}^F 582 nm



408

The P coordination to the AuCl salt induces more pronounced effects on the optical properties, that is, the larger bathochromic shifts in absorption and emission spectra ($\Delta\lambda_{\text{abs}} = 25\text{--}52$ nm; $\Delta\lambda_{\text{em}} = 24\text{--}66$ nm) and a considerable decrease in emission efficiency.

The UV/Vis data show that the compounds **409b–410b** based on phosphine oxide nodes absorb practically at the same wavelength as the corresponding phosphine-based system **409a–410a** (08OBC3202). Comparison of the fluorescence quantum efficiencies (Φ_{em}) of compounds **409a** and **410a** with those of the corresponding terthienyls shows that the passage from the individual chains to the nonlinear molecules leads to a slight decrease of Φ_{em} . Oxidation of phosphine into phosphine oxide produces a significant increase of Φ_{em} from 4% to 15% between **409a** and **410b**.

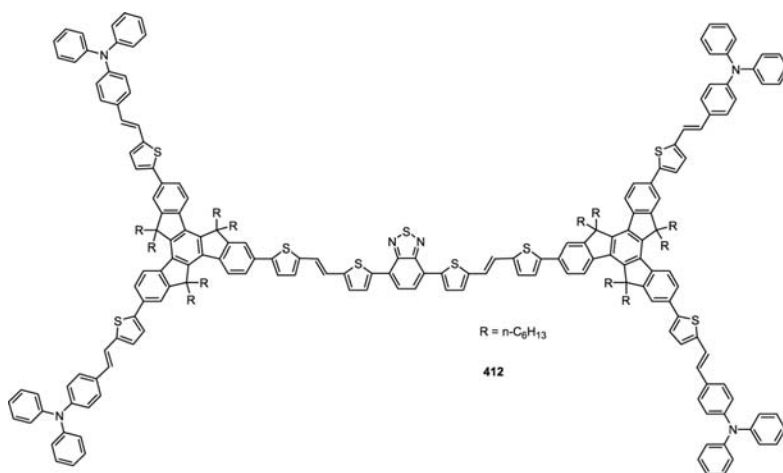
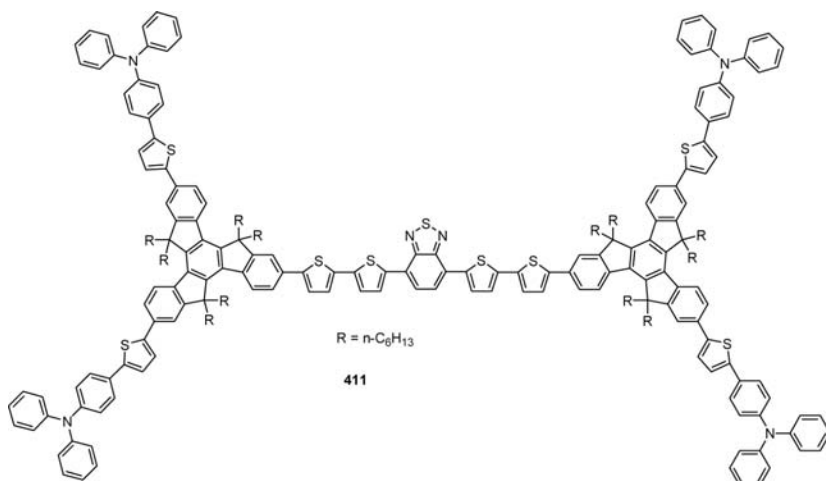


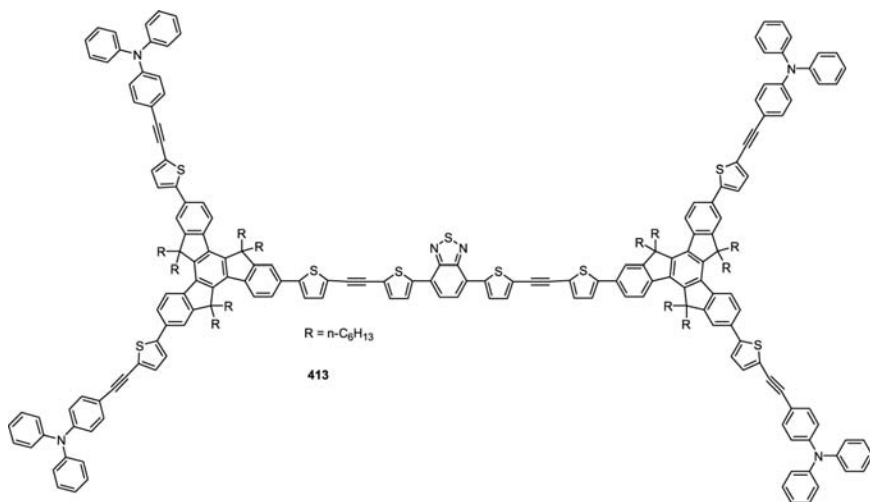
Donor-acceptor π -conjugated (D- π -A) compounds have led to numerous theoretical and experimental studies to explore the origin of intramolecular charge-transfer (ICT) fluorescence. This property can be used in order to have low bandgap materials.

A series of new D- π -A dendrimers (**411–413**) composed of four triphenylamine moieties as the donor groups share one benzothiadiazole chromophore in the middle as the acceptor, though various conjugated spacers

have been developed (08OL4271; 09OL863). The properties of donor-acceptor-substituted conjugated dendrimers have been tuned by changing the structures of the donor, acceptor, and π -conjugated moieties.

All the molecules show two distinct absorption bands. Absorption peaks were at 396 and 535 nm for **411**, 421 and 552 nm for **412**, and 391 and 512 nm for **413**. The absorption band was assigned in the shorter wavelength region to the four end-capping triphenylamine units in these dendrimers. Another absorption peak for **411** (535 nm), **412** (552 nm), and **413** (512 nm) was assigned to the π - π^* absorption band of the benzothiadiazole core. Among three dendrimers, **412** exhibited the longest effective conjugation length along the molecule. In comparison with **411**, the insertion of vinylene units results in a red shift of ca. 20 nm and a higher value of molar extinction coefficient.





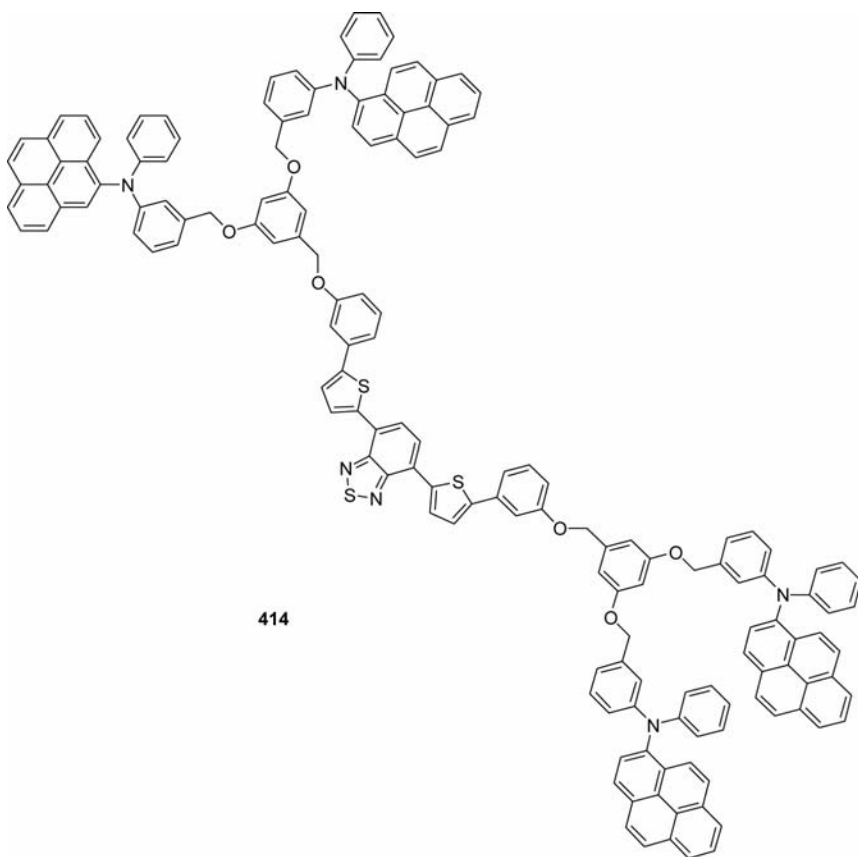
The maximum emission wavelength λ_{max} in cyclohexane solution for **411–413** were 614, 628, and 592 nm, respectively. The fluorescence quantum yields (Φ_F) of these dendrimers in dilute cyclohexane solution were measured to be 8% for **411**, 3% for **412**, and 16% for **413**. The fluorescence quantum yields for **412** were dramatically lower than the others, which might be related to the nonluminescent property of oligothiophylenevinylenes. For **412** and **413**, when excited at 394 or 391 nm, the emission came almost exclusively from the core units. The residual fluorescence from the periphery group in the range from 400 to 550 nm became very weak, which indicated a highly efficient intramolecular energy transfer process from the outside to the core. The absorption spectra are nearly independent of solvent polarity in our D- π -A dendrimers, except for a slight red shift in methanol due to aggregation. This result indicated a negligible intramolecular interaction between donor and acceptor chromophores in the ground states. However, their emission spectra exhibited distinct solvent dependence. The maximum emission peak of **412** changed from ca. 628 nm in cyclohexane to ca. 672 nm in methanol along with successively decreased fluorescence intensity. These results suggest that the excited states of our molecules possess more polar character than the ground state.

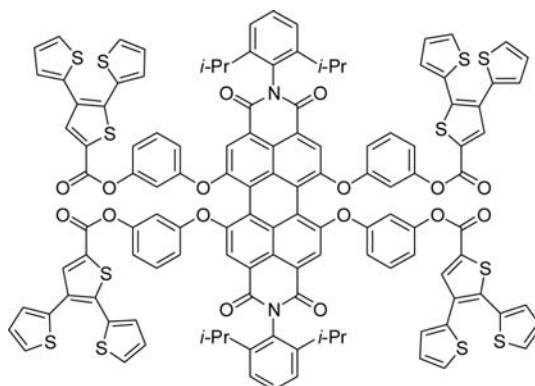
All compounds exhibited excellent film forming properties. Absorption peaks were observed for **411**, **412**, and **413** at 552 (405), 567 (426), and 521 nm (397 nm), respectively. The emission spectra of these molecules in thin film became very broad, and the maximum peaks were obviously red shifted compared with those in cyclohexane solutions. For example, red shifts of 44 nm for **411** and 36 nm for **413** were observed,

respectively, indicating the formation of excimer in the solid state. Moreover, **412** exhibits nearly nonluminescent properties in thin film.

Other dendrimers, such as **414**, were obtained from the same thiophene scaffold (05JA373): this compound showed an absorption band at 490 nm and an emission centered at 600 nm.

Dendritic oligothiophene-erylene bisimide derivatives of type **415** have been synthesized (09MI129). Its fluorescence spectrum is consistent with the perylene bisimide unit and resembles the mirror image of the longest wavelength perylene absorption band. This quenching of dendritic oligothiophene emission and the wavelength-independent emission of perylene bisimide is attributed to a fluorescence resonance energy transfer process.



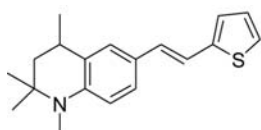
**415**

λ_{\max} 563, 533, 442, 348, and 279 nm
 λ_{\max}^F 600 nm, Φ_F 0.69, τ 6.2 ns

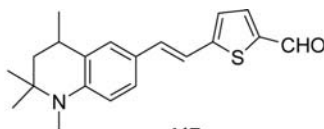
Perylene bisimide–dithienothiophene derivatives have been prepared (09JPC(A)5039). A femtosecond transient absorption study showed the presence of two positive bands at 490 nm (perylene cation radical) and at 730 nm (perylene anion radical).

Detailed evidence on the ICT state revealed that, in the electronically excited state, charge transfer from the donor moiety to the electron-withdrawing species is accompanied by an anomalous 90° twist of the donor compound relative to the thiophene π bridge (98T8469; 04JOC8239; 08CEJ6935; 08JST(876)102). The strong absorption maximum in the visible region and relatively weak absorption peak in the near UV region correspond to the $S_1 \leftarrow S_0$ and $S_2 \leftarrow S_0$ electronic transitions, respectively.

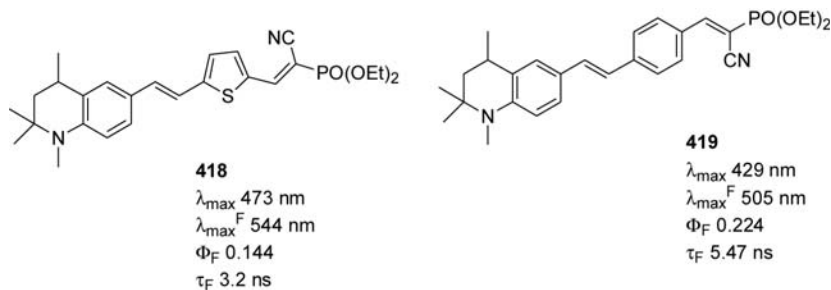
In general, an electron-withdrawing substituent at the thienyl 2-position can induce a remarkable red shift of the absorption maximum, the origin of which can be attributed to the ICT state for a strong push-pull system.

**416**

λ_{\max} 366 nm
 λ_{\max}^F 402 nm
 Φ_F 0.211
 τ_F 3.7 ns

**417**

λ_{\max} 425 nm
 λ_{\max}^F 474 nm
 Φ_F 0.066
 τ_F 3.4 ns

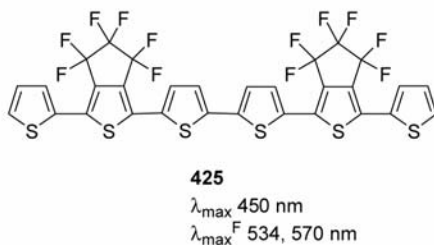
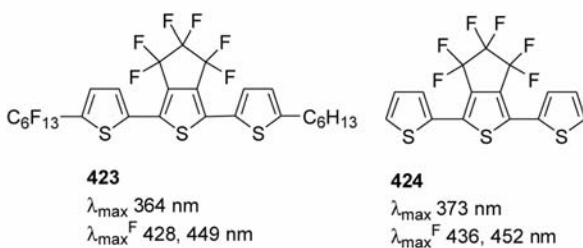
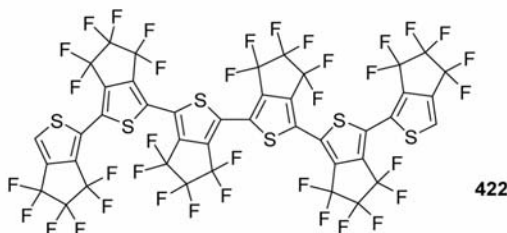
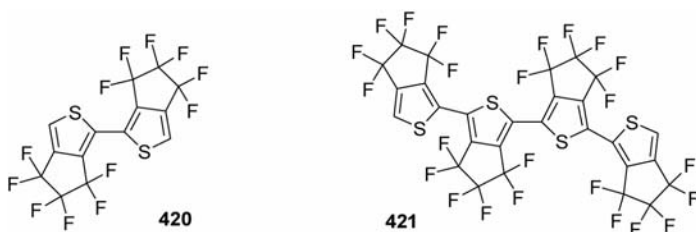


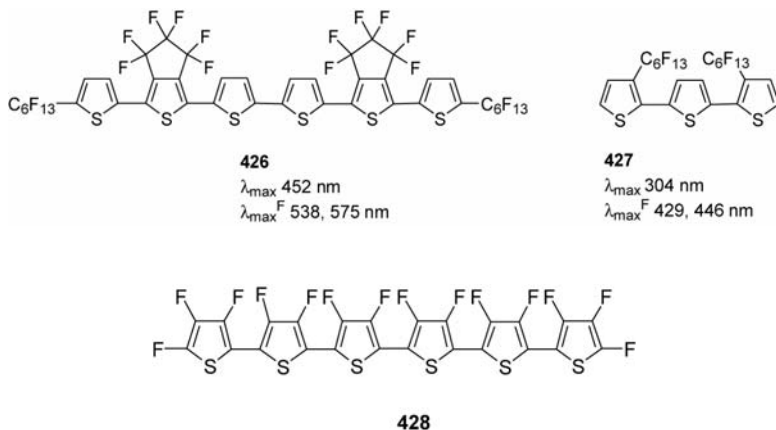
The solvatochromic shift is rather small for **416** (366 nm in hexane and 370 nm in acetonitrile). This indicates that the difference in dipole moments of the Franck–Condon (FC) excited state and the ground state of **416** is quite small. However, the solvatochromic shifts of **417**, **418**, and **419** are larger due to the larger difference in dipole moment of the FC excited state and the ground state, which is induced by the electron-withdrawing formyl and diethylcyanomethylphosphonate substituents. The fluorescence spectra of **417** and **418** exhibit significant red shifts in polar solvents, indicative of a pronounced ICT characteristic of the fluorescent state. As in the case of **416**, the maxima of the emission spectra extend from 402 nm in hexane to 464 nm in MeCN, that is, a comparatively small solvatochromic shift of 62 nm. With an electron-withdrawing formyl substituent in the thienyl 2-position, the emission maxima of **417** range widely from 474 nm (in hexane) to 666 nm (in methanol), and the solvatochromic shift of **418** becomes even large as 224 nm on changing from hexane to methanol. This indicates that the magnitude of the solvatochromic shift also depends on the electron-withdrawing substituent at the thienyl 2-position in thiophene- π -conjugated tetrahydroquinolines. The smaller solvatochromic shift of **419** with **418** confirms that a thiophene bridge can offer more effective conjugation than a benzene bridge in donor–acceptor compounds. Fluorescence is emitted from the TICT (twisted) state in polar solvent. In addition, the fluorescence of **417** and **418** in nonpolar solvents is emitted from the fluorescent states with planar conformations. The electron-donating group amine can be a triarylamine linked to three thienyl derivatives bearing an electron withdrawing group: in this case the absorption spectrum showed bands at 368 and 510 nm in solution and at 545 nm in a film (06JCS(CC)1416). Bithienyl derivatives bearing electron-withdrawing in 5'-position and an electron-donating group in 2-position have been reported (03T4891). This type of substrates was linked to a polyimide showing nonlinear optical properties (02MI67).

The compound **420** showed absorption at 312 nm, **421** at 376 nm, and **422** at 398 nm (08OL1095).

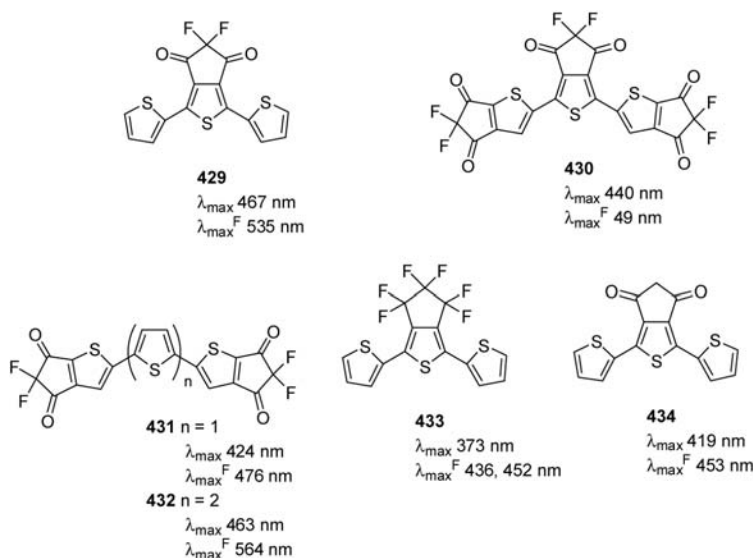
Compared to those of **427**, the absorption and emission maxima of **424** and **423** are largely red shifted and much closer to those observed for terthienyl (06OL5381).

Tetradecafluorosexithiophene **428** was considered as a potential n-type semiconductor for FETs for the following reasons: sexithiophene is an excellent p-type semiconductor with high hole mobility; perfluorination is an effective way to convert a p-type organic semiconductor to a n-type one (01JA4643). The absorption and emission maxima of **428** (421 and 471 nm, respectively) shifted to higher energies relative to those of sexithiophene (435 and 508 nm, respectively).



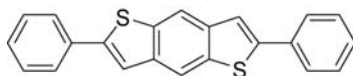


Thiophene-based oligomers and polymers have been extensively investigated for this application (OFETs). The absorption and fluorescence maxima of **429** are markedly red shifted relative to those of **433** and **434** (08OL833). This indicates that the fluoroketonic unit not only contributes to keeping the effective conjugation but also has stronger electron-accepting ability than those of the fluorine cyclopentane and ketonic units, leading to a unique donor-acceptor-donor configuration in **429**. Actually, solvent-dependent absorption shifts were observed for **429** (λ_{max} = 453 nm in cyclohexane and 459 nm in THF). The terminally annulated difluorodioxocyclopentene groups stabilize both the HOMO and LUMO levels with narrowing of the optical gap.



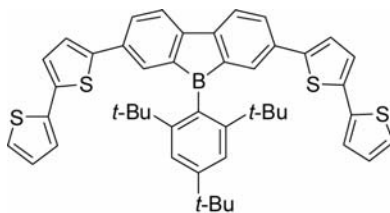
Benzodithiophene exhibits orange fluorescence in the solid state and a blue emission when irradiated in diluted solution with UV light (98JA2206). A HOMO–LUMO gap of 2.8 eV in dilute chloroform solution was observed from the absorption edge (440 nm), and 2.3 eV energy gap was obtained from the emission peak (547 nm) of a thin film.

The compound **435** showed p-type response (04JA5084).



435

In boron-containing π -conjugated molecule, the $p_{\pi}-\pi^*$ conjugation through a vacant p orbital of the boron atom endows them with intriguing photophysical and electronic properties and makes them attractive materials for organic (opto)electronics. As a representative core skeleton, dibenzoborole (9-borafluorene) is of particular interest. While its carbon and nitrogen congeners, fluorene and carbazole, have been widely used as the core skeleton for emissive and hole-transporting materials, respectively, the dibenzoborole would have significant potential as an electron-accepting building unit since the perpendicular arrangement of the vacant p orbital of the boron to the biphenyl plane in the skeleton promises an effective $p_{\pi}-\pi^*$ conjugation (08JCS(CC)579).



436

λ_{\max} 383, 466 nm

λ_{\max}^F 590 nm

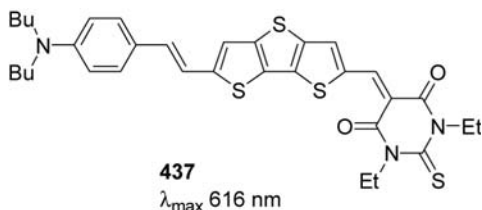
Φ_F 0.26

The extended compound **436** showed intense absorption band around 366–390 nm and weak absorption bands around 453–470 nm. In the fluorescence spectra (THF) **436** showed orange-red emissions with the maximum around 600 nm. When the nonpolar solvent cyclohexane (**436**:

590 nm) was replaced with the polar DMD (**436**: 622 nm), the emission bands shifted to a longer wavelength, while only subtle changes were observed in the absorption spectra. These results confirm that the dibenzoborole framework acts as a π -electron accepting unit only in the excited state, and the enhancement in charge transfer character in the excited state results in the large red shift in the emission.

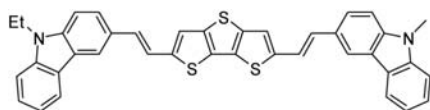
The molecular nonlinearity, $\mu\beta$ (determined by EFISH measurements in various solvents), of dithienothiophene-based chromophores is strongly influenced by solvent polarity and the acceptor strength (96CPL (255)147; 99MI2227; 02JOC205; 02MI559; 04CEJ3805).

The large $\mu\beta$ values observed suggest that dithienothiophene functions as an efficient relay in transmitting electrons from the terminal D moiety to A moiety. By contrast, in high polar solvents such as DMF, $\mu\beta$ values decrease significantly from what observed in CH_2Cl_2 and a dramatic change occurs with the strong acceptor chromophore, **437**, whose $\mu\beta$ value shifts to the negative regime.

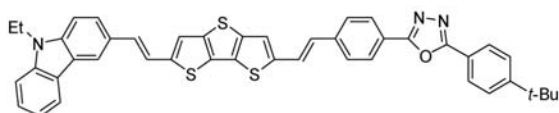


As shown in TPA (two-photon absorption) molecular structures, π -centers are attached by either a D/D or a D/A pair through conjugation: typically D is triphenylamine and A is 2-phenyl-5-(4-*ter*-butyl)-1,3,4-oxadiazole. Their (single-photon) absorption maximum, λ_{max} , is slightly (≈ 5 nm) red-shifted due to CT, relative to that of their symmetric D/D pair counterpart (**438** and **440**) (02CPL(364)432). These compounds are highly fluorescent, particularly with D/D pair chromophores relative to D/A pair counterparts as indicated by the fluorescence quantum yield (Φ_f), probably due to the presence of competing charge-transfer pathway for decay of the singlet excited state.

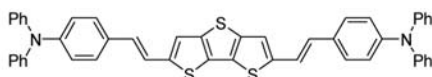
The magnitude of σ_{TPA} values is in the following order: **443** > **440** > **441** > **438** > **439**. Viewing that **275**, **277**, and **279** are a symmetric D/D structure differing in D moieties whereas **439** and **441** are an asymmetric D/A structure with the same A, this seems to implicate two things. The first is that symmetric structure is more effective for TPA than corresponding asymmetric counterpart and the second is that the effectiveness of D is different in function of the structure.

**438**

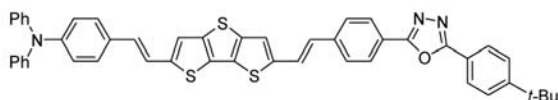
λ_{max} 440, 467 nm
 $\lambda_{\text{max}}^{\text{F}}$ 487, 518 nm
 Φ_{F} 0.47

**439**

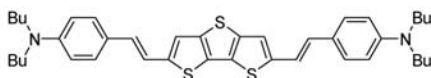
λ_{max} 446 nm
 $\lambda_{\text{max}}^{\text{F}}$ 545 nm
 Φ_{F} 0.10

**440**

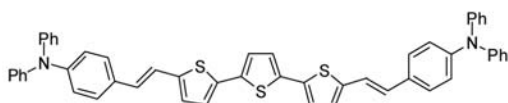
λ_{max} 453, 479 nm
 $\lambda_{\text{max}}^{\text{F}}$ 512, 543 nm
 Φ_{F} 0.31

**441**

λ_{max} 456 nm
 $\lambda_{\text{max}}^{\text{F}}$ 565 nm
 Φ_{F} 0.05

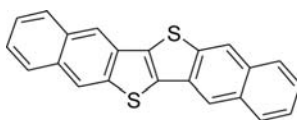
**442**

λ_{max} 456 nm
 $\lambda_{\text{max}}^{\text{F}}$ 585 nm
 Φ_{F} 0.51

**443**

λ_{max} 448, 469 nm
 $\lambda_{\text{max}}^{\text{F}}$ 535 nm
 Φ_{F} 0.07

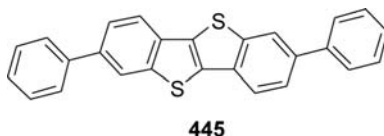
Optical HOMO–LUMO gaps estimated from the absorption edge are ca. 3.0 for **444** (07JA2224).

**444**

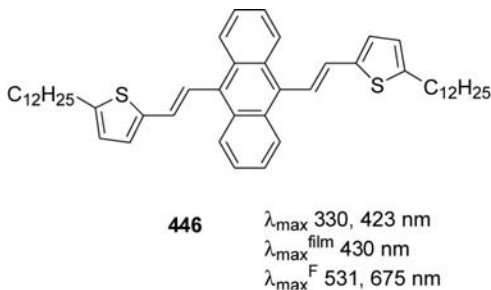
All the devices fabricated under various conditions showed typical p-channel FET characteristics with μ_{FET} higher than $0.3 \text{ cm}^2 \text{ V}^{-1} \text{ s}^{-1}$ and $I_{\text{on}}/I_{\text{off}} > 10^6$ under ambient conditions.

Excellent FET characteristics with μ_{FET} higher than $2.0 \text{ cm}^2 \text{ V}^{-1} \text{ s}^{-1}$ and $I_{\text{on}}/I_{\text{off}}$ of 10^7 were observed in **444**-based devices fabricated on the OTS-treated substrate at $T_{\text{sub}} = 60^\circ\text{C}$.

In the solution UV/Vis spectrum of **445** in THF, the absorption maximum is 336 nm with an absorption edge at 385 nm, corresponding to the HOMO–LUMO energy gap of 3.2 eV (06JA12604).

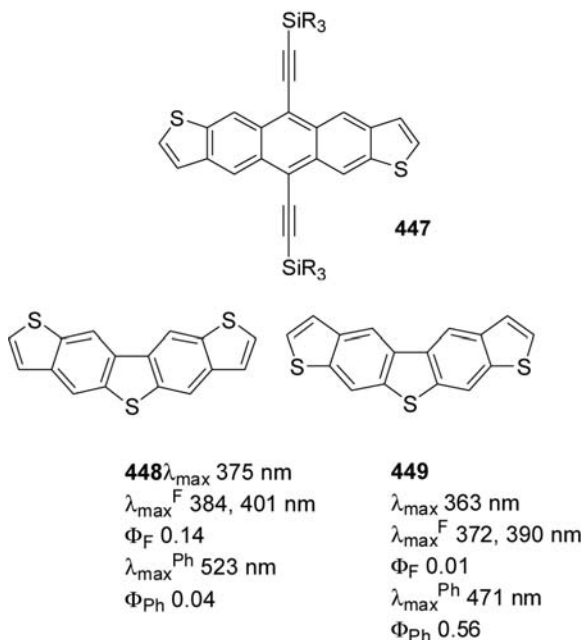


All the devices showed typical p-channel FET response under ambient conditions. On the HMDS-treated substrates, the maximum μ_{FET} was $\sim 1.2 \text{ cm}^2 \text{ V}^{-1} \text{ s}^{-1}$ at $T_{\text{sub}} = 100^\circ\text{C}$, which is almost four times higher than the μ_{FET} on the bare Si/SiO₂ substrates. The devices fabricated at $T_{\text{sub}} = 100^\circ\text{C}$ routinely showed $\mu_{\text{FET}} > 1.0 \text{ cm}^2 \text{ V}^{-1} \text{ s}^{-1}$ and $I_{\text{on}}/I_{\text{off}} > 10^7$, and the best devices with $\mu_{\text{FET}} = 2.0 \text{ cm}^2 \text{ V}^{-1} \text{ s}^{-1}$ and $I_{\text{on}}/I_{\text{off}} \sim 10^8$ were reproducibly obtained.



Anthracene linked to thiophene in 2,6-position showed an absorption band at 392 nm and emission at 431 nm (05CM1261). 9,10-bis(oligothienylvinyl)anthracene derivatives such as **446** have been studied (09MI8202).

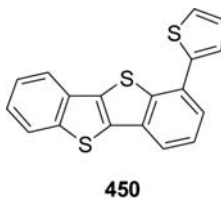
Both synthesis and properties of functionalized pentacene and anthradithiophene **447** were reported (05JA4986; 06MI3708). Anthradithiophenes functionalized on the thiophene ring were reported to yield good hole mobility from vapor-deposited films (on order of $0.1 \text{ cm}^2 \text{ V}^{-1} \text{ s}^{-1}$). Acenedithiophenes with absorption at 653 nm have been reported (04OL3325). Tetrathiophene anthracene derivatives have been described showing absorption at 431 nm and emission at 437 nm (07OL4187).



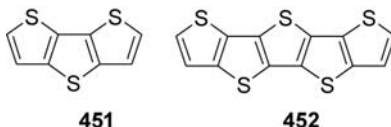
Pentacene, a member of the acene series of linear polycyclic aromatic hydrocarbons, is a fundamental component of organic field-effect transistors (OFET). The UV/Vis absorption spectra of **448** and **449** showed that the longest wavelength absorption band of the *anti*-isomer (375 nm) is 12 nm red-shifted relative to the maximum absorption of the *syn* isomer (363 nm) (05JOC4502; 06MI1121). The longest wavelength absorption band of the parent dibenzo[*b,d*]thiophene (DBT) is at 327 nm. The fluorescence emission of **449** exhibits a 12 nm blue shift from that of **448**. Both isomers show an equally small Stokes shift, indicating that they are of equal rigidity. Emission quantum yields vary significantly by isomer.

The fluorescence quantum yield of **448** is 0.14, a sixfold increase relative to that of the parent. In comparison, the fluorescence quantum yield of **449** (0.01) is comparable to that of the parent compound. The phosphorescence emission quantum yield of **449** is 0.56 in a frozen matrix as expected as a result of the intramolecular heavy atom effect. In contrast, the phosphorescence is effectively shut off in the *anti*-isomer where the quantum yield is only 0.04. This observation suggests that the electronic excited state structures and nonradiative decay channels vary considerably with constitution of the isomers. The optical gap energy was 3.1 (3.3) eV for **448** (**449**).

The structure and solvent effects upon the electronic absorption and fluorescence spectra and fluorescence quantum yields of three thienobenzothiophene derivatives, such as **450**, and benzothienoindole were investigated (06SM(156)256).



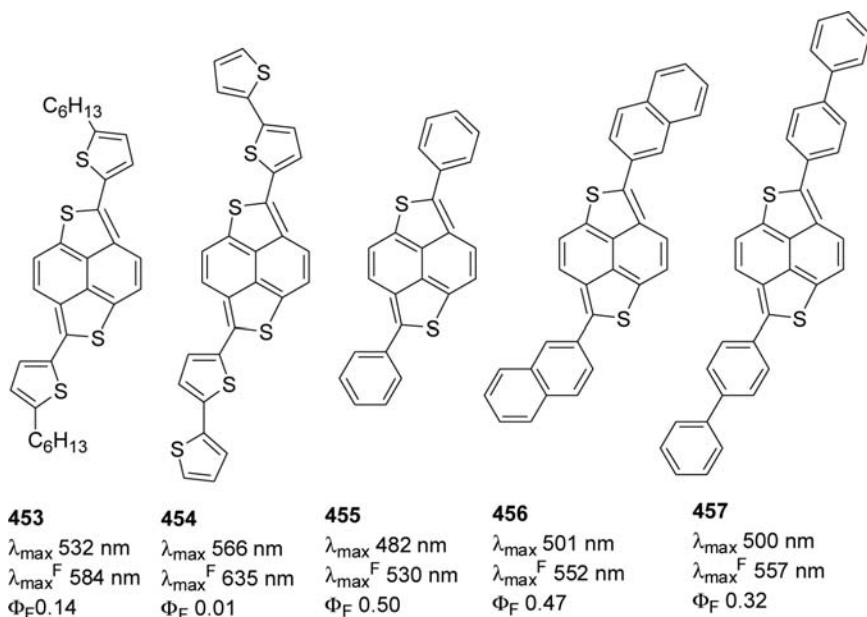
The *R*-linked dimer of dithieno[3,2-*b*:2,3-*d*]thiophene (**451**) and its alkylated derivatives have proven to be effective as the active layer in organic thin film transistors (OTFTs) (04SM(146)251; 05JA13281).



Compound **451** showed absorption at 314 nm and a photoluminescence at 384 nm (01MI1625). The UV/Vis absorption spectrum for **452** in chloroform solution shows absorption peaks at 305, 317, 339, 344, and 358 nm. The spectral absorption of vacuum-deposited thin films of **452** was slightly blue shifted, with absorption maxima at 326 and 342 nm, indicating that H-aggregates were formed. The solution photoluminescence was excited at 344 nm, and the solid-state emission was at 260 nm. **452** exhibits blue fluorescence in the solid state and a blue emission when irradiated in dilute solution with UV light. A HOMO–LUMO gap of 3.20 eV in dilute chloroform solution was estimated from the absorption edge. The mobility increases with increasing T_{sub} which is attributed to better ordered thin films and large grain sizes at elevated T_{sub} . Borane-substituted derivatives of **451** have been described (05AM34).

Two isomeric naphtho[1,8-*bc*:4,5-*b'**c'*]dithiophene (*syn*-NDT) and naphtho[1,8-*bc*:5,4-*b'**c'*]dithiophene (*anti*-NDT) and their dithienyl derivatives which served as good donor components for molecular-based conductors and conducting polymers were developed. Absorption spectra of **453–457** also provide information on the extent of π -conjugation between

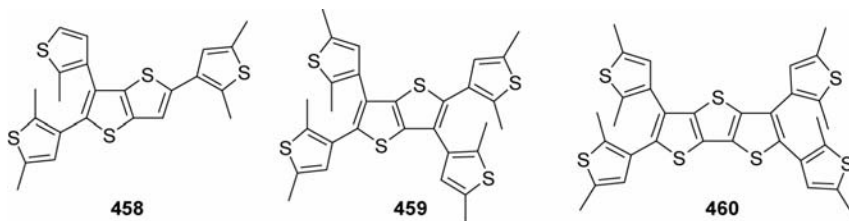
the NDT core and the substituents (93CL365; 94JCS(CC)1859; 02BCJ1795; 04JPC(B)7611; 05JA3605). Compared to that of the parent *anti*-NDT ($\lambda_{\max} = 411$ nm), the $\pi-\pi^*$ transitions of **453** ($\lambda_{\max} = 532$ nm) and **454** ($\lambda_{\max} = 566$ nm) show large bathochromic shifts.



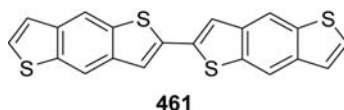
On the other hand, the $\pi-\pi^*$ transition of the phenyl derivative **455** ($\lambda_{\max} = 482$ nm) shows a less-pronounced bathochromic shift than that of **453**, evidently supporting that phenyl conjugation is not as effective as thieryl conjugation. Extension of the π -system from phenyl to naphthyl substitution (**456**) or to biphenyl substitution (**457**) causes a bathochromic shift by ca. 20 nm, which is much smaller than that (34 nm) from thieryl to bithiophenyl substitution. The fluorescence quantum yields of **453** (Φ_F 0.14) and **454** (Φ_F 0.01) bearing thieryl substituents are more markedly reduced than those (Φ_F 0.32–0.50) of **455–457** bearing phenyl or naphthyl substituents. This suggests that the photoexcited state is efficiently quenched by interactions involved with the sulfur atoms of the attached heterocyclic rings. These compounds gave p-type FET.

The compounds **458–460**, all dissolved in benzene to give colorless solutions, with intense absorption band at ca. 330 nm for **458** and **459** and at ca. 350 nm for **460**, corresponding to the $\pi-\pi^*$ transitions of the fused thiophene rings mixed with that of the dimethylthiophene moieties

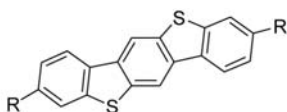
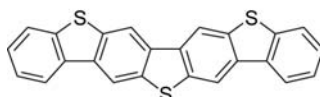
(08JCS(CC)5203). The lower absorption energy for **460** compared to that of **458** and **459** is in line with the more extended π -conjugation for dithienothiophene compared to thienothiophene. On excitation with $\lambda \leq 37$ nm, compounds **458–460** displayed intense luminescence with $\lambda_F \approx 405$ nm for **458** and **459** [**458**, $\tau_0 < 1$ ns, $\Phi_F(\lambda_{ex} 330 \text{ nm}) = 0.10$; **459**, $\tau_0 < 1$ ns, $\Phi_F(\lambda_{ex} 330 \text{ nm}) = 0.06$] and $\lambda_F \approx 420$ nm for **460** [$\tau_0 < 1$ ns, $\Phi_F(\lambda_{ex} 330 \text{ nm}) = 0.14$]. On UV excitation into the absorption bands ($\lambda \leq 370$ nm for **458** and **459**, and $\lambda \leq 392$ nm for **460**), all compounds in benzene solution displayed photochromism and became purplish red in color with the evolution of an intense absorption band at ca. 380 nm in the UV region and a moderately intense absorption band at ca. 560 nm in the visible region. For compound **459** and **460**, which consist of two diarylethene moieties, photocyclization could only take place at one of the diarylethene moieties even upon prolonged irradiation. On excitation into the absorption bands of the closed form decreased in intensity, indicative of the regeneration of the open forms **458–460**. The UV transitions in **458–460** mainly corresponds to an excitation from HOMO to LUMO, which can be assigned as the $\pi-\pi^*$ transition of oligothienoacene core, slightly mixed with $\pi-\pi^*$ transition of the peripheral thiophene rings.



A p-type organic semiconductor **461** based on benzodithiophene building blocks which has exceptional thermal stability was reported (97AM36). The highest mobility ($\mu_{FET} = 0.04 \text{ cm}^2 \text{ V}^{-1} \text{ s}^{-1}$) was obtained for transistors prepared at $T_{sub} = 100^\circ\text{C}$ because of the accompanying changes in morphology at elevated temperatures.

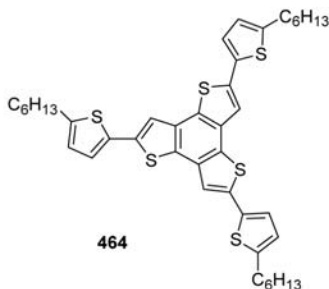
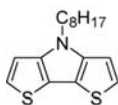
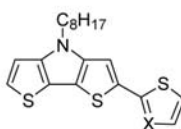
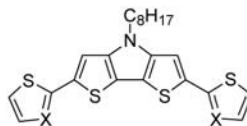


The main absorption band of **462a** was slightly blue shifted (366 nm for **462a** and 369 nm for **462b**) (08JCS(CC)1548).

**462a** R = H**462b** R = C₄H₉**463**

In dichlorobenzene, the determination of UV/Vis spectrum of **463** showed three absorption maxima at 374, 394, and 415 nm (99MI2095).

Benzofused compounds, such as **464**, showed absorption at 357–404 nm showing increasing potential properties (04OL273).

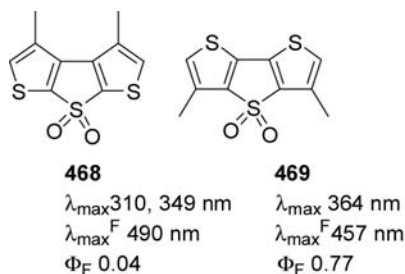
**464****465** λ_{\max} 298, 303, 310 nm λ_{\max}^F 324, 362 nm Φ_F 0.017**466a** X = CH λ_{\max} 364, 383 nm λ_{\max}^F 408, 421 nm Φ_F 0.29**466b** X = C-C₄H₉ λ_{\max} 378, 390 nm λ_{\max}^F 407, 420 nm Φ_F 0.089**466c** X = N λ_{\max} 378, 390 nm λ_{\max}^F 418 nm Φ_F 0.55**467a** X = CH λ_{\max} 405 nm λ_{\max}^F 444, 470, 506 nm Φ_F 0.49**467b** X = C-C₄H₉ λ_{\max} 382 nm λ_{\max}^F 446, 472, 508 nm Φ_F 0.36**467c** X = N λ_{\max} 413, 433 nm λ_{\max}^F 451, 478 nm Φ_F 0.54

Thienyl derivatives linked to carbazole or dibenzothiophene have been reported (09MI910). Increasing conjugation length in compounds **465–467** results in red shifts of the transitions and increased extinction coefficients. The observed DTP (dithienopyrrole) oligomer absorptions should all correspond to simple $\pi \rightarrow \pi^*$ transitions (05OL5253). The DTP quaterthiophene analogs **467a–c** exhibit a single transition ranging from a low of 382 nm for **467b** and a high of 413 nm for **467c**, which also exhibits a second lower energy peak at 433 nm. The parent quaterthiophene is in the center of this range at 392 nm. Oligomers **467a** and **467c** are red shifted in comparison to quaterthiophene presumably as a result of increased planarity due to the central DTP unit.

The fluorescence intensities of the DTP-based oligomers **467a–c** are significantly enhanced in comparison to quaterthiophene, with solution quantum efficiencies (Φ_F) of 36–54%. This was initially unexpected, as monomeric DTPs exhibit significantly less detectable fluorescence ($\Phi_F = \sim 10^{-13}$) than bithiophene ($\Phi_F = 0.017$). The often-weak fluorescence of thiophene based chromophores has been attributed to significant spin-orbit coupling due to the heavy atom effect of the sulfur, which is possibly also mediated by charge transfer mixing. The spin-orbit coupling thus results in high triplet quantum yields (0.99 for bithiophene), and highly efficient nonradiative processes between the triplet and ground states usually lead to relaxation from the triplet state without emission. However, as the length of the oligothiophene is increased, the triplet quantum yields typically decrease and Φ_F increases. Compounds bearing a phosphorus atom (-P(Ph)-) have been reported (04AGE6197; 05CEJ4687; 07CEJ7487).

A good example of the negative effect of side chains is oligothiophene **467b** that contains butyl groups on the two external thiophenes. As illustrated with the absorbance data, these side chains cause increased torsional strain and a reduction in conjugation. As a result, Φ_F is also reduced in comparison to other DTP analogs. What is interesting, however, is that while the absorbance of **467b** is blue shifted in comparison to that of quaterthiophene, its Φ_F is still twice that of it. This shows that the ring fusion still plays an important role in reducing torsional vibrations and mediating the formation of the planar excited state.

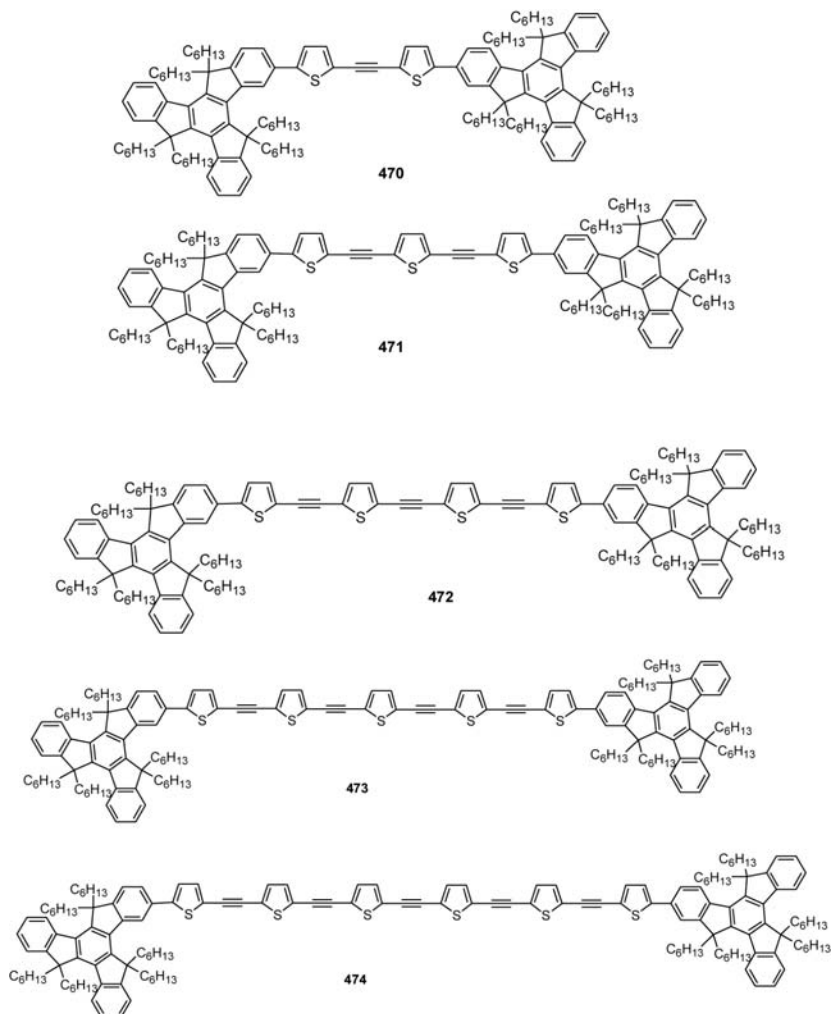
Oligomers containing thiophene *S,S*-dioxide has been described (99AM1375). They showed absorption maxima in the range 336–495 nm and fluorescence in the range 470–725 nm (00JA11971). The photoluminescence efficiency (Φ_F) of **468** is much smaller than that displayed by **469**, in solution as well as in the solid state (01CM4112; 03T5083).



The absorption spectrum of **468** in solution is characterized by the presence of an intense and structured band near 300 nm and by a broad and much weaker band around 350 nm, whereas the corresponding spectrum of **469** shows the presence of an intense featureless band at 364 nm. Dithieno derivative **469** is characterized by high emission efficiency in solution, more than two orders of magnitude greater than that of oligomers containing the thienyl-*S,S*-dioxide moiety. On the contrary, the photoluminescence efficiency of dithieno derivative **468** in solution is almost 20 times lower than that of **469**.

The synthesis of oligomers of thiophene-bearing fluorene derivatives as end cap has been reported (01JA9214; 03CM1778). The terthienyl derivative showed an absorption band at 360 nm and emission bands at 570 and 608 nm.

Oligo(thienylethynylene)s showed third-order nonlinear optical properties (94JPC10102). An efficient preparation of a family of molecular wires connecting two truxene moieties through oligo(thienylethynylene)s (OTE) units of different conjugation lengths and their photophysical properties in solution and in thin film were presented (08OL17). The investigation indicates that the introduction of the truxene units as the end group not only effectively suppresses the formation of aggregates of these molecular wires in the ground state but also converts the single-exponential of the excited-state lifetime of OTEs to biexponential with a longer lifetime component, which makes it possible to employ such compounds for optoelectronic devices. All molecular wires exhibited an identical absorption at 308 nm with the same molar extinction coefficient ($\log \epsilon = 4.92$), which was assigned to the $\pi-\pi^*$ electron absorption band of truxene units. It was also observed that their absorption λ_{max} peaked at 394 nm for **470**, 409 nm for **471**, 416 nm for **472**, 422 nm for **473**, and 424 nm for **474**, respectively, which exhibited the continual red shift in agreement with the increase of the effective conjugation length.



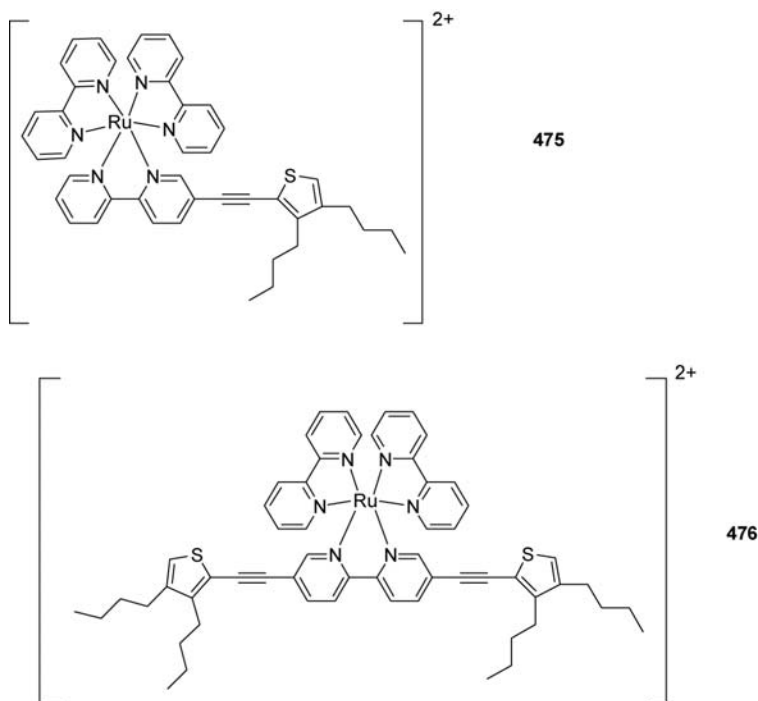
All the emission spectra in solution showed a maximum peak with a shoulder on the red side. It was observed that the photoluminescence λ_{max} in dilute THF solution red shifted from **470** to **474**. They also exhibited similar Stokes shifts (about 66 nm) due to their similar backbone. The fluorescence quantum yields (Φ_F) of these molecular wires in dilute THF solution were measured to be 0.25 for **470**, 0.22 for **471**, 0.20 for **472**, 0.20 for **473**, and 0.18 for **474**, respectively. The excited-state lifetime for OTEs was found to be single-exponential within a few hundred picoseconds. However, in THF solution (10^{-17} M), the decay of the emission maximum band for these molecular wires was found to be biexponential with two excited-state lifetimes yielding a ξ^2 of <1.2 . One excited-state lifetime ranged from 0.42 to 0.30 ns, which was in agreement with that in OTEs. Another one exhibited a

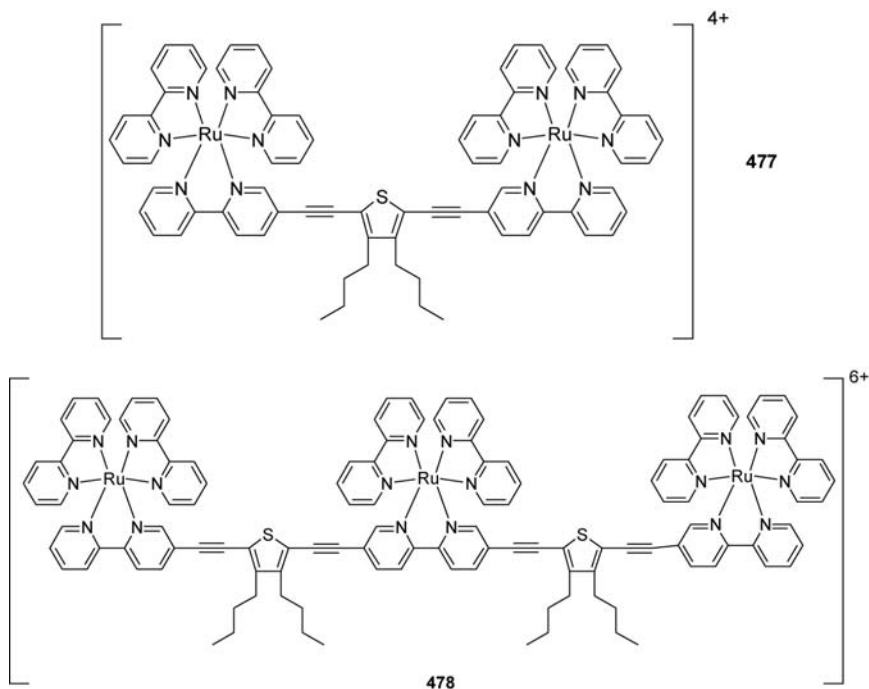
longer lifetime ranging from 1.29 to 1.85 ns. This emission was assigned to intrachain singlet excitons on the backbone. Therefore, the introduction of truxene units, which have long excited-state lifetimes (10.1 ns), might modify the excited-state lifetime of such molecular wires.

The absorption spectra of every molecular wire **470–474** in thin films were nearly identical to those in solution, which implied that the inter-chain interaction and/or intermolecular aggregation in the ground states might be suppressed in films possibly owing to truxene moieties with hexyl substituents. Their absorption spectra in films show an identical peak at about 309 nm owing to the $\pi-\pi^*$ electron absorption band of the truxene units. The absorption λ_{max} peaked at 400 nm for **470**, 410 nm for **471**, 415 nm for **472**, 418 nm for **473**, and 424 nm for **474**, respectively.

Oligo(thienylene-ethynylene) derivatives were obtained linked with [60]fullerene. A typical compound showed absorptions at 641 and 704 nm and emission at 716 and 798 nm (01T6877).

A study of a series of structurally well-defined metal complexes featuring ruthenium(II) polypyridine chromophores coordinated to a series of π -conjugated “oligomer ligands” that contain alternating 3,4-dibutylthiophene and 2,2-bipyridine units connected by ethynyl linkage was presented (03JPC(A)3476). The study explores the correlations between the conjugation length of the oligomer ligands and the nature of the lowest excited state.





All of the complexes display long-lived (i.e., microsecond time scale) and luminescent excited states. On the basis of photoluminescence and transient absorption spectroscopy, it is determined that in two systems the lowest excited state is based on $d\pi(\text{Ru}) \rightarrow \pi^*(\text{L})$ MLCT (where L = the dibutylthiophene-bipyridine ligand), while in the other two systems the lowest excited state is $^3\pi,\pi^*$ based on the oligomer ligand. Comparison of the spectra of the individual complexes allows assignment of the various absorption bands to transitions localized on the ancillary 2,2'-bpy ligands. All four complexes display a strong, narrow absorption band in the UV at ~ 286 nm. The absorption is assigned to the π,π^* transition of the auxiliary 2,2'-bpy ligands. **475**, **476**, and **477** each display strong absorption between 360 and 425 nm and a weaker band (or shoulder) between 450 and 500 nm. The higher energy band is attributed to long-axis polarized π,π^* transition of the e-T substituted bpy ligand. The MLCT absorption appears as a well-resolved band in **475** with $\lambda_{\text{max}} = 453$ nm. Inspection of the photoluminescence data reveals that the complexes fall into two categories: (1) monometallic complexes

476 and **477** both feature a broad, nearly structureless emission, with $\tau_{\text{em}} \leq 1 \mu\text{s}$; (2) polymetallic complexes **477** and **478** both feature a narrower emission band with clearly defined vibronic structure at room temperature, and $\tau > 1 \mu\text{s}$.

It is believed that **475** and **476** luminesce from MLCT manifold, while **477** and **478** emit from a $^3\pi,\pi^*$ state based on the thiophene-bipyridine oligomer ligands. The photoluminescence properties of the monometallic complexes **475** and **476** are characteristic of an MLCT excited state. First, as noted above, the emission bands are broad and nearly structureless. In addition, the values of τ_{em} , k_r , and k_{nr} for the two complexes are in accord with the MLCT assignment. In contrast to the monometallic complexes, the photoluminescence properties of polymetallic complexes **477** and **478** are atypical for MLCT states. The luminescent excited state is relatively nonpolar, consistent with a $^3\pi,\pi^*$ assignment. The emission decay lifetimes of **477** and **478** are also in accord with the $^3\pi,\pi^*$ assignment.

The transient absorption spectra of **475** and **476** are quantitatively similar. They are characterized by strong ground-state bleaching and a relatively narrow and intense transient absorption band in the mid-visible region. It is believed that the TA spectra of **475** and **476** arise from the MLCT states. The spectrum of **477** features strong ground-state bleaching in the intraligand π,π^* absorption feature, in addition to a broad excited-state absorption band with $\lambda_{\text{max}} \approx 650 \text{ nm}$. The spectrum of **478** is similar, except that the excited-state absorption appears to extend into the near-IR region.

In complexes that contain a bpy ligand that is flanked by two e-T units (i.e., **476** and **478**) the $^3\text{MLCT}$ state is at a relatively lower energy. Second, the energy of the $^3\pi,\pi^*$ state is believed to decrease with the conjugation length of the thiophene-bipyridine oligomer ligands. Specifically, the energy of the $^3\pi,\pi^*$ state is believed to follow the order **475** (3 rings) > **476** (4 rings) > **477** (5 rings) > **478** (8 rings). An interesting result of these two effects is that there is a distinct crossover in the lowest excited state for **476** and **477**. Thus, in **476** the $^3\text{MLCT}$ state is stabilized relative to $^3\pi,\pi^*$ because the chromophoric bipyridine ligand is flanked by two e-T units. Thus, this complex features photophysics that are typical of a system having a lowest $^3\text{MLCT}$ state. By contrast, in **477** the $^3\text{MLCT}$ state is destabilized relative to the $^3\pi,\pi^*$ state because each of the two chromophoric bipyridine ligands feature only one e-T substituent. In addition, the $^3\pi,\pi^*$ state is at a slightly lower energy than in **476** because of increased conjugation. As a result, in **477** the energy of the $^3\pi,\pi^*$ state is well below that of $^3\text{MLCT}$, and the observed photophysics are dominated by the intraligand $^3\pi,\pi^*$ state. It is believed that

in **478** the $^3\pi,\pi^*$ and $^3\text{MLCT}$ states are at almost the same energy. On the basis of the observed photophysics, we conclude that $^3\pi,\pi^*$ is slightly below $^3\text{MLCT}$.

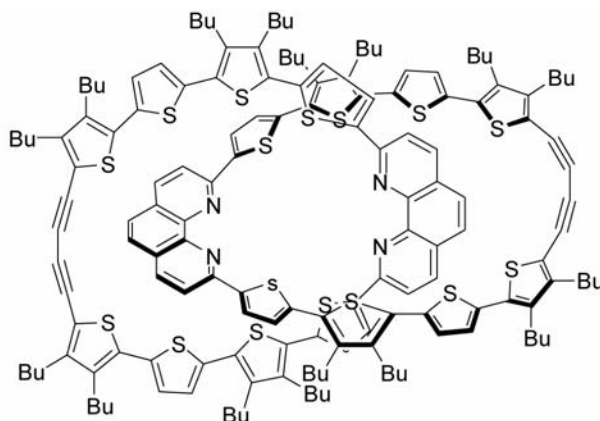
Nonradiative decay from the $^3\pi,\pi^*$ state is much faster in **477** than in **478**. This difference in decay rates arises because the dominant nonradiative decay pathway for the $^3\pi,\pi^*$ states in the two complexes is via (thermally activated) crossing to the $^3\text{MLCT}$ state.

Photoinduced electron transfer experiments were carried out using N,N' -dimethyl-4,4'-bipyridinium (MV^{2+}) as an oxidant. A key objective of these studies was to determine whether the quenching efficiency is strongly influenced by the nature of the lowest excited state. In each case, MV^{2+} was observed to quench the excited states. The k_q values generally increase with electron-transfer driving force. On the basis of this comparison, we conclude that the nature of the lowest excited state for the ruthenium-thiophene complexes does not have a strong influence on the rate of electron-transfer quenching. The spectra evolve in shape and a "long-time" spectrum is observed which persists long after excitation ($> 10 \mu\text{s}$). The species which give rise to the long-time spectrum decay according to equal concentration, second-order kinetics on a time scale of 20–50 μs .

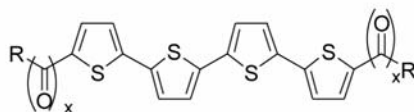
For **475**, the long-time spectrum is dominated by absorption at $\lambda_{\text{max}} = 395$ and 605 nm along with a weak ground-state bleach at $\lambda_{\text{min}} = 480$ nm. Clearly the absorption features that dominate the long-time difference spectrum for the **475**/ MV^{2+} system arise from MV^{+} , which is known to absorb at 395 and 605 nm. The structure is $[(\text{bpy})_2\text{Ru}^{\text{III}}(\text{bpy-e-T})]^{3+}$. The long-time spectrum observed for the **475**/ MV^{2+} system is distinct from that of **476**/ MV^{2+} . In particular, although the features for MV^{+} are present at 390 and 605 nm, the spectrum is dominated by a derivative-shaped bleach-absorption feature with $\lambda_{\text{min}} = 415$ nm and $\lambda_{\text{max}} = 465$ nm. On the basis of the relative intensity of the 465 nm absorption relative to the 395 nm MV^{+} absorption ($\Delta\epsilon \approx 30,000 \text{ M}^{-1} \text{ cm}^{-1}$), it is clear that the 465 nm band is very strong with $\Delta\epsilon \approx 50,000 \text{ M}^{-1} \text{ cm}^{-1}$. It is believed that the structure of the oxidized complex is $[(\text{bpy})_2\text{Ru}^{\text{III}}(\text{T-e-bpy-e-T})]^{3+}$. The long-time difference spectra of the **477**/ MV^{2+} and **478**/ MV^{2+} systems are very similar to that of **475**.

Oligothiophene derivatives were used to obtain catenanes such as **479** (07AGE363).

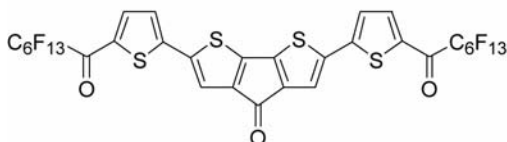
The synthesis and OFET properties of new carbonyl-functionalized quaterthiophenes **480–484** exhibiting improved stability and unique charge transport characteristics were reported (04JA13859; 05JA1348).

**479**

λ_{max} 413 nm
 $\lambda_{\text{max}}^{\text{F}}$ 565, 602 nm
 Φ_{F} 0.02



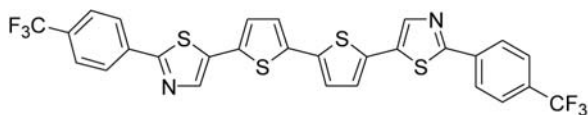
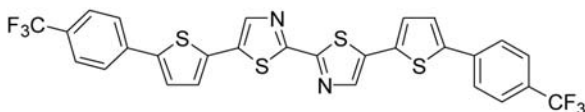
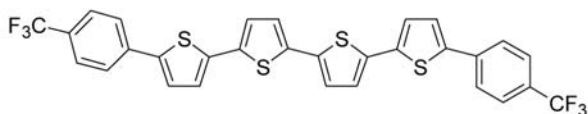
480: X = 1, R = C₆H₁₃
481: X = 1, R = C₆F₁₃
482: X = 0, R = C₆H₁₃
483: X = 0, R = C₆F₁₃

**484**

UV/Vis and photoluminescence data indicate that the C=O groups are effectively conjugated with the 4T core and give rise to substantially red-shifted absorption and emission maxima ($\lambda_{\text{abs}}/\lambda_{\text{F}}$ (nm): **480** 430/530; **481** 465/550; **484** 545/615) and HOMO–LUMO optical gap reductions (E_{g} (eV): **480** 2.6; **481** 2.4; **484** 2.2) versus quaterthiophene ($\lambda_{\text{abs}}/\lambda_{\text{em}}$: 391/450 nm; E_{g} = 2.8 eV). All of the new oligothiophenes exhibit very high electron mobilities (μ_{e}) in vacuum. **480** films also exhibit relatively large hole mobilities (μ_{h} up to 0.01 cm² V^{−1} s^{−1} at T_{D} = 70°C) at all deposition temperatures. **480** was the first organic conductor exhibiting unoptimized $\mu_{\text{e}}/\mu_{\text{h}}$ values as high as ~0.1/0.01 cm² V^{−1} s^{−1}. From the transfer plots, very high $I_{\text{on}}/I_{\text{off}}$ ratios are observed for electrons: > 10⁷. Maximum current gains for

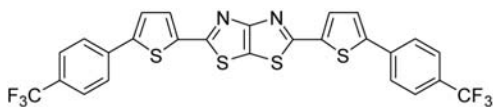
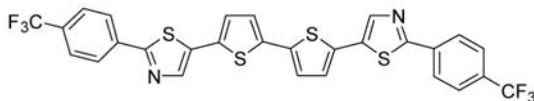
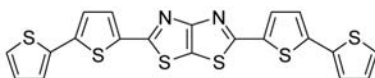
holes are $> 10^8$ for **480**. **484**-based devices can be cycled more than 20 times in air without degradation.

The HOMO–LUMO gaps obtained from the absorption onsets are 2.44 eV for **485**, 2.42 eV for **486**, and 2.45 eV for **487** (05JA14996).

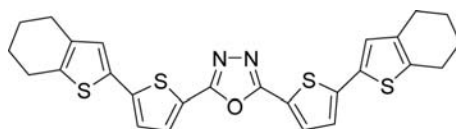
**485****486****487**

The thiazole derivative **485** also showed good n-type performance. The mobility of $0.085 \text{ cm}^2 \text{ V}^{-1} \text{ s}^{-1}$ is about three times as high as that of the quaterthiophene derivative **487**, indicating that the 2-(4-trifluoromethylphenyl)thiazole unit is more effective for electron transport than 2-(4-trifluoromethylphenyl)thiophene unit. Thienyl pyrrole derivatives showed absorption maximum at 321–384.5 nm and showed nonlinear optical properties (06OL3681). Nonlinear optical chromophores showing thiophene-benzothiazole units are been prepared (absorption bands in the range 343–417 nm) (04TL2825; 06EJO3938).

Compounds **488–490** exhibited strong photoluminescence in the solid state (λ_{max} **488**: 554 nm; **489**: 546 nm) (04MI1787; 05JA5336). The emission maxima are observed at longer wavelengths than those in solution (67–87 nm red shift), indicating the presence of strong intermolecular interaction in the solid state. **488** and **489** exhibited high n-type performances. The electron mobilities of the film **488** calculated in the saturation regime were found to be $0.12\text{--}0.30 \text{ cm}^2 \text{ V}^{-1} \text{ s}^{-1}$ depending on the substrate temperature. The mobilities are in a class with a high value. The on/off ratios were high values of $10^5\text{--}10^6$. The thiophene derivative **490** also showed high n-type FET performances. The mobility is $0.18 \text{ cm}^2 \text{ V}^{-1} \text{ s}^{-1}$ at 50°C , indicating the very effective nature of the trifluoromethylphenyl group.

**488****489****490**

Thienyl substituted 3,4-oxadiazole derivatives have been described (98CEJ2211). **491** showed an absorption peak at 402 nm and an emission at 453 and 477 nm (Φ_F 0.62).

**491**

13.2 Polythiophenes

Poly- and oligo(α -thiophene) derivatives are important compounds for biological studies, electronic semiconducting materials, nonlinear optical materials, and highly ordered molecular assemblies.

From the electronic perspective, poly(α -thiophene) is an excellent semiconducting material when doped. While poly(α -thiophene) itself is intractable and therefore not processable, the poly(3-alkyl- α -thiophene)s are soluble and still exhibit conductivities comparable to the unsubstituted derivatives.

The first electronic transition of undoped polythiophene (PT) (which strongly depends on the structure) lies between 300 and 500 nm (molar extinction coefficient, $\epsilon \sim 10,000 \text{ M}^{-1} \text{ cm}^{-1}$) (87JPC6706; 87MM212; 87SM(22)79; 89SM(28)C435; 93JOC904; 99JPC(B)7771). Upon doping, it undergoes a dramatic bathochromic shift transforming into the so-called “conducting” band, which tails from the visible to the deep-IR region.

Terthiophene polymers showed absorption peaks in the range 430–463 nm in toluene and 438–550 nm in the solid state (05CM1381). UV/Vis spectrum of P3HT (poly 3-hexylthiophene) showed a broad absorption with a maximum at ca. 435 nm, indicative of extensive π -electron delocalization. Regular polymer showed absorption at 449 nm (91MM4834; 95JA233; 98JA2047). Regioregular poly(3-alkylthiophene)s showed absorption bands in the range 448–456 nm in solution and from 527 to 558 nm in films (05SM(148)169). The film of poly(3',4'-dibutyl-2,2':5'2''-terthiophene) showed an absorption maximum at 488 nm (94CM401). Poly(3,4-dihexylthiophene) showed an absorption at 315 nm (90JCS(CC)273). Poly(3,3'''-diakylquaterthiophene) was obtained as nanoparticles by using ultrasonic agitation with peaks at 510, 545, and 585 nm in thin film (05AM1141). In contrast to undoped PTs, which exhibit reasonably strong luminescence in the visible region of the spectrum, the doped PTs are not luminescent, although partially doped PTs have been used in light-emitting electrochemical cells (LECs), and doped poly(3,4-ethylenedioxythiophene) (PEDOT) is routinely used as an electrode for PLEDs (mostly as a second layer on ITO-covered glass). Poly(thieno[3,4-*b*]thiophene) film showed a peak at 804 nm (01MM5746).

Usually, PTs emit orange-red light, consistent with their bandgap of ca. 2 eV. A film of polythiophene exhibited well-defined peaks at 2.01, 1.94, 1.84, 1.70, and 1.54 eV (90SM(38)1). The photoluminescence relaxation processes were affected by the film thickness and the polymerization conditions (95SM(69)335). The film of poly(3',4'-dibutyl-2,2':5'2''-terthiophene) showed emission at 557–620 nm (94CM401). Often the luminescence efficiency of PTs in the solid state is relatively low (87SM(21)41; 89SM(28)C293; 89SM(28)C349; 89SM(28)C393; 95CPL(241)89; 96MI1763). Poly(3-hexylthiophene), irradiated at 250 and 600 nm, showed an emission at 826 nm, assigned to the phosphorescence (94AM325). A possible explanation is a tendency of strong interchain interactions (especially for low-molecular-weight oligomers). A theoretical explanation of the electronic structure of polythiophene derivatives appeared (87SM(21)149; 05JPC(A)7197; 05JPC(B)3126). Polythiophene showed also nonlinear optical properties (89SM(28)C323).

Whereas in solution the photoluminescence efficiency (Φ_F) of poly(3-alkylthiophenes) (PATs) is ~30–40%, it drastically drops to 1–4% and lower in the solid state due to the increased contribution of nonradiative decay via interchain interactions and ISC caused by the heavy-atom effect of sulfur (97MM4608). Optoelectronic devices of this type of compounds have been studied (98SCI(280)1741; 06SM(156)1241). Fibers of poly(3-hexylthiophene) for photovoltaic applications have been described (07MI1377). Poly(3-octylthiophene) showed a TTA band at 800 nm (96JPC15309). The photophysical properties of some alkyl and aryl polythiophenes have been studied (03JCP(118)1550). The absorption maximum of poly(3-octylthiophene) is at 438 nm, while the fluorescence was

observed at 576 nm (Φ_F 0.27, τ_F 0.2 ns, k_F 1.35 ns⁻¹). The triplet quantum yield was 0.21 (τ_T 8 μ s, k_{ISC} 1.05 ns⁻¹) while the internal conversion quantum yield was 0.52. In another work, 500 ps for the triplet state lifetime and k_{ISC} of 1.2 ns were found (95JCP(103)5102).

The crystalline composites obtained between poly(3-alkylthiophene) and polystyrene showed an enhanced conductivity (07MM6579). The preparation of regioregular poly(3-alkylthiophene) and perylene diimide derivatives composites have been reported (06MI384). The photoluminescence spectra of this type of composites exhibit a significant photoluminescence quenching of the perylene diimide derivative. This result implies that the light absorbed by the perylene diimide units could also contribute to the generation of current at the photovoltaic device.

Poly(3,3'-dimethyl-2,2'-bithiophene) shows an absorption maximum at 417 nm (90MM1268). Poly(3-phenylthiophene), on the contrary, showed absorption at 425–432 nm (91MM2694). Polythienothiophene and polydithienothiophene showed absorption maxima at 2.83 and 2.67 eV, while the fluorescence maxima were at 1.95 and 1.92 eV, respectively (87SM(18)177).

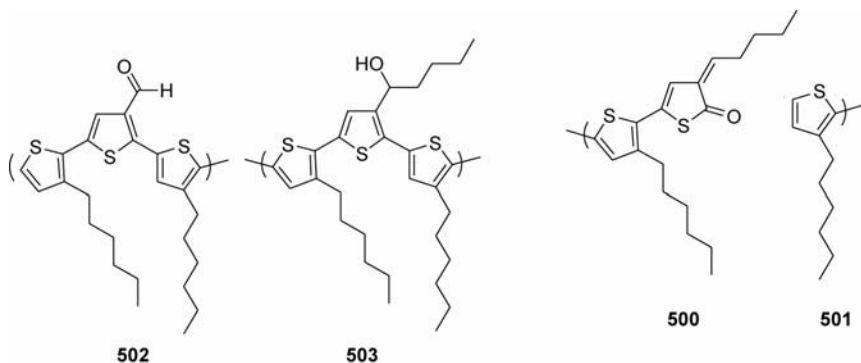
In solution, ISC from the singlet excited state is efficient, leading to triplets from which radical cations are produced in the presence of an electron acceptor. In solid films, where neighboring chains may act as an electron acceptor, radical cations can give rise to polarons and bipolarons. Poly(3-alkylthiophenes) undergo photochemical reactions including photobleaching, chain scission, and cross-linking (91MM4834; 93MM2954; 93SM(57)3587; 97JA4518). Irradiation of the polymer in air-saturated CHCl₃ results in a blue shift in λ_{max} and a decrease in the optical density. Also fluorescence was affected. Solutions and film of P3HT fluoresce at 548 nm if random and at 569 nm if regular (91MM4834; 95JA233) with a quantum yield of 0.14 in solution and 0.02 for the film. In the presence of oxygen, quantum yields are 0.07 and 0.00017, respectively. Photobleaching is attributed to disruption and shortening of the π -conjugated segments. Concurrent with photobleaching is a decrease in molecular weight of the polymer (photochain scission). Number-average molecular weights of pristine polymer were 8500. Following photolysis M_n decreased to values as low as 1400. The author observed the formation of relatively strong absorption bands in the range 3700–3200 cm⁻¹ which are characteristic of hydroxyl and hydroperoxy functionality; the evolution of a strong and complex band at 1800–1660 cm⁻¹ characteristic of various keto and/or aldehydic group, the formation of strong bands in the region 1260–1000 cm⁻¹ which indicate sulfine residues C=S=O; the decrease of the aliphatic C-H stretching peak in the region 2900 cm⁻¹ due to loss of the alkyl side chain; a decrease of the absorption bands characteristic of interannular stretching modes (1460 cm⁻¹) and disappearance of the aromatic C-H stretch and C-H out-of-plane deformation at 3055 and 823 cm⁻¹, respectively. This is attributed to disruption of the conjugated system; the formation of a signal at 3.75 ppm

and a weak broad signal at ca. 7.7 ppm (^1H NMR) assigned to CH(OH) and hydroperoxy proton, respectively; a decrease in the aliphatic proton resonance signals, the presence of signals attributable to α,β -unsaturated aldehydic protons; a decrease in aromatic proton signal indicating ring opening or loss of aromaticity.

Upon irradiation of the polymer in the presence of anthracene, the authors observed the loss of anthracene and the buildup of anthraquinone. These results provide strong arguments that photosensitized $^1\text{O}_2$ is largely responsible for loss of π -conjugation and photobleaching of the polymer.

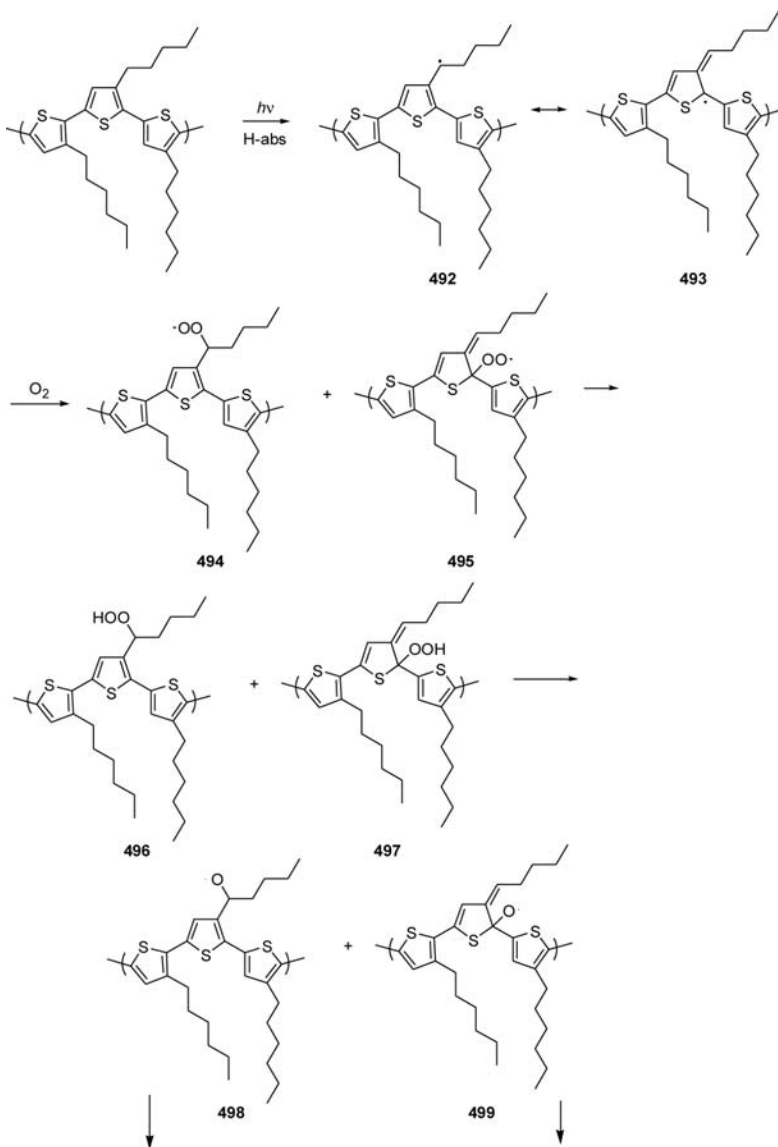
Reaction of P3HT with singlet oxygen was monitored over a period of 16 h. The OD of the solution at 435 nm decreased by ca. 30%, whereas M_n of the polymer remained constant. Clearly chain scission does not originate from reaction with $^1\text{O}_2$ in contrast to photobleaching. No hydroxyl functionality was observed.

Since singlet oxygen alone is not responsible for chain scission and the products of reaction between singlet oxygen and thiophene are photolitically inert, a classical photooxidative route has been proposed (Scheme 27). Photooxidation of polyolefins is initiated by the photosensitization of free radicals by impurities such as residual transition-metal catalysts. When O_2 was vigorously removed from solution, no photochemistry or photochain scission was observed even after 20 h of photolysis through a 300 nm cut-off filter with a 150 W Hg lamp. These trends strongly point to a photooxidative free-radical pathway in which the initial step is photolysis of FeX_3 . The resulting P3HT radical is resonance stabilized by the π -system to yield radicals **492** and **493**. Radicals **492** and **493** rapidly react with oxygen to produce peroxides **494** and **495** which can abstract a hydrogen from the polymer chain or solvent to give hydroperoxides **496** and **497**. Cleavage of the hydroperoxide group by light results in alkoxy radicals **498** and **499**. Fe^{2+} produced from previously described reaction might also take part in the cleavage of the OOH groups. In this mechanism,



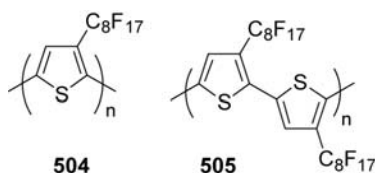
Scheme 27

only rearrangement of the alkoxy radical **499** can cause chain scission with the formation of ketones **500** and thienyl radical **501**. Alkoxy radical **498**, on the other hand, can undergo several of the following possibilities: (i) β -scission to yield an aldehyde **502** and volatile hydrocarbons; (ii) hydrogen abstraction to give a secondary alcohol **503**, (iii) radical coupling to form a cross-linked polymer.



On the contrary, films of poly(3-octylthiophene) were stable under UV irradiation (95SM(73)195). A photodegradation study of poly[2-(3-thienyl)ethoxy-4-butylsulfonate] showed that the singlet excited state produces characteristic absorption at 770 nm with a life time of 22 ps. The triplet state exhibits a broad absorption in the 650–800 nm region and has a lifetime of 18.7 μ s in deaerated water. The excited triplet is readily quenched by oxygen. The high photochemical reactivity of the triplet with oxygen is responsible for the photodegradation (09JPC(C)11507).

The direct attachment of perfluoroalkyl substituents to the backbone would provide an opportunity to influence the electronic structure of the π -system, with the potential to prepare n-dopable materials **504** and **505** (94MM1847; 04AM180).



The conjugation length of poly(3-alkylthiophene)s can be determined from the absorption maximum in the electronic spectrum. Whereas regioregular (i.e., head-tail) poly(3-octylthiophene) (POT) displays a maximum at 442 nm in CHCl_3 /Freon-113 solution, the absorbance maximum of **504** is blue shifted by 114 to 328 nm. This blue shift could arise from a particularly low molecular weight.

The electronic effect of perfluoroalkyl substituents on the absorption spectra of arenes is relatively small (e.g., λ_{max} 3-perfluorooctylthiophene = 229 nm; 3-octylthiophene = 235 nm). Thus, the anomalously low absorption maximum of **504** is the effect of twisting around the backbone. It is apparent that the difference in size of the side chains is sufficiently large to cause twisting of the conjugated backbone of **504** due to steric interactions between the perfluoroalkyl substituents and the adjacent repeat unit. **504** exhibits green fluorescence (λ_{max} = 512 nm) in solution with a maximum blue shifted by 58 nm relative to POT (570 nm). Accordingly, **504** shows a Stokes shift of ca. 1.4 eV (186 nm) compared to only 0.6 eV (126 nm) for POT.

Long-lived photoluminescence, at ~ 826 nm, is reported ($\tau \sim 15$ μ s) for thin films of the processable, π -conjugated polymer, poly(3-hexylthiophene) (93JA8447). Excitation of the $\pi-\pi^*$ transition with 518 nm light ($S_0 \rightarrow S_1$) yields only very weak luminescence of 826-nm light, even at 18 K. The emission is enhanced, to point where it can be observed at room temperature, when the excitation wavelength is 250 nm, but it is completely quenched by oxygen. Prompt fluorescence decays within

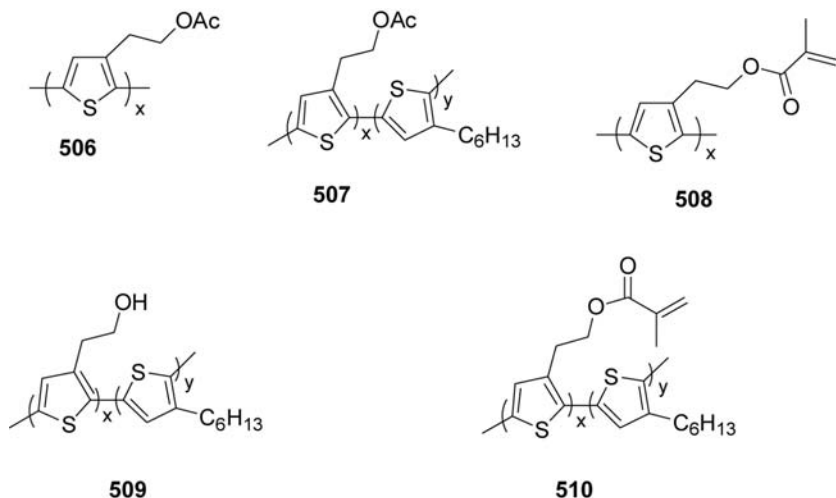
400 ps. When the sample is cooled to 18 K and data collection delayed by 30 μ s following the incident light pulse, a weak, long-wavelength emission is observed at \sim 826 nm. Irradiation with 250-nm light results in localized excitation of individual thienyl rings and enhances emission at 826 nm, compared to direct excitation of the π - π^* band. Furthermore, fluorescence of the π - π^* transition was surprisingly absent, indicating the existence of a decay manifold which can compete with internal conversion to S_1 .

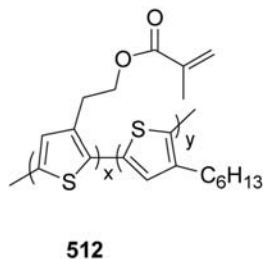
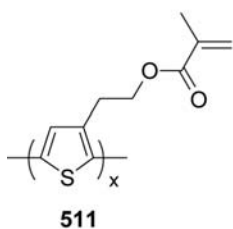
Photoluminescence at 826 nm is attributed to a radiative, spin-forbidden $T_1 \rightarrow S_0$ transition, that is, phosphorescence.

Population of T_1 via ISC from S_1 is inefficient. Phosphorescence is, therefore, extremely weak when $S_0 \rightarrow S_1$ excitation of the polymer is achieved with visible light. Excitation to a higher level singlet state (S_i) using 250-nm light, for example, affords an alternative route to T_1 . From the observation that phosphorescence increases and fluorescence decreases when λ_{ex} is changed from 518 to 250 nm, upper excited-state transfer (UEST) is inferred, a process which facilitates ISC from higher lying singlets to higher lying triplets (T_j).

A thin film of soluble poly(3-hexylthiophene) is irradiated with UV-Vis light through a photomask (91CM1003). The exposed regions undergo a photochemical process which results in insolubility, whereas the unexposed regions remain soluble. Dissolution of unexposed polymer leaves a negative image of the photomask.

The photoimaging process occurs via a photooxidation process photo-initiated by residual transition metal impurities in the presence of oxygen and terminated by coupling of polymer-bound radicals. Photoinduced cross-linking thus requires generation of a critical, and large, concentration of free radicals.



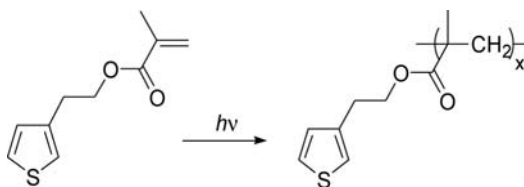


The vinyl functionality attached to the 3-position of the thienyl ring should be an excellent candidate for radical-induced cross-linking of these systems since polythiophenes are relatively inert to free radicals (95MM4608). Two different synthetic routes were used to achieve the target polymers. One of the routes leads to polymers which adhere very strongly to polar substrates. The photoluminescence properties of some of these compounds have been studied (95SM(69)377).

Spectra of the films exhibited a red shift in λ_{\max} compared to polymer solutions, indicating increased coplanarity and conjugation in the solid state (Table 11).

Polymers obtained from electropolymerization of 3-(benzyloxyethyl) thiophene have been described. They showed an absorption band at ca. 520 nm (90JCS(CC)414).

Exposure of the monomer MET to ambient lighting produced a gum-like polymer, poly[(3-thienyl)ethyl methacrylate] (Scheme 28).



Scheme 28

Table 11. Spectroscopic properties of selected compounds

Polymer	λ_{\max} (nm) Solution	Film
507	432	468
509	430	468
510	434	464
506	414	438
508	414	438
512	426	458
511	422	434

The UV/Vis spectrum of the solution exhibited a λ_{max} at 250 nm and a shoulder at 304 nm. The monomer possessed a single absorption peak at 250 nm.

The ca. 80 nm thick film was irradiated with the 313 nm band interference filter. A decrease in the vinylidene stretch at 1638 cm^{-1} was observed in conjunction with a shift in the carbonyl stretch toward higher frequency. Lithographic data were determined from gel dose curves made by plotting the residual thickness of the polymer image after solvent development as a function of the energy adsorbed by the polymer. This plot clearly shows that **512** can be cross-linked with greater efficiency than P3HT due to the presence of methacrylate side chain. The trend in conductivity indicates that higher conductivities are achieved with increasing 3HT content.

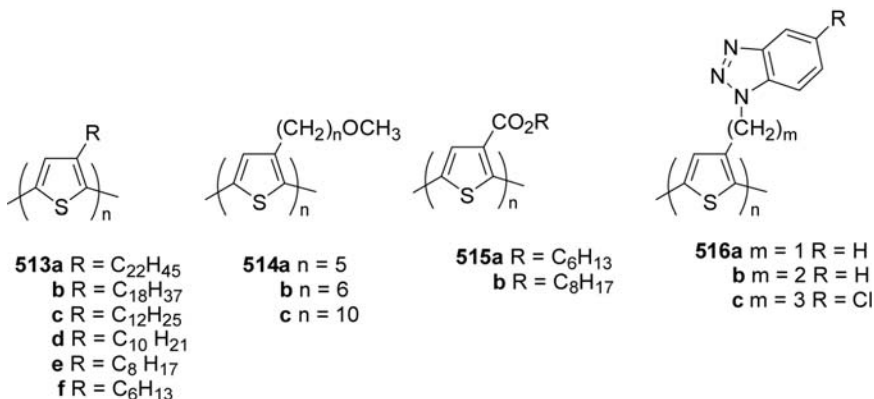
The wavelength of maximum absorption of poly(3-hexylthiophene) in the visible region was 500 nm. The absorption maximum is red shifted by ca. 60 nm compared to the same polymer dissolved in organic solvent due to restricted rotation of thienyl ring in the solid state and hence a greater degree of π -conjugation. Prior to irradiation the films were soluble in toluene. After 15 s of irradiation, the films were rendered totally insoluble in toluene. Neutral irradiated and preirradiated polymer films were non-conducting. Upon oxidative doping by immersion of the films into an anhydrous solution of nitrosonium tetrafluoroborate, the films turned blue and were found to be electronically conductive.

When the irradiation time was kept short ($< 1\text{ min}$), the change in electronic conductivity was negligible. This observation illustrates that polymer films can be photochemically insolubilized yet still exhibit high conductivity upon chemical oxidation. When long irradiation times were employed, exposed regions showed a distinct discoloration due to photochemical bleaching. When the irradiation time was short, the color contrast of the relief image was barely visible yet unexposed regions rapidly dissolved when the irradiated polymer/substrate was immersed in toluene, while exposed polymer did not. The remaining polymer appeared yellow when immersed in toluene but formed a negative red image of the photomask upon drying. Upon immersion into an acetonitrile solution of nitrosonium tetrafluoroborate, the pattern immediately turned blue.

3-Alkyloxythiophene derivatives can be connected to an azobenzene moiety and the polymer showed nonlinear optical properties (03SM(138) 409; 04MI2117; 05MI2360).

Π Conjugation alone cannot be relied upon to significantly enhance the optical nonlinearities. The conformational effects and the role of the substituents so that understanding of the molecular structure-property relation can be improved have been studied (89JPC7916). In the case of the thiophene oligomers, a rapid increase in the γ value (large microscopic nonlinearity) as a function of N is found.

PT LEDs were first reported by Ohmori et al. in 1991 (91MI1938; 91MI605; 95MM5706), who described PTs as red-orange-light-emitting materials (peak emission at 640 nm for **513a**) in single-layer ITO/PT/Mg:In devices.



It was shown that the luminescence efficiency depends on the length of the alkyl chain, showing about a fourfold increase in EL efficiency for PT **513a** with R = C₂₂H₄₅ compared to **513c** with R = C₁₂H₂₅ (93SM(55–57)4168). Polymers **514a,b** showed high (for PTs) photoluminescence quantum yields in solution (38–45% in THF); however, these quantum yields decreased in the films (00SM(111–112)187). The emission maxima for the Cu-prepared polymers **515a,b** were red shifted compared to the Ni-prepared polymers (by 13–15 nm in solution and 25–30 nm in films) (Table 12).

The presence of a carboxylate function increased air stability of the polythiophene film (λ_{max} 489 nm) (03S2255; 05CM4892).

Polymers **516b,c** endowed with longer tethers, possessed improved solubilities as well as high molecular weights and thermal stabilities.

They showed pronounced blue shifts at 50–70 nm in absorption and emission comparable to P3OT (**513e**) [01MM2522].

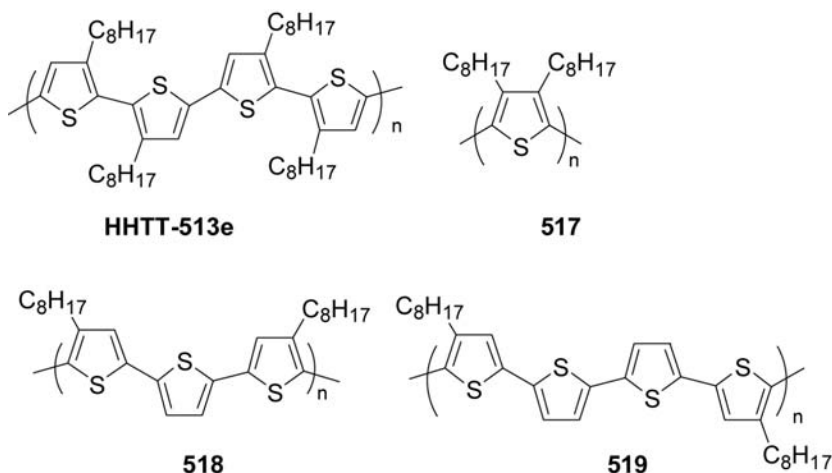
An increased planarization of regioregular HT PT facilitated aggregation, which results in a decrease of Φ_{F} emission efficiency in the solid state (from 0.8% for 50% HT to 0.2% for 80% HT).

Its regioregular HH/TT-coupled isomer **HHTT-513d** [90POLLDG1379] showed large blue shifts in its absorption, fluorescence, and electroluminescence spectra; in addition, it emits green light with one order-of-magnitude higher emission ($\Phi_{\text{F}}^{\text{film}} = 11 \pm 0.1\%$) and two orders-of-magnitude higher EL ($\Phi_{\text{EL}}^{\text{int}} = 0.001$ and 0.25–0.30%, respectively), but requires a higher turn-on voltage [98MI6279].

Table 12. Properties of PATs (93MM4457; 95MM5706; 95SM(71)2191; 96MI1763; 99MI151; 99MI2155; 00MI(111–112)187; 01MM2522)

Polymer (method)	λ_{\max} (nm) Solution (solvent)	Film	λ_{\max}^F (nm) Solution (solvent)	Film
513e (FeCl ₃)		500		655
513f (50% HT)	413 (CHCl ₃)	420	567, 600	608
513f (60% HT)	420 (CHCl ₃)	432	572, 600	608, 643
513f (70% HT)		456		650
513f (80% HT)	440 (CHCl ₃)	518	580, 614	670, 714
514a (Ni)	451 (toluene)	550		660, 730
514b (Ni)	450 (toluene)	535		670, 730
514c (Ni)	448 (toluene)	530		
514c (Ni)		470		660
515a (Cu)	423 (THF)	447	570 (THF)	620
515b (Cu)	430 (THF)	450	568 (THF)	630
515a (Ni)	408 (THF)	429	555 (THF)	595
515b (Ni)	408 (THF)	430	555 (THF)	600
515a	410 (THF)	434		600
515b	439 (THF)	460		610
HHTT-515a	387 (THF)	377		590
HHTT-515b	389 (THF)	381		600
516b (FeCl ₃)		444		580
516c (FeCl ₃)		446		588

In regioregular **HHTT-515a,b** blue shifts in photoluminescence and EL were much less pronounced (10–15 nm) [99MI2155].



Hadziioannou and coworkers synthesized a number of regioregular alkylated polymers **HHTT-513e** and **517–519** and demonstrated PL and

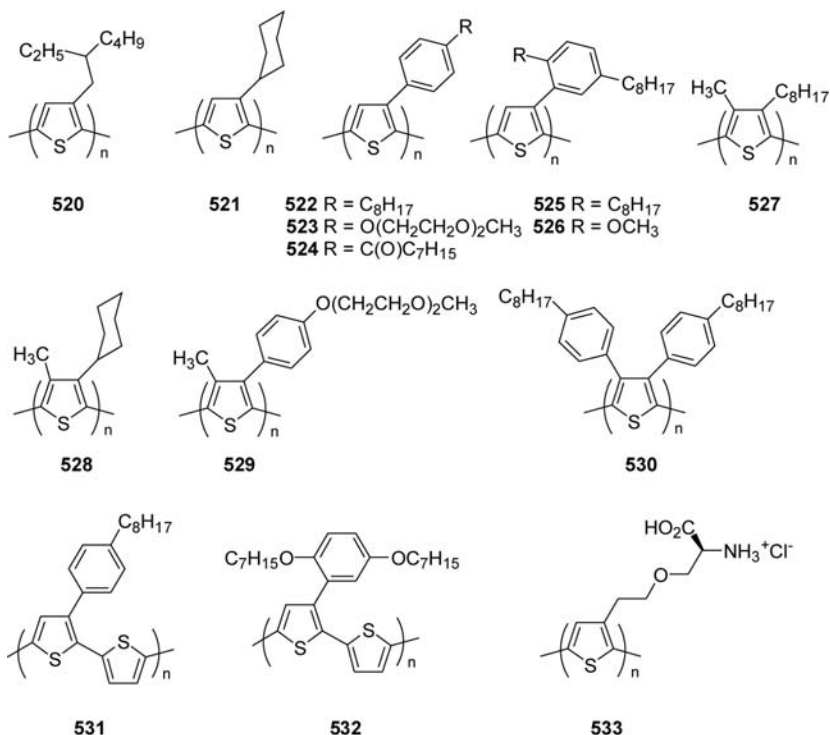
EL color tuning through a variation of the length of the coplanar blocks between the HH links (94AM132). They also found blue shifts of >100 nm in absorption, photoluminescence, and electroluminescence spectra, with decreasing I_{\max} in the sequence **519** > **518** > **HHTT-513e** > **517**, that is, an increasing HOMO–LUMO gap with increasing steric hindrance.

A large number of PTs with emissions covering the full visible region, i.e., from blue to red and into the near-IR (NIR), have been reported. EL color changes were achieved by structural variations in PT side chains, as well as by controlling the regioregularity. Such wide variations of the emission color in a homopolymer are remarkable and cannot be achieved in other conjugated polymers (except via copolymerization approaches). To understand the wide range of colors available from PTs, it is necessary to look at the underlying phenomena. The PT emission color directly depends on the effective conjugation length determined by the twist angle between thiophene units. Poly(3,3''-dialkyl-terthiophene) derivatives showed a broad absorption at ca. 470 nm, while, in thin film, absorptions at ca. 510, 540, and 583 nm were observed, showing a higher structural order in the solid state (05CM221).

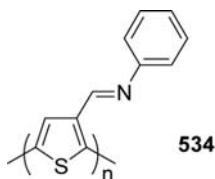
Table 13. Properties of electroluminescent PTs via conjugation control (93AM721; 95MM7525; 95MM8102; 3; 99MI1933)

Polymer	M_n (g/mol)	λ_{abs} Film (nm)	λ_{PL} Film (nm)	Φ_{PL} (CHCl ₃) (%)	Φ_{PL} Film (%)
513e	35,000	506		27	4
520		464	593	26	9
521	6000	405	574	37	9
522	8000	482	677	18	9
	23,000	485	670		
523	7800	476	616	20	8
524	9400	454	638	14	10
525	36,000	494	606	37	24
		532	659		
		577	720		
526	46,000	470	590	29	11
527	42,000	326	468	4.6	2.2
528	26,000	303	442	1.3	0.8
529	16,000	380	532	3.8	2.8
530	21,000	346	504	1.1	1.0
531	9000	513	627	27	5
532	24,500	510	598	31	4
547a	2300	332	428		
547b	3400	342	429		
			470		
			520		
547c	5000	384	524		
547d	6800	389	470, 525		
548a	4300	443	605		
548b	5600	451	620		

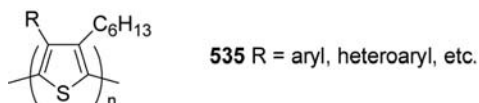
In the highly regioregular polymer **522**, in its pristine amorphous form, the absorption maximum of spin-cast films is 493 nm (2.86 eV) (94MM6503; 01JPC(B)7624). On treating the films with chloroform vapor, the maximum was shifted to 602 nm (2.06 eV), and the spectrum showed a fine vibronic structure with $\Delta E = 0.19$ eV, typical of a more-planar ordered conformation.



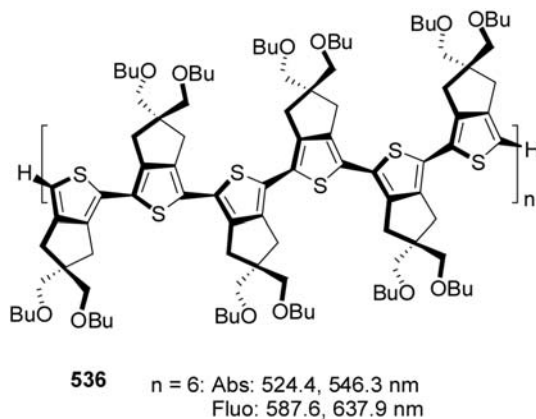
Blends between thiazole yellow and the polythiophene **534** have been reported (07MI275). The polythiophene showed an absorption band at 520 nm. Electrical and photovoltaic properties have been studied.



Functionalization with bulky aryl substituents (**535**) hindered the inter-chain interactions and allowed a substantial increase of Φ_{PL} in the films from 1.6% to 13–22% (01MM3130).



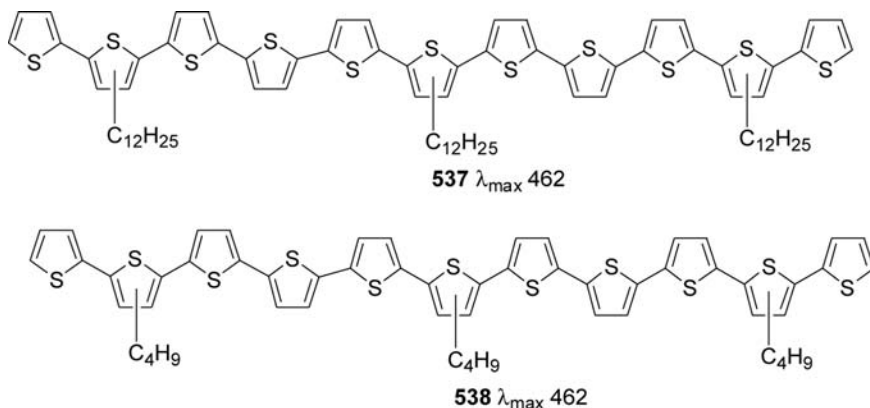
It was demonstrated that blends of 3- and 3,4-substituted PT derivatives of different bandgaps gave rise to a voltage-controlled variable-color light source (94NAT(372)444). When a relatively low voltage was applied to the polymer blend PLED, the low-bandgap polymer started to emit first, followed by higher bandgap emitters as the voltage increased. PMMA (poly(methyl methacrylate)) was used in this case to diminish the energy transfer from the high bandgap to the low bandgap polymer (**527/521/531**). Several other inert polymer matrixes (polystyrene, polycarbonate, poly(vinyl chloride), poly(2,6-dimethyl-1,4-phenyleneoxide)) showed similar effects (97MI27). Thus, efficient white-light emission of the PLED ITO/**531**/PBD/Al ($\Phi_{EL}^{ext} = 0.3\%$ at 7 V) consisted of blue (410 nm), green (530 nm), and red-orange (620 nm) bands.



Whereas the first and the last EL peaks are due to EL from PBD and the PT layers, respectively, the green-light emission probably originates from a transition between electronic states in the PBD layer and hole states in the polymer layer (94APPLAB(76)7530). It was demonstrated that even small additions of PTs can improve the device performance. $\Phi_{\text{EL}}^{\text{ex}}$ of red-light-emitting ITO/P3HT (513f)/MEH-PPV/Ca diodes (MEH-PPV = poly(2-methoxy-5-(2-ethylhexyloxy)-*p*-phenylene vinylene)) initially increased with P3HT content and went through a maximum at 1 wt% P3HT with $\Phi_{\text{EL}} = 1.7\%$ (95SM(72)249).

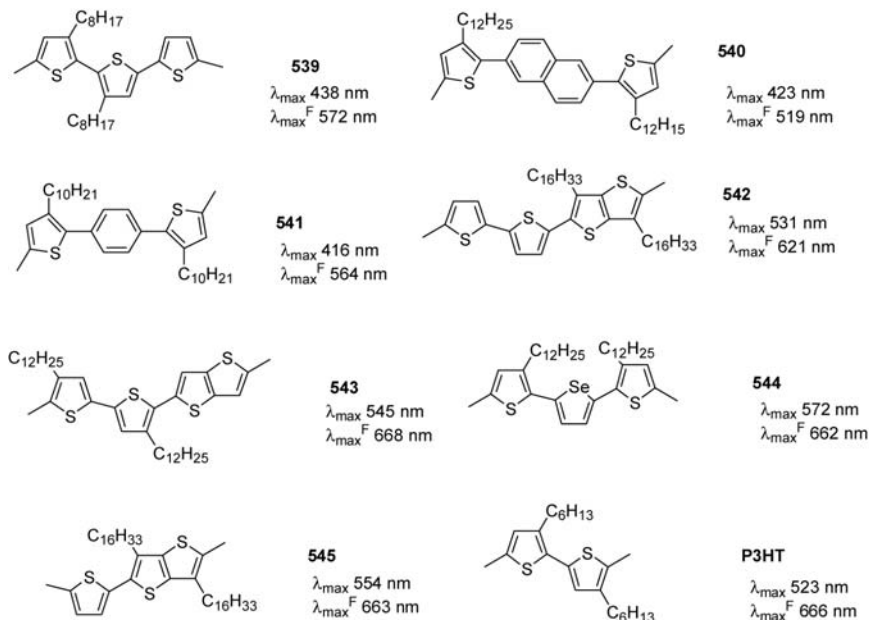
Regioregular poly(3,4-cycloalkylthiophene) derivatives, such as 536, have been reported (03JA5286).

The wavelength of the maximum absorbance of CHCl_3 solutions of the oligothiophenes, being a rather direct measure of the conjugation length, increases steadily with chain length and seems to approach saturation (at 11 units) without actually reaching it (91JA5887; 92AM107; 92AM490; 95AGE303). Absorption spectra of solid films of both 537 and 538 and poly(3-alkylthiophenes) (430–440 nm), however, are much alike, with maxima at higher wavelength (520 nm), indicating a much larger conjugation length in the solid state.



The amorphous poly(541), poly(540), and poly(539) pristine films exhibited structureless absorption bands at 416, 423, and 438 nm, respectively, which are significantly blue shifted compared with the lowest vibrational band of P3HT (~ 640 nm) (04MM6306; 07AM833; 08JA3030). On the other hand, the more crystalline poly(543), poly(542), poly(545), and poly(544) pristine films exhibited more structured, red-shifted absorption bands with a shoulder or a vibrational band corresponding to the lowest vibronic transition at ~ 635 , 612, 633, and ~ 640 nm, respectively, which is more comparable to that of

P3HT (~ 640 nm). The vibrational structure observed is characteristic of ordered polythiophene films and is consistent with interplanar π -stacking of conjugated planes.



Photoluminescence intensity of the amorphous polymers was generally much larger than that of the more crystalline polymers. The energy level of the lowest singlet excited state E_S was evaluated to be 2.5–2.7 eV for the amorphous polymer pristine films, and ~ 2.0 eV for the more crystalline polymers. The Stokes shifts were also observed to be much larger for the amorphous polymer films compared with those of the more crystalline polymer films. This indicates a larger structural relaxation of the amorphous polymers following photoexcitation.

Poly(**541**) pristine films of this polymer exhibited a photoinduced transient absorption band at around 700 nm. The transient signal decayed monoexponentially with a lifetime of 7 μs under Ar atmosphere, accelerating to ~ 1.5 μs under O_2 atmosphere. These transient bands are assigned to $T_1 \rightarrow T_n$ transitions of polymer triplet excitons ($^3\text{P}^*$) formed in the amorphous polymer pristine films.

The poly(**542**) pristine film, representative of the more crystalline polymers, exhibited a broader transient photoinduced absorption band around 900–1000 nm. This transient optical density decayed rapidly on the

hundreds of nanoseconds time scale down to $<10^{-15}$ Δ OD within 1 μ s. This fast transient was not quenched under O₂ atmosphere. These observations suggest that this absorption transient should not be assigned to triplet excitons. Poly(benzo[1,2-*b*:4,5-*b'*]dithiophene) derivatives have been synthesized. They showed absorption bands at 446 and 469 nm and emission at 545 nm (633 nm in the solid state) (06CM3237).

A similar absorption bands have been reported for a regioregular P3HT pristine film by continuous wave photoinduced absorption (PIA) measurements at 10 K. The PIA spectrum exhibits an absorption peak around 990 nm and was assigned to localized polarons in the disordered portions of the film. Similar rapid decays were observed for the other polythiophene pristine films. Thus, these rapid decays are ascribed to the charge recombination of polaron pairs formed in the pristine film.

The inclusion of 5 wt% PCBM [1-(3-methoxycarbonyl)propyl-1-phenyl-[6,6]C₆₁] in the spin-coating solutions resulted in efficient polymer emission quenching for all the polythiophenes studied. The transient absorption spectra of the amorphous poly(541)/PCBM blend film. At 10 μ s exhibited an absorption peak around 700 nm, similar to that observed for the poly(541) pristine film. The shape of the transient spectrum varied with time, with the absorption peak shifting from 700 nm at 10 μ s to \sim 900 nm for time delays \geq 100 μ s, demonstrating the formation of two distinct transient species in the blend film. The monoexponential lifetime was $\tau = 8$ μ s under Ar atmosphere and significantly shortened under O₂ atmosphere. Monoexponential phase is therefore assigned to the decay of poly(541) triplet excitons.

Turning now to more crystalline polymers, poly(542)/PCBM blend films exhibited a broad transient absorption signal around 900–1000 nm, similar to, but significantly enhanced in amplitude from, that observed for the poly(542) pristine film. This initial transient absorption decayed rapidly in <1 μ s and left a residual long-lived transient which extended up to milliseconds. The lifetime is 0.1 μ s. The amplitude of the power-law decay phase which is assigned to dissociated polarons varied by an order of magnitude between polymers and indicates large variations in charge dissociation yields between these polymers.

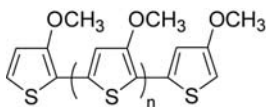
Blends obtained from polythiophene derivatives and PCBM resulted in a strong quenching of the photoluminescence (06AM572; 06JCS(CC)3939). In the P3HT/PCBM blend film, the transient spectrum exhibits a broad transient absorption signal over the wavelength range studied with an absorption maximum at \sim 1020 nm. The transient signal was not quenched under O₂ atmosphere. Therefore, the decay was assigned to the bimolecular recombination of charged species trapped in the blend films, as we have discussed previously.

The efficient triplet formation observed here for the more amorphous polymers is attributable to the twisted backbone of the amorphous polymers. On the other hand, the higher crystallinity of the second polymer group is attributed to their relatively planar backbones, resulting in a longer conjugation length of the main chain. This is consistent with the red-shifted absorption band, smaller IP, and high carrier mobility. In contrast to the amorphous polymers, excitons will be more delocalized in the partially crystalline polymers. The planar conjugated backbone, favoring interplanar interaction leading to π staking in the conjugated backbone, can be expected to reduce the ISC rate as twist motions enhancing the spin-orbit coupling are effectively suppressed in the π -stacked main chain. Such π stacking can be expected to favor interchain charge separation. The $^1P^*$ states are efficiently quenched by the addition of only 5 wt% PCBM to the polymer film. The addition of this low concentration of PCBM is unlikely to alter the ISC or internal conversion decay rates from $^1P^*$ state, consistent with there being no measurable change in polymer absorption spectra. Rather this emission quenching is assigned to the generation of polarons, P^+ and $PCBM^{-1}$.

For the polymers poly(541) and poly(539), the observation of polymer triplet formation in the blend films indicates that their triplet energies are below that of PCBM ($E_T \approx 1.5$ eV), while for poly(540), the observation of PCBM triplet rather than polymer triplet formation in the blend indicates that the poly(540) triplet state lies higher in energy than the PCBM triplet state.

The observation of long-lived charge separated states in these blend films, even when these states are thermodynamically unstable with respect to neutral triplet excitons, can be understood in terms of the kinetics of diffusion-controlled bimolecular charge recombination. Polaron trapping on localized low-energy trap sites within the polymer phase results in the slow decay dynamics observed for these dissociated polarons, extending up to millisecond time scales. The charge separated states are energetically likely to be more stable than the polymer and PCBM triplet states.

The electropolymerization of 3-methoxythiophene (MOT) was performed in an aqueous micellar medium containing sodium dodecylsulfate (SDS) as a surfactant. The electronic absorption spectra, the fluorescence excitation and emission spectra, and the quantum yields of **546**, were measured in different solvents of various polarities and hydrogen bond abilities (89SM(28)C487; 98SM(93)175; 00JF107; 00POLLDG4047; 00SA1391). Poly(3-methoxythiophene-polybithiophene composite film shows an absorption at 510 nm (99PCCP1731).



$$n = 3, 4$$

546

$$\lambda_1 \text{ 221, } \lambda_2 \text{ 264, } \lambda_3 \text{ 335, } \lambda_4 \text{ 471 nm}$$

$$\lambda_{\text{max}}^{\text{F}} \text{ 545 nm}$$

$$\Phi_{\text{F}} \text{ 0.21}$$

The electronic absorption spectra showed three or four relatively strong bands occurring at 219–221 nm (λ_1), 262–274 nm (λ_2), 333–338 nm (λ_3), and 471–487 nm (λ_4), according to the solvent used. The first two bands, which are also present in the monomer (3-methoxythiophene), have been attributed to a charge transfer transition from the methoxy group oxygen atom to the thiophene ring and to the thiophene ring local $\pi \rightarrow \pi^*$ transition, respectively. The third band (λ_3), characterized by slightly lower molar absorption coefficients, can be ascribed to a polarized transition, parallel with the long molecular axis. The longest wavelength peak (λ_4) is attributed to the delocalized $\pi \rightarrow \pi^*$ electronic transition. λ_1 and λ_3 are not solvent sensitive. In contrast, the $\pi \rightarrow \pi^*$ electronic transitions (λ_2 and λ_4) are red shifted with changing solvent polarity. λ_2 and λ_4 undergo a 12 and 16 nm red shift, respectively, when going from a nonpolar solvent (cyclohexane) to a more polar one (DMSO).

The fluorescence excitation spectra exhibit a broad band located between 461 and 465 nm, which is homothetic to the longest wavelength absorption band. The fluorescence emission spectra are characterized by a well-defined peak which is strongly red shifted from 545 to 565 nm on going from hexane to DMSO. This bathochromic shift reflects the occurrence of $\pi \rightarrow \pi^*$ electronic transitions in the **546** singlet excited state.

The fullwidth-at-half-maximum (FWHM) of the bands which are comprised in a narrow range ($1750 \pm 170 \text{ cm}^{-1}$) for the fluorescence and a larger one ($6720 \pm 1810 \text{ cm}^{-1}$) for the absorption spectra indicate that the sharpness of the curves is also slightly solvent-dependent and that more conformers are present in the ground state than in excited singlet state. These results also suggest that the relaxed excited singlet state produces more planar conformations than noted in the ground

state. The authors obtained a high μ_e/μ_g ratio value of 5.8, which indicates that **546** dipole moment is much larger in the first excited singlet state than in the ground state. This result shows that **546** is much more polar in the excited singlet state than in the ground state. The high value of 9.74 found for μ_e suggests the existence of important discrepancies in the electronic charge distribution in the excited singlet state relative to the ground state.

Some other 3-thienyl ether derivatives have been prepared. Poly[3-oligo(oxyethylene)-4-methylthiophene] showed an absorption peak at 550 nm (95JCS(CC)2293). On the other hand, poly[3-(*N*-succinimido(tetraethoxy)oxy)-4-methylthiophene] was prepared and it is able to react with amines to give the corresponding carbamate with a 15-crown-5 attached substructure. This polymer showed absorption at 429 nm and fluorescence at 543 nm (04T11169).

Poly(3-aminothiophene) derivatives have also been prepared showing absorptions in solutions at 482–535 nm and in film at 510–545 nm (05SM(152)137). The electropolymerization of 3,4-dimethoxythiophene gave the corresponding polymer showing absorptions in the 300–400 nm region. It emits at 534 and 537 nm (01SM(123)365).

Poly[(tetramethyldisilanylene)-bis(2,5-thienylene)] and poly[(hexamethyltrisilanylene)-bis(2,5-thienylene)] are photochemically inactive (93MI269). On the other hand, the silicon–silicon bonds in poly[(tetramethyldisilanylene)(2,5-thienylene)] can readily be cleaved homolytically upon irradiation with UV light (94JOM(468)55). Some silicon contained polymers (poly[(tetraethyldisilanylene)(2,5-thienylene)] $M_w = 20,000$; poly[(tetraethyldisilanylene)bis(2,5-thienylene)] $M_w = 53,000$; poly[(tetraethyldisilanylene)tris(2,5-thienylene)] $M_w = 47,000$; poly[(tetraethyldisilanylene)tetrakis(2,5-thienylene)] $M_w = 29,500$; poly[(tetraethyldisilanylene)pentakis(2,5-thienylene)] $M_w = 17,000$) show strong absorption bands in the UV region (270, 343, 389, 415, 427 nm, respectively), which are significantly red shifted relative to those of the corresponding 2,5-thienylene oligomers such as thiophene (230 nm), bithiophene (304 nm), terthiophene (353 nm), and quaterthiophene (390 nm), indicating the presence of $\sigma-\pi$ conjugation (96OM2000).

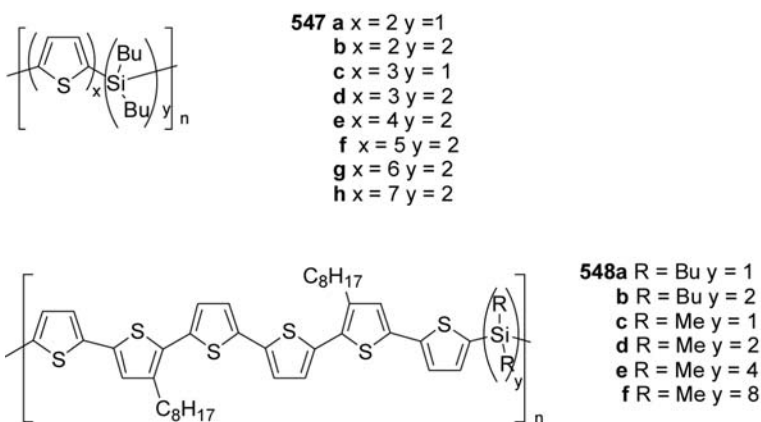
When a thin film prepared from poly[(tetraethyldisilanylene)bis(2,5-thienylene)] was irradiated in air with a 6-W low pressure mercury lamp bearing a Vycor filter, the absorption maximum near 340 nm disappeared within 40 min. Poly[(tetraethyldisilanylene)(2,5-thienylene)] also exhibited a rapid UV change when its thin film was irradiated. IR spectra of the resulting films reveal strong absorption bands due to Si–O–H and Si–O–Si bonds at 3300 and 1100 cm^{-1} . The formation of the Si–O–H and Si–O–Si bonds can be best explained by the reaction of the silyl radicals generated by homolytic scission of the silicon–silicon bonds in the polymer backbone with oxygen in air. The other polymers are also photoactive,

but they become less sensitive to UV light with expansion of the thienylene π -electron system.

Poly[(tetraethyldisilanylene)(2,5-thienylene)] and poly[(tetraethyldisilanylene)bis(2,5-thienylene)] have $\sigma-\sigma^*$ -type band gaps, whereas the other polymers have $\pi-\pi^*$ -type gaps due to an interchange of nature of the optical transition with the lowest energy. The Si-Si bond cleavage is obviously associated with the nature of their lowest unoccupied crystal orbitals. On the other hand, in poly[(tetraethyldisilanylene)tris(2,5-thienylene)], poly[(tetraethyldisilanylene)tetrakis(2,5-thienylene)], and poly[(tetraethyldisilanylene)pentakis(2,5-thienylene)], the optical energy by irradiation is rather wasted in the $\pi-\pi^*$ transition and makes the Si-Si bond cleavage slow to occur.

The reaction of 5,5'-bis(pentaethyldisilanyl)-2,2'-bithiophene was chosen as a model compounds of poly[(tetraethyldisilanylene)bis(2,5-thienylene)]. After 77 h irradiation in benzene, they obtained 5-(pentaethyldisilanyl)-2,2'-bithiophene (23%) and triethylphenylsilane (46%). The corresponding permethyl derivative was found to be photochemically inert. The inactivity of permethyl derivative is similar to the low photosensitivity of the permethyl polymer.

The photodegradation seems to involve the homolytic scission of the silicon-silicon and silicon-sp² carbon bonds in the polymer backbone.

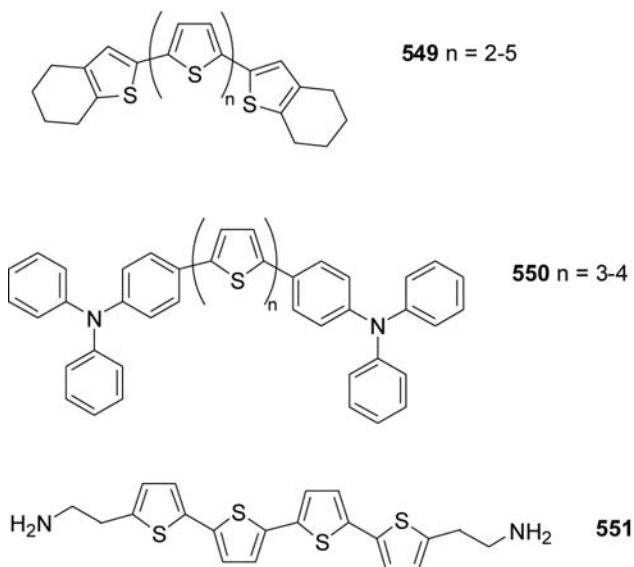


Hadzioannou and coworkers demonstrated photoluminescence and electroluminescence tuning via exciton confinement with block copolymers **547a-d** and **548a-f** containing oligothiophene and alkylsilanylene units (93AM721; 95MM8102). Precise control of the conjugation length of

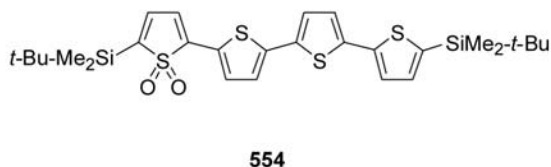
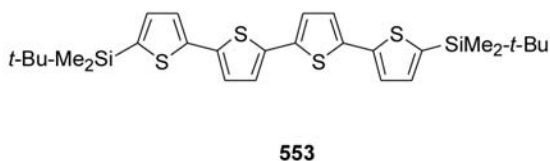
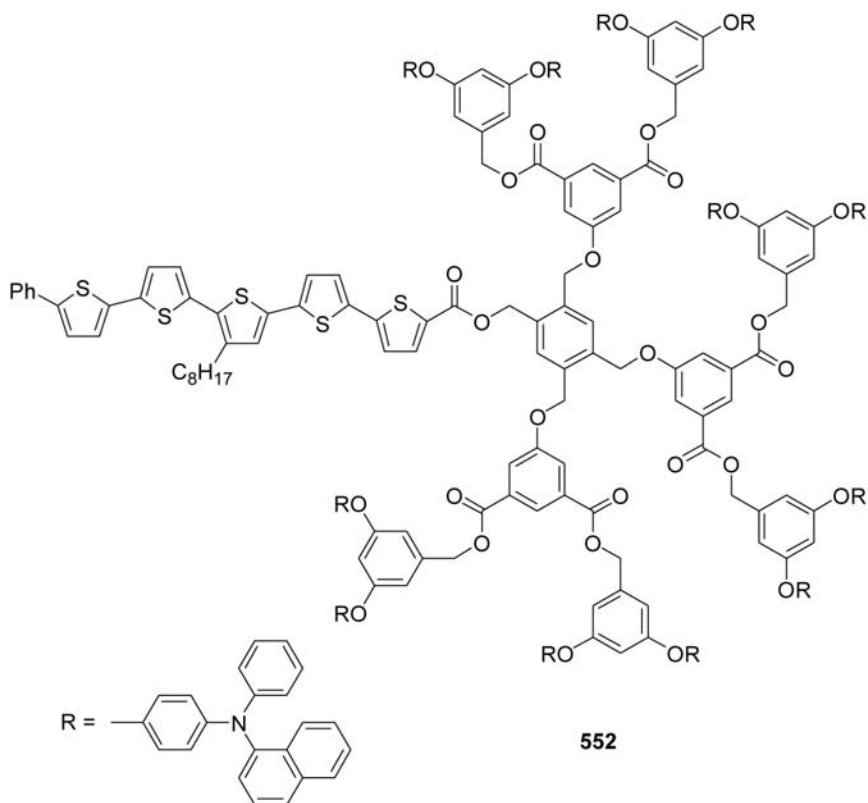
the oligothiophene blocks, interrupted by silanylene units, allowed tuning the emission from blue to orange-red (Table 13). Later, Yoshino et al. reported similar extended block-copolymer **547d–h** that showed changes in EL color from green to red with increasing oligothiophene block length (99SM(102)1158).

Poly[4-(2-thienyl)benzenamine] showed a single peak at 400 nm (97MI1738). Gieger et al. studied a series of end-capped oligothiophenes **549** (93AM922). End-capping of terthiophene and quaterthiophene with triphenylamino groups (**550**), which led to stable amorphous glasses, can afford relatively high luminescence efficiencies (97AM720; 97APPLAB(70) 699).

When **551** was incorporated within lead halide perovskite layers in an ITO/**551**:PbCl₄/OXD7/Mg/Ag device (OXD7 = 1,3-bis(4-(*tert*-butylphenyl)-1,3,4-oxadiazol-yl)phenylene), a bright green-light emission (530 nm) from the organic layer was found (Scheme 212) (99CM3028).



A quinquethiophene oligomer unit was used as a core in the light-emitting dendrite **552** (00JA12385). In this material, an excitation of the peripheral amines at 310 nm results in energy transfer to the highly luminescent fluorophore at the core of the dendrimer with subsequent green-light emission ($\lambda_{PL} = 550$ nm) exclusively from the oligothiophene.

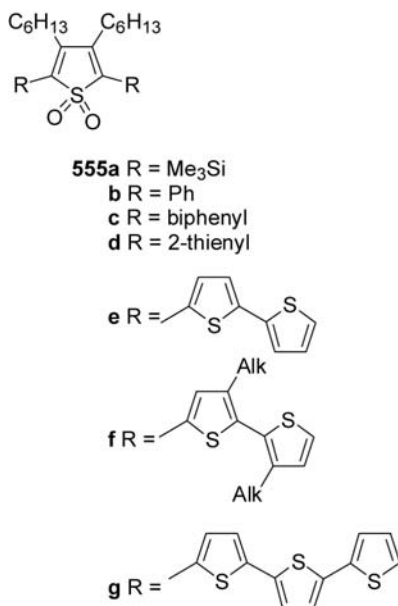


Poly- and oligothiophenes are generally p-type (hole-transporting) semiconductors. In thiophene-*S,S*-dioxide (98AM551; 98JOC5497), this modification results in “de-aromatization” of the thiophene unit and increases the electron affinity and electron-transport properties of the

material. A comparison of two quaterthiophene **553** and **554** indicates that a single thiophene-*S,S*-dioxide moiety results in a bandgap contraction of >0.7 eV (98AM551).

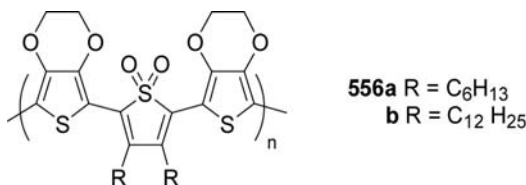
Oligomers incorporating thiophene-*S,S*-dioxide units possess good photoluminescence properties in solution and the solid state.

Photoluminescence quantum yields were reported to be as high as 37% for pentathiophene **555f** (00MI612), 45% for terthiophene **384d** (00JA9006), and even 70% for phenylenethiophene oligomer **555c** (00JA11971).



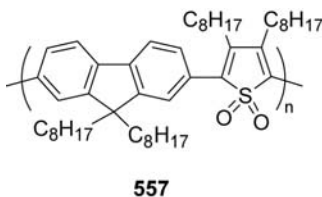
Incorporation of electron-deficient thiophene-*S,S*-dioxide units into electron-rich conjugated oligomers (**555**) predictably results in reduction of the material's bandgap. This allows variation of both absorption and photoluminescence energies over a wide range ($\lambda_{\max}^{\text{abs}} \sim 350\text{--}540$ nm, $\lambda_{\max}^{\text{F}} \sim 400\text{--}725$ nm) to cover the full visible range, from the UV to the NIR (98AM551; 98JOC5497; 00MI612; 00JA9006; 00JA11971).

Phenylene-thiophene-*S,S*-dioxide copolymers with λ_{\max} 476–484 nm appeared (00AGE2870). Thiophene-thiophene-*S,S*-dioxide copolymers **556a,b** were reported by Berlin et al. (03MI27). The polymers absorbed at 535 nm (bandgap energy $E_g = 2.3$ eV) in chloroform solution and in films and emitted at 650 nm ($\Phi_{\text{F}}^{\text{film}} \sim 1\%$). Such a high bandgap strongly suggests a disruption of the conjugation, possibly due to steric interactions.



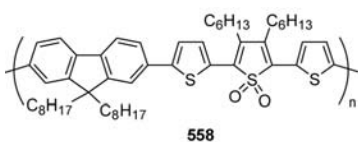
These works stimulated research activities toward incorporation of the thiophene-*S,S*-dioxide unit into various copolymers, and PLEDs built with such copolymers were reported by several authors (01JCS(CC)1216; 02MI3523; 03POLLDG1843).

Copolymer **557** (03MI807) showed a solvent-dependent green-yellow-light emission (from 545 nm in THF to 565 in chloroform). No strong decrease in emission efficiency was observed in solid state ($\Phi_F^{\text{film}} = 13\%$).

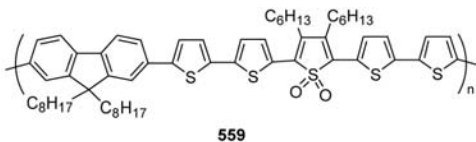


Abs 411 nm PL 511 nm

Beaupré and Leclerc reported fluorene-thiophene copolymers in which fluorene and thiophene-*S,S*-dioxide fragments **558** and **559** were separated by one or two thiophene units (02MI192).



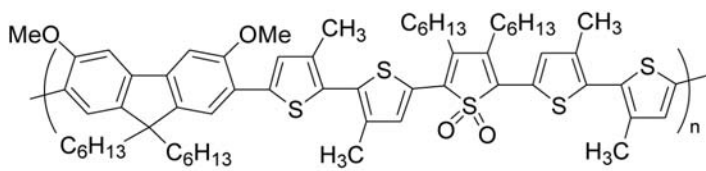
Abs 509 nm PL 610, 660 nm



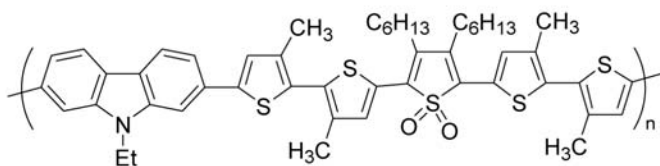
Abs 547 nm, PL 666, 708 nm

These copolymers are both p- and n-dopable, as follows from their electrochemistry, with bandgaps of 2.2 and 2.0 eV for **558** and **559**, respectively. The efficiency of similar fluorene copolymers was much lower. The combination of thiophene and thiophene-*S,S*-dioxide units in a copolymers allows tuning of the emission color from green to pure red (02MI192; 03SM(138)289).

Similar results (a significant decrease of the photoluminescence quantum yields) were observed for thiophene-thiophene-*S,S*-dioxide copolymers containing 3,6-dimethoxyfluorene **560** (03MM8986) and carbazole **561** (02MM8413) (with $\Phi_F = 20\text{--}25\%$ in solution).

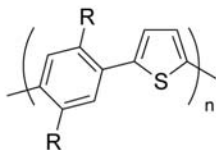
**560**

Abs 392, 478 nm, PL 662 nm

**561**Abs. 512 nm, PL 671 Φ_{PL} 25%

The largest variety of emission wavelengths was created via copolymerization of thiophene with other conjugated monomers. Thus, “diluting” the thiophene units in the polymer chain with other aromatic moieties enlarges the material bandgap, affording blue-light-emitting thiophene copolymers, and in many cases suppresses aggregation in the solid state (thus improving the emission efficiency). Copolymerization with electron-deficient co-monomers results in a bandgap reduction (well-known for alternating donor (D)-acceptor (A) polymers, DADA), thus affording NIR-emitting materials.

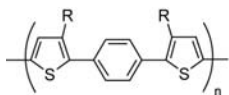
Phenylene-thiophene copolymers **562b** and **562a** emit blue light at ca. 450–475 nm, with somewhat different reported $\Phi_{\text{EL}}^{\text{ex}}$ values of 0.2% (96AM982) and 0.03% (97MM4608) respectively, for ITO/polymer/Ca configurations.



562a R = C₇H₁₅
b R = C₅H₁₁

562a Abs 330 nm PL 450 nm, **562b** Abs 335 nm, PL 455 nm.

A related series of copolymers containing thiophene-phenylene-thiophene repeat units have been reported by Huang and coworkers (00MM2462; 01MI3082; 01MM7241). By changing the steric effect of substituents, the polymer emission was tuned from greenish-yellow to pure green.



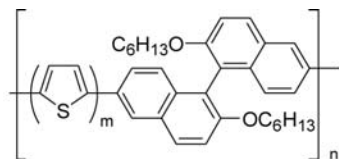
563 R = C₄H₉; λ_{max} 398 nm, $\lambda_{\text{max}}^{\text{film}}$ 420 nm, $\lambda_{\text{max}}^{\text{F}}$ 492 nm, $\lambda_{\text{max}}^{\text{F, film}}$ 512 nm, Φ_{F} 0.26
564 R = C₈H₁₇; λ_{max} 398 nm, $\lambda_{\text{max}}^{\text{film}}$ 420 nm, $\lambda_{\text{max}}^{\text{F}}$ 494 nm, $\lambda_{\text{max}}^{\text{F, film}}$ 521 nm, Φ_{F} 0.23
565 R = C₁₂H₂₅; λ_{max} 398 nm, $\lambda_{\text{max}}^{\text{film}}$ 422 nm, $\lambda_{\text{max}}^{\text{F}}$ 494 nm, $\lambda_{\text{max}}^{\text{F, film}}$ 529 nm, Φ_{F} 0.19

In solution, all the polymers depict the same absorption maxima at 398 nm in the UV/Vis spectra and the same fluorescence emission maxima at about 494 nm despite the thiophene moieties being substituted by alkyl groups of different chain lengths (98SM(92)33). However, film samples show a bathochromic shift (i.e., increasing Stokes shift) in the emission maxima on going from **563** to **565** with the increasing alkyl chain length, an effect tentatively attributed to increasing vibrational disorder in the latter polymer with consequently accentuated nonradiative loss. In addition, film samples have their absorption maxima red shifted from the corresponding solution samples. This can be ascribed to conformational changes which increase the degree of conjugation in the polymer backbone of the condensed state. The bandgap energy at about 2.5 eV of the polymers, as determined from extrapolation of the low energy absorption edge of film samples in UV/Vis absorption spectra, lies between that of polythiophene (2.0 eV) and poly(*para*-phenylene) (3.0 eV).

The polymers **563** to **565** appear highly fluorescent. The quantum yields of the solution polymers decrease slightly with increasing alkyl chain length, which is in contrast to other reported observation for polyalkylthiophenes.

Copolymer between 3-octylthiophene and 3-decyloxythiophene has been described (06JA8980). They showed an absorption band at 538 nm in chloroform and at 621 nm in film, with a bandgap of 1.64 eV.

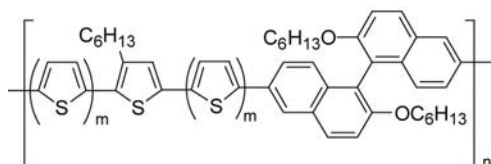
Twisted 1,1-binaphthyl units in alternating oligothiophene-containing copolymers **566a–c** and **567a–c** interrupt the conjugation, which could prevent the self-quenching processes in the solid state. A variation in the length of the oligothiophene segment from one to seven thiophene rings predictably reduced the polymer bandgap and tuned the emission color from yellow-green to red.



566a $m = 1$: λ_{\max} 368 nm, λ_{\max}^F 421, 446, 475 nm, Φ_F 0.54

b $m = 2$: λ_{\max} 406 nm, λ_{\max}^F 463, 498 nm, Φ_F 0.26

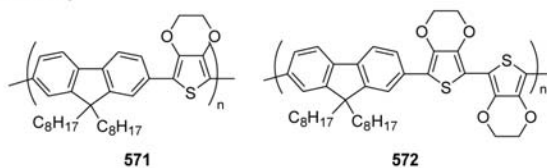
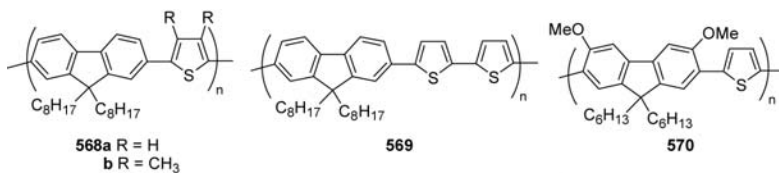
c $m = 4$: λ_{\max} 440 nm, λ_{\max}^F 515, 549 nm, Φ_F 0.23



567a $m = 2$: λ_{\max} 434 nm, λ_{\max}^F 530, 568 nm, Φ_F 0.054

b $m = 3$: λ_{\max} 454 nm, λ_{\max}^F 545, 583, 631 nm, Φ_F 0.065

A combination of electron-rich thiophene units with relatively electron-deficient fluorene units should modify the bandgap of the material (and thus tune the emission) and improve the charge injection/transport balance compared to fluorene homopolymers.



568a Abs 438 nm PL 485, 512 nm

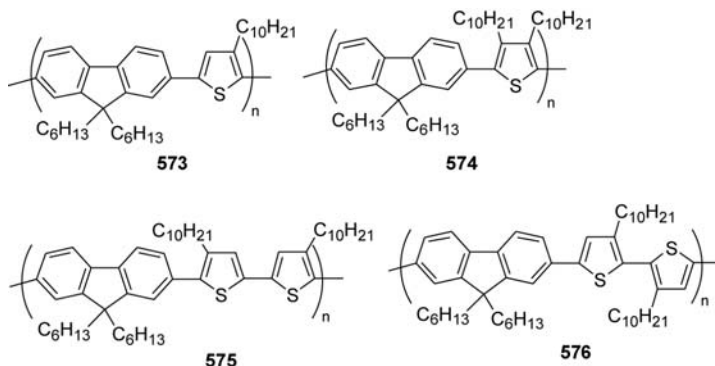
568b Abs 384 nm PL 460 nm

569 Abs 427 nm PL 548 nm

570 Abs 446 nm PL 510

571 Abs 444 nm PL 494, 526 nm

572 Abs 517 nm PL 532, 574 nm



573 Abs 412 nm PL 492, 477 nm

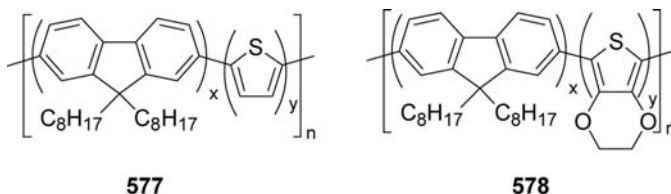
574 Abs 378 nm PL 458, 475 nm

575 Abs 403 nm PL 490, 520 nm

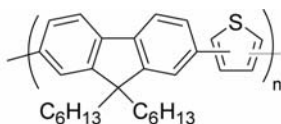
576 Abs 401 nm PL 493, 520 nm

Lévesque, Leclerc, and coworkers have efficiently tuned the emission color from blue to green and yellow by introducing various thiophene units in alternating fluorene copolymers **568–572** (00CM1931; 01SM(122) 79; 02MM8413).

Huang's group has systematically studied the structure–property relationships of fluorene-thiophene-based conjugated polymers **573–576** (00JCS(CC)1631; 00MM8945; 01MM7241). Several random fluorene-thiophene copolymers such as **577** (02APPLAB(81)634) and **578** (02APPLAB (81)634; 02SM(131)31) have been investigated.



Vamvounis and Holdcroft prepared a series of fluorene-thiophene copolymers **579** with a varying ratio of conjugated (2,5-thienylene) and nonconjugated (3,4-thienylene) thiophene moieties in the polymer chain (04AM716). The PL efficiencies in films are low (6 and 7%, respectively). Substantial increases in solid-state PL efficiencies were observed reaching a value of 43% for copolymer **579e**.

**579**

a PFT-A $\Phi_{\text{PL}}^{\text{sol}}$ 57%, $\Phi_{\text{PL}}^{\text{film}}$ 6%

b PFT-0.5A $\Phi_{\text{PL}}^{\text{sol}}$ 50%, $\Phi_{\text{PL}}^{\text{film}}$ 14%

c PFT-0.2A $\Phi_{\text{PL}}^{\text{sol}}$ 54%, $\Phi_{\text{PL}}^{\text{film}}$ 19%

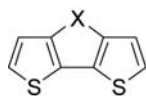
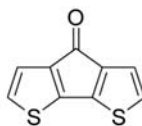
d PFT-0.1A $\Phi_{\text{PL}}^{\text{sol}}$ 47%, $\Phi_{\text{PL}}^{\text{film}}$ 19%

e PFT-0.04A $\Phi_{\text{PL}}^{\text{sol}}$ 57%, $\Phi_{\text{PL}}^{\text{film}}$ 43%

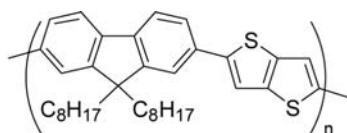
f PFT-B $\Phi_{\text{PL}}^{\text{sol}}$ 39%, $\Phi_{\text{PL}}^{\text{film}}$ 7%

This enhanced solid-state emission was rationalized in terms of a self-forming host-guest system in which excitons formed on the PFT-B host fragment transfer their energy to electronically isolated highly efficient PFT-A emitting fragments.

The polymers of 4*H*-cyclopenta[2,1-*b*;3,4-*b'*]dithiophene derivatives showed absorptions in the range 560–590 nm [03MM2705]. Some monomers are based on the nonaromatic (12 π electrons) 4*H*-cyclopenta[2,1-*b*;3,4-*b'*]dithiophen-4-yl cation **580a** ($X = \text{CH}^+$) model which was expected to display a reduced HOMO–LUMO separation, compared to related aromatic fused systems (i.e., **580**, $X = \text{S}$, O, NH) (91JCS(CC)752). Polymers of **580** ($X = \text{S}$) showed absorption at 480 nm. Poly(dithieno[3,4-*b*:3',4'-*d*]thiophene) showed an absorption at 590–610 nm (89SM(28)C507; 97MI23).

**580****581**

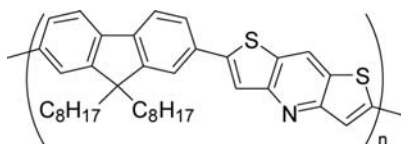
Cyclopenta[2,1-*b*;3,4-*b'*]dithiophen-4-one **581** was considered as a first approximation to it. Ketone **581** displays its lowest $\pi-\pi^*$ transition at $\lambda_{\max} = 472$ nm ($\epsilon = 1250$). Upon electropolymerization, this long wavelength absorption shifts to 740 nm in the neutral polymer, a red shift of ≥ 200 nm compared to PT. A strong absorption at 425 nm is also present in poly-**581**. If we assume that the lower energy absorption in neutral poly-**581** is derived primarily from the aromatic HOMO–LUMO transition, and the higher energy transition arises between some deeper level and the LUMO. The E_{gap} is ≤ 1.2 eV.

**582**

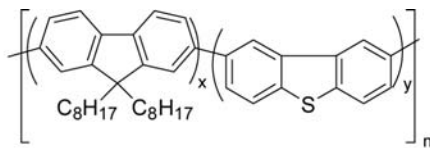
Abs 448, 471 nm PL 495, 511, 548 nm

A very efficient green-light-emitting fluorene copolymer **582** was synthesized by Shim and coworkers (03MM4288). Also, thieno[2,3-*b*]thiophene derivatives can be used to synthesize new semiconductors (05JA1078): the polymer showed λ_{\max} at 467–472 nm.

Introduction of electron-accepting bithieno[3,2-*b*:2',3'-*c*]pyridine units resulted in copolymer **583** (04MM709). Upon excitation at 420 nm ($\lambda_{\max}^{\text{abs}} = 415$ nm), copolymer **583** exhibited blue-green-light emission with two peaks at 481 and 536 nm.

**583**

Several random fluorene-dibenzothiophene copolymers **584a–e** (03JPS (A)(41)1521; 03MI1351) have been reported.

**584**

a x:y = 95:5 Abs 383 nm PL 422 nm Φ_{PL} 29%

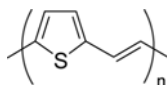
b x:y = 90:10 Abs 380 nm PL 421 nm Φ_{PL} 25%

c x:y = 80:20 Abs 373 nm PL 420 nm Φ_{PL} 18%

d x:y = 70:30 Abs 350 nm PL 419 nm Φ_{PL} 23%

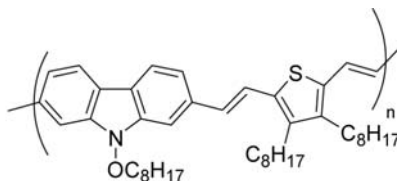
e x:y = 50:50 Abs 343 nm PL 410 nm Φ_{PL} 62%

Minor conjugation limits the emission band to the deep-blue color range ($\lambda_{\text{max}} \sim 420\text{--}440$ nm) (03MI1351). PTV, the polymer **585** (02MI200), is a fluorescent material. The UV/Vis spectrum of the oligomers showed the 0–0 transition at 487 nm (03AM306).

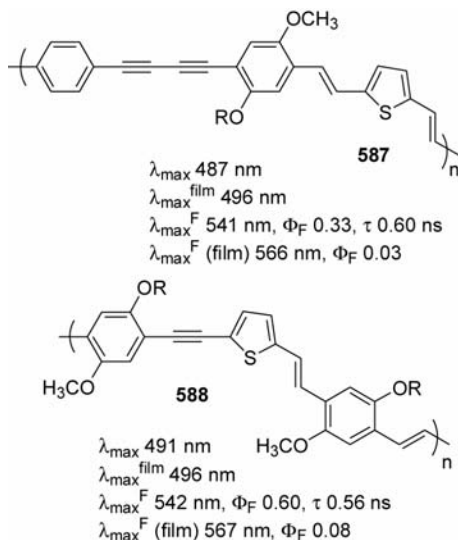
**585**

A strong NIR photo- and electroluminescence were observed in acceptor- (cyano-) substituted PTV (95SM(71)2117).

Leclerc and coworkers synthesized a 2,7-carbazolylenevinylene-thienylenevinylene copolymer **586** (04CM4619). Whereas this material showed red emission in solution ($\lambda_{\text{PL}} = 581$ nm, $\Phi_{\text{PL}} = 16\%$), it was not fluorescent in the solid state.

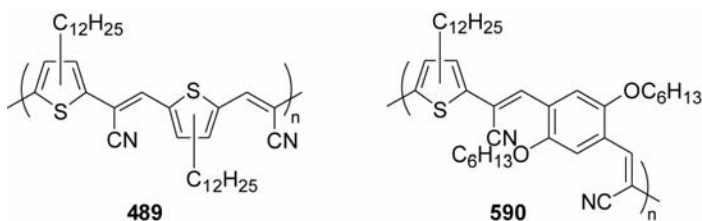
**586**

Abs 485 nm PL 581, 547 nm Φ_{PL} 16%



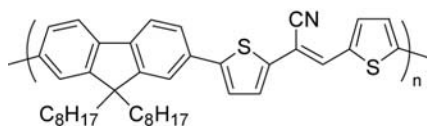
Polyvinylthiophene derivatives such as **587** and **588** has been synthesized and tested for their photophysical and electrochemical properties (09JPS(A)2243; 09SM(159)142).

A cyano group drastically improves the fluorescence of PTV materials. Two CN-PTV derivatives, **589** and **590** showed strong fluorescence in the NIR region and have been used to fabricate rarely achieved NIR PLED (95SM(71)2117).



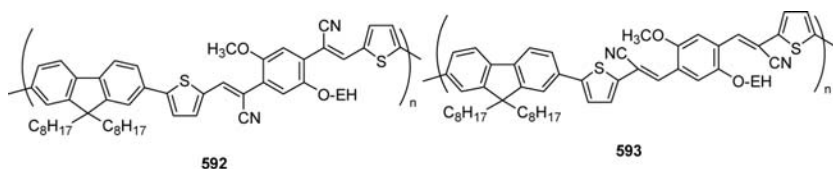
589 PL 950 nm; **590** PL 840 nm

A PLED based on the fluorene-PTV copolymer **591** emitted red-orange light (02MI192). Cyano substituted poly(thienylene-vinylene-thienylene)s have been synthesized and tested for their use in photovoltaic devices and field-effect transistors (09JPS(A)4028).

**591**

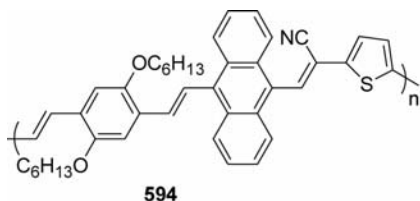
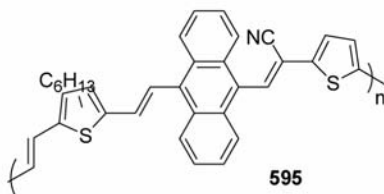
Abs 500 nm PL 610 nm

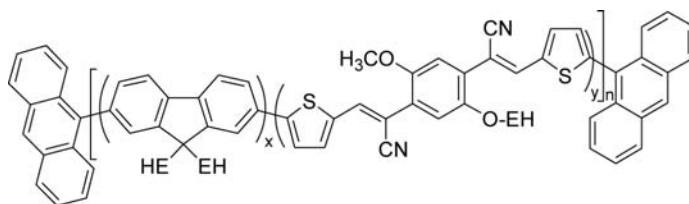
Fluorene-thiophene-phenylene copolymers **592–593** clearly demonstrate the effect of the exact position of CN groups in the vinylene fragment on the emission of the materials (04MM5265).

**592****593****592** Abs 460 nm PL 602 nm;**593** Abs 537 nm PL 674 nm

Both absorption and emission maxima of the polymer **592** with cyano groups in the β -position with respect to the thiophene nucleus are hypsochromically shifted as compared to the polymer **593** (having the cyano group in the α -position), which can be explained by steric interactions between the cyano and alkoxy groups. Nevertheless, both copolymers **592** and **593** exhibit pure red-light emission with chromaticity values very close to standard red.

Anthracene containing thienylene-vinylene copolymers, such as **594** and **595**, have been reported and photovoltaic properties have been described (09JAPNAB(113)1173).

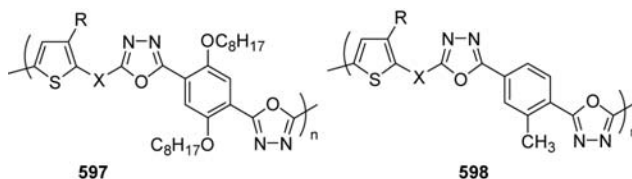
**594**
 λ_{\max} 403 nm
 $\lambda_{\max}^{\text{film}}$ 433 nm
 $\lambda_{\max}^{\text{F}}$ 518 nm
**595**
 λ_{\max} 390 nm
 $\lambda_{\max}^{\text{film}}$ 395 nm
 $\lambda_{\max}^{\text{F}}$ 455 nm

**596****a** x:y = 99:1 Abs 380 nm PL 536 nm**b** x:y = 97:3 Abs 380 nm PL 544 nm**c** x:y = 95:5 Abs 380 nm PL 583 nm**d** x:y = 85:15 Abs 379 nm PL 620 nm

Random copolymers **596a–d** synthesized by Yamamoto coupling of a fluorene and thiophene-base (02MI199; 02MM1224).

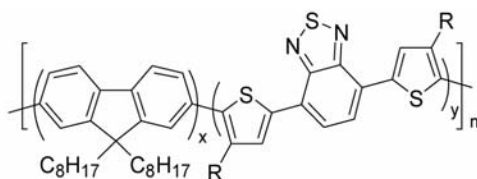
All the copolymers showed similar absorptions with λ_{\max} at ~ 470 nm, which was more intense for polymers with higher thiophene content. In contrast, their emission colors were progressively red shifted with increasing thiophene-based comonomer content. Copolymer **596a** emitted bright red light (620 nm) with reasonably high photoluminescent quantum yields (34–69%).

Several thiophene copolymers (**597–598**) containing electron-rich thiophene and electron-deficient 1,3,4-oxadiazole units (98AM593; 98CM3340; 99MM118; 00JOC3894). Structural variations, particularly different lengths of oligothiophene fragments, allowed them to tune the bandgap and PL energy of these materials: $\lambda_{\text{F}}^{\text{film}} = 489 \text{ nm} \rightarrow 530 \text{ nm} \rightarrow 580 \text{ nm}$ (**597a** \rightarrow **b** \rightarrow **c**); $462 \text{ nm} \rightarrow (498, 526 \text{ nm}) \rightarrow 568 \text{ nm}$ (**598a** \rightarrow **b** \rightarrow **c**).

**a** R = C₈H₁₇, X = none**b** R = C₁₀H₂₁, X = **c** R = C₈H₁₇, X =

Narrowing the bandgap of copolymers by alternation of electron-rich thiophene and electron-deficient benzo-1,2,3-thiadiazole units was used in the design of several LEPs whose optical and electronic properties could be tuned through such a modification. Cao and coworkers synthesized copolymers **599** and **600** (02MI2887; 04MM6299), exploiting random copolymerization.

The absorption spectra of copolymers **599** and **600** show two maxima corresponding to oligofluorene (~ 370 – 390 nm) and bisthienylbenzothiadiazole fragments (~ 520 – 550 nm). Both copolymers emit saturated red light. Decreased interchain interaction for copolymer **600**, compared to **599** (due to hexyl substituents on the thiophene rings), results in increased photoluminescence quantum yield in the solid state (44–88% for **600a–g** compared to 4–12.5% for **599a–g**).



599-600

599 R = H

600 R = C₆H₁₃

a x:y = 99:1

b x:y = 95:5

c x:y = 90:10

d x:y = 85:15

e x:y = 75:25

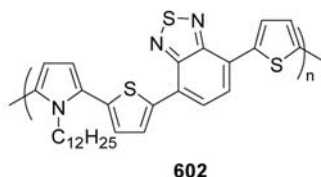
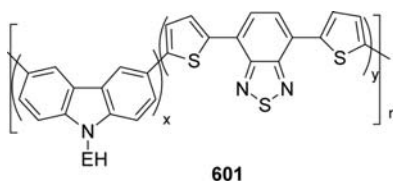
f x:y = 65:35

g x:y = 50:50

599 Abs 382–388, 535–551 nm PL 635–685 Φ_{PL} 4–12.5%

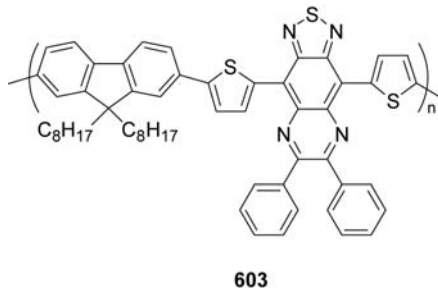
600 Abs 369–383, 520–526 nm PL 629–678 nm Φ_{PL} 19–88%

Cao and coworkers also prepared random 3,6-carbazole-benzothiadiazole-thiophene copolymers **601** (02MI709). Copolymer **601** emitted saturated red light (from 660 to 730 nm, depending on the stoichiometry).



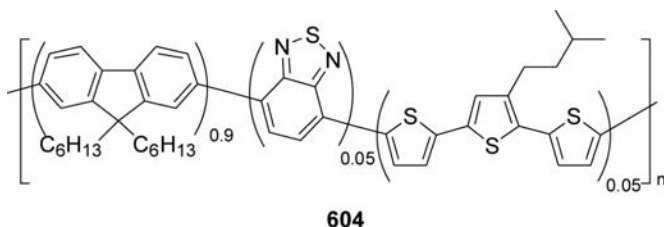
Further lowering of the bandgap ($E_g \sim 1.6$ eV) was observed for bisthierylbenzothiadiazole-pyrrole copolymer **602**, reflecting an increased conjugation through the 2,5-connected pyrrole units (01MI255).

PL and EL emissions from a very-low-bandgap copolymer **603** ($E_g = 1.27$ eV) was demonstrated (04APPLAB(84)3570; 04SM(146)233). The material had two absorption peaks at 400 and 780 nm, and emitted light in the NIR region. The PL spectrum of thin films had one peak at 1035 nm that was blue shifted by ca. 60 nm on annealing at 200°C for 10 min.



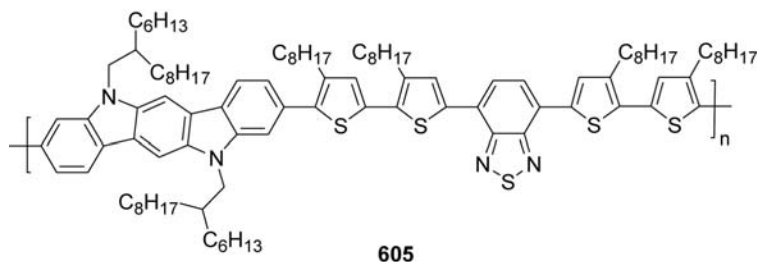
Abs 400, 780 nm, PL 1035 nm

Copolymer **604** showed an absorption with $\lambda_{\max} = 378$ nm (02MM6094). The copolymer had a green luminescence.



A further development of the approach of using multicomponent PF copolymers for tuning the emission color was recently exemplified by fabrication of fan RGB (red/green/blue color specification) prototype display, in which the pure red, green, and blue colors was achieved by variation of the feed ratio of several monomers (03NAT(421)829).

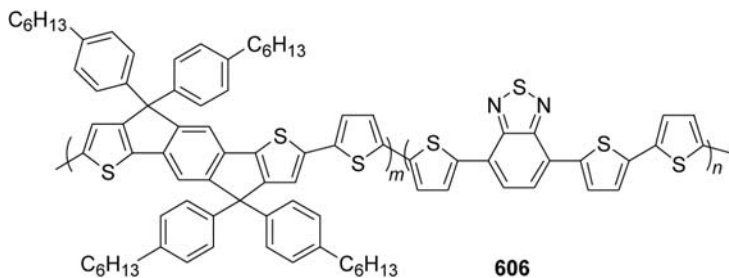
The absorption spectra of **605** measured in chloroform are characterized with a strong, broad and structureless absorption peak at 538 nm, corresponding to the intramolecular charge-transfer (ICT) transition, together with a strong absorption band at shorter wavelength (~ 395 nm) owing to higher energy transitions such as a $\pi-\pi^*$ transition (08JCS(CC) 5315). The polymer emits deep red fluorescence in CHCl_3 solution with an emission peak at 691 nm, regardless of excitation at 400 or 535 nm.

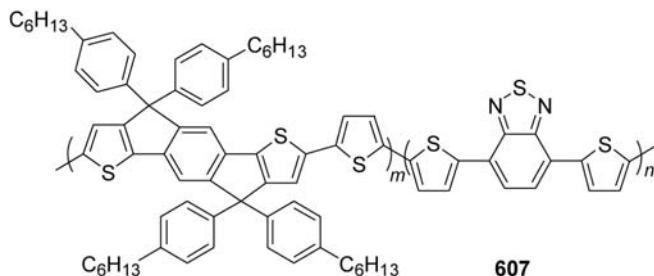


Compared with the solution absorption, the film sample prepared by spin-coating a dichlorobenzene solution using a slow solvent evaporation process showed pronounced peak broadening and a significant shift of ~ 100 nm of the absorption edge.

Thin films only exhibited very weak fluorescence. This suggests the formation of strong interchain interaction in the solid state, leading to fluorescence self-quenching.

PCE = 3.6%, V_{oc} = 0.69 V, short circuit current (J_{sc}) = 9.17 mA cm^{-2} , and fill factor (FF) = 0.57 have been obtained in some preliminary devices.

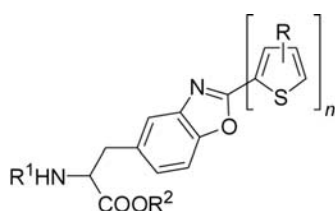




To improve the PCE (power conversion efficiency) of PSCs (polymer solar cells), development of new semiconducting polymers with high absorption coefficient and broader solar absorption are of critical importance. For these reasons, low bandgap (LBG) polymers have been developed to harvest the solar spectrum efficiently in order to generate more photocurrent. **606** film shows broad $\pi-\pi^*$ absorption from 350 to 700 nm and λ_{\max} is around 520 nm (08JA12828; 08MM5519; 09JPC(B)15928). The optical bandgap (E_g^{opt}) determined from the onset of absorption of **606** is 1.76 eV. The strong red shift from absorption edge from 590 to 700 nm was obtained via introducing the strong electron accepting benzothiadiazole group. **607** film possesses a broad and strong absorption band in the region from 350 to 730 nm with a λ_{\max} at around 590 nm, which shows approximately 20 nm red shifted compared to that of P3HT. The absorption edge also shows a red shift from 650 (P3HT) to 730 nm, corresponding to a bandgap of 1.70 eV for **607**.

Additional attractive characteristic of **606** or **607** is that they have high absorption coefficients that are comparable with P3HT in THF solution. **606** and **607** have $1.1 \times 10^6 \text{ cm}^{-1}$ at λ_{\max} (~ 520 nm) and $7.7 \times 10^5 \text{ cm}^{-1}$ at λ_{\max} (~ 570 nm), respectively, which are comparable to that ($\alpha \approx 1.2 \times 10^6 \text{ cm}^{-1}$) of P3HT at its λ_{\max} (~ 450 nm). In order to evaluate the absorption property of pSC, the absorption coefficients of solid films are investigated. The absorption coefficients (α) of the polymer films are measured to be $1.6 \times 10^5 \text{ cm}^{-1}$ at λ_{\max} (~ 520 nm) and $1.4 \times 10^5 \text{ cm}^{-1}$ at λ_{\max} (~ 590 nm) for **606** and **607**, respectively, and $1.9 \times 10^5 \text{ cm}^{-1}$ at λ_{\max} (~ 510 nm) for P3HT. The absorption coefficient of P3HT falls in the reasonable range of $1.75\text{--}2.5 \times 10^5 \text{ cm}^{-1}$ at λ_{\max} . The absorption coefficients at λ_{\max} for **606** and **607** are slightly lower than for P3HT, but in the same order of magnitude. The solid film photoluminescence (PL) of **607** lies near the red region with an emission maximum at 730 nm. The solid film PL of polymer **606** shows the same tendency in our experiment. The cell performance of P3HT is comparable with the earlier literature results, with the optimum efficiency being around 3.9%. The **607** cell has highest AM1.5G power conversion efficiency (PCE) of 4.4%, with a short circuit current density (J_{sc}) of 10.2 mA cm^{-2} , an open circuit voltage (V_{oc}) of 0.81 V, and a fill factor (FF) of 0.53.

The insertion of amino acids into the backbone of both natural and synthetic polymers can lead to the development of macromolecules possessing biomimetic characteristics (08TL5258). The nature of the thiophenic substituent at position 2 of the benzoxazole has a clear influence on the absorption and emission bands of compounds **608–610** (Table 14). The wavelength of maximum absorption was shifted to longer wavelengths as the number of thiophene units increased, ca. 50 nm for each added thiophene. The same trend was observed in the emission spectra as the position of the wavelength of maximum emission was red shifted with the increase of the number of thiophene units, which varied from $\lambda_{\text{max}} = 398$ nm for **608a** to $\lambda_{\text{max}} = 490$ nm for **610a**.



608 $n = 1$, $R = -(CH_2O)_2-$

609 $n = 2$, $R = H$

610 $n = 3$, $R = H$

a $R^1 = \text{Boc}$, $R^2 = \text{Me}$

b $R^1 = \text{Boc}$, $R^2 = H$

c $R^1 = R^2 = H$

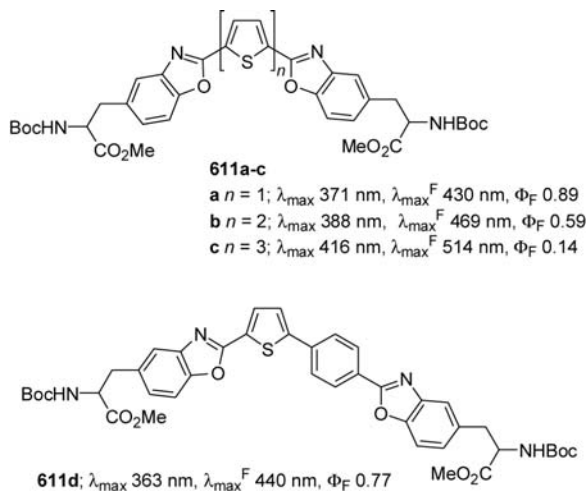
Alanines **609a–c**, with a bithiophene at position 2 of the benzoxazole, were found to be strongly emissive ($0.37 < \Phi_F < 0.13$). The ethylenedioxythienylbenzoxazolyl-alanines **608a–c** displayed residual fluorescence. For this compound, it was found that the rigidity introduced by the ethylenedioxy bridge on the thiophene ring had a strongly deleterious effect on the fluorescence quantum yield. Spectra were run in cyclohexane, dioxane, acetonitrile, and 1:1 ethanol/water and the obtained results showed that no solvatochromic effect was observed, suggesting that these compounds are solvent polarity independent.

It can be seen that the replacement of the second thiophene ring by a phenyl ring leads to a small hypsochromic shift, related to the

Table 14. Photophysical properties of compounds **608–610**

Compound	λ_{max} (log ϵ) (nm)	λ_{max}^F (nm)	Φ_F
608a	314 (4.37)	398	0.03
608b	320 (4.12)	400	0.03
608c	320 (4.28)	386	0.05
609a	365 (4.32)	445	0.46
609b	365 (4.39)	442	0.37
609c	365 (4.29)	448	0.55
610a	400 (4.57)	490	0.10
610b	400 (4.49)	480	0.13
610c	-	-	-

bathochromic effect of sulfur and an increase π -overlap between the thiophene units in **611b**. Also, **611a–d** possess very large molar absorptivity coefficients (higher than $46,000 \text{ mol}^{-1} \text{ L cm}^{-1}$) (08T9733).

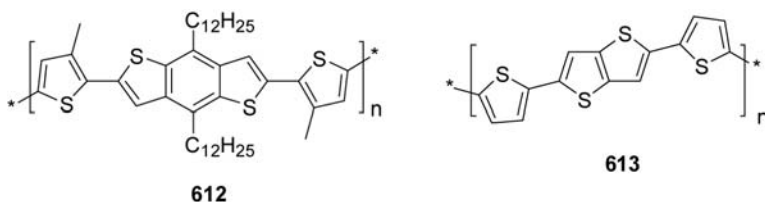


The wavelength of the maximum absorption for **611a–c** was shifted to longer wavelengths as the number of thiophene units increased.

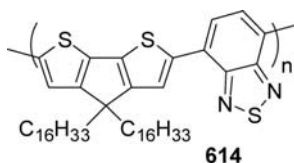
The same trend was observed in the emission spectra of these compounds as the position of the wavelength of the maximum emission was red shifted, ca. 40 nm for each added thiophene.

The highest values were obtained for bis-alanines **611a**, **611b**, and **611d**, with a thiophene, bithiophene, and a phenylthiophene at position 2 of the benzoxazole, respectively, which were found to be strongly emissive ($0.59 < \Phi_{\text{F}} < 0.89$) while **611c**, with a terthiophene bridge, displayed much lower quantum yield ($\Phi_{\text{F}} = 0.14$).

The polymers **612** showed a strong absorption at 481 nm. Two new strong shoulder absorptions at 531 and 580 nm appeared (07JA4112; 07MI3574). On the other hand, the thienothiophene derivatives **613** showed an absorption band at 467 nm, while the film displayed absorption at 496 nm (06AM3029; 07JA3226).

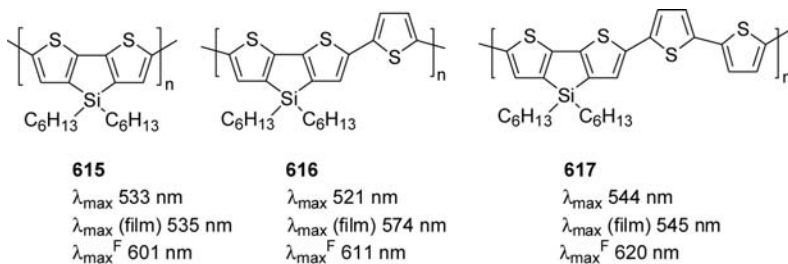


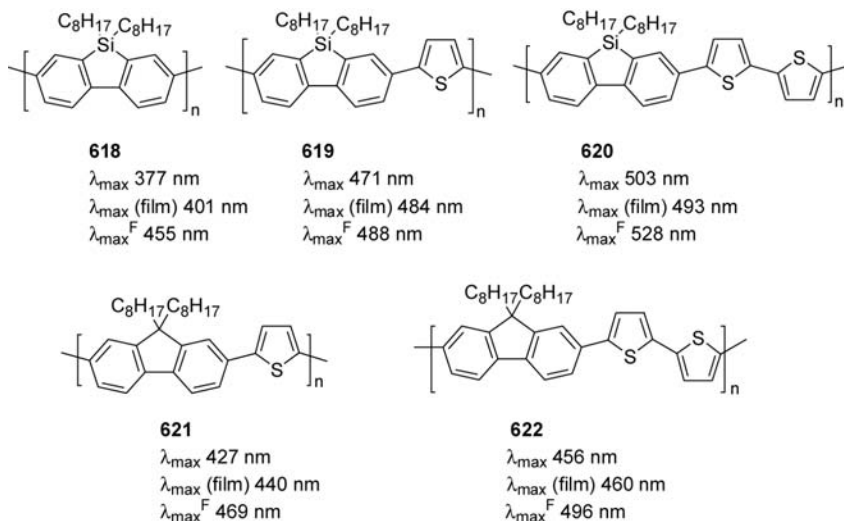
The copolymer **614**, obtained between cyclopentadithiophene and benzothiadiazole, has been reported (07JA3472).



The differences in the optical properties of the polymers reflect the differences in the chemical structures since the number-average degrees of polymerization (DPs) are sufficiently large (>15) to make contributions of the molecular weights negligible (06JA9034; 08JA7670). In THF, polymer **615** exhibits a single absorption maximum at 533 nm, while the solution-cast thin film, which is discontinuous on glass substrates, shows a similar absorption maximum at 535 nm. The absorption maxima for **616** and **617** are located at 521 and 544 nm, respectively, in THF. Polymers **616** and **617** form smooth and shiny thin films when solutions are cast on silicon wafers and exhibit absorption maxima at 574 nm for polymer **616** and 545 nm for polymer **617**. Polymers **615** and **617** exhibit little difference in absorption maxima upon going from the solution to thin film phase; however, the absorption maximum red shifts ~ 50 nm for polymer **616** in the thin film versus solution, suggesting a high degree of macromolecular organization in the thin film phase.

The optical absorption spectra of dibenzosilole-based polymers **618–620** have absorption maxima that are blue shifted compared to those of dithienylsilole **615–617**. The absorption maximum for homopolymer **618** occurs at 377 nm, corresponding to the largest $\pi-\pi^*$ transition energy in the silole-based polymer series.



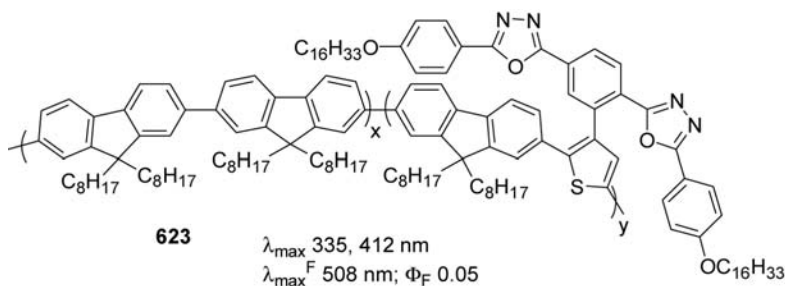


Polymers **619** and **620** exhibit two absorption maxima located at 444 and 471 nm for **619** and 473 and 503 nm for **620**. These transitions likely correspond to predominantly local transitions of the constituent dibenzosilole and mono/bithiophene copolymer building blocks. The absorption maxima of polymer **618–620** cast as thin films are 401 nm (**618**), 484 nm (**619**), and 493 nm (**620**). The fluorine-based copolymers exhibit maxima at 427 nm in solution and 440 nm as a thin film for **621** and 456 nm in solution (with strong shoulder at 502 nm) and 460 nm as a thin film for **622**. Dibenzosilole-based copolymers **619** and **620** exhibit significant bathochromic shifts of ca. 30–50 nm compared to the fluorine-based polymers **621** and **622**.

The optical band gaps of polymers **615**, **616**, and **617** are estimated to be 1.8, 1.8, and 1.9 eV, respectively, and are similar to that of P3HT (1.9 eV). Larger band gaps are observed for the dibenzosilole-based polymers versus dithienosilole-based polymers; the optical band gaps of polymers **618**, **619**, and **620** are estimated to be 2.9, 2.5, and 2.3 eV, respectively. The optical band gaps for material for **621** and **622** are estimated to be 2.5 and 2.4 eV, respectively. Similarities in the optical band gaps of pair **620** and **622** and pair **618** and **621** suggest similarly extended π -conjugation. The dithienosilole-based polymers emit orange-red light with maxima at 601, 611, and 620 nm for **615**, **616**, and **617**, respectively. The dibenzosilole-based polymers exhibit well-resolved vibronic structures for the shorter-wavelength emission maxima. While homopolymer **618** emits blue light with a maximum at 455 nm, copolymers **618** and **620** show green-yellow emission with maxima at 488 and 528 nm, respectively; these transitions are assigned to the 0–0 transition in dilute solutions. The 0–1 and 0–2 transitions in the emission spectra are observed at 477 and 512 nm for

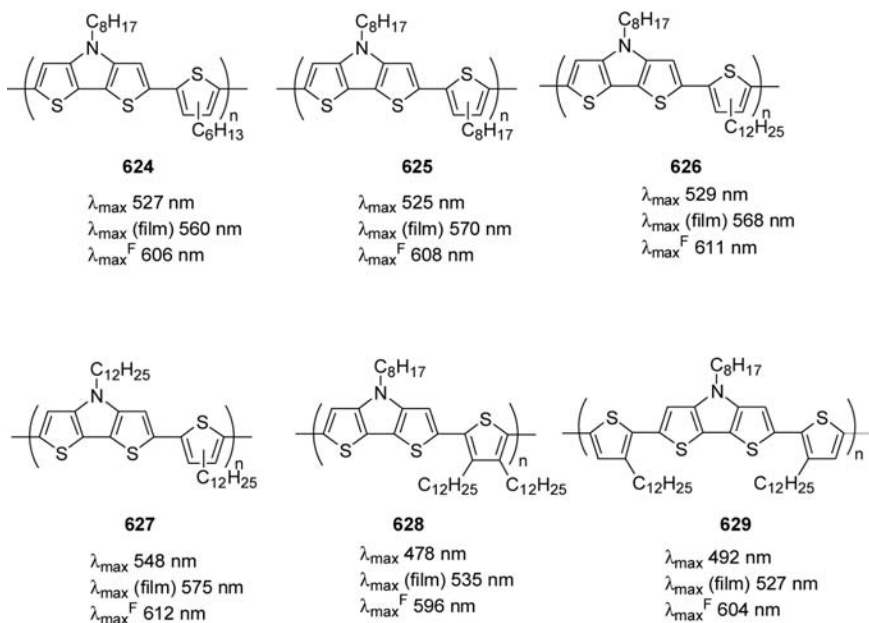
618 and at 521 and 561 nm for **619**. Polymer **620** exhibits a 0–1 transition at 555 nm. The 100–150 nm red shift of emission maxima for **615–617** versus the dibenzosilole-based polymers **618–620** likely indicates weaker π -conjugation in the latter systems. Fluorene-based polymers **621** and **622** exhibit hypsochromic shifts versus the dibenzosilole-based polymers with emission maxima at 469 and 496 nm, respectively. Polymers **619** and **620** exhibit emissions which are ~ 20 – 30 nm red-shifted compared to those of fluorine-based polymers **621** and **622**. The dithienosilole-based polymers **615–616** and homopolymer **618** exhibit large Stokes' shifts of ~ 70 – 90 nm, which are not usual for silicon-containing polymers, and may possibly be due to excimer emission. Polymers **619** and **620** exhibit modest Stokes' shifts of ~ 20 nm between the absorption and emission maxima, which are smaller than those of polymers **621** and **622** (~ 40 nm); this suggests a greater rigidity in the dibenzosilole-based polymers.

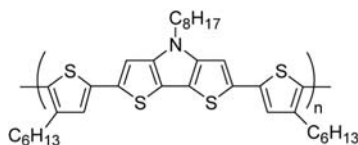
Devices of **616** spin-coated from 1,2-dichlorobenzene exhibit the highest saturated hole mobility of $0.002 \text{ cm}^2 \text{ V}^{-1} \text{ s}^{-1}$ and $I_{\text{on}}/I_{\text{off}} \approx 10^2 - 10^3$ for a channel length of $100 \text{ }\mu\text{m}$, while hole mobilities are comparable for devices having films spin-coated from the other solvents. These films of polymers **617** spin-coated from all solvents exhibit very similar saturated hole mobilities of $\sim 10^{-14} \text{ cm}^2 \text{ V}^{-1} \text{ s}^{-1}$. Devices fabricated from polymers **619** and **620** on untreated SiO_2 substrates show hole mobilities one to two orders of magnitude lower than those from devices fabricated with polymers **616** and **617**. Polymer **619** exhibits the lowest mobility of $5 \times 10^{-16} \text{ cm}^2 \text{ V}^{-1} \text{ s}^{-1}$ with $I_{\text{on}}/I_{\text{off}} = 1 \times 10^4$ for thin films spin-coated from TCB solution. Films of **620** provide the best overall performance for devices spin-coated from TCB solution, with a mobility of $1 \times 10^{-14} \text{ cm}^2 \text{ V}^{-1} \text{ s}^{-1}$ and $I_{\text{on}}/I_{\text{off}} = 1 \times 10^5$. Devices fabricated with polymers **616**, **617**, **619**, and **620** spin-coated on HMDS-passivated SiO_2/Si substrates exhibit greatly enhanced TFT response. After annealing at 150°C under nitrogen, respective mobilities of 0.01 and $0.007 \text{ cm}^2 \text{ V}^{-1} \text{ s}^{-1}$ are obtained for **616** and **617**, with $I_{\text{on}}/I_{\text{off}} = 1 \times 10^4$ for both. The TFT performance of devices with polymers **619** and **620** is also enhanced by this processing methodology, yielding mobilities of 5×10^{-15} and $0.001 \text{ cm}^2 \text{ V}^{-1} \text{ s}^{-1}$ with $I_{\text{on}}/I_{\text{off}}$ ratios of 3×10^4 and 4×10^5 , respectively. For devices annealed at 250°C , the highest mobilities of **616** and **617** are found to be 0.05 and $0.08 \text{ cm}^2/\text{V s}$, with $I_{\text{on}}/I_{\text{off}}$ ratios of 1×10^5 and 5×10^4 , respectively. For polymers **619** and **620**, the maximum mobilities are 6×10^{-15} and $0.006 \text{ cm}^2 \text{ V}^{-1} \text{ s}^{-1}$ with $I_{\text{on}}/I_{\text{off}}$ ratios of 3×10^4 and 4×10^6 , respectively. OTFT devices fabricated with fluorine-based copolymers exhibit hole mobilities of $9 \times 10^{-15} \text{ cm}^2 \text{ V}^{-1} \text{ s}^{-1}$ with $I_{\text{on}}/I_{\text{off}}$ ratios of 2×10^5 for **621** and $0.006 \text{ cm}^2 \text{ V}^{-1} \text{ s}^{-1}$ with $I_{\text{on}}/I_{\text{off}}$ ratios of 2×10^5 for **622**. OTFT devices fabricates with polymers **616**, **617**, **620**, and **622** switch on crisply at around 0.0 V . OTFTs fabricated using materials **616**, **617**, **620**, and **622** operate well in air, exhibiting very good ambient storage stability and electrical stability.



More recently, more complex structures, such as **623**, have been synthesized, showing interesting properties for OLED applications (09MM1037).

The synthesis, characterization, electrical conductivity, and field effect mobility of a series of novel soluble *N*-alkyl dithieno[3,2-*b*:2',3'-*d*]pyrrole (DTP) and thiophene (TH)-based copolymers (DTP-*co*-THs) were reported (06MM1771; 08JA13167). The incorporation of DTP units extends π conjugation, and the introduction of thiophene subunits imparts good solubility, high conductivity, and high charge carrier mobility. Therefore, the incorporation of DTP units and various substituted thiophenes into the polymer backbone affords the ability to enhance the solubility, lower the band gap, and achieve the enhanced electronic properties.



**630** λ_{max} 473 nm λ_{max} (film) 477 nm $\lambda_{\text{max}}^{\text{F}}$ 594 nm

The results suggest that the presence of highly ordered microcrystalline structures in thin films of polymeric semiconductors is not necessary for excellent performance of organic transistors. The maximum absorption (λ_{max}) corresponds to a π – π^* transition and a large λ_{max} signifies a long effective conjugation length.

629, which consists of alternating DTP- and TT-coupled alkylthiophene units, exhibited a thin film λ_{max} at 527 nm. In sharp contrast, **630**, which has HH-coupled alkylthiophene units, displayed a much shorter λ_{max} at 477 nm. This may be due to a dramatic decrease of conjugation caused by steric hindrance of the HH linkage between thiophene units. These results indicate that the effective conjugation length also depends on the twist angle of the polymer's backbone. There is no obvious influence on alkyl chain length. Interestingly, **627** with both dodecyl groups on DTP a thiophene units had the highest λ_{max} in both film and solution. Comparing **628** with **627**, polymers with dialkylthiophene units showed smaller λ_{max} than those with monoalkylthiophene units (**624**–**627**) due to the steric repulsions.

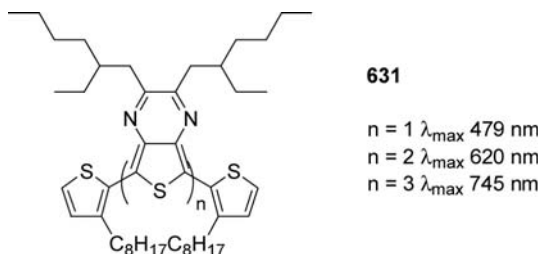
624–**627** and **629** exhibit red emission with λ_{max} of 600–615 nm along with shoulders around 660 nm. These shoulders suggest better resolved vibronic structures, indicating higher ordered polymer structures, which can also be supported by the small Stoke's shift of **624**–**627** and **629**. In the case of solid state, only **630** was detected to exhibit fluorescence, which has a λ_{max} of 642 nm. This might be because **624**–**629** have a relatively rigid structure that facilitates aggregation in the solid state, favors the interchain excitations, and hence quenches the fluorescence.

The optical band gaps (E_g) of all the polymer were determined from UV/Vis absorption onset. Polymers **624**–**629** have band gaps between 1.74 and 1.86 eV, which are smaller than *rr*-P3HT (1.90 eV). This low band gap can be due to the more coplanar structure of the polymer and the weak donor–acceptor effect of DTP and THs. Regioirregular **624**–**627** have a 1:1 ratio of TH/DTP units in the backbone. They have the band gaps between 1.74 and 1.79 eV.

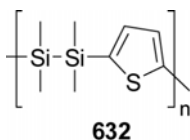
Model compounds of **627**, **629**, and **630** containing methyl side groups were designed for the calculations. The results revealed that all the

adjacent rings prefer to be *trans* to each other. If the adjacent thiophene rings have a TT linkage or if the tail of the thiophene rings is linked with adjacent DTP rings, the two adjacent rings prefer *trans* coplanarity. The calculated energy barrier for adopting a *trans* planar conformation is $<0.2 \text{ kcal mol}^{-1}$. In contrast, the minimum energy geometry of model compound **630** is highly twisted at the HH linkage with a dihedral angle γ of 120° . Up to $5.5 \text{ kcal mol}^{-1}$ is required to adopt a *trans* coplanar conformation from this minimum energy geometry. Therefore, it may be unlikely for HH coupling thiophene rings to adopt planarity. This result indicates that the HH linkages in the polymer backbone decrease conjugation, increase the band gap, and inhibit intrachain charge transfer.

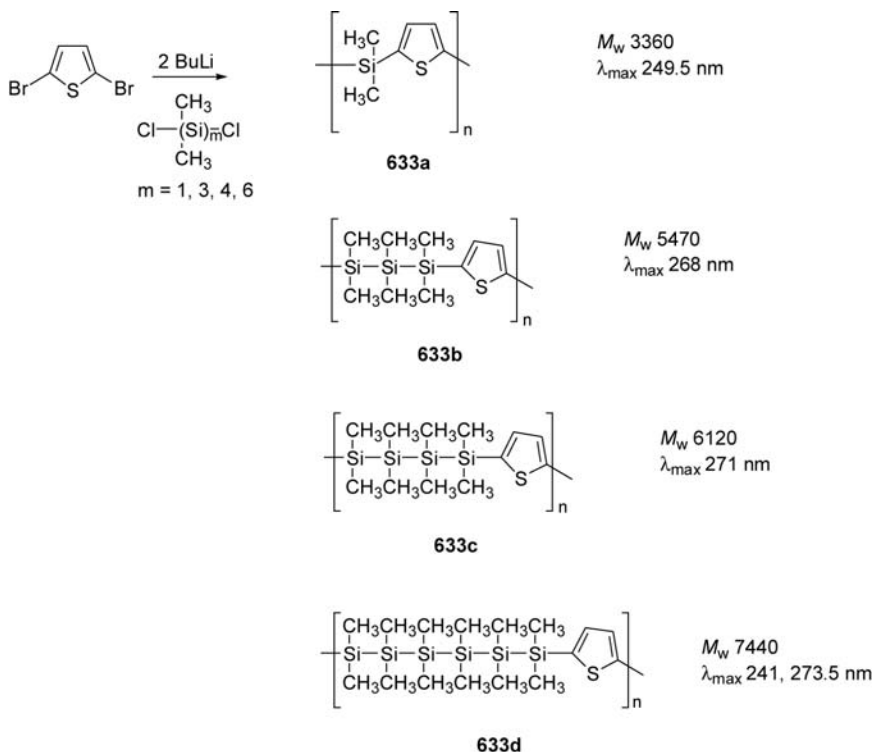
Poly(2,3-alkylthieno[3,4-*b*]pyrazine)s **631** were prepared showing that adding extra thieno[3,4-*b*]pyrazine units causes a large shift and an increase of the molar absorption coefficient of the low energy absorption band (08OL3513).



The polymer **632** was photoactive (94JOM(468)55): irradiation of thin films with a 6 W low-pressure mercury lamp bearing a Vycor filter in air for 1 h led to the disappearance of the characteristic absorption at 265 nm attributed to disilanylthienylene unit. Irradiation in benzene in the presence of *t*-butyl alcohol gave the formation of a photoproduct with lower molecular weight. On the contrary, if the photolysis was performed without *t*-butyl alcohol, cross-linking occurred during the reaction and a photoproduct with a higher molecular weight than the native polymer was isolated. The reactivity was explained assuming the homolytic fission of Si-Si bond.



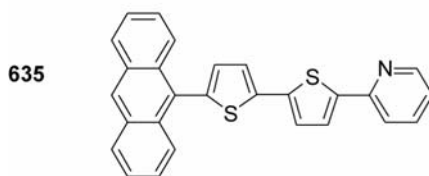
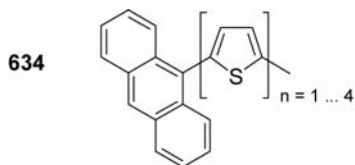
The silylene-thienylene copolymers were prepared as shown in Scheme 29 (95JOM(489)15).



Scheme 29

The thermochromism of the copolymers **633a–d** was investigated. With decreasing temperature, the absorption spectrum of **633a** does not show the red shift of the absorption peak. With **633d** the red shift is shown. The absorption maxima and the extinction coefficient ϵ per repeating unit in the solution state increase with increasing number of silylene units. This means that conjugation along the backbone is enhanced by increasing the number of silylene units. The red shift of the silylene-thienylene copolymers compared with α,ω -dichloropermethylenated oligosilanes may be caused by electron delocalization through the $\sigma-\pi$ conjugation. The thermochromism of the polysilanes is caused by the conformational change of the Si-Si chain. The red shift was scarcely observed in **633a**. The red shift was observed in **633b–d** which have dimethylsilylene chain lengths greater than 3. These results suggest the existence of $\sigma-\pi$ conjugation between dimethylsilylene units and π units and that the conjugation is enhanced by an increase in the dimethylsilylene chain length.

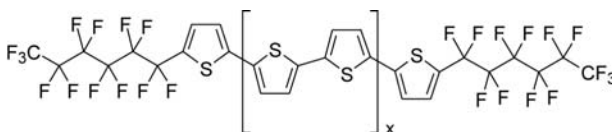
The lowest excited triplet state in anthryl-oligothiophenes (**634**) were studied (96CPL(260)125). Also, binaphthyl oligothiophenes have been studied (09MM1710). The triplet state properties are studied with respect to coupling effects between the molecular subunits for a different chain length n and also for additional pyridine substitution (**635**).



Low temperature spectra of the singlet \rightarrow triplet ($S_0 \rightarrow T_1$) absorption in crystalline samples have been measured using the photoexcitation technique.

Thiophene-perfluoroarene copolymers have been described (06JA2536). Absorptions in the range 334–360 were reported.

Optical absorption and fluorescence spectra of oligofluoroalkylthiophene **636–640** in tetrahydrofuran (THF) solution exhibit strong absorption [λ_{\max} (nm): **636** (308), **637** (360), **638** (398), **639** (421), and **640** (443)] and emission [λ_F (nm): **636** (369), **637** (417, 437), **638** (458, 489), **639** (493, 525), and **640** (515, 547)] in the UV-visible region (03AM33). Furthermore, λ_{\max} decreases monotonically across the series **636** \rightarrow **640** with decreasing numbers of thiophene units.

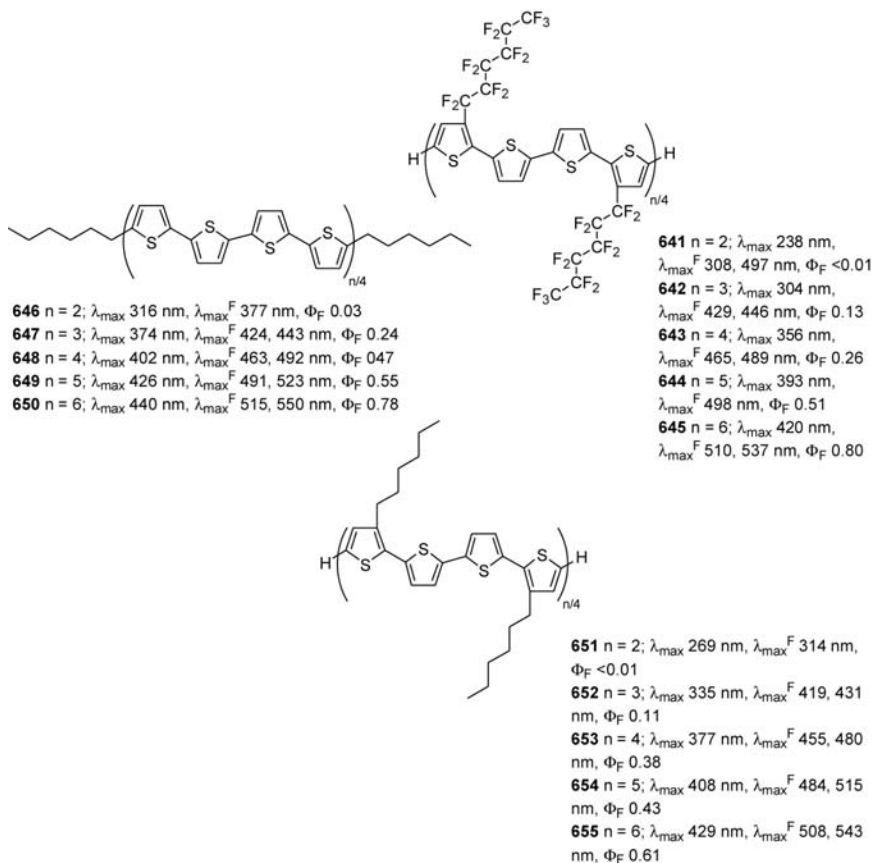


- 636:** $X = 2$
637: $X = 1.5$
638: $X = 1$
639: $X = 0.5$
640: $X = 0$

TFT devices based on **638**, **637**, and **636** have been fabricated. Mobilities (μ), current on/off ratio ($I_{\text{on}}/I_{\text{off}}$) and threshold voltages (V_T) are collected. The data clearly show that both n-type carrier mobility and $I_{\text{on}}/I_{\text{off}}$ ratios increase with decreasing π -core conjugation length (**636** \rightarrow **638**), approaching $0.05 \text{ cm}^2 \text{ V}^{-1} \text{ s}^{-1}$ and 10^5 , respectively. The threshold voltage is 35–42 V for **636** and **637** and 25–30 V for **638**. Remarkably similar trends in mobility and $I_{\text{on}}/I_{\text{off}}$ ratio are found in the p-type series. A more detailed study on this type of compounds appeared (04JA13480).

Optical absorption and fluorescence spectra of **636**–**655** were measured both in solution and as thin films to assess the effect of both fluoroalkyl- versus alkyl- and α,ω - vs β,β' -substitutions on oligothiophene absorption and emission maxima ($\lambda_{\text{abs}}/\lambda_{\text{em}}$) and the (optical) HOMO–LUMO energy gap.

The large molar absorption coefficients (ϵ) indicate the dominance in the optical spectra of the allowed conjugated core $\pi \rightarrow \pi^*$ transition. As expected, **636**–**655** λ_{abs} values increase throughout the series ($n = 2 \rightarrow 6$) for increasing numbers of thiophene units. The magnitude of this shift [$\Delta\lambda_{\text{abs}}^{2T \rightarrow 6T} = \lambda_{\text{abs}}(n = 6) - \lambda_{\text{abs}}(n = 2)$] from 2T to 6T derivatives is 135, 124, and 132 nm for **636**–**640** and **646**–**653**, respectively, with the latter value being close to the 130 and 133 nm measured for the unsubstituted oligothiophenes in CH_2Cl_2 and dioxane, respectively. A much larger displacement is observed in both **651**–**655** families with a $\Delta\lambda_{\text{abs}}^{2T \rightarrow 6T}$ of 182 and 160 nm, respectively. This result is due mainly to the short wavelength absorption of 238 and 269 nm for **641** and **651**, respectively, compared to 2T (304 nm). The former value is close to the absorption of thiophene (230 nm in THF), providing additional evidence that the **641** core is essentially deconjugated in solution. When comparing the absorption of systems with the same core [$\Delta\lambda_{\text{abs}}^{nT}(\mathbf{x} \leftrightarrow \mathbf{y}) = |\lambda_{\text{abs}}^{nT}(\mathbf{x}) - \lambda_{\text{abs}}^{nT}(\mathbf{y})|$; $\mathbf{x}, \mathbf{y} = 1\text{--}4$], with the exception of **640** and **650** for which the $\Delta\lambda_{\text{abs}}^{6T}(\mathbf{636}\text{--}\mathbf{640} \leftrightarrow \mathbf{646}\text{--}\mathbf{650})$ value shifts bathochromically by ~ 3 nm (note that the **640** spectrum was recorded at $\sim 60^\circ\text{C}$), all of the remaining fluoroalkyl-substituted systems **636**–**640** and **640**–**645** experience, compared to their alkyl analogues **646**–**650** and **651**–**655**, a hypsochromic shift (5–31 nm), which can be explained by alkyl group inductive and hyperconjugative effects. In addition, in α,ω -disubstituted n Ts **636**–**640** and **646**–**650**, λ_{abs} values are bathochromically shifted compared to those of the corresponding β,β' -isomers **641**–**645** and **651**–**655**, respectively, probably because β,β' -disubstitution engenders steric interactions that distort the conjugated π -core from planarity in solution.



Photoluminescence quantum yields (Φ_f) values are found to increase quasi-monotonically with the number of thiophene rings. This behavior is similar to that found in the n T series in dioxane, where Φ_f was found to increase up to six rings and then remain stable or even decrease for longer oligomers. With the exception of highly twisted oligomers **641** and **651**, substitution of either α,ω - or β,β' -positions is found to increase the solution quantum yield. Fluorocarbon substitution is found to markedly increase the solution photoluminescence quantum yields in all case, with the efficiency of **640** approaching unity. This effective modulation of quantum efficiency by chemical substitution must be related to changes in the relative positions of the lowest excited states within the singlet and triplet manifolds and, hence, to changes in the decay rate via efficient nonradiative channels, such as intersystem-crossing processes due to excimer formation (self-quenching) and intramolecular vibrational or rotational modes. A lower Φ_f is observed when the substituents are displaced from terminal to lateral positions.

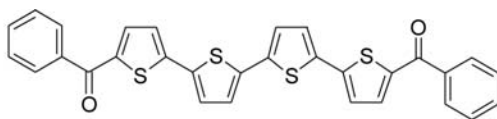
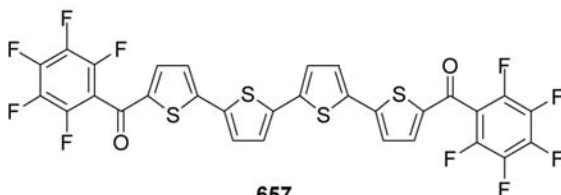
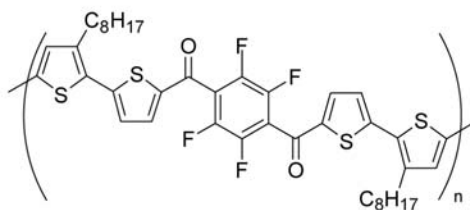
In general, the excited states of **636–655** having the same n differ less electronically than the corresponding ground states, probably because of the rigidification of the excited-state quinoid structure. The quinoid form, which has an intrinsically higher degree of coplanarity, is apparently more effective in planarizing the more sterically hindered isomers. In other words, the excited states of **641–645** and **651–655** are still less planar than those of **636–640** and **646–650**, but much more so than might be anticipated from ground-state considerations. The change in conformation to a more planar structure and energy dissipation during the excited-state lifetime are manifest in Stoke's shifts, rigorously defined as the energy difference between the 0–0 transitions in absorption and emission. The observed general trend here is that $\Delta(\lambda_{\text{em}} - \lambda_{\text{abs}})$ decreases with increasing n and the repositioning of substituents from lateral to end positions. Chemical substitution appears to have only a marginal effect. The amplitude of this shift generally tracks the lifetime of the excited state, with longer lifetimes corresponding to increase relative probability of nonradiative decay and correlates with lower PL quantum efficiency. Indeed, these results are in good agreement with the present quantitative Φ_{f} measurements.

Solution optical gaps (E_{g}^{op}) were estimated from the intercept of the normalized optical absorption and emission spectra, regarded as mirrors of the 0–0 transitions. The gaps increase with contraction of the core, from 2.52 to 2.62 eV for 6T derivatives ($n = 6$) to 3.50–4.33 eV for the shortest 2T ($n = 2$) series. E_{g}^{op} values remain in a very narrow range ($\Delta E_{\text{g}}^{\text{op}} \leq 0.11$ eV) for oligomers **636–655** ($n = 4–6$), and increase for shorter oligomers **636–655** ($n = 3$) ($\Delta E_{\text{g}}^{\text{op}} \leq 0.25$ eV) and **636–655** ($n = 2$) ($\Delta E_{\text{g}}^{\text{op}} \leq 0.83$ eV).

UV/Vis/PL data for molecules **636–640**, **646–650** ($n = 3–6$), **641–645** ($n = 4–6$), and **651–655** ($n = 5, 6$) as vacuum-deposited thin films were collected. The absorption spectra exhibit characteristic peak(s) at high energy (270–280 nm) found in the spectra of all oligothiophenes and origin from the thiophene ring. With a strong absorption at 340–380 nm followed by two weaker peaks or shoulders at 410–520 nm. The intense peak at high energies can be attributed to exciton interactions between closed-packed nearest-neighbor molecules

E_{g}^{op} values decrease as the core conjugation length increases and are larger for the β,β' -substituted systems. In general, film E_{g}^{op} values are smaller by 0.1–0.4 eV than the corresponding solution values. A similar trend has been observed for other oligothiophenes.

Nonfluorinated material **657** exhibits hole mobilities (μ_{h}) in vapor-deposited films of $0.043 \pm 0.008 \text{ cm}^2 \text{ V}^{-1} \text{ s}^{-1}$ ($I_{\text{on}}/I_{\text{off}} = 10^5$; $V_{\text{T}} \sim -20 \text{ V}$) (05JA13476). UV/Vis absorption in THF indicates that the optical band gap (E_{g}) is ~ 2.40 eV for **656** and 2.46 eV for **657**. Films of the neat polymer exhibit $\mu_{\text{e}} \sim 10^{-16} \text{ cm}^2 \text{ V}^{-1} \text{ s}^{-1}$. An initial study reveals that blends of **656** and **658** yield films with a $\mu_{\text{e}} \sim 0.01 \text{ cm}^2 \text{ V}^{-1} \text{ s}^{-1}$ ($I_{\text{on}}/I_{\text{off}} = 10^4$; $V_{\text{T}} \sim 60 \text{ V}$).

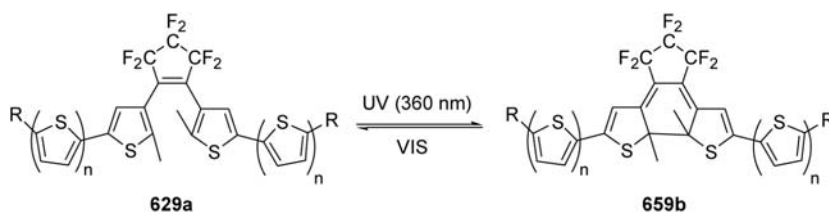
**656****657****658**

Highly efficient polymer/fullerene (both C_{61} -PCBM and C_{71} -PCBM were employed) solar cells have been described in which a 3D network of preassembled polymer-semiconductor nanowires serves as the donor component in a sea of fullerene acceptors (05MI13; 06MI2263; 07MI1071; 07SCI(317)222; 08JA5424). In addition to the absorption maximum (λ_{\max}) of the nanowire suspension ($\lambda_{\max} = 502$ nm) which is red shifted from the solution ($\lambda_{\max} = 463$ nm), two additional lower-energy shoulder peaks appear at 565 and 615 nm and are characteristic of the crystalline P3BT. The optical absorption spectra of spin-coated thin films of P3BT-nw/ C_{61} -PCBM (1/1 wt ratio) nanocomposite (70 nm) and P3BT: C_{61} -PCBM (1:1 wt ratio) blends (80 nm) are identical as well as similar to P3BT-nw suspension. Blends of oligothiophenes and C_{60} showed a large quenching of the luminescence due to an efficient energy transfer; on the contrary, in the presence of 1,2-dichlorobenzene or TCNE, electron transfer occurs (94JCP (101)9519; 95JCP(102)2628). Poly(thiophene)-fullerene blends were tested using a poly(1,3-dithienylisothanaphthene) derivatives (λ_{\max} 458–468 nm) (01JPC(B)11106). Polythiophene linked to fullerene and tetraarylporphyrin derivatives has been reported (05JA15372). A copolymer porphyrin-thiophene has been described. It showed absorptions bands 424, 451, 555, and 603 nm in solution and at 446, 561, and 615 nm in a thin film. A blend with PCBM showed absorption band at 451, 563, and 616 nm. It

emitted at 626 nm in solution, at 641 nm in the thin film, and at 820 nm in the blend. Photovoltaic properties have been studied (09JPC(C)10798).

Oligothiophene derivatives can also be inserted in a polyester matrix. A quaterthiophene derivative–polyester showed an absorption band at 407 nm and fluorescence emissions at 482 and 507 nm ($\Phi_F = 0.17$; $\tau_F = 0.41$ ns) (98MM6289).

Poly(thiophene) derivatives were obtained starting from a terthiophene unit bearing a spironaphthoxazine group with photochromic properties (95JCS(CC)471; 95MM4548). Polythiophenes bearing a dithienylethene photochromic system have been prepared (08AM1998). Other dithienylpyrrole polymers bearing a photochromic system have been prepared (05NJC1128). The UV spectrum of thiophene oligomers, such as **659a** has a peak at 326 nm (96JPC4689).



Upon UV irradiation, the spectrum has a sharp peak at 352 nm a broad absorption band at 620 nm, corresponding to the closed-ring form. The closed-ring form can be completely converted to the open-ring form by irradiation at 532 nm. In transient spectra, just after the excitation, the spectrum has a peak at around 460 nm. In addition, another absorption band at 515 nm clearly appears at a delay time of 0.2–0.4 ps. As time progresses, the absorbance at 515 nm decays rapidly and is replaced by a broad absorption band in the wavelength range from 590 to 660 nm. After 1.2 ps, the absorption maximum is positioned at ~ 620 nm. The absorption at 460 nm is due to the $S_n \leftarrow S_1$ absorption of the open-ring form of the thiophene oligomer. It is worth noting that the absorbance at 515 nm decays faster than the peak at 460 nm. At a delay time of 30 ps, the spectrum at 515 nm completely disappears, although the spectrum at 460 nm still remains, in which the absorption spectrum is composed of 460 and 620 nm bands. This result indicates that the relaxation from the S_1 state is not the main process of the ring-closure reaction.

The decay curve recorded at 515 nm was analyzed by the sum of two- or three-exponential functions. The fitting to the experimental data with a three-exponential function was always better than a two-exponential function. The fast decay component with a time constant of 1.1 ps (59%), corresponding to the fast rise time at 650 nm, and a very fast rise time of 70–110 fs (73%), were obtained in addition to the long decay component. From these results, it is concluded that the closed-ring form is mainly formed from the species with an absorbance maximum at 515 nm with a

time constant of 1.1 ps. During the relaxation process in the S_1 state, some portions of the excited open-ring form undergo a cyclization reaction, and others relax to the fluorescent state in which the conformation is unfavorable for the cyclization reaction.

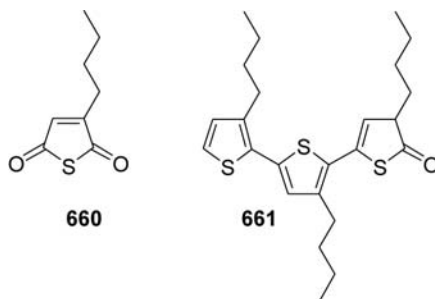
Upon excitation of the open-ring form, some intermediate with a peak at 515 nm is formed from the antiparallel conformer prior to relaxation to the vibrationally relaxed S_1 state. The closed-ring form is mainly formed from the intermediate species with a time constant of 1.1 ps. One possible interpretation of the species is a diradical-like intermediate. This result suggests deviation from a synchronous concerted reaction.

Photophysical and electron transfer properties have been studied also in poly(3-octylthiophene) linked to Ru(II) and Os(II)-bipyridine (00IC5496).

14. PHOTOOXIDATION

Despite the fact that optical applications require thin films of poly(3-alkylthiophene)s, the photochemistry of these materials has been characterized in solution but only scarcely in the solid state. The UV/Vis spectra of these films of poly(3-butylthiophene) show an absorption band in the visible range corresponding to a $\pi-\pi^*$ transition whose energy depends on π -electron delocalization.

Photoirradiation experiments of P3-BT were carried out under nitrogen, air, or oxygen atmosphere using lamps irradiating in the visible range (97CM991). Substantial differences in the electronic spectra were found only when irradiation was performed in air or oxygen, showing that the polymer itself is photochemically stable in an inert atmosphere, while degradation occurs in the presence of oxygen. A plausible mechanism of photooxidation is an energy transfer from the excited polymer to oxygen, forming singlet oxygen that in turn will react with the conjugated chain. This statement is in accordance with a recent report by Heeger et al., which confirmed the existence of the ISC in poly(3-octylthiophene); thus, this triplet state can transfer energy to oxygen forming singlet oxygen. The first molecule was identified as a thioanhydride **660** and **661**.



Indeed treatment of the irradiated plates with CHCl_3 shows the presence of insoluble material, indicating that more complex polymer systems are present. *N*-Hexadecyl-*N*-methylaniline (HMA) and 1-phenyldodecan-1-one (PDK) were studied. The plots show the effect of the addition of HMA and PDK, revealing striking differences between the two substances at least with wavelengths, concentrations, and time of irradiation used. While the protection by HMA depends on its concentration, the one of PDK seems rather insensitive to that parameter and in any case appears to give better results. From these data, it is possible to exclude that the slowing down in the degradation is due to an energy transfer from the excited polymer to the additive, but rather the reverse may occur.

In the case of the sample with PDK, acetophenone and dec-1-ene were isolated, showing that the Norrish type-II reaction is operating. A hypothesis that can be put forward is that, with different efficiency, the aniline and the ketone additives act essentially as a light screen without transfer of energy to the polymer.

Little is known on their photochemistry. It is pertinent to investigate photochemically induced reactions of poly (3-alkylthiophenes) (91MM2119).

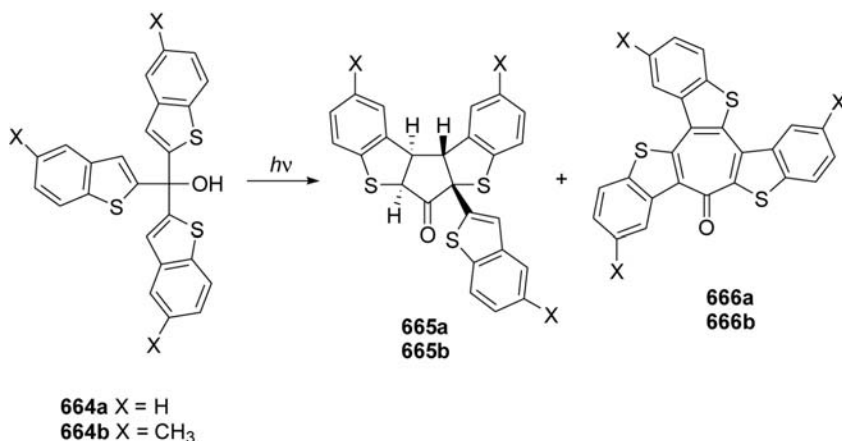
Irradiation of P3HT in O_2 -saturated organic solvents, using 313-nm light, decreases the molecular weight of the polymer. The rate of chain scission is greatly reduced when oxygen is absent. The quantum yields decrease in the order $313 > 366 > 436$ nm. In O_2 -saturated tetrahydrofuran, the quantum yields of chain scission decreased, compared to CHCl_3 , by factors of 22, 12, and 14 at 313, 366, and 436 nm, respectively. In N_2 -purged THF the quantum yield was 14 times smaller than that observed in deoxygenated CHCl_3 at 313 nm. In O_2 -saturated benzene, the quantum yield was 3.64×10^{-15} at 313 nm, slightly lower than that determined in THF at 313 nm.

The lowest triplet state of oligomeric thiophenes is an efficient singlet oxygen photosensitizer. Following photolysis of P3HT in the presence of oxygen, the residual polymer absorbs strongly at 1209 and 1161 cm^{-1} , indicating the formation of a sulfine residue. This is indirect evidence for the photosensitization of singlet oxygen by poly(3-hexylthiophene).

It is well established that singlet oxygen undergoes addition to polymeric double bonds to yield an allylic hydroperoxide and that photolysis of the hydroperoxide initiates an autocatalytic chain reaction which leads to chain scission. It is inferred that the hydroperoxide mechanism is responsible for photochain scission of P3HT since a large number of polymeric double bonds exist, singlet oxygen is produced *in situ*, and quantum yields for chain scission are low and are markedly dependent on the nature of the solvent and on the incident wavelength.

15. PHOTOCHEMICAL CYCLIZATION

An intramolecular photocyclization of tris(2-benzo[*b*]thienyl)methyl alcohol (**664a**) to afford five- and seven-membered products has been reported (02TL8669). The irradiation of **664a** gave cyclopentanone **665a** (43%) and benzo[*b*]thiophene-condensed tropone derivative **666a** (23%) along with recovered **664a** (ca. 30%).

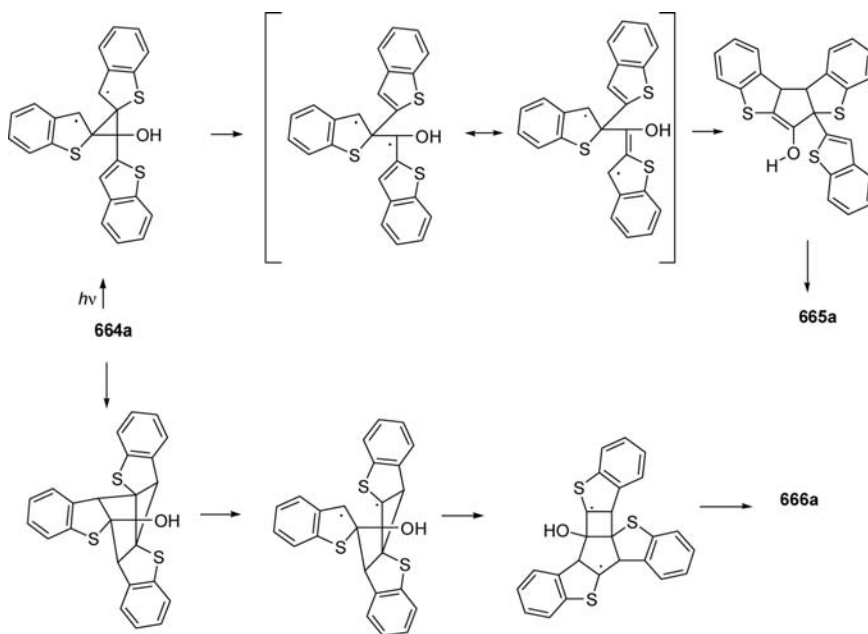


A similar photoreaction was induced also in methyl-substituted derivative **664b**, giving rise to **665b** (33%) and **666b** (30%).

The interconversion between **665a** and **666a** was not induced under the photolysis conditions. Thus, the photoproducts are not precursors to each other. The isomerization of **664a** to **665a** is interpreted based on the di- π -methane rearrangement which involved the two benzo[*b*]thiophene rings in **664a**; a resonance structure of the 1,3-diradical, which is formed via the 1,4-diradical intermediate of the di- π -methane rearrangement, could make its cyclization possible to give a cyclopentene framework.

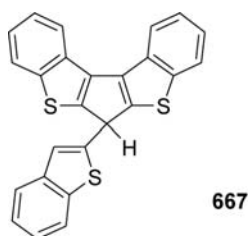
As for the formation of a novel product **666a**, the bond formation between the α and β carbons among three thiophene rings are most plausible as an initial photoprocess. The resulting 1,6-diradical intermediate of a bicyclo[2.2.0]hexane backbone could undergo rearrangement, ring expansion, and oxidation finally to produce **666a** (Scheme 30).

664a was irradiated in methanol. However, no photosolvolysis took place or give the methoxy derivative, but again **665a** and **666a** were obtained in 45 and 22% yields, respectively. In contrast, irradiation in *n*-hexane resulted in the formation of a cyclopentadiene compound **667**



Scheme 30

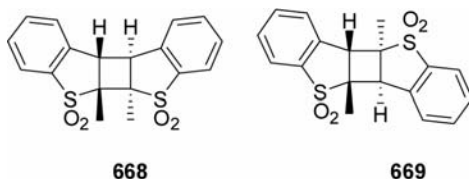
(41%). It seems most likely that **667** is formed via *tert*-carbocation and subsequent ring-closure by intramolecular electrophilic attack.



16. PHOTOCHEMISTRY OF THIOPHENE S-OXIDE AND SULPHONE

The photodimerization of 2-methylthianaphthene 1,1-dioxide (MeTND) as a function of solvent, concentration of MeTND, sensitizers, and quenchers (49JCS381; 50NAT(166)108; 56JA6174; 77AJC173; 79JA2157) showed the photodimerization gave a single product in good yield. We have found

that irradiation at 313 nm of rigorously degassed solutions of MeTND produces two dimers in about a 9:1 ratio. When oxygen is present, the quantum yield decreases and the two dimers are produced in similar proportions. The dimers of MeTND were initially assigned anti head-to-head (HH) **668** and anti head-to-tail (HT) **669** geometries.

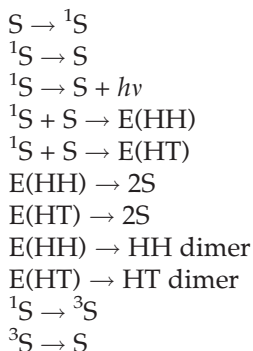


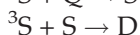
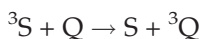
Solutions of MeTND in cyclohexane show a fluorescence maximum at 355 nm when excited at 313 nm. The fluorescence quantum yield, Φ_F , of MeTND was found to be 0.020. The Φ_F is 0.011 for 2-bromothianaphthene 1,1-dioxide. Flash spectroscopy showed that the lifetime of excited singlet MeTND was <3 ns.

The photodimerization of MeTND at 313 nm was studied as a function of substrate concentration in benzene, dibromomethane, and 1-bromobutane.

The lifetime of the precursor for the HT dimer is on order of 10^{-19} s, suggesting that this dimer arises from an excited singlet state, possibly a singlet excimer.

The curved Stern-Volmer plot for the HH isomer suggests that it arises from both an excited singlet and an excited triplet state. This suggests that about 3, 1.5, and 3% respectively of the HH isomer is singlet derived in each solvent. The 360-nm irradiation of MeTND and benzophenone was explored in a solution of benzene, dibromomethane, and 1-bromobutane. The very efficient quenching of the HH isomer formation by COT implies that the majority of this isomer is formed from a triplet-state precursor. The unquenchable part of the HH isomer appears to be derived from singlet-state precursors, possibly singlet excimers.





The TTA spectrum of benzophenone observed by laser flash photolysis indicates that strong TTA was completely quenched by the addition of MeTND. Energy transfer is indeed 100% efficient.

Triplet quencher, *trans*- α -methylstilbene has a triplet energy level about 50 kcal mol⁻¹ and does not absorb at the irradiating wavelength of 313 nm. When thianaphthene 1,1-dioxide was irradiated in the presence of this quencher, the production of photodimers was negligible. The triplet state of the starting material was quenched. Thianaphthene 1,1-dioxide was irradiated at 366 nm in the presence of a variety of triplet sensitizers [72]A8179]. At this wavelength thianaphthene 1,1-dioxide does not absorb any light; in all cases, >98% of the light is absorbed by the sensitizers. Experiments of this type have been used to support a mechanism proceeding wholly *via* the triplet excited state.

The triplet energy of thianaphthene 1,1-dioxide was determined by two indirect methods. The first involved the use of several sensitizers of decreasing triplet energy. The results summarized in Table 1 indicate that E_{triplet} lies between 53 and 49 kcal mol⁻¹. The second method is more precise and involves the use of thianaphthene 1,1-dioxide as a sensitizer to establish a photostationary state of the α -methylstilbenes. The composition of the photostationary state of α -methylstilbene has been determined as a function of the triplet energy level of the sensitizer. The results indicate a triplet energy for thianaphthene 1,1-dioxide of 50 ± 1 kcal mol⁻¹. Quantum yields of the photodimerization of thianaphthene 1,1-dioxide were determined in benzene as a function of concentration. Φ_{isc} is 0.18. The product distribution as a function of solvent polarity demonstrates the ratio of the head-to-head to head-to-tail dimer (HH/HT) increases with the polarity of the solvents. This is consistent with preferential solvation of the head-to-head transitions state.

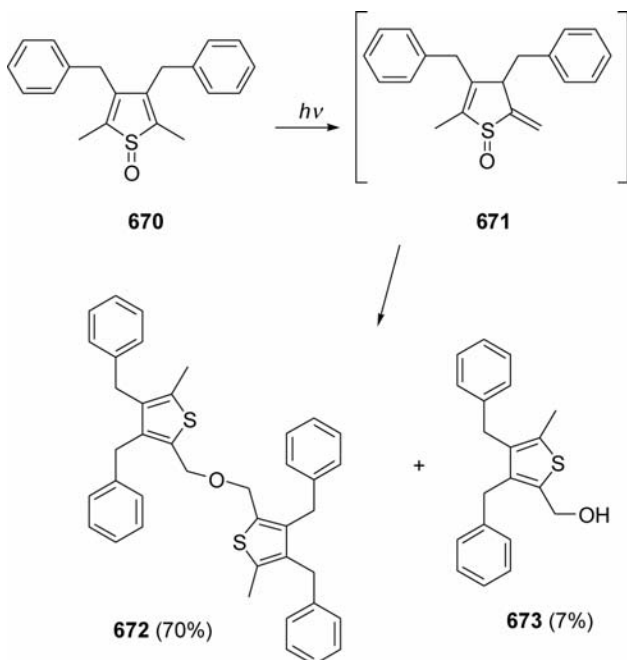
These results are consistent for a photodimerization which involves attack on the ground-state molecule by the triplet excited state.

The increase of HH over HT dimers with an increase in solvent polarity was due to the selective formation of these intermediates rather than their selective decomposition.

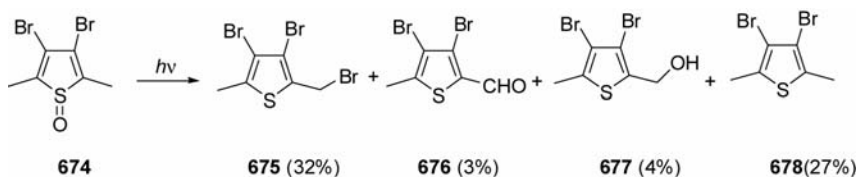
In the head-to-head transition state, the component dipoles point in the same direction and the net moment is expected to be greater than that of the head-to-tail transition state where the component dipoles lie in opposite directions. Therefore, the solvent effect appears due to the polarity differences in the transition states leading to the head-to-head and head-to-tail dimers. 2-Methylbenzothiophene oxide gave the corresponding

benzothiophene derivative, but 3-methylbenzothiophene oxide gave the corresponding dimers (78TL999; 81JOC4258).

Upon irradiation with light **670** deoxygenates rapidly (00JPO648) to two products **672** and **673**, where **671** could be formulated as an intermediate.



The irradiation of **674** leads to a number of products, where the progress of the reaction is much slower compared with **670**. While an intermediate as discussed above may be formulated once again, here, bromo radicals are formed which lead to 2-bromomethyl-3,4-dibromo-5-methylthiophene (**675**) potentially as well as to **676** by the addition of a bromo radical to **677** with subsequent cleavage of the bromohydrin.

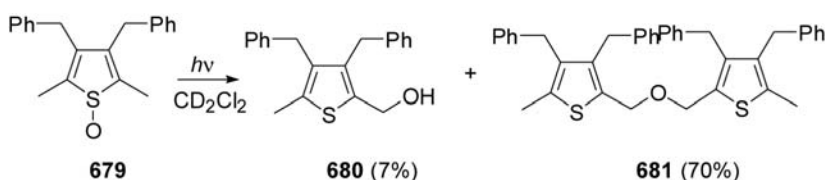


In the presence of amines or thiophenols, photoirradiation of a thiophene-S-oxide leads exclusively to the corresponding thiophene.

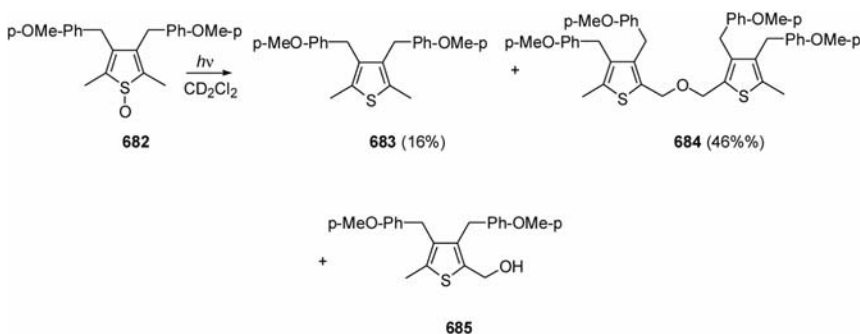
Dibenzothiophene-*S*-oxide derivatives do not deoxygenate when photoirradiated under conditions used in this study.

When standing in solution, a slow conversion of the thiophene *S*-oxide takes place and after some time a noticeable amount of the corresponding thiophenes is formed, among other products. The conversion is accelerated upon exposure to light. In order to understand the conversion processes under these conditions, the authors undertook a study on the photochemistry of thiophene *S*-oxide.

When 3,4-dibenzyl-2,5-dimethylthiophene *S*-oxide (**679**) is photoirradiated in CD_2Cl_2 with a high-pressure mercury lamp, a mixture of thienyl alcohol **680** and thienyl ether **681** is formed (05PPS808).



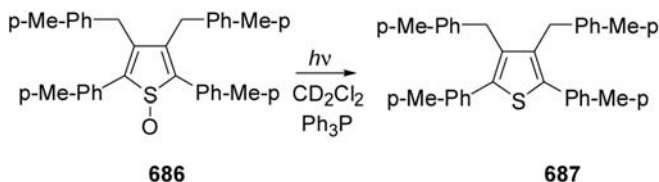
3,4-bis(*p*-methoxyphenyl)-2,5-dimethylthiophene *S*-oxide (**682**) was photoirradiated under similar conditions. Again, a thienyl ether **684** was observed, this time in addition to 3,4-bis(*p*-methoxyphenyl)dimethylthiophene (**683**) itself. The thienyl alcohol **685** could not be isolated.



The photolysis of **682** in carefully dried and distilled CD_2Cl_2 yielded a mixture of products, which is a little different in relative composition from that of the photoreaction in nondried CD_2Cl_2 . Most noticeable is the higher yield of the purely deoxygenated products, **683** (25%), and a lower yield in the total amount of hydroxylated products, **684** and **685** (27 and 12%). The formation of hydroxylated products in dried solvents, however, means that oxygen in the hydroxyl/alkoxymethyl moieties of the products stems from thiophene *S*-oxides. The addition of ethanol (5 equiv.) to the reaction mixture in nondried CD_2Cl_2 leads to the formation of 2-ethoxymethyl-5-

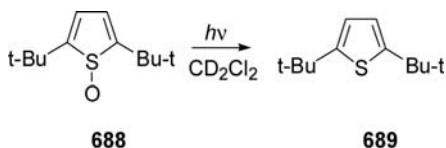
methyl-3,4-bis(*p*-methoxyphenyl)thiophene as the major product in addition to a small amount of the thiophene **683** as a deoxygenated product.

Piperidine and dibenzylamine as well as *p*-methoxythiophenol have been examined as readily oxidizable additives. In the case of the amines, no product resulting from the oxidation of the amines can be isolated. However, the conversion of the thiophene *S*-oxide to the thiophene is quantitative.

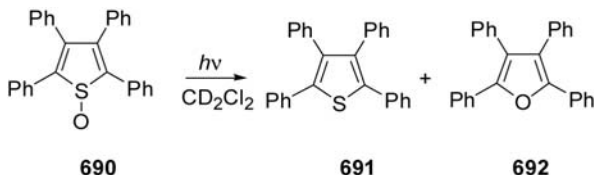


The photoirradiation of tetrakis(*p*-tolyl)thiophene *S*-oxide (**686**) in the presence of triphenylphosphine was carried out. Here, again the corresponding thiophene **687** was formed, but also significant amount of triphenylphosphide oxide could be isolated, giving evidence of a direct transfer of the oxygen from a thiophene *S*-oxide to another species of molecule.

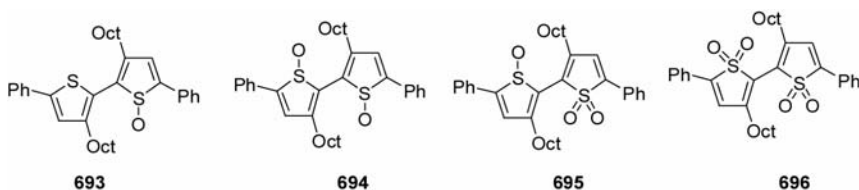
When 2,5-*tert*-butylthiophene *S*-oxide (**688**) is photoirradiated, 2,5-*tert*-butylfuran (**689**) is produced almost quantitatively. When 2,4-*tert*-butylthiophene *S*-oxide is photoirradiated, 2,4-*tert*-butylfuran is isolated. Here, however, also side products can be observed.



The photoirradiation of tetraphenylthiophene *S*-oxide (**690**) leads to an inseparable mixture of tetraphenylthiophene (**691**) and tetraphenylfuran (**692**) (**691**/**692** = 92:8).

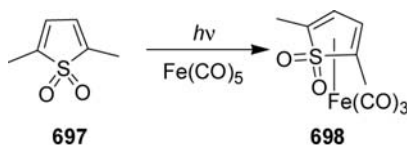


When tetrakis(*p*-tolyl)thiophene *S*-oxide is used, no furan could be isolated from the reaction. When photoirradiated **693**–**6955** deoxygenate readily. The bis(thiophene *S,S*-dioxide **696** is not photoreactive under the condition and does not deoxygenate.

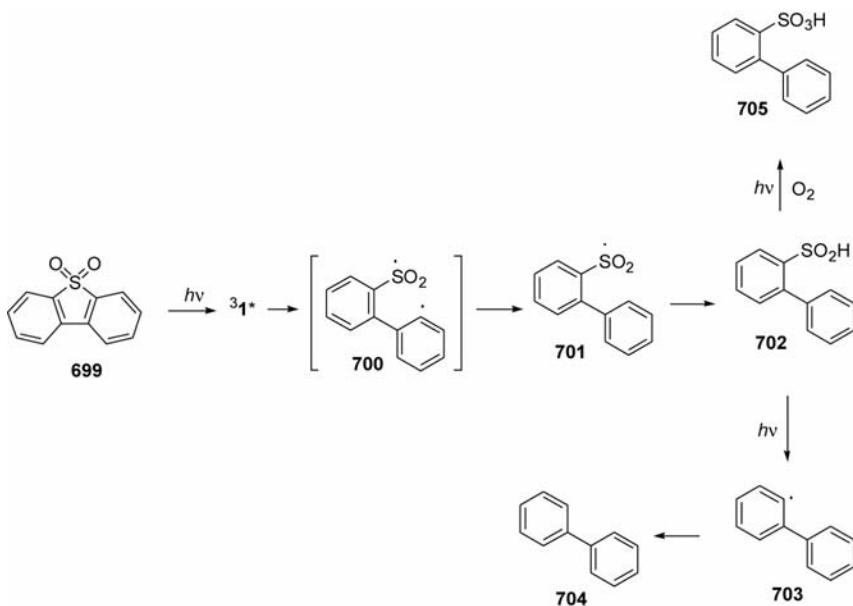


Photodeoxygenation reaction was obtained also on dibenzothiophene oxide (01JOC4576; 03JCR(S)60).

Irradiation of a benzene solution of 2,5-dimethylthiophene-1,1-dioxide (697) and $\text{Fe}(\text{CO})_5$ in a Pyrex apparatus for 50 min gave 2,5-dimethylthiophene-1,1-dioxide tricarbonyl iron (698) in 90% yield (72JCS(CC)501).



In benzene, DBT sulfone is virtually inert (94TL7155). Jenks et al. have found that DBT sulfone, when dissolved in 2-propanol, is converted quantitatively into the biphenyl by photoirradiation at wavelengths of $\lambda > 300$ nm using a Xe lamp.

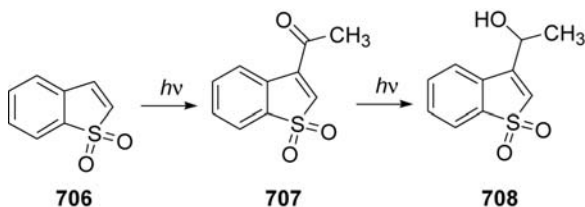


When the DBT sulfone, dissolved in 2-propanol, was photoirradiated at $\lambda > 280$ nm by a high-pressure mercury lamp under air, the concentration of DBT sulfone decreased with time and the biphenyl concentration increased accordingly (73JOC2419; 94TL7155; 95JA2667; 97JA94; 03EF(17) 95). However, when almost all the DBT sulfone disappeared following 60 h of photoirradiation, only 60% biphenyl yield was obtained. The other photoproduct of DBT sulfone **699** is biphenyl-2-sufonic acid **705**.

When the reaction was carried out under N_2 atmosphere, the biphenyl yield was increased up to $>92\%$. Compound **705** is therefore likely to be formed via the photooxidation of the intermediate **702** with an O_2 molecule dissolved in 2-propanol.

Photoreactivities of methyl-substituted DBT sulfones, such as 4-methyl-DBT sulfone and 4,6-dimethyl-DBT sulfone, gave rise to the corresponding biphenyls, as also the case for no substituted DBT sulfone. The methyl-substituted DBT sulfones were found to be photodecomposed rather faster than unsubstituted DBT sulfone **699** and the biphenyl yields were higher than those for the unsubstituted one.

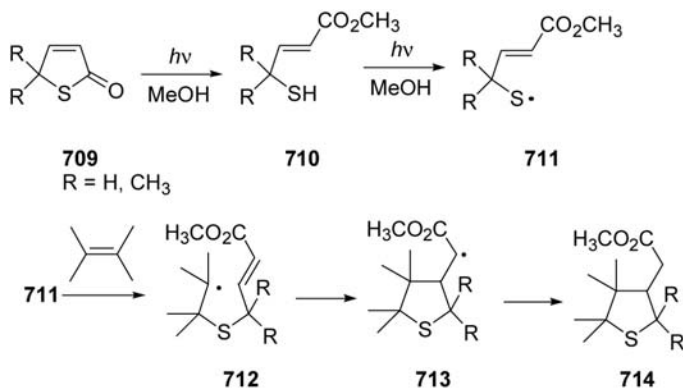
The photodecomposition of BT sulfone was seen to proceed significantly rather faster than that of DBT sulfones. GC-AED analysis showed two new peaks having molecular ions at m/z 208 and 212, both of which contain a sulfur atom. These peak compounds were identified by GC-MS analyses to be 3-acetylbenzothiophene **707** and its hydrogenated derivative **708**. Following an additional 5 h of photoirradiation, only peak compound **708** remained on the chromatogram.



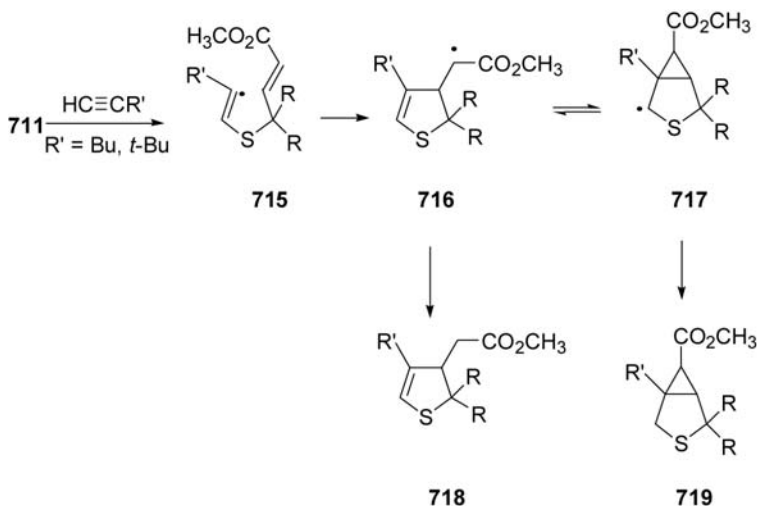
The reactivities of methyl-substituted BT sulfones were also examined. The reactivity was found to decrease with an increasing number of methyl substituents on the molecule. This tendency differs completely from that obtained for DBT sulfones.

17. DIHYDROTHIOPHENES

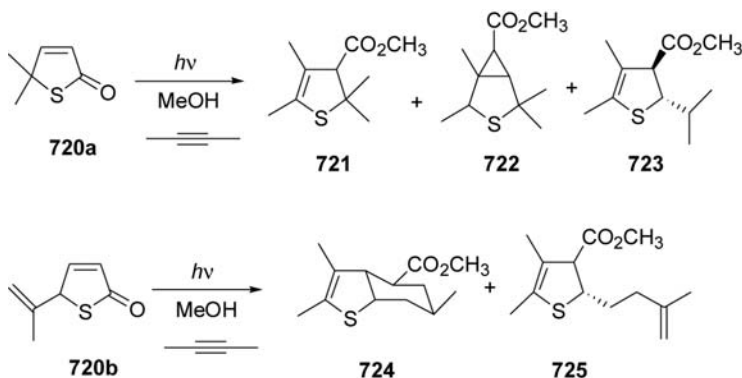
The authors reported that methyl 4-mercapto-2-alkenoates **710**, obtained by irradiation of 2(5*H*)-thiophenones **709** in MeOH, undergo light-induced S-H bond homolysis to give thio radicals **710** (84HCA2198; 85HCA2350; 87HCA125). Intermediate **710** can be trapped by alkenes to afford 3-thiahex-5-enyl radical **711**, which cyclize selectively to radicals **712**, precursors of thiolane-3-acetates **714**.



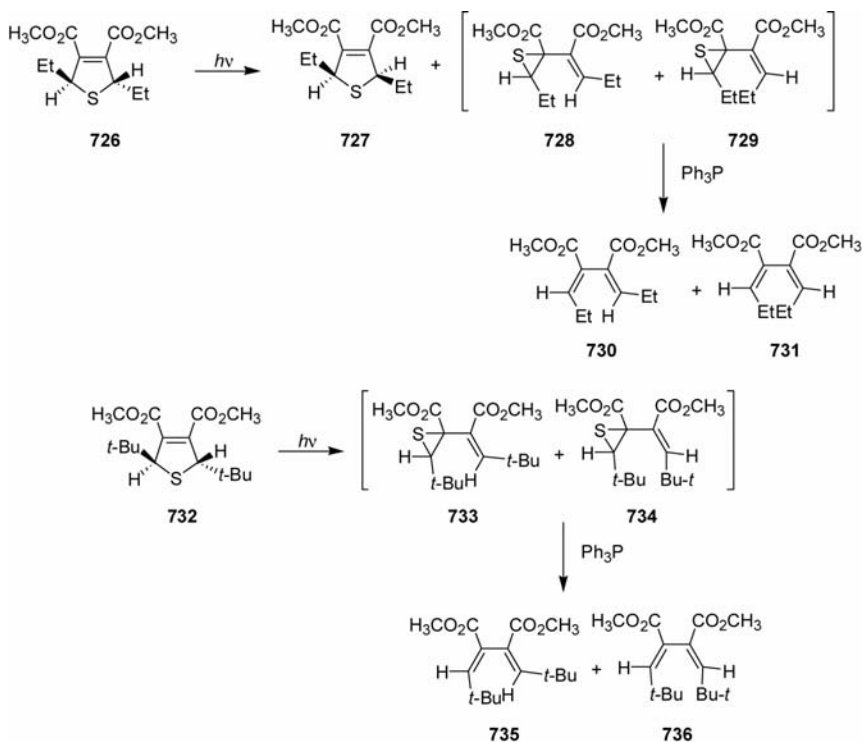
Reaction of **711** with terminal alkynes occurs regioselectively living 3-thiahexa-1,5-dienyl radicals **715** which also undergo selective 1,5-ring closure to allylcarbinyl radicals **716**. Depending on the substitution pattern, radicals **716** rearrange to cyclopropylcarbinyl radicals **717**. From **716** and **717**, 2,3-dihydrothiophene-3-acetate **718** and 3-thiabicyclo[3.1.0]hexane-6-carboxylates **719** are formed, respectively.



Irradiation of **720a** in MeOH saturated with 2-butyne affords 2,3-dihydrothiophene-3-acetate **721**, 3-thiabicyclo[3.1.0]hexane **722**, and 2,3-dihydrothiophene-3-carboxylate **723** in a 1:1:1 ratio. From **720b**, a 1:1 mixture of *trans*-fused 3a,4,5,6,7,7a-hexahydrobenzo[*b*]thiophene **724** and of 2,3-dihydrothiophene-3-carboxylate **725** is formed.



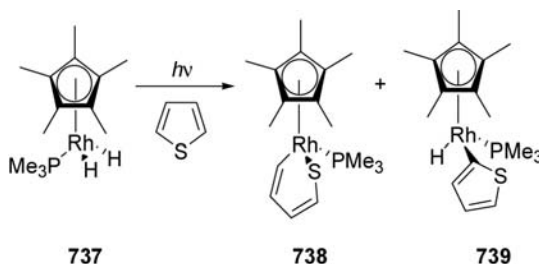
The irradiation of 2,5-dihydrothiophene derivatives in *n*-hexane or ether at 254 nm of degassed solutions leads to rapid formation of thermally and photochemically unstable products.



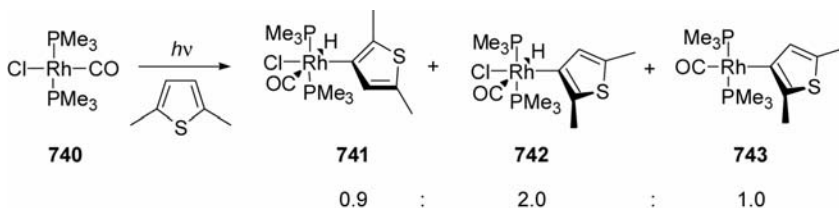
On brief treatment with triphenylphosphine in hot benzene, these intermediates are desulfurized quantitatively yielding the dienes **730–731** (or **735–736**) (71JA2344).

18. PHOTOCHEMISTRY OF INORGANIC COMPLEXES

The complex $(C_5Me_5)Rh(PMe_3)_2H_2$ was irradiated in the presence of thiophene in C_7D_{14} solution at $-40^\circ C$ in order to look for intermediates in the C–S cleavage reaction (92JA151). The major product observed was **738** (75%), although a second $(C_5Me_5)Rh(PMe_3)$ -containing product was observed by 1H NMR spectroscopy (25%). The ratio of products **738** and **739** remained 3:1 throughout the photolysis, suggesting that they are formed in parallel reactions rather than sequential reactions.



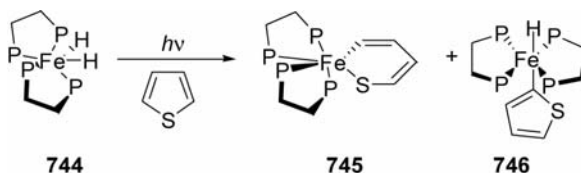
When a Rhodium complex **740** was irradiated in 2,5-dimethylthiophene, a complex mixture of products (**741–743**) was obtained.



The reaction is performed at 230 K. When the reaction mixture is warmed at room temperature, the starting material is re-formed almost quantitatively (96OM872). If the reaction mixture is taken to dryness at low temperature under high vacuum (under conditions where HCl is removed), the last product is relatively stable at room temperature. In 2,5-dimethylthiophene/THF (1:1) the ratio of the products is 1:1:1.

When thiophene-hexane or 2-methylthiophene-hexane (1:2 v/v) solutions of $[cis-Fe(H)_2(dmpe)_2]$ **744** were irradiated at 248 K, NMR

spectroscopy showed a complex reaction mixture containing a number of *cis*- and *trans*-adducts **745** and **746** (94JCS(CC)557). If the reaction mixture was warmed at 273 K (or the photolysis performed at 273 K) NMR spectra show resonances for two major products.

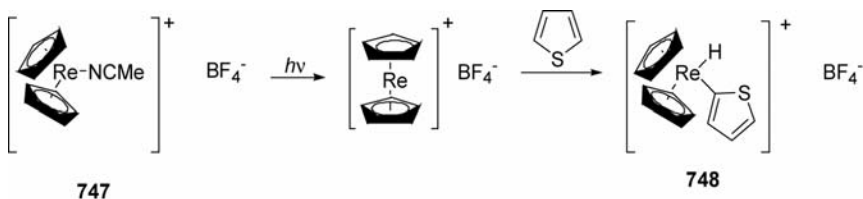


Photolysis of $[cis\text{-Fe(H)}_2(\text{dmpe})_2]$ with simple thiophenes at 273 K gives C-H and C-S insertion products. Prolonged photolysis (15 h) of the thiophene product mixture at 273 K does not appear to affect the relative ratios of the C-H and C-S adducts suggesting that they are stable under the photochemical conditions of the experiment.

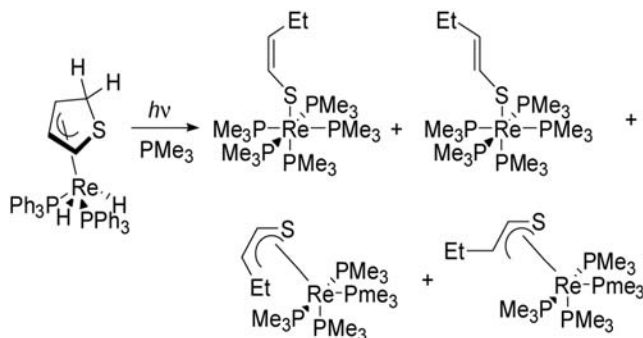
When a solution of $(\eta^4\text{-C}_4\text{H}_5\text{S})\text{ReH}_2(\text{PPh}_3)_2$ in benzene is treated with an excess trimethylphosphine and irradiated for several hours, the ^1H NMR spectrum of the reaction mixture indicates the presence of free triphenylphosphine and resonances attributable to four new organometallic complexes (Scheme 31) (92JA10767).

The sulfur ligand resonances for each of the four complexes are in a 1:1:2:3 ratios. This represents the first time that thiophene has been homogeneously transformed to a butenethiolate ligand.

Complex **747** did not react with benzene or thiophene thermally at room temperature, but under UV irradiation, **747** reacted with an excess of benzene to afford the hydrido(phenyl)rhenocene cation $[\text{Cp}_2\text{Re(H)Ph}]^+$ (BF_4^-) in 88% yield (98OM3405). Similarly, photolysis of **747** in the presence of excess thiophene yielded the 2-thienyl complex $[\text{Cp}_2\text{Re(H)(2-C}_4\text{H}_3\text{S})]^+$ (BF_4^-) (**748**) in 80% yield.



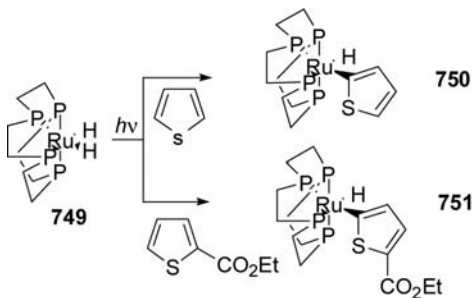
Hydrodesulfurization (HDS) is a stepwise reaction of Paramount industrial and environmental relevance whose mechanism(s), however, is still poorly understood. In this process, sulfur, contained in various



Scheme 31

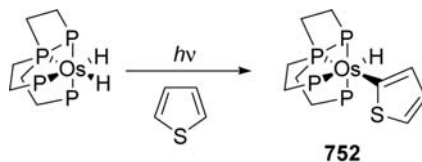
organic compounds such as thiols, sulfides, disulfides, and more refractory thiophenic molecules, is removed from fossil materials upon treatment with H₂ in the presence of heterogeneous catalysts.

Homogeneous modeling studies have recently contributed several mechanistic breakthroughs regarding most of the steps which may be involved in the metal-assisted HDS of thiophene to H₂S and hydrocarbons.

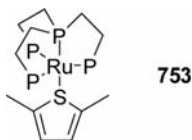


Neither of previous reported compounds was observed when the photolysis of **749** is carried out at room temperature in the presence of either thiophene or 2-carboxyethylthiophene either under N₂ or He (97OM4661). These photochemical reactions exclusively yield the (hydride)2-thienyl complexes [(PP₃)Ru(H)(2-Tyl)] **750** (Tyl = C₄H₃S) and [(PP₃)Ru(H)(2-CO₂EtTyl)] **751**.

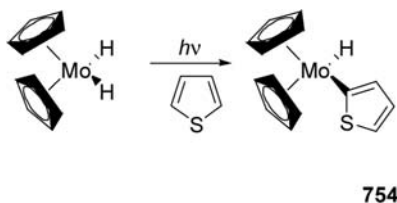
Identical regioselectivity of C-H insertion, as well as overall complex structure, is observed when transient [(PP₃)Os], photolitically generated in THF from [(PP₃)OsH₂], is reacted with thiophene. The resulting (hydride)2-thienyl complex [(PP₃)Os(H)(2-Tyl)] (**752**) exhibits spectroscopic characteristics which are fully comparable with those of the Ru derivative **750**.



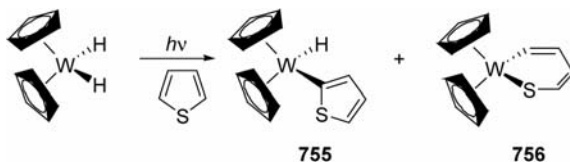
Photolysis of **749** in THF in the presence of a large excess of 2,5-dimethylthiophene for 3 h under a nitrogen atmosphere gives partial conversion of the dihydride complex to a mixture of products among which the most abundant (40%) is a new species that we assign as **753**.



Photolysis of a thiophene solution of Cp_2MoH_2 gave **754** (94OM4448).



Photolysing a mixture of Cp_2WH_2 , thiophene, and hexane, a 1:1 mixture of two products **755** and **756** was obtained.



Photolysis of Cp_2WH_2 is known to generate Cp_2W which can then insert into the C-S bond of thiophene to give the second complex.

This complex apparently undergoes a photochemical rearrangement to yield the other product. The viability of this pathway was demonstrated by the photolysis of an isolated sample of the second complex, which led to the formation of the other one. The photochemical rearrangement was intramolecular: photolysis in the presence of thiophene- d_4 led to no incorporation of thiophene- d_4 into the complex.

REFERENCES

- 47JA270
47JA273
49JCS381
50NAT(166)108
55JOC1086
56JA549

56JA5213
56JA6174

58ACSA765
58ACSA771
58MI1005
58SA350
59G540
60MI1181
62CB2934
63CB498
63MI357
65CB155
65CB876
65JA3998
65JCS6221
65JCS7109

65JOC2493
65TL301
66CB984
66JA5047
66JCS(CC)203
66MI45
66TL4227
67JA3487
67JA3495
- J.W. Sease and L. Zechmeister, *J. Am. Chem. Soc.*, **69**, 270 (1947).
L. Zechmeister and J.W. Sease, *J. Am. Chem. Soc.*, **69**, 273 (1947).
A. Mustafa and A.M. Islam, *J. Chem. Soc.*, 381 (1949).
A. Mustafa, *Nature*, **166**, 108 (1950).
J.S. Splitter and M. Calvin, *J. Org. Chem.*, **20**, 1086 (1955).
W.E. Haines, R.V. Helm, G.L. Cook, and J.S. Ball, *J. Am. Chem. Soc.*, **78**, 549 (1956).
W.E. Haines, G.L. Cook, and J.S. Ball, *J. Am. Chem. Soc.*, **78**, 5213 (1956).
A. Mustafa and S.M.A.D. Zayed, *J. Am. Chem. Soc.*, **78**, 6174 (1956).
J.S. Sørensen and N.A. Sørensen, *Acta Chem. Scand.*, **12**, 765 (1958).
J.S. Sørensen and N.A. Sørensen, *Acta Chem. Scand.*, **12**, 771 (1958).
J.H. Uhlenbrock and J.D. Bijloo, *Rec. Trav. Chi. Pays-Bas*, **77**, 1005 (1958).
R. Andrisano and G. Pappalardo, *Spectrochim. Acta*, **12**, 350 (1958).
G. Pappalardo, *Gazz. Chim. Ital.*, **89**, 540 (1959).
J.H. Uhlenbrock and J.D. Bijloo, *Rec. Trav. Chim. Pays-Bas*, **79**, 1181 (1960).
F. Bohlmann, K.M. Kleine, and H. Bornowski, *Chem. Ber.*, **95**, 2934 (1962).
G.O. Schenck, W. Hartmann, and R. Steinmetz, *Chem. Ber.*, **96**, 498 (1963).
R.A. Dalton and R.F. Curtis, *Nematologica*, **9**, 357 (1960).
F. Bohlmann, C. Arndt, K.M. Kleine, and H. Bornowski, *Chem. Ber.*, **98**, 155 (1965).
F. Bohlmann and U. Hinz, *Chem. Ber.*, **98**, 876 (1965).
H. Wynberg and H. van Driel, *J. Am. Chem. Soc.*, **87**, 3998 (1965).
W. Carruthers and H.N.M. Stewart, *J. Chem. Soc.*, 6221 (1965).
R.E. Atkinson, R.F. Curtis, and G.T. Phillips, *J. Chem. Soc.*, 7109 (1965).
W. Wolf and N. Kharasch, *J. Org. Chem.*, **30**, 2493 (1965).
W. Carruthers and H.N.M. Stewart, *Tetrahedron Lett.*, 301 (1965).
F. Bohlmann, M. Wotschokowsky, U. Hinz, and W. Lucas, *Chem. Ber.*, **99**, 984 (1966).
H. Wynberg, R.M. Kellogg, H. van Driel, and G.E. Beekhuis, *J. Am. Chem. Soc.*, **88**, 5047 (1966).
H. Wynberg and H. van Driel, *J. Chem. Soc., Chem. Commun.*, 203 (1966).
L. Benati and M. Tiecco, *Boll. Sci. Fac. Chim. Ind. Bologna*, **24**, 45 (1966).
N.R. Krishnaswamy, T.R. Seshadri, and B.R. Sharma, *Tetrahedron Lett.*, 4227 (1966).
H. Wynberg, H. van Driel, R.M. Kellogg, and J. Buter, *J. Am. Chem. Soc.*, **89**, 3487 (1967).
R.M. Kellogg and H. Wynberg, *J. Am. Chem. Soc.*, **89**, 3495 (1967).

- 67JA3498 H. Wynberg, G.E. Beekhuis, H. van Driel, and R.M. Kellogg, *J. Am. Chem. Soc.*, **89**, 3498 (1967).
- 67JA3501 H. Wynberg, R.M. Kellogg, H. van Driel, and G.E. Beekhuis, *J. Am. Chem. Soc.*, **89**, 3501 (1967).
- 67JCS(C)6221 C.E. Loader and C.J. Timmons, *J. Chem. Soc. (C)*, 6221 (1967).
- 67JOC3093 R.M. Kellogg, M.B. Groen, and H. Wynberg, *J. Org. Chem.*, **32**, 3093 (1967).
- 67T4419 R.F. Curtis and G.T. Phillips, *Tetrahedron*, **23**, 4419 (1967).
- 68AX(B)(24)467 G.J. Visser, G.J. Heeres, J. Wolters, and A. Vos, *Acta Crystallogr. B*, **24**, 467 (1968).
- 68JA5339 H. Wynberg and M.B. Groen, *J. Am. Chem. Soc.*, **90**, 5339 (1968).
- 68JCS(B)901 G. Martelli, P. Spagnolo, and M. Tiecco, *J. Chem. Soc. (B)*, 901 (1968).
- 68TL5895 R.M. Kellogg and H. Wynberg, *Tetrahedron Lett.*, 5895 (1968).
- 69CJC2965 H.A. Weibe and J. Hecklen, *Can. J. Chem.*, **47**, 2965 (1969).
- 69JCS(CC)524 A. Couture and A. Lablache-Combier, *J. Chem. Soc., Chem. Commun.*, 524 (1969).
- 69JOC3175 H. Wynberg, T.J. van Bergen, and R.M. Kellogg, *J. Org. Chem.*, **34**, 3175 (1969).
- 69TL2913 D.C. Neckers, J.H. Dopfer, and H. Wynberg, *Tetrahedron Lett.*, 2913 (1969).
- 69TL4791 W.H.F. Sasse, P.J. Collin, and D.B. Roberts, *Tetrahedron Lett.*, 4791 (1969).
- 69ZN(B)12 H. Güsten, L. Klasinc, and O. Volkert, *Z. Naturforsch. Teil B*, **24**, 12 (1969).
- 70CB834 F. Bohlmann and C. Zdero, *Chem. Ber.*, **103**, 834 (1970).
- 70JA6664 H. Wynberg and M.B. Groen, *J. Am. Chem. Soc.*, **92**, 6664 (1970).
- 70JCS(C)2504 G. De Luca, G. Martelli, P. Spagnolo, and M. Tiecco, *J. Chem. Soc. (C)*, 2504 (1970).
- 70JCS(CC)1474 C. Rivas, M. Velez, and O. Crescente, *J. Chem. Soc., Chem. Commun.*, 1474 (1970).
- 70JOC1582 D.G. Neckers, J.H. Dopfer, and H. Wynberg, *J. Org. Chem.*, **35**, 1582 (1970).
- 70JOC2737 R.M. Kellogg, J.K. Dik, H. van Driel, and H. Wynberg, *J. Org. Chem.*, **35**, 2737 (1970).
- 70MI1 S. Braslavsky, H.A. Wiebe, and J. Hecklen, "Centre for Air Environment Studies". Publication No. 164-70, Pennsylvania State University, Pennsylvania (1970).
- 70MI28 C. Rivas, S. Krestonosich, E. Payo, and L. Cortés, *Acta Cient. Venesolana*, **21**, 28 (1970).
- 71ACR65 H. Wynberg, *Acc. Chem. Res.*, **4**, 65 (1971).
- 71BSF679 A. Lablache-Combier and M.A. Remy, *Bull. Soc. Chim. Fr.*, 679 (1971).
- 71JA2344 R.M. Kellogg, *J. Am. Chem. Soc.*, **93**, 2344 (1971).
- 71JA3432 E.C. Wu and J. Hecklen, *J. Am. Chem. Soc.*, **93**, 3432 (1971).
- 71JCS(CC)891 A. Couture and A. Lablache-Combier, *J. Chem. Soc., Chem. Commun.*, 891 (1971).
- 71JCS(CC)892 P. Grandclaude and A. Lablache-Combier, *J. Chem. Soc., Chem. Commun.*, 892 (1971).
- 71JOC1011 H. Wynberg, H.J.M. Sinnige, and H.M.J.C. Creemers, *J. Org. Chem.*, **36**, 1011 (1971).

- 71JOC2797 M.B. Groen, H. Schanderberg, and H. Wynberg, *J. Org. Chem.*, **36**, 2797 (1971).
- 71JOC3755 J.H. Doppler and D.C. Neckers, *J. Org. Chem.*, **36**, 3755 (1971).
- 71MI9 C. Rivas, M. Velez, O. Crescente, and S.E. Flores, *Rev. Latinoam. Quim.*, **2**, 9 (1971).
- 71T1059 A. Couture and A. Lablache-Combier, *Tetrahedron*, **27**, 1059 (1971).
- 72CJC2821 H.A. Wiebe, S. Braslavsky, and J. Heicklen, *Can. J. Chem.*, **50**, 2821 (1972).
- 72JA8179 D.N. Harpp and C. Heitner, *J. Am. Chem. Soc.*, **94**, 8179 (1972).
- 72JCS(CC)501 Y.L. Chow, J. Fossey, and R.A. Perry, *J. Chem. Soc., Chem. Commun.*, 501 (1972).
- 72JCS(CC)879 B. Iddon, H. Suschitzky, and D.S. Taylor, *J. Chem. Soc., Chem. Commun.*, 879 (1972).
- 72MI458 F.J. Gommers, *Nematologica*, **18**, 458 (1972).
- 72TL1429 R.M. Kellogg, *Tetrahedron Lett.*, 1429 (1972).
- 72TL1909 H.J. Kuhn and K. Gollnick, *Tetrahedron Lett.*, 1909 (1972).
- 72TL3769 E.J. Corey and P.L. Fuchs, *Tetrahedron Lett.*, 3769 (1972).
- 73CB674 H.J. Kuhn and K. Gollnick, *Chem. Ber.*, **106**, 674 (1973).
- 73JA2058 A. Elgavi, B.S. Green, and G.M.J. Schmidt, *J. Am. Chem. Soc.*, **95**, 2058 (1973).
- 73JA3692 J.H. Doppler, D. Oudman, and H. Wynberg, *J. Am. Chem. Soc.*, **95**, 3692 (1973).
- 73JCS(P1)2322 T. Nakano, K. Tori, C. Rivas, and C. Pérez, *J. Chem. Soc., Perkin Trans.*, **1**, 2322 (1973).
- 73JHC967 C. Rivas and R.A. Bolivar, *J. Heterocyclic Chem.*, **10**, 967 (1973).
- 73JOC2419 G.M. Gurria and G.H. Posner, *J. Org. Chem.*, **38**, 2419 (1973).
- 73JPC1478 F.C. Thyron, *J. Phys. Chem.*, **77**, 1478 (1973).
- 73T651 P. Grandclaude and A. Lablache-Combier, *Tetrahedron*, **29**, 651 (1973).
- 74AJC315 P.G. Lehman and H. Wynberg, *Aust. J. Chem.*, **27**, 315 (1974).
- 74CJC132 C.C. Leznoff, W. Lilie, and C. Manning, *Can. J. Chem.*, **52**, 132 (1974).
- 74CJC1681 D.R. Arnold, R.J. Birtwell, and B.M. Clarke, *Can. J. Chem.*, **52**, 1681 (1974).
- 74JA1305 P. Bucci, M. Longeri, C.A. Veracini, and L. Lunazzi, *J. Am. Chem. Soc.*, **96**, 1305 (1974).
- 74TL2941 Y. Kobayashi, I. Kumadaki, A. Ohsawa, and Y. Sekine, *Tetrahedron Lett.*, 2941 (1974).
- 75CPB2772 Y. Kobayashi, I. Kumadaki, A. Ohsawa, Y. Sekine, and H. Mochizuki, *Chem. Pharm. Bull.*, **25**, 2772 (1975).
- 75CJC1 D.R. Arnold and B.M. Clarke, *Can. J. Chem.*, **53**, 1 (1975).
- 75JCS(CC)106 A. Croisy, P. Jacquignon, and F. Perin, *J. Chem. Soc., Chem. Commun.*, 106 (1975).
- 75JOC3001 Y. Kanaoka, K. Itoh, Y. Hatanaka, J.L. Flippen, I.L. Karle, and B. Witkop, *J. Org. Chem.*, **40**, 3001 (1975).
- 75P2295 G.F.Q. Chan, G.H.N. Towers, and J.C. Mitchell, *Phytochemistry*, **14**, 2295 (1975).
- 75PP(14)2295 J. Kagan, W.D. McRae, E. Yamamoto, and G.H.N. Towers, *Photochem. Photobiol.*, **14**, 2295 (1975).
- 75T785 A. Couture, A. Delevallee, A. Lablache-Combier, and C. Parkanyl, *Tetrahedron*, **31**, 785 (1975).

- 75TL1639 Y. Kobayashi, I. Kumadaki, A. Ohsawa, and Y. Sekine, *Tetrahedron Lett.*, 1639 (1975).
- 75TL4471 M. Matsumoto, S. Dobashi, and K. Kondo, *Tetrahedron Lett.*, 4471 (1975).
- 76CPL(38)489 W.M. Flicker, O.R. Mosher, and A. Kuppermann, *Chem. Phys. Lett.*, **38**, 489 (1976).
- 76CPL(41)535 E.H. Van Veen, *Chem. Phys. Lett.*, **41**, 535 (1976).
- 76MI1 O. Buchardt, "Photochemistry of Heterocyclic Compounds," Wiley, New York (1976).
- 76MI123 A. Lablache-Combier, in "Photochemistry of Heterocyclic Compounds," (O. Buchardt, ed.), Wiley, New York, 1976, p. 123.
- 76P1309 F. Bohlmann, C. Zdero, and M. Grenz, *Phytochemistry*, **15**, 1309 (1976).
- 77AJC173 W. Davies, B.C. Ennis, C. Mahavera, and Q.N. Porter, *Aust. J. Chem.*, **30**, 173 (1977).
- 77CRV473 S. Braslavsky and J. Hecklen, *Chem. Rev.*, **77**, 473 (1977).
- 77JOC1570 C.M. Camaggi, R. Leardini, and P. Zanirato, *J. Org. Chem.*, **42**, 1570 (1977).
- 77MI215 G.F.Q. Chan, M. Primoda, G.H.N. Towers, and J.C. Mitchell, *Contact Dermatitis*, **3**, 215 (1977).
- 78CJC1970 D.R. Arnold and C.P. Hadjiantoniou, *Can. J. Chem.*, **56**, 1970 (1978).
- 78JOC2493 A.H.A. Tinnemans and D.C. Neckers, *J. Org. Chem.*, **43**, 2493 (1978).
- 78P2097 A. Selva, A. Arnoni, R. Mondelli, V. Sprio, L. Ceranlo, S. Petruso, S. Plescia, and L. Lamartina, *Phytochemistry*, **17**, 2097 (1978).
- 78TL125 H. Wamhoff and H.-J. Hupe, *Tetrahedron Lett.*, 125 (1978).
- 78TL999 M. El Faghi El Amoudi, P. Geneste, and J.-L. Olivé, *Tetrahedron Lett.*, 999 (1978).
- 79JA2157 M.J. Hopkinson, W.W. Schloman Jr., B.F. Plummer, E. Wenkert, and M. Raju, *J. Am. Chem. Soc.*, **101**, 2157 (1979).
- 79JBC(254)1841 J. Bakker, F.J. Gommers, I. Nieuwenhuis, and H. Wynberg, *J. Biol. Chem.*, **254**, 1841 (1979).
- 79JCS(CC)881 J.A. Baltrop, A.C. Day, and E. Irving, *J. Chem. Soc., Chem. Commun.*, 881 (1979).
- 79JCS(CC)966 J.A. Baltrop, A.C. Day, and E. Irving, *J. Chem. Soc., Chem. Commun.*, 966 (1979).
- 79JCS(P2)393 P.B. Koster, J. Runsink, and M.J. Janssen, *J. Chem. Soc., Perkin Trans.*, **2**, 393 (1979).
- 79MI134 E. Yamamoto, C.K. Wat, W.D. McRae, G.H.N. Towers, and G.F. Q. Chan, *FEBS Lett.*, **107**, 134 (1979).
- 79MI140 G.H.N. Towers, T. Arnason, C.K. Wat, E.A. Graham, J. Lam, and J.C. Mitchell, *Contact Dermatitis*, **5**, 140 (1979).
- 80E1096 W.D. McRae, G.F.Q. Chan, C.K. Wat, G.H.N. Towers, and J. Lam, *Experientia*, **36**, 1096 (1980).
- 80JOC2968 Y. Kobayashi, A. Ando, K. Kawada, and I. Kumadaki, *J. Org. Chem.*, **45**, 2968 (1980).
- 80MI309 W.D. McRae, D.A.J. Irwin, T. Bisalputra, and G.H.N. Towers, *Photobiophys. Photobiophys.*, **1**, 309 (1980).
- 80MI369 F.J. Gommers, J. Bakker, and L. Smits, *Nematologica*, **26**, 369 (1980).

- 80MI501 A. Padwa, in "Rearrangements in Ground and Excited States," P. de Mayo, ed.), Academic Press, New York, 1980, p.501.
- 80P2760 F. Bohlmann, J. Jakupovic, H. Robinson, and R.M. King, *Phytochemistry*, **19**, 2760 (1980).
- 80PP(31)465 J. Kagan, R. Gabriel, and S.A. Reed, *Photochem. Photobiol*, **31**, 465 (1980).
- 80PP(32)167 C.K. Wat, W.D. McRae, E. Yamamoto, G.H.N. Towers, and J. Lam, *Photochem. Photobiol*, **32**, 167 (1980).
- 80T1161 A. Greenberg, J.F. Liebman, and D. van Vechten, *Tetrahedron*, **36**, 1161 (1980).
- 81JHC1065 C. Rivas, D. Pacheco, F. Vargas, and J. Ascanio, *J. Heterocyclic Chem.*, **18**, 1065 (1981).
- 81JOC3939 D.C. Neckers and F.L. Wagenaar, *J. Org. Chem*, **46**, 3939 (1981).
- 81JOC4258 M. El Faghi El Amoudi, P. Geneste, and J.-L. Olivé, *J. Org. Chem*, **46**, 4258 (1981).
- 81JP(17)91 R.A. Bolivar and C. Rivas, *J. Photochem*, **17**, 91 (1981).
- 81MI54 T. Arnason, J.R. Stein, E. Graham, C.K. Wat, and G.H.N. Towers, *Can. J. Bot*, **59**, 54 (1981).
- 81MI59 C.K. Wat, S.K. Prasad, E.A. Graham, S. Partington, T. Arnason, and G.H.N. Towers, *Biochem. System. Ecol*, **9**, 59 (1981).
- 81MI63 T. Arnason, T. Swain, C.K. Wat, E.A. Graham, S. Partington, and G.H.N. Towers, *Biochem. System. Ecol*, **9**, 63 (1981).
- 81MI67 J.B. Hudson, E.A. Graham, J. Lam, and G.H.N. Towers, *Planta Med*, **57**, 67 (1981).
- 81P743 F. Bohlmann, U. Fritz, R.M. King, and H. Robinson, *Phytochemistry*, **20**, 743 (1981).
- 81P825 F. Bohlmann, W.F. Abraham, R.M. King, and H. Robinson, *Phytochemistry*, **20**, 825 (1981).
- 81PP(33)821 T. Arnason, G.F.Q. Chan, C.K. Wat, K. Downum, and G.H. N. Towers, *Photochem. Photobiol*, **33**, 821 (1981).
- 81T75 A. Buquet, A. Couture, A. Lablache-Combier, and A. Pollet, *Tetrahedron*, **37**, 75 (1981).
- 82JHC529 C. Rivas, R.A. Bolivar, and M. Cucarella, *J. Heterocyclic Chem*, **19**, 529 (1982).
- 82JOC4520 V. Nair, S.G. Richardson, and R.E. Coffman, *J. Org. Chem*, **47**, 4520 (1982).
- 82JP(19)95 R.A. Bolivar and C. Rivas, *J. Photochem*, **19**, 95 (1982).
- 82MI961 G. Campbell, J.D.H. Lambert, T. Arnason, and G.H.N. Towers, *J. Chem. Ecol*, **8**, 961 (1982).
- 82MI2565 J. Sinclair and T. Arnason, *Can. J. Bot*, **60**, 2565 (1982).
- 82P1795 F. Bohlmann, N. Borthakur, H. Robinson, and R.M. King, *Phytochemistry*, **21**, 1795 (1982).
- 82PP(35)615 F.J. Gommers, J. Bakker, and H. Wynberg, *Photochem. Photobiol*, **35**, 615 (1982).
- 83E402 J. Kagan and G. Chan, *Experientia*, **39**, 402 (1983).
- 83H(20)174 Y. Kobayashi, K. Kawada, A. Ando, and I. Kumadaki, *Heterocycles*, **20**, 174 (1983).
- 83JHC1453 M. Sugiyura, M.L. Tedjamulia, Y. Tominaga, R.N. Castle, and M. L. Lee, *J. Heterocycl. Chem*, **20**, 1453 (1983).
- 83JP(22)91 R.A. Bolivar, R. Machado, F. Montero, F. Vargas, and C. Rivas, *J. Photochem*, **22**, 91 (1983).

- 83JPC2317 F. Bertinelli, P. Palmieri, C. Stremmenos, G. Pelizzi, and C. Taliani, *J. Phys. Chem*, **87**, 2317 (1983).
- 83MI185 W.H. Laarhoven, *Recl. Trav. Chim. Pays-Bas*, **102**, 185 (1983).
- 83MI377 J. Kagan, J.P. Beny, G. Chan, S.M. Dhawan, J.A. Jaworski, E. D. Kagan, P.D. Kassner, M. Morphy, and J.A. Rogers, *Insect Sci. Appl.*, **4**, 377 (1983).
- 83TCA(63)55 T. Matsushita, H. Tanaka, K. Nishimoto, and Y. Osamura, *Theor. Chim. Acta*, **63**, 55 (1983).
- 84BBA(802)442 J. Kagan, M. Hasson, and F. Gryndspan, *Biochim. Biophys. Acta*, **802**, 442 (1984).
- 84E577 D.E. Champagne, J.H. Arnason, B.J.R. Philogene, G. Campbell, and D.G. McLachlan, *Experientia*, **40**, 577 (1984).
- 84HCA2198 E. Anklam and P. Margaretha, *Helv. Chim. Acta*, **67**, 2198 (1984).
- 84JHC185 H. Kudo, M.L. Tedjamulia, R.N. Castle, and M.L. Lee, *J. Heterocycl. Chem*, **21**, 185 (1984).
- 84MI25 J. Kagan, I. Prakash, J.M. Dhawan, and J.A. Jaworski, *Photobiocem. Photobiophys*, **8**, 25 (1984).
- 84MI104 K.R. Sownum, G.A. Rosenthal, and G.H.N. Towers, *Pest. Biochem. Physiol.*, **22**, 104 (1984).
- 84MI124 E. Yamamoto, W.D. McRae, F.J. Garcia, and G.H.N. Towers, *Planta Med*, **50**, 124 (1984).
- 84MI1115 J. Kagan, P.A. Kagan, and N.E. Buhse, *J. Chem. Ecol.*, **10**, 1115 (1984).
- 84OR1 F.B. Mallory and C.W. Mallory, *Org. React*, **30**, 1 (1984).
- 84PP(39)177 D. McLachlan, T. Arnason, and J. Lam, *Photochem. Photobiol*, **39**, 177 (1984).
- 84TL1917 Y. Kobayashi, K. Kawada, A. Ando, and I. Kumadaki, *Tetrahedron Lett.*, **25**, 1917 (1984).
- 85BBA(821)488 D.G. McRae, E. Yamamoto, and G.H.N. Towers, *Biochim. Biophys. Acta*, **821**, 488 (1985).
- 85G595 M. D'Auria and F. D'Onofrio, *Gazz. Chim. Ital*, **115**, 595 (1985).
- 85HCA2350 R. Keisewetter and P. Margaretha, *Helv. Chim. Acta*, **68**, 2350 (1985).
- 85JA723 W.A. Rendall, M. Torres, and O.P. Strausz, *J. Am. Chem. Soc*, **107**, 723 (1985).
- 85MI745 A. Lablache-Combier, in "Chemistry of Heterocyclic Compounds," (S. Gronowitz, ed.), Vol. IV, Wiley, New York, 1985, p. 745.
- 85P615 P. Singh, A.K. Sharma, K.C. Joshi, and F. Bohlmann, *Phytochemistry*, **24**, 615 (1985).
- 85PP(41)1 J.P. Reyftmann, J. Kagan, R. Santus, and P. Morliere, *Photochem. Photobiol*, **41**, 1 (1985).
- 85TL2423 V.H. Rawal, R.J. Jones, and M.P. Cava, *Tetrahedron Lett*, **26**, 2423 (1985).
- 85ZN497 M.Z. Zander, *Naturforsch*, **40A**, 497 (1985).
- 86CJC76 R.J. Waltman and J. Bargon, *Can. J. Chem*, **64**, 76 (1986).
- 86G747 M. D'Auria, A. De Mico, and F. D'Onofrio, *Gazz. Chim. Ital*, **116**, 747 (1986).
- 86H(24)799 K.-I. Seki, K. Ohkura, M. Terashima, and Y. Kanaoka, *Heterocycles*, **24**, 799 (1986).
- 86H(24)1575 M. D'Auria, R. Antonioletti, A. De Mico, and G. Piancatelli, *Heterocycles*, **24**, 1575 (1986).

- 86JCS(CC)826 R.J. Jones and M.P. Cava, *J. Chem. Soc., Chem. Commun.*, 826 (1986).
- 86JCS(P1)1755 R. Antonioletti, M. D'Auria, F. D'Onofrio, G. Piancatelli, and A. Scettri, *J. Chem. Soc., Perkin Trans.*, **1**, 1755 (1986).
- 86JOC3453 S.P. Spyroudis, *J. Org. Chem.*, **51**, 3453 (1986).
- 86JP(32)363 R.A. Bolivar, R. Gonzales, R. Machado, C. Rivas, and M. L. Tasayco, *J. Photochem.*, **32**, 363 (1986).
- 86MI49 J. Kagan, E.D. Kagan, and E. Seigneurie, *Chemosphere*, **15**, 49 (1986).
- 86MI781 W.E. Bennett, J.L. Maas, S.A. Sweeney, and J. Kagan, *Chemosphere*, **15**, 781 (1986).
- 86PP(44)441 C. Evans, D. Weir, J.C. Scaiano, A. MacEachern, J.T. Arnason, P. Morand, B. Hallebone, L.C. Leitch, and J.R. Philogene, *Photochem. Photobiol.*, **44**, 441 (1986).
- 87BCJ1847 K. Maruyama and H. Tamiaki, *Bull. Chem. Soc. Jpn*, **60**, 1847 (1987).
- 87HCA125 R. Kieseewetter and P. Margaretha, *Helv. Chim. Acta*, **70**, 125 (1987).
- 87JCS(P1)1777 M. D'Auria, A. De Mico, F. D'Onofrio, and G. Piancatelli, *J. Chem. Soc., Perkin Trans.*, **1**, 1777 (1987).
- 87JOC5243 M. D'Auria, A. De Mico, F. D'Onofrio, and G. Piancatelli, *J. Org. Chem.*, **52**, 5243 (1987).
- 87JOC5382 M. Novi, G. Garbarino, G. Petrillo, and C. Dell'Erba, *J. Org. Chem.*, **52**, 5382 (1987).
- 87JPC6706 J. Roncali, R. Garreau, A. Yassar, P. Marque, F. Garnier, and M. Lemaire, *J. Phys. Chem.*, **91**, 6706 (1987).
- 87MI1 J.R. Heitz, in "Light-Activated Pesticides," (J.R. Heitz and K.R. Downum, eds.), American Chemical Society, Washington, DC, 1987, p. 1.
- 87MI176 J. Kagan, W.E. Bennett, E.D. Kagan, J.L. Maas, S.A. Sweeney, I.A. Kagan, E. Seigneurie, and V. Bindokas, in "Light-Activated Pesticides," (J.R. Heitz and K.R. Downum, eds.), American Chemical Society, Washington, DC, 1987, p. 176.
- 87MM212 S. Hotta, S.D.D.V. Rughooputh, A.J. Heeger, and F. Wudl, *Macromolecules*, **20**, 212 (1987).
- 87SM(18)177 C. Taliani, R. Danieli, R. Zamboni, P. Ostoja, and W. Porzio, *Synth. Met.*, **18**, 177 (1987).
- 87SM(21)41 S.D.D.V. Rughooputh, M. Nowak, S. Hotta, A.J. Heeger, and F. Wudl, *Synth. Met.*, **21**, 41 (1987).
- 87SM(21)149 B. Themans, J.M. André, and J.L. Brédas, *Synth. Met*, **21**, 149 (1987).
- 87SM(22)79 S. Hotta, S.D.D.V. Rughooputh, and A.J. Heeger, *Synth. Met*, **22**, 79 (1987).
- 88CRV183 A.O. Patil, A.J. Heeger, and F. Wudl, *Chem. Rev.*, **88**, 183 (1988).
- 88G633 M. D'Auria and F. D'Onofrio, *Gazz. Chim. Ital*, **118**, 633 (1988).
- 88H(27)1731 J. Kakayama, T. Konishi, and M. Hoshino, *Heterocycles*, **27**, 1731 (1988).
- 88JCP(89)5535 M.-T. Zhao, B.P. Singh, and P.N. Prasad, *J. Chem. Phys.*, **89**, 5535 (1988).
- 88JOC803 M. Irie and M. Mohri, *J. Org. Chem.*, **53**, 803 (1988).
- 88MI139 G.H.N. Towers and D. Champagne, in "Chemistry and Biology of Naturally-Occurring Acetylenes and Related Compounds

- (NOARC)," (J. Lam, H. Breteler, T. Arnason, and L. Hansen, eds.), Elsevier, Amsterdam, 1988, p. 139.
- 89BCJ1539 K. Yui, Y. Aso, T. Otsubo, and F. Ogura, *Bull. Chem. Soc. Jpn*, **62**, 1539 (1989).
- 89BCJ1547 K. Yui, H. Ishida, Y. Aso, T. Otsuro, F. Ogura, A. Kawamoto, and J. Tanaka, *Bull. Chem. Soc. Jpn*, **62**, 1547 (1989).
- 89G201 M. D'Auria, A. De Mico, F. D'Onofrio, and G. Piancatelli, *Gazz. Chim. Ital*, **119**, 201 (1989).
- 89G381 M. D'Auria, A. De Mico, F. D'Onofrio, and G. Piancatelli, *Gazz. Chim. Ital*, **119**, 381 (1989).
- 89G419 M. D'Auria, *Gazz. Chim. Ital*, **119**, 419 (1989).
- 89H(29)1331 M. D'Auria, A. De Mico, and F. D'Onofrio, *Heterocycles*, **29**, 1331 (1989).
- 89JCP(90)3506 D. Birnbaum and B. Kohler, *J. Chem. Phys*, **90**, 3506 (1989).
- 89JPC7916 M.-T. Zhao, M. Samoc, B.P. Singh, and P.N. Prasad, *J. Phys. Chem*, **93**, 7916 (1989).
- 89JPP(A)(47)191 M. D'Auria, A. De Mico, F. D'Onofrio, D. Mendola, and G. Piancatelli, *J. Photochem. Photobiol., A: Chem*, **47**, 191 (1989).
- 89JPP(B)(3)165 J. Kagan, M. Bazin, and R. Santus, *J. Photochem. Photobiol. B*, **3**, 165 (1989).
- 89JPP(B)(3)411 J.C. Scaiano, C. Evans, and J.T. Arnason, *J. Photochem. Photobiol. B*, **3**, 411 (1989).
- 89MI163 W.H. Laarhoven, *Org. Photochem*, **10**, 163 (1989).
- 89MI1329 J.B. Hudson, E.A. Graham, N. Miki, G.H.N. Towers, L. L. Hudson, R. Rossi, A. Carpita, and D. Neri, *Chemosphere*, **19**, 1329 (1989).
- 89SC1325 G. Karminsky-Zamola and M. Bajic, *Synth. Commun*, **18**, 1325 (1989).
- 89SM(28)C293 J.L. Sauvajol, D. Chenouni, S. Hasoon, and J.P. Lère-Porte, *Synth. Met.*, **28**, C293 (1989).
- 89SM(28)C323 T. Sugiyama, T. Wada, and H. Sasabe, *Synth. Met.*, **28**, C323 (1989).
- 89SM(28)C349 K. Yoshino, S. Nakajima, M. Onoda, and R. Sugimoto, *Synth. Met.*, **28**, C349 (1989).
- 89SM(28)C393 J.R. Linton, C.W. Frank, and S.D.D.V. Rughooputh, *Synth. Met.*, **28**, C393 (1989).
- 89SM(28)C435 J.E. Österholm, J. Laakso, P. Nyholm, H. Isotalo, H. Stubb, O. Inganas, and W.R. Salaneck, *Synth. Met.*, **28**, C435 (1989).
- 89SM(28)C487 M. Feldhues, G. Kämpf, H. Litterer, T. Macklenburg, and P. Wegener, *Synth. Met.*, **28**, C487 (1989).
- 89SM(28)C507 C. Taliani, G. Ruani, R. Zamboni, A. Bolognesi, M. Catellani, S. Destri, W. Porzio, and P. Ostoia, *Synth. Met.*, **28**, C507 (1989).
- 89SM(30)381 F. Van Bolhuis, H. Wynberg, E.E. Havinga, E.W. Meijer, and E.G. I. Staring, *Synth. Met*, **30**, 381 (1989).
- 89ZN205 M. Zander and G. Kirsch, *Z. Naturforsch*, **44A**, 205 (1989).
- 90BCJ1311 K. Uchida, Y. Nakayama, and M. Irie, *Bull. Chem. Soc. Jpn*, **63**, 1311 (1990).
- 90G793 R. Rossi, A. Carpita, M. CiofLO, and J.L. Houben, *Gazz. Chim. It*, **120**, 793 (1990).
- 90JA2694 C.H. Evans and J.C. Scaiano, *J. Am. Chem. Soc*, **112**, 2694 (1990).
- 90JCS(CC)273 M. Leclerc and G. Daoust, *J. Chem. Soc., Chem. Commun.*, 273 (1990).

- 90JCS(CC)414 J. Roncali, H.K. Youssoufi, R. Garreau, F. Garnier, and M. Lemaire, *J. Chem. Soc., Chem. Commun.*, 414 (1990).
- 90JCS(P1)2999 M. D'Auria, G. Piancatelli, and A. Vantaggi, *J. Chem. Soc., Perkin Trans. 1*, 2999 (1990).
- 90JOC4019 M. D'Auria, G. Piancatelli, and T. Ferri, *J. Org. Chem.*, **55**, 4019 (1990).
- 90MI479799 M. D'Auria, A. De Mico, F. D'Onofrio, and G. Piancatelli, *Italian Pat. Appl.*, **479799A90**, (May 18 1990).
- 90MM1268 R.M. Souto Maior, K. Hinkelmann, H. Eckert, and F. Wudl, *Macromolecules*, **23**, 1268 (1990).
- 90POLLDG1379 M. Zagórska and B. Krische, *Polymer*, **31**, 1379 (1990).
- 90PP(52)655 J.C. Scaiano, R.W. Redmond, B. Mehta, and J.T. Arnason, *Photochem. Photobiol.*, **52**, 655 (1990).
- 90SM(38)1 J.L. Sauvajol, D. Chenouni, J.P. Lère-Porte, C. Chorro, B. Moukala, and J. Petrissans, *Synt. Met.*, **38**, 1 (1990).
- 90T2367 J. Meng, D. Fu, Z. Gao, R. Wang, H. Wang, I. Saito, R. Kasatani, and T. Matsuura, *Tetrahedron*, **46**, 2367 (1990).
- 90T7831 M. D'Auria, F. D'Onofrio, and A. Vantaggi, *Tetrahedron*, **46**, 7831 (1990).
- 91CM1003 M.S.A. Abdou, G.A. Diaz-Guijada, M.I. Arroyo, and S. Holdcroft, *Chem. Mat.*, **3**, 1003 (1991).
- 91H(32)1059 M. D'Auria, *Heterocycles*, **32**, 1059 (1991).
- 91H(32)2323 G. Karminski-Zamola, D. Pavlicic, M. Bajic, and N. Blazevic, *Heterocycles*, **32**, 2323 (1991).
- 91JA600 J.V. Caspar, V. Ramamurthy, and D.R. Corbin, *J. Am. Chem. Soc.*, **113**, 600 (1991).
- 91JA5887 W. ten Hoeve, H. Wynberg, E.E. Havinga, and E.W. Meijer, *J. Am. Chem. Soc.*, **113**, 5887 (1991).
- 91JCP(95)4783 D. Birnbaum and B.E. Kohler, *J. Chem. Phys.*, **95**, 4783 (1991).
- 91JCR(S)166 N.R. Krishnaswamy, Ch.S.S.R. Kumar, and S.R. Prasanna, *J. Chem. Res. (S)*, 166 (1991).
- 91JCS(CC)752 T.M. Lambert and J.P. Ferraris, *J. Chem. Soc., Chem. Commun.*, 752 (1991).
- 91JCS(CC)1268 J.P. Ferraris and T.L. Lambert, *J. Chem. Soc., Chem. Commun.*, 1268 (1991).
- 91JCS(CC)1618 T. Iyoda, M. Kitano, and T. Shimidzu, *J. Chem. Soc., Chem. Commun.*, 1618 (1991).
- 91JHC1481 R.-J. Wang, H.-G. Wang, and T. Matsuura, *J. Heterocycl. Chem.*, **28**, 1481 (1991).
- 91JHC1997 R.N. Castle, S. Pakray, and G.E. Martin, *J. Heterocycl. Chem.*, **28**, 1997 (1991).
- 91JOC129 K. Jug and H.-P. Schluff, *J. Org. Chem.*, **56**, 129 (1991).
- 91MI87 J. Kagan, *Progr. Chem. Org. Nat. Prod.*, **56**, 87 (1991).
- 91MI605 Y. Ohmori, M. Uchida, K. Muro, and K. Yoshino, *Solid State Commun.*, **80**, 605 (1991).
- 91MI1938 Y. Ohmori, M. Uchida, K. Muro, and K. Yoshino, *Jpn J. Appl. Phys Part 2*, **30**, L1938 (1991).
- 91MM2119 S. Holdcroft, *Macromolecules*, **24**, 2119 (1991).
- 91MM2694 M. Ueda, Y. Miyaji, T. Ito, Y. Oba, and T. Sone, *Macromolecules*, **24**, 2694 (1991).
- 91MM4834 S. Holdcroft, *Macromolecules*, **24**, 4834 (1991).
- 91PP(53)181 M. D'Auria and A. Vantaggi, *Photochem. Photobiol.*, **53**, 181 (1991).

- 91PP(53)463 T.P. Wang, J. Kagan, R.W. Tuveson, and G.R. Wang, *Photochem. Photobiol.*, **53**, 463 (1991).
- 91PP(54)659 C.F. Foote, *Photochem. Photobiol.*, **54**, 659 (1991).
- 91SM(41-43)473 E.E. Havinga, I. Rotte, E.W. Meijer, W. Ten Hoeve, and H. Wynberg, *Synth. Met.*, **41-43**, 473 (1991).
- 91T9225 M. D'Auria, *Tetrahedron*, **47**, 9225 (1991).
- 92AM102 P. Bäuerle, *Adv. Mater.*, **4**, 102 (1992).
- 92AM107 D. Delabouglise, M. Hmyene, G. Horowitz, A. Yassar, and F. Garnier, *Adv. Mater.*, **4**, 107 (1992).
- 92AM490 A. Yassar, D. Delabouglise, M. Hmyene, B. Nessak, G. Horowitz, and F. Garnier, *Adv. Mater.*, **4**, 490 (1992).
- 92CB2583 F. Effenberger and J. Wonner, *Chem. Ber.*, **125**, 2583 (1992).
- 92CCA835 M. Bajić, G.M. Karminski-Zamola, and N. Blažević, *Croatica Chim. Acta*, **65**, 835 (1992).
- 92CM1106 M.G. Hill, J.-F. Penneau, B. Zinger, K.R. Mann, and L.L. Miller, *Chem. Mater.*, **4**, 1106 (1992).
- 92CPL(192)566 F. Charra, D. Fichou, J.M. Nunzi, and N. Pfeffer, *Chem. Phys. Lett.*, **192**, 566 (1992).
- 92JA151 L. Dong, S.B. Duckett, K.F. Ohman, and W.D. Jones, *J. Am. Chem. Soc.*, **114**, 151 (1992).
- 92JA2728 M.G. Hill, K.R. Mann, L.L. Miller, and J.-F. Penneau, *J. Am. Chem. Soc.*, **114**, 2728 (1992).
- 92JA10767 G.P. Rosini and W.D. Jones, *J. Am. Chem. Soc.*, **114**, 10767 (1992).
- 92JCP(96)165 D. Birnbaum, D. Fichou, and B.E. Kohler, *J. Chem. Phys.*, **96**, 165 (1992).
- 92JCP(96)2492 D. Birnbaum and B.E. Kohler, *J. Chem. Phys.*, **96**, 2492 (1992).
- 92JCS(CC)206 M. Hanazawa, R. Sumiya, Y. Horikawa, and M. Irie, *J. Chem. Soc., Chem. Commun.*, 206 (1992).
- 92JPC7671 M. Irie and K. Sayo, *J. Phys. Chem.*, **96**, 7671 (1992).
- 92MI261 M. Nivsarkar, G.P. Kumar, M. Laloraya, and M.M. Laloraya, *Arch. Insect Biochem. Physiol.*, **19**, 261 (1992).
- 92MM1901 J.M. Tour and R. Wu, *Macromolecules*, **25**, 1901 (1992).
- 92MM4297 Q. Pei, H. Järvinen, J.E. Österholm, and O. Inganäs, *Macromolecules*, **25**, 4297 (1992).
- 92NAT(355)624 J.N. Yao, K. Hashimoto, and A. Fujishima, *Nature*, **355**, 624 (1992).
- 92PP(56)479 R.J. Marles, J.B. Hudson, E.A. Graham, C. Soucy-Breau, P. Morand, R.L. Compadre, C.M. Compadre, G.H. N. Towers, and J.T. Arnason, *Photochem. Photobiol.*, **56**, 479 (1992).
- 92SM(48)167 D. Fichou, G. Horowitz, B. Xu, and F. Garnier, *Synth. Met.*, **48**, 167 (1992).
- 92SM(52)213 H. Chosrovian, D. Grebner, S. Rentsch, and H. Naarmann, *Synth. Met.*, **52**, 213 (1992).
- 92T2523 M. D'Auria and A. Vantaggi, *Tetrahedron*, **48**, 2523 (1992).
- 92T9315 M. D'Auria and D. Tofani, *Tetrahedron*, **48**, 9315 (1992).
- 92T9323 M. D'Auria, A. D'Annibale, and T. Ferri, *Tetrahedron*, **48**, 9323 (1992).
- 93AM721 G.G. Malliaras, J.K. Herrema, J. Wildeman, R.H. Wieringa, R. E. Gill, S.S. Lampoura, and G. Hadziioannou, *Adv. Mater.*, **5**, 721 (1993).
- 93AM646 B. Fabre and G. Bidan, *Adv. Mater.*, **5**, 646 (1993).

- 93AM922 F. Geiger, M. Stoldt, H. Schweizer, P. Bäuerle, and E. Umbach, *Adv. Mater.*, **5**, 922 (1993).
- 93CL365 K. Takimiya, F. Yashiki, Y. Aso, T. Otsubo, and F. Ogura, *Chem. Lett.*, 365 (1993).
- 93CPB1299 K. Oda and M. Machida, *Chem. Pharm. Bull.*, **41**, 1299 (1993).
- 93CPL(211)125 L.S. Andres, M. Merchan, M. Fulscher, and B.O. Roos, *Chem. Phys. Lett.*, **211**, 125 (1993).
- 93CPL(211)135 D.V. Lap, D. Grebner, S. Rentsch, and H. Naarmann, *Chem. Phys. Lett.*, **211**, 135 (1993).
- 93G129 M. D'Auria and F. D'Onofrio, *Gazz. Chim. Ital.*, **123**, 129 (1993).
- 93JA8447 B. Xu and S. Holdcroft, *J. Am. Chem. Soc.*, **115**, 8447 (1993).
- 93JA12158 L. De Witt, G.J. Blanchard, E. Le Goff, M.E. Benz, J.H. Liao, and M.G. Kanatzidis, *J. Am. Chem. Soc.*, **115**, 12158 (1993).
- 93JCP(97)7427 S. Hotta and K. Waragai, *J. Chem. Phys.*, **97**, 7427 (1993).
- 93JCP(98)8819a D. Beljonne, Z. Shuai, and J.L. Brédas, *J. Chem. Phys.*, **98**, 8819 (1993).
- 93JOC904 R.D. McCullough, R.D. Lowe, M. Jayaraman, and D. L. Anderson, *J. Org. Chem.*, **58**, 904 (1993).
- 93JPC513 P. Garcia, J.M. Pernaut, P. Hapiot, V. Wintgens, P. Valat, F. Garnier, and D. Delabougliuse, *J. Phys. Chem.*, **97**, 513 (1993).
- 93JPP(A)(70)59 R. Rossi, M. Ciofalo, A. Carpita, and G. Ponterini, *J. Photochem. Photobiol. A*, **70**, 59 (1993).
- 93MI33 J.B. Hudson, L. Harris, A. Teeple, and G.H.N. Towers, *Antiviral Res.*, **20**, 33 (1993).
- 93MI269 J. Ohshita, D. Kanaya, and M. Ishikawa, *Appl. Organomet. Chem.*, **7**, 269 (1993).
- 93MI447 J.B. Hudson, E.A. Graham, R. Rossi, A. Carpita, D. Neri, and G. H.N. Towers, *Planta Med.*, **59**, 447 (1993).
- 93MM4457 B. Xu and S. Holdcroft, *Macromolecules*, **26**, 4457 (1993).
- 93PP(58)49 M. Herrnreiter, J. Kagan, X. Chen, K.Y. Lau, M. D'Auria, and A. Vantaggi, *Photochem. Photobiol.*, **58**, 49 (1993).
- 93PP(58)246 J.B. Hudson, L. Harris, R.J. Marles, and J.T. Arnason, *Photochem. Photobiol.*, **58**, 246 (1993).
- 93SM(55-57)4168 M. Uchida, Y. Ohmori, C. Morishima, and K. Yoshino, *Synth. Met.*, **55-57**, 4168 (1993).
- 93SM(55-57)4740 S. Rentsch, H. Chosrovian, D. Grebner, and H. Naarmann, *Synth. Met.*, **55-57**, 4740 (1993).
- 93SM(57)3587 M. Sandberg, S. Tanaka, and K. Kaeriyama, *Synth. Met.*, **57**, 3587 (1993).
- 93SM(57)4714 C. Taliani, R. Danieli, R. Lazzaroni, N. Periasamy, G. Ruani, and R. Zamboni, *Synth. Met.*, **57**, 4714 (1993).
- 93SM(59)259 S. Samdal, E.J. Samuelson, and H. Volden, *Synth. Met.*, **59**, 259 (1993).
- 93SM(60)23 H. Chosrovian, S. Rentsch, D. Grebner, D.U. Dahm, E. Birckner, and H. Naarmann, *Synth. Met.*, **60**, 23 (1993).
- 93SM(61)143 H.-J. Egelhaaf, P. Bäuerle, K. Rauer, V. Hoffmann, and D. Oelkrug, *Synth. Met.*, **61**, 143 (1993).
- 93JCP(98)8819b D. Beljonne, Z. Shuai, and J.L. Bredas, *J. Chem. Phys.*, **98**, 8819 (1993).
- 93MM2954 M.S.A. Abdou and S. Holdcroft, *Macromolecules*, **26**, 2954 (1993).
- 93SM(60)23 H. Chosrovian, S. Rentsch, D. Grebner, U. Dahm, and E. Birckner, *Synth. Met.*, **60**, 23 (1993).

- 94AM64 D. Fichou, J.-M. Nunzi, F. Charra, and N. Pfeffer, *Adv. Mater*, **6**, 64 (1994).
- 94AM132 R.E. Gill, G.G. Malliaras, J. Wildeman, and G. Hadziioannou, *Adv. Mater*, **6**, 132 (1994).
- 94AM325 B. Xu and S. Holdcroft, *Adv. Mater*, **6**, 325 (1994).
- 94AM488 M. Berggren, G. Gustafsson, O. Inganäs, M.R. Andersson, O. Wennerström, and T. Hjerberg, *Adv. Mater*, **6**, 488 (1994).
- 94APPLAB(76)7530 M. Berggren, G. Gustafsson, O. Inganäs, M.R. Andersson, T. Hjerberg, and O. Wennerström, *Appl. Phys. Lett*, **76**, 7530 (1994).
- 94CM401 C. Wang, M.E. Benz, E. LeGoff, J.L. Schindler, J. Allbritton-Thomas, C.R. Kannewurf, and M.G. Kanatzidis, *Chem. Mater*, **6**, 401 (1994).
- 94CM1809 B. Servet, G. Horowitz, S. Ries, O. Lagorsse, P. Alnot, A. Yassar, F. Deloffre, P. Srivastava, R. Hajlaoui, P. Lang, and F. Ganier, *Chem. Mater.*, **6**, 1809 (1994).
- 94CPL(228)651 D. Grebner, D.V. Lap, S. Rentsch, and H. Naarmann, *Chem. Phys. Lett*, **228**, 651 (1994).
- 94CPL(230)249 H. Miyasaka, S. Araki, A. Tabata, T. Nobuto, N. Mataga, and M. Irie, *Chem. Phys. Lett*, **230**, 249 (1994).
- 94G195 M. D'Auria, *Gazz. Chim. Ital*, **124**, 195 (1994).
- 94JCP(98)3031 J.E. Chadwick and B.E. Kohler, *J. Chem. Phys*, **98**, 3031 (1994).
- 94JCP(100)2571 F. Negri and M.Z. Zgierski, *J. Chem. Phys*, **100**, 2571 (1994).
- 94JCP(101)1787 R.A. Janssen, L. Smilowitz, N.S. Sariciftci, and D. Moses, *J. Chem. Phys.*, **101**, 1787 (1994).
- 94JCP(101)6344 D. Oeter, H.-J. Egelhaaf, Ch. Ziegler, D. Oelkrug, and W. Göpel, *J. Chem. Phys*, **101**, 6344 (1994).
- 94JCP(101)9519 R.A.J. Janssen, D. Moses, and N.S. Sariciftci, *J. Chem. Phys*, **101**, 9519 (1994).
- 94JCS(CC)557 I.E. Buys, L.D. Field, T.W. Hambley, and E.D. McQueen, *J. Chem. Soc., Chem. Commun.*, 557 (1994).
- 94JCS(CC)1011 S.H. Kawai, S.L. Gilat, and J.-M. Lehn, *J. Chem. Soc., Chem. Commun.*, 1011 (1994).
- 94JCS(CC)1859 K. Takimiya, T. Otsubo, and F. Ogura, *J. Chem. Soc., Chem. Commun.*, 1859 (1994).
- 94JCS(CC)1911 M. Catellani, T. Caronna, and S.V. Meille, *J. Chem. Soc., Chem. Commun.*, 1911 (1994).
- 94JCS(CC)2123 T. Saika, M. Irie, and T. Shimidzu, *J. Chem. Soc., Chem. Commun.*, 2123 (1994).
- 94JCS(P1)1245 A. D'Agostini and M. D'Auria, *J. Chem. Soc., Perkin Trans*, **1**, 1245 (1994).
- 94JOM(468)55 J. Oshita, D. Kanaya, and M. Ishikawa, *J. Organomet. Chem*, **468**, 55 (1994).
- 94JPC228 V. Wintgens, P. Valat, and F. Garnier, *J. Phys. Chem*, **98**, 228 (1994).
- 94JPC2282 W.S. Jenks, W. Lee, and D. Shutters, *J. Phys. Chem*, **98**, 2282 (1994).
- 94JPC3631 J.E. Chadwick and B.E. Kohler, *J. Phys. Chem*, **98**, 3631 (1994).
- 94JPC4990 W.J. Buma, B.E. Kohler, and T.A. Shaler, *J. Phys. Chem*, **98**, 4990 (1994).
- 94JPC12893 M. Takayanagi, T. Gejo, and F. Hanazaki, *J. Phys. Chem*, **98**, 12893 (1994).

- 94JPC10102 T. Geisler, J.C. Petersen, T. Bjørnholm, E. Fisher, J. Larsen, C. Dehu, J.-L. Brédas, G.J. Tormos, P.N. Nugara, M.P. Cava, and R. Metzger, *J. Phys. Chem*, **98**, 10102 (1994).
- 94JPP(A)(79)67 M. D'Auria, *J. Photochem. Photobiol. A*, **79**, 67 (1994).
- 94JPP(A)(83)1 M. Ciofalo and G. Ponterini, *J. Photochem. Photobiol., A: Chem*, **83**, 1 (1994).
- 94MI329 J.B. Hudson, E.A. Graham, and G.H.N. Towers, *Planta Med*, **60**, 329 (1994).
- 94MI377 D. Mares, C. Romagnoli, R. Rossi, A. Carpita, M. Ciofalo, and A. Bruni, *Mycoses*, **37**, 377 (1994).
- 94MI745 A. Sharma and H.C. Goel, *Indian J. Exp. Biol*, **32**, 745 (1994).
- 94MM1847 L. Robitaille and M. Leclerc, *Macromolecules*, **27**, 1847 (1994).
- 94MM6503 M.R. Andersson, D. Selse, M. Berggren, H. Järvinen, T. Hjertberg, O. Inganäs, O. Wennerström, and J.-E. Österholm, *Macromolecules*, **27**, 6503 (1994).
- 94NAT(372)444 M. Berggren, O. Inganäs, G. Gustafsson, J. Rasmusson, M. R. Andersson, T. Hjertberg, and O. Wennerström, *Nature*, **372**, 444 (1994).
- 94OM4448 W.D. Jones, R.M. Chin, T.W. Crane, and D.M. Baruch, *Organometallics*, **13**, 4448 (1994).
- 94PP(60)591 J.B. Hudson, R.J. Marles, C. Soucy-Breau, L. Harris, and T. Arnason, *Photochem. Photobiol*, **60**, 591 (1994).
- 94TL633 M. D'Auria, *Tetrahedron Lett*, **35**, 633 (1994).
- 94TL3151 M. D'Auria, *Tetrahedron Lett*, **35**, 3151 (1994).
- 94TL7155 W.S. Jenks, L.M. Taylor, Y. Guo, and Z. Wan, *Tetrahedron Lett*, **35**, 7155 (1994).
- 95AGE303 P. Bäuerle, T. Fischer, B. Bidlingmeier, A. Stabel, and J.P. Rabe, *Angew. Chem. Int. Ed. Engl*, **34**, 303 (1995).
- 95AGE1119 M. Tsivgoulis and J.-M. Lehn, *Angew. Chem. Int. Ed. Engl*, **34**, 1119 (1995).
- 95BCJ2363 H. Higuchi, T. Nakayama, H. Koyama, J. Ojima, T. Wada, and H. Sasabe, *Bull. Chem. Soc. Jpn*, **68**, 2362 (1995).
- 95CEJ275 S.L. Gilat, S.H. Kawai, and J.-M. Lehn, *Chem. Eur. J*, **1**, 275 (1995).
- 95CEJ285 S.H. Kawai, S.L. Gilat, R. Ponsinet, and J.-M. Lehn, *Chem. Eur. J*, **1**, 285 (1995).
- 95CL69 S. Abe, A. Sugai, I. Yamazaki, and M. Irie, *Chem. Lett.*, 69 (1995).
- 95CL99 M. Fujitsuka, T. Sato, H. Segawa, and T. Shimidzu, *Chem. Lett.*, 99 (1995).
- 95CL109 M. D'Auria, *Chem. Lett.*, 109 (1995).
- 95CP(201)309 R. Colditz, D. Grebner, M. Hebig, and S. Reutsch, *Chem. Phys*, **201**, 309 (1995).
- 95CPL(241)89 N.C. Greenham, I.D.W. Samuel, G.R. Hayes, R.T. Phillips, Y.A.R. R. Kessener, S.C. Moratti, A.B. Holmes, and R.H. Friend, *Chem. Phys. Lett*, **241**, 89 (1995).
- 95H(41)1659 J. Dogan, G. Karminski-Zamola, and D.W. Boykin, *Heterocycles*, **41**, 1659 (1995).
- 95H(41)2691 M. Malešević, G. Karminski-Zamola, M. Bajić, and D.W. Boykin, *Heterocycles*, **41**, 2691 (1995).
- 95JA233 T.-A. Chen, X. Wu, and R.D. Rieke, *J. Am. Chem. Soc*, **117**, 233 (1995).
- 95JA2667 Z. Wan and W.S. Jenks, *J. Am. Chem. Soc*, **117**, 2667 (1995).

- 95JCP(102)2628 R.A.J. Janssen, M.P.T. Christiaans, K. Pakbaz, D. Moses, J. C. Hummelen, and N.S. Sariciftci, *J. Chem. Phys.*, **102**, 2628 (1995).
- 95JCP(103)5102 B. Kraabel, D. Moses, and A.J. Heeger, *J. Chem. Phys.*, **103**, 5102 (1995).
- 95JCS(CC)471 A.e. Yassar, C. Moustrou, H.K. Youssoufi, A. Samat, R. Guglielmetti, and F. Garnier, *J. Chem. Soc., Chem. Commun.*, 471 (1995).
- 95JCS(CC)2293 I. Lévesque and M. Leclerc, *J. Chem. Soc., Chem. Commun.*, 2293 (1995).
- 95JF165 D. Oelkrug, H.-I. Egelhaaf, and F. Wilkinson, *J. Fluoresc.*, **5**, 165 (1995).
- 95JOC2082 F. Effenberger, F. Würthner, and F. Steybe, *J. Org. Chem.*, **60**, 2082 (1995).
- 95JOC8360 M. D'Auria and T. Ferri, *J. Org. Chem.*, **60**, 8360 (1995).
- 95JOM(489)15 M.-C. Fang, A. Watanabe, and M. Matsuda, *J. Organomet. Chem.*, **489**, 15 (1995).
- 95JPC5365 F. Elisei, L. Latterini, G.G. Aloisi, and M. D'Auria, *J. Phys. Chem.*, **99**, 5365 (1995).
- 95JPC9155 A. Yassar, G. Horowitz, P. Valat, V. Wintgens, M. Hmyene, F. Deloffre, P. Srivastava, P. Lang, and F. Garnier, *J. Phys. Chem.*, **99**, 9155 (1995).
- 95JPC16991 D. Grebner, H. Helbig, and S. Rentsch, *J. Phys. Chem.*, **99**, 16991 (1995).
- 95JPP(A)(91)187 M. D'Auria, *J. Photochem. Photobiol., A: Chem.*, **91**, 187 (1995).
- 95JST(348)405 H.-J. Egelhaaf, D. Oelkrug, D. Oeter, Ch. Ziegler, and W. Göpel, *J. Mol. Struct.*, **348**, 405 (1995).
- 95MI536 C. Rivas and F. Vargas, in "CRC Handbook of Organic Photochemistry and Photobiology," (W.M. Horspool and P.-S. Song, eds.), CRC Press, Boca Raton, FL, 1995 p. 536.
- 95MI803 A. Lablache-Combier, in "CRC Handbook of Organic Photochemistry and Photobiology," (W. Horspool, ed.), CRC Press, Boca Raton, FL, 1995, p. 803.
- 95MI1063 A. Lablache-Combier, in "CRC Handbook of Organic Photochemistry and Photobiology," (W. Horspool, ed.), CRC Press, Boca Raton, FL, 1995, p. 1063.
- 95MM4548 A. Yassar, C. Moustrou, H. Korri Youssoufi, A. Samat, R. Guglielmetti, and F. Garnier, *Macromolecules*, **28**, 4548 (1995).
- 95MM4608 J. Lowe and S. Holdcroft, *Macromolecules*, **28**, 4608 (1995).
- 95MM5706 M. Pomerantz, H. Yang, and Y. Cheng, *Macromolecules*, **28**, 5706 (1995).
- 95MM7525 M.R. Andersson, M. Berggren, O. Inganäs, G. Gustafsson, J. C. Gustafsson-Carlberg, D. Selse, T. Hjertberg, and O. Wennerström, *Macromolecules*, **28**, 7525 (1995).
- 95MM8102 J.K. Herrema, P.F. van Hutten, R.E. Gill, J. Wildeman, R. H. Wieringa, and G. Hadziioannou, *Macromolecules*, **28**, 8102 (1995).
- 95PAC9 R.S. Becker, J. Seixas de Melo, A.L. Maçanita, and F. Elisei, *Pure Appl. Chem.*, **67**, 9 (1995).
- 95PP(60)542 M. D'Auria and G. Mauriello, *Photochem. Photobiol.*, **60**, 542 (1995).

- 95SM(69)309 M. Fujitsuka, T. Sato, H. Segawa, and T. Shimidzu, *Synth. Met*, **69**, 309 (1995).
- 95SM(69)335 T. Sato, M. Fujitsuka, H. Segawa, and T. Shimidzu, *Synth. Met*, **69**, 335 (1995).
- 95SM(69)377 T.J. Kang, J.Y. Kim, K.J. Kim, C. Lee, and S.B. Rhee, *Synth. Met*, **69**, 377 (1995).
- 95SM(69)401 J. Poplawski, E. Ehrenfreund, J. Cornil, J.L. Bredas, R. Pugh, M. Ibrahim, and A.J. Frank, *Synth. Met*, **69**, 401 (1995).
- 95SM(71)2117 S.C. Moratti, R. Cervini, A.B. Holmes, D.R. Baigent, R.H. Friend, N.C. Greenham, J. Grüner, and P.J. Hamer, *Synth. Met*, **71**, 2117 (1995).
- 95SM(71)2191 A. Bolognesi, C. Botta, Z. Geng, C. Flores, and L. Denti, *Synth. Met*, **71**, 2191 (1995).
- 95SM(72)249 G. Yu, H. Nishino, A.J. Heeger, T.-A. Chen, and R.D. Rieke, *Synth. Met*, **72**, 249 (1995).
- 95SM(73)195 B.H. Cumpston and K.F. Jensen, *Synth. Met*, **73**, 195 (1995).
- 95TL3177 R.M. El-Shishtawy, K. Fukunishi, and S. Mixi, *Tetrahedron Lett*, **36**, 3177 (1995).
- 95TL6567 M. D'Auria, *Tetrahedron Lett*, **36**, 6567 (1995).
- 96ACSA71 J. Larsen and K. Bechgaard, *Acta Chem. Scand*, **50**, 71 (1996).
- 96ACSA77 J. Larsen and K. Bechgaard, *Acta Chem. Scand*, **50**, 77 (1996).
- 96ACSA83 J. Larsen, A. Dolbecq, and K. Bechgaard, *Acta Chem. Scand*, **50**, 83 (1996).
- 96AM982 J. Birgersson, K. Kaeriyama, P. Barta, P. Bröms, M. Fahlman, T. Granlund, and W.R. Salaneck, *Adv. Mater*, **8**, 982 (1996).
- 96CCA261 M. Bajić and G. Karmiski-Zamola, *Croatica Chim. Acta*, **69**, 261 (1996).
- 96CEJ1399 G.M. Tsivgoulis and J.-M. Lehn, *Chem. Eur. J*, **2**, 1399 (1996).
- 96CL285 M. Fujitsuka, T. Sato, A. Watanabe, O. Ito, and T. Shimidzu, *Chem. Lett.*, 285 (1996).
- 96CM819 I.D.W. Samuel, I. Ledoux, C. Delporte, D.L. Pearson, and J. M. Tour, *Chem. Mater*, **8**, 819 (1996).
- 96CPL(255)147 O.-K. Kim and J.-M. Lehn, *Chem. Phys. Lett*, **255**, 147 (1996).
- 96CPL(260)125 P. Landwehr, H. Port, and H.C. Wolf, *Chem. Phys. Lett*, **260**, 125 (1996).
- 96H(43)959 M. D'Auria, *Heterocycles*, **43**, 959 (1996).
- 96H(43)1305 M. D'Auria, *Heterocycles*, **43**, 1305 (1996).
- 96H(43)1529 M. D'Auria, *Heterocycles*, **43**, 1529 (1996).
- 96JCS(P2)1377 M. Blenkle, P. Boldt, C. Bräuchle, W. Grahn, I. Ledoux, H. Nerenz, S. Stadler, J. Wichern, and J. Zyss, *J. Chem. Soc., Perkin Trans*, **2**, 1377 (1996).
- 96JPC4689 N. Tamai, T. Saika, T. Shimidzu, and M. Irie, *J. Phys. Chem*, **100**, 4689 (1996).
- 96JPC15309 T. Kodaira, A. Watanabe, O. Ito, M. Watanabe, H. Saito, and M. Koishi, *J. Phys. Chem*, **100**, 15309 (1996).
- 96JPC18683 R.S. Becker, J. Seixas de Melo, A.L. Maçanita, and F. Elisei, *J. Phys. Chem*, **100**, 18683 (1996).
- 96JPP(A)(93)39 R. Boch, B. Mehta, T. Connolly, T. Durst, J.T. Arnason, R. W. Redmond, and J.C. Scaiano, *J. Photochem. Photobiol., A: Chem*, **93**, 39 (1996).
- 96JPP(A)(93)169 F. Vargas, C. Rivas, M. Navarro, and Y. Alvarado, *J. Photochem. Photobiol., A: Chem*, **93**, 169 (1996).

- 96L6167 M.H. Dishner, J.C. Hemminger, and F.J. Feher, *Langmuir*, **12**, 6176 (1996).
- 96MI374 M. Ciofalo, S. Petruso, and D. Schillaci, *Planta Med*, **62**, 374 (1996).
- 96MI1763 F. Chen, P.G. Mehta, L. Takiff, and R.D. McCullough, *J. Mater. Chem.*, **6**, 1763 (1996).
- 96OM872 M.G. Partridge, L.D. Field, and B.A. Messerle, *Organometallics*, **15**, 872 (1996).
- 96OM2000 A. Kunai, T. Ueda, K. Horata, E. Toyoda, I. Nagamoto, J. Ohshita, M. Ishikawa, and K. Tanaka, *Organometallics*, **15**, 2000 (1996).
- 96SM(76)249 D. Oelkrug, H.-J. Egelhaaf, J. Gierschner, and A. Tompert, *Synth. Met*, **76**, 249 (1996).
- 96SM(83)227 W. Gebauer, M. Bäßler, A. Soukopp, C. Väterlein, R. Fink, M. Sokolowski, and E. Umbach, *Synth. Met*, **83**, 227 (1996).
- 96T14253 M. D'Auria, V. Esposito, and G. Mauriello, *Tetrahedron*, **52**, 14253 (1996).
- 96TSF(284/85)267 D. Oelkrug, H.-J. Egelhaaf, and J. Haiber, *Thin Solid Films*, **284–285**, 267 (1996).
- 97AM36 J.G. Laquindanum, H.E. Katz, A.J. Lovinger, and A. Dodabalapur, *Adv. Mater*, **9**, 36 (1997).
- 97AM233 S.E. Döttinger, M. Hohloch, J.L. Segura, E. Steinhuber, M. Hanack, A. Tompert, and D. Oelkrug, *Adv. Mater*, **9**, 233 (1997).
- 97AM389 R. Hajlaoui, G. Horowitz, F. Garnier, A. Arce-Bouchet, L. Laigrem, A. El Kassmi, F. Demanze, and F. Kouki, *Adv. Mater*, **9**, 389 (1997).
- 97AM720 T. Noda, H. Ogawa, N. Noma, and Y. Shirota, *Adv. Mater*, **9**, 720 (1997).
- 97APPLAB(70)699 T. Toda, H. Ogawa, N. Noma, and Y. Shirota, *Appl. Phys. Lett*, **70**, 699 (1997).
- 97CM981 T.M. Barclay, A.W. Cordes, C.D. MacKinnon, R.T. Oakley, and R.W. Reed, *Chem. Mater*, **9**, 981 (1997).
- 97CM991 T. Caronna, M. Forte, M. Catellani, and S.V. Meille, *Chem. Mater*, **9**, 991 (1997).
- 97CPL(278)146 G. Bongiovanni, C. Botta, J.L. Brédas, J. Cornil, D.R. Ferro, A. Mura, A. Piaggi, and R. Tubino, *Chem. Phys. Lett*, **278**, 146 (1997).
- 97CRV173 J. Roncali, *Chem. Rev.*, **97**, 173 (1997).
- 97DP(33)319 G. Hallas and A.D. Towns, *Dyes Pigments*, **33**, 319 (1997).
- 97DP(35)219 G. Hallas and H.D. Towns, *Dyes Pigments*, **35**, 219 (1997).
- 97JA94 D.D. Gregory, Z. Wan, and W.S. Jenks, *J. Am. Chem. Soc.*, **119**, 94 (1997).
- 97JA4518 M.S.A. Abdou, F.P. Orfino, Y. Son, and A. Holdcroft, *J. Am. Chem. Soc.*, **119**, 4518 (1997).
- 97JOC1376 D.L. Pearson and J.M. Tour, *J. Org. Chem*, **62**, 1376 (1997).
- 98JOC3105 A.K. Mohanakrishnan, M.V. Lakshmikanthan, C. McDougal, M. P. Cava, J.W. Baldwin, and R.M. Metzger, *J. Org. Chem*, **63**, 3105 (1998).
- 97JPC107 D.V. Lap, D. Grebner, and S. Rentsch, *J. Phys. Chem*, **101**, 107 (1997).
- 97JPC(A)1056 M. Fujutsuka, T. Sato, T. Shimidzu, A. Watanabe, and O. Ito, *J. Phys. Chem. A*, **101**, 1056 (1997).

- 97JPC(B)4553 F. Demanze, J. Cornil, F. Garnier, G. Horowitz, P. Valat, A. Yassar, R. Lazzaroni, and J.-L. Brédas, *J. Phys. Chem. B*, **101**, 4553 (1997).
- 97L3434 R. Ricceri, A. Abboto, A. Facchetti, G.A. Pagani, and G. Gabrielli, *Langmuir*, **13**, 3434 (1997).
- 97L4182 R. Ricceri, A. Abboto, A. Facchetti, G.A. Pagani, and G. Gabrielli, *Langmuir*, **13**, 4182 (1997).
- 97MI23 C. Arbizzani, M. Catellani, M. Mastragostino, and M.G. Cerroni, *J. Electroanal. Chem*, **423**, 23 (1997).
- 97MI27 M. Granström, M. Berggren, D. Pede, O. Inganäs, M. R. Andersson, T. Hjertberg, and O. Wennerström, *Supramol. Sci*, **4**, 27 (1997).
- 97MI1738 S.C. Ng, L.G. Xu, and H.S.O. Chan, *J. Mater. Sci. Lett.*, **16**, 1738 (1997).
- 97MM4608 H. Saadeh, T. Goodson, and L. Yu, *Macromolecules*, **30**, 4608 (1997).
- 97OM4661 C. Bianchini, J.A. Casares, R. Osman, D.I. Pattison, M. Peruzzini, R.N. Perutz, and F. Zanobini, *Organometallics*, **16**, 4611 (1997).
- 97SM(85)1383 M.R. Andersson, M. Berggren, T. Olinga, T. Hjertberg, O. Inganäs, and O. Wennerström, *Synth. Met*, **85**, 1383 (1997).
- 97SM(87)127 W. Gebauer, C. Väterlein, A. Soukopp, M. Sokolowski, R. Hock, H. Port, P. Bäuerle, and E. Umbach, *Synth. Met*, **87**, 127 (1997).
- 97T1157 M. D'Auria, E. De Luca, V. Esposito, G. Mauriello, and R. Racioppi, *Tetrahedron*, **53**, 1157 (1997).
- 98AGE402 A. Kraft, A.C. Brimsdale, and A.B. Holmes, *Angew. Chem. Int. Ed*, **37**, 402 (1998).
- 98AM93 R.D. McCullough, *Adv. Mater*, **10**, 93 (1998).
- 98AM365 G. Horowitz, *Adv. Mater*, **10**, 365 (1998).
- 98AM551 G. Barbarella, L. Favaretto, M. Zambianchi, O. Pudova, C. Arbizzani, A. Bongini, and M. Mastragostino, *Adv. Mater*, **10**, 551 (1998).
- 98AM593 W. Huang, H. Meng, W.-L. Yu, J. Gao, and A.J. Heeger, *Adv. Mater*, **10**, 593 (1998).
- 98BCJ985 M. Irie and K. Uchida, *Bull. Chem. Soc. Jpn*, **71**, 985 (1998).
- 98BCJ2229 H. Higuchi, S. Yoshida, Y. Uraki, and J. Ojima, *Bull. Chem. Soc. Jpn*, **71**, 2229 (1998).
- 98CEJ2211 U. Mitschke, E.M. Osteritz, T. Debaerdemaeker, M. Sokolowski, and P. Bäuerle, *Chem. Eur. J*, **4**, 2211 (1998).
- 98CM3340 W. Huang, W.-L. Yu, H. Meng, J. Pei, and S.F.Y. Li, *Chem. Mater*, **10**, 3340 (1998).
- 98CP(227)33 W. Gebauer, M. Sokolowski, and E. Umbach, *Chem. Phys*, **227**, 33 (1998).
- 98CPB1522 K. Oda, H. Tsujita, M. Sakai, and M. Machida, *Chem. Pharm. Bull*, **46**, 1522 (1998).
- 98CPL(292)607 W. Paa, J.-P. Yang, M. Helbig, J. Hein, and S. Rentsch, *Chem. Phys. Lett*, **292**, 607 (1998).
- 98JA2047 T. Yamamoto, D. Komarudin, M. Arai, B.-L. Lee, H. Suganuma, N. Asakawa, Y. Inoue, K. Kubota, S. Sasaki, T. Fukuda, and H. Matsuda, *J. Am. Chem. Soc.*, **120**, 2047 (1998).
- 98JA2206 X.-C. Li, H. Sirringhaus, F. Garnier, A.B. Holmes, S.C. Moratti, N. Feeder, W. Clegg, S.J. Teat, and R.H. Friend, *J. Am. Chem. Soc*, **120**, 2206 (1998).

- 98JCP(109)2543 V. Hernandez, S. Hotta, and J.T.L. Navarrete, *J. Chem. Phys.*, **109**, 2543 (1998).
- 98JCS(F)3331 M. Fujitsuka, T. Sato, F. Sezaki, K. Tanaka, A. Watanabe, and O. Ito, *J. Chem. Soc., Faraday Trans.*, **94**, 3331 (1998).
- 98JOC5497 G. Barbarella, L. Favaretto, G. Sotgiu, M. Zambianchi, L. Antolini, O. Pudova, and A. Bongini, *J. Org. Chem.*, **63**, 5497 (1998).
- 98MI6279 P. Barta, F. Cacialli, R.H. Friend, and M. Zagórska, *J. Appl. Phys.*, **84**, 6279 (1998).
- 98MM6289 N. DiCésare, M. Belletête, A. Donat-Bouillud, M. Leclerc, and G. Durocher, *Macromolecules*, **31**, 6289 (1998).
- 98OM3405 H. Tobita, K. Hashidzume, K. Endo, and H. Ogino, *Organometallics*, **17**, 3405 (1998).
- 98S1303 P. Brooks, D. Donati, A. Pelter, and F. Ponticelli, *Synthesis*, 1303 (1998).
- 98SCI(280)1741 H. Sirringhaus, N. Tessler, and R.H. Friend, *Science*, **280**, 1741 (1998).
- 98SM(92)33 S.C. Ng, J.M. Xu, and H.S.O. Chan, *Synth. Met.*, **92**, 33 (1998).
- 98SM(93)175 M. Fall, J.J. Aaron, N. Sakmeche, M.M. Dieng, M. Jouini, S. Aeiya, J.C. Lacroix, and P.C. Lacaze, *Synth. Met.*, **93**, 175 (1998).
- 98SM(94)185 S.C. Ng, L.G. Xu, and H.S.O. Chan, *Synth. Met.*, **94**, 185 (1998).
- 98SM(95)107 T. Sato, M. Fujitsuka, H. Segawa, T. Shimidzu, and K. Tanaka, *Synth. Met.*, **95**, 107 (1998).
- 98T8469 F. Steybe, F. Effenberger, U. Gubler, C. Bosshard, and P. Günter, *Tetrahedron*, **54**, 8469 (1998).
- 99ACR209 F. Garnier, *Acc. Chem. Res.*, **32**, 209 (1999).
- 99AM452 A.K.-Y. Jen, Y. Liu, L. Zheng, S. Liu, K.J. Drost, Y. Zhang, and L. R. Dalton, *Adv. Mater.*, **11**, 452 (1999).
- 99AM910 A. Fernandez-Acebes and J.-M. Lehn, *Adv. Mater.*, **11**, 910 (1999).
- 99AM1375 G. Barbarella, L. Favaretto, G. Sotgiu, M. Zambianchi, V. Fattori, M. Cocchi, F. Cacialli, G. Gigli, and R. Cingolani, *Adv. Mater.*, **11**, 1375 (1999).
- 99CM3028 K. Chondroudis and D.B. Mitzi, *Chem. Mater.*, **11**, 3028 (1999).
- 99DP(42)249 G. Hallas and J.-H. Choi, *Dyes Pigments*, **42**, 249 (1999).
- 99H(50)1115 M. D'Auria, *Heterocycles*, **50**, 1115 (1999).
- 99JCP(111)5427 J. Seixas de Melo, L.M. Silva, L.G. Arnaut, and R.S. Becker, *J. Chem. Phys.*, **111**, 5427 (1999).
- 99JCS(CC)747 M. Irie, T. Lifka, K. Uchida, S. Kobatake, and Y. Shindo, *J. Chem. Soc., Chem. Commun.*, 747 (1999).
- 99JCS(P1)3691 S. Yuquan, Z. Yuxia, L. Zao, W. Jianghong, Q. Ling, L. Shixiong, Z. Jianfeng, and Z. Jiayun, *J. Chem. Soc., Perkin Trans.*, **1**, 3691 (1999).
- 99JPC(A)795 N. DiCésare, M. Belletête, C. Marrano, M. Leclerc, and G. Durocher, *J. Phys. Chem. A*, **103**, 795 (1999).
- 99JPC(A)3864 N. DiCésare, M. Belletête, E.R. Garcia, M. Leclerc, and G. Durocher, *J. Phys. Chem. A*, **103**, 3864 (1999).
- 99JPC(B)7771 M. Theander, O. Inganäs, W. Mammo, T. Olinga, M. Svensson, and M. Andersson, *J. Phys. Chem. B*, **103**, 7771 (1999).
- 99MI151 A. Bolognesi, W. Porzio, G. Bajo, G. Zannoni, and L. Fanning, *Acta Polym.*, **50**, 151 (1999).

- 99MI233 M. D'Auria, in "Targets in Heterocycles Systems, Chemistry and Properties," (O.A. Attanasi and D. Spinelli, eds.) Vol. 2, Italian Society of Chemistry, Rome, 1999, p. 233.
- 99MI259 M. Maiti, S. Sinha, C. Deb, A. De, and T. Ganguly, *J. Lumin.*, **82**, 259 (1999).
- 99MI395 H.-J. Egelhaaf, J. Gierschner, J. Haiber, and D. Oelkrug, *Opt. Mater.*, **12**, 395 (1999).
- 99MI1875 J. Roncali, *J. Mat. Chem.*, **9**, 1875 (1999).
- 99MI1933 M.R. Andersson, O. Thomas, W. Mammo, M. Svensson, M. Theander, and O. Inganäs, *J. Mater. Chem.*, **9**, 1933 (1999).
- 99MI2095 H. Sirringhaus, R.H. Friend, C. Wang, J. Leuninger, and K. Müllen, *J. Mater. Chem.*, **9**, 2095 (1999).
- 99MI2155 M. Pomerantz, Y. Cheng, R.K. Kasim, and R.L. Elsenbaumer, *J. Mater. Chem.*, **9**, 2155 (1999).
- 99MI2227 O.-K. Kim, A. Fort, M. Barzoukas, M. Blanchard-Desce, and J.-M. Lehn, *J. Mater. Chem.*, **9**, 2227 (1999).
- 99MM118 W. Huang, H. Meng, W.-L. Yu, J. Pei, Z.-K. Chen, and Y.-H. Lai, *Macromolecules*, **32**, 118 (1999).
- 99OL1039 J.-Y. Wu, J.-H. Ho, S.-M. Shih, T.-L. Hsieh, and T.-I. Ho, *Org. Lett.*, **1**, 1039 (1999).
- 99OL1847 C. Cai, I. Liakatas, M.-S. Wong, M. Büsch, C. Bosshard, P. Gunter, S. Concilio, N. Tirelli, and U.W. Suter, *Org. Lett.*, **1**, 1847 (1999).
- 99PCCP1707 S. Rentsch, J.P. Yang, W. Paa, E. Birkner, J. Schiedt, and R. Weinkauff, *Phys. Chem. Chem. Phys.*, **1**, 1707 (1999).
- 99PCCP1731 D. Gningue-Sall, M. Fall, M.M. Dieng, J.J. Aaron, and P. C. Lacaze, *Phys. Chem. Chem. Phys.*, **1**, 1731 (1999).
- 99SM(101)11 M.R. Andersson, W. Mammo, T. Olinga, M. Svensson, M. Theander, and O. Inganäs, *Synth. Met.*, **101**, 11 (1999).
- 99SM(101)624 J.P. Yang, W. Paa, and S. Rentsch, *Synth. Met.*, **101**, 624 (1999).
- 99SM(102)1158 K. Yoshino, M. Hirohata, T. Sonoda, R. Hidayat, A. Fujii, A. Naka, and M. Ishikawa, *Synth. Met.*, **102**, 1158 (1999).
- 99T14985 M. Pasini, S. Destri, C. Botta, and W. Porzio, *Tetrahedron*, **55**, 14985 (1999).
- 99TSF(340)218 R. Ricceri, A. Abbotto, A. Facchetti, G.A. Pagani, and G. Gabrielli, *Thin Solid Films*, **340**, 218 (1999).
- 00AGE2870 M.C. Suh, B. Jiang, and T.D. Tilley, *Angew Chem. Int. Ed.*, **39**, 2870 (2000).
- 00AGE4547 A. Facchetti, Y. Deng, A. Wang, Y. Koide, H. Sirringhaus, T. J. Marks, and R.H. Friend, *Angew. Chem. Int. Ed.*, **39**, 4547 (2000).
- 00AM227 Z. Bao, *Adv. Mater.*, **12**, 227 (2000).
- 00AM481 L.B. Groenendaal, F. Jonas, D. Freitag, H. Pielartzik, and J. R. Reynolds, *Adv. Mater.*, **12**, 481 (2000).
- 00CM1931 A. Donat-Bouillud, I. Lévesque, Y. Tao, M. D'Iorio, S. Beaupré, P. Blondin, M. Ranger, J. Bouchard, and M. Leclerc, *Chem. Mater.*, **12**, 1931 (2000).
- 00CR1685 M. Irie, *Chem. Rev.*, **100**, 1685 (2000).
- 00EJO1327 K. Eckert, A. Schröder, and H. Hartmann, *Eur. J. Org. Chem.*, 1327 (2000).
- 00H(52)159 S. Inoue, T. Jigami, H. Nozoe, Y. Aso, F. Ogura, and T. Otsubo, *Heterocycles*, **52**, 159 (2000).

- 00IC5496 K.A. Walters, L. Trouillet, S. Guillerez, and K.S. Schanze, *Inorg. Chem*, **39**, 5496 (2000).
- 00JA4871 M. Irie, T. Lifka, S. Kobatake, and N. Kato, *J. Am. Chem. Soc*, **122**, 4871 (2000).
- 00JA9006 L. Antolini, E. Tadesco, G. Barbarella, L. Favaretto, G. Sotgiu, M. Zambianchi, D. Casarini, G. Gigli, and R. Cingolani, *J. Am. Chem. Soc*, **122**, 9006 (2000).
- 00JA11971 G. Barbarella, L. Favaretto, G. Sotgiu, M. Zambianchi, A. Bongini, C. Arbizzani, M. Mastragostino, M. Anni, G. Gigli, and R. Cingolani, *J. Am. Chem. Soc*, **122**, 11971 (2000).
- 00JA12385 A.W. Freeman, S.C. Koene, P.R.L. Malenfant, M.E. Thompson, and J.M.J. Fréchet, *J. Am. Chem. Soc*, **122**, 12385 (2000).
- 00JCP(112)383 S. Tan, A.K. Bhowmik, M. Thakur, M.V. Lakshmikantham, and M.P. Cava, *J. Chem. Phys*, **112**, 383 (2000).
- 00JCS(CC)1139 T. Caronna, R. Sinisi, M. Catellani, L. Malpezzi, S.V. Meille, and A. Mele, *Chem. Commun.*, 1139 (2000).
- 00JCS(CC)1631 J. Pei, W.-L. Yu, W. Huang, and A.J. Heeger, *Chem. Commun.*, 1631 (2000).
- 00JCS(P1)4316 H. Hartmann and I. Zug, *J. Chem. Soc., Perkin Trans*, **1**, 4316 (2000).
- 00JF107 M. Fall, J.J. Aaron, and D. Gningue-Sall, *J. Fluoresc*, **10**, 107 (2000).
- 00JOC2494 M. D'Auria, *J. Org. Chem*, **65**, 2494 (2000).
- 00JOC3894 H. Meng and W. Huang, *J. Org. Chem*, **65**, 3894 (2000).
- 00JPO523 N. Rebiere, C. Moustrou, M. Meyer, A. Samat, R. Guglielmetti, J.-C. Micheau, and J. Aubard, *J. Phys. Org. Chem*, **13**, 523 (2000).
- 00JPO648 T. Thiemann, D. Ohira, K. Arima, T. Sawada, S. Mataka, F. Marken, R.G. Compton, S.D. Bull, and S.G. Davies, *J. Phys. Org. Chem*, **13**, 648 (2000).
- 00MI612 G. Gigli, M. Ani, G. Barbarella, L. Favaretto, F. Cacialli, and R. Cingolani, *J. Phys. E*, **7**, 612 (2000).
- 00MM2462 J. Pei, W.-L. Yu, W. Huang, and A.J. Heeger, *Macromolecules*, **33**, 2462 (2000).
- 00MM8945 B. Liu, W.-L. Yu, Y.-H. Lai, and W. Huang, *Macromolecules*, **33**, 8945 (2000).
- 00POLLDG4047 M. Fall, J.J. Aaron, M.M. Dieng, and C. Parkanyi, *Polymer*, **41**, 4047 (2000).
- 00SA1391 J.J. Aaron and M. Fall, *Spectrochim. Acta*, **56**, 1391 (2000).
- 00SM(111-112)187 A. Bolognesi, C. Botta, and L. Cecchinato, *Synth. Met.*, **111-12**, 187 (2000).
- 00SM(113)129 M. Pasini, S. Destri, C. Botta, and W. Porzio, *Synth. Met*, **113**, 129 (2000).
- 00SM(115)213 I. Ledoux, J. Zyss, E. Barni, C. Barolo, N. Diulgheroff, P. Quagliotto, and G. Viscardi, *Synth. Met*, **115**, 213 (2000).
- 00T9383 B. Guizzardi, M. Mella, M. Fagnoni, and A. Albini, *Tetrahedron*, **56**, 9383 (2000).
- 00TAL807 A. Ghauch, J. Rima, C. Fachinger, J. Suptil, and M. Martin-Bouyer, *Talanta*, **51**, 807 (2000).
- 00TL1951 K. Song, L.-Z. Wu, C.-H. Yang, and C.-H. Tung, *Tetrahedron Lett.*, **41**, 1951 (2000).
- 01ACR359 H.E. Katz, Z. Bao, and S.L. Gilat, *Acc. Chem. Res*, **34**, 359 (2001).

- 01AHC41 M. D'Auria, in "Advances in Heterocyclic Chemistry," (A.R. Katritzky, ed.) Vol. 79, Academic Press, San Diego, CA, 2001, p. 41.
- 01AM1201 H. Ma and A.K.-Y. Jen, *Adv. Mater*, **13**, 1201 (2001).
- 01BCJ1789 T. Otsubo, Y. Aso, and K. Takimiya, *Bull. Chem. Soc. Jpn*, **74**, 1789 (2001).
- 01CL618 K. Shibata, S. Kobatake, and M. Irie, *Chem. Lett.*, 618 (2001).
- 01CM3906 T. Caronna, M. Catellani, S. Luzzati, L. Malpezzi, S.V. Meille, A. Mele, C. Richter, and R. Sinisi, *Chem. Mater*, **13**, 3906 (2001).
- 01CM4112 G. Barbarella, L. Favaretto, G. Sotgiu, L. Antolini, G. Gigli, R. Cingolani, and A. Bongini, *Chem. Mater*, **13**, 4112 (2001).
- 01JA1784 T.B. Norsten and N.R. Branda, *J. Am. Chem. Soc.*, **123**, 1784 (2001).
- 01JA4643 Y. Sakamoto, S. Komatsu, and T. Suzuki, *J. Am. Chem. Soc.*, **123**, 4643 (2001).
- 01JA9214 H. Meng, Z. Bao, A.J. Lovinger, B.-C. Wang, and A.M. Muijsce, *J. Am. Chem. Soc.*, **123**, 9214 (2001).
- 01JCS(CC)711 T. Kawai, T. Sasaki, and M. Irie, *J. Chem. Soc., Chem. Commun.*, 711 (2001).
- 01JCS(CC)759 L.N. Lucas, J. van Esch, R.M. Kellog, and B.L. Feringa, *J. Chem. Soc., Chem. Commun.*, 759 (2001).
- 01JCS(CC)1216 A. Charas, J. Morgado, J.M.G. Martinho, L. Alcácer, and F. Cacialli, *Chem. Commun.*, 1216 (2001).
- 01JCS(P1)740 U. Mitschke and P. Bäuerle, *J. Chem. Soc., Perkin Trans*, **1**, 740 (2001).
- 01JOC4576 E. Lucien and A. Greer, *J. Org. Chem*, **66**, 4576 (2001).
- 01JOC5419 K. Yagi, C.F. Soong, and M. Irie, *J. Org. Chem*, **66**, 5419 (2001).
- 01JPC(A)1741 J. Ern, A.T. Bens, H.-D. Martin, S. Mukamel, S. Tretiak, K. Tsyganenko, K. Kuldova, H.P. Trommsdorff, and C. Krysch, *J. Phys. Chem. A*, **105**, 1741 (2001).
- 01JPC(B)7624 A. Ruseckas, E.B. Namadas, T. Ganguly, M. Theander, M. Svensson, M.R. Andersson, O. Inganäs, and V. Sundström, *J. Phys. Chem. B*, **105**, 7624 (2001).
- 01JPC(B)11106 D.L. Vangeneugden, D.J.M. Vanderzande, J. Salbeck, P.A. van Hal, R.A.J. Janssen, J.C. Hummelen, C.J. Brabec, S.E. Shaheen, and N.S. Sariciftci, *J. Phys. Chem. B*, **105**, 11106 (2001).
- 01MI1 H.A.M. van Mullekom, J.A.J.M. Vakemans, E.E. Havinga, and E. W. Meijer, *Mater. Sci. Eng*, **32**, 1 (2001).
- 01MI255 A. Dhanabalan, J.K.J. van Duren, P.A. van Hal, J.L.J. van Dongen, and R.A.J. Janssen, *Adv. Funct. Mater*, **11**, 255 (2001).
- 01MI445 Z. Yuxia, L. Zhao, Q. Ling, Z. Jianfen, Z. Jiayun, S. Yuquan, X. Gang, and Y. Peixian, *Eur. Polym. J*, **37**, 445 (2001).
- 01MI1625 F. Osterod, L. Peters, A. Kraft, T. Sano, J.J. Morrison, N. Feeder, and A.B. Holmes, *J. Mater. Chem*, **11**, 1625 (2001).
- 01MI3082 A.-L. Ding, J. Pei, Y.-H. Lai, and W. Huang, *J. Mater. Chem*, **11**, 3082 (2001).
- 01MM2522 A.-H. Ahn, M.-Z. Czae, E.-R. Kim, H. Lee, S.-H. Han, J. Noh, and M. Hara, *Macromolecules*, **34**, 2522 (2001).
- 01MM5746 K. Lee and G.A. Sotzing, *Macromolecules*, **34**, 5746 (2001).
- 01MM7241 J. Pei, W.-L. Yu, J. Ni, Y.-H. Lai, W. Huang, and A.J. Heeger, *Macromolecules*, **34**, 7241 (2001).
- 01PCCP2765 L. Latterini, F. Elisei, G.G. Aloisi, and M. D'Auria, *Phys. Chem. Chem. Phys.*, **3**, 2765 (2001).

- 01SCI(291)1769 M. Irie, S. Kobatake, and M. Horichi, *Science*, **291**, 1769 (2001).
- 01SM(119)79 T. Caronna, R. Sinisi, M. Catellani, S. Luzzati, S. Abbate, and G. Longhi, *Synth. Met.*, **119**, 79 (2001).
- 01SM(121)1647 S. Destri, W. Porzio, C. Botta, M. Pasini, and F. Bertini, *Synth. Met.*, **121**, 1647 (2001).
- 01SM(122)79 I. Lévesque, A. Donat-Bouillud, Y. Tao, M. D'Iorio, S. Beaupré, P. Blondin, M. Ranger, J. Bouchard, and M. Leclerc, *Synth. Met.*, **122**, 79 (2001).
- 01SM(123)365 M. Fall, L. Assogba, J.-J. Aaron, and M.M. Dieng, *Synth. Met.*, **123**, 365 (2001).
- 01T6877 Y. Obara, K. Takimiya, Y. Aso, and T. Otsubo, *Tetrahedron*, **42**, 6877 (2001).
- 02AM918 H. Tian, B. Chen, H. Tu, and K. Müllen, *Adv. Mater.*, **14**, 918 (2002).
- 02APPLAB(81)634 Y. Niu, Q. Hou, and Y. Cao, *Appl. Phys. Lett.*, **81**, 634 (2002).
- 02BCJ1795 K. Takimiya, K.-I. Kato, Y. Aso, F. Ogura, and T. Otsubo, *Bull. Chem. Soc. Jpn.*, **75**, 1795 (2002).
- 02CL984 J. Yu and Y. Shirota, *Chem. Lett.*, 984 (2002).
- 02CM1884 Y.Z. Su, J.T. Lin, Y.-T. Tao, C.-W. Ko, S.-C. Lin, and S.-S. Sun, *Chem. Mater.*, **14**, 1884 (2002).
- 02CPL(364)432 O.-K. Kim, H.Y. Woo, J.-K. Kim, W.B. Heuer, K.-S. Lee, and C.-Y. Kim, *Chem. Phys. Lett.*, **364**, 432 (2002).
- 02JA4184 T.M. Pappenfus, R.J. Chesterfield, C.D. Frisbie, K.R. Mann, J. Casado, J.D. Raff, and L.L. Miller, *J. Am. Chem. Soc.*, **124**, 4184 (2002).
- 02JA12380 J. Casado, L.L. Miller, K.R. Mann, T.M. Pappenfus, H. Higuchi, E. Ortí, B. Milián, R. Pou-Américo, V. Hernández, and J.T. L. Navarrete, *J. Am. Chem. Soc.*, **124**, 12380 (2002).
- 02JCC(23)824 M. Kleinschmidt, J. Tatchen, and C.M. Marian, *J. Comput. Chem.*, **23**, 824 (2002).
- 02JCP(116)10503 G. Rothe, S. Hintschich, A.P. Monkman, M. Svensson, and M. R. Anderson, *J. Chem. Phys.*, **116**, 10503 (2002).
- 02JF231 J.-J. Aaron, Z. Mechbal, A. Adenier, C. Parkanyi, V. Kozmik, and J. Svoboda, *J. Fluoresc.*, **12**, 231 (2002).
- 02JOC205 J.-M. Raimundo, P. Blanchard, N. Gallego-Planas, N. Mercier, I. Ledoux-Rak, R. Hierle, and J. Roncali, *J. Org. Chem.*, **67**, 205 (2002).
- 02JOC4574 K. Morimitsu, K. Shibata, S. Kobatake, and M. Irie, *J. Org. Chem.*, **67**, 4574 (2002).
- 02JOC5208 S.-M. Yang, J.-J. Shie, J.-M. Fang, S.K. Nandy, H.-Y. Chang, S.-H. Lu, and G. Wang, *J. Org. Chem.*, **67**, 5208 (2002).
- 02JOC6015 T.M. Pappenfus, J.D. Raff, E.J. Hukkanen, J.R. Burney, J. Casado, S.M. Drew, L.L. Miller, and K.R. Mann, *J. Org. Chem.*, **67**, 6015 (2002).
- 02JPP(A)(149)31 M. D'Auria, *J. Photochem. Photobiol. A: Chem.*, **149**, 31 (2002).
- 02JPP(A)(152)41 M. Maiti, T. Misra, T. Bhattacharya, C. Basu (nee Deb), A. De, S. K. Srkar, and T. Ganguly, *J. Photochem. Photobiol. A: Chem.*, **152**, 41 (2002).
- 02JPP(A)(152)141 K. Higashiguchi, K. Matsuda, M. Matsuo, T. Yamada, and M. Irie, *J. Photochem. Photobiol. A: Chem.*, **152**, 141 (2002).
- 02MI34 C. Wochnowski and S. Metev, *Appl. Surf. Sci.*, **186**, 34 (2002).

- 02MI65 M. D'Auria, L. Emanuele, V. Esposito, and R. Racioppi, *Arkivoc*, **11**, 65 (2002).
- 02MI67 C.A. Samyn, K. Van den Broeck, E. Gubbelmans, W. Ballet, T. Verbiest, and A. Persoons, *Opt. Mater.*, **21**, 67 (2002).
- 02MI192 S. Beaupré and M. Leclerc, *Adv. Funct. Mater.*, **12**, 192 (2002).
- 02MI199 D.-H. Hwang, N.S. Cho, B.-J. Jung, H.-K. Shim, J.-I. Lee, L.-M. Do, and T. Zyung, *Opt. Mater.*, **21**, 199 (2002).
- 02MI200 W.J. Mitchell, C. Pena, and P.L. Burn, *J. Mater. Chem.*, **12**, 200 (2002).
- 02MI271 M.-S. Kim, T. Kawai, and M. Irie, *Opt. Mater.*, **21**, 271 (2002).
- 02MI709 J. Huang, Y. Xu, Q. Hou, W. Yang, M. Yuan, and Y. Cao, *Macromol. Rapid Commun.*, **23**, 709 (2002).
- 02MI2565 T. Otsubo, Y. Aso, and K. Takimiya, *J. Mater. Chem.*, **12**, 2565 (2002).
- 02MI3523 A. Charas, J. Morgado, J.M.G. Martinho, A. Fedorov, L. Alcácer, and F. Cacialli, *J. Mater. Chem.*, **12**, 3523 (2002).
- 02MI37 M. Pasini, S. Destri, C. Botta, and W. Porzio, *Mater. Sci. Eng. C*, **19**, 37 (2002).
- 02MI167 A.J. Myles and N.R. Branda, *Adv. Funct. Mater.*, **12**, 167 (2002).
- 02MI192 S. Beaupré and M. Leclerc, *Adv. Funct. Mater.*, **12**, 192 (2002).
- 02MI559 O.-K. Kim, K.-S. Lee, Z. Huang, W.B. Heuer, and C.S. Paik-Sung, *Opt. Mater.*, **21**, 559 (2002).
- 02MI699 A. Yassar, F. Demanze, A. Jaafari, M. El Idrissi, and C. Coupry, *Adv. Funct. Mater.*, **12**, 699 (2002).
- 02MI2887 Q. Hou, Y. Xu, W. Yang, M. Yuan, J. Peng, and Y. Cao, *J. Mater. Chem.*, **12**, 2887 (2002).
- 02MM1224 N.S. Cho, D.-H. Hwang, J.-I. Lee, B.-J. Jung, and H.-K. Shim, *Macromolecules*, **35**, 1224 (2002).
- 02MM6094 P. Herguth, X. Jiang, M.S. Liu, and A.K.-Y. Jen, *Macromolecules*, **35**, 6094 (2002).
- 02MM8413 J.-F. Morin and M. Leclerc, *Macromolecules*, **35**, 8413 (2002).
- 02MM8684 H. Cho and E. Kim, *Macromolecules*, **35**, 8684 (2002).
- 02OL1099 J.-J. Shie, S.-M. Yang, C.-T. Chen, and J.-M. Fang, *Org. Lett.*, **4**, 1099 (2002).
- 02SM(127)221 H.-J. Egelhaaf, J. Gierschner, and D. Oelkrug, *Synth. Met.*, **127**, 221 (2002).
- 02SM(131)31 O. Stéphane, F. Tran-Van, and C. Chevrot, *Synth. Met.*, **131**, 31 (2002).
- 02TL8669 N. Tanifuji, H. Huang, Y. Shinagawa, and K. Kobayashi, *Tetrahedron Lett.*, **43**, 8669 (2002).
- 03AGE3537 K. Higashiguchi, K. Matsuda, and M. Irie, *Angew. Chem. Int. Ed.*, **42**, 3537 (2003).
- 03AM33 A. Facchetti, M. Mushrush, H.E. Katz, and T.J. Marks, *Adv. Mater.*, **15**, 33 (2003).
- 03AM306 C. Videlot, J. Ackermann, P. Blanchard, J.-M. Raimundo, P. Frère, M. Allain, R. de Bettignies, E. Levillain, and J. Roncali, *Adv. Mater.*, **15**, 306 (2003).
- 03CEJ1991 A. Abbotto, L. Beverina, S. Bradamante, A. Facchetti, C. Klein, G. A. Pagani, M. Redi-Abshiro, and R. Wortmann, *Chem. Eur. J.*, **9**, 1991 (2003).

- 03CEJ3670 M.C.R. Delgado, V. Hernández, J. Casado, J.T.L. Navarrete, J.-M. Raimundo, P. Blanchard, and J. Roncali, *Chem. Eur. J.*, **9**, 3670 (2003).
- 03CL1178 K. Matsuda, Y. Shinkai, T. Yamaguchi, K. Nomiyama, M. Isayama, and M. Irie, *Chem. Lett.*, **32**, 1178 (2003).
- 03CM1778 H. Meng, J. Zheng, A.J. Lovinger, B.-C. Wang, P.G. Van Patten, and Z. Bao, *Chem. Mater.*, **15**, 1778 (2003).
- 03EF(17)95 Y. Shiraishi, K. Tachibana, T. Hirai, and I. Komasaawa, *Energy Fuel*, **17**, 95 (2003).
- 03HAC218 K. Starčević, D.W. Boykin, and G. Karminski-Zamola, *Heteroat. Chem.*, **14**, 218 (2003).
- 03JA2524 J. Casado, T.M. Pappenfus, L.L. Miller, K.R. Mann, E. Ortí, P. M. Viruela, R. Pou-Amérigo, V. Hernández, and J.T. L. Navarrete, *J. Am. Chem. Soc.*, **125**, 2524 (2003).
- 03JA3404 A. Peters and N.R. Branda, *J. Am. Chem. Soc.*, **125**, 3404 (2003).
- 03JA5286 T. Izumi, S. Kobashi, K. Takimiya, Y. Aso, and T. Otsubo, *J. Am. Chem. Soc.*, **125**, 5286 (2003).
- 03JA8104 N. Satoh, J.-S. Cho, M. Higuchi, and K. Yamamoto, *J. Am. Chem. Soc.*, **125**, 8104 (2003).
- 03JA9414 M. Mushrush, A. Facchetti, M. Lefenfeld, H.E. Katz, and T. J. Marks, *J. Am. Chem. Soc.*, **125**, 9414 (2003).
- 03JCP(118)1550 J. Seixas de Melo, H.D. Burrows, M. Svensson, M.R. Andersson, and A.P. Monkman, *J. Chem. Phys.*, **118**, 1550 (2003).
- 03JCR(S)60 K. Kumazoe, K. Arima, S. Mataka, D.J. Walton, and T. Thiemann, *J. Chem. Res. (S)*, 60 (2003).
- 03JMC4516 J.D. Koružnjak, M. Grdiša, B. Zamola, K. Pavelić, and G. Karminski-Zamola, *J. Med. Chem.*, **46**, 4516 (2003).
- 03JOC2921 K. Ogawa and S.C. Rasmussen, *J. Org. Chem.*, **68**, 2921 (2003).
- 03JOC8008 C. Sanchez-Martinez, M.M. Faul, C. Shih, K.A. Sullivan, J. L. Grutsch, J.T. Cooper, and S.P. Kolis, *J. Org. Chem.*, **68**, 8008 (2003).
- 03JOC9813 X. Zhang and A.J. Matzger, *J. Org. Chem.*, **68**, 9813 (2003).
- 03JPC(A)3476 Y. Liu, A. De Nicola, O. Reiff, R. Ziessel, and K.S. Schanze, *J. Phys. Chem. A*, **107**, 3476 (2003).
- 03JPS(A)(41)1521 N. Nemoto, H. Kameshima, Y. Okano, and T. Endo, *J. Polym. Sci., Part A: Polym. Chem.*, **41**, 1521 (2003).
- 03MI27 A. Berlin, G. Zotti, S. Zecchin, G. Schiavon, M. Cocchi, D. Virgili, and C. Sabatini, *J. Mater. Chem.*, **13**, 27 (2003).
- 03MI807 M. Passini, S. Destri, W. Porzio, C. Botta, and U. Giovannella, *J. Mater. Chem.*, **13**, 807 (2003).
- 03MI1351 W. Yang, Q. Hou, C. Liu, Y. Niu, J. Huang, R. Yang, and Y. Cao, *J. Mater. Chem.*, **13**, 1351 (2003).
- 03MM2705 P. Coppo, D.C. Cupertino, S.G. Yeates, and M.L. Turner, *Macromolecules*, **36**, 2705 (2003).
- 03MM4288 E. Lim, B. Jung, and H. Shim, *Macromolecules*, **36**, 4288 (2003).
- 03MM8986 S. Beaupré and M. Leclerc, *Macromolecules*, **36**, 8986 (2003).
- 03NAT(421)829 C.D. Müller, A. Falcou, N. Reckefuss, M. Rojahn, V. Widerhirn, P. Rudati, H. Frohne, O. Nuyken, H. Becker, and K. Meerholz, *Nature*, **421**, 829 (2003).
- 03OL1535 T.M. Pappenfus, M.W. Burand, D.E. Janzen, and K.R. Mann, *Org. Lett.*, **5**, 1535 (2003).

- 03POLLDG1843 A. Charas, J. Morgado, J.M.G. Martinho, L. Alcácer, S.F. Lim, R. H. Friend, and F. Cacialli, *Polymer*, **44**, 1843 (2003).
- 03PP(77)121 J. Seixas de Melo, L.M. Rodrigues, C. Serpa, L.G. Arnaut, I.C.F. R. Ferreira, and M.-J.R.P. Queiroz, *Photochem. Photobiol.*, **77**, 121 (2003).
- 03S2255 A.S. Amarasekara and M. Pomerantz, *Synthesis*, 2255 (2003).
- 03SM(138)289 S. Destri, M. Pasini, W. Porzio, G. Gigi, D. Pisignano, and C. Capolupo, *Synth. Met.*, **138**, 289 (2003).
- 03SM(138)409 C. Della-Casa, P. Costa-Bizzarri, M. Lanzi, L. Paganin, F. Bertinelli, R. Pizzoferrato, F. Sarcinelli, and M. Casalboni, *Synth. Met.*, **138**, 409 (2003).
- 03T4891 M.M.M. Raposo and G. Kirsch, *Tetrahedron*, **59**, 4891 (2003).
- 03T5083 G. Sotgiu, L. Favaretto, G. Barbarella, L. Antolini, G. Gigli, M. Mazzeo, and A. Bongini, *Tetrahedron*, **59**, 5083 (2003).
- 04AGE6197 T. Baumgartner, T. Neumann, and B. Wirges, *Angew. Chem. Int. Ed.*, **43**, 6197 (2004).
- 04AM180 L. Li, K.E. Counts, S. Kurosawa, A.S. Teja, and D.M. Collard, *Adv. Mater.*, **16**, 180 (2004).
- 04AM716 G. Vamvounis and S. Holdcroft, *Adv. Mater.*, **16**, 716 (2004).
- 04APPLAB(84)3570 M. Chen, E. Perzon, M.R. Andersson, S.K.M. Jönsson, M. Fahlman, and M. Berggren, *Appl. Phys. Lett.*, **84**, 3570 (2004).
- 04BCJ195 S. Kobatake and M. Irie, *Bull. Chem. Soc. Jpn.*, **77**, 195 (2004).
- 04CEJ3805 J. Casado, V. Hernandez, O.-K. Kim, J.-M. Lehn, J.T. L. Navarrete, S.D. Ledesma, R.P. Ortiz, M.C.R. Delgado, Y. Vida, and E. Pérez-Inestrosa, *Chem. Eur. J.*, **10**, 3805 (2004).
- 04CM4413 T.W. Kelly, P.F. Baude, C. Gerlach, D.E. Ender, D. Muyres, M. A. Haase, D.E. Vogel, and S.D. Theiss, *Chem. Mater.*, **16**, 4413 (2004).
- 04CM4436 C.R. Newman, C.D. Frisbie, D.A. de Silva Filho, J.-L. Brédas, P. C. Ewbank, and K.R. Mann, *Chem. Mater.*, **16**, 4436 (2004).
- 04CM4619 J.-F. Morin, N. Drolet, Y. Tao, and M. Leclerc, *Chem. Mater.*, **16**, 4619 (2004).
- 04CM4715 A. Facchetti, J. Letizia, M.-H. Yoon, M. Mushrush, H.E. Katz, and T.J. Marks, *Chem. Mater.*, **16**, 4715 (2004).
- 04CM4824 M.M. Ling and Z. Bao, *Chem. Mater.*, **16**, 4824 (2004).
- 04CSR85 H. Tian and S. Yang, *Chem. Soc. Rev.*, **33**, 85 (2004).
- 04JA5084 K. Takimiya, Y. Kunugi, Y. Konda, N. Nihara, and T. Otsubo, *J. Am. Chem. Soc.*, **126**, 5084 (2004).
- 04JA13480 A. Facchetti, M.-H. Yoon, C.L. Stern, G.R. Hutchison, M. A. Ratner, and T.J. Marks, *J. Am. Chem. Soc.*, **126**, 13480 (2004).
- 04JA13859 A. Facchetti, M. Mushrush, M.-H. Yoon, G.R. Hutchison, M. A. Ratner, and T.J. Marks, *J. Am. Chem. Soc.*, **126**, 13859 (2004).
- 04JA15382 M. Frigoli, C. Welch, and G.H. Mehl, *J. Am. Chem. Soc.*, **126**, 15382 (2004).
- 04JCS(CC)72 T. Kawai, T. Iseda, and M. Irie, *J. Chem. Soc., Chem. Commun.*, 72 (2004).
- 04JCS(CC)1010 T. Yamaguchi, Y. Fujita, and M. Irie, *J. Chem. Soc., Chem. Commun.*, 1010 (2004).
- 04JOC8239 C.R. Moylan, B.J. McNelis, L.C. Nathan, M.A. Marques, E. L. Hermstad, and B.A. Brichler, *J. Org. Chem.*, **69**, 8239 (2004).
- 04JPC(B)7611 J. Casado, J.J. Quirante, V. Hernández, J.T.L. Navarrete, K. Takimiya, and T. Otsubo, *J. Phys. Chem. B*, **108**, 7611 (2004).

- 04JPC(B)8626 Z.-Y. Hu, A. Fort, M. Barzoukas, A.K.-Y. Jen, S. Barlow, and S. R. Marder, *J. Phys. Chem. B*, **108**, 8626 (2004).
- 04JPP(C)(5)169 K. Matsuda and M. Irie, *J. Photochem. Photobiol. C: Photochem. Rev.*, **5**, 169 (2004).
- 04MI23 M. Morimoto, S. Kobatake, and M. Irie, *Chem. Rec.*, **4**, 23 (2004).
- 04MI1077 C. Winder and N.S. Sariciftci, *J. Mater. Chem.*, **14**, 1077 (2004).
- 04MI1787 S. Ando, J.-I. Nishida, Y. Inoue, S. Tokito, and Y. Yamashita, *J. Mater. Chem.*, **14**, 1787 (2004).
- 04MI2117 M. Lanzi, L. Paganin, and P. Costa-Bizzarri, *Eur. Polym. J.*, **40**, 2117 (2004).
- 04MM709 P. Sonar, J. Zhang, A.C. Grimsdale, K. Müllen, M. Surin, R. Lazzaroni, P. Leclère, S. Tierney, M. Heeney, and I. McCulloch, *Macromolecules*, **37**, 709 (2004).
- 04MM5265 N.S. Cho, D.-H. Hwang, B.-J. Jung, E. Lim, J. Lee, and H.-K. Shim, *Macromolecules*, **37**, 5265 (2004).
- 04MM6299 Q. Hou, Q. Zhou, Y. Zhang, W. Yang, R. Yang, and Y. Cao, *Macromolecules*, **37**, 6299 (2004).
- 04MM6306 X. Zhang, M. Köhler, and A.J. Matzger, *Macromolecules*, **37**, 6306 (2004).
- 04OL273 Y. Nicolas, P. Blanchard, E. Levillain, M. Allain, N. Mercier, and J. Roncali, *Org. Lett.*, **6**, 273 (2004).
- 04OL2523 J.-I. Nishida, T. Miyagawa, and Y. Yamashita, *Org. Lett.*, **6**, 2523 (2004).
- 04OL3325 M.M. Payne, S.A. Odom, S.R. Parkin, and J.E. Anthony, *Org. Lett.*, **6**, 3325 (2004).
- 04SCI(304)278 J.J.D. de Jong, L.N. Lucas, R.M. Kellogg, J.H. van Esch, and B. L. Feringa, *Science*, **304**, 278 (2004).
- 04SM(146)233 M.X. Chen, E. Perzon, N. Robisson, S.K.M. Jönsson, M. R. Andersson, M. Fahlman, and M. Berggren, *Synth. Met.*, **146**, 233 (2004).
- 04SM(146)251 M.D. Iosip, S. Destri, M. Pasini, W. Porzio, K.P. Pernstich, and B. Batlogg, *Synth. Met.*, **146**, 251 (2004).
- 04T4071 M.M.M. Raposo, A.M.C. Fonseca, and G. Kirsch, *Tetrahedron*, **60**, 4071 (2004).
- 04T11169 M. Béra-Abérem, H.-A. Ho, and M. Leclerc, *Tetrahedron*, **60**, 11169 (2004).
- 04TL2825 R.M.F. Batista, S.P.G. Costa, and M.M.M. Raposo, *Tetrahedron Lett.*, **45**, 2825 (2004).
- 05AGE2373 J.J.D. de Jong, P.R. Hania, A. Pugžlys, L.N. Lucas, M. de Loos, R. M. Kellogg, B.L. Feringa, K. Duppen, and J.H. van Esch, *Angew. Chem. Int. Ed.*, **44**, 2373 (2005).
- 05AM34 M. Mazzeo, V. Vitale, F. Della Sala, M. Anni, G. Barbarella, L. Favaretto, G. Sotgiu, R. Cingolani, and G. Gigli, *Adv. Mater.*, **17**, 34 (2005).
- 05AM1141 B.S. Ong, Y. Wu, P. Liu, and S. Gardner, *Adv. Mater.*, **17**, 1141 (2005).
- 05AM1581 G. Barbarella, M. Melucci, and G. Sotgiu, *Adv. Mater.*, **17**, 1581 (2005).
- 05AM1705 A. Facchetti, M.-H. Yoon, and T.J. Marks, *Adv. Mater.*, **17**, 1705 (2005).
- 05AM2281 I.F. Perepichka, D.F. Perepichka, H. Meng, and F. Wudl, *Adv. Mater.*, **17**, 2281 (2005).

- 05CEJ4687 T. Baumgartner, W. Bergmans, T. Kárpáti, T. Neumann, M. Nieger, and L. Nyulászi, *Chem. Eur. J.*, **11**, 4687 (2005).
- 05CEJ6414 W. R. Browne, J.J.D. de Jong, T. Kudernac, M. Walko, L.N. Lucas, K. Uchida, J.H. van Esch, and B.L. Feringa, *Chem. Eur. J.*, **11**, 6414 (2005).
- 05CM221 Y. Wu, P. Liu, S. Gardner, and B.S. Ong, *Chem. Mater.*, **17**, 221 (2005).
- 05CM1261 S. Ando, J. Nishida, E. Fujiwara, H. Tada, Y. Inoue, S. Tokito, and Y. Yamashita, *Chem. Mater.*, **17**, 1261 (2005).
- 05CM1381 I. McCulloch, C. Bailey, M. Giles, M. Heeney, I. Love, M. Shkunov, D. Sparrowe, and S. Tierney, *Chem. Mater.*, **17**, 1381 (2005).
- 05CM4892 A.R. Murphy, J. Liu, C. Luscombe, D. Kavulak, J.M.J. Fréchet, R. J. Kline, and M.D. McGehee, *Chem. Mater.*, **17**, 4892 (2005).
- 05JA373 K.R.J. Thomas, A.L. Thompson, A.V. Sivakumar, C.J. Bardeen, and S. Thayumanavan, *J. Am. Chem. Soc.*, **127**, 373 (2005).
- 05JA1078 M. Heeney, C. Bailey, K. Genevicius, M. Shkunov, D. Sparrowe, S. Tierney, and I. McCulloch, *J. Am. Chem. Soc.*, **127**, 1078 (2005).
- 05JA1348 M.-H. Yoon, S.A. DiBenedetto, A. Facchetti, and T.J. Marks, *J. Am. Chem. Soc.*, **127**, 1348 (2005).
- 05JA3605 K. Takimiya, Y. Kunugi, Y. Toyoshima, and T. Otsubo, *J. Am. Chem. Soc.*, **127**, 3605 (2005).
- 05JA4986 M.M. Payne, S.R. Parkin, J.E. Anthony, C.-C. Kuo, and T. N. Jackson, *J. Am. Chem. Soc.*, **127**, 4986 (2005).
- 05JA5336 S. Ando, J.I. Nishida, H. Tada, Y. Inoue, S. Tokito, and Y. Yamashita, *J. Am. Chem. Soc.*, **127**, 5336 (2005).
- 05JA8922 K. Higashiguchi, K. Matsuda, N. Tanifuji, and M. Irie, *J. Am. Chem. Soc.*, **127**, 8922 (2005).
- 05JA13476 J.A. Letizia, A. Facchetti, C.L. Stern, M.A. Ratner, and T.J. Marks, *J. Am. Chem. Soc.*, **127**, 13476 (2005).
- 05JA13804 J.J.D. de Jong, T.D. Tiemersma-Wegman, J.H. van Esch, and B. L. Feringa, *J. Am. Chem. Soc.*, **127**, 13804 (2005).
- 05JA13281 K. Xiao, Y. Liu, T. Qi, W. Zhang, F. Wang, J. Gao, W. Qiu, Y. Ma, G. Cui, S. Chen, X. Zhan, G. Yu, J. Qin, W. Hu, and D. Zhu, *J. Am. Chem. Soc.*, **127**, 13281 (2005).
- 05JA14996 S. Ando, R. Murakami, J.-I. Nishida, H. Tada, Y. Inoue, S. Tokito, and Y. Yamashita, *J. Am. Chem. Soc.*, **127**, 14996 (2005).
- 05JA15372 T. Oike, T. Kurata, K. Takimiya, T. Otsubo, Y. Aso, H. Zhang, Y. Araki, and O. Ito, *J. Am. Chem. Soc.*, **127**, 15372 (2005).
- 05JCS(CC)2503 Y.-C. Jeong, S.I. Yang, K.-H. Ahn, and E. Kim, *J. Chem. Soc., Chem. Commun.*, 2503 (2005).
- 05JOC4502 B. Wex, B.R. Kaafarani, K. Kirschbaum, and D.C. Neckers, *J. Org. Chem.*, **70**, 4502 (2005).
- 05JPC(A)7197 Y. Wang, J. Ma, and Y. Jiang, *J. Phys. Chem. A*, **109**, 7197 (2005).
- 05JPC(A)7343 F.M. Raymo and M. Tomasulo, *J. Phys. Chem. A*, **109**, 7343 (2005).
- 05JPC(B)3126 G.R. Hutchison, M.A. Ratner, and T.J. Marks, *J. Phys. Chem. B*, **109**, 3126 (2005).
- 05JPP(A)(170)181 M. Venanzi, G. Bocchinfuso, A. Palleschi, A.S. Abreu, P.M. T. Ferreira, and M.-J.R.P. Queiroz, *J. Photochem. Photobiol., A: Chem.*, **170**, 181 (2005).

- 05MI13 M. Al-Ibrahim, H.-K. Roth, U. Zhokhavets, G. Gobsch, and S. Sensfuss, *Sol. Ener. Sol. Cells*, **85**, 13 (2005).
- 05MI53 Y. Sun, Y. Liu, and D. Zhu, *J. Mater. Chem*, **15**, 53 (2005).
- 05MI2360 C. Della-Casa, A. Fraleoni-Morgera, M. Lanzi, P. Costa-Bizzarri, L. Paganin, F. Bertinelli, L. Schenetti, A. Mucci, M. Casalboni, F. Sarcinelli, and A. Quatela, *Eur. Polym. J.*, **41**, 2360 (2005).
- 05NJC1128 B.C. Thompson, K.A. Abboud, J.R. Reynolds, K. Nakatani, and P. Audebert, *New. J. Chem*, **29**, 1128 (2005).
- 05OL3315 Y. Moriyama, K. Matsuda, N. Tanifuji, S. Irie, and M. Irie, *Org. Lett*, **7**, 3315 (2005).
- 05OL3777 N. Tanifuji, K. Matsuda, and M. Irie, *Org. Lett*, **7**, 3777 (2005).
- 05OL5253 K.R. Radke, K. Ogawa, and S.C. Rasmussen, *Org. Lett*, **7**, 5253 (2005).
- 05PPS808 K. Arima, D. Ohira, M. Watanabe, A. Miura, S. Mataka, T. Thiemann, J.I. Valcarcel, and D.J. Walton, *Photochem. Photobiol. Sci*, **4**, 808 (2005).
- 05SM(148)169 A. Babel and S.A. Jenekhe, *Synth. Met.*, **148**, 169 (2005).
- 05SM(152)137 K. Ogawa, J.A. Stafford, S.D. Rothstein, D.E. Tallman, and S. C. Rasmussen, *Synth. Met*, **152**, 137 (2005).
- 05T8249 M.M.M. Raposo, A.M.R.C. Sousa, A.M.C. Fonseca, and G. Kirsch, *Tetrahedron*, **61**, 8249 (2005).
- 05T11055 T. Ozturk, E. Ertas, and O. Mert, *Tetrahedron*, **61**, 11055 (2005).
- 05T11991 M.M.M. Raposo, A.M.R.C. Sousa, G. Kirsch, F. Ferreira, M. Belsley, E. de Matos Gomes, and M.C. Fonseca, *Tetrahedron*, **61**, 11991 (2005).
- 05TL4225 A.K. Mohanakrishnan and P. Amaladas, *Tetrahedron Lett*, **46**, 4225 (2005).
- 05TL5409 X. Li and H. Tian, *Tetrahedron Lett*, **46**, 5409 (2005).
- 05TSF(474)230 M. Cerninara, F. Meinardi, A. Borghesi, A. Sassella, and R. Tubino, *Thin Solid Films*, **474**, 230 (2005).
- 06AM572 J.Y. Kim, S.H. Kim, H.-H. Lee, K. Lee, W. Ma, X. Gong, and A. J. Heeger, *Adv. Mater*, **18**, 572 (2006).
- 06AM3029 Y. Li, Y. Wu, P. Liu, M. Birau, H. Pand, and B.S. Ong, *Adv. Mater*, **18**, 3029 (2006).
- 06CL628 S. Kobatake and H. Kuratani, *Chem. Lett*, **35**, 628 (2006).
- 06CL1204 K. Matsuda and M. Irie, *Chem. Lett*, **35**, 1204 (2006).
- 06CM3237 H. Pan, Y. Li, Y. Wu, P. Liu, B.S. Ong, S. Zhu, and G. Xu, *Chem. Mater*, **18**, 3237 (2006).
- 06CPL(429)180 S.Y. Yang, Y.H. Kan, G.C. Yang, Z.M. Su, and L. Zhao, *Chem. Phys. Lett*, **429**, 180 (2006).
- 06CRV5028 J.E. Anthony, *Chem. Rev*, **106**, 5028 (2006).
- 06EJO3938 S.P.G. Costa, R.M.F. Batista, P. Cardoso, M. Belsley, and M.M. M. Raposo, *Eur. J. Org. Chem.*, 3938 (2006).
- 06JA2536 Y. Wang and M.D. Watson, *J. Am. Chem. Soc*, **128**, 2536 (2006).
- 06JA8980 C. Shi, Y. Yao, Y. Yang, and Q. Pei, *J. Am. Chem. Soc*, **128**, 8980 (2006).
- 06JA9034 H. Usta, G. Lu, A. Facchetti, and T.J. Marks, *J. Am. Chem. Soc*, **128**, 9034 (2006).
- 06JA12604 K. Takimiya, H. Ebata, K. Sakamoto, T. Izawa, T. Otsubo, and Y. Kunugi, *J. Am. Chem. Soc*, **128**, 12604 (2006).
- 06JCS(CC)1416 A. Cravino, S. Roquet, P. Leriche, O. Alévêque, P. Frère, and J. Roncali, *J. Chem. Soc., Chem. Commun.*, 1416 (2006).

- 06JCS(CC)3939 H. Ohkita, S. Cook, Y. Astuti, W. Duffy, M. Heeney, S. Tierney, I. McCulloch, D.d.C. Bradley, and J.R. Durrant, *J. Chem. Soc., Chem. Commun.*, 3939 (2006).
- 06JPC(A)13754 B. Wex, B.R. Kaafarani, E.O. Danilov, and D.C. Neckers, *J. Phys. Chem. A*, **110**, 13754 (2006).
- 06MI384 W.S. Shin, H.-H. Jeong, M.-K. Kim, S.-H. Jin, M.-R. Kim, J.-K. Lee, J.W. Lee, and Y.-S. Gal, *J. Mater. Chem.*, **16**, 384 (2006).
- 06MI1121 B. Wex, B.R. Kaafarani, Schroeder, L.A. Majewski, P. Burckel, M. Grell, and D.C. Neckers, *J. Mater. Chem.*, **16**, 1121 (2006).
- 06MI2263 R.C. Hiorns, R. de Bettignies, J. Leroy, S. Bailly, M. Firon, C. Sentein, A. Khoukh, H. Preud'homme, and C. Dagron-Lartigau, *Adv. Fnct. Mater.*, **16**, 2263 (2006).
- 06MI3040 S. Roquet, R. de Bettignies, P. Leriche, A. Cravino, and J. Roncali, *J. Mater. Chem.*, **16**, 3040 (2006).
- 06MI3177 A. Bilge, A. Zen, M. Forster, H. Li, F. Galbrecht, B.S. Nehls, T. Farrell, D. Neher, and U. Scherf, *J. Mater. Chem.*, **16**, 3177 (2006).
- 06MI3685 Y. Feng, Y. Yan, S. Wang, W. Zhu, S. Qian, and H. Tian, *J. Mater. Chem.*, **16**, 3685 (2006).
- 06MI3708 R. Schmidt, S. Göttling, D. Leusser, D. Stalke, A.-M. Krause, and F. Würthner, *J. Mater. Chem.*, **16**, 3708 (2006).
- 06MM1771 K. Ogawa and S.C. Rasmussen, *Macromolecules*, **39**, 1771 (2006).
- 06OL3681 M.M.M. Raposo, A.M.R.C. Sousa, G. Kirsch, P. Cardoso, M. Beisley, E. de Matos Gomes, and M.C. Fonseca, *Org. Lett.*, **8**, 3681 (2006).
- 06OL3911 Z. Zhou, S. Xiao, J. Xu, Z. Liu, M. Shi, F. Li, T. Yi, and C. Huang, *Org. Lett.*, **8**, 3911 (2006).
- 06OL5381 Y. Ie, Y. Umemoto, T. Kaneda, and Y. Aso, *Org. Lett.*, **8**, 5381 (2006).
- 06SM(156)256 Ch. Lô, A. Adenier, K.I. Chane-Ching, F. Maurel, J.J. Aaron, B. Kosata, and J. Svoboda, *Synth. Met.*, **156**, 256 (2006).
- 06SM(156)1241 B.A. Mattis, P.C. Chang, and V. Subramanian, *Synth. Met.*, **156**, 1241 (2006).
- 06T5855 Y.-C. Jeong, S.I. Yang, E. Kim, and K.-H. Ahn, *Tetrahedron*, **62**, 5855 (2006).
- 06T6814 E. Kim, M. Kim, and K. Kim, *Tetrahedron*, **62**, 6814 (2006).
- 06TL3711 P.J. Coelho, L.M. Carvalho, A.M.C. Fonseca, and M.M. Raposo, *Tetrahedron Lett.*, **47**, 3711 (2006).
- 07AGE363 P. Bäuerle, M. Ammann, M. Wilde, G. Götz, E. Mena-Osteritz, A. Range, and C.A. Schalley, *Angew. Chem. Int. Ed.*, **46**, 363 (2007).
- 07AGE1679 C.-Q. Ma, E. Mena-Osteritz, T. Debaerdemaeker, M.M. Wienk, R.A.J. Janssen, and P. Bäuerle, *Angew. Chem. Int. Ed.*, **46**, 1679 (2007).
- 07AGE4273 A. Wakamiya, K. Mori, and S. Yamaguchi, *Angew. Chem. Int. Ed.*, **46**, 4273 (2007).
- 07AM833 D.M. DeLongchamp, R.J. Kline, E.K. Lin, D.A. Fischer, L. J. Richter, L.A. Lucas, M. Heeney, I. McCulloch, and J. E. Nothrup, *Adv. Mater.*, **19**, 833 (2007).
- 07AM2045 J. Roncali, P. Leriche, and A. Cravino, *Adv. Mater.*, **19**, 2045 (2007).

- 07CEJ7487 Y. Dienes, S. Durben, T. Kárpáti, T. Neumann, U. Englert, L. Nyulászi, and T. Baumgartner, *Chem. Eur. J.*, **13**, 7487 (2007).
- 07CM4864 M.-H. Yoon, S.A. DiBenedetto, M.T. Russell, A. Facchetti, and T. J. Marks, *Chem. Mater.*, **19**, 4864 (2007).
- 07CRV1066 A.R. Murphy and J.M.J. Fréchet, *Chem. Rev.*, **107**, 1066 (2007).
- 07DP(75)11 H. Dinçalp, F. Toker, İ. Durucasu, N. Avcıbai, and S. Icli, *Dyes Pigments*, **75**, 11 (2007).
- 07EJO3212 T. Nakashima, K. Atsumi, S. Kawai, T. Nakagawa, Y. Hasegawa, and T. Kawai, *Eur. J. Org. Chem.*, 3212 (2007).
- 07JA3226 M.L. Chabiny, M.F. Toney, R.J. Kline, I. McCulloch, and M. Heeney, *J. Am. Chem. Soc.*, **129**, 3226 (2007).
- 07JA3472 M. Zhang, H.N. Tsao, W. Pisula, C. Yang, A.K. Mishra, and K. Müllen, *J. Am. Chem. Soc.*, **129**, 3472 (2007).
- 07JA4112 H. Pan, Y. Li, Y. Wu, P. Liu, B.S. Ong, S. Zhu, and G. Xu, *J. Am. Chem. Soc.*, **129**, 4112 (2007).
- 07JA12590 A.C. Whalley, M.L. Steigerwald, X. Guo, and C. Nuckolis, *J. Am. Chem. Soc.*, **129**, 12590 (2007).
- 07JA2224 T. Yamamoto and K. Takimiya, *J. Am. Chem. Soc.*, **129**, 2224 (2007).
- 07JCS(CC)781 H. Tian and S. Wang, *J. Chem. Soc., Chem. Commun.*, 781 (2007).
- 07JCS(CC)1169 Y. Tanaka, A. Inagaki, and M. Akita, *J. Chem. Soc., Chem. Commun.*, 1169 (2007).
- 07JOC8332 P. Leriche, P. Frère, A. Cravino, O. Alévêque, and J. Roncali, *J. Org. Chem.*, **72**, 8332 (2007).
- 07MI275 G.D. Sharma, V.S. Choudhary, and M.S. Roy, *Sol. Ener. Mater. Sol. Cells*, **91**, 275 (2007).
- 07MI954 W. Bundgaard and F.C. Krebs, *Sol. Ener. Sol. Cells*, **91**, 954 (2007).
- 07MI1071 L.H. Nguyen, H. Hoppe, T. Erb, S. Günes, G. Gobsch, and N. S. Sariciftci, *Adv. Funct. Mater.*, **17**, 1071 (2007).
- 07MI1163 S. Karpe, A. Cravino, P. Frère, M. Allain, G. Mabon, and J. Roncali, *Adv. Funct. Mater.*, **17**, 1163 (2007).
- 07MI1377 S. Berson, R. De Bettignies, S. Bailly, and S. Guillerez, *Adv. Funct. Mater.*, **17**, 1377 (2007).
- 07MI2096 S.P.G. Costa, E. Oliveira, C. Lodeiro, and M.M.M. Raposo, *Sensors*, **7**, 2096 (2007).
- 07MI3574 H. Pan, Y. Wu, Y. Li, P. Liu, B.S. Ong, S. Zhu, and G. Xu, *Adv. Funct. Mater.*, **17**, 3574 (2007).
- 07MI4477 A.S. Matharu, S. Jeeva, P.R. Huddleston, and P.S. Ramanujam, *J. Mater. Chem.*, **17**, 4477 (2007).
- 07MM6579 G. Lu, H. Tang, Y. Qu, L. Li, and X. Yang, *Macromolecules*, **40**, 6579 (2007).
- 07NAT(446)778 S. Kobatake, S. Takami, H. Muto, T. Ishikawa, and M. Irie, *Nature*, **446**, 778 (2007).
- 07OL2115 Y. Ie, M. Nitani, M. Ishikawa, K.-I. Nakayama, H. Tada, T. Kaneda, and Y. Aso, *Org. Lett.*, **9**, 2115 (2007).
- 07OL3201 R.M.F. Batista, E. Oliveira, S.P.G. Costa, C. Lodeiro, and M.M. M. Raposo, *Org. Lett.*, **9**, 3201 (2007).
- 07OL4187 W.-J. Liu, Y. Zhou, Y. Ma, Y. Cao, J. Wang, and J. Pei, *Org. Lett.*, **9**, 4187 (2007).
- 07OL4351 M.J.E. Resendiz, J. Taing, and M.A. Garcia-Garibay, *Org. Lett.*, **9**, 4351 (2007).
- 07OL4499 H. Ebata, E. Miyazaki, T. Yamamoto, and K. Takimiya, *Org. Lett.*, **9**, 4499 (2007).

- 07OM5165 O.V. Borshchev, S.A. Ponomarenko, N.M. Surin, M.M. Kaptyug, M.I. Buzin, A.P. Pleshkova, N.V. Demchenko, V. D. Myakushev, and A.M. Muzafarov, *Organometallics*, **26**, 5165 (2007).
- 07SCI(317)222 J.Y. Kim, K. Lee, N.E. Coates, D. Moses, T.-Q. Nguyen, M. Dante, and A.J. Heeger, *Science*, **317**, 222 (2007).
- 07T4258 R.M.F. Batista, S.P.G. Costa, E.L. Malheiro, M. Belsley, and M.M. M. Raposo, *Tetrahedron*, **63**, 4258 (2007).
- 07T9482 A. El Yahyaoui, G. Félix, A. Heynderckx, C. Moustrou, and A. Samat, *Tetrahedron*, **63**, 9482 (2007).
- 07TL779 A.K. Mohanakrishnan, P. Amaladass, and J.A. Clement, *Tetrahedron Lett*, **48**, 779 (2007).
- 08AGE5034 V. Lemieux, M.D. Spantulescu, K.K. Baldrige, and N.R. Branda, *Angew. Chem. Int. Ed*, **47**, 5034 (2008).
- 08AM1998 J. Finden, T.K. Kunz, N.R. Branda, and M.O. Wolf, *Adv. Mater.*, **20**, 1998 (2008).
- 08CEJ4201 O.J. Dautel, M. Robitzer, J.-C. Flores, D. Tondelier, F. Serein-Spirau, J.-P. Lère-Porte, D. Guérin, S. Lenfant, M. Tillard, D. Vuillaume, and J.J.E. Moreau, *Chem. Eur. J*, **14**, 4201 (2008).
- 08CEJ459 T. Benincori, M. Capaccio, F. De Angelis, L. Falciola, M. Muccini, P. Mussini, A. Ponti, S. Toffanin, P. Traldi, and F. Sannicolò, *Chem. Eur. J*, **14**, 459 (2008).
- 08CEJ4766 B.S. Ong, Y. Wu, Y. Li, P. Liu, and H. Pan, *Chem. Eur. J*, **14**, 4766 (2008).
- 08CEJ6935 G.-J. Zhao, R.-K. Chen, M.-T. Sun, J.-Y. Liu, G.-Y. Li, Y.-L. Gao, K.-L. Han, X.-C. Yang, and L. Sun, *Chem. Eur. J*, **14**, 6935 (2008).
- 08CEJ8102 Y. Matano, T. Miyajima, T. Fukushima, H. Kaji, Y. Kimura, and H. Imahori, *Chem. Eur. J*, **14**, 8102 (2008).
- 08DP(77)657 K. Guo, J. Hao, T. Zhang, F. Zu, J. Zhai, L. Qiu, Z. Zhen, X. Liu, and Y. Shen, *Dyes Pigm*, **77**, 657 (2008).
- 08DP(78)89 A. Matharu, P. Huddleston, S. Jeeva, M. Wood, and D. Chambers-Asman, *Dyes Pigm*, **78**, 89 (2008).
- 08EJO255 T. Miyajima, Y. Matano, and H. Imahori, *Eur. J. Org. Chem.*, 255 (2008).
- 08EJO2031 C.D. Gabutt, B.M. Heron, S.B. Kolla, and M. McGivern, *Eur. J. Org. Chem.*, 2031 (2008).
- 08EJO2531 S.F. Yan, V.N. Belov, M.L. Bossi, and S.W. Hell, *Eur. J. Org. Chem.*, 2531 (2008).
- 08EJO3798 P. Amaladass, J.A. Clement, and A.K. Mohanakrishnan, *Eur. J. Org. Chem.*, 3798 (2008).
- 08JA3030 H. Ohkita, S. Cook, Y. Astuti, W. Duffy, S. Tierney, W. Zhang, M. Heeney, I. McCulloch, J. Nelson, D.D. Bradley, and J. R. Durrant, *J. Am. Chem. Soc*, **130**, 3030 (2008).
- 08JA5424 H. Xin, F.S. Kin, and S.A. Jenekhe, *J. Am. Chem. Soc*, **130**, 5424 (2008).
- 08JA7670 G. Lu, H. Usta, C. Risko, L. Wang, A. Facchetti, M.A. Ratner, and T.J. Marks, *J. Am. Chem. Soc*, **130**, 7670 (2008).
- 08JA9202 H. Qin, S. Wenger, M. Xu, F. Gao, X. Jing, P. Wang, S. M. Zakeeruddin, and M. Grätzel, *J. Am. Chem. Soc*, **130**, 9202 (2008).

- 08JA12828 C.-P. Chen, S.-H. Chan, T.-C. Chao, C. Ting, and B.-T. Ko, *J. Am. Chem. Soc.*, **130**, 12828 (2008).
- 08JA12850 J. Areephong, T. Kudernac, J.J.D. de Jong, G.T. Carroll, D. Pantorott, J. Hjelm, W.R. Browne, and B.L. Feringa, *J. Am. Chem. Soc.*, **130**, 12850 (2008).
- 08JA13167 J. Liu, R. Zhang, G. Sauvé, T. Kawalewski, and R. D. McCullough, *J. Am. Chem. Soc.*, **130**, 13167 (2008).
- 08JA13840 S.R. Diegelmann, J.M. Gorham, and J.D. Tovar, *J. Am. Chem. Soc.*, **130**, 13840 (2008).
- 08JCS(CC)335 M. Morimoto, S. Kobatake, and M. Irie, *J. Chem. Soc., Chem. Commun.*, 335 (2008).
- 08JCS(CC)579 A. Wakamiya, K. Mishima, K. Ekawa, and S. Yamaguchi, *J. chem. Soc., Chem. Commun.*, 579 (2008).
- 08JCS(CC)1548 P. Gao, D. Beckmann, H.N. Tsao, X. Feng, V. Enkelmann, W. Pisula, and K. Müllen, *J. Chem. Soc., Chem. Commun.*, 1548 (2008).
- 08JCS(CC)3281 M. Oshumi, M. Hazama, T. Fukaminato, and M. Irie, *J. Chem. Soc., Chem. Commun.*, 3281 (2008).
- 08JCS(CC)5203 C. Ko, W.H. Lam, and V.W.-W. Yam, *J. Chem. Soc., Chem. Commun.*, 5203 (2008).
- 08JCS(CC)5315 J. Lu, F. Liang, N. Drolet, J. Ding, Y. Tao, and R. Movileanu, *J. Chem. Soc., Chem. Commun.*, 5315 (2008).
- 08JCS(CC)5812 K. Motoyama, T. Koike, and M. Akita, *J. Chem. Soc., Chem. Commun.*, 5812 (2008).
- 08JST(876)102 R. Chen, G. Zhao, X. Yang, X. Jiang, J. Liu, H. Tian, Y. Gao, X. Liu, K. Han, M. Sun, and L. Sun, *J. Mol. Struct.*, **876**, 102 (2008).
- 08JOC638 M.J.E. Resendiz, J. Taing, S.I. Khan, and M. Garcia-Garibay, *J. Org. Chem.*, **73**, 638 (2008).
- 08JPP(A)(194)67 J. Seixas de Melo, J. Pina, L.M. Rodrigues, and R.S. Becker, *J. Photochem. Photobiol., A: Chem.*, **194**, 67 (2008).
- 08JPP(A)(200)74 H. Zhao, U. Al-Atar, T.C.S. Pace, C. Bohne, and N.R. Branda, *J. Photochem. Photobiol. A: Chem.*, **200**, 74 (2008).
- 08MI122 A.K.D. Diaw, A. Yassar, D. Gningue-Sall, and J.-J. Aaron, *Arkivoc*, **17**, 122 (2008).
- 08MI528 M. Gaber, S.A. El-Daly, T.A. Fayed, and Y.S. El-Sayed, *Opt. Laser Technol.*, **40**, 528 (2008).
- 08MI973 J. Hao, M.-J. Han, K. Guo, Y. Zhao, L. Qiu, Y. Shen, and X. Meng, *Mater. Lett.*, **62**, 973 (2008).
- 08MI1617 H. Tian and Y. Feng, *J. Mater. Chem.*, **18**, 1617 (2008).
- 08MM5519 S.-H. Chan, C.-P. Chen, T.-C. Chao, C. Ting, C.-S. Lin, and B.-T. Ko, *Macromolecules*, **41**, 5519 (2008).
- 08OBC1544 M. Akazawa, K. Uchida, J.J.D. de Jong, J. Areephong, M. Stuart, G. Caroli, W.R. Browne, and B.L. Feringa, *Org. Biomol. Chem.*, **6**, 1544 (2008).
- 08OBC3202 P. Leriche, D. Aillerie, S. Roquet, M. Allain, A. Cravino, P. Frère, and J. Roncali, *Org. Biomol. Chem.*, **6**, 3202 (2008).
- 08OL17 J.-L. Wang, Z.-M. Tang, Q. Xiao, Q.-F. Zhou, Y. Ma, and J. Pei, *Org. Lett.*, **10**, 17 (2008).
- 08OL833 Y. Ie, Y. Umemoto, M. Okabe, T. Kusunoki, K.-I. Nakayama, Y.-J. Pu, J. Kido, H. Tada, and Y. Aso, *Org. Lett.*, **10**, 833 (2008).
- 08OL1095 Y. Umemoto, Y. Ie, A. Saeki, S. Seki, S. Tagawa, and Y. Aso, *Org. Lett.*, **10**, 1095 (2008).

- 08OL2051 K. Yumoto, M. Irie, and K. Matsuda, *Org. Lett.*, **10**, 2051 (2008).
- 08OL2735 Y.N. Luponosov, S.A. Ponomarenko, N.M. Surin, and A. M. Muzafarov, *Org. Lett.*, **10**, 2735 (2008).
- 08OL2991 S.T. Meek, E.E. Nesterov, and T.M. Swager, *Org. Lett.*, **10**, 2991 (2008).
- 08OL3179 H. Maeda, Y. Mihashi, and Y. Haketa, *Org. Lett.*, **10**, 3179 (2008).
- 08OL3513 B.P. Karsten and R.A.J. Janssen, *Org. Lett.*, **10**, 3513 (2008).
- 08OL3639 X. Li, Y. Ma, B. Wang, and G. Li, *Org. Lett.*, **10**, 3639 (2008).
- 08OL3785 X. Li, A. Liu, S. Xun, W. Qiao, X. Wan, and Z.Y. Wang, *Org. Lett.*, **10**, 3785 (2008).
- 08OL4271 J.-L. Wang, Z.-M. Tang, Q. Xiao, Y. Ma, and J. Pei, *Org. Lett.*, **10**, 4271 (2008).
- 08PPS257 M. Gaber, T.A. Fayed, S.A. El-Daly, and Y.S. El-Sayed, *Photochem. Photobiol. Sci.*, **7**, 257 (2008).
- 08T5878 M.M.M. Raposo, A.M.F.P. Ferreira, M. Belsley, and J.C.V. P. Moura, *Tetrahedron*, **64**, 5878 (2008).
- 08T7611 S. Kobatake and I. Yamashita, *Tetrahedron*, **64**, 7611 (2008).
- 08T8292 H.D. Samachetty, V. Lemieux, and N.R. Branda, *Tetrahedron*, **64**, 8292 (2008).
- 08T8324 J.J.D. de Jong, P. van Rijn, T.D. Tiemersma-Wegeman, L. N. Lucas, W.R. Browne, R.M. Kellogg, K. Uchida, J.H. van Esch, and B.L. Feringa, *Tetrahedron*, **64**, 8324 (2008).
- 08T9108 F.-S. Han, M. Higuchi, and D.G. Kurth, *Tetrahedron*, **64**, 9108 (2008).
- 08T9464 S. Pu, C. Fan, W. Miao, and G. Liu, *Tetrahedron*, **64**, 9464 (2008).
- 08T9733 S.P.G. Costa, R.M.F. Batista, and M.M.M. Raposo, *Tetrahedron*, **64**, 9733 (2008).
- 08TL5258 S.P.G. Costa, E. Oliveira, C. Lodeiro, and M.M.M. Raposo, *Tetrahedron Lett.*, **49**, 5258 (2008).
- 09CM287 W.J. Mitchell, A.J. Ferguson, M.E. Köse, B.L. Rupert, D.S. Ginley, G. Rumbles, S.E. Shaheen, and N. Kopidakis, *Chem. Mater.*, **21**, 287 (2009).
- 09H(78)737 M. D'Auria and R. Racioppi, *Heterocycles*, **78**, 737 (2009).
- 09JAPNAB(113)1173 P.D. Vellis, J.A. Mikroyannidis, D. Bagnis, L. Valentini, and J. M. Kenny, *J. Appl. Polym. Sci.*, **113**, 1173 (2009).
- 09JPC(A)5039 J. Huang, Y. Wu, H. Fu, X. Zhan, J. Yao, S. Barlow, and S. R. Marder, *J. Phys. Chem. A*, **113**, 5039 (2009).
- 09JPC(B)15928 J. Pina, J. Seixas de Melo, H.D. Burrows, T.W. Bünnagel, C. J. Kudla, and U. Scherf, *J. Phys. Chem. B*, **113**, 15928 (2009).
- 09JCS(CC)6300 B. Aydogan, A.S. Gundogan, T. Ozturk, and Y. Yagci, *J. Chem. Soc. Chem. Commun.*, 6300 (2009).
- 09JPC(C)10798 T. Umeyama, T. Takamatsu, N. Tezuka, Y. Matano, Y. Araki, T. Wada, O. Yoshikawa, T. Sagawa, S. Yoshikawa, and I. Imahori, *J. Phys. Chem. C*, **113**, 10798 (2009).
- 09JPC(C)11507 M. Kock, R. Nicolaescu, and P.V. Kamat, *J. Phys. Chem. C*, **113**, 11507 (2009).
- 09JPC(C)19677 A.N. Bourque, S. Dufresne, and W.G. Skene, *J. Phys. Chem. C*, **113**, 19677 (2009).
- 09JPS(A)2243 A. Wild, D.A.M. Egbe, E. Birkner, V. Cimrová, R. Baumann, U.-W. Grummt, and U.S. Schubert, *J. Polym. Sci., Polym. Chem., Part A*, **47**, 2243 (2009).

- 09JPS(A)4028 M. Wan, W. Wu, G. Sang, Y. Zou, Y. Liu, and Y. Li, *J. Polym. Sci., Polym. Chem., Part A*, **47**, 4028 (2009).
- 09MI910 Y.-X. Li, X.-T. Tao, F.-J. Wang, T. He, and M.-H. Jiang, *Org. Electr*, **10**, 910 (2009).
- 09MI1129 M.K.R. Fischer, T.E. Kaiser, F. Würthner, and Bäuerle, *J. Mater. Chem*, **19**, 1129 (2009).
- 09MI1533 W. Zhang, Z. Fang, M. Su, M. Saeys, and B. Liu, *Macromol. Rapid Commun*, **30**, 1533 (2009).
- 09MI8202 J. Luo, H. Qu, J. Yin, X. Zhang, K.-W. Huang, and C. Chi, *J. Mater. Chem*, **19**, 8202 (2009).
- 09MM1037 Q. Yang, H. Jin, Y. Xu, P. Wang, X. Liang, Z. Shen, X. Chen, D. Zou, X. Fan, and Q. Zhou, *Macromolecules*, **42**, 1037 (2009).
- 09MM1710 J. Pina, J. Seixas de Melo, H.D. Burrows, A.L. Maçanita, F. Galbrecht, T. Bünnagel, and U. Scherf, *Macromolecules*, **42**, 1710 (2009).
- 09OL863 J.-L. Wang, Z.-M. Tang, Q. Xiao, Y. Ma, and J. Pei, *Org. Lett*, **11**, 863 (2009).
- 09PCCP8706 J. Pina and J.S. Seixas de Melo, *Phys. Chem. Chem. Phys*, **11**, 8706 (2009).
- 09SM(159)142 J.A. Mikroyannidis, M.M. Stylianakis, K.Y. Cheung, M.K. Fung, and A.B. Djurišić, *Synth. Met*, **159**, 142 (2009).
- 09SM(159)1471 J.A. Mikroyannidis, M.M. Stylianakis, Q. Dong, Y. Zhou, and W. Tian, *Synth. Met*, **159**, 1471 (2009).
- 09T822 N.S. Kumar, J.A. Clement, and A.K. Mohanakrishnan, *Tetrahedron*, **65**, 822 (2009).
- 09T5062 F. Shibahara, E. Yamaguchi, A. Kitagawa, A. Imai, and T. Murai, *Tetrahedron*, **65**, 5062 (2009).
- 10CR3 A.C. Arias, J.D. MacKenzie, I. McCulloch, J. Rivnay, and A. Salleo, *Chem. Rev*, **110**, 3 (2010).

CHAPTER 3

Organometallic Complexes of Phosphinopyridines and Related Ligands

Alexander P. Sadimenko

Contents	1. Introduction	392
	2. Monophosphinopyridine Ligands	392
	2.1 Early transition metals	392
	2.2 Iron group	393
	2.3 Cobalt group	402
	2.4 Nickel group	409
	3. Bis(Phosphino)Pyridines	414
	4. Bis- and Tris-Pyridyl Phosphines	416
	5. Pyridylphosphinooxides (Selenides)	420
	6. Pyridylphosphinoalkane Ligands	422
	6.1 Early transition metals	422
	6.2 Iron group	423
	6.3 Cobalt group	428
	6.4 Nickel group	433
	7. P,N-Pyridine Ligands	438
	7.1 Iminophosphoranes	438
	7.2 Combination of phosphino and amino groups	441
	7.3 Phosphinoamino pyridines	442
	8. P,O-(S-,Se-) Pyridine Ligands	449
	9. Conclusions	457
	Abbreviations	461
	References	462

Department of Chemistry, University of Fort Hare, Alice 5701, Republic of South Africa

Advances in Heterocyclic Chemistry, Volume 104
ISSN 0065-2725, DOI 10.1016/B978-0-12-388406-0.00003-8

© 2011 Elsevier Inc.
All rights reserved

1. INTRODUCTION

This chapter continues the review series on organometallic complexes of heterocycles (10AHC175). Within this series, there is a section devoted to the chelating pyridine ligands. In the previous two parts (09AHC225, 11AHC227), hydroxy- and aminopyridines as well as related ligands were described. Another important and broad class of chelating ligands is constituted by phosphinopyridines and related compounds including bis (phosphino)pyridines, bis- and tris-pyridyl phosphines, pyridyl phosphinoxides (selenides), pyridylphosphinoalkanes, P,N- and P,O- (P,S- and P, Se-) forms of various nature. Attention to these compounds is related to the simultaneous presence of the hard (pyridine nitrogen) and soft (phosphorus) sites, which makes them attractive in catalysis and materials chemistry. We concentrate basic attention on preparation and coordination, grouped by moving from early to late transition metals. Coordination modes are highlighted in conclusion. An attempt is made to cover publications up to the end of 2010.

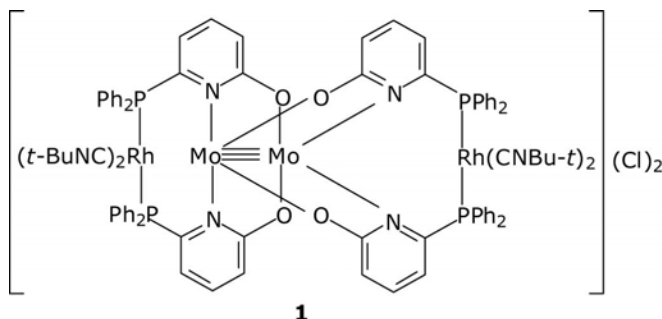
2. MONOPHOSPHINOPYRIDINE LIGANDS

2.1 Early transition metals

2-Diphenylphosphinopyridine with $[W(CO)_4(py)_2]$ in benzene gives $[W(CO)_4(\eta^1(P)-L)_2]$ (01EJI2255). Similarly, $[W(CO)_4(py)(PPh_3)]$ is converted into $[W(CO)_4(\eta^1(P)-L)(PPh_3)]$. Protonation using perchloric acid occurs *via* the pyridine nitrogen and leads to $[W(CO)_4(\eta^1(P)-LH)(\eta^1(P)-L)](ClO_4)$ where the proton is shared between the two pyridine nitrogen atoms and $[W(CO)_4(\eta^1(P)-LH)(PPh_3)](ClO_4)$, respectively. 4-Diphenylphosphinopyridine with $[W(CO)_4(py)_2]$, in contrast, gives dinuclear $[(OC)_4W(\mu, \eta^2(N,P)-L)W(CO)_4]$ (01JOM(633)66). $[W(CO)_4(\eta^1(P)-L)_2]$ and the protonation product $[W(CO)_4(\eta^1(P)-LH)_2](ClO_4)$ ($L = 2$ -diphenyl-phosphino)pyridine) are P-coordinated (00ICC508). 2-Diphenylphosphino-pyridine with $[(\eta^5-Me_3SiC_5H_4)CrCl_2(THF)]$ gives $(LH)^+[(\eta^5-Me_3SiC_5H_4)CrCl_3]^-$ along with minor amounts of $[(\eta^5-Me_3SiC_5H_4)CrCl_2(L)]$, where the ligand is tentatively assigned the N-coordination mode (04JOM2268). 2-(6-*t*-Butylpyridyl)diphenylphosphine and 2-(6-*t*-butylpyridyl)dimethylphosphine with $[W(AN)_3(CO)_2(NO)](BF_4)$ lead to *cis-cis*- $[W(CO)_2(NO)(\eta^1(P)-L)(\eta^2(N,P)-L)](BF_4)$, *cis-cis*- $[W(CO)(NO)(\eta^2(N,P)-L)_2](BF_4)$, *trans*-, *trans*- $[W(CO)(NO)(\eta^2(N,P)-L)_2](BF_4)$, *fac*- $[W(CO)_2(NO)(\eta^1(P)-L)_3](BF_4)$, and *cis-cis*- $[W(CO)_2(AN)(NO)(\eta^1(P)-L)_2]BF_4$ (00EJI1411).

2-Diphenylphosphinopyridine (L) with $[(\eta^5-Cp)_2Mo_2(CO)_4]$ in *m*-xylene affords dinuclear $[(\eta^5-Cp)(OC)_2(\eta^1(P)-L)Mo-Mo(\eta^1(P)-L)(CO)_2(\eta^5-Cp)]$ (92JCS(D)1847). Reaction of $[Mo(CO)_4L_2]$ ($L = 2$ -diphenylphosphino-

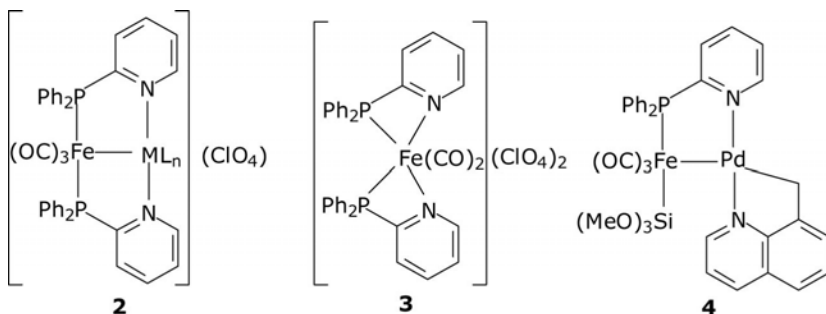
pyridine) with $[(\eta^4\text{-cod})\text{PdCl}_2]$ gives $[\text{PdMo}(\mu\text{-L})_2(\mu\text{-CO})(\text{CO})_2]$ (86JOM (314)357) with a $\text{Pd}^{\text{I}}\text{--Mo}^{\text{I}}$ bond. 2-Diphenylphosphinopyridine with $[\text{Mn}_2(\text{CO})_{10}]$ affords $[\text{Mn}_2(\text{CO})_8(\eta^1(\text{P})\text{-L})]$, $[\text{Re}_2(\text{CO})_{10}] - [\text{Re}(\text{CO})_4(\eta^1(\text{P})\text{-L})]_2$, $[\text{Cr}(\text{CO})_6]$ and $[\text{Mn}(\text{CO})_6] - [\text{M}(\text{CO})_5(\eta^1(\text{P})\text{-L})]$ ($\text{M} = \text{Cr}, \text{Mo}$) (90POL1479). 2-Diphenylphosphinopyridine with $(\text{N}(n\text{-Bu})_4)_2[\text{MX}_3(\text{CO})_3]$ ($\text{M} = \text{Re}, \text{Tc}$; $\text{X} = \text{Cl}, \text{Br}$) forms the $\eta^1(\text{P})$ -coordinated anionic $(\text{N}(n\text{-Bu})_4)[\text{MX}_2\text{CO}_3(\text{L})]$ ($\text{M} = \text{Re}, \text{Tc}$; $\text{X} = \text{Cl}, \text{Br}$) and neutral $[\text{MX}(\text{CO})_3\text{L}_2]$ ($\text{M} = \text{Re}, \text{X} = \text{Br}$; $\text{M} = \text{Tc}, \text{X} = \text{Cl}$) (99POL2995). $[\text{Mo}_2\text{L}_4]$ ($\text{L} = 6\text{-(diphenylphosphino)-2-pyridonate}$) with $[\text{Rh}(\mu\text{-Cl})(\text{CO})_2]_2$ and $t\text{-BuNC}$ forms cluster **1** without direct σ -bonding $\text{Rh}(\text{I})\text{--Mo}$ (04JA12244). Chemical oxidation of the product by $[\text{Cp}_2\text{Fe}](\text{PF}_6)$ affords $[\text{Mo}_2\text{Rh}_2(\text{Cl})_2(t\text{-BuNC})_4\text{L}_4](\text{PF}_6)_2$ of similar structure but with two $\text{Mo}\text{--Rh}(\text{II})$ single bonds and reduced $\text{Mo}\text{--Mo}$ bond orders. The 2-diphenylphosphinopyridine (L) $\text{Re}(\text{II})\equiv\text{Re}(\text{II})$ complex eliminates hydrogen chloride to yield the *ortho*-metalated $[\text{Re}_2\text{Cl}_3(\mu\text{-L})_2((\text{Ph})(\text{C}_6\text{H}_4)\text{PC}_5\text{H}_4\text{N})]$ (83JA4090, 84JA1323).

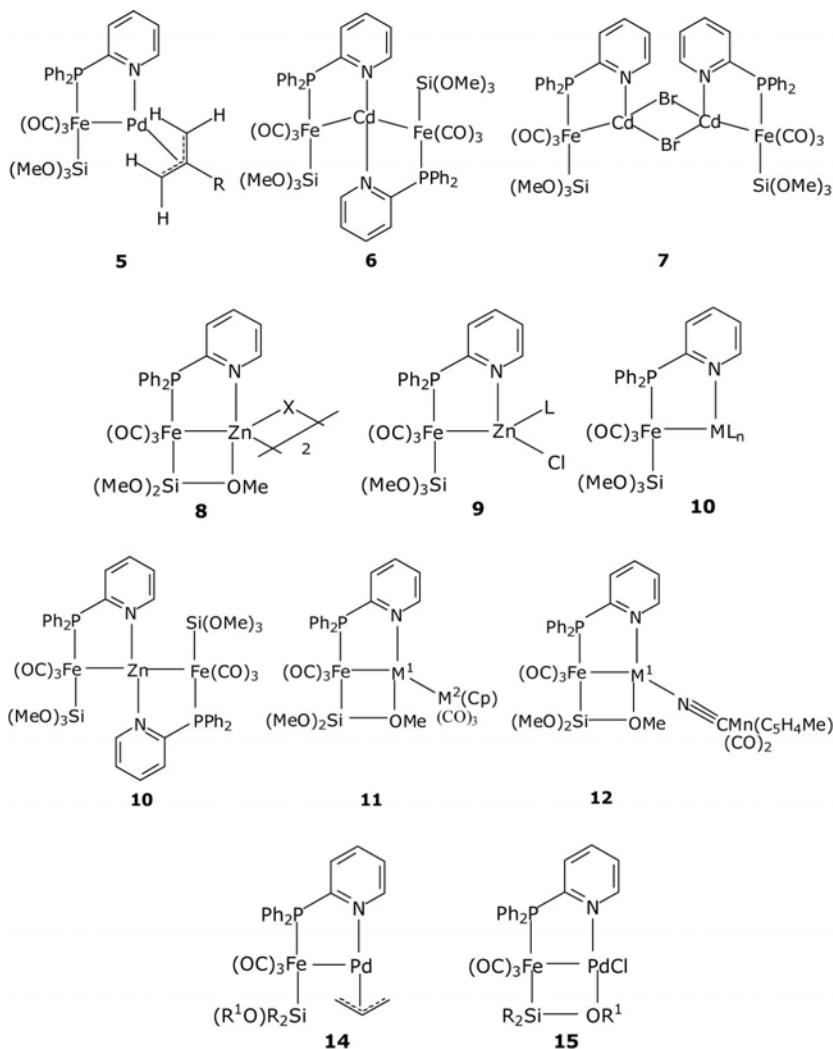


2.2 Iron group

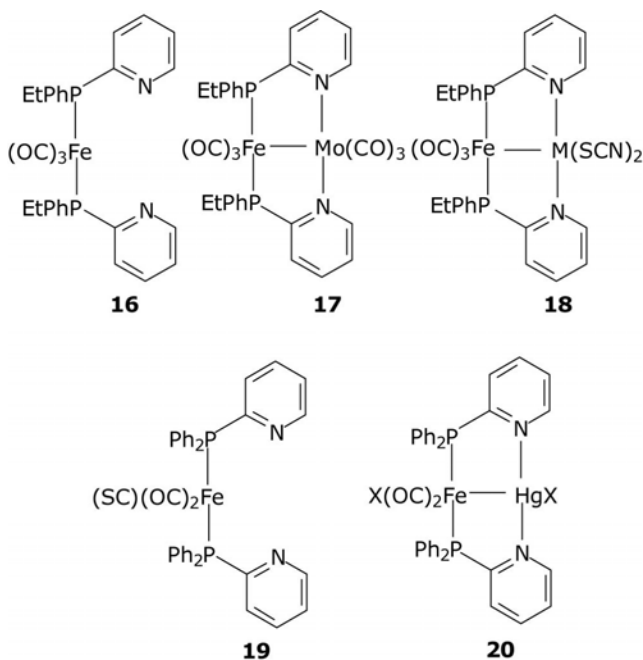
2-Diphenylphosphinopyridine with $[\text{Fe}(\text{CO})_5]$ affords $[\text{Fe}(\text{CO})_4(\eta^1(\text{P})\text{-L})]$ (90POL1479). 2-Diphenylphosphinopyridine reacts with $[\text{Fe}(\text{CO})_5]$ in *n*-pentane to yield the P-coordinated $[\text{Fe}(\text{CO})_3\text{L}_2]$. *Trans*- $[\text{Fe}(\eta^1(\text{P})\text{-Ph}_2\text{PC}_5\text{H}_4\text{N})_2(\text{CO})_3]$ functions as a neutral ligand with respect to $[\text{Mo}(\text{CO})_6]$, $\text{Ni}(\text{NCS})_2$, $[\text{Rh}(\text{CO})_2\text{Cl}]_2$, CuX ($\text{X} = \text{Cl}, \text{Br}, \text{I}$), and $\text{Hg}(\text{SCN})_2$ to form dinuclear complexes with an $\text{Fe}\text{--M}$ bond where the second metal in the form of $\text{Mo}(\text{CO})_3$, $\text{Ni}(\text{NCS})_2$, CuX ($\text{X} = \text{Cl}, \text{Br}, \text{I}$), $\text{Hg}(\text{SCN})_2$ is coordinated by the pyridine nitrogen atoms (93JOM(454)221, 96CCR(147)1, 99CCR499, 09CCR1793). In the case of rhodium precursor, $[(\text{OC})_3\text{Fe}(\mu\text{-L})_2(\mu\text{-CO})\text{Rh}(\text{Cl})]$ results. With $[\text{Cu}(\text{AN})_4](\text{ClO}_4)$ in methylene chloride–acetone the product is **2** ($\text{ML}_n = \text{Cu}(\text{OCMe}_2)$), with $\text{Cu}(\text{ClO}_4)_2 \cdot 6\text{H}_2\text{O}$ in methylene chloride–methanol, **2** ($\text{ML}_n = \text{Cu}(\text{OH}_2)$), with AgClO_4 in methylene chloride–methanol, **2** ($\text{ML}_n = \text{Ag}(\eta^1(\text{P})\text{-Ph}_2\text{PC}_5\text{H}_4\text{N})$), with $\text{Hg}_2(\text{ClO}_4)_2 \cdot 8\text{H}_2\text{O}$ in methylene chloride–THF and further in methylene chloride–methanol-2

($M = \text{Hg}(\text{OH}_2)(\text{OCIO}_3)$) (96JCS(D)3475). Reaction with $\text{Fe}(\text{ClO}_4)_2 \cdot 6\text{H}_2\text{O}$ in methylene chloride–acetone, in contrast, does not lead to the dinuclear iron(0)–iron(II) but to mononuclear **3** with two four-membered chelate rings. $\text{K}[\text{Fe}(\text{Si}(\text{OMe})_3)(\text{CO})_3(\eta^1(\text{P})\text{-Ph}_2\text{PC}_5\text{H}_4\text{N})]$ (89AGE1361) with $[\text{Pd}(\text{8-methylquinoline})(\mu\text{-Cl})_2]$ forms heterodinuclear **4** containing the N,P-chelated and cyclometalated moieties (93JOM(462)271). The product of reaction with $[(\eta^3\text{-allyl})\text{Pd}(\mu\text{-Cl})_2]$ is **5** ($R = \text{H}, \text{Me}$). Reaction of the anionic $[\text{Fe}(\text{CO})_3(\text{Si}(\text{OMe})_3)(\text{L})]^-$ with CdCl_2 yields $[(\text{MeO})_3\text{Si}(\text{OC})_3\text{Fe}(\mu\text{-L})_2]\text{Cd}$ **6** (93IC1656, 98CCR(178)903). In contrast, with CdBr_2 it affords $[(\eta^2(\text{N,P})\text{-L})(\text{MeO})_3\text{Si})\text{FeCd}(\mu\text{-Br}_2)_2]$ **7**. With ZnCl_2 and ZnI_2 , tetranuclear **8** ($X = \text{Cl}, \text{I}$) result, and the chloro-derivative under 4-methylpyridine or *t*-butylisocyanide transforms into dinuclear **9** ($L = 4\text{-Mepy}, t\text{-BuNC}$) (94JCS(D)117). With ZnEt_2 , GaCl_2 , and InCl_3 , heterodinuclear **10** ($\text{ML}_n = \text{ZnEt}, \text{GaCl}_2, \text{InCl}_2$) follow. $[\text{Fe}(\text{CO})_3(\text{H})(\text{Si}(\text{OMe})_3)(\text{L})]$ with twofold excess of zinc chloride produces the trimetallic chain **11**. Tetranuclear **7** and **8** further react with $\text{Na}[(\eta^5\text{-Cp})\text{M}(\text{CO})_3]$ ($M = \text{Mo}, \text{W}$) to yield heterotrimetallic **12** ($M^1 = \text{Zn}, \text{Cd}, M^2 = \text{W}; M^1 = \text{Cd}, M^2 = \text{Mo}$). $\text{K}[\text{Fe}(\text{Si}(\text{OMe})_3)(\text{CO})_3(\eta^1(\text{P})\text{-Ph}_2\text{PC}_5\text{H}_4\text{N})]$ with $[(\eta^5\text{-Cp})\text{W}(\text{CO})_3\text{HgCl}]$ affords **12** ($M^1 = \text{Hg}, M^2 = \text{W}$). Heterodinuclear **10** ($\text{ML}_n = \text{InCl}_2$) with $\text{Na}[(\eta^5\text{-Cp})\text{W}(\text{CO})_3]$ forms heterotrinuclear **12** ($M^1 = \text{InCl}, M^2 = \text{W}$). Another transformation of this kind occurs when **7** and **8** interact with $\text{Na}[(\eta^5\text{-C}_5\text{H}_4\text{Me})\text{Mn}(\text{CO})_2(\text{CN})]$ forming **13** ($M = \text{Zn}, \text{Cd}$). A similar general pathway allows the preparation of $[(\text{OC})_3\text{Fe}(\mu\text{-Ph}_2\text{PC}_5\text{H}_4\text{N})_2\text{ML}_n]$ ($\text{ML}_n = \text{Mn}(\text{SCN})_2, \text{Co}(\text{SCN})_2, \text{CoCl}_2, \text{NiCl}_2, \text{Cr}(\text{CO})_3, \text{Mo}(\text{CO})_3, \text{Zn}(\text{SCN})_2, \text{ZnCl}_2, \text{Cs}(\text{SCN})_2, \text{CdCl}_2, \text{HgCl}_2, \text{HgI}_2, \text{AgClO}_4, \text{SnCl}_2$) containing Fe–M bond (96JOM(516)1, 96POL3417). Heterobimetallic alkoxy-silyls **14** and siloxy-silyls **15** ($R_2 = (\text{OMe})_2, R^1 = \text{Me}; R_2 = (\text{OSiMe}_3)_2, R^1 = \text{SiMe}_3; R_2 = \text{Me}(\text{OSiMe}_3), R^1 = \text{SiMe}_3; R_2 = \text{Me}_2, R^1 = \text{SiHMe}_2$) catalyze dehydrogenative coupling of hydrostannanes (00CRV3541). $[(\text{OC})_3\text{Fe}(\mu\text{-Ph}_2\text{PC}_5\text{H}_4\text{N})(\text{SnPh}_2)(\mu\text{-Cl})(\text{SnClPh}_2)]$, can be prepared from a Si–Fe–Sn precursor (97CC1911).

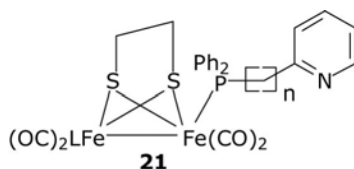




2-Ethylphenylphosphinopyridine with $[\text{Fe}(\text{CO})_5]$ in the presence of sodium hydroxide in *n*-butanol gives the P-coordinated ligand **16** (97JOM(540)55). In refluxing benzene, with $[\text{Mo}(\text{CO})_6]$ it yields heterodinuclear **17**, and with $\text{M}(\text{SCN})_2$ ($\text{M} = \text{Mn}, \text{Fe}, \text{Co}, \text{Ni}, \text{Zn}, \text{Cd}, \text{Hg}$) – a series of heterodinuclear **18**, with HgCl_2 a similar HgCl_2 derivative can be prepared (99ICA(293)106). Complex **19** reacts with HgX_2 ($\text{X} = \text{Cl}, \text{SCN}$) to yield heterodinuclear **20** ($\text{X} = \text{Cl}, \text{SCN}$) containing an iron(I)–mercury(II) bond (97JOM(534)15).

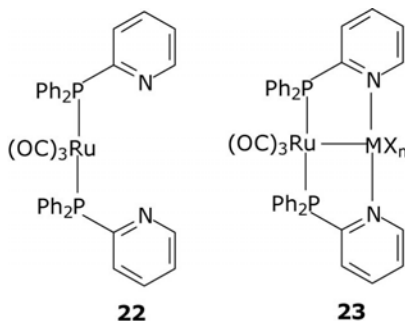


2-Diphenylphosphinopyridine reacts with $[\text{Fe}_2(\text{CO})_6(\mu_3\text{-S})_2\text{Pt}(\eta^4\text{-cod})]$ to yield $[\text{Fe}_2(\text{CO})_6(\mu_3\text{-S})_2\text{Pt}(\eta^1(\text{P})\text{-L})_2]$ (**96JCC273**). 2-Diphenylphosphinopyridine and 2-phosphinomethylpyridine with $[(\text{OC})_3\text{Fe}(\mu\text{-S}(\text{CH}_2)_3\text{S})\text{Fe}(\text{CO})_3]$ or $[(\text{OC})_3\text{Fe}(\mu\text{-S}(\text{CH}_2)_3\text{S})\text{Fe}(\text{CO})_2(\text{PMe}_3)]$ in the presence of $\text{Me}_3\text{NO}\cdot 2\text{H}_2\text{O}$ in acetonitrile give the P-coordinated products of CO-substitution **21** ($n = 0, 1$; $\text{L} = \text{CO}, \text{Me}_3\text{P}$) (**09JCS(D)1919**).



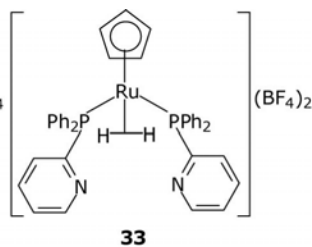
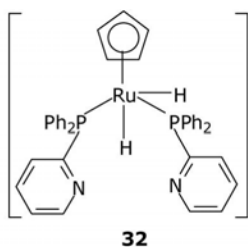
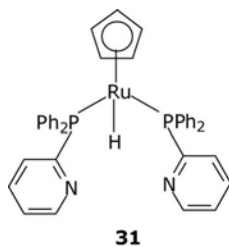
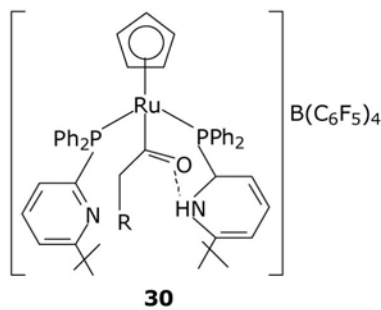
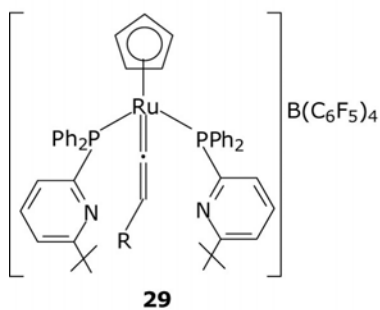
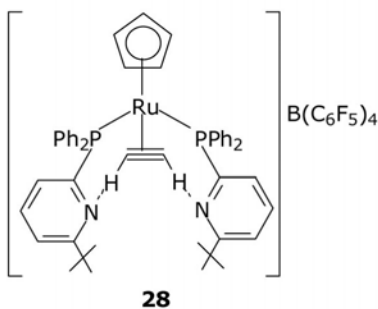
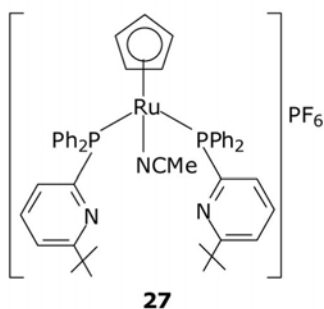
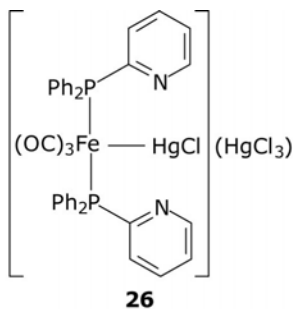
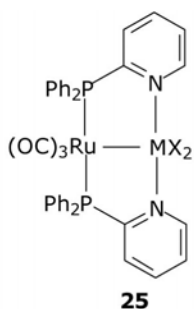
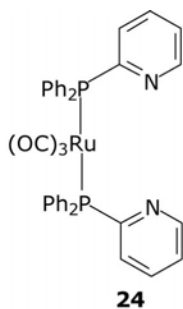
The products of interaction of 2-phenylphosphinopyridine (L) with $[\text{Ru}_3(\text{CO})_{12}]$ are $[\text{Ru}_3(\text{CO})_9\text{L}_3]$ and mononuclear species. One of them, $[\text{RuL}_2(\text{CO})_3]$, further reacts with $[(\eta^4\text{-cod})\text{PdCl}_2]$ and gives $[\text{RuPd}(\text{Ph}_2\text{PC}_5\text{H}_4)_2(\text{CO})_2\text{Cl}_2]$ and some other products (**82IC3961**). One more cluster product, $[\text{Ru}_3(\text{CO})_{11}\text{L}]$, can be isolated provided a catalyst like $(\text{PPN})(\text{CN})$ is used (**86IC7**). It gradually transforms to the μ -benzoyl cluster $[\text{Ru}_3(\mu, \eta^2\text{-C}(\text{O})\text{Ph})(\mu_3, \eta^2(\text{N}, \text{P})\text{-P}(\text{Ph})(\text{C}_5\text{H}_4\text{N})(\text{CO})_9)]$ by oxidative cleavage of a P–C bond. This cluster enters CO substitution reactions with phosphines to yield $[\text{Ru}_3(\mu, \eta^2\text{-C}(\text{O})\text{Ph})(\mu_3, \eta^2(\text{N}, \text{P})\text{-P}(\text{Ph})(\text{C}_5\text{H}_4\text{N})(\text{CO})_8(\text{PR}_3)]$

($R_3 = Ph_3, Ph_2H, Cy_2H$) (87IC585). The PR_2H ($R = Ph, Cy$) complexes under thermolysis yield $[Ru_3(\mu_3-P(Ph)(C_5H_4N))(\mu-PR_2)(\mu-CO)_2(CO)_6]$ ($R = Ph, Cy$) (88JA5369). The parent $(CO)_9$ complex with molecular hydrogen affords $[Ru_3(\mu-H)(\mu_3-P(Ph)(C_5H_4N))(CO)_9]$ and with $(PPN)(BH_4)$ gives $(PPN)[Ru_3(\mu_3-P(Ph)(C_5H_4N))(CO)_9]$. $[Ru_3(CO)_9(\mu-I)(\mu_3-PPh(2-C_5H_4N))]$ has a closely related structure (92AX(C)999). Acyl $[Ru_3(Ph)(\mu_3,\eta^2-P(Ph)(C_5H_4N))(CO)_9]$ incorporates diphenylphosphido groups of PPh_2H leading to $[Ru_3(\mu_3,\eta^2-P(Ph)(C_5H_4N))(\mu-PPh_2)_3(CO)_6]$ (93IC1363). $[Ru(CO)_3(L)]_3$ adds molecular chlorine to yield $[Ru(\eta^2(N,P)-L)(CO)_2Cl_2]$ (81IC4060). $[Ru(\eta^1(P)-Ph_2PC_5H_4N)(\eta^2(N,P)-Ph_2PC_5H_4N)_2Cl]Cl$ with carbon monoxide gives the substitution product $[Ru(\eta^1(P)-Ph_2PC_5H_4N)(\eta^2(N,P)-Ph_2PC_5H_4N)_2(CO)]Cl_2$ (94ICA(221)109). $[Ru_3(CO)_9L_3]$ with $HgBr_2$ in methylene chloride gives *cis*- $[Ru(CO)_3(\mu-L)(HgBr)_2]$ (98JOM(559)31). $[Os_3(CO)_{11}L]$ with $HgCl_2$ gives similar *cis*- $[Os(CO)_3(\mu-L)(HgCl)_2]$. In contrast, $[Ru_3(CO)_9L_3]$ with CdI_2 results in $[I(OC)_2Ru(\mu-L)Ru(CO)_2I]$. 2-Diphenylphosphinopyridine with $Na[Ru(H)(CO)_4]$ gives the P-coordinated **22**, which reveals its properties of a ligand with $AgOTf$, HgI_2 , and CdI_2 yielding heterodinuclear **23** ($MX_n = AgOTf, HgI_2, CdI_2$) (02NJC113).

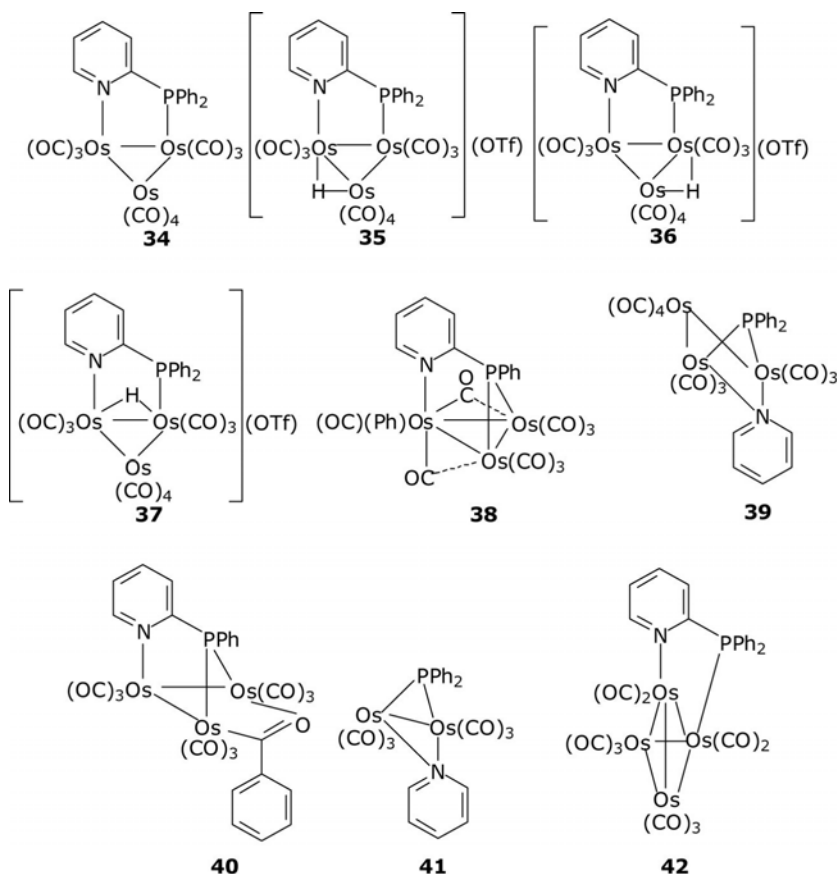


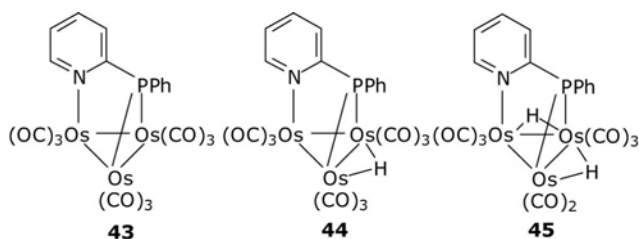
2-Diphenylphosphinopyridine with $[(\eta^4-cod)Ru(CO)_3]$ gives the P-coordinated **24** (98JCS(D)803, 06JOM1927) and then treatment with $ZnCl_2$, $CdCl_2$, or $Cd(ClO_4)_2 \cdot 4H_2O$ leads to the heterodinuclear **25** ($M = Zn, Cd, X = Cl$; $M = Cd, X = ClO_4$). Mercury(II) chloride leads to the cationic **26**. P-coordinated **27** is an efficient catalyst for anti-Markovnikov hydration of terminal alkynes to aldehydes (04JA12232, 07SYN1121, 08JCS(D)6497) as well as for one-pot cyclization and hydration to give functionalized indoles and benzofurans (10CEJ7992). Alkyne π -coordinated **28** serve as intermediates in anti-Markovnikov alkyne hydration (08JA20), where the role of hydrogen bonding between each acetylenic proton and pyridine N-atom is noted. Structures **29** ($R = Me, Ph$) and the product of hydration **30** ($R = Me, Ph$) may also be intermediates of anti-Markovnikov alkyne hydration to give an aldehyde (08JA10860). NMR coupling and isotopic labeling studies elucidate the location of this proton and its involvement in hydrogen bonding.

Ruthenium(II) **31** with tetrafluoroboric acid gives the monocationic dihydride **32** and subsequently the η^2 -molecular hydrogen dicationic **33** (98CC1879, 05JA15364, 10OM4682).

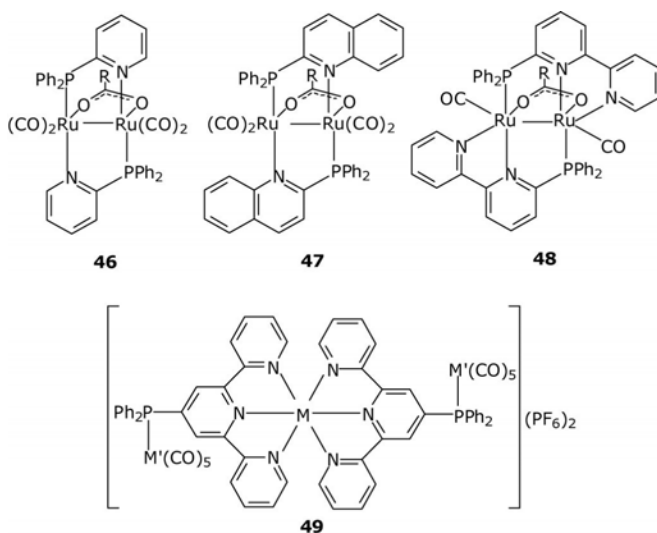


2-Diphenylphosphinopyridine (L) with $[\text{Os}_3(\text{CO})_{10}(\text{AN})_2]$ affords monodentate $\eta^1(\text{P})$ -coordinated $[\text{Os}_3(\text{CO})_{11}\text{L}]$ and $[\text{Os}_3(\text{CO})_{10}\text{L}_2]$ along with the major product **34** containing the N,P-bridging ligand (93CC844, 93JCS(D)3383). Under triflic acid, protonation of **34** yields a mixture of cationic **35**–**37**. Reflux of **34** in *n*-pentane leads to various products. Cluster **38** is the product of decarbonylation, **39** and **40** are the results of isomerization, and dinuclear **41** stems from degradation. 2-Diphenylphosphinopyridine (L) with $[\text{Os}_3(\text{H})_2(\text{CO})_{10}]$ gives $[\text{Os}_3(\text{H})_2(\text{CO})_{10}(\eta^1(\text{P})\text{-L})]$ (96ICA(248)257). With $[\text{Os}_4(\mu\text{-H})_4(\text{CO})_{10}(\text{AN})_2]$, the product is **42** (99JOM(573)189). Thermolysis of **34** at 100 °C yields merely product **43**, and its interaction with molecular hydrogen gives the product of splitting on one of the phosphorus–phenyl groups **44** containing the bridging hydride (06JOM111). 2-Diphenylphosphinopyridine with $[\text{H}_2\text{Os}_3(\text{CO})_{10}]$ at room temperature gives the P-coordinated $[\text{H}_2\text{Os}_3(\text{CO})_{10}(\eta^1(\text{P})\text{-L})]$, which on thermolysis produces **45**, and on carbonylation at elevated temperature product **44**.



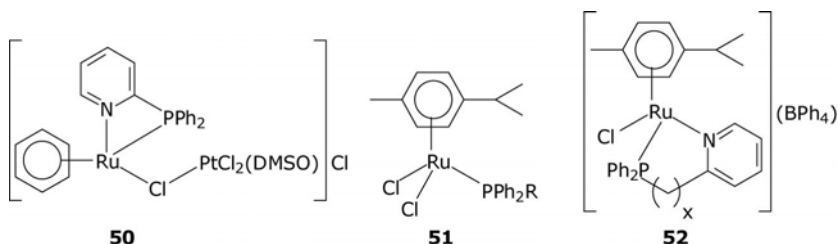


2-Diphenylphosphinopyridine with $[(\eta^5\text{-Cp})(\eta^4\text{-cod})\text{Ru}(\text{Cl})]$ gives $[(\eta^5\text{-Cp})\text{Ru}(\eta^1(\text{P})\text{-L})_2]$ (01JOM(628)1). Complexes derived *in situ* from 6-aryl-2-diphenylphosphinopyridines (aryl = Ph, Mes, 2,4,6-*i*-Pr₃C₆H₂, 2,4,6-Ph₃C₆H₂) and $[(\eta^5\text{-Cp})\text{Ru}(\eta^6\text{-naphthalene})]\text{PF}_6$ efficiently catalyze the anti-Markovnikov hydration of terminal alkynes to aldehydes (06OL5853, 09CEJ7167). 2-Diphenylphosphinopyridine with $[(\eta^5\text{-Cp})\text{Ru}(\text{PPh}_3)_2\text{Cl}]$ in benzene gives the P-coordinated $[(\eta^5\text{-Cp})\text{Ru}(\eta^1(\text{P})\text{-L})(\text{PPh}_3)\text{Cl}]$, in methanol the P,N-chelate $[(\eta^5\text{-Cp})\text{Ru}(\eta^2(\text{N,P})\text{-L})(\text{PPh}_3)]\text{Cl}$, and in acetonitrile in the presence of silver tetrafluoroborate $[(\eta^5\text{-Cp})\text{Ru}(\eta^1(\text{P})\text{-L})(\text{PPh}_3)(\text{AN})](\text{BF}_4)$ (09JOM3643). 2-Diphenylphosphinopyridine, 2-diphenylphosphinoquinoline, and 6-diphenylphosphino-2,2'-bipyridine react with the carboxylate-bridged polymers $[\text{Ru}_2(\mu, \eta^2\text{-OC(R)O})_2(\text{CO})_4]_n$ (R = H, Me, Et) giving rise to dinuclear **46–48** (97JCS(D)2843). Iron(II) and ruthenium(II) dications of 4-diphenylphosphino-2,2':6',2''-terpyridine with $[\text{M}(\text{CO})_5(\text{THF})]$ (M = Mo, W) form the P-coordinated **49** (M = Fe, Ru; M' = Mo, W) (99JOM(573)101).

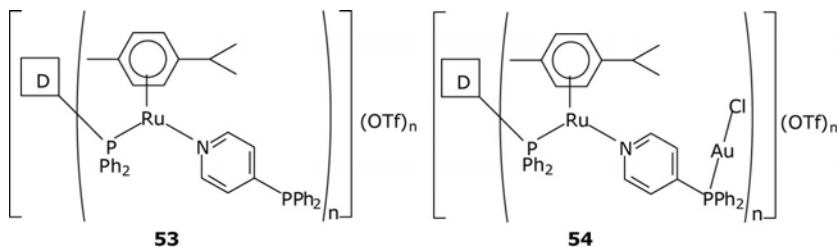


2-Diphenylphosphinopyridine with the dimer $[(\eta^6\text{-C}_6\text{H}_6)\text{RuCl}_2]_2$ in benzene gives P-coordinated $[(\eta^6\text{-C}_6\text{H}_6)\text{Ru}(\eta^1(\text{P})\text{-L})\text{Cl}_2]$ (95JOM(485)

115). Treatment with silver hexafluorophosphate causes elimination of one of the chloride ligands and formation of the P,N-chelate $[(\eta^6\text{-C}_6\text{H}_6)\text{Ru}(\eta^2(\text{N,P})\text{-L})\text{Cl}]$. The P-coordinated precursor with *cis*- $[\text{Pd}(\text{DMSO})_2\text{Cl}_2]$ forms dinuclear **50**, where the ligand is chelated around the ruthenium site only. 2-Diphenylphosphinopyridine and 2-diphenylphosphino-methylpyridine with $[(\eta^6\text{-p-cymene})\text{RuCl}_2]_2$ gives P-coordinated **51** ($\text{R} = \text{C}_5\text{H}_4\text{N}$, $\text{CH}_2\text{C}_5\text{H}_4\text{N}$) (98JOM(566)165). With sodium tetraphenylborate, both are converted to chelates **52** ($x = 0, 1$). The tetrafluoroborate analog of **52** ($x = 0$) is known (05ICA273). A system based on 2,6-bis[1-(diphenylphosphino)ethyl]pyridine and $[(\eta^6\text{-C}_6\text{H}_6)\text{RuCl}_2]$ is a promoter of asymmetric transfer hydrogenation (96TL797).

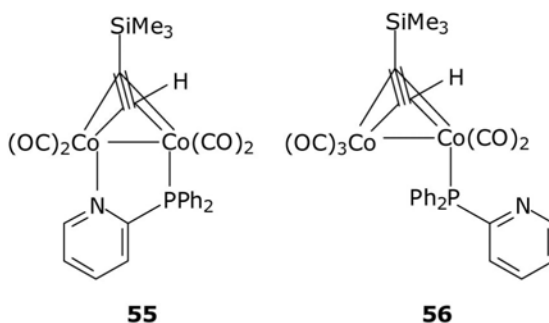


2-Diphenylphosphinopyridine with $[\text{Os}_5\text{C}(\text{CO})_{15}]$ yields $[\text{Os}_5(\mu_5\text{-CO})_{14}(\eta^1(\text{P})\text{-L})]$ (99JCL91). Treatment of the latter with $[\text{Pd}(\text{AN})_2\text{Cl}_2]$ gives $[\text{Os}_5\text{Pd}(\mu_5\text{-C})(\text{CO})_{14}\text{Cl}_2(\mu\text{-}\eta^2(\text{N,P})\text{-L})]$. The reaction of 4-diphenylphosphinopyridine with the ruthenium-*p*-cymene-based phosphino-terminated dendrimers (D) yields polymeric structures **53** containing the $\eta^1(\text{N})$ -coordinated ligand, which then further reacts with $(\text{PPh}_4)\text{Cl}$ and $[(\text{THT})\text{Au}(\text{Cl})]$ to give **54** (05OM6365). Instead of the $\text{Au}\text{-Cl}$ moiety, $\text{Pd}(\eta^3\text{-allyl})$ or $\text{Rh}(\eta^4\text{-cod})\text{Cl}$ may be $\eta^1(\text{P})$ -coordinated in the appropriate reactions. 4-Diphenylphosphinopyridine in combination with $[\text{Pd}(\eta^3\text{-2-MeC}_3\text{H}_4)(\text{cod})](\text{OTf})$, and $[\text{Pd}(\text{H}_2\text{O})_2(\text{dppp})](\text{OTf})_2$ forms metallamacrocycles of composition $[(\eta^3\text{-2-MeC}_3\text{H}_4)\text{Pd}(\mu\text{-P}(\text{Ph}_2)(\text{C}_5\text{H}_4\text{N})\text{Pd}(\eta^2\text{-dppp}))_2](\text{OTf})_6$ (10CEJ13960). Another illustration of complex catalytic systems is encapsulated $[(\eta^1\text{-L})_2\text{Rh}(\text{CO})(\text{acac})]$ ($\text{L} = 3\text{- or }4\text{-diphenylphosphinopyridine}$ and other similar ligands) into three zinc or ruthenium porphyrin molecules (01AGE4271, 04JA1526).

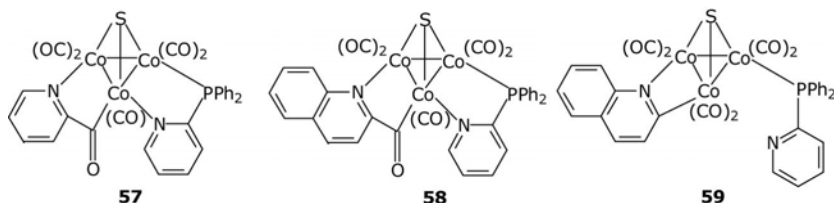


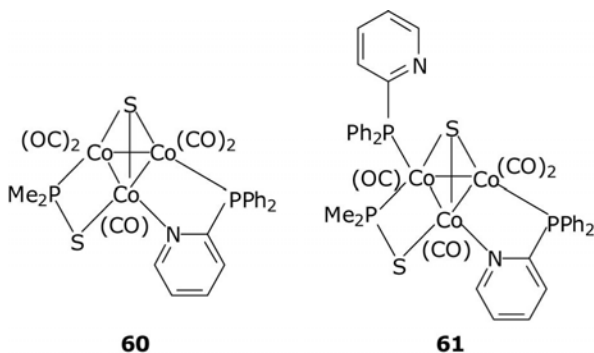
2.3 Cobalt group

Reaction of $[\text{L}_2\text{CoCl}_2]$ or 2-diphenylphosphinopyridine (L) and $\text{CoCl}_2 \cdot 6\text{H}_2\text{O}$ with carbon monoxide and zinc powder gives a dinuclear $[\text{Co}^0\text{Co}^1(\mu\text{-L})_2(\mu\text{-CO})(\text{CO})\text{Cl}]$ (89JOM(376)123). $[(\eta^5\text{-C}_5\text{H}_4\text{COOMe})\text{Co}(\text{CO})\text{I}_2]$ reacts with 2-diphenylphosphinopyridine to yield the neutral $[(\eta^5\text{-C}_5\text{H}_4\text{COOMe})\text{Co}(\eta^5\text{-L})\text{I}_2]$ (90JOM(397)93). Complexes prepared *in situ* from 2-diphenylphosphinopyridine and $[\text{Rh}(\text{H})(\text{CO})(\text{PPh}_3)_3]$, $\eta^1(\text{P})$ -coordinated $[\text{Rh}(\text{H})(\text{CO})(\text{L})(\text{PPh}_3)_2]$ and $[\text{Rh}(\text{H})(\text{CO})(\text{L})_2(\text{PPh}_3)]$, are efficient hydroformylation catalysts (91JMC(66)183). 2-Diphenylphosphinopyridine with $[\text{Co}_2(\text{CO})_8]$ and trimethylsilyl acetylene gives two products, one with bridging **55** and another with P-coordinated ligand **56** (99JOM(588)160).

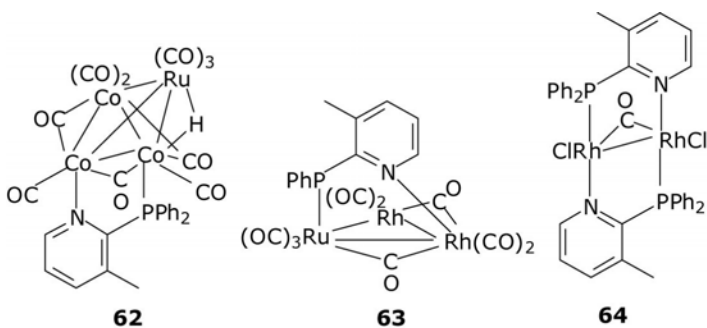


2-Mercaptopyridine with $[\text{Co}_2(\text{CO})_8]$ forms cluster $[(\mu_3\text{-S})\text{Co}_3(\text{CO})_7(\mu\text{-C},\text{N-C}_5\text{H}_4\text{N})]$, which with 2-diphenylphosphinopyridine forms bridged **57** (02JOM(655)172). A similar cluster $[(\mu_3\text{-S})\text{Co}_3(\text{CO})_7(\mu\text{-C},\text{N-C}_9\text{H}_6\text{N})]$ derived from 2-mercaptoquinoline reacts with 2-diphenylphosphinopyridine slightly differently, forming along with the bridged product of CO-insertion into the quinoline moiety **58**, a routine P-coordinated **59**. 2-Diphenylphosphinopyridine with sulfido-cluster $[(\mu_3\text{-S})\text{Co}_3(\text{CO})_7(\mu\text{-S},\text{P-SPMe}_2)]$ affords the N,P-bridged **60** and mixed bridged-P-coordinated **61** (03JOM(677)80).



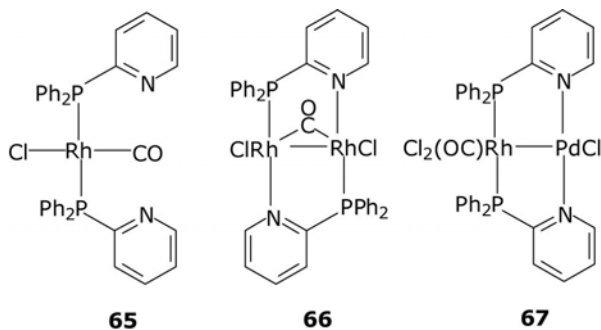


2-Dimethylphosphino-3-methylpyridine with $[\text{HRuCo}_3(\text{CO})_{12}]$ gives bridging **62** [04JOM1064]. Rhodium analog of **62** is a primary product of the reaction with $[\text{HRuRh}_3(\text{CO})_{10}]$. However, with longer reaction times, another product is formed, a trinuclear **63**, where the ligand loses one phenyl group. The product of interaction of the same ligand with $[\text{Rh}_4(\text{CO})_{12}]$ is $[\text{Rh}_6(\text{CO})_{14}\text{L}_2]$, where the ligand behaves as in **62**. 2-Diphenylphosphinopyridine with $[\text{Rh}_6(\text{CO})_{15}(\text{AN})]$ gives the monosubstitution $[\text{Rh}_6(\text{CO})_{15}(\eta^1(\text{P})\text{-L})]$, which can readily be transformed to the more stable clusters $[\text{Rh}_6(\text{CO})_{15}(\mu, \eta^2(\text{N}, \text{P})\text{-L})]$ [03JCS(D)2457]. The dimer $[\text{Rh}(\text{CO})_2\text{Cl}]_2$ also leads to the bridged **64**.

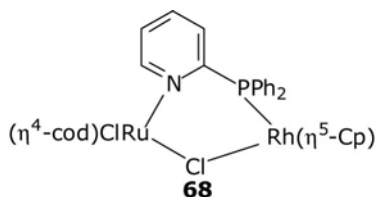


The product of interaction of 2-diphenylphosphinopyridine with $[\text{Rh}(\text{CO})_2(\mu\text{-Cl})_2]$, **65**, is an attractive ligand system [80JA6654, 93CRV2067, 94PIC238, 95MI1]. With $[\text{Rh}(\text{CO})_2(\mu\text{-Cl})_2]$ it gives $[\text{Rh}_2(\mu\text{-L})_2(\mu\text{-CO})\text{Cl}_2]$ **66**, which under SO_2 forms $[\text{Rh}_2(\mu\text{-L})_2(\mu\text{-SO}_2)\text{Cl}_2]$ [81IC1182, 81ICA(53)L217]. Under electrochemical conditions, this rhodium(I)–rhodium(I) species is transformed to rhodium(II)–rhodium(II) [86IC3534]. Dirhodium(I) **66** on reaction with Cl^- in the presence of carbon monoxide leads to the monomeric $[\text{RhL}_2(\text{CO})\text{Cl}]$ [88POL1751]. Electrochemical oxidation of **66** in the presence of Cl^- affords dirhodium(II) $[\text{Rh}_2(\mu\text{-L})_2(\text{CO})\text{Cl}_4]$, which with CO produces $[\text{Rh}_2(\mu\text{-L})_2(\text{CO})_2\text{Cl}_4]$, and with $t\text{-BuNC}$ forms $[\text{Rh}_2(\mu\text{-L})_2(t\text{-BuNC})_2\text{Cl}_4]$. **65**

interacts with $[(\eta^4\text{-cod})\text{PdCl}_2]$ to yield heterodinuclear Rh(II)–Pd(I) **67** by way of oxidative addition of the Pd–Cl bond. An alternative preparation of **67** is the reaction between $[\text{Pd}(\eta^1(\text{P})\text{-L})_2\text{Cl}_2]$ and $[\text{Rh}(\text{CO})_2(\mu\text{-Cl})_2]$ (**83IC1229**). Another synthesis of heterodinuclear products is based on the reaction between *cis*- $[\text{PtL}_2\text{Cl}_2]$ and $[\text{Rh}_2(\mu\text{-X})_2(\text{CO})_4]$ (X = Cl, Br) to yield $[\text{RhPtL}_2(\text{CO})\text{X}_3]$, which can add molecular halogen and form $[\text{RhPtL}_2(\text{CO})\text{X}_5]$ (**83JA792**). Complex **66** with NaBH_4 in THF gives the substitution product $[\text{Rh}_2(\mu\text{-L})_2(\mu\text{-CO})(\text{BH}_4)_2]$ (**93IC3287**). It also reacts with acetylenes to give the dimetalated alkene derivatives $[\text{Rh}_2\text{Cl}_2(\mu\text{-RC}=\text{CR}^1)\text{L}_2]$, which add carbon monoxide to produce $[\text{Rh}_2\text{Cl}_2(\text{CO})_2(\mu\text{-RC}=\text{CR}^1)\text{L}_2]$ (R = R¹ = COOMe, CF₃; R = COOMe, R¹ = H) (**86OM918**). 7-Diphenylphosphino-2,4-dimethyl-1,8-naphthyridine with *cis*- $[\text{Ir}(\text{CO})_2(p\text{-toluidine})\text{Cl}]$ give the P-monodentate *trans*- $[\text{Ir}(\text{CO})(\eta^1(\text{P})\text{-L})_2\text{Cl}]$ and *cis*- $[\text{Ir}(\text{CO})_2(\eta^1(\text{P})\text{-L})\text{Cl}]$ (**94ICA(216)209**). With $[(\eta^4\text{-cod})\text{Ir}(\text{Cl})_2]$, the mononuclear complex $[(\eta^4\text{-cod})\text{Ir}(\eta^1(\text{P})\text{-L})\text{Cl}]$ is obtained. Treatment of the latter with silver perchlorate leads to $[(\eta^4\text{-cod})\text{Ir}(\eta^2(\text{N},\text{P})\text{-L})]\text{ClO}_4$. 2-Diphenylphosphino-3-methylpyridine appeared inefficiently in rhodium-catalyzed propene hydroformylation (**01JC302**). Ligands 2-Ph₂PC₅H₄N, 2,2'-PhP(C₅H₄N)₂ and 2,2',2''-P(C₅H₄N)₃ with $[\text{Rh}(\text{acac})(\text{CO})_2]$ give the P-coordinated $[\text{Rh}(\text{acac})(\text{CO})\text{L}]$ (**98JOM(570)63**).

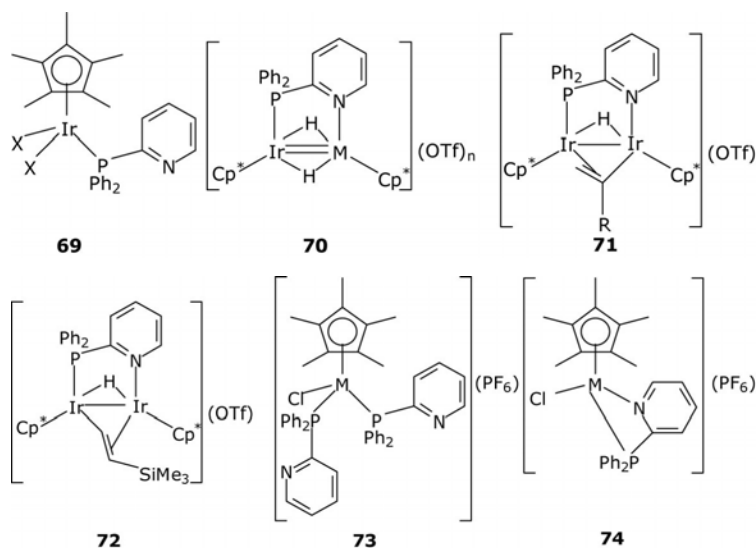


2-Diphenylphosphinopyridine with $[(\eta^5\text{-Cp}^*)\text{RhCl}_2]_2$ in dichloromethane give the P-coordinated $[(\eta^5\text{-Cp}^*)\text{Rh}(\eta^1(\text{P})\text{-L})\text{Cl}_2]$ (**95JOM(485)115**). Addition of silver hexafluorophosphate leads to the chelate $[(\eta^5\text{-Cp}^*)\text{Rh}(\eta^2\text{-N},\text{P})\text{-L})\text{Cl}](\text{PF}_6)$. $[(\eta^5\text{-Cp}^*)\text{Rh}(\text{Ph}_2\text{Ppy})(\text{CO})]$ with *cis*- $[\text{Pd}(t\text{-BuNC})_2\text{Cl}_2]$ and *cis*- $[\text{Pt}(\text{DMSO})_2\text{Cl}_2]$ give dinuclear $[(\eta^5\text{-Cp}^*)\text{Rh}(t\text{-BuNC})(\mu\text{-Ph}_2\text{Ppy})\text{Pd}(t\text{-BuNC})\text{Cl}]$ and rhodium(II)–platinum(I) $[(\eta^5\text{-Cp}^*)\text{Rh}(\text{Cl})(\mu\text{-Ph}_2\text{Ppy})\text{Pt}(\text{CO})\text{Cl}]$, respectively. The same rhodium precursor with $[(\eta^4\text{-cod})\text{RuCl}_2]_n$ in dichloromethane gives Ru–Rh **68**. 2-Diphenylphosphino-pyridine with $[(\eta^5\text{-Cp}^*)\text{Ir}(\text{N}_3)_2]_2$ gives $[(\eta^5\text{-Cp}^*)\text{Ir}(\text{N}_3)(\eta^1\text{-P})\text{-L}]$ (**09POL2287**) and with silver triflate or hexafluorophosphate $[(\eta^5\text{-Cp}^*)\text{Ir}(\text{N}_3)(\eta^2\text{-P},\text{N})\text{-L})\text{X}]$ (X = OTf, PF₆).

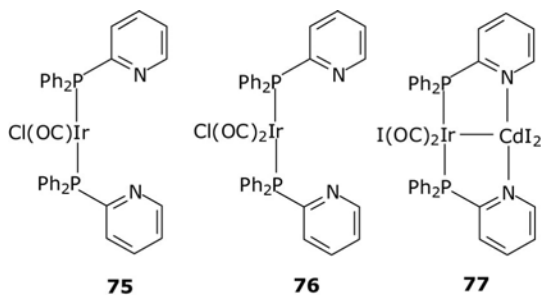


2-Diphenylphosphinopyridine (L) with $[(\eta^5\text{-Cp})\text{Rh}(\text{CO})_2]$ or $[(\eta^5\text{-Cp})_2\text{Rh}_2(\text{CO})_3]$ yields mononuclear $[(\eta^5\text{-Cp})\text{Rh}(\text{CO})(\eta^1(\text{P})\text{-L})]$, which serves as an efficient metalloligand for various dinuclear complexes (89OM886). Thus, on reaction with $[\text{Rh}(\text{CO})_2\text{Cl}]_2$, it gives $[(\eta^5\text{-Cp})\text{Rh}(\mu\text{-CO})(\mu\text{-L})\text{Rh}(\text{CO})\text{Cl}]$ containing a rhodium–rhodium bond, where the ligand performs a $\mu_2\text{-}\eta^2(\text{N,P})$ bridging function. The product with sulfur dioxide yields $[(\eta^5\text{-Cp})\text{Rh}(\mu\text{-SO}_2)(\mu\text{-L})\text{Rh}(\text{CO})\text{Cl}]$ and with molecular chlorine and bromine affords rhodium(III) $[(\eta^5\text{-Cp})\text{X}_2\text{Rh}(\mu\text{-L})\text{Rh}(\text{CO})\text{X}_2]$ ($\text{X} = \text{Cl}, \text{Br}$), and with molecular iodine it generates a mixture of $\text{Rh}(\text{II})\text{--Rh}(\text{II})$ $[(\eta^5\text{-Cp})\text{Rh}(\mu\text{-I})(\mu\text{-L})\text{Rh}(\text{CO})\text{I}_2]$ and $[(\eta^5\text{-Cp})\text{I}_2\text{Rh}(\mu\text{-L})\text{Rh}(\text{CO})\text{I}_3]$. With dimethylacetylene dicarboxylate and diethylacetylene dicarboxylate (L^1) in methylene chloride tetranuclear products $[(\eta^5\text{-Cp})\text{Rh}(\mu\text{-L}^1)(\mu\text{-L})\text{Rh}(\text{CO})(\mu\text{-Cl})_2]$ are generated where the dinuclear units are linked by chloro-bridges and the acetylenes are in a cis-metalated olefinic bonding mode (89IC2944). The starting $\eta^1(\text{P})$ -coordinated rhodium(I) also reacts with $[\text{Ir}(\text{CO})_2(p\text{-toluidine})\text{Cl}]$ to generate rhodium–iridium bond $[(\eta^5\text{-Cp})\text{Rh}(\mu\text{-CO})(\mu\text{-L})\text{Ir}(\text{CO})\text{Cl}]$ (89OM886). Heterodinuclear complexes are formed in the following reactions of $[(\eta^5\text{-Cp})\text{Rh}(\text{CO})(\eta^1(\text{P})\text{-L})]$: with $[\text{Pd}(\text{CNBu-}t)_2\text{Cl}_2]$ and hexafluorophosphate – $[(\eta^5\text{-Cp})(\text{CNBu-}t)\text{Rh}(\mu\text{-L})\text{Pd}(\text{CNBu-}t)](\text{PF}_6)$ containing a rhodium–palladium bond; with $[(\eta^4\text{-cod})\text{PdCl}_2] - [(\eta^5\text{-Cp})(\text{Cl})\text{Rh}(\mu\text{-L})\text{PdCl}_2]$, with $[\text{Pt}(\text{DMSO})_2\text{Me}_2] - [(\eta^5\text{-Cp})\text{Rh}(\mu\text{-CO})(\mu\text{-L})\text{PtMe}_2]$ with rhodium–platinum bond; and with $[\text{Pt}(\text{DMSO})_2\text{Cl}_2] - \text{rhodium(II)–platinum(I)}$ $[(\eta^5\text{-Cp})(\text{Cl})\text{Rh}(\mu\text{-L})\text{Pt}(\text{CO})\text{Cl}]$ (91OM1613). $[(\eta^5\text{-Cp})\text{Rh}(\mu\text{-CO})(\mu\text{-L})\text{Rh}(\text{CO})\text{Cl}]$ reacts with $\text{Na}[(\eta^5\text{-Cp})\text{Mo}(\text{CO})_3]$ in THF by replacement of the terminal chloride by $[\text{Mo}(\eta^5\text{-C}_5\text{H}_5)(\text{CO})_3]^-$, to give trinuclear $[(\eta^5\text{-Cp})\text{Rh}(\mu\text{-CO})(\mu\text{-L})\text{Rh}(\text{CO})\text{Mo}(\text{CO})_3(\eta^5\text{-Cp})]$ (90JOM(387)357).

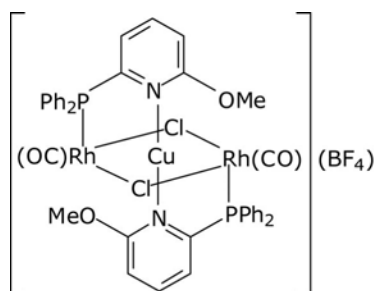
2-Diphenylphosphinopyridine with $[(\eta^5\text{-Cp}^*)\text{IrCl}_2]_2$ gives P-coordinated **69** ($\text{X} = \text{Cl}$) (09JCS(D)2029), which with lithium triethyl borohydride transforms to **69** ($\text{X} = \text{H}$). The resultant ligand with $[(\eta^5\text{-Cp}^*)\text{M}(\text{AN})_3(\text{OTf})_n]$ ($n = 2, \text{M} = \text{Rh}, \text{Ir}; n = 1, \text{M} = \text{Ru}$) gives the triply bridged **70** ($n = 2, \text{M} = \text{Rh}, \text{Ir}; n = 1, \text{M} = \text{Ru}$). Terminal alkynes $\text{RC}\equiv\text{CH}$ ($\text{R} = \text{H}, \text{COOMe}$) insert into **70** ($\text{M} = \text{Ir}, n = 2$) to yield μ -vinyls **71** ($\text{R} = \text{H}, \text{COOMe}$). The reaction with trimethylsilylacetylene gives the β -isomer **72**. Rhodium analog **69** ($\text{X} = \text{Cl}$) can be prepared similarly (06JCI319). If the reaction is conducted in methanol in the presence of ammonium hexafluorophosphate, cationic **73** ($\text{M} = \text{Rh}, \text{Ir}$) or chelated **74** ($\text{M} = \text{Rh}, \text{Ir}$) follow.



Another case study starts with 2-diphenylphosphinopyridine (L) and $[(\eta^4\text{-cod})\text{Rh}(\mu\text{-Cl})_2]$ leading to $[(\eta^4\text{-cod})\text{Rh}(\eta^1(\text{P})\text{-L})(\text{Cl})]$ ([91JOM\(419\)399](#), [91OM3877](#), [09OM6383](#)). The ligand can be transformed into the chelating form with silver perchlorate or hexafluorophosphate leading to cationic $[(\eta^4\text{-cod})\text{Rh}(\eta^2(\text{N,P})\text{-L})](\text{X})$ ($\text{X} = \text{ClO}_4, \text{PF}_6$). Protonation using HPF_6 occurs on the pyridine nitrogen giving $[(\eta^4\text{-cod})\text{Rh}(\eta^1(\text{P})\text{-LH})(\text{Cl})](\text{PF}_6)$. Under carbon monoxide in methylene chloride, A-frame $[\text{Rh}_2\text{Cl}_2\text{L}_2(\mu\text{-CO})]$ follows, but in the presence of triphenylphosphine the mononuclear $[\text{Rh}(\text{CO})(\text{PPh}_3)(\eta^1(\text{P})\text{-L})(\text{Cl})]$ results. $[(\eta^4\text{-cod})\text{Rh}(\eta^1(\text{P})\text{-L})(\text{Cl})]$ reacts with $[\text{Pd}(\text{CNBu-}t)_2\text{Cl}_2]$ in methylene chloride to give tetranuclear $[(t\text{-BuNC})_2\text{Cl}_2\text{Rh}(\mu\text{-L})\text{Pd}(\mu\text{-Cl})_2]$ containing a $\text{Rh}^{\text{II}}\text{-Pd}^{\text{I}}$ bond, where the heterocyclic ligand is coordinated by its nitrogen atom to rhodium and by its phosphorus site to palladium. The product of interaction of $[(\eta^4\text{-cod})\text{Rh}(\eta^1(\text{P})\text{-L})(\text{Cl})]$ with $[(\eta^4\text{-cod})\text{PdCl}_2]$ is dinuclear $[(\eta^4\text{-cod})\text{Rh}(\mu\text{-Cl})(\mu\text{-L})\text{PdCl}_2]$. 2-Diphenylphosphinopyridine with $[(\eta^4\text{-cod})\text{Ir}(\mu\text{-Cl})_2]$ gives P-coordinated **75**, which on carbonylation turns into **76** and on further reaction with CdI_2 forms heterodinuclear **77** ([97JCS\(D\)3409](#)).

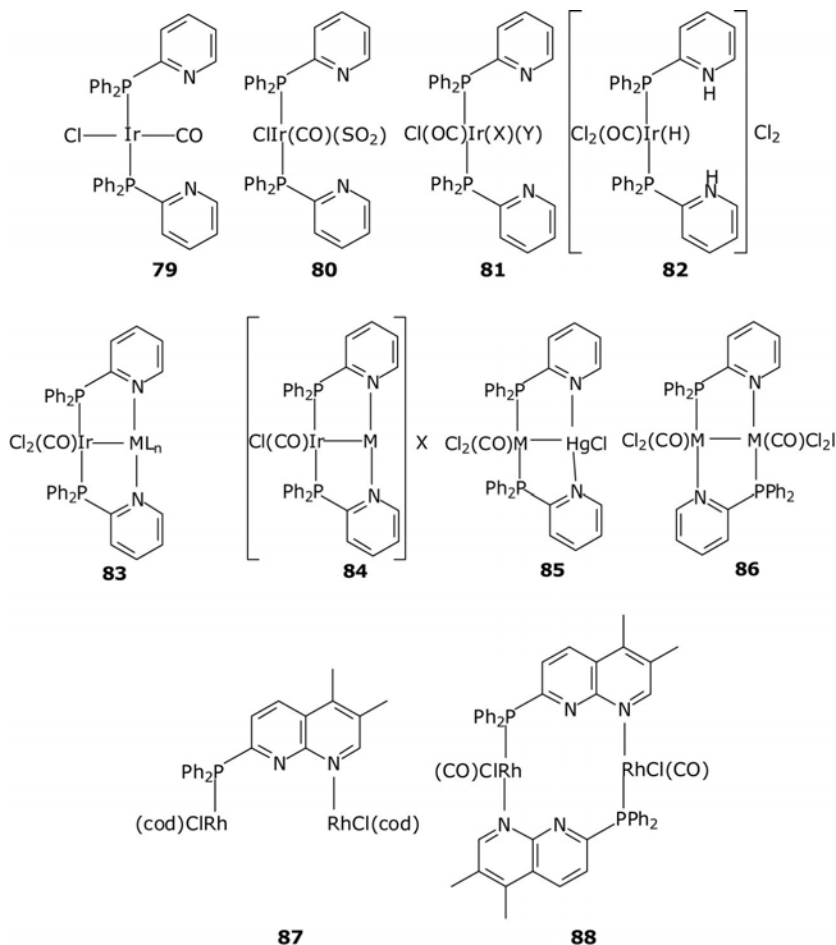


2-Dimethylphosphino-4-methoxypyridine (L) with $[(\eta^4\text{-cod})\text{Rh}(\mu\text{-Cl})_2]$ in benzene gives $\eta^1(\text{P})$ -coordinated $[(\eta^4\text{-cod})\text{Rh}(\eta^1(\text{P})\text{-L})(\text{Cl})]$ (92IC4797). Under carbon monoxide in methylene chloride $[\text{Rh}(\text{CO})_2(\eta^1(\text{P})\text{-L})(\text{Cl})]$ is generated. In an excess of the ligand, *trans*- $[\text{Rh}(\text{CO})(\eta^1(\text{P})\text{-L})_2(\text{Cl})]$ can be obtained. The product reacts with $[\text{Cu}(\text{AN})_4](\text{BF}_4)$ to give trinuclear **78** where the ligand performs a bridging function. Tris(3-(2,6-dimethoxypyridyl))phosphine, bis(3-(2,6-dimethoxypyridyl))phenylphosphine, and 3-(2,6-dimethoxypyridyl)diphenylphosphine rhodium(I) P-coordinated complexes are active in the catalytic hydrogenation of olefins, aldehydes, and imines (97OM3469).

**78**

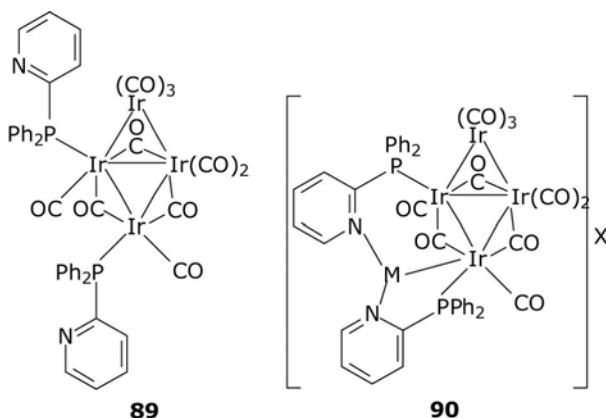
2-Diphenylphosphinopyridine with $[\text{Ir}(\text{CO})_2(p\text{-toluidine})\text{Cl}]$ gives another ligand **79** (98OM338). It adds sulfur dioxide forming **80**, molecular halogens, molecular hydrogen, and methyl iodide affording **81** ($\text{X} = \text{Y} = \text{Br}, \text{I}, \text{H}$; $\text{X} = \text{Me}, \text{Y} = \text{I}$), and hydrogen chloride yielding **82**. With $[\text{Pd}(\text{PhCN})_2\text{Cl}_2]$ and HgCl_2 in benzene, heterodinuclear Ir(II)-Pd(I), **83** ($\text{ML}_n = \text{PdCl}$) and Ir(II)-Hg(I), **83** ($\text{ML}_n = \text{HgCl}$) follow. With $[\text{Cu}(\text{AN})_4](\text{BF}_4)$ and TIPF_6 cationic **84** ($\text{M} = \text{Cu}, \text{X} = \text{BF}_4$; $\text{M} = \text{Tl}, \text{X} = \text{PF}_6$) result. Metallocomplex ligand **79** and its rhodium analog can also be prepared from 2-dimethylphosphinopyridine and $[(\eta^4\text{-cod})\text{M}(\mu\text{-Cl})_2]$ ($\text{M} = \text{Rh}, \text{Ir}$) in the presence of carbon monoxide (99ICA(284)119). Their reaction with mercury(II) chloride results in heterodinuclear **85** and homodinuclear **86**. $[\text{Ir}(p\text{-toluidine})(\text{CO})_2\text{Cl}]$ with 2-diphenylphosphinopyridine gives *trans*- $[\text{Ir}(\text{CO})\text{Cl}(\eta^1(\text{P})\text{-L})_2]$ (98OM338). The addition of hydrochloric acid is a two-step process, first the pyridine nitrogens are protonated and then the iridium-hydrogen bond is formed, and the final product is $[\text{Ir}(\text{CO})\text{H}(\text{Cl})_2(\eta^1(\text{P})\text{-LH})_2]\text{Cl}_2$. The addition of $[\text{Pd}(\text{PhCN})_2\text{Cl}_2]$ gives the iridium(II)-palladium(I) $[\text{Ir-Pd}(\text{CO})\text{Cl}_3(\mu\text{-Ph}_2\text{PPy})_2]$, of HgCl_2 - $[\text{Ir}(\text{CO})\text{Cl}_2(\text{HgCl}_2)(\mu\text{-Ph}_2\text{PPy})_2\text{HgCl}]$, of $[\text{Cu}(\text{AN})_4](\text{BF}_4)$ - $[\text{Ir}(\text{CO})\text{Cl}(\mu\text{-Ph}_2\text{PPy})_2\text{Cu}](\text{BF}_4)$, and with thallium hexafluorophosphate - $[\text{Ir}(\text{CO})\text{Cl}(\mu\text{-Ph}_2\text{PPy})_2\text{Tl}](\text{PF}_6)$ containing iridium-thallium bond. 7-Diphenylphosphino-2,4-dimethyl-1,8-naphthyridine (L) with $[(\eta^4\text{-cod})\text{Rh}(\mu\text{-Cl})_2]$ in a molar ratio 2:1 gives the monodentate $[(\eta^4\text{-cod})\text{Rh}(\eta^1(\text{P})\text{-L})\text{Cl}]$ (92JCS(D)2367). If the

reactant molar ratio is 1:1, dinuclear **87** is formed. With $[\text{Rh}(\text{CO})_2(\mu\text{-Cl})]_2$, the only product isolated is dinuclear **88**.



2-Diphenylphosphinopyridine, phenylbis(2-pyridyl)phosphine, and tris-(2-pyridyl)phosphine (L) with $[\text{Ir}_4(\text{CO})_{12}]$ in methanol in basic medium, in the presence of carbon monoxide give $[\text{Ir}_4(\text{CO})_9(\eta^1(\text{P})\text{-L})_3]$ (**90AOC173**). 2-Diphenylphosphinopyridine with $[\text{Ir}_4(\text{CO})_{12}]$ in the presence of potassium hydroxide in methanol gives $[\text{Ir}_4(\mu\text{-CO})_3(\text{CO})_5(\mu\text{-}\eta^2(\text{N}, \text{P})\text{-L})(\eta^1(\text{P})\text{-L})_2]$ (**95ICA(232)207**). Pyridylphosphines $\text{PPh}_x\text{py}_{3-x}$ ($x = 0\text{--}2$) with $[\text{Ir}_4(\text{CO})_{12}]$ give $[\text{Ir}_4(\mu\text{-CO})_3(\text{CO})_5(\mu\text{-L})\text{L}_2]$, where one ligand plays the role of an N,P-bridge and the other two are P-coordinated (**96JOM(508)75**). 2-Diphenylphosphinopyridine (L) with $(\text{NEt}_4)[\text{Ir}_4(\text{CO})_{11}\text{Br}]$ in methylene chloride gives $\eta^1(\text{P})$ -coordinated **89** (**96OM3170**). It further reacts with [Cu

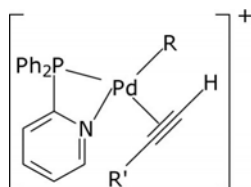
(AN)₄](BF₄) or AgPF₆ to yield heteropolynuclear cationic **90** (M = Cu, X = BF₄; M = Ag, X = PF₆).



2.4 Nickel group

An alkylphosphine ligand containing a pyridyl group is applied in the Ni(0)-catalyzed cycloaddition reactions (**89CC9**). P-coordinated [Ni(CO)₂L₂] (L = 2-diphenylphosphinopyridine, 1,2-bis(bis(2-pyridylphosphino)ethane) result from the substitution of triphenylphosphine in [Ni(CO)₂(PPh₃)₂] by the corresponding ligand (**95ICA(235)291**). Platinum(0) [PtL₄] (L = tri(2-pyridyl)phosphine), and [PtL₃] (L = 2-diphenylphosphinopyridine) with olefins (ethylene, maleic anhydride, diethyl maleate, and olefinic nitriles) give [(η²-olefin)Pt(η¹(P)-L)₂] (**91JOM(417)277**). Methyl iodide oxidatively adds and gives [Pt(I)(Me)(L)₂]. [PtL₂Cl₂] (L = 2-diphenylphosphinopyridine) reacts with [(bicycloheptadiene)Mo(CO)₄] or [(AN)₃W(CO)₃] to yield [PtM(μ-L)₂(μ-CO)(CO)₂Cl₂] (M = Mo, W) (**83OM1758**). A molybdenum complex may also form in the reaction between [Mo(CO)₄L₂] and [(η⁴-cod)PtCl₂]. The coordination units are PtClP₂ and MC₂N₂Cl, and Pt–M bonds are formed. [PtL₂(C≡CPh)₂] with two equivalents of [M(AN)₄]⁺ (M = Cu, Ag) in methylene chloride gives heterotrinnuclear [Pt(μ-L)₂(μ,η²-PhC≡C)₂(M(AN)_x)₂]²⁺ (M = Cu, x = 1, 2; M = Ag, x = 1) isolated as hexafluorophosphate or tetrafluoroborate salts (**93JCS(D)2075**). Two phosphorus atoms are coordinated to platinum, and pyridine nitrogen to one of the copper (silver) sites. Carbonylation of the nonfunctionalized 1-alkynes can be promoted by cationic palladium containing chelated 2-diphenylphosphinopyridine, where formation of **91** (R = H, COOMe; R' = (CH₂)_nOH) can be postulated (**02TL753**).

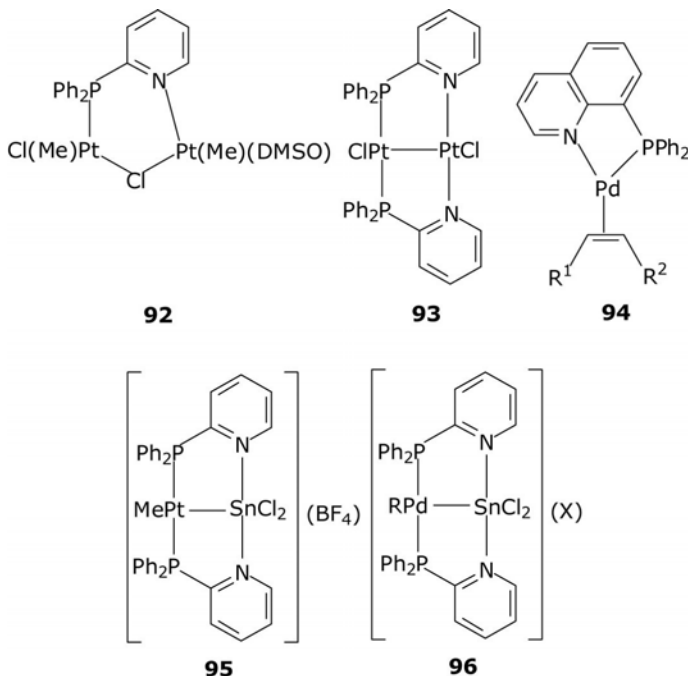
Treatment of $[\text{Pd}(\eta^1\text{-Ph}_2\text{PC}_5\text{H}_4\text{N})_2(\text{dba})]$ with *p*-benzoquinone affords $[\text{Pd}(\eta^1\text{-Ph}_2\text{PC}_5\text{H}_4\text{N})_2(\eta^2\text{-p-benzoquinone})]$ (10JCS(D)7921). Palladium-catalyzed distannylation of *o*-quinodimethanes in the presence of 2-diphenylphosphinopyridine involves the formation of organometallic forms (06OL4157).



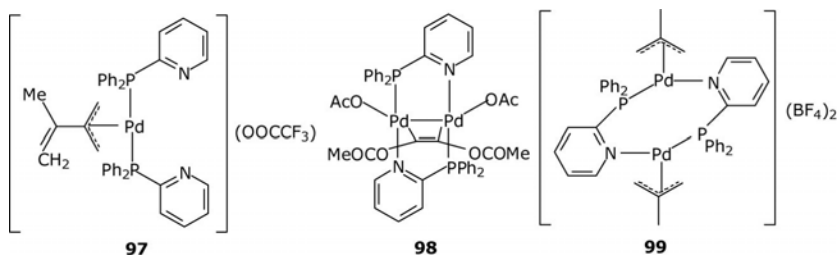
91

$[\text{Pt}(\text{DMSO})(\eta^1(\text{P})\text{-L})_2\text{Cl}_2]$ reacts with $[\text{Pt}(\text{DMSO})_2\text{Me}_2]$ to yield two dinuclear products **92** and **93** (93IC1601). Carbon monoxide with **92** gives $[(\text{MeCO})(\text{Cl})\text{Pt}(\mu\text{-Cl})(\mu\text{-Ph}_2\text{PC}_5\text{H}_4\text{N})\text{Pt}(\text{Me})(\text{DMSO})]$ with retention of the structural pattern (94JOM(484)171). It slowly transforms into cationic $[(\text{Me})(\text{Cl})\text{Pt}(\mu\text{-Ph}_2\text{PC}_5\text{H}_4\text{N})_2\text{Pt}(\text{COMe})][\text{Pt}(\text{CO})(\text{COMe})\text{Cl}_2]$ containing a platinum–platinum bond. The *cis*–*trans* isomerization of alkenes bearing strong electron-withdrawing substituents occurs within palladium(0) complexes of type **94** (08OM3577). The reaction of 2-diphenylphosphinopyridine (L) with $[(\eta^4\text{-cod})\text{Pt}(\text{Me})\text{X}]$ yields $[\text{Pt}(\text{Me})\text{X}(\text{L})_2]$ (X = Me, Cl, or I) (90JOM(389)417). Reaction of $[(\eta^4\text{-cod})\text{Pt}(\text{Me})\text{Cl}]$ with an excess of L gives the dinuclear $[\text{Pt}(\text{Me})\text{Cl}(\text{L})]_2$. Treatment of the latter with sodium tetraphenylborate or tetrafluoroborate yields cationic $[\text{Pt}(\text{Me})(\eta^2\text{-L})(\text{L})](\text{Y})$ (Y = BPh₄, BF₄). The product with SnCl₂ gives **95** (10JCS(D)2423). A palladium analog can be made starting from $[(\eta^4\text{-cod})\text{Pd}(\text{Me})(\text{Cl})]$. $[(\eta^1(\text{P})\text{-L})_3\text{Pd}]$ with RSnCl_3 (R = Me, *n*-Bu, Ph) gives first ionic **96** (X = Cl) and then **96** (X = RSnCl₄) (10OM5904). An efficient catalytic system for the carbonylation of alkynes is prepared from 2-diphenylphosphinopyridine, palladium(II) species and a proton source containing weakly coordinating anions (93JOM(455)247, 94JOM(475)55, 95TL9015, 96RCT248, 01CRV3435). $[(\text{Cl})\text{Pd}(\mu\text{-}\eta^2(\text{N,P})\text{-L})_2\text{Pd}(\text{Cl})]$ inserts dimethylacetylene dicarboxylate to yield $[(\text{Cl})\text{Pd}(\mu\text{-}\eta^2(\text{N,P})\text{-L})_2(\mu\text{-MeOOC}\text{C}\equiv\text{CCOOMe})\text{Pd}(\text{Cl})]$ (92CJC751). $\text{Pd}(\text{OAc})_2$ /2-diphenylphosphinopyridine/triflic acid is a catalytic system for the carbonylation of alkynes, which is postulated to form the Pd–C(Ph) = CH₂ moiety (98OM630, 02ASC543). $[(\eta^3\text{-CH}_2\text{C}(\text{Me})\text{CH}_2)\text{Pd}(\eta^1(\text{P})\text{-L})\text{Cl}]$ (L = 2-diphenylphosphinopyridine) with silver tetrafluoroborate gives dinuclear $[(\eta^3\text{-CH}_2\text{C}(\text{Me})\text{CH}_2)\text{Pd}(\mu, \eta^2(\text{N,P})\text{-L})_2\text{Pd}(\eta^3\text{-CH}_2\text{C}(\text{Me})\text{CH}_2)](\text{BF}_4)_2$, which in excess ligand gives cationic $[(\eta^3\text{-CH}_2\text{C}(\text{Me})\text{CH}_2)\text{Pd}(\eta^1(\text{P})\text{-L})_2](\text{BF}_4)$ (09JOM131). Treatment of the latter with

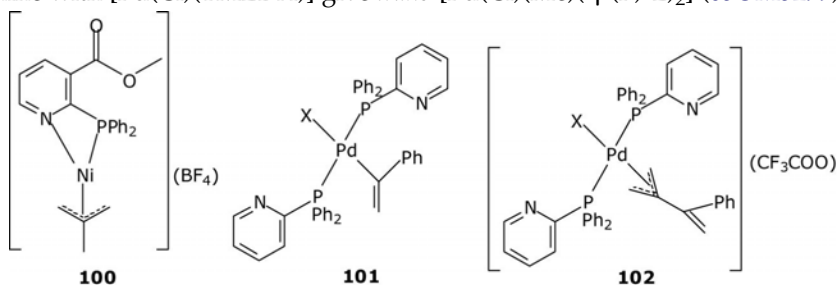
diethylamine in the presence of fumaronitrile gives neutral $[(\eta^2\text{-CNCH=CHCN})\text{Pd}(\eta^1(\text{P})\text{-L})_2]$.



2-Diphenylphosphinopyridine with palladium(II) acetate in an appropriate alcohol under carbon monoxide yields $[\text{Pd}(\eta^1(\text{P})\text{-L})_2(\text{COOR})(\text{OAc})]$ ($\text{R} = \text{Me}, \text{Et}, i\text{-Pr}$) (99JCS(D)1113). In the presence of trifluoroacetic acid, the product is $[\text{Pd}(\eta^1(\text{P})\text{-L})_2(\text{COOMe})(\text{OOCF}_3)]$ in methanol. From $[\text{Pd}(\eta^1(\text{P})\text{-L})_2\text{Cl}_2]$ and sodium methoxide $[\text{Pd}(\eta^1(\text{P})\text{-L})_2(\text{COOMe})\text{Cl}]$ can also be prepared. The latter two complexes with phenylacetylene give the σ -alkynyl $[\text{Pd}(\eta^1(\text{P})\text{-L})_2(\text{C}\equiv\text{CPh})(\text{OOCF}_3)]$ and $[\text{Pd}(\eta^1(\text{P})\text{-L})_2(\text{C}\equiv\text{CPh})\text{Cl}]$, respectively. $[\text{Pd}(\eta^1(\text{P})\text{-L})_2(\text{COOMe})(\text{OOCF}_3)]$ with allene gives π -allyl 97. $[\text{Pd}_2(\mu\text{-}\eta^2(\text{P},\text{N})\text{-Ph}_2\text{PC}_5\text{H}_4\text{N})_2(\text{OAc})_2]$ with $\text{MeOOC}\equiv\text{COOMe}$ gives the dimetalated alkene 98 (98JCS(D)3771). $[(\eta^3\text{-CH}_2\text{C}(\text{Me})\text{CH}_2)\text{Pd}(\text{Ph}_2\text{PPy})\text{Cl}]$ with *cis*- $[\text{Pd}(t\text{-BuNC})_2\text{Cl}_2]$ in dichloromethane affords *cis*- $[\text{Pd}(t\text{-BuNC})(\eta^1(\text{P})\text{-Ph}_2\text{PPy})\text{Cl}_2]$ along with $[(\eta^3\text{-CH}_2\text{C}(\text{Me})\text{CH}_2)\text{PdCl}_2]$ (93JOM(450)263). 2-Diphenylphosphinopyridine with $[(\eta^3\text{-2-Me-allyl})\text{Pd}(\text{Cl})]_2$ gives $\eta^1(\text{P})$ -coordinated $[(\eta^3\text{-2-Me-allyl})\text{Pd}(\eta^1(\text{P})\text{-L})\text{Cl}]$, which in the presence of silver tetrafluoroborate yields the dinuclear cationic 99 (07JOM3577). The product reacts with further 2-diphenylphosphinopyridine to afford $[(\eta^3\text{-2-Me-allyl})\text{Pd}(\eta^1(\text{P})\text{-L})_2](\text{BF}_4)$.

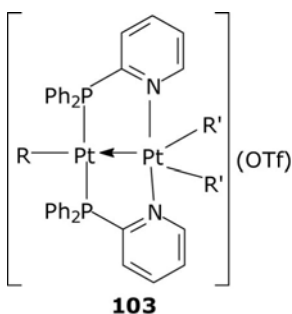


N-(2-(Diphenylphosphino)benzylidene)(2-(2-pyridyl)ethyl)amine (L) contains phosphine, imine, and pyridyl donor groups and in alkyl, allyl, and acyl-palladium as well as methyl platinum it coordinates in a terdentate fashion, as in $[(L)M(R)]Y$ ($M = Pd, Pt, R = Me, Y = Cl, OTf$; $M = Pd, R = C(O)Me, Y = OTf$; $M = Pd, R = \eta^1-CH_2C(H)=CH_2, Y = Cl, OTf$) (96OM3022). Methyl(2-diphenylphosphino)nicotinate forms P,N-chelated η^3 -methallyl nickel(II) tetrafluoroborate **100** (94CC615, 95OM5302, 04JOM3953). Palladium(0) homoleptic of 2-diphenylphosphinopyridine (L), $[Pd(\eta^1(P)-L)_3]$ with dimethylacetylene dicarboxylate (L^1) gives $[Pd(\eta^1(P)-L)_2(\eta^2-L^1)]$ (00JCS(D)523). In the presence of a proton source (hydrochloric or trifluoroacetic acid), oxidative addition of phenylacetylene becomes possible yielding **101** ($X = Cl, CF_3COO$). Oxidative addition of methylacryloyl chloride $Cl(CO)(Me)C=CH_2$ affords $[Pd(\eta^1(P)-L)_2(CO)(Me)C=CH_2]Cl$. **101** ($X = CF_3COO$) with propadiene produces cationic π -allyl **102** as a result of insertion of allene into the palladium–carbon bond. 2-Diphenylphosphinopyridine, 2-bis(4-(bromophenyl)phosphino)pyridine, and 2-bis(4-((2-perfluorohexyl)ethyl)dimethylsilyl)phenylphosphinopyridine with $[Pd(Cl)(TMEDA)]$ give *trans*- $[Pd(Cl)(Me)(\eta^1(P)-L)_2]$ (05OM5299).

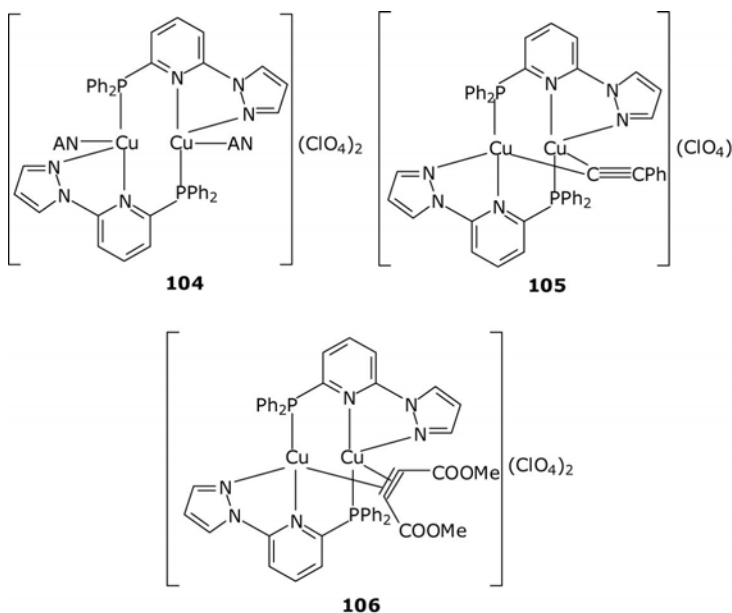


2-Diphenylphosphinopyridine (L) with $[Pt(Me_2S)_2R_2]$ ($R = Ph, p-Tol, p-FC_6H_4$) or $[Me_2Pt(\mu-SMe_2)_2PtMe_2]$ produces the P-coordinated $[PtR_2(\eta^1(P)-L)_2]$ ($R = Me, Ph, p-Tol, p-FC_6H_4$) (07JCS(D)4715). Triflic acid causes elimination of RH and formation of $[Pt(R)(OTf)(\eta^1(P)-L)_2]$ and mixed chelate-P-coordinated $[Pt(R)(\eta^1(P)-L)(\eta^2(N,P)-L)](OTf)$. Both products with $[Me_2Pt(\mu-SMe_2)_2PtMe_2]$ or $[Pt(Me_2S)_2(p-Tol)_2]$ lead to dinuclear Pt-Pt compounds with a bridging L, **103** ($R = Ph, p-Tol, p-C_6H_4F, R' = Me; R = R' = Me$;

$R = \text{Me}$, $R' = p\text{-Tol}$). In the process of interaction, the *cis-trans* mutual disposition of the two bridges changes. 2-Diphenylphosphinopyridine with of $[\text{Pt}_2\text{Me}_4(\mu\text{-SMe}_2)_2]$ gives *cis,cis*- $[\text{Pt}_2\text{Me}_4(\mu\text{-SMe}_2)(\mu\text{-}\eta^2(\text{P,N})\text{-L})]$, which with trifluoroacetic acid forms $[\text{Me}_2\text{Pt}(\mu\text{-SMe}_2)(\mu\text{-}\eta^2(\text{P,N})\text{-L})\text{Pt}(\text{Me})(\text{OOCF}_3)]$ and after isomerization - $[\text{Me}(\text{CF}_3\text{COO})\text{Pt}(\mu\text{-}\eta^2(\text{P,N})\text{-L})\text{PtMe}_2(\text{SMe}_2)]$ containing the Pt–Pt donor–acceptor bond (03OM2612). In excess ligand, this bond splits resulting in $[\text{Me}(\eta^2(\text{N,P})\text{-L})\text{Pt}(\mu\text{-SMe}_2)(\mu\text{-}\eta^2(\text{P,N})\text{-L})\text{PtMe}_2](\text{CF}_3\text{COO})$ and after elimination of dimethyl sulfide $[(\text{Me})\text{Pt}(\mu\text{-}\eta^2(\text{P,N})\text{-L})_2\text{PtMe}_2](\text{CF}_3\text{COO})$ it tends to isomerize to $[(\text{Me})\text{Pt}(\mu\text{-}\eta^2(\text{P,N})\text{-L})(\mu\text{-}\eta^2(\text{N,P})\text{-L})\text{PtMe}_2](\text{CF}_3\text{COO})$. Both isomers contain donor–acceptor Pt–Pt bonds.

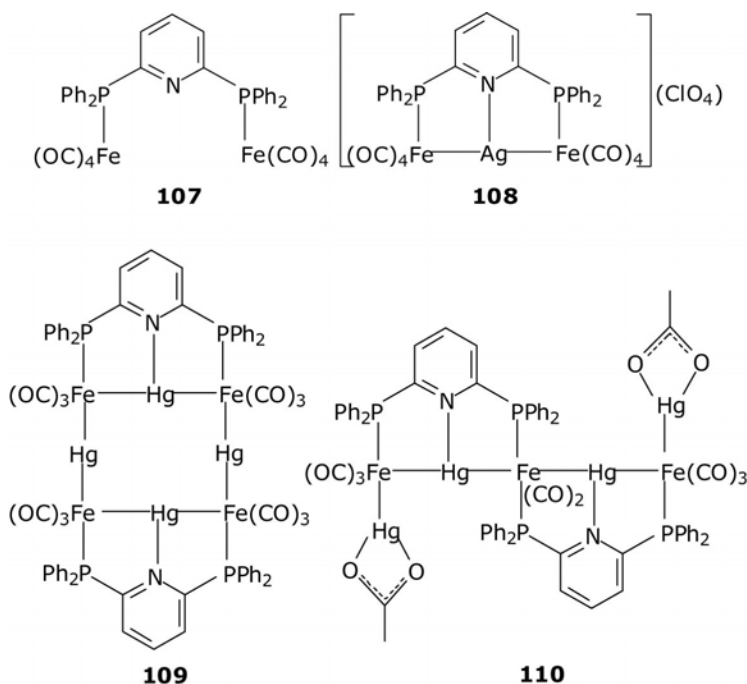


Reactivity of copper dicationic **104** with alkynes is of interest (98JCS(D) 1115). Thus, with lithium phenylacetylide, the acetylide counterpart constitutes a μ, η^1 -bridge between two copper sites as in **105**, while $\text{MeOOC}\equiv\text{CCOOMe}$ performs the μ, η^2 -bridging function **106** as a whole.



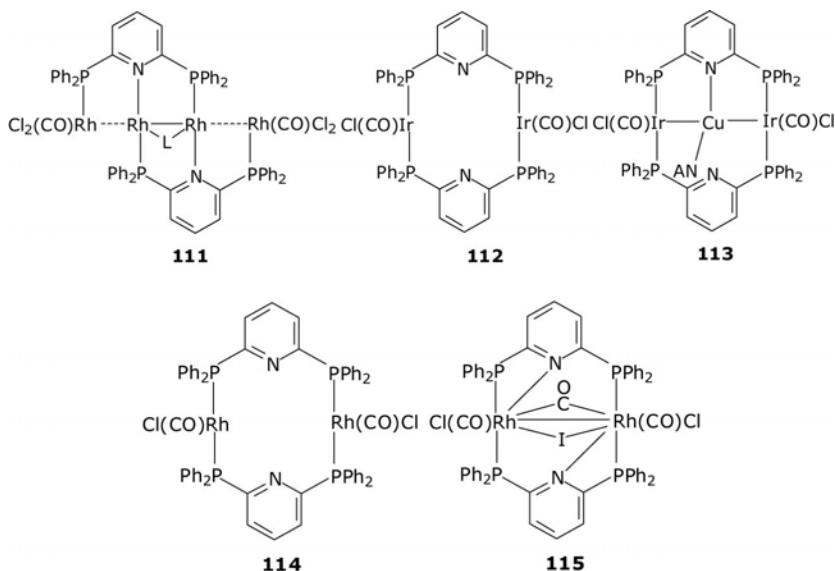
3. BIS(PHOSPHINO)PYRIDINES

2,6-Bis(diphenylphosphino)pyridine is the basis of the organometallic ligand **107** prepared from the pyridine derivative and $[\text{Fe}(\text{CO})_5]$ with sodium hydroxide in *n*-butanol (96POL2583). With mercury(II) chloride, $[\text{Fe}_2\text{Hg}(\mu\text{-L})_2(\text{CO})_6\text{Cl}_2] \cdot \text{HgCl}_2$ has two iron–mercury bonds in **107** that then reacts with silver perchlorate to form the heterotrinnuclear **108**, where the silver(I) bridges two iron(0) atoms (01IC5928). With mercury(II) acetate, a heterooctanuclear **109** and after addition of a silver salt a heteroheptanuclear **110** result. 2,2'-Bis(diphenylphosphino)-4,4'-bipyridine with $[\text{Rh}_6(\text{CO})_{15}(\text{AN})]$ or $[\text{Ru}_6\text{C}(\text{CO})_{17}]$ affords $[(\text{Rh}_6(\text{CO})_{14})_2(\text{L})]$ or $[(\text{Ru}_6\text{C}(\text{CO})_{15})_2(\text{L})]$ where the ligand forms a P,N-bridge to the hexanuclear metal cores (05OM3516).

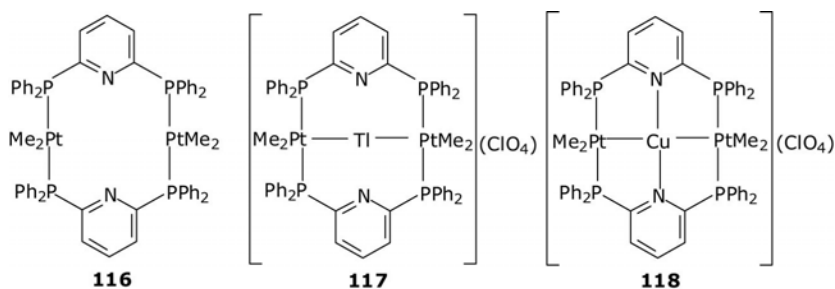


2,6-Bis(diphenylphosphino)pyridine forms tetranuclear **111** ($\text{L} = \text{CO}$, SO_2) (83JA6332), and the carbonyl complex on interaction with carbon monoxide and ammonium hexafluorophosphate in chloroform produces $[\text{Rh}_2(\mu\text{-L})_2(\text{CO})_2(\text{MeOH})\text{Cl}](\text{PF}_6)$ (83JA6986). $[\text{RhAu}(\mu\text{-L})_2](\text{BF}_4)(\text{NO}_3)$ under carbon monoxide gives $[\text{RhAu}(\mu\text{-L})_2(\text{CO})_2](\text{BF}_4)(\text{NO}_3)$ (85IC1935, 86IC4717). With $[(\eta^4\text{-cod})\text{Ir}(\mu\text{-Cl})_2]$ in acetonitrile, the ligand gives dinuclear **112** (98POL493). The product with $[\text{Cu}(\text{AN})_4](\text{ClO}_4)$ gives heterotrinnuclear **113**. 2,6-Bis(diphenylphosphino)pyridine with $[\text{Rh}(\text{CO})_2(\mu\text{-Cl})_2]$ in

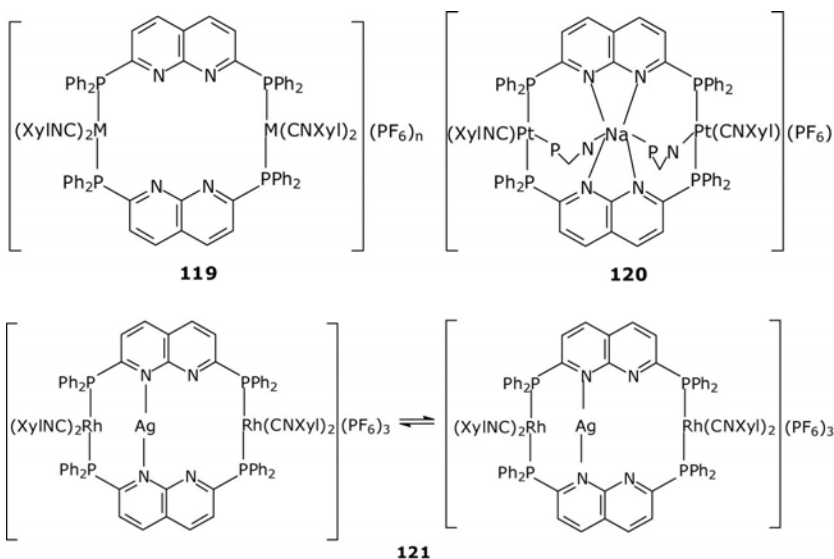
benzene gives dinuclear **114**, which with tin(II) chloride affords $[\text{Rh}_2\text{Sn}_2(\text{CO})_2\text{Cl}_6(\mu\text{-L})_2]$ containing the Rh–Sn–Rh–SnCl₃ chain where the central tin atom is coordinated *via* the pyridine nitrogen (85JA6936, 88PAC555). Treatment of **114** with sodium iodide and sodium tetraphenylborate leads to a drastic alteration of the bridging mode of the ligand and formation of **115** (86IC4526).



2,6-Diphenylphosphinopyridine with $[(\eta^4\text{-cod})\text{PtMe}_2]$ in methylene chloride gives dinuclear **116** where the ligands perform the function of a P,P-bridge (02IC3146). The product with thallium(I) perchlorate in methylene chloride yields **117**, which reacts with $[\text{Cu}(\text{AN})_4]\text{X}$ ($\text{X} = \text{ClO}_4, \text{BF}_4$) to give **118** ($\text{X} = \text{ClO}_4, \text{BF}_4$) where copper is coordinated *via* both pyridine nitrogen atoms. The ligand also gives rise to similar $[\text{Me}_2\text{Pt}(\mu\text{-L})_2\text{Ag}_2(\text{AN})_2](\text{BF}_4)_2$ and $[(\text{OC})_3\text{Fe}(\mu\text{-L})_2\text{Ag}(\text{Et}_2\text{O})](\text{ClO}_4)_2$.



2,7-Bis(diphenylphosphino)-1,8-naphthyridine can be used to construct metallocryptands (**03CIC39**). A typical scheme includes the reaction of this ligand with $[(\eta^4\text{-cod})\text{Rh}(\text{Cl})_2]_2$ or $[(\eta^4\text{-cod})\text{PtCl}_2]_2$ and 2,6-xylyl isocyanide in the presence of ammonium hexafluorophosphate to yield dinuclear **119** ($\text{M} = \text{Rh}$, $n = 2$; $\text{M} = \text{Pt}$, $n = 4$) (**07JOM175**). For rhodium(I) further reaction with silver hexafluorophosphate gives heterotrinnuclear **120**, best described by the coexisting structures. 2,7-Bis(diphenylphosphino)-1,8-naphthyridine with $[\text{Pt}(2,6\text{-XylNC})_4](\text{PF}_6)_2$ and sodium borohydride gives diplatinum(0)metallocryptate **121**, where the middle moiety is shown only partially (**04OM6042**). The palladium analog is based on $[\text{Pd}_3(2,6\text{-XylNC})_6]$ and sodium hexafluorophosphate. Under carbon monoxide, $[\text{M}_2\text{Na}(\mu\text{-L})_3(\text{CO})_2](\text{PF}_6)$ ($\text{M} = \text{Pt}$, Pd) is formed having the same framework.

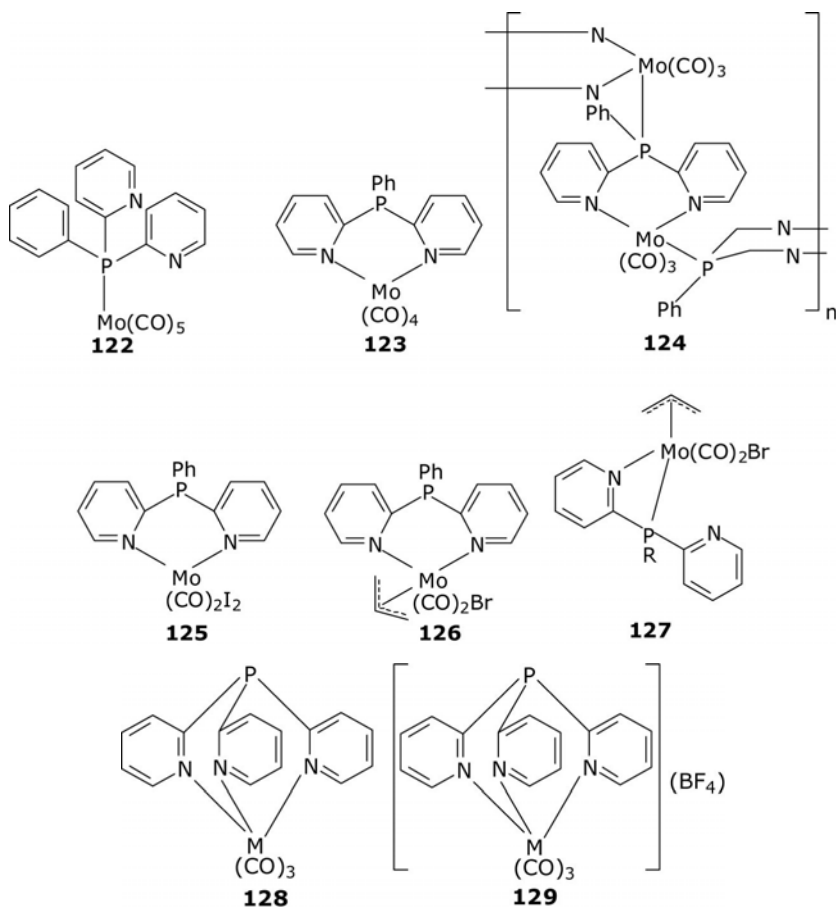


4. BIS- AND TRIS-PYRIDYL PHOSPHINES

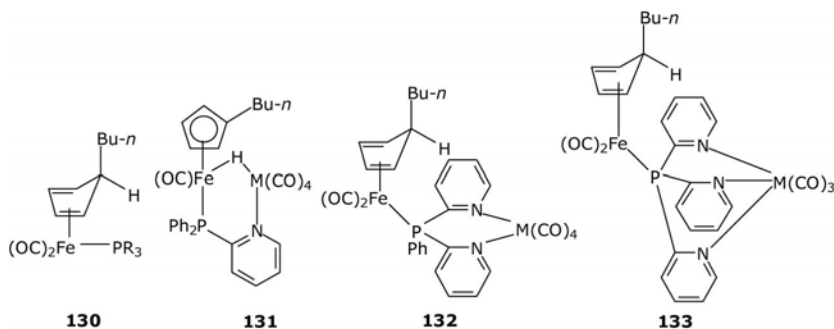
Bis(2-pyridyl)phosphine with trimethyl aluminum first gives $[\text{Me}_3\text{Al}(\mu\text{-C}_5\text{H}_4\text{N})(\text{PC}_5\text{H}_4\text{N})_2]$ and on deprotonation phosphide $[\text{Me}_3\text{Al}(\mu\text{-C}_5\text{H}_4\text{N})\text{P}]$ (**93CC444**, **95OM2422**). Similarly, $[\text{Me}_3\text{Al}(\mu\text{-C}_5\text{H}_4\text{N})\text{As}]$ and $[\text{Me}_3\text{Al}(\mu\text{-C}_5\text{H}_4\text{N})\text{Ga}]$ can be prepared. Bis(2-pyridyl)phosphine with trimethyl aluminum gives $[\text{Me}_2\text{Al}(\eta^2(\text{N},\text{N})\text{-L})]$ (**02JOM(661)111**).

Phenylbis(2-pyridyl)phosphine with $[\text{Mo}(\text{CO})_5(\text{AN})]$ yields $\eta^1(\text{P})$ -coordinated **122** (**93JOM(450)145**). Two equivalents of the ligand with $[(\eta^4\text{-nbd})\text{Mo}(\text{CO})_4]$ also give $\eta^1(\text{P})$ -coordinated $[\text{Mo}(\text{CO})_4\text{L}_2]$ but

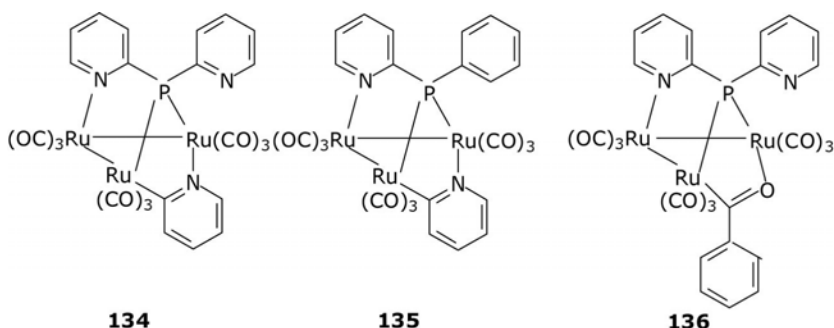
containing two ligands. An equimolar mixture of reagents in methylene chloride, in contrast, leads to $\eta^2(N,N)$ -coordinated **123**. Thermolysis of **122**, $[\text{Mo}(\text{CO})_4\text{L}_2]$, **123**, as well as refluxing the ligand with $[\text{Mo}(\text{CO})_6]$ in toluene gives polymeric **124**, where the bridging ligands are P-coordinated to one Mo-site and *N,N*-coordinated to another. The product with molecular iodine or allyl bromide leads to *N,N*-coordinated **125** and **126**. Tri-2-pyridylphosphine with $[\text{Mo}(\text{CO})_6]$ or $[(\eta^4\text{-nbd})\text{Mo}(\text{CO})_4]$ yields $[\text{Mo}(\text{CO})_3(\eta^3(N,N,N)\text{-L})]$ (**97IC44**). $\text{P}(\text{C}_5\text{H}_4\text{N})_2\text{Ph}$ or $\text{P}(\text{C}_5\text{H}_4\text{N})_3$ with $[(\eta^3\text{-allyl})\text{Mo}(\text{Br})(\text{CO})_2(\text{AN})_2]$ gives *N,P*-mono-chelates **127** (*R* = Ph, $\text{C}_5\text{H}_4\text{N}$) (**00EJI1031**). Tris-2-pyridylphosphine with $[\text{Mo}(\text{CO})_6]$ or $[\text{M}(\text{CO})_3(\text{AN})_3]$ (*M* = Cr, W) gives *N,N,N*-coordinated **128** (*M* = Cr, Mo, W) (**99JOM(588)260**). Molybdenum and tungsten products **122** with NOBF_4 in methylene chloride give cationic **129** (*M* = Mo, W). Bis(6-methylquinolin-8-yl)phenylarsine and tris(6-methylquinolin-8-yl)arsine are tridentate in $[\text{Mo}(\text{CO})_3(\eta^3\text{-As},N,N)\text{-L}]$ (**82AJC2193**).



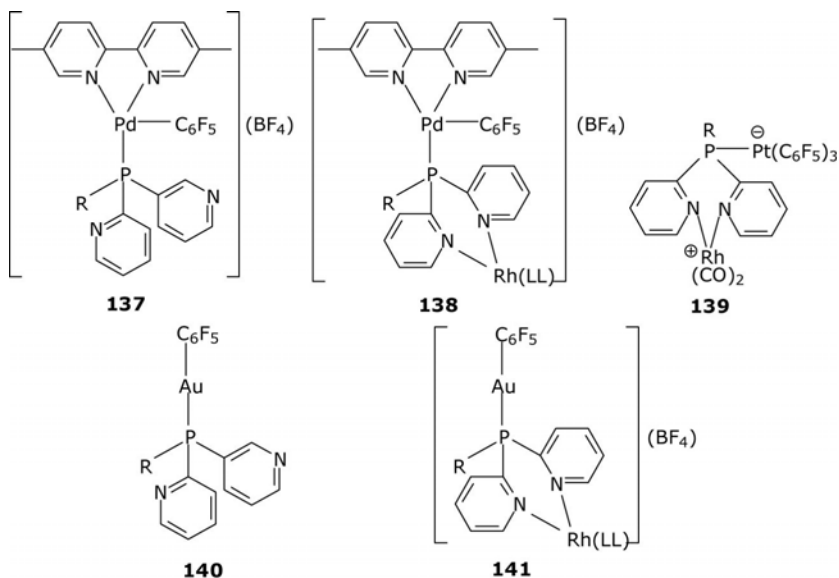
Strained $[\text{Ru}(\text{Cl})(\text{PPh}_3)_2(\eta^3(\text{P},\text{N},\text{N})\text{-L})](\text{PF}_6)$ ($\text{L} = \text{PPh}_{3-x}(\text{C}_5\text{H}_4\text{N})_x$) ($x = 2, 3$) with carbon monoxide displace the coordinated pyridyl and yield $[\text{Ru}(\text{Cl})(\text{CO})(\text{PPh}_3)(\eta^2(\text{P},\text{N})\text{-L})](\text{PF}_6)$ (**97IC5809**). $\text{PPh}_{3-n}(\text{C}_5\text{H}_4\text{N})_n$ ($n = 1-3$) with $[(\eta^5\text{-Cp})\text{Fe}(\text{CO})_2]$ and *n*-butyl lithium gives the η^4 -coordinated **130** ($\text{PR}_3 = \text{PPh}_2\text{C}_5\text{H}_4\text{N}$, $\text{PPh}_2(\text{C}_5\text{H}_4\text{N})_2$, $\text{P}(\text{C}_5\text{H}_4\text{N})_3$) where the ligands are P-monodentate (**09ICA477**). The 2-diphenylphosphinopyridine product **131** ($\text{R}_2 = \text{PPh}_2\text{C}_5\text{H}_4\text{N}$) with $[\text{M}(\text{CO})_3(\text{AN})_3]$ ($\text{M} = \text{Mo}, \text{W}$) gives heterobimetallic **132** ($\text{M} = \text{Mo}, \text{W}$) containing an hydrido bridge. In the case of $\text{PPh}(\text{C}_5\text{H}_4\text{N})_2$, the process in the presence of carbon monoxide occurs differently and affords bridging **131**. The same reaction course yielding **133** is observed for the tri-2-pyridylphosphine ligand.



$[\text{Rh}(\text{H})(\text{CO})(\text{PPh}_3)(\text{P}(\text{C}_5\text{H}_4\text{N})_3)_2]$ acts as a catalyst for selective hydroformylation (**80JCS(D)55**). The structure of *trans*- $[\text{Rh}(\text{Cl})(\text{CO})(\text{P}(\text{2-C}_5\text{H}_4\text{N})_3)_2]$ is also known (**80ICA(40)207**). Diphenyl(2-pyridyl)phosphine, phenylbis(2-pyridyl)phosphine, and tris(2-pyridyl)phosphine with $[\text{Rh}(\text{acac})(\text{CO})_2]$ and $[\text{Rh}(8\text{-oxy})(\text{CO})_2]$ yield $[\text{Rh}(\text{LL})(\text{CO})(\eta^1(\text{P})\text{-L})]$ (**88TMC22**). Tris(2-pyridyl)phosphine, phenylbis(2-pyridyl)phosphine, and tris(3-pyridyl)phosphine (L) with $[\text{Rh}(\text{CO})_2(\mu\text{-Cl})_2]$ give $[\text{Rh}(\text{Cl})(\text{CO})\text{L}_2]$ with P-coordination although in solution pentacoordination of the type N,P is observed (**88TMC101**). Tris(2-pyridyl)phosphine with $[\text{Ru}_3(\text{CO})_{12}]$ in THF in the presence of $(\text{PPN})(\text{Cl})$ as a catalyst gives cluster **134** (**93JCS(D)2041**) followed by cleavage of the P–C bond and generation of the μ -2-pyridyl three-electron and μ_3 -2-pyridylphosphido five-electron bridge. Phenylbis(2-pyridyl)phosphine and $[\text{Ru}_3(\text{CO})_{12}]$ under identical conditions form **135** and **136**. Phenylbis(2-pyridyl)phosphine and tris(2-pyridyl)phosphine (L) with $[\text{Os}_3(\text{CO})_{10}(\text{AN})_2]$ form clusters with bridging N,P-ligand of composition $[\text{Os}_3(\text{CO})_{10}(\mu\text{-L})]$ (**93CC844**, **93JCS(D)3383**). $[\text{Pt}_2\text{I}_2(\mu\text{-L})_2]$ ($\text{L} = \text{tris}(2\text{-pyridyl})\text{phosphine}$) inserts dimethyl acetylene dicarboxylate (L^1) into the Pt–Pt bond to give the A-frame $[\text{Pt}_2\text{I}_2(\mu\text{-L})_2(\mu\text{-L}^1)]$ (**94ICA(217)209**). Tri-2-pyridylphosphine derivative $[\text{RuCl}_2(\text{PPh}_3)(\eta^3(\text{N},\text{N},\text{N})\text{-PPy}_3)]$ reacts with carbon monoxide and ammonium hexafluorophosphate in methanol to afford cationic $[\text{Ru}(\text{Cl})(\text{CO})(\text{PPh}_3)(\eta^3(\text{N},\text{N},\text{N})\text{-PPy}_3)](\text{PF}_6)$ (**96CJC2064**). In benzene, however, the neutral product follows, $[\text{RuCl}_2(\text{CO})(\eta^3(\text{N},\text{N},\text{N})\text{-PPy}_3)]$

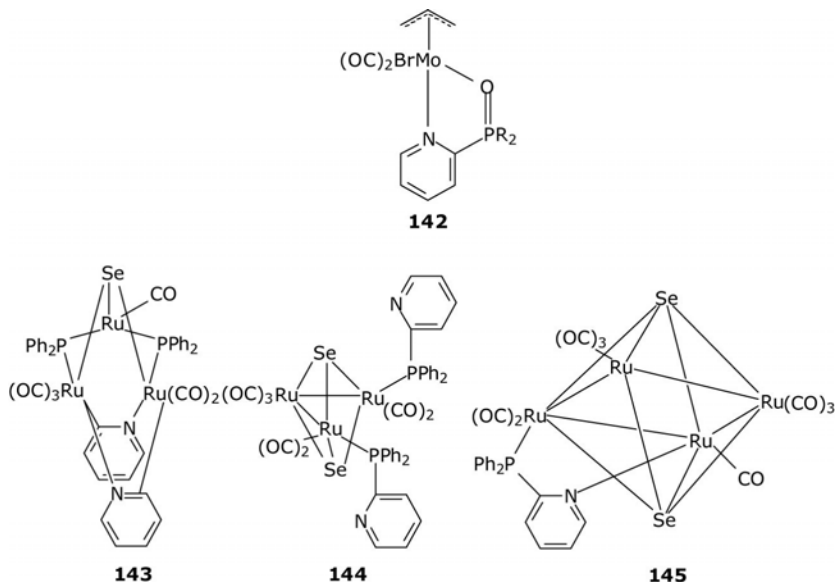


[Pd(C₆F₅)Br(4,4'-Me₂-bipy)] undergoes substitution of bromide by PPh (C₅H₄N)₂ or P(C₅H₄N)₃ with silver tetrafluoroborate to yield cationic **137** (R = Ph, C₅H₄N) (**06IC6628**). The products are good nitrogen-donor ligands and with dimers [(η⁴-LL)Rh(μ-Cl)]₂ and silver tetrafluoroborate, heterodinuclear **138** (R = Ph, C₅H₄N; LL = cod, tfb) follow. P(C₅H₄N)_nPh_{3-n} (*n* = 2, 3) with (NBu₄-*n*)[Pt(C₆F₅)₃(THT)] give the P-coordinated (N-Bu₄-*n*)₄[Pt(C₆F₅)₃(η¹(P)-L)] (**04IC189**). The products serve as *N,N*-ligands for [Rh(CO)₂(μ-Cl)]₂ and [(η⁴-diolefin)Rh(μ-Cl)]₂ (diolefin = cod, *n* = 2; nbd, *n* = 2, 3) to yield bridging **139** (R = Ph, C₅H₄N) with separation of charge as in zwitterionic complexes. Neutral gold(I) **140** (R = Ph, C₅H₄N) are similar ligands for rhodium(I) when heterodinuclear **141** (R = Ph, py; LL = cod, tfb) are formed in the presence of AgBF₄.



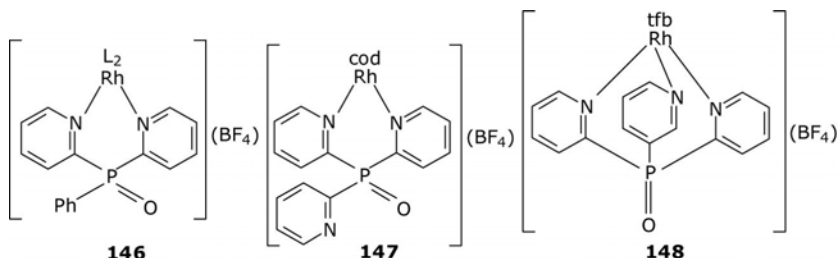
5. PYRIDYLPHOSPHINOXIDES (SELENIDES)

$\text{Ph}_2(2\text{-C}_5\text{H}_4\text{N})\text{P}(\text{O})$, $\text{Ph}_2(2\text{-C}_5\text{H}_4\text{N})_2\text{P}(\text{O})$, and $(2\text{-C}_5\text{H}_4\text{N})_3\text{P}(\text{O})$ with $[(\eta^3\text{-allyl})\text{Mo}(\text{CO})_2\text{Br}(\text{AN})_2]$ give N,O-coordinated **142** ($\text{R}^1 = \text{Ph}$, $\text{R}^2 = \text{C}_5\text{H}_4\text{N}$; $\text{R}^1 = \text{R}^2 = \text{C}_5\text{H}_4\text{N}$) ([00EJI1031](#)). $\text{Ph}_2(2\text{-C}_5\text{H}_4\text{N})\text{P}(\text{Se})$ with $[\text{Ru}_3(\text{CO})_{12}]$ gives the mixture **143–145**, where the ligand is destroyed ([01EJI721](#)). In **143**, it is split into a selenium elemental bridge, pyridine, and pyridyl bridges, as well as two diphenylphosphino bridges. Clusters **144** and **145** are formed by selenium bridges and P-coordinated diphenylphosphinopyridine ligands, the latter formed in the presence of Me_3NO . $\text{Ph}_2(2\text{-C}_5\text{H}_4\text{N})\text{PSe}$ and $[\text{Pt}(\text{Fe}(\text{CO})_3)(\text{NO})_2(\text{PhCN})_2]$ similarly give $[(\text{OC})_3\text{Fe}(\mu_3\text{-Se})[\text{Pt}(\text{CO})\text{P}(2\text{-C}_5\text{H}_4\text{N})\text{Ph}_2)_2]$ ([02ICA\(330\)95](#)). $[\text{Pd}(\text{C}_6\text{F}_5)\text{Br}(\text{C}_5\text{H}_4\text{N}-2\text{-P}(\text{S})\text{Ph}_2)]$ contains the S,N-chelating ligand; $[\text{Pd}(\text{C}_6\text{F}_5)\text{X}(\text{C}_5\text{H}_4\text{N}-2\text{-P}(\text{S})\text{Ph})]$ ($\text{X} = \text{Cl}, \text{Br}, \text{I}$), and $[\text{Pd}(\text{C}_6\text{F}_5)\text{Br}(\text{C}_5\text{H}_4\text{N}-2\text{-P}(\text{S})\text{Ph})]$ are represented by N,N- and N,S-bonded isomers ([95OM3058](#)). $[\text{M}(\text{C}_6\text{F}_5)\text{X}(\text{OP}(\text{C}_5\text{H}_4)_n\text{Ph}_{3-n})]$ ($\text{M} = \text{Pd}, \text{Pt}$; $\text{X} = \text{C}_6\text{F}_5, \text{Cl}, \text{Br}, \text{I}$; $n = 1\text{--}3$) contain N,N-chelating ligands ([97OM770](#)). $[\text{K}(\text{Et}_2\text{O})][\text{L}]$ ($\text{L} = \text{bis}(2,6\text{-diphenylphosphino-sulfido-3,5-diphenyl})\text{pyridine}$) with $[(\eta^5\text{-Cp}^*)\text{U}(\text{BH}_4)_3]$ or $[(\eta^8\text{-COT})\text{U}(\text{BH}_4)_2(\text{THF})]$ in THF gives substitution products $[(\eta^5\text{-Cp}^*)\text{U}(\text{BH}_4)_2(\eta^2(\text{S,S})\text{-L})]$ and $[(\eta^8\text{-COT})\text{U}(\text{BH}_4)(\eta^2(\text{S,S})\text{-L})]$, respectively ([08OM4158](#)).

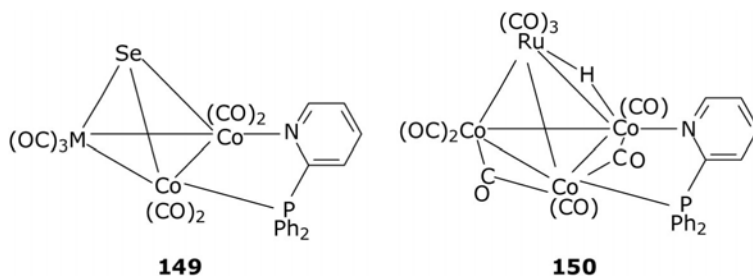


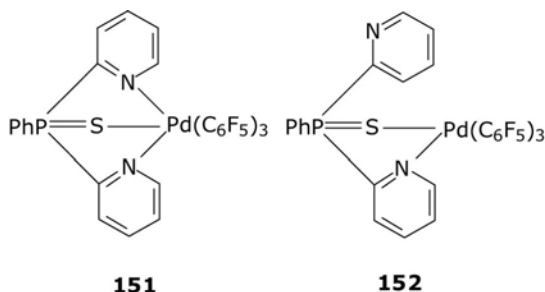
OPPy_2Ph with $[(\eta^4\text{-L}_2)\text{Rh}(\mu\text{-Cl})_2]$ in the presence of TlBF_4 gives **146** ($\text{L}_2 = \text{cod}, \text{tfb}$) ([01EJI289](#)). Bubbling carbon monoxide through a dichloromethane solution of **146** ($\text{L}_2 = \text{cod}$) gives dicarbonyl $[(\eta^2(\text{N,N})\text{-L})\text{Rh}(\text{CO})_2](\text{BF}_4)$. In contrast, the ligand with $[\text{Rh}(\mu\text{-Cl})(\text{CO})_2]_2$ gives neutral $[(\eta^2(\text{N},$

N)-L)Rh(CO)₂Cl]. OPPy₃ reacts differently with $[(\eta^4\text{-cod})\text{Rh}(\mu\text{-Cl})_2]$ and $[(\eta^4\text{-tfb})\text{Rh}(\mu\text{-Cl})_2]$ giving $\eta^2(N,N)$ -mode **147** in the first case and $\eta^3(N,N,N)$ **148** mode in the second instance. Carbonylation of both complexes gives a mixture of $[(\eta^2(N,N)\text{-L})\text{Rh}(\text{CO})_2](\text{BF}_4)$ and $[(\eta^3(N,N,N)\text{-L})\text{Rh}(\text{CO})_2](\text{BF}_4)$ in solution and further $[(\eta^3(N,N,N)\text{-L})\text{Rh}(\mu\text{-CO})_3\text{Rh}(\eta^3(N,N,N)\text{-L})](\text{BF}_4)_2$ in the solid state.



$\text{Ph}_2(2\text{-C}_5\text{H}_4\text{N})\text{PSe}$ with $[\text{HRuCo}_3(\text{CO})_{12}]$ gives two types of clusters, both with cleavage of the $\text{P}=\text{Se}$ bond (**02IC1372**). In the first, **149** ($\text{M} = \text{Ru}$), selenium plays the role of a bridge and pyridylphosphine moiety forms a chelate unit. In the second, **150**, a substituted tetranuclear hydride is formed, also containing a P,N -chelate and two bridging carbon monoxide ligands. For the iron analog, only the Se -bridged **149** ($\text{M} = \text{Fe}$) follows. The same phosphinoselenide reacts with $(\text{NEt}_4)[\text{RuCo}_3(\text{CO})_{12}]$ in the presence of Me_3NO and further with $[\text{Au}(\text{PPh}_3)\text{Cl}]$ and thallium hexafluorophosphate to yield $[(\text{Ph}_3\text{P})\text{AuRuCo}_3(\text{CO})_8(\mu\text{-CO})_3(\eta^4(\text{P})\text{-L})]$ where L is the P -coordinated 2-diphenylphosphinopyridine, so that the $\text{P}=\text{Se}$ bond is again split. Similar trends are observed for $[\text{MR}_2\text{L}_2]$ ($\text{M} = \text{Pd}, \text{Pt}$; $\text{R} = 3,5\text{-C}_6\text{Cl}_2\text{F}_3$, $\text{L}_2 = \text{OPC}_5\text{H}_4\text{NPh}_2$, $\text{SPC}_5\text{H}_4\text{NPh}_2$, $\text{OP}(\text{C}_5\text{H}_4\text{N})_2\text{Ph}$, $\text{OP}(\text{C}_5\text{H}_4\text{N})\text{Ph}$ ($\text{NHTol-}p$), $p\text{-TolNP}(\text{C}_5\text{H}_4\text{N})_2\text{Ph}$) prepared from $\text{cis-}[\text{MR}_2(\text{THF})_2]$ (**98EJ1745**). $[\text{PdR}_2(\text{SPPy}_n\text{Ph}_{3-n})]$ ($n = 1$, $\text{R} = \text{C}_6\text{F}_5$; $n = 2$, $\text{R} = \text{C}_6\text{F}_5$, $\text{C}_6\text{F}_3\text{Cl}_2$; $n = 3$, $\text{R} = \text{C}_6\text{F}_5$) are characterized by the N,N,S - and N,S -isomers being in slow equilibrium in solution, for example, **151** and **152** (**97IC5428**).

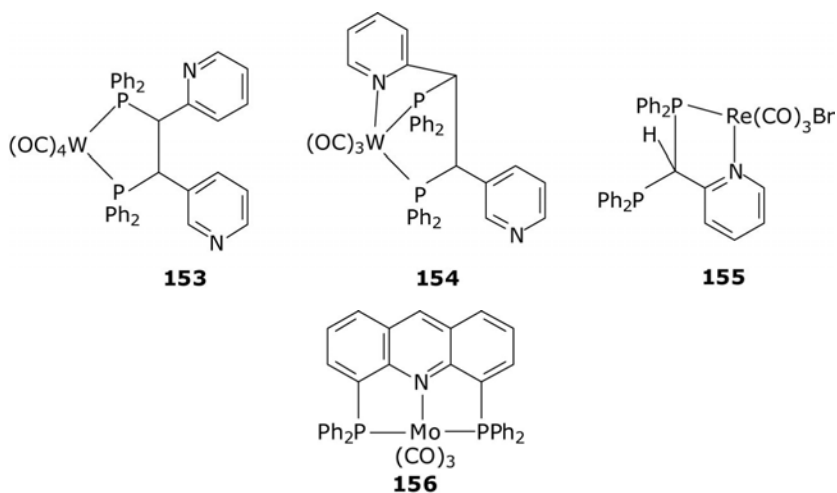




6. PYRIDYLPHOSPHINOALKANE LIGANDS

6.1 Early transition metals

1,2-Di(2-pyridyl)-1,2-bis(diphenylphosphino)ethane (L) with $[\text{Mo}(\text{CO})_4(\text{piperidine})_2]$ gives $[\text{Mo}(\text{CO})_4(\eta^2(\text{P,P})\text{-L})]$ (**99JOM(577)305**). 2-Diphenylphosphinomethylpyridine with $[(\eta^4\text{-nbd})\text{Mo}(\text{CO})_4]$ gives $[\text{Mo}(\text{CO})_4(\eta^2(\text{N,P})\text{-L})]$ (**89ZAAC74**). With $[(\eta^3\text{-C}_3\text{H}_5)\text{Mo}(\text{CO})_2(\text{AN})_2\text{Br}]$, the product is $[(\eta^3\text{-C}_3\text{H}_5)(\eta^2(\text{N,P})\text{-L})\text{Mo}(\text{CO})_2\text{Br}]$. 1,2-Di(2-pyridyl)-1,2-bis(diphenylphosphino)ethane with $[\text{W}(\text{CO})_4(\text{piperidine})_2]$ give P-coordinated **153** (**98ICC309**, **99JOM(577)305**). Thermolysis allows **153** to transform into the P,N,P-coordinated **154**. 2-(Bis(diphenylphosphino)methyl)pyridine with $[\text{Re}_2(\text{CO})_8(\mu\text{-H})(\mu\text{-CH=CHBu-}n)]$ in methylene chloride provides $[\text{Re}_2(\eta^2(\text{P,P})\text{-L})(\text{CO})_8]$ where each rhenium site is coordinated *via* two phosphorus atoms of the same ligand and the pyridyl group is switched off coordination (**89OM391**). Thermal decarbonylation of the product in toluene gives $[\text{Re}_2(\mu\text{-PPh}_2)(\mu\text{-}\eta^1, \eta^2\text{-CHPPh}_2\text{C}_5\text{H}_4\text{N})(\text{CO})_7]$ with P–C bond activation where the heterocyclic ligand is $\eta^2(\text{N,P})$ -coordinated to one rhenium center and $\eta^1(\text{C})$ -coordinated to another using its methine carbon atom. Thus the P–C bond cleavage is accompanied by the oxidative addition *via* the Re–Re bond, which also splits and is not present in the final product. 2-Pyridylbis(diphenylphosphino)methane with $[\text{Re}(\text{CO})_3\text{Br}(\text{AN})_2]$ gives N,P-coordinated **155** (**01IC1962**). A similar product follows from $[\text{Fe}(\text{CO})_4(\eta^2\text{-MA})]$, formulated as $[\text{Fe}(\text{CO})_2(\eta^2\text{-MA})(\eta^2(\text{N,P})\text{-L})]$ together with $[\text{Fe}(\text{CO})_3(\eta^2(\text{P,P})\text{-L})]$ when the pyridine ring is excluded from coordination. The product of interaction of the ligand with $[\text{Cr}(\text{CO})_3(\eta^6\text{-C}_7\text{H}_8)]$ results in substitution of cycloheptatriene by the N,P,P-coordinated ligand, $[\text{Cr}(\text{CO})_3(\eta^3(\text{N,P,P})\text{-L})]$. 4,5-Diphenylphosphinoacridine with $[\text{Mo}(\text{CO})_4(\text{nbd})]$ yields chelate **156** (**98TL813**).

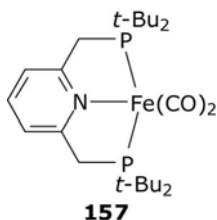


6.2 Iron group

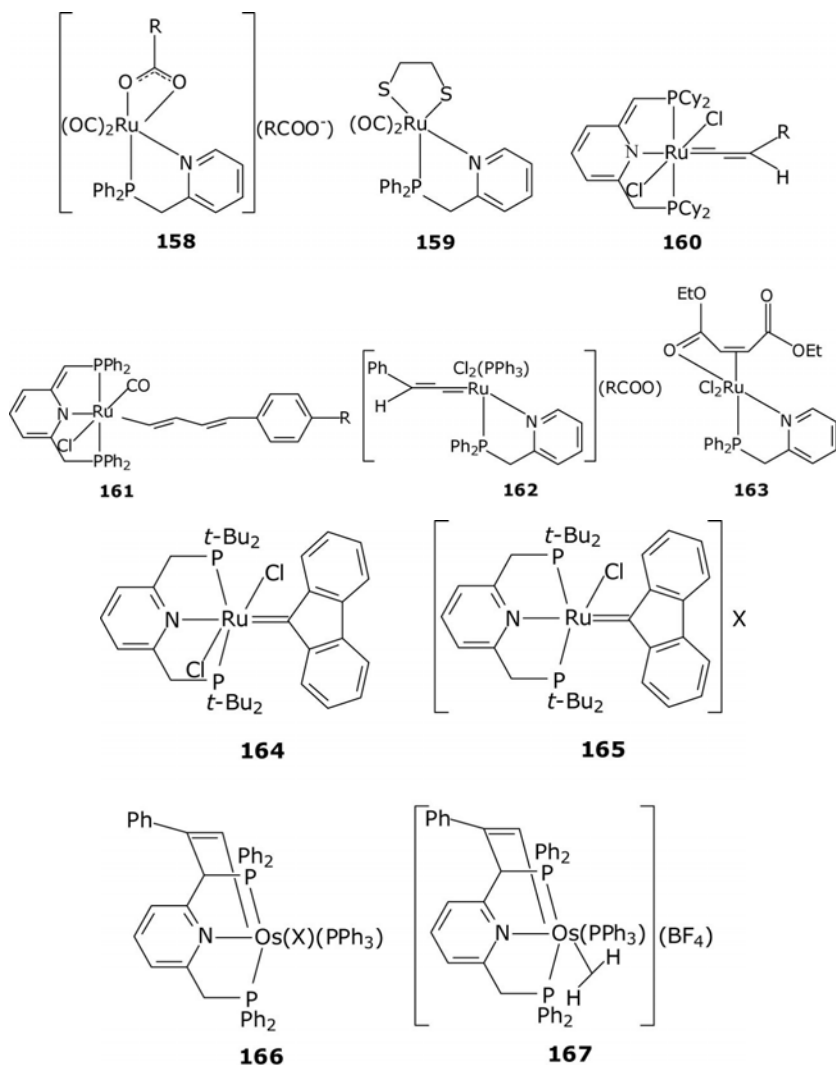
2,6-Bis-(di-*t*-butylphosphinomethyl)pyridine and 2-(di-*t*-butylphosphinomethyl)-6-diethylaminomethylpyridine reveal various reactivity patterns in the process of complexation. In particular, dearomatization of the pyridine ring followed by deprotonation of one of the P-containing groups may occur. Dearomatization may extend to the second arm of the starting ligands, which may have further implications in homogeneous catalytic reactions. These include addition of amines to acrylic acid derivatives (01OM1960). The role of dearomatization of 2,6-bis(dimethylphosphinomethyl)pyridine in the ruthenium(II) carbonyl species was assessed theoretically for the decomposition of water (09JA13584).

Photochemical reaction of 2-diphenylphosphinomethylpyridine with [Fe(CO)₅] gives the P-coordinated [Fe(CO)₄(η¹(P)-L)] and then *trans*-[Fe(CO)₃(η¹(P)-L)₂]. In both cases, L is bonded *via* the phosphorus atom only. Prolonged irradiation affords chelated tricarbonyl [Fe(CO)₃(η²(N,P)-L)]. [(η³-P,N,P)-L]FeCl₂ under carbon monoxide gives [(η³(P,N,P)-L)Fe(CO)₂] (L = 2,6-di-*i*-propylphosphinomethylpyridine (06IC7252). 2,6-Di-*t*-butylphosphinomethylpyridine (L) product [Fe(L)(CO)₂] **157** is close to square pyramidal (08OM5759, 09CEJ5491). Treatment of 2,6-(Ph₂PCH₂)₂C₅H₃N with [Ru(H)Cl(CO)(PPh₃)₃] in benzene produces [Ru(H)Cl(CO)(η³(P,N,P)-L)] (97OM3941). With HBF₄·Et₂O the molecular dihydrogen complex [Ru(Cl)(η²-H₂)(CO)(η³(P,N,P)-L)]

(BF₄) results. 2,6-Bis(diphenylphosphino-methyl)pyridine with Na₂[OsCl₆]·6H₂O and formaldehyde gives [Os(η³(P,N,P)-L)Cl₂(CO)] (96JNS230).

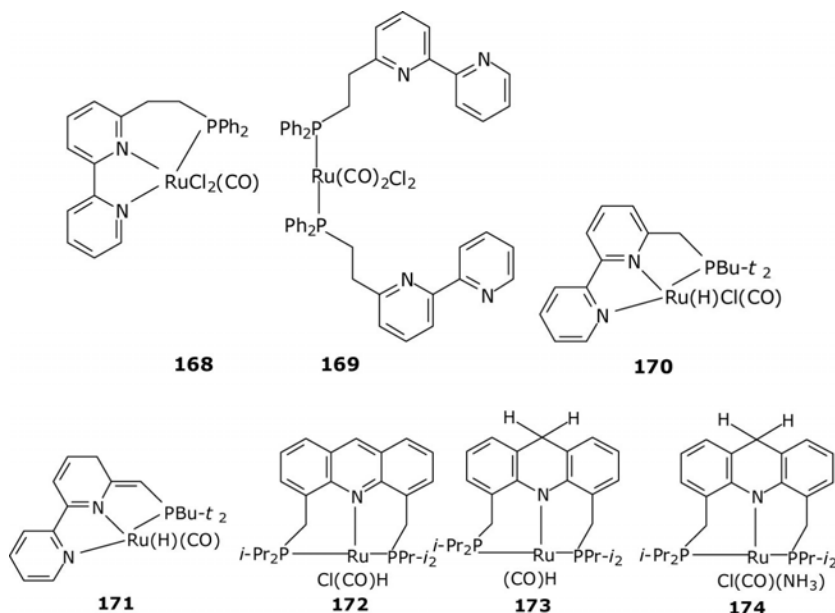


PPh₂CH₂C₅H₄N with [Ru₃(CO)₁₂] and RCOOH (R = H, Me) gives bis-chelate **158** (06ICA745). The carboxylate bridge can be displaced by HS (CH₂)₂SH to give neutral bis-chelate **159**. 2,6-Dicyclohexyl-phosphino-methylpyridine forms [Ru(η³(P,N,P)-L)Cl₂(AN)], which reacts with terminal alkynes to give vinylidenes **160** (R = *p*-MeOC₆H₄, *p*-Tol, Ph, *p*-BrC₆H₄, *t*-Bu, Fc), perhaps, through the stage of the η²-coordinated alkyne (02OM3285). 2,6-Diphenylphosphinomethylpyridine with [Ru(CO)₂(PPh₃)₂(-CH=CHCH=CHC₆H₄R-4)] (R = NO₂, NMe₂, OMe) gives **161** (R = NO₂, NMe₂, OMe) possessing NLO properties (07OM196). [Ru(η²(N,P)-L)Cl₂(PPh₃)] (L = 2-diphenylphosphinomethyl-6-methylpyridine) with phenylacetylene produces vinylidenes **162** (08OM1193). With ethyl diazoacetate, a less-common η²-alkene-η¹-O **163** results. 2-Diphenylphosphinopyridine with [(η⁶-C₆Me₆)Ru(μ-Cl)Cl]₂ in methylene chloride gives [(η⁶-C₆Me₆)Ru(η¹(P)-L)Cl₂] (04POL3115). In methanol, in the presence of ammonium tetrafluoroborate, [(η⁶-C₆Me₆)Ru(η²(P,N)-L)Cl](BF₄) is formed. With 1,1-diphenyl-2-propyn-1-ol, the product is [(η⁶-C₆Me₆)Ru(η²(P,N)-L)(C≡C=CPh₂)](BF₄)₂. RuCl₂(PPh₃)₃ when treated with 9-diazafluorene followed by 2-di-*t*-butylphosphinomethylpyridine gives Ru(II) carbene **164** (08OM3526). With silver tetrafluoroborate in THF, the product forms cationic Ru(II) fluorenylidene **165** (X = BF₄). Thermolysis of **164** gives **165** (X = Cl). [OsCl₂(PPh₃)(η³-P,N,P-L)] (L = 2,6-(Ph₂PCH₂)₂C₅H₃N) and with PhC≡CLi in THF it gives the alkynyl insertion product **166** (X = Cl) (01OM667). The product reacts with molecular hydrogen in the presence of potassium carbonate and sodium tetrafluoroborate in methanol and is converted to alkenyl-hydride **166** (X = H) and further under protonation using HBF₄·Et₂O in methylene chloride to molecular dihydrogen **167**.



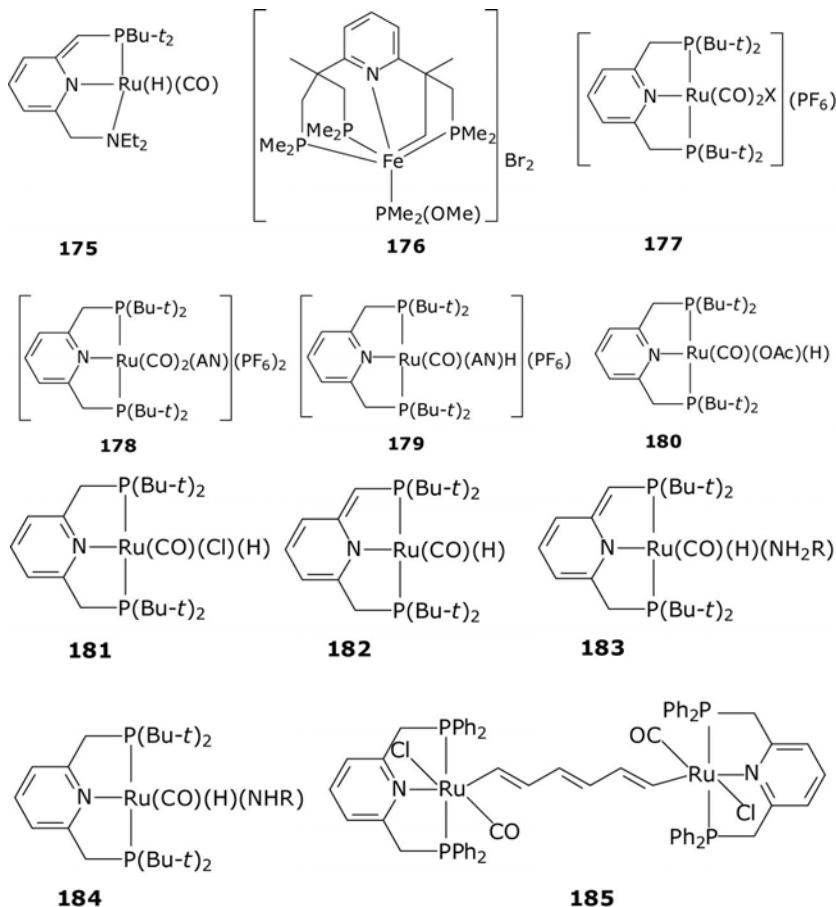
6-(Diphenylphosphinoethyl)-2,2'-bipyridine with $[\text{Ru}(\text{CO})_2\text{Cl}_2]_n$ in the presence of triethylamine in methanol gives mononuclear chelate **168** (97JCS(D)3777), while in the absence of NEt_3 the product is mononuclear **169**. 6-Di-*t*-butylphosphinomethyl-2,2'-bipyridine with $[\text{Ru}(\text{H})\text{Cl}(\text{PPh}_3)_3(\text{CO})]$ in THF yields the hydrido chloride pincer **170** (10JA16756). It can be deprotonated using potassium *t*-butylate affording dearomatized and coordinatively unsaturated **171**, catalytically active for hydrogenation of amides to amines. The 4,5-bis-(di-*i*-propylphosphinomethyl)acridine

ruthenium **172** is a catalyst for transformation of primary alcohols to acetals (09AGE8832, 09CCC72, 09JA3146, 10TC915). Hydrogenation of the product in the presence of potassium hydroxide in toluene gives **173**, where the central ring of acridine is dearomatized (10JA14763). The same reaction course is taken by ammonia when dearomatized **174** results.



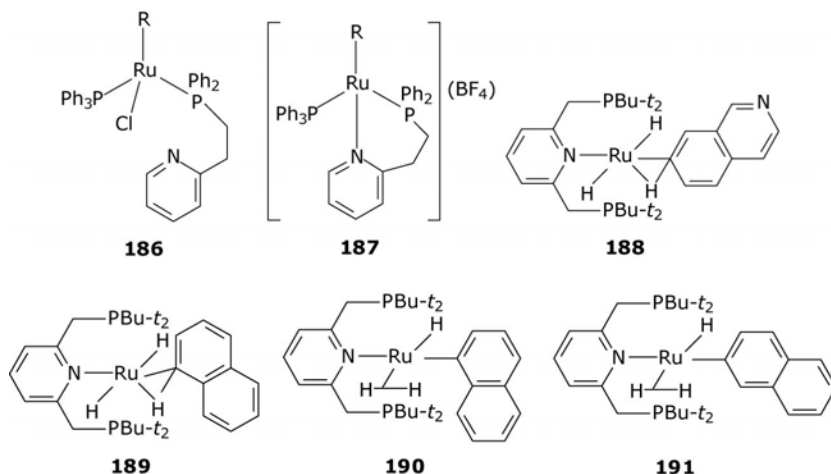
The electron-rich tridentate PNP ligand with [Ru(H)Cl(PPh₃)₃(CO)] gives pincer **175**, attractive as a catalyst in the synthesis of primary amines from alcohols and ammonia (08AGE8661). It is a potential photocatalytic system for solar hydrogen production from water, for which the detailed mechanism was proposed on the basis of DFT calculations (10JA120). The carbon–phosphorus bond cleavage of the pyridine tetraphosphine ligand C₅H₃N(CMe(CH₂PMe₂)₂)₂ occurs on interaction of anhydrous ferric bromide in methanol followed by cyclometalated iron(III) **176** (06JCS(D)5583). 2,6-Bis(di-*t*-butylphosphinomethyl)pyridine with [Ru(CO)₂Cl₂]_{*n*} in the presence of ammonium hexafluorophosphate gives cationic **177** (X = Cl) (04OM2510). Treatment of the product with silver tetrafluoroborate, acetonitrile, and finally ammonium hexafluorophosphate gives dicationic **178**. Under water, **177** (X = Cl) gives not the aqua-, but hydroxo-complex **177** (X = OH), and under potassium hydroxide, the monocationic hydride **179**. 2,6-Bis(di-*t*-butylphosphinomethyl) pyridine with [Ru₂(OAc)₄] in methanol gives **180** (04OM4026). 2,6-Bis(di-*t*-butylphosphinomethyl)pyridine with [Ru(H)Cl(CO)(PPh₃)₃] forms the hydridochloride **181** and after deprotonation with KOBu-*t* – dearomatized **182** active in direct synthesis

of imines from alcohols and amines (10AGE1468) and hydrogenation of esters (06AGE1113). It N–H activates a series of anilines RNH_2 ($\text{R} = p\text{-NO}_2\text{-C}_6\text{H}_4$, $p\text{-NO}_2\text{-}o\text{-Cl-C}_6\text{H}_3$, $o\text{-Br-C}_6\text{H}_4$, $m\text{-Cl-}p\text{-Cl-C}_6\text{H}_3$), the process occurring in two steps: coordination of an aniline derivative **183** and N–H activation accompanied by activation of the pyridine ring **184** (10JA8542). 2,6-Bis(diphenylphosphino-methyl)pyridine with $[\text{Ru}(\text{Cl})(\text{CO})(\text{PPh}_3)_2]_2(\mu\text{-CH=CHCH=CHCH=CH})$ gives six-coordinated dinuclear **185** (03OM737).



2-(2-Diphenylphosphinoethyl)pyridine with $[(\eta^5\text{-Cp})\text{Ru}(\text{PPh}_3)_2\text{Cl}]$ in benzene yields P-coordinated neutral **186** ($\text{R} = \eta^5\text{-Cp}$), but if the reaction is conducted in methanol containing ammonium tetrafluoroborate, the result is cationic chelate **187** ($\text{R} = \eta^5\text{-Cp}$) (10EJI704). The same ligand with $[(\eta^6\text{-arene})\text{Ru}(\mu\text{-Cl})\text{Cl}]_2$ ($\eta^6\text{-arene} = \text{C}_6\text{H}_6$, $\text{C}_{10}\text{H}_{14}$, and C_6Me_6) in methylene chloride gives **186** ($\text{R} = \eta^6\text{-arene}$) and the products with ammonium

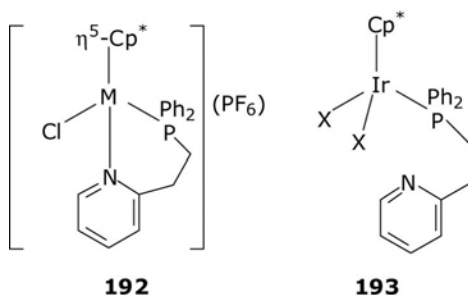
hexafluorophosphate in methanol give **187** ($R = \eta^6\text{-arene}$, PF_6 instead of BF_4). In the process of catalytic H/D exchange by inorganic $[(\eta^3\text{-P,N,P})\text{-L})\text{Ru}(\eta^2\text{-H}_2)(\text{H})]$ ($L = 2\text{-di-}t\text{-butylphosphinomethylpyridine}$) for isoquinoline and naphthalene, formation of the organometallic intermediates, **188–191**, was postulated (08EJ13493). The same type of behavior was proposed for benzene and toluene (07AGE2269). $[\text{Ru}(\eta^2(\text{N,P})\text{-L})\text{X}_2]$ ($L = 1\text{-(diphenylphosphino)-2-(2-pyridyl)ethane}$; $X = \text{Cl, Br, I}$) with carbon monoxide give $[\text{Ru}(\eta^1(\text{P})\text{-L})_2(\text{CO})\text{X}_2]$ with the cleavage of the ruthenium–nitrogen bond (93JCS(D)3001). $[\text{OsX}_2(\eta^2(\text{P,N})\text{-L})_2]$ ($L = 1\text{-(diphenylphosphino)-2-(2-pyridyl)ethane}$; $X = \text{Cl, Br}$) with carbon monoxide yields $[\text{OsX}_2(\text{CO})(\eta^1(\text{P})\text{-L})(\eta^2(\text{P,N})\text{-L})]$ or $[\text{Os}(\text{X})(\text{CO})(\eta^2(\text{P,N})\text{-L})_2]^+$ depending on the nature of the solvent (94JCS(D)2257). $[\text{Ru}(\eta^2(\text{N,P})\text{-L})_2(\text{AN})_2](\text{PF}_6)_2$ ($L = 1\text{-(diphenylphosphino)-2-(2-pyridyl)ethane}$) under a CO atmosphere in methylene chloride or acetone gives the monocarbonyl $[\text{Ru}(\eta^2(\text{N,P})\text{-L})_2(\text{AN})(\text{CO})](\text{PF}_6)_2$ (00ICA(299)180).



6.3 Cobalt group

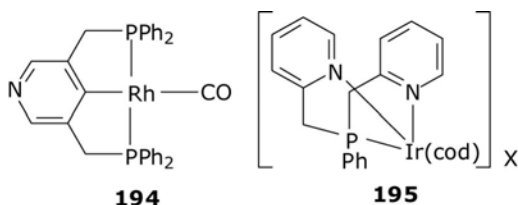
With $[(\eta^5\text{-Cp}^*)\text{M}(\mu\text{-Cl})\text{Cl}]_2$ ($M = \text{Rh}$ or Ir) and NH_4PF_6 , chelates **192** ($M = \text{Rh, Ir}$) follow (10EJ1704). The iridium chelates **192** ($M = \text{Ir}$) with excess sodium chloride or sodium azide give the neutral P-coordinated **193** ($X = \text{Cl, N}_3$). $[(\eta^3\text{-P,N,P,L})\text{Rh}(\text{OTf})]$ ($L = 2\text{-di-}t\text{-butylphosphinomethylpyridine}$) enters transmetalation with dimethyl zinc, which first gives $[(\eta^3\text{-P,N,P,L})\text{Rh}(\text{Me})\text{Zn}(\text{Me})(\text{OTf})]$ and then on interaction with 2,2'-bipyridine $[(\eta^3\text{-P,N,P,L})\text{Rh}(\text{Me})]$ (08OM1454). With diphenyl zinc, in a similar way $[(\eta^3\text{-P,N,P,L})\text{Rh}(\text{Ph})]$ can be prepared. Complexes of 2-diphenylphosphinomethylpyridine (L), $[\text{Rh}(\eta^3(\text{P,N,P})\text{-L})\text{R}]$ ($R = \text{Me, Ph}$) oxidatively add molecular iodine to yield $[\text{Rh}(\eta^3(\text{P,N,P})\text{-L})(\text{R})(\text{I})_2]$ and

methyl iodide to afford $[\text{Rh}(\eta^3(\text{P},\text{N},\text{P})\text{-L})(\text{R})(\text{Me})\text{I}]$ (99EJ1435). The latter reductively eliminate hydrocarbons RMe on reaction with thallium hexafluorophosphate in acetone. The complex of 2,6-di-*t*-butylphosphinomethylpyridine (L) $[(\eta^3(\text{P},\text{N},\text{P})\text{-L})\text{Rh}(\text{CN})]$ oxidatively adds methyl iodide to afford rhodium(III) $[(\eta^3(\text{P},\text{N},\text{P})\text{-L})\text{Rh}(\text{CN})(\text{Me})\text{I}]\text{I}$ (08JA14374). In aprotic solvents, methyl isonitrile rhodium(I) $[(\eta^3(\text{P},\text{N},\text{P})\text{-L})\text{Rh}(\text{CNMe})]\text{I}$ follows. 2-Diphenylphosphinomethylpyridine with $[\text{Rh}(\text{Cl})(\mu\text{-CO})]_2$ and sodium tetrafluoroborate in ethanol gives $[\text{Rh}_2(\text{CO})(\mu\text{-L})_2](\text{BPh}_4)$ (83OM1246). $\text{C}_5\text{H}_3\text{N}(2,6\text{-CHRPPH}_2)$ ($\text{R} = \text{H}, \text{Me}$) and $\text{C}_5\text{H}_3\text{N}(2,6\text{-CH(R)OPPh}_2)$ ($\text{R} = \text{H}, \text{Me}$) with $[(\eta^4\text{-cod})\text{Ir}(\text{Cl})]_2$ and sodium perchlorate give iridium(I) $[(\eta^4\text{-cod})\text{Ir}(\eta^3(\text{P},\text{N},\text{P})\text{-L})](\text{ClO}_4)$ (96TL4617). In a similar fashion, $[(\eta^4\text{-nbd})\text{Rh}(\eta^3(\text{P},\text{N},\text{P})\text{-L})](\text{ClO}_4)$ can be prepared. Iridium species reveal high catalytic activity in hydrogenation of imines.

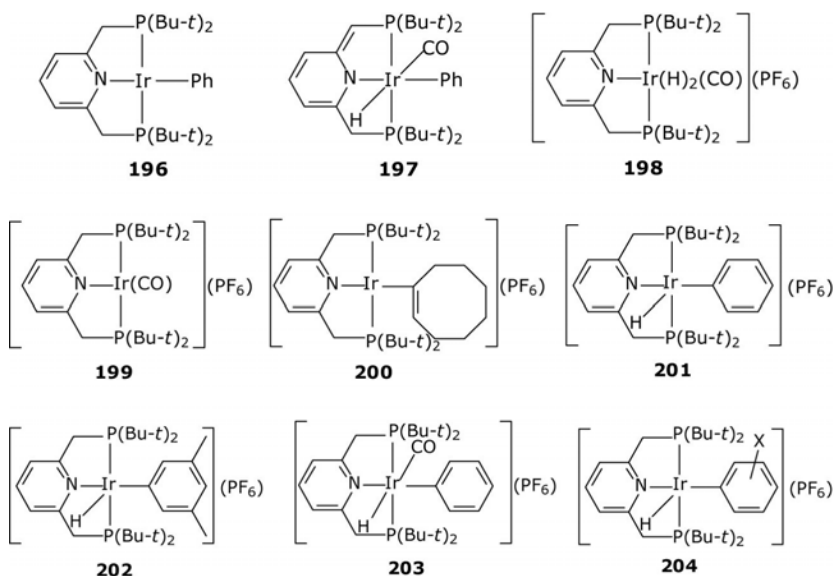


Diphosphine ligands $\text{Ph}_2\text{PCH}(2\text{-C}_5\text{H}_4\text{N})\text{CH}(2\text{-C}_5\text{H}_4\text{N})\text{PPh}_2$, $\text{Ph}_2\text{PCH}(\text{Ph})\text{CH}(\text{C}_5\text{H}_4\text{N}-2)\text{PPh}_2$ with $[(\eta^4\text{-cod})\text{Rh}(\mu\text{-Cl})]_2$ in methylene chloride in the presence of ammonium hexafluorophosphate give cationic $[(\eta^4\text{-cod})\text{Rh}(\eta^3(\text{P},\text{P},\text{N})\text{-L})](\text{PF}_6)$ (00JCS(D)975). 3,5-Bis((diphenylphosphino)methyl)pyridine with $[\text{Rh}(\text{H})(\text{PPh}_3)_4]$ in THF and further under CO in *n*-pentane gives the C,P,P-coordinated **194** with potential ligating ability (96IC1792). 1-(2-Pyridyl)-2-(diphenylphosphino)ethane with $[(\eta^4\text{-cod})\text{Ir}(\text{acetone})_2]^+$ gives $[(\eta^4\text{-cod})\text{Ir}(\eta^2(\text{P},\text{N})\text{-L})]^+$ (88IC325). $(\text{Ph}_2\text{P})_2\text{C}(\text{H})(\text{C}_5\text{H}_4\text{N})$ with $[(\eta^4\text{-nbd})\text{Rh}(\mu\text{-Cl})]_2$ in the presence of silver tetrafluoroborate yields $[(\eta^4\text{-nbd})\text{Rh}(\eta^2\text{-N},\text{P})\text{-L}](\text{BF}_4)$ (83IC2644). 2-(Bis(diphenylphosphino)methyl)pyridine forms dinuclear $[\text{Rh}_2(\text{CO})_2(\mu\text{-}(\eta^2(\text{N},\text{P})\text{-L}))_2](\text{PF}_6)_2$ and $[\text{Ir}(\mu\text{-CO})(\text{CO})_2(\mu\text{-}(\eta^2(\text{N},\text{P})\text{-L}))_2](\text{BF}_4)_2$ with an iridium-iridium bond (83IC3267). The iridium product readily evolves carbon monoxide and forms an analog of the rhodium complex. 1-(2-Pyridyl)-2-diphenylphosphino ethane with $[\text{Ir}(\text{CO})_2\text{Cl}_2]$ in 2-methoxyethanol gives four-coordinate $[\text{Ir}(\text{CO})\text{Cl}(\eta^2(\text{N},\text{P})\text{-L})]$ and $[\text{Ir}(\text{CO})\text{Cl}(\eta^1(\text{P})\text{-L})_2]$ (88IC1649). The latter with potassium hexafluorophosphate gives four-coordinate cationic $[\text{Ir}(\text{CO})(\eta^2(\text{N},\text{P})\text{-L})(\eta^1(\text{P})\text{-L})](\text{PF}_6)$, where each ligand is coordinated differently. 2,6-Bis(diphenylphosphinomethyl)pyridine with $[(\eta^2\text{-C}_2\text{H}_4)_2\text{Rh}(\text{solv})_2]\text{X}$ ($\text{solv} = \text{acetone}, \text{THF}; \text{X} = \text{BF}_4, \text{PF}_6, \text{OTf}$) under ethylene gives cationic rhodium(I) $[(\eta^2\text{-C}_2\text{H}_4)\text{Rh}(\eta^3(\text{P},\text{N},\text{P})\text{-L})]\text{X}$

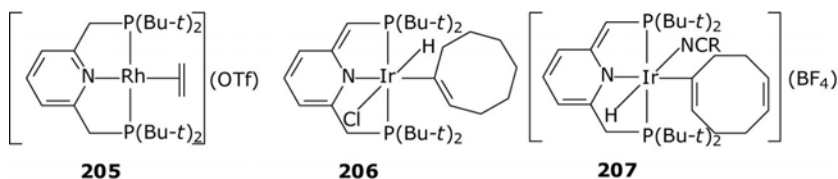
(97CB939, 98POL1183). $[(\eta^2\text{-C}_2\text{H}_4)\text{Rh}(\eta^3(\text{P,N,P})\text{-L})](\text{BF}_4)]$ ($\text{L} = 2,6\text{-bis}(\text{diphenylphosphinomethyl})\text{pyridine}$) with methyl or phenyl lithium produce $[\text{Rh}(\eta^3(\text{P,N,P})\text{-L})\text{R}]$ ($\text{R} = \text{Me}, \text{Ph}$) (98EJ11425). Under ethylene in THF the products give rhodium(I) $[(\eta^2\text{-C}_2\text{H}_4)\text{Rh}(\eta^3(\text{P,N,P})\text{-L})\text{(R)}]$. $[(^3(\text{P,N,P})\text{-L})\text{Rh}(\text{acetone})](\text{BF}_4)_2$ ($\text{L} = 2,6\text{-di-}t\text{-butylphosphinomethylpyridine}$) with carbon monoxide gives rhodium(I) $[(^3(\text{P,N,P})\text{-L})\text{Rh}(\text{CO})](\text{BF}_4)$ (07IC10479). $\text{P}(\text{CH}_2\text{CH}_2\text{C}_5\text{H}_4\text{N})_2\text{Ph}$ (L) with $[\text{Rh}(\text{CO})_2(\mu\text{-Cl})_2]_2$ gives $[\text{Rh}(\text{Cl})(\text{CO})(\eta^2(\text{P,N})\text{-L})]$ (00IC705). The product reacts with sodium iodide to yield the ligand-substituted $[\text{Rh}(\text{I})(\text{CO})(\eta^2(\text{P,N})\text{-L})]$ and with silver or thallium tetrafluoroborate to afford cationic dinuclear $[\text{Rh}_2(\text{CO})_2(\eta^2(\text{P,N})\text{-L})_2](\text{BF}_4)_2$. $\text{P}(\text{CH}_2\text{CH}_2\text{C}_5\text{H}_4\text{N})\text{Ph}_2$ and $\text{P}(\text{CH}_2\text{CH}_2\text{C}_5\text{H}_4\text{N})_2\text{Ph}$ (L) with $[(\eta^4\text{-diene})\text{Rh}(\mu\text{-Cl})_2]$ in the presence of thallium hexafluorophosphate or thallium or silver tetrafluoroborate give a series $[(\eta^4\text{-diene})\text{Rh}(\eta^2(\text{P,N})\text{-L})](\text{A})$ ($\text{L} = \text{P}(\text{CH}_2\text{CH}_2\text{C}_5\text{H}_4\text{N})\text{Ph}_2$, diene = tfb, $\text{A} = \text{PF}_6$, diene = cod, $\text{A} = \text{BF}_4$; $\text{L} = \text{P}(\text{CH}_2\text{CH}_2\text{C}_5\text{H}_4\text{N})_2\text{Ph}$, diene = nbd, tfb, $\text{A} = \text{PF}_6$; diene = cod, $\text{A} = \text{BF}_4$). (8-methyl-2-quinolylmethyl)di-*t*-butyl-phosphine $[\text{Rh}_2\text{Cl}_2(\text{CO})_3(\eta^2(\text{N,P})\text{-L})]$ contains the bidentate ligand (80JCS(D)1974). N,P,N-Bis(pyridine) phenylphosphine and $[(\eta^4\text{-cod})\text{Ir}(\mu\text{-Cl})_2]$ gives cationic **195** ($\text{X} = \text{Cl}$) (10JCS(D)2563). In the presence of NaBAR^{F} , the same reaction leads to **195** ($\text{X} = \text{BAR}^{\text{F}}$).



The product of activation of benzene **196** is oxidized under carbon monoxide to **197** where a proton has migrated from the ligand CH_2 group to the iridium site, followed by dearomatization of the ligand (06JA15390). $[\text{Ir}(\eta^3(\text{P,N,P})\text{-L})(\text{Ph})\text{H}](\text{PF}_6)$ ($\text{L} = 2,6\text{-bis}(\text{di-}t\text{-butylphosphinomethyl})\text{pyridine}$) when heated in methanol, reductively eliminates benzene and gives iridium(III) **198** (06OM3007, 09JCS(D)9433). The product in an atmosphere of hydrogen reductively eliminates molecular hydrogen and forms iridium(I) **199**. 2,6-Bis(*t*-butylphosphinomethyl)pyridine with $[(\eta^2\text{-COE})_2\text{Ir}(\text{I})(\text{acetone})_2](\text{PF}_6)$ gives cationic **200** (06OM3190). Thermolysis of **200** in benzene gives aryl hydride **201** and *m*-xylene-*m*-xylyl hydride **202**. Under carbon monoxide, **201** gives **203**, while under prolonged heating in anisole it gives **199**. In a similar fashion, starting from **200**, aryl halides **204** ($\text{X} = o\text{-F}, p\text{-F}, o\text{-}, m\text{-}, p\text{-Cl}, o\text{-}, m\text{-}, p\text{-Br}$) and anisoles **204** (*o*-, *m*-, *p*-MeO) can be prepared. The role of molecular hydrogen activation by $[\text{Ir}(\eta^3(\text{P,N,P})\text{-L})(\text{Ph})]$ ($\text{L} = 2,6\text{-bis}(\text{di-}t\text{-butylphosphinomethyl})\text{pyridine}$) consists in proton transfer from the CH_2 moiety to the metal center to yield an iridium(III) intermediate, followed by dearomatization of the ligand (09IC10257).

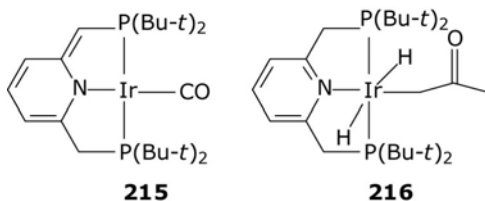
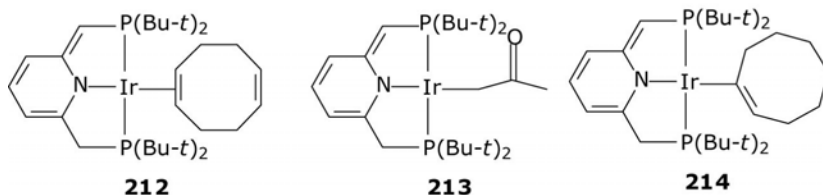
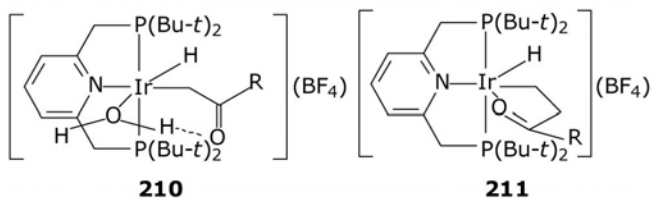
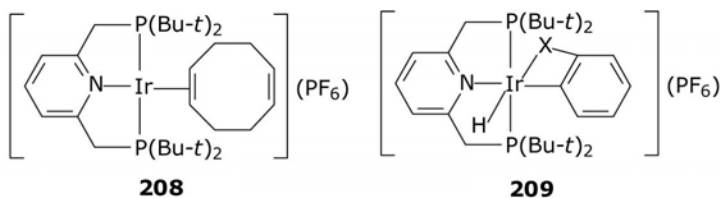


2,6-Di-*t*-butylphosphinomethylpyridine with $[(\eta^2\text{-C}_2\text{H}_4)_2\text{Rh(soln)}_2](\text{OTf})$ gives cationic **205** (02OM812). The same ligand with $[(\eta^2\text{-COE})\text{Ir}(\text{Cl})]_2$ reacts by insertion of iridium into the $\text{C}(\text{sp}^2)\text{-H}$ bond of cyclooctene to yield hydridovinyl **206**. A similar type of coordination is realized with $[(\eta^4\text{-cod})\text{Ir}(\text{RCN})_2](\text{BF}_4)$ ($\text{R} = \text{Me}, i\text{-Pr}, t\text{-Bu}$) where the products are C-H activated, **207** ($\text{R} = \text{Me}, i\text{-Pr}, t\text{-Bu}$). 2,6-Di-*t*-butylphosphinomethylpyridine with $[\eta^2\text{-COE}]_2\text{Rh}(\text{Cl})_2$ and silver triflate gives the rhodium(I) triflate $[(\eta^3(\text{P},\text{N},\text{P})\text{-L})\text{Rh}(\text{OTf})]$ (07AGE4736). The rhodium(I) methyl $[(\eta^3(\text{P},\text{N},\text{P})\text{-L})\text{Rh}(\text{Me})]$ can be prepared from the triflate and dimethyl zinc. When it was heated in benzene, phenyl $[(\eta^3(\text{P},\text{N},\text{P})\text{-L})\text{Rh}(\text{Ph})]$ followed.

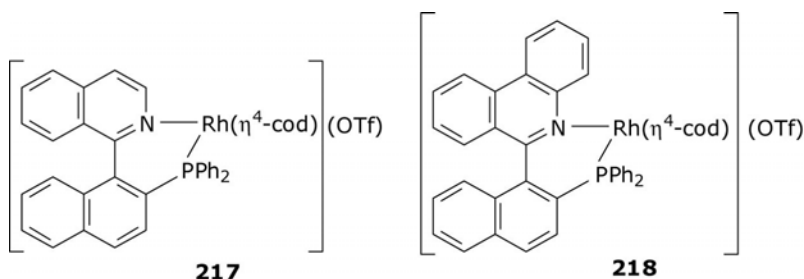


Cationic **208** in benzene gives the product of C-H activation **204** ($\text{X} = \text{H}$) (03JA4714). Heating **208** in fluorobenzene gives a mixture **204** ($\text{X} = o\text{-F}, m\text{-F}, p\text{-F}$). In contrast, chloro- and bromobenzene yield a mixture of products **204** ($\text{X} = m\text{-Cl}, m\text{-Br}, p\text{-Cl}, p\text{-Br}$) and **204** ($\text{X} = \text{Cl}, \text{Br}$) where the *o*-products **209** clearly predominate and become the sole products when thermolysis is conducted at higher temperature. The same starting complex **208** taken as a tetrafluoroborate salt is the source of C-H activation in ketones. Thus,

it reacts with acetone or 2-butanone and water at elevated temperatures to give ketonyl hydrides **210** (R = Me, Et) (06JA12400). However, **210** (R = Et) is not the only product but it co-exists with the product of β -C-H activation **211** (R = Me). The latter becomes a sole product, when the reaction is conducted in the absence of water, and 3-pentanone follows only this route to yield **211** (R = Et). Heating an acetone solution of nonaromatic **212** gives the product of C-H activation of acetone **213** along with the product of intramolecular C-H activation of COE **214** (10OM3817). Treatment of iridium(I) acetonyl **213** with CO results in elimination of acetone and formation of nonaromatic **215**. The reaction of **213** with molecular H_2 gives only the *trans*-dihydride acetonyl **216**. Heating **213** in cyclooctene results in the oxidative addition of cyclooctene followed by acetonyl group substitution yielding cyclooctenyl iridium(I) **212**. Likewise, in benzene the acetonyl moiety is replaced by a phenyl group to give **196**.

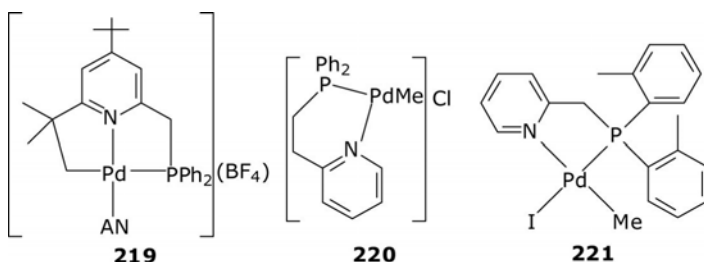


8-Diphenylphosphinoquinoline, similarly, affords $[(\eta^5\text{-Cp}^*)\text{Ir}(\text{N}_3)(\eta^2\text{-P,N-L})](\text{PF}_6)$. Rhodium(I) **217** derived from 1-(2-diphenylphosphino-1-naphthyl)isoquinoline is a catalyst for hydroboration of alkenes (93CC1673). Rhodium(I) **218** possesses much higher stereoselectivity (95T(A)2593). 8-Diphenylarsino- and 8-diphenylphosphinoquinoline (L) react with $[\text{Rh}(\text{CO})_2\text{Cl}_2]^-$ in ethanol-acetone to yield rhodium(II) $[\text{Rh}(\text{L})(\text{CO})(\mu\text{-Cl})_2]_2$ with rhodium-rhodium bonds (79IC1391). Cationic rhodium(I) complexes incorporating $\eta^2(\text{P,N})$ -coordinated 2-(1-menthoxy-diphenylphosphino)pyridine are the catalysts in hydroformylation (94CC2251) and those of 1-(2-diphenylphosphino-1-naphthyl)isoquinoline catalyze hydroboration (93CC1673). Similar rhodium and iridium complexes catalyze hydrosilylation (85CB3380).

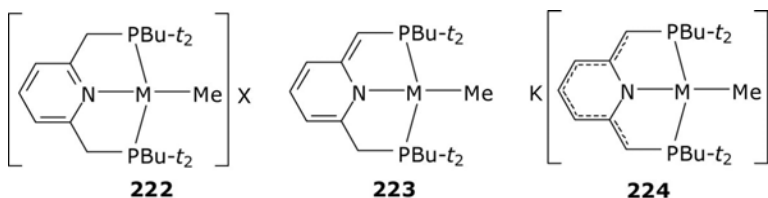


6.4 Nickel group

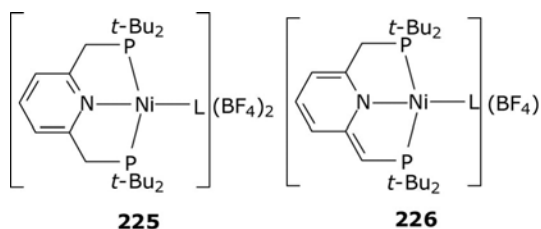
2,4-Di-*t*-butyl-6-methyldiphenylphosphinopyridine with $[(\eta^4\text{-cod})\text{Pd}(\text{Me})\text{Cl}]$ yields the chloro-bridged dipalladium $[(\eta^1(\text{P})\text{-L})\text{Pd}(\text{Me})(\mu\text{-Cl})]_2$ (03JCS(D)1419). Treatment of the latter with silver tetrafluoroborate in acetonitrile gives C–H activated **219**. Pyridine-phosphine ligands 2-aryl-6-(2-(diphenylphosphino)ethyl)pyridine (aryl = phenyl, 1-naphthyl, 9-phenanthryl, 9-anthracyl, and ferrocenyl) and 2-(2-(diarylphosphino)ethyl)pyridine form the basis of methyl palladium cationic, for example **220**, hardly active in oligomerization of ethylene (00CRV1169, 03CRV283, 05ACR784, 09OM3264, 09OM3272). 2-Bis(2-methylphenyl) phosphinomethylpyridine with $[\eta^4\text{-cod})\text{Pd}(\text{Cl})\text{Me}]$ and sodium iodide gives chelate **221** (02ZN(B)803). 2-Diphenylphosphinomethylpyridine, 2-(2-(diphenylphosphino)ethyl)pyridine, 2-(3-(diphenylphosphino)propyl)pyridine, 2-(2-(diphenylphosphino)phenyl)pyridine, 2-((1*S*,2*S*,3*R*,4*S*)-3-(diphenylphosphino)-1,7,7-trimethylbicyclo[2.2.1]hept-2-yl)pyridine with $[(\eta^4\text{-cod})\text{Pd}(\text{Me})\text{Cl}]$ give neutral $[\text{Pd}(\eta^2(\text{N,P})\text{-L})(\text{Me})(\text{Cl})]$ (09OM1180). On reaction with NaBAR^{F} and acetonitrile in methylene chloride cationic $[\text{Pd}(\eta^2(\text{N,P})\text{-L})(\text{Me})(\text{AN})](\text{BAR}^{\text{F}})$ result.

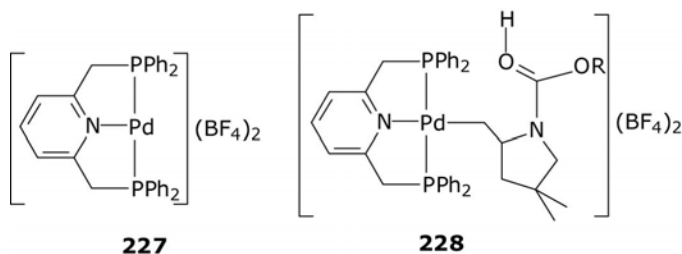


2,6-Di-*t*-butylphosphinomethylpyridine with $[(\eta^4\text{-cod})\text{M}(\text{Me})\text{Cl}]$ (M = Pd, Pt) in methylene chloride give cationic **222** (M = Pd, Pt; X = Cl) (10IC1615). Under *t*-BuOK or KN(SiMe₃)₂ in THF, dearomatization of the pincer ligand occurs in two steps to yield first neutral **223** (M = Pd, Pt) and then anionic **224** (M = Pd, Pt). In methanol at low temperatures neutral **223** (M = Pd, Pt) may be protonated to **222** (M = Pd, Pt; X = OMe), the process is reversible and deprotonation occurs at room temperature. Step-by-step double deprotonation was also observed for platinum **222** (M = Pt, X = Cl) by methyl lithium.



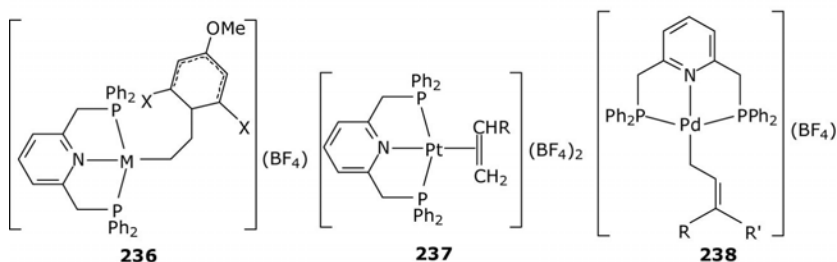
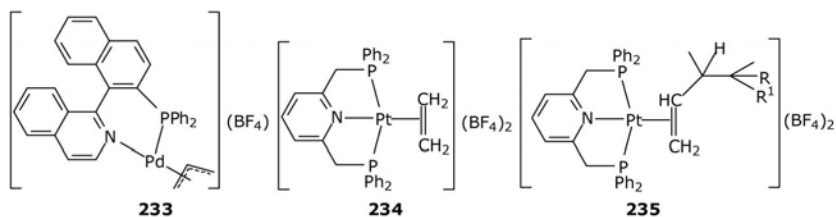
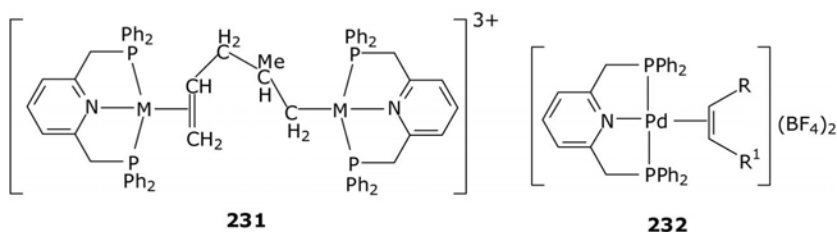
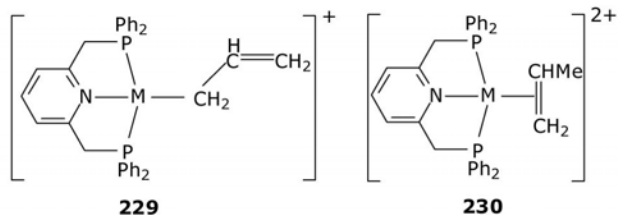
2,6-Di-*t*-butylphosphinomethylpyridine with [Ni(AN)₄](BF₄)₂ forms dicationic **225** (L = AN), which gives rise to a number of organometallic compounds (09JCS(D)1016). Thus, with *t*-butylisocyanide in acetonitrile, the product is **225** (L = CNBu-*t*). When the reaction is conducted in the presence of base NaN(SiMe₃)₂, deprotonation at the *ortho* position of a heteroring occurs, and **226** (L = CNBu-*t*) follows. The chloride precursor **226** (L = Cl) reacts with LiR (R = Me, Ph) to yield **226** (R = Me, Ph). Palladium dicationic **227** serves as a catalyst of hydroamination, forming intermediates of type **228** (R = Me, *p*-Tol, OBu-*t*, OCH₂Ph) (06JA4246, 08JA2786, 08OL793).



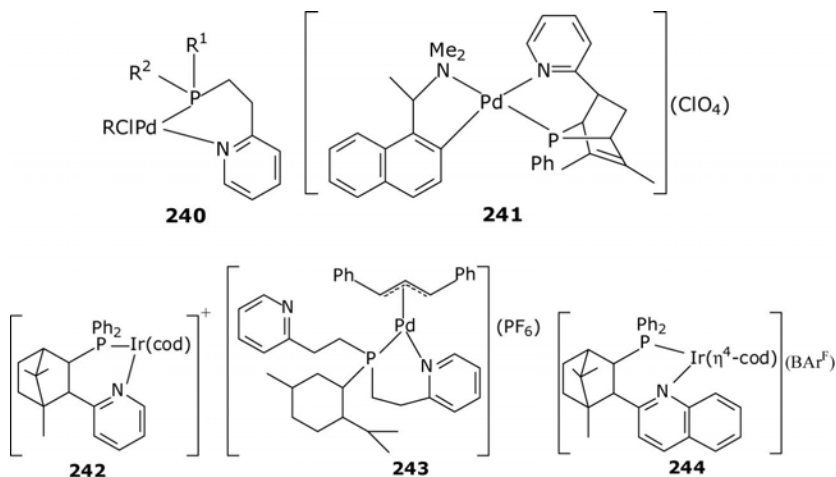


η^1 -Allyl platinum and palladium cationic complexes of 2,6-bis-diphenylphosphinomethylpyridine **229** react with dicationic platinum and palladium $\eta^2(\pi)$ -allyls of the same ligand **230** to produce dinuclear **231** where the π -coordinated metal becomes σ -bonded and vice versa (08OM6360). The reaction involves attack of the terminal (γ) carbon atom of **229** on the coordinated olefin of **230**. $[(\eta^3(\text{P,N,P})\text{-L})\text{Ag}](\text{BF}_4)$ (L = 2-di-*t*-butylphosphinomethylpyridine) enters a transmetalation reaction with $[(\eta^3\text{-C}_3\text{H}_5)\text{Pd}(\mu\text{-Cl})_2]$ affording $[(\eta^3(\text{P,N,P})\text{-L})\text{Pd}(\eta^1\text{-CH}_2\text{CH}=\text{CH}_2)](\text{BF}_4)$, $[(\eta^4\text{-cod})\text{Pd}(\text{Cl})(\text{Me})] - [(\eta^3(\text{P,N,P})\text{-L})\text{Pd}(\text{Me})](\text{BF}_4)$, and $[\text{Pd}(\text{P}(p\text{-Tol})_3)(4\text{-CNC}_6\text{H}_5)(\mu\text{Cl})_2] - [(\eta^3(\text{P,N,P})\text{-L})\text{Pd}(\eta^1\text{-C}_6\text{H}_5\text{CN})](\text{BF}_4)$ (09OM7025). $[\text{Pd}(\eta^3(\text{P,N,P})\text{-L-Cl}_2)]$ (L = 2,6-diphenylphosphinomethylpyridine) with C_2H_4 or $\text{CH}_2=\text{CHPh}$ and silver tetrafluoroborate in methylene chloride give dicationic $[(\eta^2\text{-C}_2\text{H}_4)\text{Pd}(\eta^3(\text{P,N,P})\text{-L})](\text{BF}_4)_2$ and $[(\eta^2\text{-CH}_2=\text{CHPh})\text{Pd}(\eta^3(\text{P,N,P})\text{-L})](\text{BF}_4)_2$ (98OM2060). $[(\eta^3\text{-P,N,P})\text{L-Pd}(\text{Cl})\text{Cl}]$ (L = 2-diphosphinomethylpyridine) with silver tetrafluoroborate in excess alkene $\text{RCH}=\text{CHR}^1$ (R = R¹ = H; R = Me, R¹ = H; R = Ph, R¹ = H; R = R¹ = Me) or norbornene gives a series of dicationic **232** (01EJ419). Allyl palladium complexes of 1-(2-diphenylphosphino-1-naphthyl)isoquinoline of type **233** are catalysts of allylic alkylation (94T4493) as well as palladium complexes of 2-(phosphinoaryl)pyridine (99SL1563) or phosphine/phosphoramidite ligands derived from quinoline (00AGE1428). In the process of catalysis of co-dimerization of ethylene with internal alkenes by dicationic **234**, free internal alkenes enter nucleophilic attack on the coordinated ethylene to give **235** (R, R¹ = H, Me) (02JA9038), and palladium analogs are described as well (05OM3359). Dicationic platinum(II) and palladium(II) $[(\eta^2\text{-alkene})\text{M}(\eta^3(\text{P,N,P})\text{-L})](\text{SbF}_6)_2$ (M = Pt, Pd; L = 2,6-diphenylphosphinomethylpyridine; alkene = ethene, propene) are active promoters of the catalytic hydroarylation of alkenes due to the electrophilic reaction of the coordinated alkene with benzene rings activated by methoxy substituents to yield **236** (X = H, Me, OMe) (07OM5216). 2,6-Diphenylphosphinomethylpyridine forms $[\text{Pt}(\eta^3(\text{P,N,P})\text{-L})\text{I}]$, which reacts further with alkenes in the presence of silver tetrafluoroborate to yield dicationic **237** (R = H, Me, Et, Ph) (02OM1807). 2,6-Diphenylphosphinomethylpyridine with $[(\eta^3\text{-CH}_2\text{CHCRR}')\text{Pd}(\text{Cl})]_2$ (R = R' = H; R = H, R' = Me; R = R' = Me) and silver tetrafluoroborate give products with an η^1 -coordinated allyl moiety **238** (R = R' = H; R = H, R' = Me; R = R' = Me) (00EJ12523). They are fluxional

but the depicted structure clearly predominates in solution and the solid state. $[(\eta^3\text{-P,N,P})\text{-L})\text{M}(\eta^2\text{-C}_2\text{H}_4)](\text{SbF}_6)_2$ ($\text{M} = \text{Pd}, \text{Pt}$; $\text{L} = 2,6\text{-diphenylphosphino-methylpyridine}$) with pentane-2,4-dione or methyl-3-oxobutanoate give $\eta^1(\text{C})$ -coordinated alkylation products **239** (10OM5878).

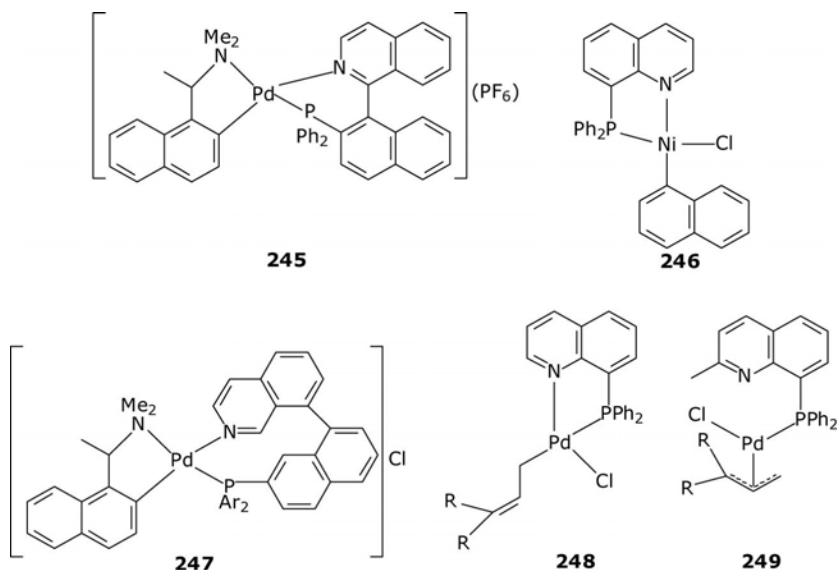


2-Pyridylethylphosphines react with $[\text{Pd}_2(\mu\text{-Cl})_2\text{R}_2(\text{THT})_2]$ to generate mononuclear chelates **240** ($\text{R} = \text{C}_6\text{F}_5$, $\text{C}_6\text{F}_3\text{Cl}_2$; $\text{R}^1 = \text{R}^2 = \text{Ph}$, $\text{CH}_2\text{CH}_2\text{C}_5\text{H}_4\text{N}$, $\text{R}^1 = \text{Ph}$, $\text{R}^2 = \text{CH}_2\text{CH}_2\text{C}_5\text{H}_4\text{N}$) (97IC5251). Some products **240** ($\text{R} = \text{C}_6\text{F}_5$, $\text{C}_6\text{F}_3\text{Cl}_2$; $\text{R}^1 = \text{R}^2 = \text{CH}_2\text{CH}_2\text{C}_5\text{H}_4\text{N}$, $\text{R}^1 = \text{Ph}$, $\text{R}^2 = \text{CH}_2\text{CH}_2\text{C}_5\text{H}_4\text{N}$) with silver hexafluorophosphate give cations of two types $[\text{Pd}_2\text{R}_2(\mu\text{-L})_2](\text{PF}_6)_2$, where all the pyridine nitrogen donor sites are engaged. *N*-(2-Diphenylphosphinobenzylidene)-2-(2-pyridyl)ethylamine (L) forms $\eta^3(\text{P}, \text{N}, \text{N})$ methyl(chloro)- and η^1 - allyl(chloro)palladium (II) cationic complexes (95CC331). The organopalladium *ortho*-metalated **241** is a promoter of asymmetric [4 + 2] Diels–Alder reactions (98OM3931). Note the hydrogenation catalyst **242** (04JOC4595). Bi(pyrid-2-ylethyl)methylphosphine with $[\text{Pd}_2(\text{dba})_3]$ and (E)-1,3-diphenyl-3-acethoxyprop-1-ene and ammonium hexafluorophosphate yield cationic **243** used in palladium-catalyzed allylic alkylations (06JOM2483). 6-Mesityl-2-diphenylphosphinomethylpyridine readily forms palladium square-planar $[\text{Pd}(\eta^2\text{-(N,P)})(\text{Me})(\text{Cl})]$ on treatment with $[(\eta^4\text{-cod})\text{Pd}(\text{Me})\text{Cl}]$ (03OM4893). Chelate **244** is a catalyst for hydrogenation (03AGE3941). $\text{C}_5\text{H}_4\text{N}(\text{CH}_2)_n\text{PPh}_2$ ($n = 1\text{--}3$) form $\eta^2(\text{N,P})$ -chelates with $[(\eta^3\text{-C}_4\text{H}_7)\text{Pd}(\text{Cl})]_2$ or $[(\eta^3\text{-C}_9\text{H}_9)\text{Pd}(\text{Cl})]_2$ of composition $[(\eta^3\text{-allyl})\text{Pd}(\eta^2(\text{N,P})\text{-L})]$ (00JCS(D)1549).



1-(2-Diphenylphosphino-1-naphthyl)isoquinoline forms P,N-chelate **245** (93T(A)743). 8-Diphenylphosphinoquinoline with *trans*-chloro(1-naphthyl)bis(triphenylphosphine)nickel gives chelate **246** (02NJC1474). 8-Dimethylphosphinoquinoline and -2-methylquinoline with $[(\eta^4\text{-cod})\text{Pd}(\text{Me})\text{Cl}]$ give $[\text{Pd}(\eta^2(\text{N,P})\text{-L})(\text{Me})\text{Cl}]$, which with 2,6-Me₂C₆H₃NC

afford $[\text{Pd}(\eta^2(\text{N},\text{P})\text{-L})(\text{Me})\text{Cl}(\text{CNC}_6\text{H}_3\text{Me}_2\text{-2,6})]$ (**07OM5550**). 1'-(2-Diarylphosphino)(1-naphthyl)isoquinolines with a palladacycle derived from palladium(II) chloride and *N,N*-dimethylnaphthylethylamine gives chelates **247** ($\text{Ar} = 3\text{-MeC}_6\text{H}_4$, $3,5\text{-Me}_2\text{C}_6\text{H}_3$, 2-furyl , $\text{Ar}_2 = \text{biphenyl}$) (**97T(A) 3775**). 8-Diphenylphosphinoquinoline and 8-diphenylphosphino-2-methyl quinoline with allyl dimers $[\text{Pd}(\mu\text{-Cl})(\eta^3\text{-C}_3\text{H}_5)]_2$ and $[\text{Pd}(\mu\text{-Cl})(\eta^3\text{-C}_3\text{H}_3\text{Me}_2)]_2$ give two different neutral products, **248** ($\text{R} = \text{R}^1 = \text{H}$; $\text{R} = \text{H}$, $\text{R}^1 = \text{Me}$) and **249** ($\text{R} = \text{R}^1 = \text{H}$; $\text{R} = \text{H}$, $\text{R}^1 = \text{Me}$), respectively (**10OM3027**).

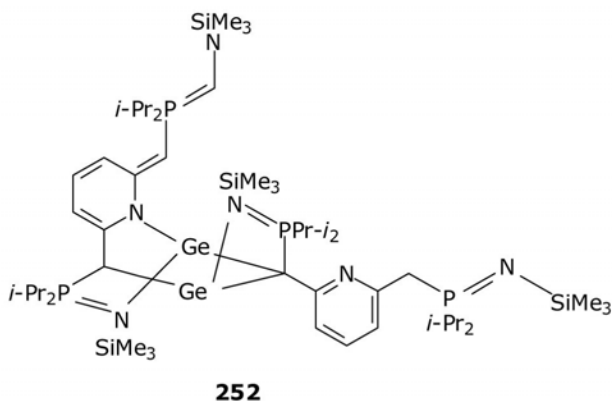
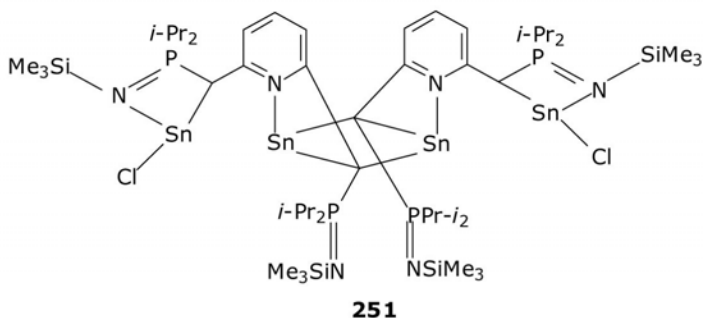
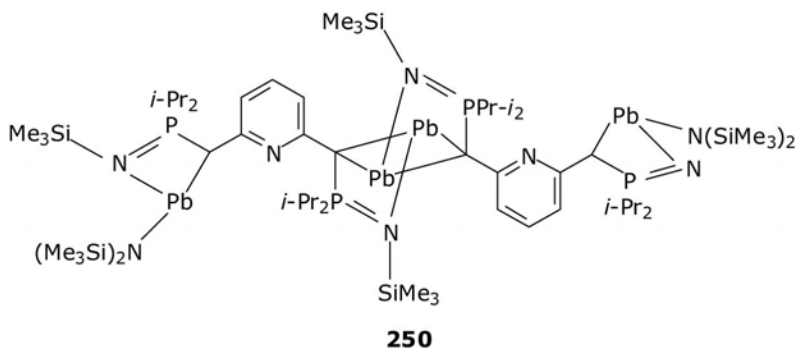


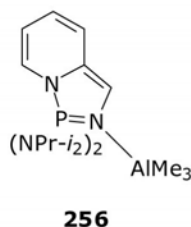
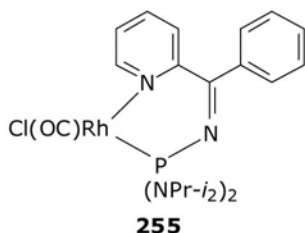
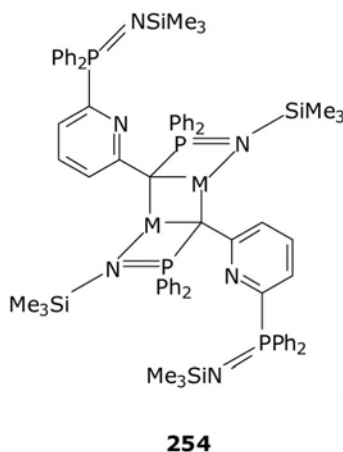
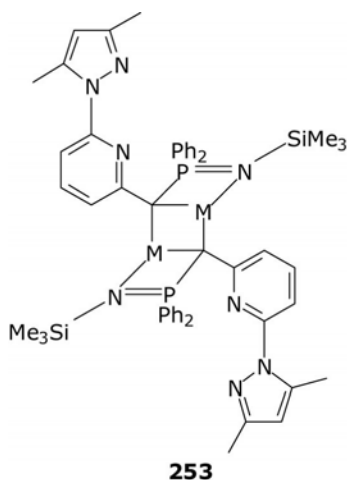
7. P,N-PYRIDINE LIGANDS

7.1 Iminophosphoranes

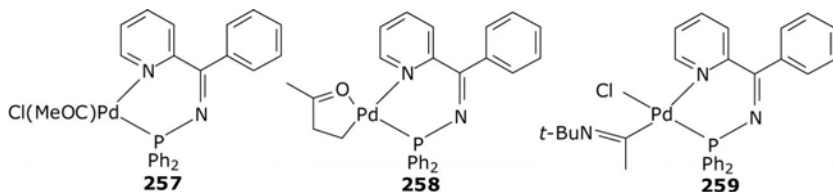
2,6-Lutidine-functionalized bis(phosphoranimine) with $[\text{Pb}(\text{N}(\text{SiMe}_3)_2)_2\cdot\text{Et}_2\text{O}]$ affords 1,3-diplumbacyclobutane **250** (**03OM4604**). The magnesium derivative of this ligand $[\text{Mg}((\text{Me}_3\text{SiN}=\text{PPr-}i_2\text{CH})_2\text{C}_5\text{H}_3\text{N-2,6})(\text{THF})]$ with $\text{SnCl}_2\cdot\text{Et}_2\text{O}$ yields 1,3-distannacyclobutane **251**, and with $\text{GeCl}_2(\text{dioxane})\cdot\text{Et}_2\text{O}$ – germanium(II) **252**. Iminophosphorane 2-(3,5-dimethyl-6-(2-(diphenylphosphino)-1-naphthyl)-1H-pyridin-2-yl)-2-methyl-1H-pyridine with $[\text{M}(\text{N}(\text{SiMe}_3)_2)]$ ($\text{M} = \text{Sn}$, Pb) gives 1,3-dimetallacyclobutadienes **253** ($\text{M} = \text{Sn}$, Pb) where neither phosphorus nor pyridine nitrogen center participates in coordination

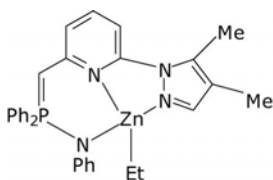
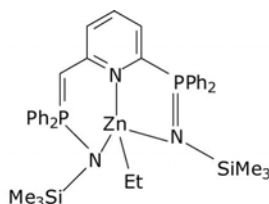
(09JCS(D)8005). The same is realized when 2-(*p*-C₆H₄(N=PPh₂)-6-(Me₃SiN=PPh₂CH₂)C₅H₄N is used as a ligand to yield **254** (M = Sn, Pb). Pyridyl-*N*-iminophosphorane undergoes reversible intramolecular cyclization in solution. As a result, it behaves differently with respect to [Rh(CO)₂(μ-Cl)]₂ forming chelate **255** based on an acyclic form and adduct **256** with AlMe₃ based on a cyclic tautomer (08AGE8674).





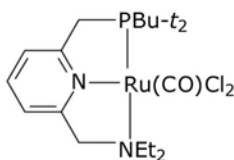
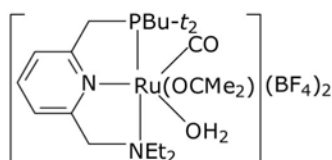
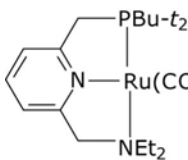
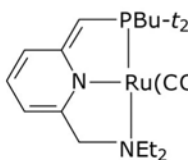
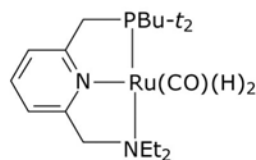
With diphenylphosphino(phenylpyridin-2-yl methylene)amine and $[(\eta^4\text{-cod})\text{M}(\text{Cl})\text{Me}]$ species similar to **255** result, $[(\eta^2(\text{N}, \text{P})\text{-L})\text{M}(\text{Cl})\text{Me}]$ ($\text{M} = \text{Pd}, \text{Pt}$) ([05JOM5264](#)). $[(\eta^2\text{-N}, \text{P})\text{-L})\text{M}(\text{Cl})\text{Me}]$ with sodium salts of B $(3,5\text{-(CF}_3)_2\text{C}_6\text{H}_3)_4$ and PF_6 anions (X) in acetonitrile gives cationic $[(\eta^2\text{-N}, \text{P})\text{-L})\text{M}(\text{AN})\text{Me}](\text{X})$. Under carbon monoxide, the insertion product $[(\eta^2\text{-N}, \text{P})\text{-L})\text{M}(\text{AN})(\text{COMe})](\text{B}(3,5\text{-(CF}_3)_2\text{-C}_6\text{H}_3)_4)$ follows. The neutral complex also inserts carbon monoxide to produce **257** and then further ethylene to yield palladacycle **258**. It also inserts *t*-butylisocyanide to generate **259**. 2-(3,5-Me₂C₃HN₂)-6-(PhN=P(Ph)₂CH₂)C₅H₃N with diethyl zinc gives **260** ([08OM1626](#)). 2-(Me₃SiN=P(Ph)₂)-6-(Me₃SiN=P(Ph)₂CH₂)C₅H₃N with triethyl aluminum or diethyl zinc gives chelates **261**, shown for the zinc derivative.



**260****261**

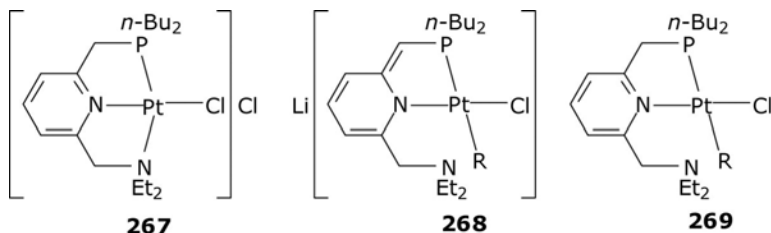
7.2 Combination of phosphino and amino groups

$[(\eta^3(\text{P},\text{N},\text{N})\text{-L})\text{Cl}_2\text{Ru}(\mu\text{-N}\equiv\text{N})\text{RuCl}_2(\eta^3(\text{P},\text{N},\text{N})\text{-L})]$ (L = di-*t*-butylphosphinomethyl-6-dimethylaminopyridine) under carbon monoxide in THF gives ruthenium(II) carbonyl **262** (07JCS(D)107). In excess silver tetrafluoroborate in acetone–water, dicationic **263** is formed. Addition of (2-(di-*t*-butylphosphinomethyl)-6-diethylaminomethyl)pyridine to $[\text{Ru}(\text{H})\text{Cl}(\text{PPh}_3)_3(\text{CO})]$ resulted in ruthenium(II) **264** (05JA10840, 09AGE8178). The product in the presence of a base such as *t*-BuOK is an efficient catalyst of dehydrogenative esterification. The base deprotonates in **264** the phosphine moiety to yield the dearomatized Ru(II) **265**. With excess molecular hydrogen, aromaticity is restored, the *trans*-dihydride **266** being the result. However, on standing **266** slowly loses H_2 and regenerates **265**, which catalyzes the dehydrogenation of primary alcohols to esters (05JA10840, 06AGE1113) and the synthesis of amides from alcohols and amines (07SCI790, 08AGE1814, 09SCI74).

**262****263****264****265****266**

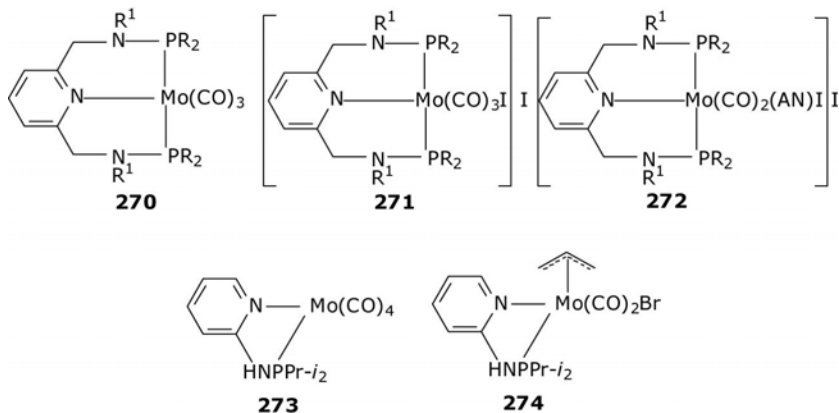
Complex **267** with methyl or phenyl lithium results in the opening of one of the chelate rings in bis-chelate **267** and the formation of anionic dearomatized **268** ($\text{R} = \text{Me}, \text{Ph}$) (08OM2627). The products are readily

protonated by aqueous hydrochloric acid to give neutral aromatic **269** ($R = \text{Me}, \text{Ph}$), where the diethylamino group remains intact. The platinum(II) $[\text{PtMe}_2(\eta^2(\text{N},\text{P})\text{-L})]$ ($\text{L} = 2\text{-di-}t\text{-butylphosphinomethylpyridine}$) with molecular oxygen in benzene or methylene chloride forms platinum(II) methylperoxo $[\text{Pt}(\text{Me})(\eta^2(\text{N},\text{P})\text{-L})]$ (**09OM953**).

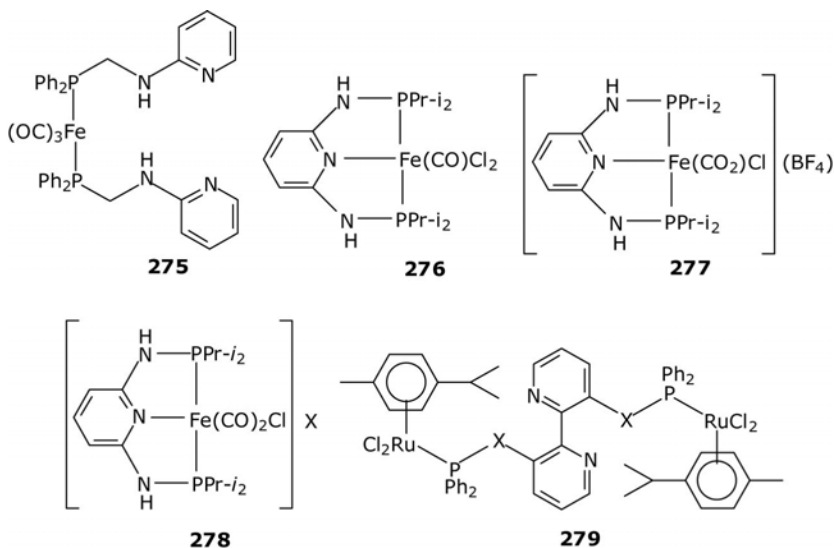


7.3 Phosphinoamino pyridines

2,6-(NHPR_2) $_2\text{C}_5\text{H}_3\text{N}$ ($R = \text{Ph}, t\text{-Bu}$) and 2,6- $\text{N}(n\text{-C}_6\text{H}_{13})\text{PPh}_2\text{C}_5\text{H}_3\text{N}$ with $[\text{Mo}(\text{CO})_3(\text{AN})_3]$ give pincers **270** ($R^1 = \text{H}, R = \text{Ph}, i\text{-Pr}, t\text{-Bu}; R = n\text{-C}_6\text{H}_{13}, R = \text{Ph}$) (**06OM1900, 08ACR201**). With iodine, in methanol some form seven-coordinate **271** and in acetonitrile form **272**. 2-Amino(di-*i*-propylphosphino)pyridine with $[\text{Mo}(\text{CO})_6]$ gives chelate **273**, which oxidatively adds allyl bromide to yield **274** (**09EJ14085**). Metal carbonyls $[\text{M}(\text{CO})_4(\eta^2(\text{P},\text{N})\text{-L})]$ ($\text{M} = \text{Cr}, \text{Mo}, \text{W}; \text{L} = \text{Ph}_2\text{PCH}_2\text{C}_5\text{H}_4\text{N}, \text{Ph}_2\text{PCH}_2\text{CH}_2\text{C}_5\text{H}_4\text{N}, \text{Ph}_2\text{PCH}_2\text{CH}_2\text{CH}_2\text{C}_5\text{H}_4\text{N}$ and $\text{Ph}_2\text{PN}(\text{H})\text{C}_5\text{H}_4\text{N}$ are mononuclear chelates (**73ICA(7)713**). $\text{Ph}_2\text{PNHC}_5\text{H}_4\text{N}$, $\text{Ph}_2\text{P}(\text{CH}_2)_n\text{NHC}_5\text{H}_4\text{N}$ ($n = 1\text{--}3$) form $[\text{Mo}(\text{CO})_4(\eta^2(\text{P},\text{N})\text{-L})]$, which react with carbon monoxide to yield $[\text{Mo}(\text{CO})_5(\eta^1(\text{P})\text{-L})]$ (**74IC632**). *N,N'*-Bis-(diphenylphosphino)-2,6-diaminopyridine forms chelates *mer*- $[\text{M}(\eta^2(\text{N}_{\text{py}}, \text{P})\text{-L})(\text{CO})_3]$ ($\text{M} = \text{Cr}, \text{Mo}, \text{W}$) (**87ZAAC83**).

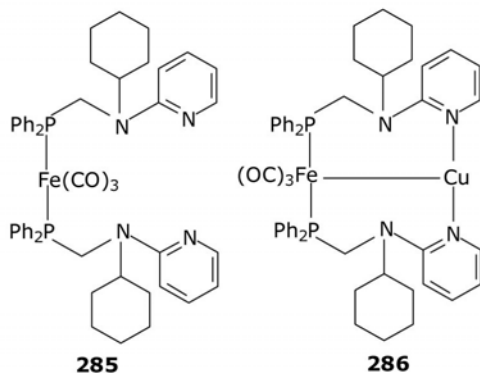
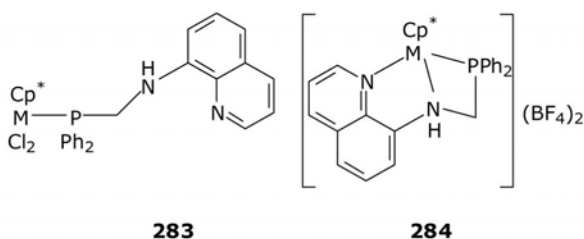
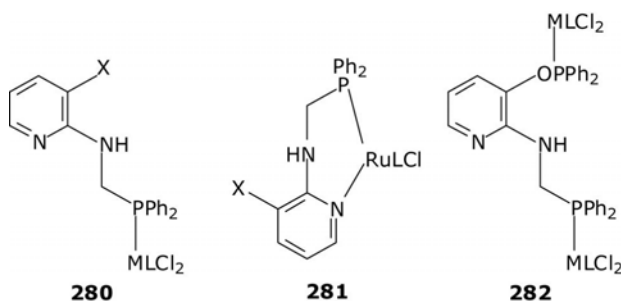


N-((Diphenylphosphino)methyl)-2-pyridylamine with $[\text{Fe}(\text{CO})_5]$ in the presence of potassium hydroxide gives **275** (02JCS(D)1336). $[(\eta^3(\text{P,N,P})\text{-L})\text{FeX}_2]$ ($\text{L} = 2,6\text{-(NHPPr-}i\text{)}_2\text{C}_5\text{H}_3\text{N}$; $\text{X} = \text{Cl, Br}$) under carbon monoxide give **276** and its bromo-analog (08AGE9142, 09OM6902). Treatment of neutral **276** with silver tetrafluoroborate in nitromethane in the presence of CO afforded cationic **277** (10OM4932). $[\text{Fe}(\text{L})\text{Cl}_2]$ ($\text{L} = 2,6\text{-diaminopyridine}$ based di-*i*-propylphosphine ligand) with a respective silver or sodium salts in the presence of carbon monoxide gives series **278** ($\text{X} = \text{NO}_3, \text{CF}_3\text{COO, CF}_3\text{SO}_3, \text{BF}_4, \text{PF}_6, \text{SbF}_6, \text{and BAR}^{\text{F}}$) (10EJI3160), among which the tetrafluoroborate is an efficient pre-catalyst for the coupling of aromatic aldehydes with ethyl diazoacetate. *N,N'*-Bis(diphenylphosphino)-3,3'-diamine and *P,P'*-diphenylphosphinous acid - *P,P'*-(2,2'-bipyridine)-3,3'-diyl ester with $[(\eta^6\text{-}p\text{-cymene})\text{RuCl}_2]_2$ gives *P,P*-coordinated **279** ($\text{X} = \text{NH, O}$), active catalyst precursors for the transfer hydrogenation of acetophenones (09JOM2488).

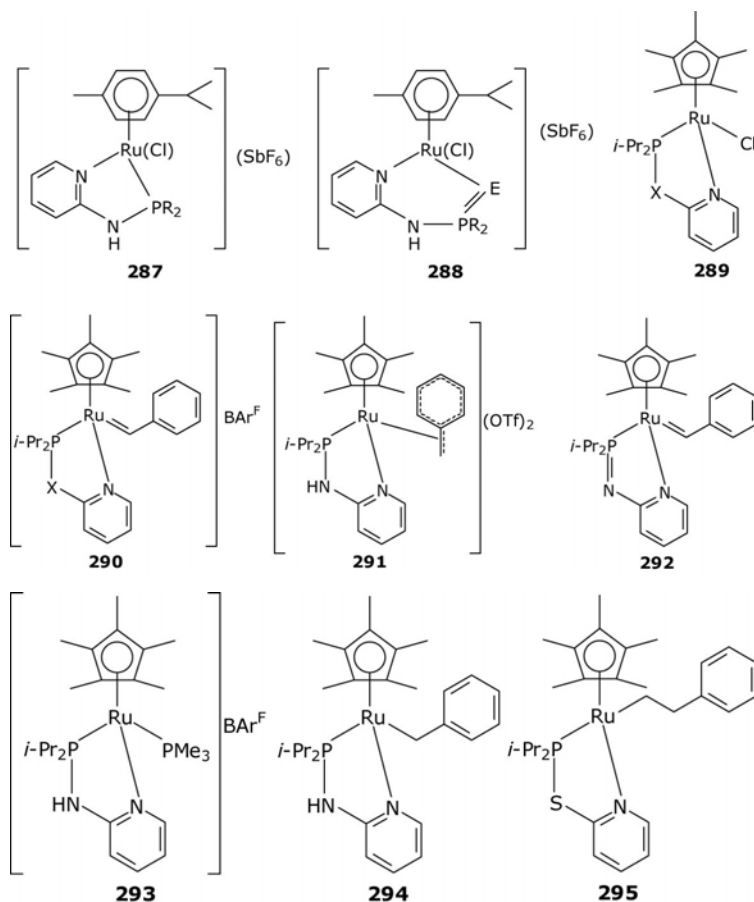


$\text{Ph}_2\text{PCH}_2\text{N}(\text{H})\text{C}_5\text{H}_3(\text{OH})\text{N}$, $\text{Ph}_2\text{PCH}_2\text{N}(\text{H})\text{C}_5\text{H}_4\text{N}$, $\text{Ph}_2\text{PCH}_2\text{N}(\text{H})\text{C}_5\text{H}_3(\text{OP}(\text{P})\text{Ph}_2)\text{N}$, and $\text{Ph}_2\text{PCH}_2\text{N}(\text{H})\text{C}_5\text{H}_3(\text{OP}(\text{P})(\text{OPh})_2)\text{N}$, with $[(\eta^6\text{-}p\text{-cymene})\text{Ru}(\mu\text{-Cl})\text{Cl}_2]$ or $[(\eta^5\text{-Cp}^*)\text{Rh}(\mu\text{-Cl})\text{Cl}_2]$ give mononuclear **280** ($\text{M} = \text{Ru, L} = p\text{-cymene, X} = \text{H, OH, OP}(\text{O})\text{Ph}_2, \text{OP}(\text{O})(\text{OPh})_2$; $\text{M} = \text{Rh, L} = \text{Cp}^*, \text{X} = \text{OH, OP}(\text{O})\text{Ph}_2, \text{OP}(\text{O})(\text{OPh})_2$) (00JCS(D)2771). Two products ($\text{M} = \text{Ru, L} = p\text{-cymene, X} = \text{H, OH}$) on standing isomerize to chelates **281** ($\text{X} = \text{H, OH}$). $\text{Ph}_2\text{PCH}_2\text{N}(\text{H})(\text{C}_5\text{H}_3(\text{OPPh}_2)\text{N})$ with $[(\eta^6\text{-}p\text{-cymene})\text{Ru}(\mu\text{-Cl})\text{Cl}_2]$, $[(\eta^6\text{-}p\text{-C}_6\text{Me}_6)\text{Ru}(\mu\text{-Cl})\text{Cl}_2]$, or $[(\eta^5\text{-Cp}^*)\text{M}(\mu\text{-Cl})\text{Cl}_2]$ ($\text{M} = \text{Rh, Ir, L} = \text{Cp}^*$) yield dimetallic **282** ($\text{M} = \text{Ru, L} = p\text{-cymene, C}_6\text{Me}_6$; $\text{M} = \text{Rh, Ir, L} = \text{Cp}^*$). 8-Diphenylphosphinomethylaminoquinoline with $[(\eta^5\text{-Cp}^*)\text{M}(\mu\text{-Cl})\text{Cl}_2]$

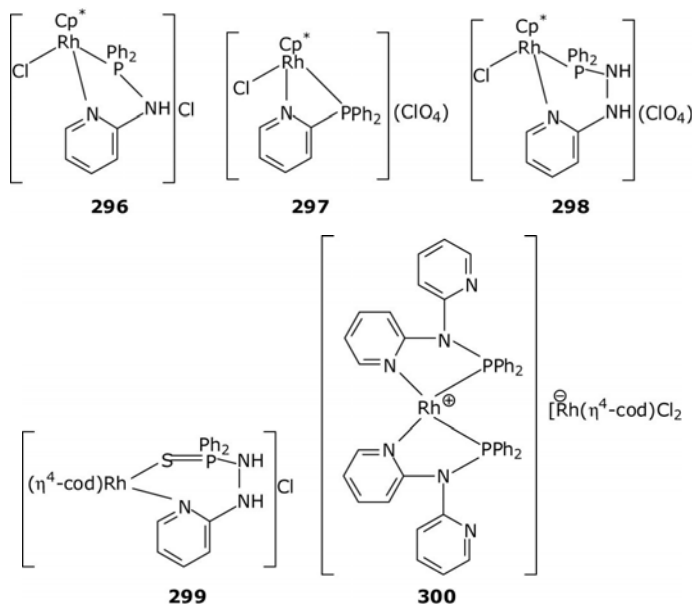
(M = Rh, Ir) gives monodentate **283** (M = Rh, Ir) (02JCS(D)1618). [$(\eta^6\text{-}p\text{-cymene})\text{Ru}(\mu\text{-Cl})\text{Cl}_2$] gives an analog of **283** (M = Ru, *p*-cymene instead of Cp^{*}). C₅H₃N(2,6-NHPR₂)₂ (R = Ph, *i*-Pr) form [Fe(η^3 (P,N,P)-L)(AN)₃](BF₄)₂, which under carbon monoxide give the monocarbonyls *cis*-[Fe(η^3 (P,N,P)-L)(CO)(AN)₂](BF₄)₂ (07OM217). The phenyl ligand with [Fe(CO)₄Br₂] and sodium tetraphenylborate gives [Fe(η^3 (P,N,P)-L)(CO)₂](BPh₄). The products are active catalysts for coupling aromatic aldehydes with ethyl diazoacetate. Under silver tetrafluoroborate in methylene chloride they transform to dicationic bis-chelates **284** (M = Rh, Ir). 2-(*N*-Diphenylphosphinomethyl-*N*-cyclohexyl)aminopyridine with [Fe(CO)₅] and KOH in refluxing ethanol forms P-coordinated **285** (01OM4126). The product with [Cu(AN)₄](ClO₄) in methylene chloride gives iron(0)–copper (I) heterodinuclear **286** containing an Fe–Cu bond.



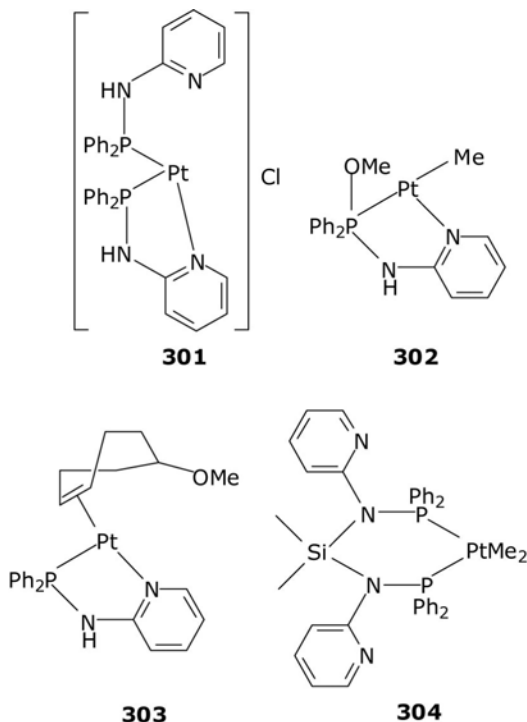
N-Diorganophosphino-2-aminopyridines with $[\text{Ru}(\eta^6\text{-}p\text{-cymene})(\mu\text{-Cl})\text{Cl}]_2$ and silver hexafluoroantimonate or triflate afford cations exemplified by **287** ($\text{R} = i\text{-Pr}$, Ph) (10POL3097). Deprotonation occurs at the amino nitrogen atom. *N*-(2-Pyridinyl)diorganophosphinoxides or selenides with $[\text{Ru}(\eta^6\text{-}p\text{-cymene})(\mu\text{-Cl})\text{Cl}]_2$ and silver hexafluoroantimonate produce *S*, *N*- or *Se*, *N*-chelates **288** ($\text{R} = i\text{-Pr}$, Ph; $\text{E} = \text{S}$, Se). Di-*i*-propylphosphinylpyrid-2-ylamine and 2-di-*i*-propylphosphinylmercaptopyridine with $[(\eta^5\text{-Cp}^*)\text{Ru}(\text{Cl})]_4$ give neutral half-sandwiches **289** ($\text{X} = \text{NH}$, S) (10EJI1767). The products with phenyldiazomethane in the presence of NaBAR'_4 [$\text{Ar}' = 3,5\text{-bis(trifluoromethyl)phenyl}$] give the benzylidenes **290** ($\text{X} = \text{NH}$, S). Protonation of **290** ($\text{X} = \text{NH}$) with triflic acid gives dicationic **291** with the η^2 -coordinated benzyl moiety. Deprotonation with $\text{KN}(\text{SiMe}_3)_2$ occurs on the NH-moiety of **290** ($\text{X} = \text{NH}$) and produces neutral **292**. With trimethylphosphine, nucleophilic substitution of the carbene ligand occurs affording **293**, and with NaBH_4 in methanol, the $\eta^1(\text{C})$ -benzyl **294** is the main product. Carbene **290** ($\text{X} = \text{S}$) with methyl lithium gives the alkene insertion product **295**.



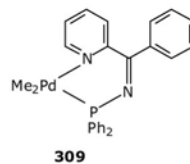
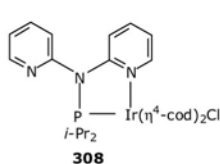
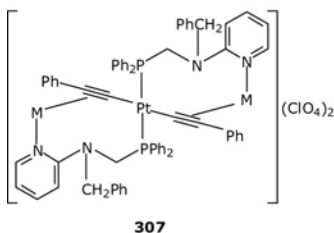
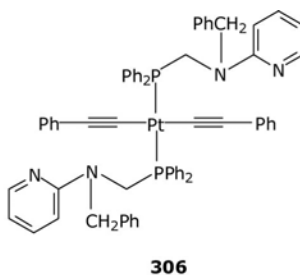
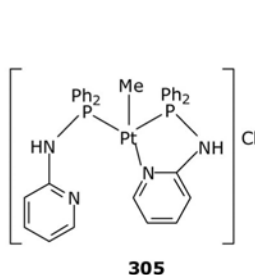
2-Diphenylphosphinopyridine, 2-diphenylphosphinohydrazinopyridine, and 2-(*N*-diphenylphosphino)piperazinopyridine with $[(\eta^5\text{-Cp}^*)\text{RhCl}_2]_2$ give monodentate $[(\eta^5\text{-Cp}^*)\text{RhCl}_2(\eta^1(\text{P})\text{-L})]$ (01JCS(D)3421). 2-Diphenylphosphinoaminopyridine in the same reaction gives cationic chelate **296**. Two more chelate derivatives **297** and **298** can be prepared from monodentate species and silver perchlorate in methylene chloride. $\text{Ph}_2\text{PNHNHC}_5\text{H}_4\text{N}$ with $[(\eta^4\text{-cod})\text{PtMe}_2]$ gives $[\text{PtMe}_2(\eta^1(\text{P})\text{-L})]$, with $[(\eta^4\text{-cod})\text{Pt}(\text{Me})\text{Cl}]$ - $[\text{Pt}(\text{Me})(\text{Cl})(\eta^1(\text{P})\text{-L})]$, with $[(\eta^3\text{-C}_3\text{H}_5)\text{Pd}(\mu\text{-Cl})_2]$ - $[(\eta^3\text{-C}_3\text{H}_5)\text{Pd}(\text{Cl})(\eta^1(\text{P})\text{-L})]$, with $[(\eta^4\text{-cod})\text{Rh}(\mu\text{-Cl})_2]$ - $[(\eta^4\text{-cod})\text{Rh}(\text{Cl})(\eta^1(\text{P})\text{-L})]$, with $[(\eta^3:\eta^3\text{-C}_{10}\text{H}_6)\text{RuCl}_2]_2$ - $[(\eta^3:\eta^3\text{-C}_{10}\text{H}_6)\text{RuCl}_2(\eta^1(\text{P})\text{-L})]$, with $[(\eta^5\text{-Cp}^*)\text{Ir}(\mu\text{-Cl})_2]$ - $[(\eta^5\text{-Cp}^*)\text{IrCl}_2(\eta^1(\text{P})\text{-L})]$ (03POL1397). $\text{Ph}_2\text{P}(\text{S})\text{NHNHC}_5\text{H}_4\text{N}$ with $[(\eta^4\text{-cod})\text{Rh}(\mu\text{-Cl})_2]$ gives chelate **299**. A similar chelate follows from $[(\eta^6\text{-cymene})\text{RuCl}_2]$; the product is $[(\eta^6\text{-cymene})\text{Ru}(\eta^2(\text{Se},\text{N})\text{-L})]\text{Cl}_2$. (Bis(2-pyridyl)amino)diphenylphosphine with $[(\eta^4\text{-cod})\text{Rh}(\text{Cl})_2]$ leads to cationic **300** (07AGE3135), the catalyst of the nondirected direct arylation of benzene with aryl iodides. $\text{Ph}_2\text{PCH}_2\text{N}(\text{H})\text{C}_5\text{H}_3(\text{Cl}-5)\text{N}$ with $[(\eta^6\text{-}p\text{-MeC}_6\text{H}_4\text{Pr}-i)\text{Ru}(\mu\text{-Cl})\text{Cl}_2]$ or $[(\eta^5\text{-Cp}^*)\text{Rh}(\text{Cl})(\mu\text{-Cl})_2]$ gives P-coordinated $[(\eta^6\text{-}p\text{-MeC}_6\text{H}_4\text{Pr}-i)\text{RuCl}_2(\eta^1(\text{P})\text{-L})]$ or $[(\eta^5\text{-Cp}^*)\text{RhCl}_2(\eta^1(\text{P})\text{-L})]$ (01NJC416). The reaction with silver tetrafluoroborate is chloride abstraction and leads to cationic chelates $[(\eta^6\text{-}p\text{-MeC}_6\text{H}_4\text{Pr}-i)\text{Ru}(\text{Cl})(\eta^2(\text{P},\text{N})\text{-L})](\text{BF}_4)$ and $[(\eta^5\text{-Cp}^*)\text{Rh}(\text{Cl})(\eta^2(\text{P},\text{N})\text{-L})](\text{BF}_4)$, where N is the pyridyl nitrogen. 5- $\text{Ph}_2\text{PCH}_2\text{N}(\text{H})\text{C}_5\text{H}_3(2\text{-X})\text{N}$ (X = Cl, Br) with $[(\eta^6\text{-}p\text{-cymene})\text{RuCl}_2]_2$ or $[(\eta^5\text{-Cp}^*)\text{MCl}_2]_2$ (M = Rh, Ir) give the $\eta^1(\text{P})$ -coordinated $[(\eta^6\text{-}p\text{-cymene})\text{RuCl}_2(\eta^1(\text{P})\text{-L})]$ or $[(\eta^5\text{-Cp}^*)\text{MCl}_2(\eta^1(\text{P})\text{-L})]$ (06ICA2980). $[(\eta^4\text{-cod})\text{Pd}(\text{Me})\text{Cl}]$ under these conditions leads to P,N-chelates $[\text{Pd}(\text{Me})\text{Cl}(\eta^2(\text{N},\text{P})\text{-L})]$ where the pyridine nitrogen participates in coordination.



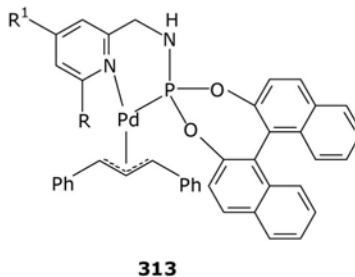
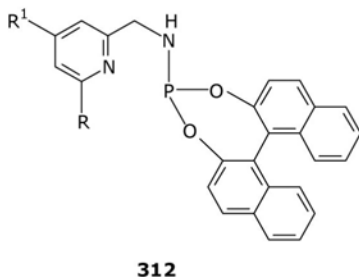
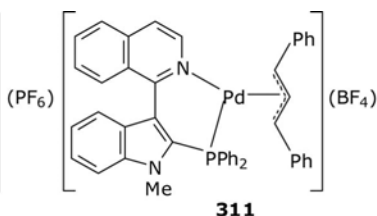
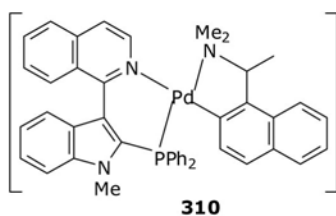
2-(Diphenylphosphinoamino)pyridine with $[(\eta^4\text{-cod})\text{Pt}(\text{Me})(\text{Cl})]$ in methylene chloride gives cationic **301**, which is further transformed into **302** by *t*-BuOK in methanol (00JCS(D)2559). Moreover, the interaction of the same ligand with $[\text{Pt}(\mu\text{-OMe})(\text{C}_8\text{H}_{12}\text{OMe})_2]$ and *t*-BuOK when mononuclear mono-chelate **303** is the product. Bis((diphenylphosphino)(2-pyridyl)amino)dimethylsilane with $[(\eta^4\text{-cod})\text{PtMe}_2]$ gives P,P-coordinated **304** (01JCS(D)972).



With $[(\eta^4\text{-cod})\text{Pt}(\text{Me})(\text{Cl})]$, a mixed coordination situation **305** is realized as represented by monodentate and neutral chelate modes (97PSS473). Deprotonation gives a mixture of the monodentate and anionic chelates, and neutral $[\text{Pt}(\text{Me})(\eta^1(\text{P})\text{-L})(\eta^2(\text{N,P})\text{-L-H})]$ is formed. 2-(*N*-Diphenylphosphinomethyl-*N*-benzyl)aminopyridine with $[(\eta^4\text{-cod})\text{Pt}(\text{C}\equiv\text{CPh})_2]$ gives **306** (03JCS(D)1551). The product realizes its ligating potential with $[\text{M}(\text{AN})_4]\text{ClO}_4$ ($\text{M} = \text{Cu}, \text{Ag}$) to yield heterobimetallic Pt(II)-M(I) eight-membered macrocycles **307** ($\text{M} = \text{Cu}, \text{Ag}$). Complex **308** is a catalyst for the alkylation of methyl-*N*-heteroaromatics with alcohols (10JA924). Pyridyl-*N*-phosphinoimine with two phenyl substituents with $[\text{PdMe}_2(\text{TMEDA})]$ gives dimethyl **309** (10AGE7046).

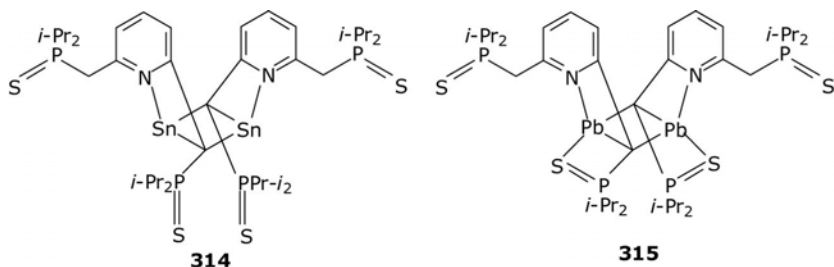


1-Methyl-2-diphenylphosphino-3-(1'-isoquinolyl)indole with palladacycle derived from dimethyl-1-naphthyl ethylamine and potassium hexafluorophosphate yields chelate **310** (97T4035). With $[(\eta^3\text{-PhCH}=\text{CH}=\text{CHPh})\text{Pd}(\mu\text{-Cl})_2]$, allyl **311** follows in the presence of silver tetrafluoroborate. Addition of ligands **312** ($R = R^1 = \text{H, Me}$) to $[(\eta^3\text{-PhCHCHCHPh})\text{Pd}(\text{Cl})_2]$ under conditions of allylic alkylation of 1,3-diphenylprop-2-enyl acetate with dimethyl malonate leads to the formation of P,N-chelates **313** ($R = R^1 = \text{H, Me}$), the active species of the catalytic reaction (00T(A)4753).

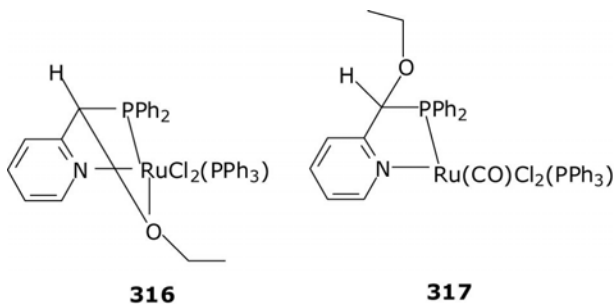


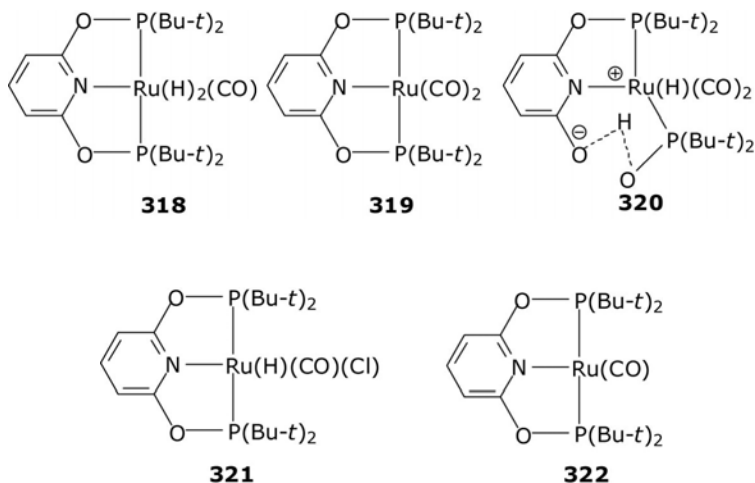
8. P,O-(S,Se-) PYRIDINE LIGANDS

2,6-Lutidylbis(phosphoranosulfide) with $M(N(SiMe_3)_2)_2$ ($M = Sn, Pb$) afforded 1,3-distannacyclobutane **314** and 1,3-diplumbacyclobutane **315** (100M1890), where coordination modes differ drastically: the sulfur donor site is involved only in the organolead derivative.

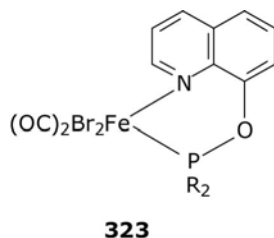


1-(Diphenylphosphino)-2-ethoxy-1-(2-pyridyl)ethane forms *fac*-[Mo(CO)₃(η^3 (N,P,O)-L)], which evolves to *cis*-[Mo(CO)₄(η^2 (N,P)-L)] (94JCS(D)2755). $P(OCH_2)_3CCH_2O_2CR$ ($R = 3$ -pyridyl, 4-pyridyl) form bridges in $[((\eta^5$ -MeCp)Mn(CO)₂)₂(μ -L)] (04OM1986). Interaction of the inorganic complex **316** with carbon monoxide leads to the organometallic derivative **317** (97OM1401). The process is accompanied by the switch of the coordination mode from η^3 (P,N,O) to η^2 (P,N). This rearrangement is due to the increased soft character of the Ru site containing coordinated CO. [η^4 -cod)Rh(η^2 (N,P)-L)](ClO₄) under carbon monoxide transforms into [Rh(CO)₂(η^2 (N,P)-L)](ClO₄) and dinuclear [Rh(CO)(μ - η^2 (P,O)-L)]₂(ClO₄)₂ (94JCS(D)2755). *Trans*-dihydride **318** under carbon monoxide forms dicarbonyl **319**, which under water gives zwitterion **320** (09OM4791). An alternative way to dicarbonyl **319** is based on chlorocarbonyl **321**, which on deprotonation with potassium *t*-butylate yields monocarbonyl **322** and then under carbon monoxide **319**.

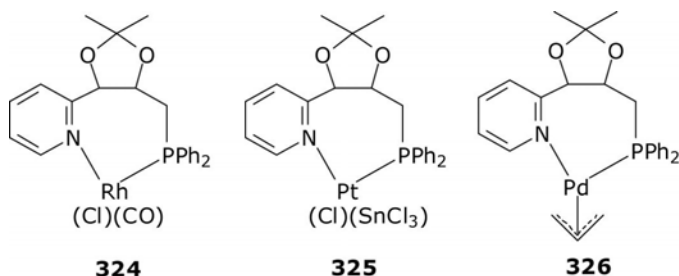




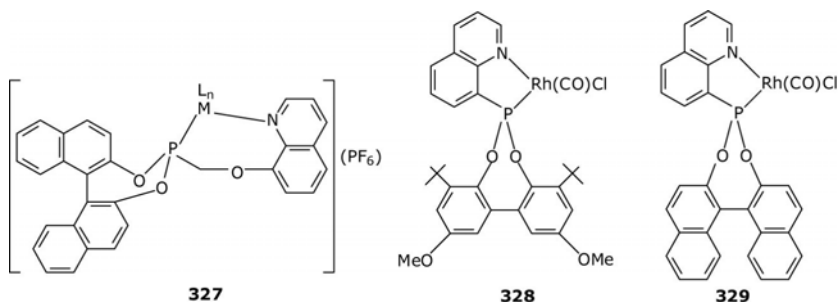
Phosphine ligands based on 8-hydroxyquinoline with *cis*-[Fe(CO)₄Br₂] afford *cis,cis*-dicarbonyl dibromo **323** (R = *i*-Pr, Ph) (10ICA3674). Similar chelates are formed from [(η⁵-Cp)Ru(AN)₃](PF₆) where the products are cationic [(η⁵-Cp)Ru(η²(N,P)-L)(AN)](PF₆) and from [(η⁶-*p*-cymene)Ru(μ-Cl)Cl]₂ in the presence of silver triflate – [(η⁶-*p*-cymene)Ru(η²(N,P)-L)Cl](OTf). Similar ligands are participants in palladium-catalyzed allylic substitutions (01T(A)1345).

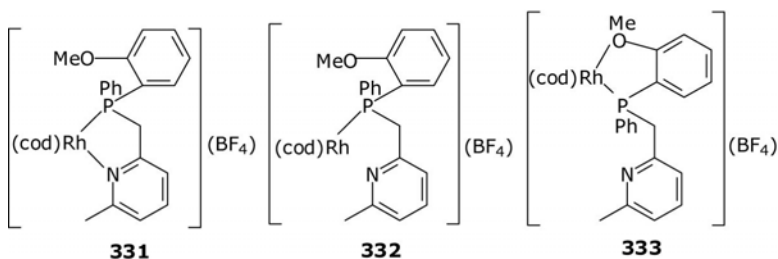
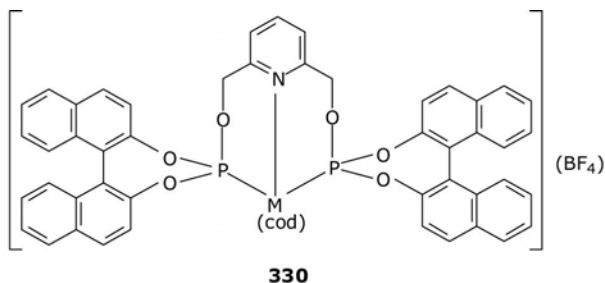


Pyridylphosphine 4-(diphenylphosphinomethyl)-2,2-dimethyl-5-(2-pyridyl)-1,3-dioxolane is predominantly η¹(P)-coordinated in [Rh(η¹(P)-L)(CO)Cl] (96JCS(D)1295). Pyridylphosphine and bipyridylphosphino derivatives of 2,2'-dimethyl-1,3-dioxolane, for example, **324–326**, are catalysts for asymmetric addition, hydroformylation, hydrocarboethoxylation, and allylic alkylation (96T(A)885).

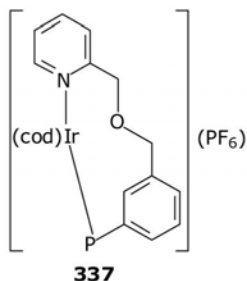
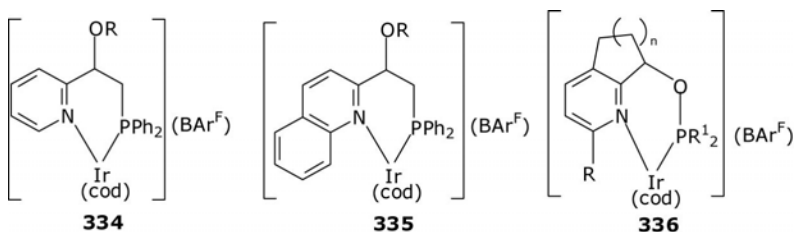


Phosphito-*N*-(8-((3,5-dioxa-4-phosphacyclohepta[2,1-*a*;3,4-*a'*]dinaphthalen-4-yl)oxy)quinoline reacts with $[(\eta^6\text{-cymene})\text{RuCl}_2]_2$ or $[(\eta^5\text{-Cp}^*)\text{RhCl}_2]_2$ to yield first the $\eta^1(\text{P})$ -coordinated and then in the presence of ammonium hexafluorophosphate the $\eta^2(\text{N,P})$ -chelates **327** ($\text{ML}_n = (\eta^6\text{-p-cymene})\text{Ru}(\text{Cl})$, $(\eta^5\text{-Cp}^*)\text{Rh}(\text{Cl})$) ([02OM761](#)). Meanwhile, phosphonito-*N*-(8-(3,5-dioxa-4-phosphacyclohepta[2,1-*a*;3,4-*a'*]dinaphthalen-4-yl)oxy)quinoline forms chelates of composition $[(\eta^6\text{-cymene})\text{Ru}(\eta^2(\text{N,P})\text{-L})\text{Cl}]\text{Cl}$ or $[(\eta^5\text{-Cp}^*)\text{Rh}(\eta^2(\text{N,P})\text{-L})\text{Cl}]\text{Cl}$ in one stage. 8-(4,8-Di-*t*-butyl-1,11-dimethoxy-5,7-dioxa-6-phosphadibenzo[*a,c*]cyclohepten-6-yl)quinoline and 8-(3,5-dioxa-4-phosphacyclohepta[2,1-*a*;3,4-*a'*]dinaphthalen-4-yl)quinoline with $[\text{Rh}(\text{CO})_2\text{Cl}]_{32}$ yield chelates **328** and **329**, respectively ([02ICA\(338\)59](#)). Similar to **329** are chelates **330** ($\text{M} = \text{Rh}, \text{Ir}$) ([96TL4933](#)). Chelates $[(\eta^4\text{-cod})\text{Rh}(\text{C}_5\text{H}_3\text{N}(2\text{-R}')(\text{6-CH}_2\text{PPhR}))](\text{BF}_4)$ ($\text{R} = \text{Me}$, $\text{R}' = \text{H}$, Me ; $\text{R} = o\text{-anisyl}$, $\text{R}' = \text{H}$, Me), for example, **331**, are characterized by the lengthened rhodium nitrogen bond and in the solid state tend to be in dynamic equilibrium with the P-coordinated isomers, for example **332** and **333** ([97OM2089](#)).

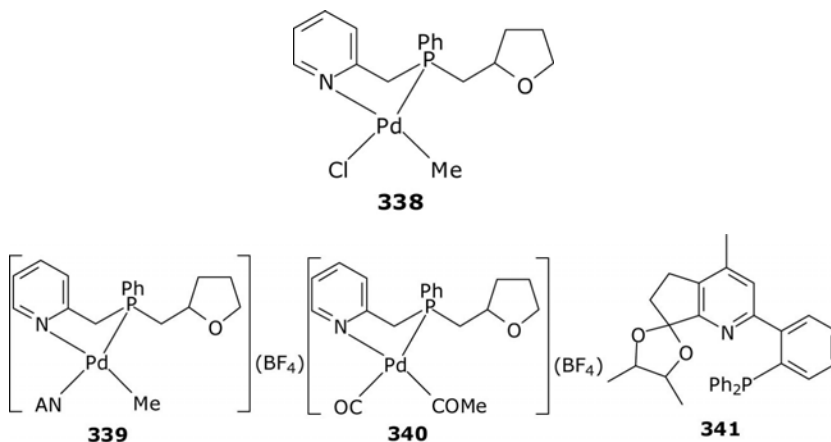




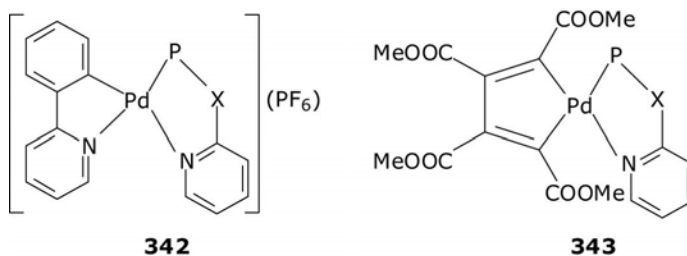
Cationic series **334**, **335** ($R = \text{Si}(t\text{-Bu})\text{Me}_2, \text{Si}(i\text{-Pr})_3, \text{Si}(t\text{-Bu})\text{Ph}_2$), and **336** ($n = 1, R = \text{H, Ph, R}^1 = \text{Ph, } o\text{-Tol, Cy, } t\text{-Bu}$; $n = 2, R = \text{H, R}^1 = \text{Ph, } o\text{-Tol, Cy, } t\text{-Bu, furyl}$; $R = \text{Me, Ph, R}^1 = \text{Ph, } o\text{-Tol, Cy, } t\text{-Bu}$; $n = 3, R = \text{H, R}^1 = \text{Ph}$), which follow from appropriate ligand, $[(\eta^4\text{-cod})\text{Ir}(\mu\text{-Cl})_2]$, and sodium tetrakis(3,5-Bis(trifluoromethyl)phenyl)borane, offer potential as asymmetric catalysts ([04AGE70](#), [06AGE5194](#)). Hybrid N,O,P-ligand occurs in iridium chelate **337** ([99OM3563](#)).

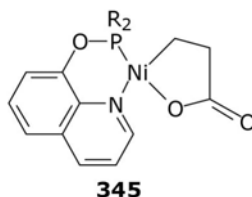
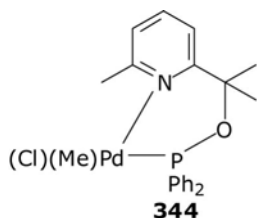


The N,P,O-ligand depicted in **338** in the N,P-chelate unit follows from $[(\eta^4\text{-cod})\text{Pd}(\text{Cl})\text{Me}]$ ([04JCS\(D\)3251](#)). With silver tetrafluoroborate in acetonitrile/methylene chloride, cationic **339** follows, which under carbon monoxide is transformed to acetylated **340**. The product of interaction of ligand **341** with $[(\eta^3\text{-C}_3\text{H}_5)\text{Pd}(\text{Cl})]_2$ is an efficient catalyst of asymmetric allylic substitutions ([04JOC5060](#)).

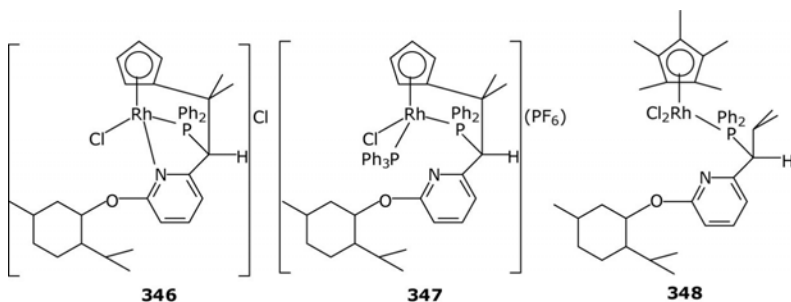


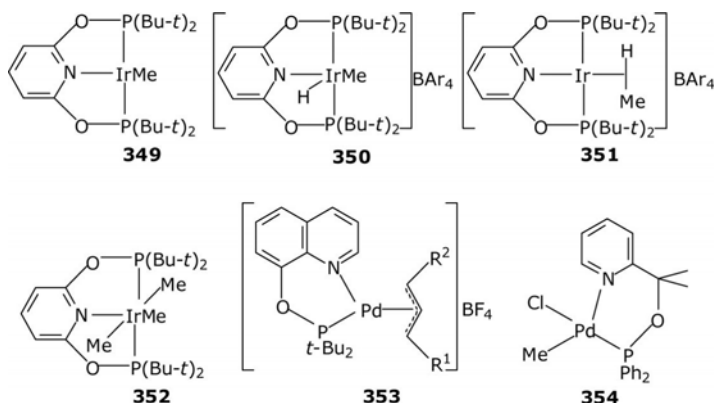
$\text{C}_5\text{H}_4\text{CH}_2\text{OPPh}_2$ and $\text{C}_5\text{H}_4\text{NHPPH}_2$ (L) react with cyclometalated $[\text{Pd}(\eta^2(\text{C},\text{N})\text{-L}^1)(\mu\text{-Cl})]_2$ ($\text{L}^1 = 2\text{-phenylpyridine}, 7,8\text{-benzoquinoline}, 2\text{-phenyloxazoline}$) and potassium hexafluorophosphate to yield cationic chelates **342** ($\text{X} = \text{CH}_2\text{O}, \text{NH}$) ([04ICA4568](#)). Palladacyclopentadiene $[\text{Pd}_4(\text{C}_4(\text{COOMe})_4)(\text{AN})_2]$ with the same ligands gives **343** ($\text{X} = \text{CH}_2\text{O}, \text{NH}$). O-Diphenylphosphino-2-hydroxypyridine with $[(\eta^4\text{-cod})\text{PtMe}_2]$ gives $[\text{PtMe}_2(\eta^1(\text{P})\text{-L})_2]$, but with $[(\eta^5\text{-Cp}^*)\text{RhCl}_2]_2$ chelate $[(\eta^5\text{-Cp}^*)\text{Rh}(\eta^2(\text{N},\text{P})\text{-L})\text{Cl}]\text{Cl}$ results ([02ICC803](#)). Complex **344** contains a P,N-chelate represented by tris(chloro((1-methyl-1-(6-methyl-2-pyridyl)ethoxy)diphenylphosphine- $\eta^2\text{-N},\text{P}$)) ([06AX\(C\)81](#)). Di-*i*-propyl- and diphenyl-8-oxyquinolyolphosphinite with the nickelacycle $[(\text{py})_2\text{Ni-CH}_2\text{CH}_2\text{-COO}]$ give nickelalactones **345** ($\text{R} = i\text{-Pr}, \text{Ph}$) ([05ZAAC2719](#)).



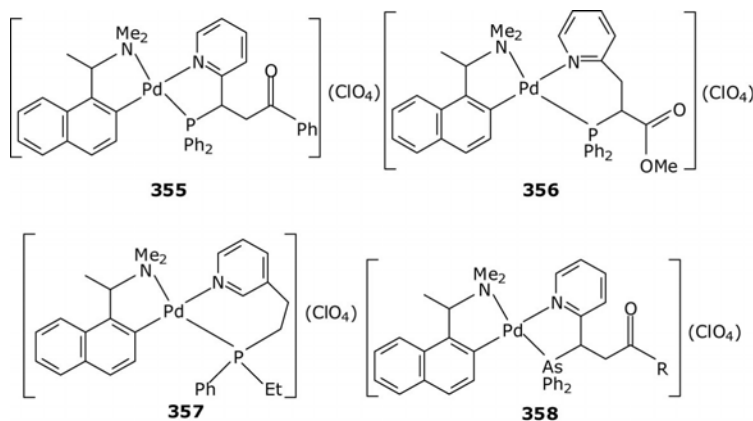


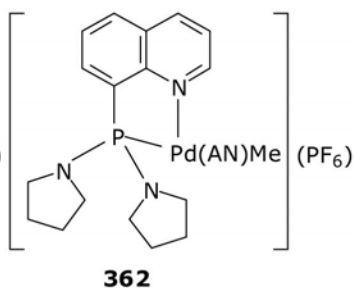
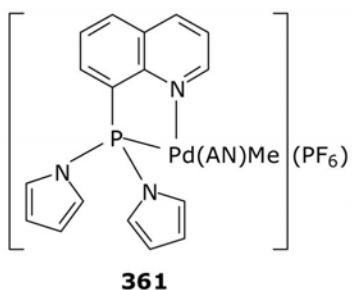
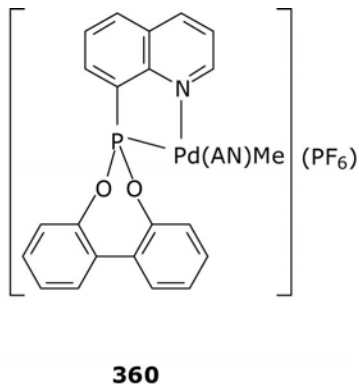
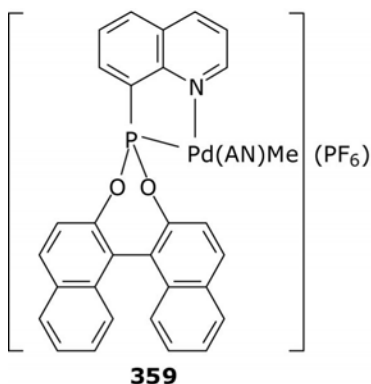
2-(2-Cyclopentadienyl-1-diphenylphosphinyl-2-methylprop-1-yl)-6-(1-menthoxy)pyridine furnishes an original approach to the half-sandwich of rhodium **346**, the result of interaction of the cyclopentadienyl ligand and rhodium(III) chloride (04JOM4244). The product contains the N,P-chelated ligand, which, however, transforms to P-coordinated **347** on reaction with triphenylphosphine and ammonium hexafluorophosphate. 2-(1-Diphenylphosphinyl-2-methylprop-1-yl)-6-(1-menthoxy)pyridine forms predominantly the half-sandwich **348** by the classical scheme of reacting with $[(\eta^5\text{-Cp}^*)\text{Rh}(\text{Cl})(\mu\text{-Cl})_2]$. 2,6-Bis(di-*t*-butylphosphinito)pyridine forms iridium(I) methyl **349**, which on protonation with HBAr^{F} yields the iridium(III) methyl hydride, cationic **350**, undergoing in solution C–H bond coupling to give **351** and reductive elimination (09JA8603). When the reaction with molecular hydrogen is conducted in benzene at -196°C and the mixture is warmed to ambient temperature, *trans*-dihydride **352** is the product (10JA4534). 2,6-($\text{Ph}_2\text{PCH}(\text{R})_2\text{C}_5\text{H}_3\text{N}$ and 2,6-($\text{Ph}_2\text{POCH}(\text{R})_2\text{C}_5\text{H}_3\text{N}$ ($\text{R} = \text{H}, \text{Me}$) with $[(\eta^4\text{-cod})\text{Ir}(\mu\text{-Cl})_2]$ and potassium perchlorate give $[(\eta^4\text{-cod})\text{Ir}(\eta^3(\text{P},\text{N},\text{P})\text{-L})\text{Ir}](\text{ClO}_4)$, active catalysts in hydrogenation of imines (96TL4937). 8-(Di-*t*-butylphosphinoloxo)quinoline with $[(\eta^3\text{-C}_3\text{H}_3\text{R}^1\text{R}^2)\text{Pd}(\mu\text{-Cl})_2]$ ($\text{R}^1 = \text{R}^2 = \text{H}$; $\text{R}^1 = \text{H}, \text{R}^2 = \text{Ph}$; $\text{R}^1 = \text{R}^2 = \text{Ph}$) in the presence of sodium tetrafluoroborate gives cationic **353**, one of which with $\text{R}^1 = \text{R}^2 = \text{H}$ serves as an efficient catalyst precursor for the coupling of aryl halides with boronic acid (08JOM3932). The structures of palladium (II) methyl complexes of 1-methyl-1-(6-methyl-2-pyridyl)ethoxydiphenylphosphine and 2-(2,6-dimethylphenyl)-6-(diphenylphosphinomethyl)pyridine are square-planar, for example, **354** (06AX(C)81).



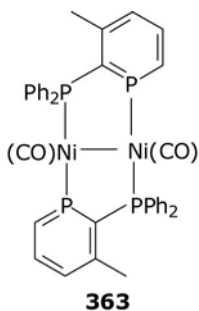


Organopalladium *ortho*-metalated (1-(dimethylamino)ethyl)naphthalene serves as a promoter of hydrophosphination of 1-phenyl-3-pyridin-2-yl-2-propenone and 1-methyl-3-pyridin-2-yl-2-propenoate with diphenylphosphine to generate P–N chelates **355** and **356** (09OM3941). 2-Vinylpyridine and phenylethylphosphine enter hydrophosphination reaction with an *ortho*-metalated [(1-(dimethylamino)ethyl)-2-naphthyl- $\text{C}_{2,2}\text{N}$]palladium(II) unit containing two acetonitrile ligands as a perchlorate salt to yield **357** (10OM3374). 1-Phenyl-3-(pyridin-2-yl)-2-propenone or 1-methyl-3-(pyridin-2-yl)-2-propenoate with diphenylarsine and organopalladium *o*-metalated (1-(dimethylamino)ethyl)naphthalene give the arsinopyridine-based $\eta^2(\text{As},\text{N})$ -chelates **358** ($\text{R} = \text{Ph}, \text{Me}$) (09EJ14134). The P,N-ligands based on quinoline with $[(\eta^4\text{-cod})\text{Pd}(\text{Cl})\text{Me}]$ in the presence of silver hexafluorophosphate give **359–362** (06JOM1143). A similar organometallic series follows from *trans*-chloro(1-naphthyl)bis(triphenylphosphine)nickel. Neutral products $[(1\text{-naphthyl})\text{Ni}(\eta^2(\text{N},\text{P})\text{-L})\text{Cl}]$ are active in oligomerization of ethylene.



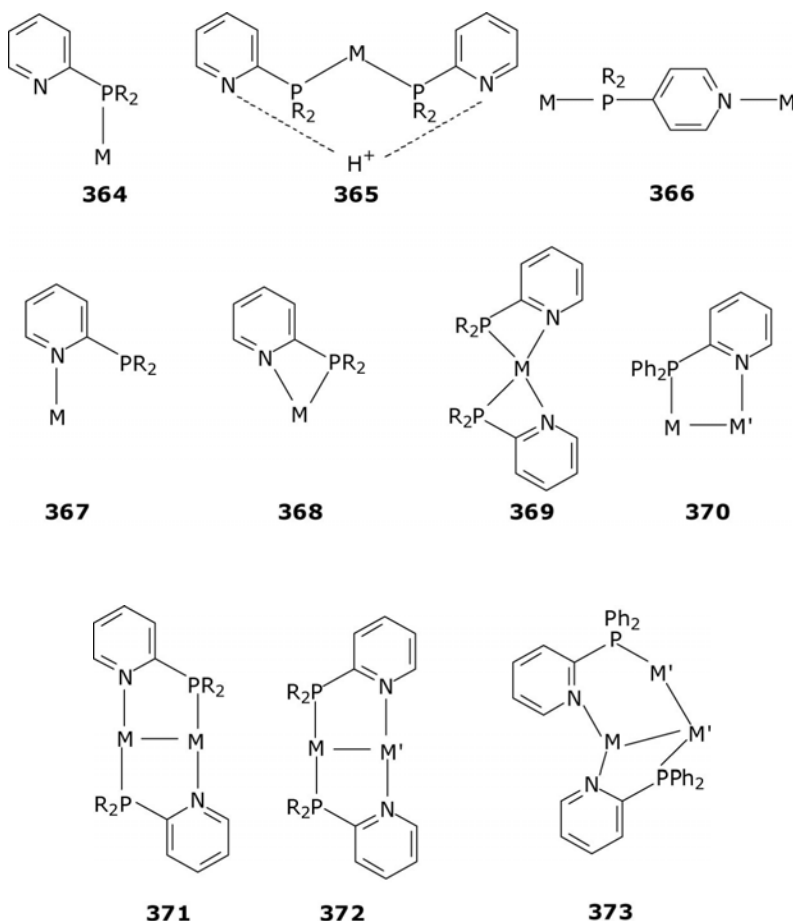


2-Diphenylphosphinophosphinine forms PPh_2 -coordinated pentacarbonyl tungsten (91OM2432). 2-Diphenylphosphino-3-methyl-phosphinine react with $[(\eta^4\text{-cod})\text{Ni}]_2$ in THF and further with carbon monoxide to produce dinuclear **363** (97JOM(541)277). An alternate way of preparation utilizes $\text{NiBr}_2\cdot\text{DME}$, zinc powder, and carbon monoxide in THF.

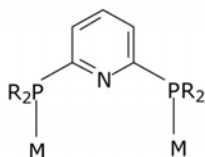
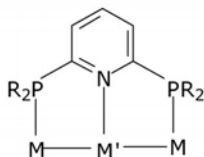
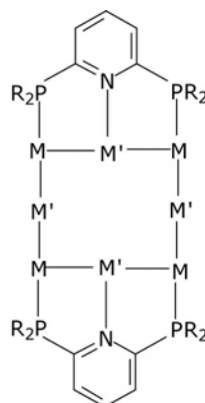
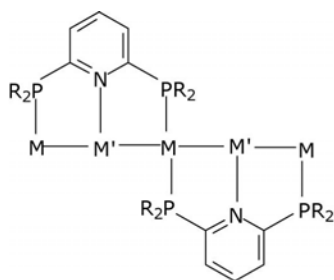
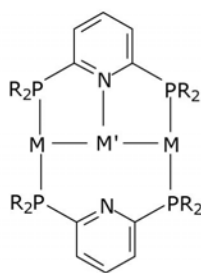
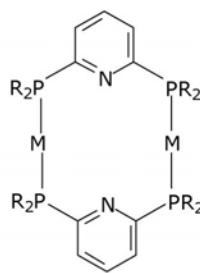


9. CONCLUSIONS

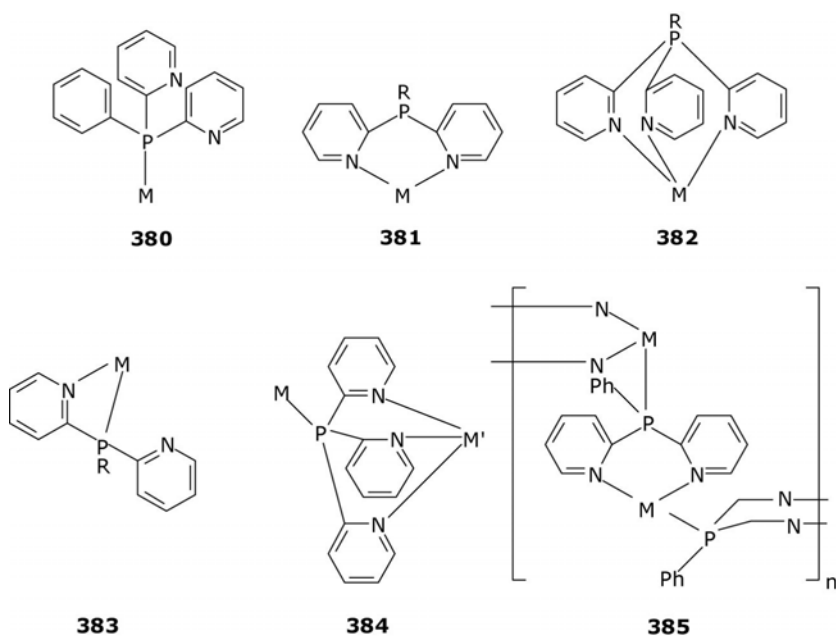
Monophosphinopyridines frequently exhibit the $\eta^1(\text{P})$ -coordination mode **364**, and may form P,P-coordinated dinuclear **365**, which is shown in a protonated form. The proton is delocalized among the pyridine heteroatoms of adjacent ligands. Dinuclear complex formation may be served by one ligand, **366**. N-Coordination **367**, although sometimes stated, always tentative and of low probability, in organometallic chemistry. Chelation of **368** and **369** is also relatively rare due to the formation of a strained four-membered metallocycle. The most widely spread case is a bridging function, which may occur in various versions, **370–372**. Another opportunity is a combination of chelation and bridging as in trinuclear **373**.



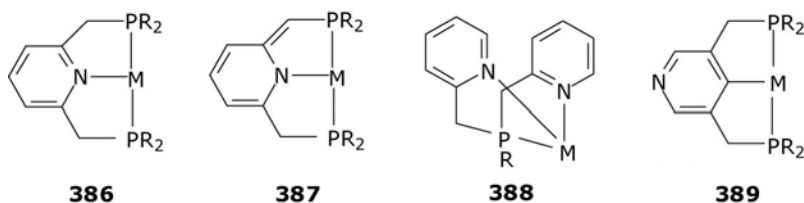
Bis(phosphino)pyridines are typically P,P-coordinated initially as in **374**. However, subsequently, they form various bridges in which pyridine heteroatoms may be fully involved as in **375–377**, partially involved in **378**, or not involved in **379** as polynuclear complexes.

**374****375****376****377****378****379**

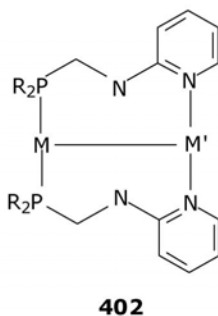
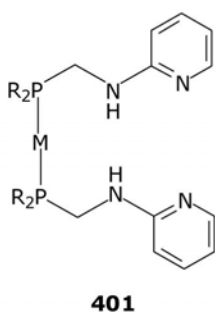
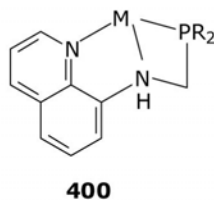
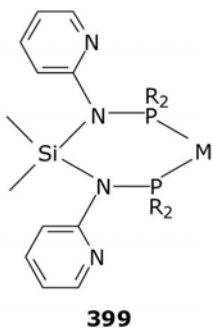
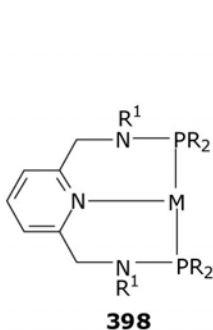
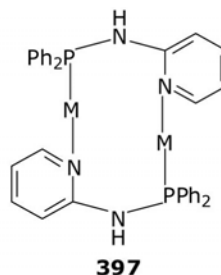
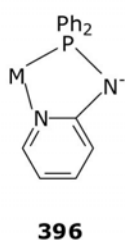
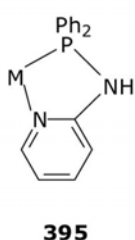
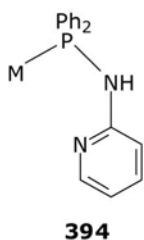
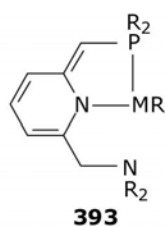
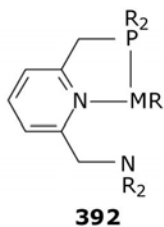
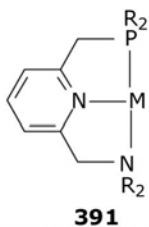
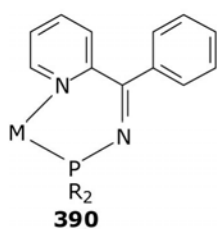
Bis- and tris-pyridyl phosphines often initiate P-coordination, **380**. However, cases of *N,N*-**381** or *N,N,N*-**382** coordination without a phosphorus atom also occur, as well as strained chelation with the exclusion of one or two pyridine nitrogens, **383**. Bridging cases may be straightforward, **384**, and complicated, **385**.



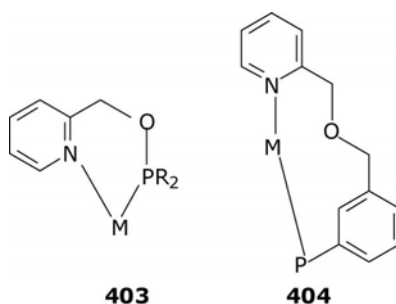
Pyridylphosphinoalkane ligands are typical chelate-forming compounds, **386**, extremely popular in homogenous catalysis when sometimes dearomatization of one, **387**, or both arms in the pincer occurs. The chelate function may combine with the bridging mode, **388**. In some specific ligands P,C,C-coordination **389** is possible.



Iminophosphoranes typically form N,P-chelates **390**. For the compounds with mixed phosphino- and amino-functions, apart from expected N,N,P-chelation **391**, there are frequent cases when an amino group is excluded from coordination, **392** and **393**. Diphenylphosphino-2-amino-pyridine may exhibit various co-ordination modes, monodentate **394**, neutral and anionic chelating, **395** and **396**, and bridging **397**. Other chelating environments may be classical pincer **398**, P,P- **399**, or double **400**. Also, transformation from the monodentately coordinated **401** to the bridging heterodinuclear **402** occurs quite frequently.



Oxygen containing phosphinopyridines is more rare but some interesting and useful chelates of type **403** and **404** may be considered representative.



ABBREVIATIONS

Ac	acetyl
acac	acetylacetonate
AN	acetonitrile
BAr ^F	tetra(3,5-di(trifluoromethyl)phenyl)borate
bipy	bipyridine
Bu	butyl
cod	cyclooctadiene-1,4
COE	cyclooctene
Cp	cyclopentadienyl
Cp [*]	pentamethylcyclopentadienyl
Cy	cyclohexyl
dba	dibenzoylacetone
DMSO	dimethylsulfoxide
dppp	diphenylphosphinopropane
Fc	ferrocenyl
Et	ethyl
MA	maleic anhydride
Me	methyl
Mes	mesityl
nbd	norbornadiene
NLO	non-linear optics
OTf	triflate
oxy	oxyquinoline
Ph	phenyl
PPN	N(PPh ₃) ₂
Pr	propyl
py	pyridine

solv	solvent
tfb	tetrafluorobenzobarrelene
THF	tetrahydrofuran
THT	tetrahydrothiophene
TMEDA	<i>N,N,N',N'</i> -tetramethylethylenediamine
Tol	tolyl
Xyl	xylyl

REFERENCES

- 73ICA(7)713 W.J. Knebel and R.J. Angelici, *Inorg. Chim. Acta*, **7**, 713 (1973).
- 74IC632 W.J. Knebel and R.J. Angelici, *Inorg. Chem.*, **13**, 632 (1974).
- 79IC1391 H.A. Hudali, J.V. Kingston, and H.A. Tayim, *Inorg. Chem.*, **18**, 1391 (1979).
- 80ICA(40)207 K. Wajda, F. Pruchnik, and T. Lis, *Inorg. Chim. Acta*, **40**, 207 (1980).
- 80JA6654 J.P. Farr, M.M. Olmstead, and A.L. Balch, *J. Am. Chem. Soc.*, **102**, 6654 (1980).
- 80JCS(D)55 K. Kurtev, D. Ribola, R.A. Jones, D.J. Cole-Hamilton, and G. Wilkinson, *J. Chem. Soc., Dalton Trans.*, 55 (1980).
- 80JCS(D)1974 A.J. Deeming, I.P. Rothwell, M.B. Hursthouse, and K.M.A. Malik, *J. Chem. Soc., Dalton Trans.*, 1974 (1980).
- 81IC1182 J.P. Farr, M.M. Olmstead, C.H. Hunt, and A.L. Balch, *Inorg. Chem.*, **20**, 1182 (1981).
- 81IC4060 M.M. Olmstead, A. Maisonnat, J.P. Farr, and A.L. Balch, *Inorg. Chem.*, **20**, 4060 (1981).
- 81ICA(53)L217 A. Maisonnat, J.P. Farr, and A.L. Balch, *Inorg. Chim. Acta*, **53**, L217 (1981).
- 82AJC2193 G.L. Roberts, B.W. Skelton, A.H. White, and S.B. Wild, *Aust. J. Chem.*, **35**, 2193 (1982).
- 82IC3961 A. Maisonnat, J.P. Farr, M.M. Olmstead, C.H. Hunt, and A.L. Balch, *Inorg. Chem.*, **21**, 3961 (1982).
- 83IC1229 J.P. Farr, M.M. Olmstead, and A.L. Balch, *Inorg. Chem.*, **22**, 1229 (1983).
- 83IC2644 M.P. Anderson, B.M. Mattson, and L.H. Pigolet, *Inorg. Chem.*, **22**, 2644 (1983).
- 83IC3267 M.P. Anderson, C.C. Tso, B.M. Mattson, and L.H. Pigolet, *Inorg. Chem.*, **22**, 3267 (1983).
- 83JA792 J.P. Farr, M.M. Olmstead, F.E. Wood, and A.L. Balch, *J. Am. Chem. Soc.*, **105**, 792 (1983).
- 83JA4090 T.J. Barder, S.M. Tetrack, and R.A. Walton, *J. Am. Chem. Soc.*, **105**, 4090 (1983).
- 83JA6332 F.E. Wood, M.M. Olmstead, and A.L. Balch, *J. Am. Chem. Soc.*, **105**, 6332 (1983).
- 83JA6986 F.E. Wood, J. Hvoslef, and A.L. Balch, *J. Am. Chem. Soc.*, **105**, 6986 (1983).
- 83OM1246 M.P. Anderson and L.H. Pigolet, *Organometallics*, **2**, 1246 (1983).
- 83OM1758 J.P. Farr, M.M. Olmstead, N.M. Rutherford, F.E. Wood, and A. L. Balch, *Organometallics*, **2**, 1758 (1983).
- 84JA1323 T.J. Barder, F.A. Cotton, G.L. Powell, S.M. Terrick, and R.A. Walton, *J. Am. Chem. Soc.*, **106**, 1323 (1984).

- 85CB3380 H. Brunner and H. Weber, *Chem. Ber.*, **118**, 3380 (1985).
- 85IC1935 R.J. McNair, P.V. Nilsson, and L.H. Pignolet, *Inorg. Chem.*, **24**, 1935 (1986).
- 85JA6936 A.L. Balch, H. Hope, and F.E. Wood, *J. Am. Chem. Soc.*, **107**, 6936 (1985).
- 86IC7 N. Lugan, G. Lavigne, and J.J. Bonnet, *Inorg. Chem.*, **25**, 7 (1986).
- 86IC3534 L.J. Tortorelli, C.A. Tucker, and C. Woods, *Inorg. Chem.*, **25**, 3534 (1986).
- 86IC4526 A.L. Balch, A.L. Fossett, and M.M. Olmstead, *Inorg. Chem.*, **25**, 4526 (1986).
- 86IC4717 R.J. McNair and L.H. Pignolet, *Inorg. Chem.*, **25**, 4717 (1986).
- 86JOM(314)357 Z.Z. Zhang, H.K. Wang, H.G. Wang, and R.J. Wang, *J. Organomet. Chem.*, **314**, 357 (1986).
- 86OM918 J.T. Mague, *Organometallics*, **5**, 918 (1986).
- 87IC585 N. Lugan, G. Lavigne, and J.J. Bonnet, *Inorg. Chem.*, **26**, 585 (1987).
- 87ZAAC83 W. Schirmer, U. Florke, and H.J. Haupt, *Z. Anorg. Allg. Chem.*, **545**, 83 (1987).
- 88IC325 H.H. Wang, A.L. Casalnuovo, B.J. Johnson, A.M. Mueting, and L. H. Pignolet, *Inorg. Chem.*, **27**, 325 (1988).
- 88IC1649 M.P. Anderson, A.L. Casalnuovo, B.J. Johnson, B.M. Mattson, A. M. Mueting, and L.H. Pignolet, *Inorg. Chem.*, **27**, 1649 (1988).
- 88JA5369 N. Lugan, G. Lavigne, J.J. Bonnet, R. Reau, D. Neibecker, and I. Tkatchenko, *J. Am. Chem. Soc.*, **110**, 5369 (1988).
- 88PAC555 A.L. Balch, *Pure Appl. Chem.*, **60**, 555 (1988).
- 88POL1751 C. Woods and L.J. Tortorelli, *Polyhedron*, **7**, 1751 (1988).
- 88TMC22 K. Wajda-Hermanowicz and F.P. Pruchnik, *Transit. Met. Chem.*, **13**, 22 (1988).
- 88TMC101 K. Wajda-Hermanowicz and F.P. Pruchnik, *Transit. Met. Chem.*, **13**, 101 (1988).
- 89AGE1361 P. Braunstein, M. Knorr, A. Tiripicchio, and M. Tiripicchio-Camellini, *Angew. Chem., Int. Ed. Engl.*, **28**, 1361 (1989).
- 89CC9 T. Tsuda, S. Morikawa, and T. Saegusa, *J. Chem. Soc., Chem. Commun.*, **9**, (1989).
- 89IC2944 E. Rotondo, S. Lo Schiavo, G. Bruno, C.G. Arena, R. Gobetto, and F. Faraone, *Inorg. Chem.*, **28**, 2944 (1989).
- 89JOM(376)123 Z.Z. Zhang, H.K. Wang, Z. Xi, R.J. Wang, and X.K. Yao, *J. Organomet. Chem.*, **376**, 123 (1989).
- 89OM391 B.M. Mattson and L.N. Ito, *Organometallics*, **8**, 391 (1989).
- 89OM886 G. Bruno, S. Lo Schiavo, E. Rotondo, C.G. Arena, and F. Faraone, *Organometallics*, **8**, 886 (1989).
- 89ZAAC74 H. tom Dieck and G. Hahn, *Z. Anorg. Allg. Chem.*, **577**, 74 (1989).
- 90AOC173 K. Wajda-Hermanowicz, M. Koralewicz, and F.P. Pruchnik, *Appl. Organomet. Chem.*, **4**, 173 (1990).
- 90JOM(387)357 S. Lo Schiavo, F. Faraone, M. Lanfranchi, and A. Tiripicchio, *J. Organomet. Chem.*, **387**, 357 (1990).
- 90JOM(389)417 V.K. Jain, V.S. Jakkal, and R. Bohra, *J. Organomet. Chem.*, **389**, 417 (1990).
- 90JOM(397)93 C. Moreno, M.J. Macazaga, and S. Delgado, *J. Organomet. Chem.*, **397**, 93 (1990).
- 90POL1479 H.G. Ang, W.L. Kwik, and P.T. Lau, *Polyhedron*, **9**, 1479 (1990).
- 91JMC(66)183 S. Gladiali, L. Pinna, C.G. Arena, E. Rotondo, and F. Faraone, *J. Mol. Catal.*, **66**, 183 (1991).
- 91JOM(417)277 Y. Xie and B.R. James, *J. Organomet. Chem.*, **417**, 277 (1991).

- 91JOM(419)399 E. Rotondo, G. Battaglia, C.G. Arena, and F. Faraone, *J. Organomet. Chem.*, **419**, 399 (1991).
- 91OM1613 S. Lo Schiavo, E. Rotondo, G. Bruno, and F. Faraone, *Organometallics*, **10**, 1613 (1991).
- 91OM2432 P. Le Floch, D. Carmichael, and F. Mathey, *Organometallics*, **10**, 2432 (1991).
- 91OM3877 C.G. Arena, E. Rotondo, F. Faraone, M. Lanfranchi, and A. Tiripicchio, *Organometallics*, **10**, 3877 (1991).
- 92AX(C)999 N. Lugan, G. Lavigne, and J.J. Bonnet, *Acta Crystallogr.*, **C48**, 999 (1992).
- 92CJC751 Y. Xie, C.L. Lee, Y. Yang, S.J. Rettig, and B.R. James, *Can. J. Chem.*, **70**, 751 (1992).
- 92IC4797 C.G. Arena, F. Faraone, M. Lanfranchi, E. Rotondo, and A. Tiripicchio, *Inorg. Chem.*, **31**, 4797 (1992).
- 92JCS(D)1847 C.G. Arena, F. Faraone, M. Fochi, M. Lanfranchi, C. Meali, R. Seeber, and A. Tiripicchio, *J. Chem. Soc., Dalton Trans.*, 1847 (1992).
- 92JCS(D)2367 M. Grassi, G. de Muno, F. Nicolo, and S. Lo Schiavo, *J. Chem. Soc., Dalton Trans.*, 2367 (1992).
- 93CC444 A. Steiner and D. Stalke, *J. Chem. Soc., Chem. Commun.*, **444**, (1993).
- 93CC844 A.J. Deeming and M.B. Smith, *J. Chem. Soc., Chem. Commun.*, 844 (1993).
- 93CC1673 J.M. Brown, D.I. Hulmes, and T.P. Layzell, *J. Chem. Soc., Chem. Commun.*, 1673 (1993).
- 93CRV2067 G.R. Newkome, *Chem. Rev.*, **93**, 2067 (1993).
- 93IC1363 N. Lugan, P.L. Fahre, D. de Montauzon, G. Lavigne, J.J. Bonnet, J.I. Saillard, and J.F. Halet, *Inorg. Chem.*, **32**, 1363 (1993).
- 93IC1601 C.G. Arena, G. Bruno, G. De Munno, R. Rotondo, D. Drommi, and F. Faraone, *Inorg. Chem.*, **32**, 1601 (1993).
- 93IC1656 G. Reinhard, B. Hirle, U. Schubert, M. Knorr, P. Braunstein, A. DeCian, and J. Fischer, *Inorg. Chem.*, **32**, 1656 (1993).
- 93IC3287 F. Shafiq and R. Eisenberg, *Inorg. Chem.*, **32**, 3287 (1993).
- 93JCS(D)2041 A.J. Deeming and M.B. Smith, *J. Chem. Soc., Dalton Trans.*, 2041 (1993).
- 93JCS(D)2075 V.W.W. Yam, L.P. Chan, and T.F. Lai, *J. Chem. Soc., Dalton Trans.*, 2075 (1993).
- 93JCS(D)3001 L. Costella, A. Del Zotto, A. Mezzetti, E. Zangrando, and P. Rigo, *J. Chem. Soc., Dalton Trans.*, 3001 (1993).
- 93JCS(D)3383 A.J. Deeming and M.B. Smith, *J. Chem. Soc., Dalton Trans.*, 3383 (1993).
- 93JOM(450)145 P. Espinet, P. Gomez-Eliphe, and F. Villafane, *J. Organomet. Chem.*, **450**, 145 (1993).
- 93JOM(450)263 G. De Munno, G. Bruno, C.G. Arena, D. Drommi, and F. Faraone, *J. Organomet. Chem.*, **450**, 263 (1993).
- 93JOM(454)221 Z.Z. Zhang, H.P. Xi, W.J. Zhao, K.Y. Jiang, R.J. Wang, H.G. Wang, and Y. Wu, *J. Organomet. Chem.*, **454**, 221 (1993).
- 93JOM(455)247 E. Drent, P. Arnoldy, and P.H.M. Budzelaar, *J. Organomet. Chem.*, **455**, 247 (1993).
- 93JOM(462)271 P. Braunstein, T. Faure, M. Knorr, F. Balegroune, and D. Grandjean, *J. Organomet. Chem.*, **462**, 271 (1993).
- 93T(A)743 N.W. Alcock, J.M. Brown, and D.I. Hulmes, *Tetrahedron: Asymmetry*, **4**, 743 (1993).
- 94CC615 M.C. Bonnet, F. Dahan, A. Ecke, W. Kein, R.P. Schulz, and I. Tkachenko, *J. Chem. Soc., Chem. Commun.*, 615 (1994).

- 94CC2251 C.G. Arena, F. Nicolo, D. Drommi, G. Bruno, and F. Faraone, *J. Chem. Soc., Chem. Commun.*, 2251 (1994).
- 94ICA(216)209 S. Lo Schiavo, M. Grassi, G. De Munno, F. Nicolo, and G. Tresoldi, *Inorg. Chim. Acta*, **216**, 209 (1994).
- 94ICA(217)209 L.Y. Xie and B.R. James, *Inorg. Chim. Acta*, **217**, 209 (1994).
- 94ICA(221)109 D. Drommi, F. Nicolo, C.G. Arena, G. Bruno, F. Faraone, and R. Gobetto, *Inorg. Chim. Acta*, **221**, 109 (1994).
- 94JCS(D)117 P. Braunstein, M. Knorr, M. Stampfer, A. DeCian, and J. Fischer, *J. Chem. Soc., Dalton Trans.*, **117**, (1994).
- 94JCS(D)2257 A. Del Zotto, A. Mezzetti, and P. Rigo, *J. Chem. Soc., Dalton Trans.*, 2257 (1994).
- 94JCS(D)2755 M. Alvarez, N. Lugan, and R. Mathieu, *J. Chem. Soc., Dalton Trans.*, **2755**, (1994).
- 94JOM(475)55 E. Drent, P. Arnoldy, and P.H.M. Budzelaar, *J. Organomet. Chem.*, **475**, 55 (1994).
- 94JOM(484)171 C.G. Arena, G. Ciani, D. Drommi, F. Faraone, D.M. Proserpio, and E. Rotondo, *J. Organomet. Chem.*, **484**, 71 (1994).
- 94PIC238 A.L. Balch, *Progr. Inorg. Chem.*, **41**, 238 (1994).
- 94T4493 J.M. Brown, D.I. Hulmes, and P.J. Guiry, *Tetrahedron*, **50**, 4493 (1994).
- 95CC331 P. Wehman, R.E. Rulke, V.E. Kaasjager, P.C.J. Kamer, H. Kooijman, A. L. Spek, C.J. Elsevier, K. Vrieze, and P.W.N.M. van Leeuwen, *J. Chem. Soc., Chem. Commun.*, 331 (1995).
- 95ICA(232)207 K. Wajda-Hermanowicz, F. Pruchnik, M. Zuber, G. Rusek, E. Galdecka, and Z. Galdecki, *Inorg. Chim. Acta*, **232**, 207 (1995).
- 95ICA(235)291 I.R. Baird, M.B. Smith, and B.R. James, *Inorg. Chim. Acta*, **235**, 291 (1995).
- 95JOM(485)115 D. Drommi, C.G. Arena, F. Nicolo, G. Bruno, and F. Faraone, *J. Organomet. Chem.*, **485**, 115 (1995).
- 95MI1 P.R. Sharp, In: *Comprehensive Coordination Chemistry* (E.W. Abel, F.G.A. Stone, and G. Wilkinson, eds.), Vol. 8, Chapter 2, p. 152, Pergamon Press, Oxford, 1995.
- 95OM2422 A. Steiner and D. Stalke, *Organometallics*, **14**, 2422 (1995).
- 95OM3058 J.A. Casares, S. Coco, P. Espinet, and Y.S. Lin, *Organometallics*, **14**, 3058 (1995).
- 95OM5302 A. Ecke, W. Keim, M.C. Bonnet, I. Tkachenko, and F. Dahan, *Organometallics*, **14**, 5302 (1995).
- 95T(A)2593 J.M. Valk, G.A. Whitlock, T.P. Layzell, and J.M. Brown, *Tetrahedron (Asymmetry)*, **6**, 2593 (1995).
- 95TL9015 A. Scrivanti and U. Matteoli, *Tetrahedron Lett.*, **36**, 9015 (1995).
- 96CCR(147)1 Z.Z. Zhang and H. Cheng, *Coord. Chem. Rev.*, **147**, 1 (1996).
- 96CJC2064 R.P. Schutte, S.J. Rettig, and B.R. James, *Can. J. Chem.*, **74**, 2064 (1996).
- 96IC1792 A. Weisman, M. Gozin, H.B. Kraatz, and D. Milstein, *Inorg. Chem.*, **35**, 1792 (1996).
- 96ICA(248)257 R. Gobetto, C.G. Arena, D. Drommi, and F. Faraone, *Inorg. Chim. Acta*, **248**, 257 (1996).
- 96JCC273 M.J. Don, K. Yang, S.J. Bott, and M.J. Richmond, *J. Coord. Chem.*, **40**, 273 (1996).
- 96JCS(D)1295 S. Stoccoro, G. Chelucci, A. Zucca, M.A. Cinellu, G. Minghetti, and M. Manassero, *J. Chem. Soc., Dalton Trans.*, 1295 (1996).
- 96JCS(D)3475 S.L. Li, T.C.W. Mak, and Z.Z. Zhang, *J. Chem. Soc., Dalton Trans.*, 3475 (1996).
- 96JNS230 Z. Li, C. Chiming, and P. Chungkwong, *J. Nat. Sci.*, **1**, 230 (1996).

- 96JOM(508)75 K. Wajda-Hermanowitz, F. Pruchnik, and M. Zuber, *J. Organomet. Chem.*, **509**, 75 (1996).
- 96JOM(516)1 Z.Z. Zhang, H. Chen, S.M. Kuang, Y.Q. Zhou, Z.X. Liu, J.K. Zhang, and H.G. Wang, *J. Organomet. Chem.*, **516**, 1 (1996).
- 96OM3022 R.E. Rulke, V.E. Kaasjager, P. Wehman, C.J. Elsevier, P.W.N.M. van Leeuwen, and K. Vrieze, *Organometallics*, **15**, 3022 (1996).
- 96OM3170 C.G. Arena, D. Drommi, F. Faraone, M. Lanfranchi, F. Nicolo, and A. Tiripicchio, *Organometallics*, **15**, 3170 (1996).
- 96POL2583 J.K. Zhang, Z.M. Zhang, A. Yu, S.L. Zhao, and W.D. Zhang, *Polyhedron*, **15**, 2583 (1996).
- 96POL3417 S.M. Kuang, H. Cheng, L.J. Sun, Z.Z. Zhang, Z.Y. Zhou, B.M. Wu, and T.C.W. Mak, *Polyhedron*, **15**, 3417 (1996).
- 96RCT248 J. Keijsper, P. Arnoldy, M.J. Doyle, and E. Drent, *Recl. Trav. Chim. Pays-Bas*, **115**, 248 (1996).
- 96T(A)885 G. Chelucci, M.A. Cabras, C. Botteghi, C. Basoli, and M. Marchetti, *Tetrahedron (Asymmetry)*, **7**, 885 (1996).
- 96TL797 Q. Jiang, D. Van Plew, S. Murtuza, and X. Zhang, *Tetrahedron Lett.*, **37**, 797 (1996).
- 96TL4617 R. Sablong and J.A. Osborn, *Tetrahedron Lett.*, **37**, 4617 (1996).
- 96TL4933 R. Sablong, C. Newton, P. Dierkes, and J.A. Osborn, *Tetrahedron Lett.*, **37**, 4933 (1996).
- 96TL4937 R. Sablong and J.A. Osborn, *Tetrahedron Lett.*, **37**, 4937 (1996).
- 97CB939 C. Hahn, J. Sieler, and R. Taube, *Chem. Ber.*, **130**, 939 (1997).
- 97CC1911 P. Braunstein, C. Charles, C. Charles, G. Kickelbick, and U. Schubert, *Chem. Commun.*, 1911 (1997).
- 97IC44 J.A. Casares, P. Espinet, R. Hernando, G. Iturbe, F. Villafane, D. D. Ellis, and A.G. Orpen, *Inorg. Chem.*, **36**, 44 (1997).
- 97IC5251 J.A. Casares, P. Espinet, K. Soulantica, I. Pascual, and A.G. Orpen, *Inorg. Chem.*, **36**, 5251 (1997).
- 97IC5428 J.A. Casares and P. Espinet, *Inorg. Chem.*, **36**, 5428 (1997).
- 97IC5809 R.P. Schutte, S.J. Rettig, A.M. Joshi, and B.R. James, *Inorg. Chem.*, **36**, 5809 (1997).
- 97JCS(D)2843 J.S. Field, R.J. Haines, and C.J. Parry, *J. Chem. Soc., Dalton Trans.*, 2843 (1997).
- 97JCS(D)3409 S.M. Kuang, F. Xue, Z.Z. Zhang, W.M. Xue, C.M. Che, and T.C. W. Mak, *J. Chem. Soc., Dalton Trans.*, 3409 (1997).
- 97JCS(D)3777 R. Ziessel, L. Toupet, S. Chardon-Noblat, A. Deronzier, and D. Matt, *J. Chem. Soc., Dalton Trans.*, 3777 (1997).
- 97JOM(534)15 S.M. Kuang, F. Xue, C.Y. Duan, T.C.W. Mak, and Z.Z. Zhang, *J. Organomet. Chem.*, **534**, 15 (1997).
- 97JOM(540)55 S.M. Kuang, Z.Z. Zhang, B.M. Wu, and T.C.W. Mak, *J. Organomet. Chem.*, **540**, 55 (1997).
- 97JOM(541)277 N. Mezailles, P. Le Floch, K. Waschbusch, L. Ricard, F. Mathey, and C. P. Kubiak, *J. Organomet. Chem.*, **541**, 277 (1997).
- 97OM770 J.A. Casares, P. Espinet, J.M. Martinez-Ilarduya, and Y.S. Lin, *Organometallics*, **16**, 770 (1997).
- 97OM1401 H. Yang, M. Alvarez-Gressier, N. Lugan, and R. Mathieu, *Organometallics*, **16**, 1401 (1997).
- 97OM2089 H. Yang, N. Lugan, and R. Mathieu, *Organometallics*, **16**, 2089 (1997).
- 97OM3469 A.S.C. Chan, C.C. Chen, R. Cao, M.R. Lee, S.M. Peng, and G.H. Lee, *Organometallics*, **16**, 3469 (1997).

- 97OM3941 G. Jia, H.M. Lee, I.D. Williams, C.P. Lau, and Y. Chen, *Organometallics*, **16**, 3941 (1997).
- 97PSS473 S.M. Aucott, A.M.Z. Slawin, and J.D. Woollins, *Phosph., Sulfur, Silicon*, **124–125**, 473 (1997).
- 97T4035 T.D.W. Claridge, J.M. Long, J.M. Brown, D. Hibbs, and M. B. Hursthouse, *Tetrahedron*, **53**, 4035 (1997).
- 97T(A)3775 H. Doucet and J.M. Brown, *Tetrahedron (Asymmetry)*, **8**, 3775 (1997).
- 98CC1879 A. Caballero, F.A. Jalon, and B.R. Manzano, *Chem. Commun.*, 1879 (1998).
- 98CCR(178)903 P. Braunstein, M. Knorr, and C. Stern, *Coord. Chem. Rev.*, **178–180**, 903 (1998).
- 98EJI1425 C. Hahn, M. Spiegler, E. Herdtweck, and R. Taube, *Eur. J. Inorg. Chem.*, 1425 (1998).
- 98EJI1745 M.A. Alonso, J.A. Casares, P. Espinet, J.M. Martínez-Ilarduya, and C. Perez-Briso, *Eur. J. Inorg. Chem.*, 1745 (1998).
- 98ICC309 J.L. Bookham, *Inorg. Chem. Commun.*, **1**, 309 (1998).
- 98JCS(D)803 W.H. Chan, Z.Z. Zhang, T.C.W. Mak, and C.M. Che, *J. Chem. Soc., Dalton Trans.*, 803 (1998).
- 98JCS(D)1115 S.M. Kuang, Z.Z. Zhang, Q.G. Wang, and T.C.W. Mak, *J. Chem. Soc., Dalton Trans.*, 1115 (1998).
- 98JCS(D)3771 A. Dervisi, P.E. Edwards, P.D. Neuman, R.P. Tooze, S.J. Coles, and M. B. Hursthouse, *J. Chem. Soc., Dalton Trans.*, 3771 (1998).
- 98JOM(559)31 S.M. Kuang, F. Xue, Z.Y. Zhang, T.C.W. Mak, and Z.Z. Zhang, *J. Organomet. Chem.*, **559**, 31 (1998).
- 98JOM(566)165 I. Moldes, E. de la Encarnacion, J. Ros, A. Alvarez-Larena, and J.F. Piniella, *J. Organomet. Chem.*, **566**, 165 (1998).
- 98JOM(570)63 F.P. Pruchnik, P. Smolenski, and K. Wajda-Hermanowicz, *J. Organomet. Chem.*, **570**, 63 (1998).
- 98OM338 G. Francio, R. Scopelliti, C.G. Arena, G. Bruno, D. Drommi, and F. Faraone, *Organometallics*, **17**, 338 (1998).
- 98OM630 A. Scriveranti, V. Beghetto, E. Campagna, M. Zanato, and U. Matteoli, *Organometallics*, **17**, 630 (1998).
- 98OM2060 C. Hahn, A. Vitagliano, F. Giordano, and R. Taube, *Organometallics*, **17**, 2060 (1998).
- 98OM3931 G. He, S.K. Loh, J.J. Vittal, K.F. Mok, and P.H. Leung, *Organometallics*, **17**, 3931 (1998).
- 98POL493 S.M. Kuang, Z.Z. Zhang, Q.C. Wang, and T.C.W. Mak, *Polyhedron*, **17**, 493 (1998).
- 98POL1183 C. Hahn, J. Sieler, and R. Taube, *Polyhedron*, **17**, 1183 (1998).
- 99CCR499 P. Espinet and K. Soulantica, *Coord. Chem. Rev.*, **193–195**, 499 (1999).
- 99EJI435 C. Hahn, M. Spiegler, E. Herdtweck, and R. Taube, *Eur. J. Inorg. Chem.*, 435 (1999).
- 99ICA(284)119 S.M. Kuang, F. Xue, T.C.W. Mak, and Z.Z. Zhang, *Inorg. Chim. Acta*, **284**, 119 (1999).
- 99ICA(293)106 S.M. Kuang, Z.Z. Zhang, K. Chinnakali, H.K. Fun, and T.C.W. Mak, *Inorg. Chim. Acta*, **293**, 106 (1999).
- 99JCL91 J.W.S. Hui and W.T. Wong, *J. Cluster Sci.*, **10**, 91 (1999).
- 99JCS(D)1113 A. Dervisi, P.G. Edwards, P.D. Newman, R.P. Tooze, S.J. Coles, and M. B. Hursthouse, *J. Chem. Soc., Dalton Trans.*, 1113 (1999).
- 99JOM(573)101 E.C. Constable, C.E. Housecroft, and A.G. Schneider, *J. Organomet. Chem.*, **573**, 101 (1999).
- 99JOM(573)189 Y.Y. Choi and W.T. Wong, *J. Organomet. Chem.*, **573**, 189 (1999).

- 99JOM(577)305 J.L. Bookham and D.M. Smithies, *J. Organomet. Chem.*, **577**, 305 (1999).
- 99JOM(588)160 F.E. Hong, Y.C. Chang, R.E. Chang, C.C. Lin, S.L. Wang, and F.L. Liao, *J. Organomet. Chem.*, **588**, 160 (1999).
- 99JOM(588)260 C.Y. Kuo, Y.S. Fuh, J.J. Shiue, S.J. Yu, G.H. Lee, and S.M. Peng, *J. Organomet. Chem.*, **588**, 260 (1999).
- 99OM3563 Y. Kataoka, M. Imanishi, T. Yamagata, and K. Tani, *Organometallics*, **18**, 3563 (1999).
- 99POL2995 U. Abram, R. Alberto, J.R. Dilworth, Y. Zheng, and K. Ortnert, *Polyhedron*, **18**, 2995 (1999).
- 99SL1563 K. Ito, R. Kashiwagi, K. Iwasaki, and T. Katsuki, *Synlett*, 1563 (1999).
- 00AGE1428 F. Faraone and W. Leitner, *Angew. Chem., Int. Ed.*, **39**, 1428 (2000).
- 00CRV1169 S.D. Ittel, L.K. Johnson, and M. Brookhart, *Chem. Rev.*, **100**, 1169 (2000).
- 00CRV3541 P. Braunstein and X. Morise, *Chem. Rev.*, **100**, 3541 (2000).
- 00EJI1031 P. Espinet, R. Hernando, G. Iturbe, F. Villafane, A.G. Orpen, and I. Pascual, *Eur. J. Inorg. Chem.*, 1031 (2000).
- 00EJI1411 J. Baur, H. Jacobsen, P. Burger, G. Artus, H. Berke, and L. Dahlenburg, *Eur. J. Inorg. Chem.*, 1411 (2000).
- 00EJI2523 L. Barloy, S. Ramdeehul, J.A. Osborn, C. Carlotti, F. Taulelle, A. De Cian, and J. Fischer, *Eur. J. Inorg. Chem.*, 2523 (2000).
- 00IC705 M.A. Alonso, J.A. Casares, P. Espinet, K. Soulantica, J.P.H. Charmant, and A.G. Orpen, *Inorg. Chem.*, **39**, 705 (2000).
- 00ICA(299)180 A. Del Zotto, E. Rocchini, F. Pichierri, E. Zangrando, and P. Rigo, *Inorg. Chim. Acta*, **299**, 180 (2000).
- 00ICC508 L. Hirsivaara, M. Haukka, and J. Pursiainen, *Inorg. Chem. Commun.*, **3**, 508 (2000).
- 00JCS(D)523 A. Dervisi, P.G. Edwards, P.D. Newman, and R.P. Tooze, *J. Chem. Soc., Dalton Trans.*, 523 (2000).
- 00JCS(D)975 J.L. Bookham, D.M. Smithies, and M.T. Pett, *J. Chem. Soc., Dalton Trans.*, 975 (2000).
- 00JCS(D)1549 R.J. van Haaren, C.J.M. Duijven, G.P.F. van Strijdonck, H. Oevering, J.N.H. Reek, P.C.J. Kamer, and P.W.N.M. van Leeuwen, *J. Chem. Soc., Dalton Trans.*, 1549 (2000).
- 00JCS(D)2559 S.M. Aucott, A.M.Z. Slawin, and J.D. Woollins, *J. Chem. Soc., Dalton Trans.*, 2559 (2000).
- 00JCS(D)2771 S.E. Durrant, M.B. Smith, A.M.Z. Slawin, and J.W. Steed, *J. Chem. Soc., Dalton Trans.*, 2771 (2000).
- 00T(A)4753 C.G. Arena, D. Drommi, and F. Faraone, *Tetrahedron: Asymmetry*, **11**, 4753 (2000).
- 01AGE4271 V.F. Slagt, J.N.H. Reek, P.C.J. Kamer, and P.W.N.M. van Leeuwen, *Angew. Chem., Int. Ed.*, **40**, 4271 (2001).
- 01CRV3435 G. Kiss, *Chem. Rev.*, **101**, 3435 (2001).
- 01EJI289 J.A. Casares, P. Espinet, J.M. Martin-Alvarez, G. Espino, M. Perez-Manrique, and F. Vattier, *Eur. J. Inorg. Chem.*, 289 (2001).
- 01EJI419 C. Hahn, P. Morvillo, and A. Vitagliano, *Eur. J. Inorg. Chem.*, 419 (2001).
- 01EJI721 D. Cauzzi, C. Graiff, C. Massera, G. Predieri, and A. Tiripicchio, *Eur. J. Inorg. Chem.*, 721 (2001).
- 01EJI2255 L. Hirsivaara, M. Haukka, and J. Pursiainen, *Eur. J. Inorg. Chem.*, 2255 (2001).
- 01IC1962 J.T. Mague and J.L. Krinsky, *Inorg. Chem.*, **40**, 1962 (2001).
- 01IC5928 H.B. Song, Z.Z. Zhang, and T.C.W. Mak, *Inorg. Chem.*, **40**, 5928 (2001).
- 01JC302 H.K. Reinius, P. Suomalainen, H. Riihimäki, E. Karvinen, J. Pursiainen, and A.O.I. Krause, *J. Catal.*, **199**, 302 (2001).

- 01JCS(D)972 S.M. Aucott, M.L. Clarke, A.M.Z. Slawin, and J.D. Woollins, *J. Chem. Soc., Dalton Trans.*, 972 (2001).
- 01JCS(D)3421 M.L. Clarke, A.M.Z. Slawin, M.V. Wheatley, and J.D. Woollins, *J. Chem. Soc., Dalton Trans.*, 3421 (2001).
- 01JOM(628)1 M.A. Rida, C. Coperet, and A.K. Smith, *J. Organomet. Chem.*, **628**, 1 (2001).
- 01JOM(633)66 L. Hirsivaara, M. Haukka, and J. Pursiainen, *J. Organomet. Chem.*, **633**, 66 (2001).
- 01NJC416 S.J. Coles, S.E. Durran, M.B. Hursthouse, A.M.Z. Slawin, and M. B. Smith, *New J. Chem.*, **25**, 416 (2001).
- 01OM667 S.H. Liu, S.T. Lo, T.B. Wen, Z.Y. Zhou, C.P. Lau, and G. Jia, *Organometallics*, **20**, 667 (2001).
- 01OM1960 M. Kawatsura and J.F. Hartwig, *Organometallics*, **20**, 1960 (2001).
- 01OM4126 D.J. Cui, Q.S. Li, F.B. Xu, X.B. Leng, and Z.Z. Zhang, *Organometallics*, **20**, 4126 (2001).
- 01T(A)1345 G. Delapierre, J.M. Brunel, T. Constantieux, and G. Buono, *Tetrahedron: Asymmetry*, **12**, 1345 (2001).
- 02ASC543 A. Scrivanti, V. Beghetto, and U. Matteoli, *Adv. Synth. Catal.*, **344**, 543 (2002).
- 02IC1372 P. Braunstein, C. Graiff, C. Hassera, G. Predieri, J. Rose, and A. Tiripicchio, *Inorg. Chem.*, **41**, 1372 (2002).
- 02IC3146 H.B. Song, Z.Z. Zhang, Z. Hui, C.M. Che, and T.C. Mak, *Inorg. Chem.*, **41**, 3146 (2002).
- 02ICA(330)95 C. Graiff, A. Ienco, C. Massera, C. Mealli, G. Predieri, A. Tiripicchio, and F. Uguzzoli, *Inorg. Chim. Acta*, **330**, 95 (2002).
- 02ICA(338)59 G. Francio, D. Drommi, C. Graiff, F. Faraone, and A. Tiripicchio, *Inorg. Chim. Acta*, **338**, 59 (2002).
- 02ICC803 P. Cheshire, A.M.Z. Slawin, and J.D. Woollins, *Inorg. Chem. Commun.*, **5**, 803 (2002).
- 02JA9038 C. Hahn, M.E. Cucciolito, and A. Vitagliano, *J. Am. Chem. Soc.*, **124**, 9038 (2002).
- 02JCS(D)1336 H.B. Song, Z.Z. Zhang, and T.C.W. Mak, *J. Chem. Soc., Dalton Trans.*, 1336 (2002).
- 02JCS(D)1618 M.L. Clarke, D.J. Cole-Hamilton, D.F. Foster, A.M.Z. Slawin, and J.D. Woollins, *J. Chem. Soc., Dalton Trans.*, 1618 (2002).
- 02JOM(655)172 F.E. Hong, S.C. Chen, Y.T. Tsai, and Y.C. Chang, *J. Organomet. Chem.*, **655**, 172 (2002).
- 02JOM(661)111 F. Baier, Z. Fei, H. Gornitzka, A. Murso, S. Neufeld, M. Pfeiffer, I. Rudenauer, A. Steiner, T. Stey, and D. Stalke, *J. Organomet. Chem.*, **661**, 111 (2002).
- 02NJC113 H.B. Song, Z.Z. Zhang, and T.C.W. Mak, *New J. Chem.*, **26**, 113 (2002).
- 02NJC1474 W.H. Sun, Z. Li, H. Hu, B. Wu, H. Yang, N. Zhu, X. Leng, and H. Wang, *New J. Chem.*, **26**, 1474 (2002).
- 02OM761 D. Drommi, F. Faraone, G. Francio, D. Beletti, C. Graiff, and A. Tiripicchio, *Organometallics*, **21**, 761 (2002).
- 02OM812 D. Hermann, M. Gandelman, H. Rozenberg, L.J.W. Shimon, and D. Milstein, *Organometallics*, **21**, 812 (2002).
- 02OM1807 C. Hahn, P. Morwillo, E. Herdtweck, and A. Vitagliano, *Organometallics*, **21**, 1807 (2002).
- 02OM3285 H. Katayama, C. Wada, K. Taniguchi, and F. Ozawa, *Organometallics*, **21**, 3285 (2002).

- 02TL753 C.S. Consorti, G. Ebeling, and J. Dupont, *Tetrahedron Lett.*, **43**, 753 (2002).
- 02ZN(B)803 G. Muller, M. Klinga, P. Oswald, M. Leskela, and R. Rieger, *Z. Naturforsch.*, **B57**, 803 (2002).
- 03AGE3941 T. Bunlaksananusorn, K. Polborn, and P. Knochel, *Angew. Chem., Int. Ed. Engl.*, **42**, 3941 (2003).
- 03CIC39 V.J. Catalano, B.L. Bennett, M.A. Malwitz, R.L. Yson, H.M. Kar, S. Muratidis, and S.J. Horner, *Comments Inorg. Chem.*, **24**, 39 (2003).
- 03CRV283 V.C. Gibson and S.K. Spitzmesser, *Chem. Rev.*, **103**, 283 (2003).
- 03JA4714 E. Ben-Ari, M. Gandelman, H. Rozenberg, L.J.W. Shimon, and D. Milstein, *J. Am. Chem. Soc.*, **125**, 4714 (2003).
- 03JCS(D)1419 H.P. Chen, Y.H. Liu, S.M. Peng, and S.T. Liu, *Dalton Trans.*, 1419 (2003).
- 03JCS(D)1551 Q.S. Li, F.B. Xu, D.J. Cui, K. Yu, X.S. Zeng, X.B. Leng, H.B. Song, and Z. Zhang, *Dalton Trans.*, 1551 (2003).
- 03JCS(D)2457 S.P. Tunik, I.O. Koshevoy, A.J. Poe, D.H. Farrar, E. Nordlander, M. Haukka, and T.A. Pakkanen, *Dalton Trans.*, 2457 (2003).
- 03JOM(677)80 F.E. Hong, C.P. Chang, H. Chang, Y.L. Huang, and Y.C. Chang, *J. Organomet. Chem.*, **677**, 80 (2003).
- 03OM737 S.H. Liu, H. Xia, T.B. Wen, Z. Zhou, and G. Jia, *Organometallics*, **22**, 737 (2003).
- 03OM2612 M. Rashidi, M.C. Jennings, and R.J. Puddephatt, *Organometallics*, **22**, 2612 (2003).
- 03OM4604 W.P. Leung, Q.W.Y. Ip, S.Y. Wong, and T.C.W. Mak, *Organometallics*, **22**, 4604 (2003).
- 03OM4893 H.P. Chen, Y.H. Liu, S.M. Peng, and S.T. Liu, *Organometallics*, **22**, 4893 (2003).
- 03POL1397 A.M.Z. Slawin, J. Wheatley, and J.D. Woollins, *Polyhedron*, **22**, 1397 (2003).
- 04AGE70 W.J. Drury, N. Zimmermann, M. Keenan, M. Hayashi, S. Kaiser, R. Goddard, and A. Pfaltz, *Angew. Chem., Int. Ed. Engl.*, **43**, 70 (2004).
- 04IC189 J.A. Casares, P. Espinet, J.M. Martin-Alvarez, and V. Santos, *Inorg. Chem.*, **43**, 189 (2004).
- 04ICA4568 G. Sanchez, J. Garcia, D. Meseguer, J.L. Serrano, L. Garcia, J. Perez, and G. Lopez, *Inorg. Chim. Acta*, **357**, 4568 (2004).
- 04JA1526 V.F. Slagt, P.C.J. Kamer, P.W.N.M. van Leeuwen, and J.N.H. Reek, *J. Am. Chem. Soc.*, **126**, 1526 (2004).
- 04JA12232 D.B. Grotjahn and D.A. Lev, *J. Am. Chem. Soc.*, **126**, 12232 (2004).
- 04JA12244 T. Ruffer, M. Ohashi, A. Shima, H. Mizomoto, Y. Kaneda, and K. Mashima, *J. Am. Chem. Soc.*, **126**, 12244 (2004).
- 04JCS(D)3251 M.J. Green, K.J. Cavell, P.G. Edwards, R.P. Tooze, B.W. Skelton, and A.H. White, *Dalton Trans.*, 3251 (2004).
- 04JOC4595 T. Bunlaksananusorn and P. Knochel, *J. Org. Chem.*, **69**, 4595 (2004).
- 04JOC5060 M.P.A. Lyle, A.A. Narine, and P.D. Wilson, *J. Org. Chem.*, **69**, 5060 (2004).
- 04JOM1064 S. Jaaskelainen, M. Haukka, H. Riihimaki, J.T. Pursiainen, and T. A. Pakkanen, *J. Organomet. Chem.*, **689**, 1064 (2004).
- 04JOM2268 R. Rojas and M. Valderrama, *J. Organomet. Chem.*, **689**, 2268 (2004).
- 04JOM3953 P. Braunstein, *J. Organomet. Chem.*, **689**, 3953 (2004).
- 04JOM4244 H. Brunner, A. Kollnberger, A. Mehmood, T. Tsuno, and M. Zabel, *J. Organomet. Chem.*, **689**, 4244 (2004).

- 04OM1986 R.D. Pike, B.A. Reinecke, M.E. Dellinger, A.B. Wiles, J.D. Harper, J.R. Cole, K.A. Dendramis, B.D. Borne, J.L. Harris, and W. T. Pennington, *Organometallics*, **23**, 1986 (2004).
- 04OM2510 D.H. Gibson, C. Pariya, and M.S. Mashuta, *Organometallics*, **23**, 2510 (2004).
- 04OM4026 J. Zhang, M. Gandelman, L.J.W. Shimon, H. Rozenberg, and D. Milstein, *Organometallics*, **23**, 4026 (2004).
- 04OM6042 E. Goto, M. Usuki, H. Takenaka, K. Sakai, and T. Tanase, *Organometallics*, **23**, 6042 (2004).
- 04POL3115 P. Govindaswamy, Y.A. Mozharivskiy, and M.R. Kollipara, *Polyhedron*, **23**, 3115 (2004).
- 05ACR784 F. Speiser, P. Braunstein, and L. Saussine, *Acc. Chem. Res.*, **38**, 784 (2005).
- 05ICA273 E. de la Encarnation, J. Pons, R. Yanez, and J. Ros, *Inorg. Chim. Acta*, **358**, 273 (2005).
- 05JA10840 J. Zhang, G. Leitus, Y. Ben-David, and D. Milstein, *J. Am. Chem. Soc.*, **127**, 10840 (2005).
- 05JA15364 F.A. Jalon, B.R. Manzano, A. Caballero, M. Carmen Carrion, L. Santos, G. Espino, and M. Moreno, *J. Am. Chem. Soc.*, **127**, 15364 (2005).
- 05JOM5264 P.W. Dyer, J. Fawcett, and M.J. Hanton, *J. Organomet. Chem.*, **690**, 5264 (2005).
- 05OM3359 M.E. Cucciolito, A. D'Amora, and A. Vitagliano, *Organometallics*, **24**, 3359 (2005).
- 05OM3516 I.O. Koshevoy, M. Haukka, T.A. Pakkanen, S.P. Tunik, and P. Vainiotalo, *Organometallics*, **24**, 3516 (2005).
- 05OM5299 J.J.M. de Pater, C.E.P. Maljaars, E. de Wolf, M. Lutz, A.L. Spek, B. J. Deelman, C.J. Elsevier, and G. van Koten, *Organometallics*, **24**, 5299 (2005).
- 05OM6365 I. Angurell, O. Rossell, M. Seco, and E. Ruiz, *Organometallics*, **24**, 6365 (2005).
- 05ZAAC2719 J. Langer, H. Gorls, G. Gillies, and D. Walther, *Z. Anorg. Allg. Chem.*, **631**, 2719 (2005).
- 06AGE1113 J. Zhang, G. Leitus, Y. Ben-David, and D. Milstein, *Angew. Chem., Int. Ed.*, **45**, 1113 (2006).
- 06AGE5194 S. Kaiser, S.P. Smidt, and A. Pfaltz, *Angew. Chem., Int. Ed.*, **45**, 5194 (2006).
- 06AX(C)81 M. Agostinho, A. Banu, P. Braunstein, R. Welter, and X. Morise, *Acta Crystallogr.*, **C62**, m81 (2006).
- 06IC6628 J.A. Casares, P. Espinet, J.M. Martin-Alvarez, and V. Santos, *Inorg. Chem.*, **45**, 6628 (2006).
- 06IC7252 R.J. Trovitch, E. Lobkovsky, and P.J. Chirik, *Inorg. Chem.*, **45**, 7252 (2006).
- 06ICA745 E. de la Encarnation, J. Pons, R. Yanez, and J. Ros, *Inorg. Chim. Acta*, **359**, 745 (2006).
- 06ICA2980 S.E. Durrán, M.B. Smith, S.H. Dale, S.J. Coles, M.B. Hursthouse, and M.E. Light, *Inorg. Chim. Acta*, **359**, 2980 (2006).
- 06JA4246 F.E. Michael and B.M. Cochran, *J. Am. Chem. Soc.*, **128**, 4246 (2006).
- 06JA12400 M. Feller, A. Karton, G. Leitus, J.M.L. Martin, and D. Milstein, *J. Am. Chem. Soc.*, **128**, 12400 (2006).
- 06JA15390 E. Ben-Ari, G. Leitus, L.J.W. Shimon, and D. Milstein, *J. Am. Chem. Soc.*, **128**, 15390 (2006).

- 06JCI319 P.V. Govindaswamy, P.J. Carroll, Y.A. Mozharivskyj, and M. R. Kollipara, *J. Chem. Sci.*, **118**, 319 (2006).
- 06JCS(D)5583 S.W. Kohl, F.W. Heinemann, M. Hummert, W. Bauer, and A. Grohmann, *Dalton Trans.*, 5583 (2006).
- 06JOM111 V.I. Ponomarenko, T.S. Pilyugina, V.D. Khripun, E.V. Grachova, S. P. Tunik, M. Haukka, and T.A. Pakkanen, *J. Organomet. Chem.*, **691**, 111 (2006).
- 06JOM1143 D. Sirbu, G. Consiglio, and S. Gischig, *J. Organomet. Chem.*, **691**, 1143 (2006).
- 06JOM1927 X. Xu, L. Fang, Z.X. Chen, G.C. Yang, S.L. Sun, and Z.M. Su, *J. Organomet. Chem.*, **691**, 1927 (2006).
- 06JOM2483 M. Minato, T. Kaneko, S. Masauji, and T. Ito, *J. Organomet. Chem.*, **691**, 2483 (2006).
- 06OL4157 H. Yoshida, S. Nakano, Y. Yamaryo, J. Ohshita, and A. Kunai, *Org. Lett.*, **8**, 4157 (2006).
- 06OL5853 A. Labonne, T. Kribber, and L. Hintermann, *Org. Lett.*, **8**, 5853 (2006).
- 06OM1900 D. Benito-Garagorri, E. Bocker, J. Widermann, W. Lackner, M. Poliak, K. Mereiter, J. Kisala, and K. Kirchner, *Organometallics*, **25**, 1900 (2006).
- 06OM3007 S.M. Klok, D.M. Heinekey, and K.I. Goldberg, *Organometallics*, **25**, 3007 (2006).
- 06OM3190 E. Ben-Ari, R. Cohen, M. Gandelman, L.J.W. Shimon, J.M.L. Martin, and D. Milstein, *Organometallics*, **25**, 3190 (2006).
- 07AGE2269 M.H.G. Precht, M. Holscher, Y. Ben-David, N. Theysen, R. Loschen, D. Milstein, and W. Leitner, *Angew. Chem., Int. Ed.*, **46**, 2269 (2007).
- 07AGE3135 S. Proch and R. Kempe, *Angew. Chem., Int. Ed.*, **46**, 3135 (2007).
- 07AGE4736 S.M. Klok, D.M. Heinekey, and K.I. Goldberg, *Angew. Chem., Int. Ed.*, **46**, 4736 (2007).
- 07IC10479 M. Feller, E. Ben-Ari, T. Gupta, L.J.W. Shimon, G. Leitun, Y. Diskin-Posner, L. Weiner, and D. Milstein, *Inorg. Chem.*, **46**, 10479 (2007).
- 07JCS(D)107 J. Zhang, M. Gandelman, L.J.W. Shimon, and D. Milstein, *Dalton Trans.*, 107 (2007).
- 07JCS(D)4715 B. Shafaatian, A. Akbari, S.M. Nabavizadeh, F.W. Heinemann, and M. Rashidi, *Dalton Trans.*, 4715 (2007).
- 07JOM175 T. Tanase, H. Takenaka, and E. Goto, *J. Organomet. Chem.*, **692**, 175 (2007).
- 07JOM3577 A. Scrivanti, F. Benetollo, A. Venzo, M. Bertoldini, V. Beghetto, and U. Matteoli, *J. Organomet. Chem.*, **692**, 3577 (2007).
- 07OM196 P. Yuan, J. Yin, G. Yu, Q. Hu, and S.H. Liu, *Organometallics*, **26**, 196 (2007).
- 07OM217 D. Benito-Garagorri, J. Widermann, M. Pollak, K. Mereiter, and K. Kirchner, *Organometallics*, **26**, 217 (2007).
- 07OM5216 M.E. Cucciolito, A. D'Amora, A. Tuzi, and A. Vitagliano, *Organometallics*, **26**, 5216 (2007).
- 07OM5550 L. Canovese, F. Visentin, C. Santo, C. Levi, and A. Dolmella, *Organometallics*, **26**, 5550 (2007).
- 07SCI790 C. Gunanathan, Y. Ben-David, and D. Milstein, *Science*, **317**, 790 (2007).
- 07SYN1121 A. Labonne and L. Hintermann, *Synthesis*, 1121 (2007).
- 08ACR201 D. Benito-Garagorri and K. Kirchner, *Acc. Chem. Res.*, **41**, 201 (2008).
- 08AGE1814 H. Grrutzmacher, *Angew. Chem., Int. Ed.*, **47**, 1814 (2008).
- 08AGE8661 C. Gunanathan and D. Milstein, *Angew. Chem., Int. Ed.*, **47**, 8661 (2008).

- 08AGE9142 D. Benito-Garagorri, M. Puchberger, K. Mereiter, and K. Kirchner, *Angew. Chem., Int. Ed.*, **47**, 9142 (2008).
- 08AGE8674 D.A. Smith, A.S. Batsanov, K. Miqueu, J.M. Sotiropoulos, D. C. Apperley, J.A.K. Howard, and P.W. Dyer, *Angew. Chem. Int. Ed.*, **47**, 8674 (2008).
- 08EJI3493 M.H.G. Prechtel, M. Holscher, Y. Ben-David, N. Theyssen, D. Milstein, and W. Leitner, *Eur. J. Inorg. Chem.*, **3493**, (2008).
- 08JA20 D.B. Grotjahn, V. Miranda-Soto, E.J. Kragulj, D.A. Lev, G. Erdogan, X. Zeng, and A.L. Cooksy, *J. Am. Chem. Soc.*, **130**, 20 (2008).
- 08JA2786 B.M. Cochran and F.E. Michael, *J. Am. Chem. Soc.*, **130**, 2786 (2008).
- 08JA10860 D.B. Grotjahn, E.J. Kragulj, C.D. Zeinalipour-Yazdi, V. Miranda-Soto, D.A. Lev, and A.L. Cooksy, *J. Am. Chem. Soc.*, **130**, 10860 (2008).
- 08JA14374 M. Feller, M.A. Iron, L.J.W. Shimon, Y. Diskin-Posner, G. Leitun, and D. Milstein, *J. Am. Chem. Soc.*, **130**, 14374 (2008).
- 08JCS(D)6497 D.B. Grotjahn, *Dalton Trans.*, 6497 (2008).
- 08JOM3932 B. Crociani, S. Antonasroli, M. Burattini, F. Benetollo, A. Scrivanti, and M. Bertoldini, *J. Organomet. Chem.*, **693**, 3932 (2008).
- 08OL793 F.E. Michael, P.A. Sibbald, and B.M. Cochran, *Org. Lett.*, **10**, 793 (2008).
- 08OM1193 E. Mothes, S. Senters, M.A. Liquin, and G. Lavigne, *Organometallics*, **27**, 1193 (2008).
- 08OM1454 S.K. Hanson, D.M. Heinekey, and K.I. Goldberg, *Organometallics*, **27**, 1454 (2008).
- 08OM1626 Z.Y. Chai, C. Zhang, and Z.X. Wang, *Organometallics*, **27**, 1626 (2008).
- 08OM2627 D. Vuzman, E. Poverenov, L.J.W. Shimon, Y. Diskin-Posner, and D. Milstein, *Organometallics*, **27**, 2627 (2008).
- 08OM3526 J. Zhang, M. Gandelman, L.J.W. Shimon, and D. Milstein, *Organometallics*, **27**, 3526 (2008).
- 08OM3577 L. Canovese, C. Santo, and F. Visentin, *Organometallics*, **27**, 3577 (2008).
- 08OM4158 T. Arliguie, M. Blug, P. Le Floch, N. Mezaillies, P. Thuery, and M. Ephritikhine, *Organometallics*, **27**, 4158 (2008).
- 08OM5759 E.M. Pelczar, T.J. Emge, K. Krogh-Jespersen, and A.S. Goldman, *Organometallics*, **27**, 5759 (2008).
- 08OM6360 M.E. Cucciolito and A. Vitagliano, *Organometallics*, **27**, 6360 (2008).
- 09AHC225 A. Sadimenko, *Adv. Heterocycl. Chem.*, **98**, 225 (2009).
- 09AGE8178 D.G.H. Hetterscheid, J.I. van der Vlugt, B. de Bruin, and J.N.H. Reek, *Angew. Chem., Int. Ed.*, **48**, 8178 (2009).
- 09AGE8832 J.I. van der Vlugt and J.N.H. Reek, *Angew. Chem., Int. Ed.*, **48**, 8832 (2009).
- 09CCC72 A. Friedrich and S. Schneider, *ChemCatChem*, **1**, 72 (2009).
- 09CCR1793 S. Maggini, *Coord. Chem. Rev.*, **253**, 1793 (2009).
- 09CEJ5491 A.A. Danopoulos, D. Pugh, H. Smith, and J. Sassannshausen, *Chem. Eur. J.*, **15**, 5491 (2009).
- 09CEJ7167 L. Hintermann, T.T. Dang, A. Labonne, T. Kribber, L. Xiao, and P. Naumov, *Chem. Eur. J.*, **15**, 7167 (2009).
- 09EJI4085 C.M. Standfest-Hauser, G. Dazinger, J. Wiedermann, K. Mereiter, and K. Kirchner, *Eur. J. Inorg. Chem.*, 4085 (2009).
- 09EJI4134 F. Liu, S.A. Pullarkat, Y. Li, S. Chen, and P.H. Leung, *Eur. J. Inorg. Chem.*, 4134 (2009).
- 09ICA477 O.G. Adeyemi and L.K. Li, *Inorg. Chim. Acta*, **362**, 477 (2009).
- 09IC10257 G. Zeng, Y. Guo, and S. Li, *Inorg. Chem.*, **48**, 10257 (2009).
- 09JA3146 C. Gunanathan, L.J.W. Shimon, and D. Milstein, *J. Am. Chem. Soc.*, **131**, 3146 (2009).

- 09JA8603 W.H. Bernskoetter, S.K. Hanson, S.K. Buzak, Z. Davis, P.S. White, R. Swartz, K.I. Goldberg, and M. Brookhart, *J. Am. Chem. Soc.*, **131**, 8603 (2009).
- 09JA13584 J. Li, Y. Shiota, and K. Yoshizawa, *J. Am. Chem. Soc.*, **131**, 13584 (2009).
- 09JCS(D)1016 J.I. van der Vlugt, M. Lutz, E.A. Pidko, D. Voght, and A.L. Spek, *Dalton Trans.*, 1016 (2009).
- 09JCS(D)1919 P. Li, M. Wang, L. Chen, J. Liu, Z. Zhao, and L. Sun, *Dalton Trans.*, 1919 (2009).
- 09JCS(D)2029 Y. Takahashi, N. Murakami, K. Fujita, and R. Yamaguchi, *Dalton Trans.*, 2029 (2009).
- 09JCS(D)8005 Z.Y. Chai and Z.X. Wang, *Dalton Trans.*, 8005 (2009).
- 09JCS(D)9433 M.A. Iron, E. Ben-Ari, R. Cohen, and D. Milstein, *Dalton Trans.*, 9433 (2009).
- 09JOM131 A. Scrivanti, M. Bertoldini, V. Beghetto, U. Matteoli, and A. Venzo, *J. Organomet. Chem.*, **694**, 131 (2009).
- 09JOM2488 M. Aydemir, A. Baysal, N. Meric, and B. Gumgum, *J. Organomet. Chem.*, **694**, 2488 (2009).
- 09JOM3643 P. Kumar, A.K. Singh, S. Sharma, and D.S. Pandey, *J. Organomet. Chem.*, **694**, 3643 (2009).
- 09OM953 K.A. Grice and K.I. Goldberg, *Organometallics*, **28**, 953 (2009).
- 09OM1180 J. Flapper, H. Kooijman, M. Lutz, A.L. Spek, P.W.N.M. Van Leeuwen, C.J. Elsevier, and P.C.J. Kamer, *Organometallics*, **28**, 1180 (2009).
- 09OM3264 J. Flapper, P.W.N.M. van Leeuwen, C.J. Elsevier, and P.C.J. Kamer, *Organometallics*, **28**, 3264 (2009).
- 09OM3272 J. Flapper, H. Kooijman, M. Lutz, A.L. Spek, P.W.N.M. van Leeuwen, C.J. Elsevier, and P.C.J. Kamer, *Organometallics*, **28**, 3272 (2009).
- 09OM3941 F. Liu, S.A. Pullarkat, Y. Li, S. Chen, M. Yuan, Z.Y. Lee, and P. H. Leung, *Organometallics*, **28**, 3941 (2009).
- 09OM4791 H. Salem, L.J.W. Shimon, Y. Diskin-Posner, G. Leitus, Y. Ben-David, and D. Milstein, *Organometallics*, **28**, 4791 (2009).
- 09OM6383 A. Bruck and K. Ruhland, *Organometallics*, **28**, 6383 (2009).
- 09OM6902 D. Benito-Garagorri, L.G. Alves, M. Puchberger, K. Mereiter, L.F. Veiros, M.J. Calhorda, M.D. Carvalho, L.P. Ferreira, M. Godinho, and K. Kirchner, *Organometallics*, **28**, 6902 (2009).
- 09OM7025 J.I. van der Vlugt, M.A. Siegler, M. Janssen, D. Vogt, and A.L. Spek, *Organometallics*, **28**, 7025 (2009).
- 09POL2287 T. Suzuki, M. Kotera, A. Takayama, and M. Kojima, *Polyhedron*, **28**, 2287 (2009).
- 09SCI74 S.W. Kohl, L. Weiner, L. Schwartzburd, L. Konstantinovski, L.J.W. Shimon, Y. Ben-David, M.A. Iron, and D. Milstein, *Science*, **324**, 74 (2009).
- 10AHC175 A. Sadimenko, *Adv. Heterocycl. Chem.*, **100**, 175 (2010).
- 10AGE1468 B. Gnanaprakasam, J. Zhang, and D. Milstein, *Angew. Chem., Int. Ed.*, **49**, 1468 (2010).
- 10AGE7046 D.A. Smith, A.S. Batsanov, K. Costuas, R. Edge, D.C. Apperley, D. Collison, J.F. Halet, J.A.K. Howard, and P.W. Dyer, *Angew. Chem., Int. Ed.*, **49**, 7046 (2010).
- 10CEJ7992 R.N. Nair, P.J. Lee, A.L. Rheingold, and D.B. Grotjahn, *Chem. Eur. J.*, **16**, 7992 (2010).
- 10CEJ13960 I. Angurell, M. Ferrer, A. Gutierrez, M. Martinez, L. Rodriguez, O. Rossell, and M. Engeser, *Chem. Eur. J.*, **16**, 13960 (2010).

- 10EJI704 P. Kumar, M. Yadav, A.K. Singh, and D.S. Pandey, *Eur. J. Inorg. Chem.*, 704 (2010).
- 10EJI1767 I. Macias-Arce, M.C. Puerta, and P. Valerga, *Eur. J. Inorg. Chem.*, 1767 (2010).
- 10EJI3160 L.G. Alves, G. Dazinger, L.F. Veiros, and K. Kirchner, *Eur. J. Inorg. Chem.*, 3160 (2010).
- 10IC1615 M. Feller, E. Ben-Ari, M.A. Iron, Y. Diskin-Posner, G. Leitus, L.J. W. Shimon, L. Konstantinovski, and D. Milstein, *Inorg. Chem.*, **49**, 1615 (2010).
- 10ICA3674 D. Benito-Garagorri, W. Lackner-Warton, C.M. Standfest-Hauser, K. Mereiter, and K. Kirchner, *Inorg. Chim. Acta*, **363**, 3674 (2010).
- 10JA120 X. Yang and M.B. Hall, *J. Am. Chem. Soc.*, **132**, 120 (2010).
- 10JA924 B. Blank and R. Kempe, *J. Am. Chem. Soc.*, **132**, 924 (2010).
- 10JA4534 M. Findlater, W.H. Bernskoetter, and M. Brookhart, *J. Am. Chem. Soc.*, **132**, 4534 (2010).
- 10JA8542 E. Khaskin, M.A. Iron, L.J.W. Shimon, J. Zhang, and D. Milstein, *J. Am. Chem. Soc.*, **132**, 8542 (2010).
- 10JA14763 C. Gunanathan, B. Gnanaprakasam, M.A. Iron, L.J.W. Shimon, and D. Milstein, *J. Am. Chem. Soc.*, **132**, 14763 (2010).
- 10JA16756 E. Balaraman, B. Gnanaprakasam, L.J.W. Shimon, and D. Milstein, *J. Am. Chem. Soc.*, **132**, 16756 (2010).
- 10JCS(D)2423 Y. Cabon, H. Kleijn, M.A. Siegler, A.L. Spek, R.J.M.K. Gebbink, and B. J. Deelman, *Dalton Trans.*, 2423 (2020).
- 10JCS(D)2563 S. Liu, R. Peloso, and P. Braunstein, *Dalton Trans.*, 2563 (2010).
- 10JCS(D)7921 J. Liu, C. Jacob, K.J. Sheridan, F. Al-Mosule, B.T. Heaton, J.A. Iggo, M. Matthews, J. Pelletier, R. Whyman, J.F. Bickley, and A. Steiner, *Dalton Trans.*, 7921 (2010).
- 10OM1890 W.P. Leung, K.W. Kan, and T.C.W. Mak, *Organometallics*, **29**, 1890 (2010).
- 10OM3027 L. Canovese, F. Visentin, C. Santo, G. Chessa, and V. Bertolasi, *Organometallics*, **29**, 3027 (2010).
- 10OM3374 S. Chen, J.K.P. Ng, S.A. Pullarkat, F. Liu, Y. Li, and P.H. Leung, *Organometallics*, **29**, 3374 (2010).
- 10OM3817 L. Schwartsburd, M.A. Iron, L. Konstantinovski, Y. Diskin-Posner, G. Leitus, L.J.W. Shimon, and D. Milstein, *Organometallics*, **29**, 3817 (2010).
- 10OM4682 J.C. Gordon and G.J. Kubas, *Organometallics*, **29**, 4682 (2010).
- 10OM4932 D. Benito-Garagorri, L.G. Alves, L.F. Veiros, C.M. Standfest-Hauser, S. Tanaka, K. Mereiter, and K. Kirchner, *Organometallics*, **29**, 4932 (2010).
- 10OM5878 M.E. Cucciolito, A. D'Amora, and A. Vitagliano, *Organometallics*, **29**, 5878 (2010).
- 10OM5904 Y. Cabon, I. Reboule, M. Lutz, R.J.M.K. Gebbink, and B.J. Deelman, *Organometallics*, **29**, 5904 (2010).
- 10POL3097 W. Lackner-Warton, S. Tanaka, C.M. Standfest-Hauser, O. Oztöpcü, J.C. Hsieh, K. Mereiter, and K. Kirchner, *Polyhedron*, **29**, 3097 (2010).
- 10TC915 D. Milstein, *Top. Catal.*, **53**, 915 (2010).
- 11AHC227 A. Sadimenko, *Adv. Heterocycl. Chem.*, **102**, 227 (2011).

SUBJECT INDEX

A

- 5-Acceptor-substituted 2-amino- or 2-alkoxy-(oligo)thiophenes, extremely large positive solvatochromism, 237
- 8-Acetoxymethyl-5,6,7,8-tetrahydro-1H,4aH-pyrido[1,2-a]pyrimidin-1-one, methanolysis, 23
- 2-Acetyl-5-iodothiophene, irradiation with 2-ethynyl-5-trimethylsilylthiophene, 192
- Actisomide, 2
 - computerised prediction of human drug clearance, 13
- 2-Acyl-1,2,3,4,11,11a-6H-hexahydropyrazino[1,2-b]isoquinoline-1,4-diones, reaction with aromatic aldehydes, 58
- 2-Acyl-1,3,4,6,7,11b-hexahydro-2H-pyrazino[2,1-a]isoquinolin-4-ones, 117
- 5'-Alkoxy-2,2'-bithiophene azo dyes, 238
- N-Alkyl dithieno[3,2-b:2',3'-d]pyrrole, in polymers and copolymers with thiophene, 329
- Alkyl 7-oxo-1H,3H,7H-pyrido[3,2,1-ij][3,1]benzoxazine-6-carboxylates, hydrolysis, 21
- 3-Alkyloxythiophene derivatives, polymers with azobenzenes, 293
- Alkylthiophenes, irradiation, 169
- (+)-Allosedridine alkaloids, 34
- Allyl palladium complexes of 1-(2-diphenylphosphino-1-naphthyl)isoquinoline, 435
- 8-Allyl-perhydropyrido[1,2-c][1,3]-oxazin-1-ones, asymmetric dihydroxylation, 22
- 3-Allylpiperazin-2-ones, cyclizations, 107
- 2(3)-Allylthiophene, 179
- 3-Amino-2-(aryloxymethyl)quinoxalin-4(3H)-ones, N-acylation, 77
- 7-Amino-3-aryl-2,3,6,7-tetrahydro-1H,5H-pyrido[3,2,1-ij]quinazolin-1-ones, 17
- 4-Aminobenzo[b]thiophene, 229
- 2-[(Aminocarbonyl)cyclopropylmethyl]pyridine, cyclization, 31
- 3-(Aminocarbonylmethylthio)-4-cyano-1-(4-methylphenyl)-1-trifluoromethyl-1H-pyrido[1,2-c]pyrimidine, 23
- 2-Amino-6-chloro-4-cyclopropyl-7-fluoro-5-methoxy-1H,3H-pyrido[1,2-c]pyrimidine-1,3-dione, 21
- 8-Amino-6-cyano-9,10-difluoro-3(S)-methyl-2,3-dihydro-7H-pyrido[1,2,3-de][1,4]benzoxazin-7-one, reaction with sodium azide, 71
- 8-Amino-7-cyano-2,6-dihydro-1H-pyrido[1,2-c]pyrimidin-1-one, reaction with hydrazine, 21
- 10-Amino-2-cyclohexylcarbonyl-1,3,4,6,7,11b-hexahydro-2H-pyrazino[1,2-b]isoquinolin-4-one, 57
 - acylation, 69
- 8-Amino-9,10-difluoro-6-cyano-2,3-dihydro-7H-pyrido[1,2,3-de][1,4]benzoxazine-7-ones, reaction with 3-substituted propylamines, 60
- 8-Amino-9,10-difluoro-7-oxo-2,3-dihydro-7H-pyrido[1,2,3-de][1,4]benzoxazine-6-carboxamides, reaction with phosphoryl chloride, 71, 77
- 2-Amino-5-(2,4-difluorophenyl)-6H-pyrido[1,2-b]pyridazin-6-one, reaction with (2-fluorophenyl)isocyanate and 2,4-difluorobenzoyl chloride, 8

- 8-Amino-9,10-difluoro-6-(1H-tetrazol-5-yl)-2,3-dihydro-7H-pyrido[1,2,3-de][1,4]benzoxazine-7-ones, reaction with 3-substituted propylamines, 60
- 2-Amino(di-i-propylphosphino)pyridine, reaction with molybdenum carbonyls, 442
- 2-Aminoethanol, reaction with cycloheptatriene-1,2,3,4,5,6,7-heptacarboxylate, 114
- 3-Amino-6,6a,7,8,9,10-hexahydropyrido[2,1-c][1,4]benzoxazine, acetylation, 59
- 4-Amino-4,4a,5,6,7,8-hexahydro-3H-pyrido[1,2-c]pyrimidin-3-ones, 19
- (+)-(3R,7R)-7-Amino-3-(4-methoxyphenyl)-6,7-dihydro-3H,5H-pyrido[3,2,1-ij]quinazoline-1(2H)-one, stereostructures, 14
- 7-Amino-3-(4-methoxyphenyl)-2,3,6,7-tetrahydro-1H,5H-pyrido[3,2,1-ij]quinazolin-1-one, reaction with 4-dimethylaminobenzaldehyde, 20
- 1-Aminomethyl-1,2,3,4-tetrahydroquinoline, cyclocondensation with 3-aryol-2-hydroxyacrylates, 106
- 3-Aminomethyl-5,6,7-trihydroxy-1-oxoperhydropyrido[1,2-c][1,3]oxazine-8-carboxylic acid, 17
- 8-Amino-7-oxo-2,3-dihydro-7H-pyrido[1,2,3-de][1,4]oxazine-6-carboxylic acids, 77
- 1-(4-Aminophenyl)-2-[2-(hydroxymethyl)piperidin-1-yl]ethanol, 52
reaction with aqueous hydrogen bromide, 90
- 3-(4-Aminophenyl)perhydropyrido[2,1-c][1,4]oxazine, 90
sulfonation, 71
- 2-(4-Aminophenyl)perhydropyrido[1,2-a]pyrazine, arylation, 73
- 1-Aminopiperidine-2-carboxylates, reaction with (benzo[1,2,4]thiadiazin-3-yl)acetic acid, 10
- 6-(Amino-1-piperidiny)-8-fluoro-6,7-dihydro-3H,5H-pyrido[1,2,3-de]quinoxalin-3-one, separation of enantiomers, 38
- 3-[-(Aminopiperidin-1-yl)methyl]-5-oxo-2,3-dihydro-5H-pyrido[1,2,3-de][1,4]benzoxazine-10-carbonitrile, separation of enantiomers, 119
- 9-(3-Aminopropyl)-3,3-dimethyl-1H,3H,7H-[1,3]oxazino[5,4,3-ij]quinoline-3-carboxylic acid, amination, 22
- 4-Amino-1,2,3,4-tetrahydroquinoline-8-carboxamide, reaction with 2H-chromene-3-carbaldehydes, 31
- Amlopidine, structures of degradation products, 47
thermal degradation, 50
- Amorphous polymers, photoluminescence intensity, 300
- Anthracene, linked to thiophene in 2,6-position, 270
- Anthracene containing thienylene-vinylene copolymers, 318
- Antofloxacin, 2
use in human antibiotic activity, 122
- 3-Aryolmethylene-1,3,4,6,7,11b-hexahydro-2Hpyrazino[2,1-a]isoquinolin-4-ones, 106
- 3-Arylamino-4-arylimino-4H-pyrido[1,2-a]pyrazines, reaction with 1,4-naphthoquinone, 79
- N-Aryl-5-bromo-1,2,3,4-tetrahydroquinoline-8-carboxamides, reaction with phenoxychloroformate, 31
- 1-Aryl-4-cyano-1-trifluoromethyl-2,3-dihydro-1H-pyrido[1,2-c]pyrimidine-3-thiones, 21
- 4-Aryl-2,3-dihydro-1H-pyrido[1,2-c]pyrimidine-1,3-diones hydrochlorides, solid state structure, 14
- 2-Aryl-6-(2-(diphenylphosphino)ethyl)pyridine, 433

4-Aryl-2-{4-[4-(het)aryl]piperazino}butyl-2,3-dihydro-1H-pyrido[1,2-c]pyrimidine-1,3-diones, receptor binding, 13,33

4-Aryl-1,3,4,6,7,9a-hexahydropyrido[2,1-c][1,4]oxazin-6-ones, catalytic hydrogenation, 54

3-Aryl-1,2,3,5,6,7-hexahydropyrido[3,2,1-ij]quinazolin-1,7-ones, 32

3-Aryl-3-hydroxyperhydropyrido[2,1-c][1,4]oxazines, 104

3-Arylidene-1,2,3,4,11,11b-hexahydro-6Hpyrazino[1,2-b]isoquinoline-1,4-diones, 56

4-Aryl-2-{4-[4-(1H-indol-3-yl)piperidin-1-yl]butyl}-2,3-dihydro-1H-pyrido[1,2-c]pyrimidine-1,3-diones, receptor binding activity, 34

4-Aryl-7-iodoperhydropyrido[2,1-c][1,4]oxazin-6-ones, 65

1-Arylmethylene-3,4-dihydro-1H-pyrido[2,1-c][1,4]thiazinium salts, 93

1-(2-Aryl-2-oxoethyl)-2-piperidinemethanol, cyclization, 104

4(6)-Aryl-6(4)-oxo-(Z)-3-{1-[3-methoxy-4-(4-methyl-1H-imidazol-1-yl)phenyl]methylidene}-4-arylperhydropyrido[2,1-c][1,4]oxazines, enantiomers, 36

5-Aryl-2-phenoxy-6H-pyrido[1,2-b]pyridazin-6-ones, formation, 7

5-Aryl-6H-pyrido[1,2-b]pyridazin-6-ones, formation, 9

Arylthiophenes, photoisomerization, 170

Asymmetric [4 + 2] Diels-Alder reactions, organopalladium complexes, 437

4-Azidobenzo[b]thiophene, photolysis, 229

5-Azidobenzo[b]thiophene, photolysis, 229

(4R,9aR)-7-Azido-9a-methyl-4-phenyl-3,4,9,9a-tetrahydro-1H,6H-pyrido[2,1-c][1,4-oxazine-1,6-dione, 58

hydrogenation, 54

3-Azidomethyl-5,6,7-tribenzyloxy-8-benzyloxymethylperhydropyrido[1,2-c][1,3]oxazin-1-one, hydrogenation, 17

oxidation, 16

reaction with acetic anhydride, 22

3-Azidomethyl-5,6,7-tribenzyloxy-1-oxoperhydropyrido[1,2-c][1,3]oxazine-8-carboxylic acid, reduction, 17

trans-6H,9aH-3-Azidoperhydropyrido[2,1-c][1,4]oxazin-1-ones, 78

B

Benzannelated sexithienyl systems, 236

Benzodithiophene building blocks, in p-type organic semiconductors, 274

orange fluorescence in the solid state, 267

(Benzo[1,2,4]thiadiazin-3-yl)acetic acid, reaction with 1-aminopiperidine-2-carboxylates, 10

6-(Benzothiazol-2-yl)-10-(4-methylpiperazin-1-yl)-9-fluoro-3-(S)-methyl-2,3-dihydro-7H-pyrido[1,2,3-de][1,4]benzoxazin-7-one, nitration, 75

Benzothienindole, 272

4-(4-Benzo[b]thienyl)azobenzo[b]thiophene, 229

cis-7H,9aH-7-{2-[(2-Benzo[b]thienyl)carbonylamino]ethyl}-2-(2,3-dichlorophenyl)perhydropyrido[1,2-a]pyrazine, 6

Benzo[b]thiopyne, ready loss of sulphur, 178

Benzothienophene, decomposition in light, 167

femtosecond laser excitation, 153

reaction with diphenylacetylene, 177

reaction with a secondary amine, 195

Benzo[b]thiophene derivatives, spectra, 150

reaction with acetylenes, 176

Benzo[c]thiophene analogs, photoluminescence spectra, 236

- Benzylamine, reaction with methyl 1-(2-chloroacetyl)piperidine-2-carboxylate, 106
- 2-Benzyloxycarbonyl
benzylperhydropyrido[1,2-a]pyrazine-3-carboxylate, 55
- 5-Benzyloxy-6,7-dihydropyrido[1,2-c][1,3]oxazin-1-one, catalytic reduction, 17
- 9-Benzyloxy-3,4-dihydro-1H,8H-pyrido[1,2-a]pyrazine-1,8-diones, reduction, 55
- 5-Benzyloxy-6,7-(dihydroxy)perhydropyrido[1,2-c][1,3]oxazine, 19
- 5-Benzyloxy-6,7-(dimethylmethylenedioxy)perhydropyrido[1,2-c][1,3]oxazine, reaction with acid, 19
- 3-(Benzyloxyethyl)thiophene, electropolymerisation, 292
- 9-Benzyloxy-2-(4-fluorobenzyl)-6-methoxy-3,4-dihydro-1H,8H-pyrido[1,2-a]pyrazine-1,8-dione, fluorination, 58
- cis*-6H,11aH-6-Benzyloxymethyl-9-methyl-7,8,10-trimethoxy-2-pivaloyl-1,2,3,4,11,11a-6H-hexahydropyrazino[1,2-b]isoquinoline-1,4-dione, 58
- 8-(3-Benzyloxyphenyl)perhydropyrido[1,2-a]pyrazine, 64
- 2-Benzylperhydropyrido[1,2-a]pyrazines, 55
- 2-Benzylperhydropyrido[1,2-a]pyrazine-1,4-dione, 106
- Binaphthyl oligothiophenes, 333
- Biopharmaceutics Classification System, 44
- Biopharmaceutics Drug Disposition Classification System, 44
- Bi(pyrid-2-ylethyl)menthylphosphine, 437
- 1,2-Bis(bis(2-pyridylphosphino)ethane), 409
- 2,6-Bis(*t*-butylphosphinomethyl)pyridine, 430, 431
- 2,6-Bis-(di-*t*-butylphosphinomethyl)pyridine, 423, 430
with ruthenium complexes, 426, 427
- 2,6-Bis(di-*t*-butylphosphinito)pyridine, 454
- Bis(dicyanoethylene) oligothiophene derivatives, 149
- Bis(3-(2,6-dimethoxypyridyl))phenylphosphine, 407
- 2,6-Bis(dimethyl-phosphinomethyl)pyridine, dearomatization in ruthenium(II) carbonyls, 423
with ruthenium carbonyls, 425
- 2,2'-Bis(diphenylphosphino)-4,4'-bipyridine, with ruthenium complexes, 414
- N,N'-Bis(diphenylphosphino)-3,3'-diamine, 443
- N,N'-Bis-(diphenylphosphino)-2,6-diaminopyridine, 442
- 2,6-Bis[1-(diphenylphosphino)ethyl]pyridine, 401
- 2-(Bis(diphenylphosphino)methyl)pyridine, 422
formation of dinuclear complexes, 429
- 2,6-Bis-diphenylphosphinomethylpyridine, 435
- 3,5-Bis((diphenylphosphino)methyl)pyridine, 429
- 2,7-Bis(diphenylphosphino)-1,8-naphthyridine, in construction of metallocryptands, 416
- 2,6-Bis(diphenylphosphino)pyridine, 414
with rhodium carbonyls, 414
with platinum complexes, 415
formation of thallium and copper complexes, 415
- Bis((diphenylphosphino)(2-pyridyl)amino)dimethylsilane, 447
- Bis(2,6-diphenylphosphino-sulfido-3,5-diphenyl)pyridine, 420
- 4,5-Bis-(di-*i*-propylphosphinomethyl)acridine ruthenium, 426
- 3,4-Bis(*p*-methoxyphenyl)dimethylthiophene, 347

- 3,4-Bis(p-methoxyphenyl)-2,5-dimethylthiophene S-oxide, photoirradiation, 347
- 2-Bis(2-methylphenyl)phosphinomethylpyridine, 433
- 1,2-Bis(2-methyl-5-phenyl-3-thienyl)perfluorocyclopentene, 226
- Bis(6-methylquinolin-8-yl)phenylarsine, 417
- 9,10-Bis(oligothienylvinyl)anthracene derivatives, 270
- 5,5'-Bis(pentaethyldisilanyl)-2,2'-bithiophene, 305
- Bis(phosphino)pyridines, coordination mode, 458
- N,P,N-Bis(pyridine) phenylphosphine, 430
- (Bis(2-pyridyl)amino)diphenylphosphine, 446
- Bis(2-pyridyl)phosphine, reaction with trimethyl aluminium, 416
- Bis(2-tellurienyl)thiophene, UV spectra, 129
- Bisthienylbenzothiadiazole fragments, 320
- Bisthienylbenzothiadiazole-pyrrole copolymer, 321
- 2,5-Bis(2-thienyl)tellurophene, UV spectra, 129
- Bithieno[3,2-b:2',3'-e]pyridine units, in polymers, 315
- Bithienyl derivatives, photophysical properties, 158
- electron transfer process in the presence of dinitrobenzene derivatives, 159
- 2,2'-Bithienyl derivatives, UV and IR spectra, 128
- energy of trans conformer, 134
- two-photon spectroscopy, 135
- Bithienyl-imidazo-anthraquinone derivatives, 149
- 2,2'-Bithiophene, fluorescence-excitation, hole-burning, and dispersed-fluorescence spectra in a supersonic jet, 128
- excitation profile, 132
- fluorescence excitation and fluorescence spectra seeded into a supersonic helium expansion, 143
- Bithiophene, insertion into a polypeptide scaffold, 239
- isolation, 162
- Bithiophene-substituted photochromic dithienyl perfluorocyclopentenenes, reversible switches, 221
- 3-Borylbithiophene derivatives, spectra, 145
- 2-Bromoacetophenone, reaction with 2-cyanopyridine, 103
- (S)-2-(2-Bromoacetyl)tetrahydroisoquinoline-3-carboxylate, cyclocondensation with amines, 109
- 2-Bromoanilines, copper-catalyzed coupling with pipecolic acid, 103
- 8-Bromo-2-aryl-2,3,6,7-tetrahydro-1H,5H-pyrido[3,2,1-ij]quinazoline-1,3-diones, 31
- 7-Bromo-2-bromomethyl-6-methoxy-11b-cyano-1,6,7,11b-tetrahydro-2H,4H-[1,3]oxazino[4,3-a]isoquinolin-one, stereostructures, 15
- 2-(4-Bromobutyl)-4-aryl-2,3-dihydro-1Hpyrido[1,2-c]pyrimidine-1,3-diones, reaction with piperazines, 21
- 3-Bromo-2,6-diallyl-tetrahydropyridine, cyclization reactions, 26
- 8-Bromo-6,7-dihydro-1H,3H,5H-pyrido[3,2,1-ij][3,1]benzoxazine-1,3-dione, 31
- reaction with methyl 3-amino-5-chlorobenzoate, 15
- 6-Bromo-3,4-dihydro-1H,8H-pyrido[1,2-a]pyrazine-1,8-diones, reaction with nucleophiles, 58
- 8-Bromo-6,7-dihydro-1H,3H,5H-pyrido[3,2,1-ij]quinazoline-1,3-diones, reaction with 4-amino-1-benzylpiperidine, 20

- 5-Bromo-2-(*cis*-2,6-dimethylmorpholin-4-yl)benzaldehyde, reaction with malononitrile, 108
- (S)-8-Bromo-9-fluoro-10-(1-aminocyclopropyl)-7-oxo-2,3-dihydro-7H-pyrido[1,2,3-de][1,4]benzoxazine-6-carboxylic acid, reaction with amines, 68
- 6-Bromo-9-hydroxy-2-(4-fluorophenyl)-3,4-dihydro-1H,8H-pyrido[1,2-a]pyrazine-1,8-diones, 85
- 7-Bromo-8-hydroxyquinolin-2(1H)-ones, reaction with epichlorohydrin, 104
- 2-Bromomethyl-3,4-dibromo-5-methylthiophene, 346
- 5(7-)-Bromo-3-methylene-tetrahydro-1H-pyrido[1,2-c][1,3]oxazin-1-ones, 26
- 2-Bromomethyl-[1,3]oxazino[4,3-a]isoquinoline-4-ones, 27
- 3-(4-Bromophenylamino)-4-(4-bromophenylimino)-4H-pyrido[1,2-a]pyrazine, 105
- 5-Bromo-1,2,3,4-tetrahydroquinoline-8-carboxylic acid, reaction with carbonyl chloride, 31
- 5-Bromo-2-thienyl-thiophene-2-carbaldehyde, 184
reaction with methyltriphenylphosphonium bromide, 185
- 5-Bromothiophene-2-carbaldehyde, irradiation, 180
- 1-(*t*-Butoxycarbonyl)-2-(2-hydroxyethyl)piperidine, 25
- trans*-7H,9aH-2-*t*-Butoxycarbonyl-7-hydroxymethylperhydropyrido[1,2-a]pyrazine, O-alkylation, 72
- 10-(*t*-Butyl)-3-methylene-3,4,4a,5-tetrahydro-3H-[1,3]oxazino[3,4-b]isoquinolin-1-one, ring opening, 15
- 2-(6-*t*-Butylpyridyl)dimethylphosphine, reaction with tungsten complexes, 392
- 2-(6-*t*-Butylpyridyl)diphenylphosphine, reaction with tungsten complexes, 392

C

- 3,6-Carbazole-benzothiadiazole-thiophene copolymers, 320
- 2,7-Carbazolylenevinylene-thienylenevinylene copolymer, 316
- Carbonylation of alkynes, efficient catalytic systems, 410
- Catenanes, from oligothiophene derivatives, 282
- Charge-transfer complexes in spectra of bichromophores, 154
- 2-Chloro-5-aryl-6H-pyrido[1,2-b]pyridazin-6-ones, reaction with phenols, 7
- 2-(4-Chloro-5-cyclopentyloxy-2-fluorophenyl)perhydropyrido[1,2-a]pyrazine-1,4-dione, herbicidal activity, 120
- 6-Chloro-4-cyclopropyl-7-fluoro-5-methoxy-1H,3H-pyrido[1,2-c]pyrimidine-1,3-dione, reaction with hydroxylamines, 18
- 6-(4-Chloro-3-hydroxybutyl)-2,4-dimethoxy-5-methylpyrimidine, reaction with ammonia, 24
- 2-Chloromercuriomethylperhydrofuro[3,2-b]pyridine, 29
- 3-(Chloromercuriomethyl)perhydropyrido[1,2-c]pyrimidine, 29
- N-(3-Chloro-5-methoxycarbonylphenyl)-5-bromo-1,2,3,4-tetrahydroquinoline-8-carboxamide, 15
- trans*-Chloro(1-naphthyl)bis(triphenylphosphine)nickel, 455
reaction with 8-diphenylphosphinoquinoline, 437
- 2-(3-Chlorophenyl)-8-fluoro-2,3,6,7-tetrahydro-1H,5H-pyrido[3,2,1-ij]quinazoline-1,3-dione, 30
reaction with ethanolamine, 20
- 6-[5-(3-Chlorophenyl)-3-isoxazoly]-2-(3-cyanopyrazin-2-yl)perhydropyrido[1,2-a]pyrazine, 67
- 1-(6-Chloropyridazin-3-yl)-1-aryl-but-3-yn-2-ones, cyclization, 9

- 3-Chloro-1H-pyrido[1,2-c]pyrimidine, 18
- Cholesterol-tethered
trans-stylbenes, 250
- 2H-Chromene-3-carbaldehydes,
reaction with 4-amino-1,2,3,4-
tetrahydroquinoline-8-
carboxamide, 31
- Columnar mesophase liquid
crystals, 249
- Complexes with iron(I)–mercury(II)
bond, 395
- Continuous wave photoinduced
absorption, in polythiophene
pristine films, 301
- Copolymer between 3-octylthiophene
and 3-decyloxythiophene, 311
- Copolymer of cyclopentadithiophene
and benzothiadiazole, 326
- (-)-Cribrostatin, 120
- 4-Cyano-2,3-dihydro-1H-pyrido[1,2-c]
pyrimidin-1-ones, N-alkylation, 18
- 10-Cyano-3-hydroxymethyl-2,3-
dihydro-5H-pyrido[1,2,3-de][1,4]
benzoxazin-5-ones, 61
- 10-Cyanomethyl-9-fluoro-3(S)-methyl-
7-oxo-2,3-dihydro-7H-pyrido
[1,2,3-de][1,4]oxazine-6-carboxylic
acid, 61
phase transfer alkylation, 76
- 4-Cyano-1-(4-methylphenyl)-1-
trifluoromethyl-2,3-dihydro-1H-
pyrido[1,2-c]pyrimidin-3-one,
phosphorylation, 18
- Cyclooctenyl iridium(I), 432
- 4-Cyano-1-oxo-2,3-dihydro-1H-pyrido
[1,2-c]pyrimidine-3-thione, 28
reaction with halogeno ketones, 20
- 4-Cyano-3-phenyl-3-trifluoromethyl-
2,3-dihydro-1H-pyrido[1,2-c]
pyrimidin-1-one, ring opening, 15
- 2-(3-Cyanopyrazin-2-yl)-6-
hydroxymethylperhydropyrido
[1,2-a]pyrazine, Swern
oxidation, 53
- 2-Cyanopyridine, reaction with
2-bromoacetophenone, 103
- (Z)-2-[Cyano-(2-pyridyl)methylene]-
1,3-thiazolidin-4-one, 23
- Cyano substituted poly(thienylene-
vinylene-thienylene)s, 317
- Cyanosubstituted terthiophene
derivatives, 235
- 2(3)-Cyanothiophene, irradiation, 170
- 4-Cyano-3-trichloromethyl-1H-pyrido
[1,2-c]pyrimidin-1-one, reaction
with primary amines, 18
- Cyclopentabithiophene derivatives, 241
- 2-(2-Cyclopentadienyl-1-
diphenylphosphinyl-2-
methylprop-1-yl)-6-(1-menthoxy)
pyridine, 454
- 4H-Cyclopenta[2,1-b;3,4-b']
dithiophene, polymers, 314
- Cyclopentadithiophenone derivatives,
spectra, 160
- Cyclopenta[2,1-b;3,4-b']dithiophen-
4-one, 315
- Cyclopropanediester, reaction
with 1-iminoquinolinium ylides, 10
- D**
- Dendrimers, 252
- Dendrimers of bithiophene or
terthiophene units linked directly
to silicon atoms, 257
- Dendritic oligothiophene-perylene
bisimide derivatives, 262
- N-Desmethyl-levofloxacin, N-
alkylation, 74
- Dewar thiophene, 168
- α,ω -Dialkylsexithiophenes, spectra, 234
- trans*-2,6-Diallyl-1-(methoxycarbonyl)
perhydropyridine,
iodocyclocarbamation, 26
- Diarylethenes with thiophene or
benzothiophene moieties, exhibit
thermal stability, 208
photochromism in
polymethylmethacrylate
amorphous film, 214
- Diarylethene switch, with photochromism
and self-assembly, 221
two conformations, 222
- 1'-(2-Diarylphosphino)(1-naphthyl)
isoquinolines, 438
- 9-Diazafluorene, 424

- Dibenzo[b,d]phospholes, 257
- Dibenzosilole-based polymers, 326
- Dibenzothienylethene structures,
effect of donor-acceptor
substituents, 210
- Dibenzothienylethene sulfone
derivatives, 229
- Dibenzothiophene emission
maxima, 150
excitation spectra, 153
- Dibenzo[b,d]thiophene, absorption
band, 271
- Dibenzothiophene oxide,
photodeoxygenation, 349
- Dibenzothiophene-S-oxide derivatives,
photoirradiation, 347
- Dibenzothiophene sulfone,
photoirradiation, 350
- 3,4-Dibenzyl-2,5-dimethylthiophene
S-oxide, photoirradiation, 347
- 3,5-Dibromothiophene-2-carbaldehyde,
180
- 8-(4,8-Di-*t*-butyl-1,11-dimethoxy-5,7-
dioxo-6-phosphadibenzo[a,c]
cycohepten-6-yl)quinoline, 451
- 2,4-Di-*t*-butylfuran, 348
- 2,5-Di-*t*-butylfuran, 348
- 2,4-Di-*t*-butyl-6-
methyldiphenylphosphinopyridine,
433
- 6-Di-*t*-butylphosphinomethyl-2,2'-
bipyridine, with ruthenium
complexes, 425
- 2-(Di-*t*-butyl-phosphinomethyl)-6-
diethyl-aminomethylpyridine,
423, 441
- 2-Di-*t*-butylphosphinomethylpyridine,
424, 442
- 2,6-Di-*t*-
butylphosphinomethylpyridine,
with palladium and platinum
complexes, 434
- 2,4-Di-*t*-butylthiophene S-oxide,
photoirradiation, 348
- 2,5-Di-*t*-butylthiophene S-oxide,
photoirradiation, 348
- 2,3-Dichlorobenzo[b]thiophene,
reaction with bromoethene, 175
- 4-[5-(Dicyanomethanido)thien-2-yl]-N-
(*n*-hexadecyl)pyridinium, film
formation, 161
- α,ω -Dicyanoterthiophene, UV spectra,
129
- 2,6-Dicyclohexyl-
phosphinomethylpyridine, 424
- Diethylacetylene dicarboxylate, in
complexes of rhodium, 405
- Diethyl (4-oxoperhydropirido[2,1-*c*]
[1,4]oxazin-4-yl) malonate, free
energy difference between 4,9*a*-*cis*
and 4,9*a*-*trans* isomers, 41
- 9,10-Difluoro-3,3-dimethyl-7-oxo-2,3-
dihydro-7H-pyrido[1,2,3-*de*][1,4]
benzoxazine-6-carboxylic
acid, 118
- 9,10-Difluoro-3(S)-methyl-2,3-dihydro-
7H-pyrido[1,2,3-*de*][1,4]
benzoxazin-7-one, 69
- 9,10-Difluoro-3(S)-methyl-7-oxo-2,3-
dihydro-7H-pyrido[1,2,3-*de*][1,4]
benzoxazine-6-carboxylic acid,
reaction with
p-methoxybenzylamine, 60
reaction with 4-methylpiperazine
dihydrochloride, 61
- 9,10-Difluoro-3(S)-methyl-7-oxo-2,3-
dihydro-7H-pyrido[1,2,3-*de*][1,4]
oxazine-6-carboxylate, 57
- 9,10-Difluoro-7-oxo-2,3-dihydro-7H-
pyrido[1,2,3-*de*][1,4]benzoxazine-
6-carboxylic acids, nitration, 60
- 9,10-Difluoro-7-oxo-2,3-dihydro-7H-
pyrido[1,2,3-*de*][1,4]oxazine-6-
carboxylic acids, reaction with
amides, 60
- 8,9,10-Difluoro-7-oxo-2,3-dihydro-7H-
pyrido[1,2,3-*de*][1,4]oxazine-6-
carboxylate, 100
- 2-(2,4-Difluorophenoxy)-5-{2-[(1*E*)-
prop-1-enyl]phenyl}-6H-pyrido[1,2-
b]pyridazin-6-ones, reduction, 7
- 2-(2,4-Difluorophenoxy)-5-{2-
vinylphenyl}-6H-pyrido[1,2-*b*]
pyridazin-6-ones,
reduction, 7
- α,ω -Di-*n*-hexylquaterthiophene, 245

- 2(E)-3-[3(R)-((4-[(2,3-Dihydro[1,4]dioxino[2,3-c]pyridin-7-ylmethyl)amino]-1-piperidinyl)methyl)-10-fluoro-5-oxo-2,3-dihydro-5H-pyrido[1,2,3-de][1,4]benzoxazin-8-yl]-2-propenoic acid, 76
- Dihydronaphtho-[1,2-b]thiophene, 200
- (+)-2-*epi*-Dihydropinidine, 34
- 3,4-Dihydro-5H-pyrazino[1,2-b]isoquinolin-5-one, 96
- 3,4-Dihydro-10H-pyridazino[1,6-b]isoquinolin-10-ones, 11, 12
- oxidation, 7
- patented as electron-transferring agents in photoreceptors, 12
- 2,3-Dihydropyrido[1,2,3-de]-1,4-benzothiazinium betaine, 87
- 2,3-Dihydropyrido[1,2,3-de]-1,4-benzothiazinium chloride, reaction with methylmercurium ions, 43
- 2,3-Dihydropyrido[1,2,3-de]-1,4-benzothiazinium perchlorates, 105
- 2,3-Dihydro-5H-pyrido[1,2,3-de][1,4]benzoxazin-5-ones, 88
- 3,4-Dihydro-1H,6H-pyrido[2,1-c][1,4]oxazine-1,6-dione, 114
- 1,2-Dihydro-8H-pyrido[1,2-a]pyrazine-1,8-dione, 107
- 3,4-Dihydro-1H,8H-pyrido[1,2-a]pyrazine-1,8-diones, 112
- 5,6-Dihydro-10H-pyrido[1,2-a]quinoxaline-6,10-dione, 112
- 1,11b-Dihydro-2H,4H-pyrimido[6,1-a]isoquinolin-4-one, configuration, 14
- 6,7-Dihydro-4H-pyrimido[6,1-a]isoquinolin-4-one, 34
- 2,5-Dihydrothiophene, irradiation, 352
- 2,3-Dihydrothiophene-3-acetate, 351
- 2,3-Dihydrothiophene-3-carboxylate, 351
- 8,9-Dihydroxy-3,4-dihydro-1H,6H-pyrido[1,2-a]pyrazine-1,6-dione, 93
- 4,5-Diiodo-2-acetylthiophene, irradiation, 181
- 3,5-Diiodothiophene-2-carbaldehyde, irradiation, 181
- Dimerization of one-end-blocked benzo[c]thiophenes, 236
- Dimers of dithienylethene derivatives, irradiation, 229
- 5-Dimesitylboryl-2,2'-bithiophene, 145
- 1,3-Dimetallacyclobutadienes, 438
- 7,10-Dimethoxy-3-[(2,4-dimethoxyphenyl)methyl]-6-methyl-1,2,3,4,11,11a-hexahydro-6H-pyrazino[1,2-b]isquinoxaline-1,4-dione, acylation, 64
- 9,10-Dimethoxy-2-(2,6-di-i-propylphenoxy)-6,7-dihydro-2H-pyrimido[6,1-a]isoquinolin-4-ones, are long-acting PDE3/4 inhibitors, 34
- 3-(2,6-Dimethoxypyridyl)diphenylphosphine rhodium(I) P-coordinated complexes, 407
- 9,10-Dimethoxy-1,6,7,11b-tetrahydro-2H,4H-[1,3]oxazino[4,3-a]isoquinoline, 32
- 9,10-Dimethoxy-1,6,7,11b-tetrahydro-2H,4H-[1,3]oxazino[4,3-a]isoquinolin-4-one, 25
- structure, 14
- 9,10-Dimethoxy-2-[(2,4,6-trimethylphenyl)imino]-3-(N-carbamoyl-2-aminoethyl)-3,4,6,7-tetrahydro-2H-pyrimido[6,1-a]isoquinolin-4-ones, are long-acting PDE3/4 inhibitors, 34
- Dimethylacetylene dicarboxylate, in complexes of rhodium, 405
- insertion into Pt-Pt bonds, 418
- 3-(4'-Dimethylaminophenyl)-1-(2-thienyl)prop-2-en-1-one, 160
- 2,3-Dimethylbenzo[b]thiophene, addition to cis- or trans-1,2-dichloroethylene, 175
- Dimethyl 1,2,4,4a,5,6-hexahydro-[1,4]oxazino[4,3-a]quinoline-5,5-dicarboxylate, 89
- 2-(2,6-Dimethylphenyl)-6-(diphenylphosphinomethyl)pyridine, 454
- 2-Dimethylphosphino-3-methylpyridine, with ruthenium carbonyls, 403

- Dimethylterthiophene, dimerisation of cation radicals, 146
UV/Vis spectroelectrochemical oxidation, 147
- 2,5-Dimethylthiophene, reaction with benzophenone, 174
irradiation in presence of Rhodium complexes, 353
- 2,5-Dimethylthiophene-1,1-dioxide, irradiation, 349
tricarbonyl iron, 349
- 2,9-Dimethyl-7,8,10-trimethoxy-2,3,4,6,11,11a-hexahydro-1H-pyrazino[1,2-b]isoquinoline-1,4-dione, 110
- Dimethyl zinc, reaction with rhodium complexes, 428
- N-Diorganophosphino-2-aminopyridines, 445
- 8-(3,5-Dioxa-4-phosphacyclohepta[2,1-a;3,4-a0]dinaphthalen-4-yl)quinoline, 451
- 1,6-Dioxo-3,4,7,8-tetrahydro-1H,6H-pyrido[2,1-c][1,4]oxazine-carboxylate, 114
- α,ω -Diperfluorohexylquaterthiophene 245
- α,ω -Diperfluorohexylsexithiophene, the first n-type sexithiophene conductor, 247
- 8-Diphenylarsinoquinoline, 433
- 2,3-Diphenylbenzothiophene, irradiation, 201
- 2-[1-(-Diphenylmethyl)azetidin-3-yl]perhydropyrido[1,2-a]pyrazines, hydrogenolysis, 55
- Diphenyl-8-oxyquinolylphosphinite, reaction with nickelacycles, 453
- Diphenylphosphinoacridine, with molybdenum carbonyls, 422
- Diphenyl-phosphinoaminopyridine, 446
- 2-(Diphenylphosphinoamino)pyridine, reaction with platinum complexes, 447
- N-(2-Diphenylphosphinobenzylidene)-2-(2-pyridyl)ethylamine, 437
- 6-Diphenylphosphino-2,2'-bipyridine, with ruthenium complexes, 400
- 7-Diphenylphosphino-2,4-dimethyl-1,8-naphthyridine, 407
with iridium carbonyls, 404
- 1-(Diphenyl-phosphino)-2-ethoxy-1-(2-pyridyl)ethane, 449
- 6-(Diphenylphosphinoethyl)-2,2'-bipyridine, with ruthenium carbonyls, 425
- 2-(2-Diphenylphosphinoethyl)pyridine, with ruthenium complexes, 427
in palladium complexes, 433
- 2-Diphenyl-phosphinohydrazinopyridine, 446
- O-Diphenylphosphino-2-hydroxypyridine, 453
- 8-Diphenyl-phosphinomethylaminoquinoline, 443
- 2-(N-Diphenylphosphinomethyl-N-benzyl)aminopyridine, 447
- 2-(N-Diphenylphosphino-methyl-N-cyclohexyl)aminopyridine, 444
- 2-Diphenylphosphinomethyl-6-methylpyridine, 424
- 2-Diphenylphosphino-3-methylphosphinine, 456
- 2-Diphenylphosphino-3-methylpyridine, inefficient in rhodium-catalyzed propene hydroformylation, 404
- N-((Diphenylphosphino) methyl)-2-pyridylamine, 443
- 8-Diphenylphosphino-2-methylquinoline, 438
- 1-(2-Diphenylphosphino-1-naphthyl)isoquinoline, 433, 437
- 2-(2-(Diphenylphosphino)phenyl)pyridine, in palladium complexes, 433
- Diphenylphosphino(phenylpyridin-2-yl methylene) amine, 440
- 2-(N-Diphenylphosphino)piperazinopyridine, 446
- 2-(3-(Diphenylphosphino)propyl)pyridine, in palladium complexes, 433
- 1-(Diphenylphosphino)-2-(2-pyridyl)ethane, 428

- 4-Diphenylphosphino-2,2':6',2"-terpyridine, 400
- 2-((1S,2S,3R,4S)-3-(Diphenylphosphino)-1,7,7-trimethylbicyclo[2.2.1]hept-2-yl)pyridine, in palladium complexes, 433
- 1,1-Diphenyl-2-propyn-1-ol, 424
- Diphenyl(2-pyridyl)phosphine, 418
- Diphenyl-(2'-pyridyl)phosphine oxide, 420
- Diphenyl-(2'-pyridyl)phosphine selenide, 421
- 2-Diphenylphosphinomethylpyridine, 422
- in palladium complexes, 433
- with rhodium complexes, 429
- with ruthenium complexes, 401
- 2,6-Diphenylphosphinomethylpyridine, 424
- 2-Diphenylphosphinophosphinine, 456
- 2-Diphenylphosphinopyridine, 446
- in formation of iron-metal mixed complexes, 394
- reaction with tungsten complexes, 392
- with allylpalladium complexes, 394
- with chromium complexes, 392
- with cobalt complexes, 402
- with cyclopentadienylruthenium complexes, 400
- with iridium complexes, 405, 406, 407
- with iron pentacarbonyl, 393
- with iron-platinum complexes, 396
- with manganese, rhenium, chromium and molybdenum carbonyls, 393
- with molybdenum complexes, 392
- with osmium carbonyls, 399
- with palladium acetate, 411
- with palladium complexes, 407
- with rhodium carbonyls, 403, 404
- with rhodium complexes, 406, 407
- with ruthenium carbonyls, 403, with ruthenium complexes, 397, 401
- 4-Diphenylphosphinopyridine, reaction with tungsten complexes, 392
- 2-Diphenylphosphinoquinoline, with ruthenium complexes, 400
- 8-Diphenylphosphinoquinoline, 433, 438
- with trans-chloro(1-naphthyl)bis(triphenylphosphine)nickel, 437
- P,P'-Diphenylphosphinous acid-P,P'-(2,2'-bipyridine)-3,3'-diyl ester, 443
- 2-(1-Diphenylphosphinyl-2-methylprop-1-yl)-6-(1-menthoxy)pyridine, 454
- 2,3-Diphenylthiophene, photocyclization, 203
- 1,3-Diplumbacyclobutane, 438, 449
- Di-i-propyl-8-oxyquinolylphosphinite, reaction with nickelacycles, 453
- 2,6-Di-i-propylphosphinomethylpyridine, 423
- 2-Di-i-propylphosphinyl-mercaptopyridine, 445
- Di-i-propylphosphinyl-pyrid-2-ylamine, 445
- 1,2-Di(2-pyridyl)-1,2-bis(diphenylphosphino)ethane, 422
- 1,3-Distannacyclobutane, 438, 449
- Di-2-thienylethylene, oxidative photocyclization, 198
- Dithieno[3,2-b:2,3-d]thiophene, R-linked dimer, 272
- Dithieno[3,2-b:2',3'-d]thiophene, as a monomer for a conducting polymer, 240
- Dithieno[3,4-b:3',4'-d]thiophene, 240
- Dithieno[b,d]phospholes, 257
- Dithienothiophenes, radical cations, 240
- flash photolysis in carbon tetrachloride, 241
- 1,3-Dithienylbenzo[c]thiophene, photoluminescence, 235
- Dithienylcyclopentene backbone compounds, photoresponsivity, 209
- Dithienylethene derivatives with Fe(η^5 -C₅Me₅(dppe) termini, 221
- derivatives bearing oligothiophenes in position five of the thienyl rings, 214
- derivatives with imino nitroxide and nitronyl nitroxide moieties, 212

- linked to a fluorescent bis
(phenylethynyl)-anthracene
residue, 215
- photochromic systems linked to
single-walled nanotubes, 229
- with phthalimido groups, 213
- Dithiophene, photochemical
polymerisation, 231
- 2,3-Dithiophenylbutane, formation, 171
- 2,3-Di(trifluoromethyl)thiophene,
irradiation, 169
- 2,5-Di(trifluoromethyl)thiophene,
irradiation, 169
- 3,4-Di(trifluoromethyl)thiophene,
irradiation, 169
- Dodecylsexithiophene, 139
- femtosecond time-resolved study, 144
- Donor-acceptor π -conjugated
compounds, 259
- E
- (\pm)-Epipinidinone alkaloid, synthesis, 34
- 5-(3-Ethoxy-1,3-butadienyl)benzo[b]
thiophene, 205
- 2-Ethoxymethyl-5- methyl-3,4-bis(p-
methoxyphenyl)thiophene, 348
- p-Ethoxystyrylthiophene, irradiation,
205
- Ethyl 10-[2-(t-butoxycarbonyl)-
1,2,3,4,6,8a-hexahydropyrrolo[1,2-
a]pyrazin-7-yl]-9-fluoro-3(S)-
methyl-7-oxo-2,3-dihydro-7H-
pyrido[1,2,3-de][1,4]oxazine-6-
carboxylates, dehydrogenation, 54
- Ethyl 2-[(4-cyano-1-aryl-1-
trifluoromethyl-1H-pyrido[1,2-c]
pyrimidin-3-yl)thio]acetates, 23
- Ethyl 9,10-difluoro-7-oxo-2,3-dihydro-
7H-pyrido[1,2,3-de]-1,4-
benzothiazine-6-carboxylate,
reaction with 1-methylpiperazine,
67
- Ethyl 9,10-difluoro-7-oxo-2,3-dihydro-
7H-pyrido[1,2,3-de][1,4]oxazine-6-
carboxylates, reaction with
MeNO₂, 61
- Ethylenedioxythienylbenzoxazolyl-
alanines, 324
- Ethyl 9-fluoro-10-
[(trifluoromethylsulfonyl)oxy-3(S)-
methyl-7-oxo-2,3-dihydro-7H-
pyrido[1,2,3-de][1,4]oxazine-6-
carboxylate, coupling with boronic
esters, 62
- Ethyl *cis*- and *trans*-4H,9aH-6-oxo-4-
(3,4,5-trifluorophenyl)-7(E)-[[3-
methoxy-4-(4-methyl-1H-
imidazol-1-yl)phenyl]methylene]
perhydropyrido[1,2-a]
pyrazine-2-carboxylates ,
separation, 83
- 2-Ethylphenylphosphinopyridine, with
iron pentacarbonyl, 395
- with molybdenum hexacarbonyl, 395
- Ethyl pyrido[1,2-b][1,2]benzothiazine-
2-carboxylate, decarboxylation, 7
- Ethyl 4-substituted 6-methyl-2-oxo-
1,2,3,4-tetrahydropyrimidine-5-
carboxylates, formation and
reaction of lithium salts, 28
- 1-Ethylthio-1,2,3,4,11,11ahexahydro-
6H-pyrazino[1,2-b]isoquinolin-4-
one, 113
- 6-Ethynyl-2-(3-cyano-2-pyrazinyl)
perhydropyrido[1,2-a]pyrazine,
reaction with 3-iodobenzonitrile, 67
- 2-Ethynyl-5-trimethylsilylthiophene,
irradiation with 2-hydroxyacetyl-5-
iodothiophene, 192
- Excited state absorption, 137
- Experimental blood-brain partition
coefficients, 44
- F
- Fibers of poly(3-hexylthiophene) for
photovoltaic applications, 286
- Fleroxacin, flash photolysis, 99
- Fluorene-dibenzothiophene
copolymers, 315
- Fluorene-thiophene copolymers, 313
- Fluorene-thiophene-phenylene
copolymers, 318
- (S)-9-Fluoro-10-(1-aminocyclopropyl)-
7-oxo-2,3-dihydro-7H-pyrido
[1,2,3-de][1,4]benzoxazine-6-
carboxylic acid, nitration, 60

- Fluorocarbon substitution, found to markedly increase the solution photoluminescence quantum yields, 335
- 7-Fluoro-8-hydroxyquinolin-2(1H)-ones, reaction with epichlorohydrin, 104
- 9-Fluoro-10-[(p-methoxyphenyl)methyl]amino-7-oxo-3-methyl-2,3-dihydro-7H-pyrido[1,2,3-de][1,4]oxazine-6-carboxylic acid, 76
- 3-Fluoromethyl-9,10-difluoro-8-amino-7-oxo-2,3-dihydro-7H-pyrido[1,2,3-de][1,4]oxazine-6-carboxylic acid, reaction with N-2-pyridyl-1,2-ethylenediamine, 61
- 9-Fluoro-10-(4-methylpiperazin-1-yl)-8-methyl-1H,3H,7H-pyrido[3,2,1-ij][3,1]benzoxazine-6-carboxylic acid, amidation, 21
- 9-Fluoro-10-nitromethyl-7-oxo-2,3-dihydro-7H-pyrido[1,2,3-de][1,4]oxazine-6-carboxylates, oxidation, 71
- 9-Fluoro-7-oxo-2,3-dihydro-7H-pyrido[1,2,3-de][1,4]oxazine-6-carboxylate, reaction with tert-butyl (2-mercaptoethyl)carbamate, 61
- 8-Fluoro-3-oxo-2,3,6,7-tetrahydro-5H-pyrido[1,2,3-de][1,4]benzoxazin-7-carbaldehyde, reaction with cyclic amines, 71
- 4-(4-Fluorophenyl)-2-[4-(4-(3-trifluoromethylphenyl)piperazino)butyl]-2,3-dihydro-1H-pyrido[1,2-c]pyrimidine-1,3-dione, chemical shifts in C^{13} CPMASSNMR spectra, 13 structure, 15
- 9-Fluoro-10-(piperazin-1-yl)-7-oxo-2,3-dihydro-7H-pyrido[1,2,3-de][1,4]benzoxazine-6-carboxylic acids, reaction with sodium nitrite, 76
- 8-Fluoro-5H-pyrido[1,2,3-de][1,4]benzoxazine-3,7(2H,6H)-dione, 62
- 6-Formyl-2-(3-cyano-2-pyrazinyl)perhydropyrido[1,2-a]pyrazine, reaction with hydroxylamine, 67
- Four-component Ugi/Pictet-Spengler two-step procedure, 118
- Franck-Condon state, in dithienylethene derivatives, 216
- Fused benzothiophene oligomers, fluorescence excitation and emission spectra, 156 phosphorescence lifetimes, 157
- ## G
- (S)-Glycidyl nosylate, cyclocondensation with 2-methoxy-8-quinolinols, 103
- Gold complexes, 419
- ## H
- Halogenoheterocyclic compounds, reactivity, 187
- 2-(Het)arylperhydropyrido[1,2-a]pyrazines, 63
- Heterohelicenes, 201
- N-Hexadecyl-N-methylaniline, photooxidation, 340
- 1-[N-(n-Hexadecyl-4-pyridinio)]-2-[5-(dicyanomethanido)thien-2-yl]ethane, film formation, 161
- Hexafluorocyclopenta[c]thiophenes, 242
- trans-fused* 3a,4,5,6,7,7a-Hexahydrobenzo[b]thiophene, 351
- 1,3,4,6,7,11b-Hexahydro[1,4]oxazino[4,3-a]isoquinolin-4-ones, Dess-Martin oxidation, 53
- Hexahydro[1,4]oxazino[4,3-a]quinoline-5-carboxylic acid, 108
- 1,2,4,4a,5,6-Hexahydro[1,4]oxazino[4,3-a]quinoline-5,5-dinitrile, 108 epimerization, 58
- 1,3,4,6,7,11b,-Hexahydro[1,4]oxazino[4,3-a]quinoline-1,4-diones, effect of heat, 53
- Hexahydro-1H-pyrazino[1,2-b]isoquinolines, 96
- 1,2,3,4,11,11a-Hexahydro-6H-pyrazino[1,2-b]isoquinoline-1,4-diones, 110

- trans*-6H,11aH-1,2,3,4,11,11a-6H-Hexahydropyrazino[1,2-b]isoquinoline-1,4-dione, epimerization, 58
- 1,3,4,6,7,11b-Hexahydro-2H-pyrazino[1,2-a]isoquinolin-4-one, N(2)-acylation, 65
- reductive N(2)-cycloalkylation, 64
- resolution, 83
- 1,2,3,4,6,11,11a-Hexahydro-1H-pyrazino[1,2-b]isoquinolin-4-ones, 56, 98
- 1,3,4,6,7,11b-Hexahydro-2H-pyrazino[2,1-a]isoquinolin-4-one, 117
- 1,2,3,4,11,11a-Hexahydro-6H-pyrazino[1,2-b]isoquinolin-1-ones, 109
- 1,2,3,4,11,11a-Hexahydro-6H-pyrazino[1,2-b]isoquinolin-4-one, 68
- 3-(2,3,4,4a,5,6-Hexahydro-1H-pyrazino[1,2-a]quinolin-3-yl)propionitrile, 64
- 3-(2,3,4,4a,5,6-Hexahydro-1H-pyrazino[1,2-a]quinolin-3-yl)propylamine, 56, 73
- 2-[3-(2,3,4,4a,5,6-Hexahydro-1H-pyrazino[1,2-a]quinolin-3-yl)propyl]-3a,4,7,7a-tetrahydroisindole-1,3-dione, 74
- 1,3,4,6,7,8-Hexahydropyrido[2,1-c][1,4]oxazin-1-one, 111
- 1,2,3,4,9,9a-Hexahydro-5H-pyrido[1,2-a]pyrazin-1,4-diones, interaction energy to PDE-5 receptors, 42
- Hexahydropyrido[1,2-b]pyridazines, calculated partition coefficients, 5
- 2,3,5,6,7,8-Hexahydro-1H-pyrido[1,2-c]pyrimidine-1,3-diones, receptor binding, 13
- 4,4a,5,6,7,8-Hexahydro-3H-pyrido[1,2-c]pyrimidin-3-ones, 32
- Hexahydropyrido[3,2,1-ij]quinoxaline, separation of diastereomers and optical isomers, 12
- 6,6a,7,8,9,10-Hexahydro-5H-pyrido[1,2-a]quinoxalin-6-ones, 103
- 2,3,5,6,7,8-Hexahydro-1H-pyrimido[5,6,1-jk][1,4]benz diazepine-1,8-one, 24
- 1,3,4,6,7,11b-Hexahydro-2H-pyrimido[6,1-a]isoquinolin-4-one, 25, 26
- 5(E)-(Hex-1-enyl)-2,3-dihydro-5H-pyrido[1,2,3-de][1,4]oxazine-3-one, 99
- 5-Hexyl-2,2'-bithiophene, 257
- Highly oriented pyrolytic graphite, 142
- High-resolution energy-loss spectroscopy spectra, 141
- Hologram QSAR models, 45
- HPLC methods for determination of antibiotics, 36
- Hydroformylation catalysts, 433
- 2-Hydroxyacetyl-5-iodothiophene, irradiation with 2-ethynyl-5-trimethylsilylthiophene, 192
- 1-Hydroxy-4-arylperhydropyrido[2,1-c][1,4]oxazin-6-ones, 93
- 7-Hydroxy-3-aryl-2,3,6,7-tetrahydro-1H,5H-pyrido[3,2,1-ij]quinazolin-1-ones, 17
- Hydroxycarbonyl-methylenemalonates, cyclocondensation with 2-piperidinemethanol, 104
- 6-(4-Hydroxy-2,3-dimethylphenyl)perhydropyrido[1,2-a]pyrazines, 72
- 1-(2-Hydroxyethyl)-2-ethoxycarbonyl-6,7-dimethoxy-1,2,3,4-tetrahydroisoquinoline, heating with sodium methoxide, 25
- cis*-6H,9aH-3-Hydroxy-6-(4-fluorophenyl)perhydropyrido[2,1-c][1,4]oxazin-4-one, 93
- 6-(5-Hydroxyheptyl)piperidin-2-one, formation, 6, 9
- cis*-1H,11aH-1-Hydroxy-1,2,3,4,11,11a-hexahydro-6H-pyrazino[1,2-b]isoquinolin-4-one, 56
- 1-Hydroxy-1,2,3,4,11,11a-hexahydro-6H-pyrazino[1,2-b]isoquinolin-4-ones, 99
- reaction with thiols, 69
- reaction with thiophenol, 82
- 7-Hydroxyimino-3-(4-methoxyphenyl)-2,3,6,7-tetrahydro-1H,5H-pyrido[3,2,1-ij]quinazolin-1-one, formation, 20

- 7-Hydroxy-3-methoxy-4-methyl-5,6,7,8-tetrahydro-1H-pyrido[1,2-c]pyrimidin-1-one, 24
- 7-Hydroxymethyl-2-(2,3-dichlorophenyl)perhydropyrido[1,2-a]pyrazine, mesylation, 72
- 3-Hydroxymethyl-2,3-dihydro-5H-pyrido[1,2,3-de][1,4]benzoxazin-5-ones, 54, 103
sulfonylation, 76
- 3-Hydroxy-3-methyl-3,4-dihydro-1H-pyrido[2,1-c][1,4]oxazinium chloride, 42
equilibrium mixtures, 46
- 3-Hydroxymethyl-6,6a,7,8,9,10-hexahydro-5H-pyrido[1,2-a]quinoxalin-6-one, reaction with secondary amines, 73
- 8-Hydroxymethyl-4-oxo-1,4-dihydroquinoline-3-carboxylates, reaction with one carbon units, 31
- 6-Hydroxymethylperhydropyrido[1,2-a]pyrazine, 56
- 7-Hydroxymethylperhydropyrido[1,2-a]pyrazine, arylation, 63
- 2-Hydroxymethylpyridine, reaction with chloroacetone and bromoacetophenone, 102
- 9-Hydroxy-1-methyl-1,2,3,4-tetrahydro-8H-pyrido[1,2-a]pyrazin-8-one, discovery in pork, 116
- 3-Hydroxy-3-phenyl-3,4-dihydro-1H-pyrido[2,1-c][1,4]oxazinium bromide, 42
- 8-(3-Hydroxyphenyl)perhydropyrido[1,2-a]pyrazine, 73
- 3-(3-Hydroxypropyl)-1,2,3,4,11,11a-hexahydro-6H-pyrazino[1,2-b]isoquinolin-4-ones, chemoselective Swern oxidation, 74
- 8-Hydroxyquinoline, 450
- 1-Hydroxy-2,3,4,6-tetrahydro-1H-pyrazino[1,2-b]isoquinolin-4-one, reaction with silanols, 80
- 4-Hydroxy-1,2,3,4-tetrahydro-8H-pyrido[1,2-a]pyrazine-1,8-dione, 86
- 1-Hydroxy-4-(3,4,5-trifluorophenyl)perhydropyrido[2,1-c][1,4]oxazin-6-one, methylation, 66
- Hyperspine, 3, 19
- ## I
- Iminophosphoranes, as chelators, 459
- 1-Iminoquinolinium ylides, reaction with cyclopropanediester, 10
- Indolo[2,3-a]pyrrolo[3,4-c]carbazolo alkaloids, 205
- 2-(1H-Indol-6-yl)perhydropyrido[1,2-a]pyrazine, 73
- Intramolecular charge-transfer (ICT) fluorescence, 259
- 2-Iodo-5-acetylthiophene, reaction with arylalkenes with functional groups, 188
- 9-Iodo-3,3-dimethyl-7-oxo-1H,3H,7H-pyrido[3,2,1-ij][3,1]benzoxazine-6-carboxylate, reaction with S-[2-(2-tert-butoxycarbonylaminoethoxy)ethyl thioacetate, 21
- trans*-4aH,8H-3-Iodomethyl-8-allylperhydropyrido[1,2-c][1,3]oxazin-1-one, 26
- cis*-3H,4aH-3-Iodomethylperhydropyrido[1,2-c][1,3]oxazin-1-one, 26
reaction with sodium azide, 22
- 6(S)-(-Iodomethyl-4(R)-phenyl-9a-(trifluoromethyl)-9-iodoperhydropyrido[2,1-c][1,4]oxazin-1-one, 77
- 3-Iodomethyl-5,6,7-tribenzyloxy-8-benzyloxymethylperhydropyrido[1,2-c][1,3]oxazin-1-one, reaction with acetonitrile, 19
- 5-Iodo-2-nitrothiophene, irradiation, 181
irradiation in presence of naphthalene, 181
irradiation with indene, 190
irradiation with styrene, 190
reaction with indole, 189
reaction with phenylacetylene, 194

9-Iodo-7-oxo-2,3-dihydro-7H-pyrido
[1,2,3-de][1,4]benzoxazine-6-
carboxylate, 101

9-Iodo-7-oxo-2,3-dihydro-7H-pyrido
[1,2,3-de][1,4]oxazine-6-carboxylic
acids, 61

9-Iodo-7-oxo-1H,3H,7H-pyrido[3,2,1-ij]
[3,1]benzoxazine-6-carboxylates,
Heck couplings, 21
Sonogashira couplings, 21

7-Iodo-6-oxo-4-(3,4,5-trifluorophenyl)
perhydropyrido[2,1-a]pyrazine-2-
carboxylate, reduction, 65

2-Iodothiophene, reaction with
thiophenolate, 180
photolysis of film in hydrogen iodide,
230

3-Iodothiophene-2-carbaldehyde,
irradiation, 181

5-Iodothiophene-2-carbaldehyde,
irradiation, 181
irradiation in presence of benzene,
184
reaction with benzimidazole, 189
reaction with benzofuran, 189
reaction with 2,5-diethynylthiophene,
191
reaction with 2-ethynyl-5-
trimethylsilylthiophene, 191
reaction with indole, 189
reaction with β -methoxystyrene, 191
reaction with 2-propynylthiophene, 193
reaction with 2-thienyl-1-propyn-
3-ol acetate, 193

5-Iodothiophene-2-carbonitrile,
irradiation, 181

1-Iodovinylbenzenes, palladium-
catalysed two component cascade
cyclizations with sulphonamides,
116

Iridium(I) acetonys, 432

Iridium species, catalytic activity in
hydrogenation of imines, 429

Iron complexes, photolysis in presence
of thiophenes, 354

3-Isopropylthiophene, 171

Isoquinoline, catalytic H/D exchange,
428

K

Ketones, C-H activation, 431
Ketonyl hydrides, 432

L

Langmuir-Blodgett films, 161

(-)-Lemonomycin, 120

(-)-Lemonomycin alkaloid, 80

Lemonomycinone amide, 120

(3S)-(+)-Levofloxacin, 2
conversion of carboxylic acid
groups, 70
detection in presence of other
fluoroquinolones, 40
enantiomeric purity, 38
formation, 61
formation of hydrates of levofloxacin
hydrochloride, 83
spectral properties, 35

Levofloxacin ethyl ester, 100

Levofloxacin hemihydrates,
preparation, 68

Lifetime of the triplet state in
polythienyls, 136

Light-emitting electrochemical cells, 286

Lithium phenylacetylide, reaction with
copper complexes, 413

Long-lived charge separated states, 302

Low molecular-weight gelators, 222
containing responsive
perhydrodithienylcyclopentene
photochromic switches, 223

Low-temperature phosphorescence
spectroscopy, 138

2,6-Lutidine-functionalized bis
(phosphoranimine), 438

2,6-Lutidylbis(phosphoranosulfide), 449

M

anti-Markovnikov hydration of terminal
alkynes to aldehydes, 397

2-Mercaptopyridine, with cobalt
carbonyls, 402

8-Mercaptoquinolinium
bromide, 105

6-Mesityl-2-diphenyl-
phosphinomethylpyridine, 437

- 8-Methoxy-3-[2-(*trans*-4-aminocyclohexyl)acetyl]-2,3,4,4a,5,6-hexahydro-1H-pyrazino[1,2-a]quinoline, 56
- 4-Methoxybenzo[b]thiophene, spectra in presence of *p*-chloroacetophenone, 153
- 1-(3-Methoxycarbonyl)propyl-1-phenyl-[6,6]C61, 301
- cis*-6H,9aH-6-(4-Methoxy-2,3-dimethylphenyl)perhydropyrido[1,2-a] pyrazines, acylation, 63, 85
- 9-Methoxy-2-(4-fluorophenyl)-3,4-dihydro-1H,8H-pyrido[1,2-a]pyrazine-1,8-diones, 85
- hydrolysis, 66
- 8-Methoxy-2,3,4,4a,5,6-hexahydro-1H-pyrazino[1,2-a]quinoline, N(3)-acylation, 64
- 10-Methoxy-2,3,4,4a,5,6-hexahydro-1H-pyrazino[1,2-a]quinoline, 88
- alkylation, 64
- 8-Methoxy-2-[(2-hydroxyethyl)aminomethyl]-1,2,3,4-tetrahydroquinoline, 88
- 10-Methoxy -3-hydroxymethyl-2,3-dihydro-5H-pyrido[1,2,3-de][1,4]benzoxazin-5-ones, 61
- (E)-7-[[3-Methoxy-4-(4-methyl-1H-imidazol-1-yl)phenyl]methylene]-4-aryl-3,4,6,7,8,9-hexahydropyrido[2,1-c][1,4]oxazin-6-ones, 58
- 7-[1-[3-Methoxy-4-(4-methyl-1H-imidazol-1-yl)phenyl]-(E)-methylidene]-4-phenylperhydropyrido[2,1-c][1,4]oxazin-6-one, 66
- 10-Methoxy-3-((4-[(3-oxo-3,4-dihydro-2H-pyrido[3,2-b][1,4]oxazin-6-yl)methylamino] piperid-1-yl)methyl)-2,3-dihydro-5H-pyrido[1,2,3-de][1,4]benzoxazin-5-one, separation of enantiomers, 119
- 6-(4-Methoxyphenyl)-1,3,4,8,9,9a-hexahydropyrido[2,1-c][1,4]oxazin-8-one, 113
- 2-Methoxy-8-quinolinols, reaction with (S)-glycidyl nosylate, 103
- 3-Methoxythiophene, electropolymerization, 302
- 2-Methylbenzo[b]thiophene, reaction with alkenes, 175
- 2-Methylbenzothiophene oxide, photodimerization, 345
- 3-Methylbenzothiophene oxide, photodimerization, 346
- Methyl 1-(2-chloroacetyl)piperidine-2-carboxylate, reaction with benzylamine, 106
- Methyl 9-chloro-2,3-dione-2,3,6,7-tetrahydro-1H,5Hpyrido[1,2,3-de]quinoxalin-5-ylacetate, hydrolysis, 74
- 3-Methyl-2,3-dihydro-7-oxo-7H-pyrido[1,2,3-de][1,4]benzoxazine-5-carboxylic chlorides, 70
- 6-Methyl-3,4-dihydro-1H,6H-pyrido[1,2-c][1,3]oxazine-1,4-dione, 14
- 2-[[2-Methyl- and 3,4-dimethylphenyl]amino]carbonyl]perhydropyrido[1,2-a]pyrazines, as serotonin receptor ligands, 42
- Methyl *cis*-6H,9aH-1,4-dioxoperhydropyrido[1,2-a]pyrazine-6-carboxylate, 111
- Methyl (4R,9R,9Sa)-1,6-dioxo-4-phenylperhydropyrido[2,1-c][1,4]oxazine-9-carboxylate, reduction, 52
- 1-Methyl-2-diphenylphosphino-3-(10-isoquinolyl)indole, 448
- trans*-4aH,8H-3-Methylene-8-methyl-3,4,4a,5-tetrahydro-1H,8H-pyrido[1,2-c][1,3]oxazin-1-one, use in alkaloid synthesis, 34
- 5-Methyleneperhydropyrido[1,2-c][1,3]oxazine, dihydroxylation, 19
- cis*-4(R)H,9a(S)H-Methyleneperhydropyrido[2,1-c][1,4]oxazin-1-one, 65
- trans*-4H,9aH-(4R,9aR)-4-Methyleneperhydropyrido[2,1-c][1,4]oxazin-1-one, 65
- trans*-4(R)H,9(R)aH-8-Methylene-perhydropyrido[2,1-c][1,4]oxazin-1-one, oxidation, 53

- 3-Methylene-3,4,4a,5-tetrahydro-1H,8H-pyrido[1,2-c][1,3]oxazin-1-ones, ring opening, 15
- 3-Methylene-5,6,7-tribenzyloxy-8-benzyloxymethylperhydropyrido[1,2-c][1,3]oxazin-1-one, 17
- Methyl 5-fluoro-1,2,3,4-tetrahydroquinoline-8-carboxylate, reaction with isocyanates, 30
- 5-(2-Methylfuran-2-yl)-7-bromo-3,4-dihydropyridazino[1,6-b]isoquinolin-10-one, structure, 6
- Methyl 5-iodothiophene-2-carboxylate, irradiation, 181
reaction with 2-chlorothiophene, 186
- Methyl 4-mercapto-2-alkenoates, 350
- 1-Methyl-1-(6-methyl-2-pyridyl)ethoxydiphenylphosphine, 454
- Methyl 6-oxo-6,6a,7,8,9,10-hexahydro-5H-pyrido[1,2-a]quinoxaline-3-carboxylate, reduction, 56
- Methyl (4R*,9aS*)-6-oxo-4-(3,4,5-trifluorophenyl)-1,2,3,4,6,7-hexahydropyrido[1,2-a]pyrazine-2-carboxylate, 92
- 5-Methylperhydropyrido[1,2-c][1,3]oxazine, 24
- 4-Methylperhydropyrido[1,2-a]pyrazin-1-one N-oxide, NOE measurements, 48
- Methyl 4(R)-phenyl-1,6-dioxo-3,4,7,8-tetrahydro-1H,6H-pyrido[2,1-c][1,4]oxazine-9-carboxylate, catalytic reduction, 54
- 1-Methyl-2-(2-phenyl-2-hydroxyethyl)-1,2,5,6-tetrahydropyridine, formation, 17
- Methyl 3-propynoate, reaction with anion of 3-methylpyridazine, 10
- 3-Methylpyridazine, generation of anion and reaction with methyl 3-propynoate, 10
- 1-Methyl-3-(pyridin-2-yl)-2-propenoate, 455
- 8-Methyl 6H-pyrido[1,2-b]pyridazin-6-one, 10
- 6-Methyl-8H-pyrido[1,2-b]pyridazin-8-one, 102
- 8-Methyl-6H-pyrido[2,1-c]pyrimidin-6-one, 28
- (8-Methyl-2-quinolylmethyl)di-t-butylphosphine, 430
- (3S,4aS)-3-Methyl-4,4a,7,8-tetrahydro-1H,3H-pyrido[1,2-c][1,3-oxazin-1-one, catalytic hydrogenation, 16
- 2-Methylthianaphthene 1,1-dioxide, photodimerisation, 343
- 2(3)-Methylthiophene, decomposition in light, 167
- (1R,6S,9aR)- and (1SR,6S,9aR)-1-Methyl-6-(3,4,5-trifluorophenyl)perhydropyrido[2,1-c][1,4]oxazine-3,4-diones, 104
- 3-Methyl-5,6,7-trihydroxy-8-hydroxymethyl-perhydropyrido[1,2-c][1,3]oxazin-1-one, 17
- Molybdenum complexes, photolysis in presence of thiophenes, 356
- Monobenzilized dithienylcyclopentene backbone compounds, synthesis, 212
- Monomeric benzo[c]thiophene analogs, absorption band around 400 nm, 235
- (-)-Monomorphine I, synthesis, 12
- Monophosphinopyridines, coordination mode, 457
- Myrioxazine A, 3
- N**
- Nano-sized electronic and optoelectronic devices, 250
- Naphthalene, catalytic H/D exchange, 428
- Naphtho[1,8-bc:4,5-b'c']dithiophene, 272
- Naphtho[1,8-bc:5,4-b'c']dithiophene, 272
- 8-Nitro-9,10-difluoro-7-oxo-2,3-dihydro-7H-pyrido[1,2,3-de][1,4]benzoxazine-6-carboxamides, reduction, 57
- 8-Nitro-9,10-difluoro-7-oxo-2,3-dihydro-7H-pyrido[1,2,3-de][1,4]benzoxazine-6-carboxylic acids, reaction with thionyl chloride, 70
formation of carboxamides, 77

- 3-Nitro-6,6a,7,8,9,10-hexahydro-5H-pyrido[1,2-a]quinoxalin-6-one, 121
- 3-(4-Nitrophenyl)perhydropyrido[2,1-c][1,4]oxazin-3-ol, catalytic reduction, 52
- Nitro-substituted oligothiophenes, display of large bathochromic shifts, large Stokes shifts, high fluorescent quantum yields, and long lifetimes for excited states, 146
- Nonlinear optical chromophores showing thiophene-benzothiazole units, 284
- O**
- (3S,R)-Ofloxacin, 2
- binding to silica gel, 69
 - complexes with metal ions, 47
 - detection in human urine, 39
 - detection of residues, 40
 - determination of residues in food, 50
 - electrochemical behaviour, 37
 - heating in methylene chloride, 75
 - interaction with metal ions, 37
 - magnesium complexes, 49
 - metal complexes, 84
 - optical activity, 36
 - separation by RP-HPLC, 37
 - solubility, 35
 - UV spectroscopy, 46
- Ofloxacin ethyl ester, 100
- Oligofluorene, 320
- Oligofluoroalkylthiophene, 333
- Oligomers of thiophene-bearing fluorene derivatives, 277
- Oligothiénylethynylenes, 254, 277
- derivatives, 279
- Oligo(α -thiophene) derivatives, 285
- formation of self-organised films, 148
 - UV-visible spectra, 234
- Oligothiophenes, most important radiationless decay process, 140
- tendency to form several polymorphic phases, 142
- Organic thin-film transistors, 232
- Organopalladium ortho-metalated (1-(dimethylamino)ethyl) naphthalene, 455
- Osmium complexes, photolysis in presence of thiophenes, 355
- [1,2]Oxazino[2,3-a]quinoline-6-carboxylates, 12
- 7-Oxo-2,3-dihydro-7H-pyrido[1,2,3-de]-1,4-benzothiazine-6-carboxylate, 116
- 5-Oxo-2,3-dihydro-5H-pyrido[1,2,3-de][1,4]benzoxazine-3-carbaldehydes, 71
- 7-Oxo-2,3-dihydro-7H-pyrido[1,2,3-de][1,4]benzoxazine-6-carboxylate, 101, 118
- formation of anhydrides, 70
- 7-Oxo-2,3-dihydro-7H-pyrido[1,2,3-de][1,4]oxazine-6-carboxylic acid, 99
- 4-Oxo-1,4-dihydroquinolone-3-carboxylic acids, 99
- 1-(2-Oxoethyl)-4-oxo-1,4-dihydropyridine-2-carboxylate, reaction with 2-methoxyethanol, 107
- 6-Oxo-6,6a,7,8,9,10-hexahydro-5H-pyrido[1,2-a]quinoxaline-3-carboxylate, 95
- 6-(1'-Oxo-3'-hydroxy-1',3'-dihydro-2'-isoindolylmethyl)-1-hydroxy-2,3,4,6-tetrahydro-1H-pyrazino[1,2-b]isoquinolin-4-one, 57
- 4-Oxoperhydropyrido[1,2-a]pyrazine-1-carboxylate, 94
- 1-Oxo-3-phenyl-1,2-dihydropyrido[1,2-a]pyrazin-5-ium hexafluorophosphate, 103
- 10-Oxopyrido[1,2-b][1,2]benzothiazine-5,5-dioxide, reaction with arylhydrazines, 8
- 7-Oxo-1H,3H,7H-pyrido[3,2,1-ij][3,1]benzoxazine-6-carboxylates, 31
- 6-Oxopyrido[1,2-c]quinazolinium chloride, structure, 15
- 3-Oxo-3,4,7,8-tetrahydro-1H,6H-pyrido[2,1-c][1,4]oxazine-9-carboxylates, 114
- 3-Oxo-3,4,7,8-tetrahydro-1H,6H-pyrido[2,1-a]pyrazine-9-carboxylate, 114
- ring opening, 52
- Oxygen containing phosphinopyridines, as chelators, 460

P

- Palladacyclopentadiene, 453
- Palladium acetate/
2-diphenylphosphino-pyridine/
triflic acid, a catalytic system for the
carbonylation of alkynes, 410
- (S)-Pazufloxacin, 2
detection, 40, 41
mesylate, 84
- Pentacene, 271
- 8-Pentylperhydropyrido[1,2-c][1,3]
oxazin-6-one, formation, 18
- Perhydropyrido[3,2,1-ij][3,1]
benzoxazines, 31
- Perhydropyrido[2,1-c][1,4]oxazine-1,4-
diones, 91
- Perhydropyrido[2,1-c][1,4]oxazine-3,4-
diones, reduction with
L-selectride, 54
- Perhydropyrido[1,2-c][1,3]oxazin-1-
ones, in alkaloid syntheses, 34
reduction with Zn, 15
- Perhydropyrido[2,1-c][1,4]oxazin-1-
ones, 101
- cis*-4H,9aH-Perhydropyrido[2,1-c][1,4]
oxazin-3-ones, 104
- Perhydropyrido[1,2-c][1,3]oxazin-6-
ones, 30
- Perhydropyrido[1,2-b][1,2]oxazin-8-
one, N-O cleavage, 6
- (6R,9aS)-Perhydropyrido[1,2-a]
pyrazin-8-ones, 85
- Perhydropyrido[1,2-a]pyrazin-1-one N-
oxide, 85
- 4-[4-Perhydropyrido[1,2-a]pyrazin-2-
yl]phenylamino]-2,3-
dimethylquinoline, receptor
activity, 120
- trans*-4H,4aH-Perhydropyrido[1,2-c]
pyrimidine-1,3-diones, receptor
binding, 13
- Perylene bisimide-dithienothiophene
derivatives, 263
- Phenylbis(2-pyridyl)phosphine, 408, 418
reaction with molybdenum
complexes, 416
- 5-Phenyl-3-bromothiophene-3-
carbaldehyde, 180
- 2-Phenyl-5-(4-*t*-butyl)-1,3,4-oxadiazole,
268
- Phenyl-cored dendrimers, 252
- Phenyldiazomethane, 445
- Phenyl-di(2'-pyridyl)phosphine oxide, 420
- 1-Phenyldodecan-1-one,
photooxidation, 340
- Phenyleneethienylene chromophores, 251
- Phenylene-thiophene copolymers, 310
- Phenylene-thiophene-S,S-dioxide
copolymers, 308
- 1-[1(R)-Phenyl-2-hydroxyethyl]-2(S),3
(R)-bis(hydroxymethyl)piperidine,
52
- 4-Phenyl-9-
hydroxymethylperhydropyrido
[2,1-c][1,4]oxazin-1-ol, silylation, 71
- 2-(2'-Phenyl-2'-methoxy-2'-
trifluoromethylacetyl)-
1,3,4,6,7,11b-hexahydro-1H-
pyrazino[1,2-a]isoquinolin-4-one,
separation of diastereomers, 35
- 2-(2'-Phenyl-2'-methoxy-2'-
trifluoromethylacetyl)-
1,3,4,5,6,11b-hexahydro-1H-
pyrazino[1,2-b]isoquinolin-4-one,
hydrolysis, 65
- 4-Phenylperhydropyrido[2,1-c][1,4]
oxazin-1-ones, formation of
optically active, 84
- 4-Phenylperhydropyrido[2,1-c][1,4]
oxazin-6-one, 93
- (4R,9aS)- and (4S,9aS)-4-
Phenylperhydropyrido[1,2-a]
pyrazine-1,3-diones, 103
- 1-Phenylperhydropyrido[1,2-a]
pyrazine-2,4-diones, 94
- 2-Phenylphosphinopyridine, with
ruthenium carbonyls, 396
- 1-Phenyl-3-(pyridin-2-yl)-2-propenone,
455
hydrophosphination, 455
- Phenyl pyrrol-substituted bithiophene,
spectra, 144
- (3S,4aR)-(+)-3-Phenyl-4,4a,7,8-
tetrahydro-1H,3H-pyrido[1,2-c]
[1,3]oxazin-1-one, reduction with
LAH, 17

- (4S)-[4 β ,7 α ,8 β ,9 α ,9a β]-4-Phenyl-7,8,9-tribenzyloxyperhydropyrido[2,1-c][1,4]oxazin-1-one, 91
- 2-Phenylthiophene,
photoisomerization, 170
- 2-(Phosphinoaryl)pyridine, palladium complexes, 435
- 2-Phosphinomethylpyridine, with iron-platinum complexes, 396
- Phosphito-N-(8-((3,5-dioxa-4-phosphacyclohepta[2,1-a;3,4-a']dinaphthalen-4-yl)oxy)quinoline, 451
- Phospholipid-tethered trans-stylbenes, 250
- Phosphonito-N-(8-(3,5-dioxa-4-phosphacyclohepta[2,1-a;3,4-a']dinaphthalen-4-yl)oxy)quinoline, 451
- Photocatalytic system for solar hydrogen production from water, 426
- Photochemical isomerization of pentaatomic heterocyclic compounds, 165
unified description, 166
- Photochemical polymerization, 231
- Photochromic compounds,
classification, 208
- Photochromic properties of thiophene derivatives, 206
- Photochromism, from two porphyrinic groups linked to a dithienylethene scaffold, 229
- Photodetachment photoelectron spectroscopy, 138
- Photoimaging, using a thin film of soluble poly(3-hexylthiophene), 291
- Photoluminescence properties of the monometallic complexes, 281
- Photoluminescence quantum yields values, increase quasi-monotonically with the number of thiophene rings, 335
- Photooxidation of polyolefins, 288
of poly(3-alkylthiophene)s films, 339
- Photooxidative free-radical pathway, 288
- Photopolymerization of thienyl derivatives, in the presence of phenyliodonium hexafluorophosphate, 231
- Photoresponsive compounds, 209
- 3-[4-(Phthalimido)butyl]-10-methoxy-2,3,4,4a,5,6-hexahydro-1H-pyrazino[1,2-a]quinoline, 73
- 6-(Phthalimidomethyl)-2-(isopropoxycarbonyl)-2,3,4,6-tetrahydro-1H-pyrazino[1,2-b]isoquinoline-1,4-dione, reduction, 57
- Picosecond laser flash photolysis of dithienylethenes, 217
- Pipecolic acid, cyclocondensation with isoleucine, 102
- Pipecolic acid, copper-catalyzed coupling with 2-bromoanilines, 103
- 10-(Piperazin-1-yl)-9-fluoro-7-oxo-2,3-dihydro-7H-pyrido[1,2,3-de][1,4]oxazine-6-carboxylic acids, N-alkylation, 75
- 2-Piperidinemethanol,
cyclocondensation with hydroxycarbonyl-methylenemalonates, 104
reaction with bromomethyl aryl ketones, 104
reaction with oxalyl acid bis(4-bromophenylimidoyl) chloride, 105
- 2-(2-Piperidinoethyl)-1,2,3,4,11,11a-hexahydro-6H-pyrazino[1,2-b]isoquinoline-1,4-dione,
electrostatic potential map, 43
- Poly(2,3-alkylthieno[3,4-b]pyrazine)s, 331
- Poly(3-alkylthiophene), 233
crystalline composites with polystyrene, 287
conjugation length determined from absorption maximum, 290
photoinduced reactions of, 340
photoluminescence efficiency, 286
soluble and semiconductors, 285
- Poly(3-aminothiophene) derivatives, 304
- Poly(benzo[1,2-b:4,5-b']dithiophene) derivatives, 301

- Poly[1,4-bis(3-alkyl-2-thienyl)phenylenes], fluorescence, 147
- Poly(3,4-dialkylthiophene)s, 234
- Poly(3',4'-dibutyl-2,2':5',2''-terthiophene), 143
- film, spectra, 286
- Poly(3,3'-dimethyl-2,2'-bithiophene), spectra, 287
- Poly(1,3-dithienylisothanaphthene) derivatives, 337
- Poly[(hexamethyltrisilanylene)-bis(2,5-thienylene)], 304
- Poly(3-hexylthiophene), long lived photoluminescence, 290
- UV/vis spectra, 286
- wavelength of maximum absorption, 293
- Polymers from diarylethene and benzothiophenes, 227
- from electropolymerization of 3-(benzyloxyethyl)thiophene, 292
- solar cells, 323
- Poly(3-methoxythiophene) films, 147
- Poly(3-methoxythiophene-polybithiophene composite film, 302
- electronic absorption spectra, 303
- fluorescence excitation spectra, 303
- Poly(3-octylthiophene), 286
- photooxidation, 339
- stability of films, 290
- Poly[3-oligo(oxyethylene)-4-methylthiophene], 304
- Poly[3-(N-succinimido(tetraethoxyoxy)-4-methylthiophene)], 304
- Poly[(tetraethyldisilanylene)-pentakis(2,5-thienylene)], 304
- Poly[(tetraethyldisilanylene)tetrakis(2,5-thienylene)], 304
- Poly[(tetraethyldisilanylene)(2,5-thienylene)], 304
- Poly[(tetraethyldisilanylene)tris(2,5-thienylene)], 304
- Poly[(tetramethyldisilanylene)-bis(2,5-thienylene)], 304
- Poly(thieno[3,4-b]thiophene) film, 286
- Poly[4-(2-thienyl)benzenamine], 306
- Poly[2-(3-thienyl)ethoxy-4-butylsulfonate], photodegradation, 290
- Poly[(3-thienyl)ethyl methacrylate], 292
- Polythiophene, blended with thiazole yellow, 298,
- derivatives, biological activity, 162
- derivatives, theoretical explanation of the electronic structure, 286
- phototoxic insecticidal activity, 163
- pristine films, 301
- Poly(α -thiophene) derivatives, 285
- in semiconductors, 285
- Poly(thiophene)-fullerene blends, 337
- (-)-Porantheridine, 334
- (-)-2-*epi*-Porantheridine, 34
- Porphyrinic groups linked to a dithienylethene scaffold, 229
- Potassium 9-fluoro-3-methyl-10-(4-methylpiperazin-1-yl)-2,3-dihydro-7H-pyrido[1,2,3-de][1,4]benzoxazine-6-carboxylate, 77
- Power conversion efficiency, of solar cells, 323
- (1R)-(-)-Praziquantel, 2, 106
- absolute configuration of single enantiomer, 51
- determination of residues in food, 50
- nitration, 59
- solubility, 34
- structure determination by NMR, 49
- synthesis, 64
- use in treatment of schistosomiasis, 121
- Precoccinelline
- 1-Propargyl-6-oxo-1,6-dihydropyridine-2-carboxamide, methylation, 93
- 3-(Propen-2-yl)thiophene, 171
- N-(2-Pyridinyl)
- diorganophosphinoxides, 445
- Pyrido[1,2-b][1,2]benzothiazine-5,5-dioxide, 9
- 6H-Pyrido[2,1-j]-3,1-benzoxacin-6-ones, 29
- 5H-Pyrido[1,2,3-de][1,4]benzoxazine-3,7(2H,6H)-dione, 99

6H,10H-Pyrido[2,1-c][1,4]benzoxazine-6,10-diones, 113
6H-Pyrido[2,1-c][1,4]benzoxazinium inner salts, 90
Pyrido[1,2-a]pyrazine-1,6-diones, HIV-integrase activity, 120
2-Pyridylbis(diphenylphosphino) methane, 422
1-(2-Pyridyl)-2-(diphenylphosphino) ethane, with iridium complexes and carbonyls, 429
2-Pyridylethylphosphines, with palladium complexes, 437
Pyridyl-N-iminophosphorane, 439
Pyridyl-N-phosphinoimine, 447
Pyridylphosphine 4-(diphenylphosphinomethyl)-2,2-dimethyl-5-(2-pyridyl)-1,3-dioxolane, 450
Pyridylphosphinoalkane ligands, 459
Pyrrolo[2,1-a]isoquinolines, 107
Pyrrolo[1,2-a]quinoline-5-carboxylates, 12

Q
QSAR modeling of human serum protein binding, 44
Quantitative structure-pharmacokinetic/pharmacodynamic relationships of fluoroquinolones, 45
Quaterthiophene, spectra, 132
 observation of the second triplet state T2, 138
 solid-state photoluminescence, 142
 X-ray data, 134
(-)- Quinocarcin, 120
Quinodimethane derivatives of terthiophene, 149
Quinoids, 228
Quinoline-4-carboxylates, 12
Quinque thiophene, inclusion complex in perhydrotriphenylene, 160
 oligomer unit, 306
 optical constants of
 vapor-deposited films, 142

R
Regioregular poly(3-alkylthiophene)s, spectra, 286
Regioregular poly(3,4-cycloalkylthiophene) derivatives, 299
Rhenium complexes, photolysis in presence of thiophenes, 354
Rufloxacin, 2
 phototoxicity, 83
Ruthenium complexes, photolysis in presence of thiophenes, 355
Ruthenium(II) polypyridine chromophores, coordinated to π -conjugated oligomer ligands, 279

S
Sedamine, 34
Selenium, as a bridge in clusters, 421
 α -Sexithiophene, in organic semiconductor device fabrication, 233
 spectra, 132
 X-ray data, 134
Silylene-thienylene copolymers, 331
(-)-Solenopsin A,,34
Solvent polarity, effect on emission bands, 156
2-Styrylnaphthalene, photocyclization, 203
Styrylthiophene derivatives, photochemical formation, 204
 photochemical reactivity, 197
3-Styrylthiophene, oxidative photocyclization, 199
 isomers, 200
cis and *trans*-3H,7H-3-Substituted 7-amino-1,2,3,5,6,7-hexahydropyrido[3,2,1-ij]quinazolin-1-ones, 32, 33
3-Substituted 4-aminopyrido[1,2-a]pyrazinium salts, 111
(6R,9aS)-2-Substituted 6-arylperhydropyrido[1,2-a]pyrazines, 55
10-Substituted 3-hydroxymethyl-2,3-dihydro-5H-pyrido[1,2,3-de][1,4]benzoxazin-5-ones, 104

- 10-Substituted 3(S)-methyl-9-fluoro-7-oxo-2,3-dihydro-7H-pyrido[1,2,3-de][1,4]oxazine-6-carboxylic acids, 60
- 3-[(Substituted methyl)thio]-1H-pyrido[1,2-c]pyrimidines, 21
- 3-Substituted 1-oxo-2,3,5,6,7,8-hexahydropyrido[1,2-c]pyrimidine-4-carboxylates, 28
- 9-(3-Substituted prop-1-2-enyl)-7-oxo-1H,3H,7H-pyrido[3,2,1-ij][3,1]benzoxazine-6-carboxylic acids, catalytic hydrogenation, 17
- 9-(3-Substituted prop-1-ynyl)-7-oxo-1H,3H,7H-pyrido[3,2,1-ij][3,1]benzoxazine-6-carboxylates, catalytic hydrogenation, 17
- 2-Substituted thiophenes, irradiation, 167
- 3-Substituted thiophenes, by irradiation of 2-substituted isomers, 167
- 6-Substituted 2-tosyl-11-methylene-2,3,4,6,11,11a-hexahydro-1H-pyrazino[1,2-b]isoquinolines, 116
- Sunepirton, 2
- Supramolecular chirality, 222
- T**
- Terthienyl derivatives, femtosecond-spectroscopic investigation, 140
- laser excitation, 132
- observation of the second triplet state T₂, 138
- S₀-T₁ spectrum, 137
- UV spectra, 128
- X-ray data, 134
- Terthiophenes, isolation, 162
- polymers, 286
- Tetradecafluorosexithiophene, 265
- Tetrahydroisoquinoline-3-carboxylic acid, reaction with primary amines and isonitriles, 109
- 3,4,11,11a-Tetrahydro-1H,6H-[1,4-oxazino[4,3-b]isoquinoline, as enzyme inhibitors, 122
- 3-(2-Tetrahydropyranyloxymethyl)-9,10-difluoro-7-oxo-2,3-dihydro-7H-pyrido[1,2,3-de][1,4]benzoxazine-6-carboxylate, hydrolysis, 71
- 1,6,7,11b-Tetrahydro-2H-pyrazino[1,2-b]isoquinoline-3-carboxylate, 89
- 2,3,4,6-Tetrahydro-1H-pyrazino[1,2-b]isoquinolin-4-one, 97
- reduction, 81
- 3,4,6,11-Tetrahydro-2H-pyrazino[1,2-b]isoquinolin-4-one, 57
- 1,2,3,4-Tetrahydro-11bH-pyridazino[6,1-a]isoquinoline-1,1-dicarboxylate, 11
- cis*-1,2,3,4-Tetrahydro-4aH-pyridazino[1,6-a]quinoline-3,3-dicarboxylates, 10
- Tetrahydro-1H,3H-pyrido[1,2-c][1,3]oxazin-1,6-diones, 30
- 3,4,7,8-Tetrahydro-1H,6H-pyrido[2,1-c][1,4]oxazin-1-ol, 84
- Tetrahydro-1H,3H-pyrido[1,2-c][1,3]oxazin-1-ones, 27
- 3,4,4a,5-Tetrahydro-1H,8H-pyrido[1,2-c][1,3]oxazin-1-one, conformation, 15
- Tetrahydro-1H,3H-pyrido[1,2-c][1,3]oxazin-6-ones, 30
- 3,4,4a,5-Tetrahydro-1H,6H-pyrido[1,2-c][1,3]oxazin-6-one, conjugate addition with dipentylcuprate, 18
- 6,7,8,9-Tetrahydro-4H-pyrido[1,2-a]pyrazin-4-one, 89
- 1,2,3,4-Tetrahydro-6H-pyrido[1,2-a]pyrazin-6-ones, 116
- 2,3,5,6-Tetrahydro-1H,7H-pyrido[3,2,1-ij]quinazoline-1,7-dione, reaction with sodium azide, 24
- 2,3,6,7-Tetrahydro-1H,5H-pyrido[1,2,3-de]quinoxaline-2,3-diones, 96
- NMDA receptor antagonist activity, 122
- 1,2,3,4-Tetrahydro-11bH-pyridazino[6,1-a]isoquinoline-1,1-dicarboxylate, 11
- 7,8,9,10-Tetrahydro-6aH-pyrido[1,2-a]quinoxaline, 105
- Tetrakis(p-tolyl)thiophene S-oxide, photoirradiation in presence of triphenylphosphine, 348
- Tetrakis(trifluoromethyl)Dewar thiophene, isolation, 169

- Tetraphenylfuran, 348
Tetraphenylthiophene, 348
 failure to undergo oxidative
 photocyclization, 204
Tetraphenylthiophene S-oxide,
 photoirradiation, 348
Tetrathiophene anthracene derivatives,
 270
Thermochromism of polysilanes, 332
3-Thiabicyclo[3.1.0]hexane, 351
3-Thiabicyclo[3.1.0]hexane-6-
 carboxylates, 351
Thianaphthene 1,1-dioxide, irradiation
 in the presence of quencher, 345
 triplet energy, 345
[1,4]Thiazino[3,4-a]isoquinoline-1-
 imines, 107
Thienothiophene derivatives, nonlinear
 optical properties, 257
Thienyl alkenes, photochemical
 isomerisation, 165
Thienyl azodyes, linked to a polyester
 matrix as optical storage materials,
 238
Thienyl chalcones, solvatochromic
 properties, 149
Thienyl derivatives hexarylethane
 unit, 243
 linked to carbazole, 276
 linked to dibenzothiophene, 276
 UV properties, 128
Thienyl imines, spectra, 149
Thienyl pyrrole derivatives,
 spectra, 284
Thienylpyrrolylbenzothiazoles, 240
1-(2-Thienyl)-2-(2-pyrrolyl)ethylene
 derivatives, reduction, 198
Thienyl-styrene, arylation, 198
Thienyl-substituted
 benzoxazoles, 149
 imidazopyridines, 149
 3,4-oxadiazole derivatives, 285
Thienyl-thiazolyl derivatives, 248
2-Thienylthioamide, reaction with
 alkenes, 174
2-Thienyl-trimethylsilylacetylene,
 isomerisation to 3-isomer, 193
Thiohelicenes, 202
Thiophene, containing dendrimers, 252
 2+2 cycloaddition reaction when
 irradiated in the presence of maleic
 anhydride, 171
 2+2 cycloaddition reaction when
 irradiated in the presence of
 phthalimide, 172
 decomposition in light, 167
 $^3\pi-\pi^*$ transition, 133
 photochemical Diels–Alder reaction
 with alkynes, 173
 photochemical reaction with
 benzophenone, reaction with allyl
 iodide, 179
 reaction with p-
 chlorodimethylaniline, 194
Thiophene-S,S-dioxide,
 in oligomers, 307
2-Thiophenemethanol, irradiation, 171
Thiophene-perfluoroarene
 copolymers, 333
Thiophene-thiophene-S,S-dioxide
 copolymers containing 3,6-
 dimethoxyfluorene, 309
2(5H)-Thiophenones, irradiation, 350
Time-resolved pump-probe
 experiments, 138
Time-resolved spectra of the
 oligothiophenes, 137
Transient absorption study by using
 femtosecond apparatus, 136
Trequinsin, 2
 as a selective PDE3 inhibitor, 34
Triarylamine dendrimers with terminal
 2,5-diarylthiophene, 257
8,9,10-Trifluoro-3(S)-benzyl-7-oxo-2,3-
 dihydro-7H-pyrido[1,2,3-de][1,4]
 oxazine-6-carboxylate, 61
cis-4(R)H,9a(S)H-4-(3,4,5-
 Trifluoromethylphenyl)
 perhydropyrido[2,1-c][1,4]oxazin-
 6-one, 84
2-(4-Trifluoromethylphenyl)thiazole
 unit, effective for electron
 transport, 284
8,9,10-Trifluoro-3-phenyl-7-oxo-2,3-
 dihydro-7H-pyrido[1,2,3-de][1,4]
 oxazine-6-carboxylate, 61

cis- and *trans*-4H,9aH-4-(3,4,5-Trifluorophenyl)perhydropyrido [2,1-c][1,4]oxazin-6-ones, 66

Trimers of dithienylethene derivatives, irradiation, 229

1,3,8-Trioxo-1,2,3,4-tetrahydro-8H-pyrido[1,2-a]pyrazine-7-carboxamide, 94

Triphenyl imidazol-substituted derivatives, 214

cis-7H,9H-*trans*-8H,9H-7,8,9-Tri (pivaloyloxy)perhydropyrido[2,1-c][1,4]thiazine, 55

cis-7H,9H-*trans*-8H-7,8,9-Tri (pivaloyloxy)perhydropyrido[2,1-c][1,4]thiazin-6-ones, separation of epimers, 36

Triplet state lifetimes, 134

2,3,4-Tri(trifluoromethyl)thiophene, irradiation, 169

Tris(2-benzo[b]thienyl)methyl alcohol, intramolecular photocyclization, 342

Tris(chloro((1-methyl-1-(6-methyl-2-pyridyl) ethoxy) diphenylphosphine- η^2 -N,P), 453

Tris(3-(2,6-dimethoxypyridyl)) phosphine, 407

Tris(6-methylquinolin-8-yl)arsine, 417

Tris(2-pyridyl)phosphine, 408, 418
 reaction with molybdenum carbonyls, 417

Tris(2'-pyridyl)phosphine oxide, 420

Tungsten complexes, photolysis in presence of thiophenes, 356

Two-photon absorption molecular structures, 268

Two-substituted naphthalene thienyl oligomers, 144

U

2-Unsubstituted *cis*- and *trans*-4H,9aH-4-(3,4,5-trifluorophenyl)-7-{1-[3-methoxy-4-(4-methyl-1H-imidazol-1-yl)phenyl]-(E)-methylene}perhydropyrido[1,2-a]pyrazin-6-ones, 62

V

Vinylidenes, formation, 424

2-Vinylpyridine, 455

Vinylthiophene, reaction with singlet oxygen, 174

X

Xylogranatinin, 3
 isolation, 119
 structure by NMR spectra, 47